

This electronic thesis or dissertation has been downloaded from the King's Research Portal at <https://kclpure.kcl.ac.uk/portal/>



Design and Synthesis of Benzofused Biaryl Polyamides as G-Quadruplex Targeting Agents

Nahar, Kamrun

Awarding institution:
King's College London

The copyright of this thesis rests with the author and no quotation from it or information derived from it may be published without proper acknowledgement.

END USER LICENCE AGREEMENT



Unless another licence is stated on the immediately following page this work is licensed

under a Creative Commons Attribution-NonCommercial-NoDerivatives 4.0 International

licence. <https://creativecommons.org/licenses/by-nc-nd/4.0/>

You are free to copy, distribute and transmit the work

Under the following conditions:

- Attribution: You must attribute the work in the manner specified by the author (but not in any way that suggests that they endorse you or your use of the work).
- Non Commercial: You may not use this work for commercial purposes.
- No Derivative Works - You may not alter, transform, or build upon this work.

Any of these conditions can be waived if you receive permission from the author. Your fair dealings and other rights are in no way affected by the above.

Take down policy

If you believe that this document breaches copyright please contact librarypure@kcl.ac.uk providing details, and we will remove access to the work immediately and investigate your claim.

Design and Synthesis of Benzofused Biaryl Polyamides as G-Quadruplex Targeting Agents

A dissertation submitted in partial fulfilment of the requirements for the degree
of
Doctor of Philosophy

Kamrun Nahar

Institute of Pharmaceutical Sciences
School of Biomedical Sciences
King's College London



Supervisor

Dr Khondaker Miraz Rahman
Professor David E. Thurston

February 2017

Plagiarism statement

This thesis describes research conducted in the School of Pharmacy, UCL and Kings' College London, University of London between November 2009 and March 2014 under the supervision of Professor David E Thurston and Dr Khondaker Miraz Rahman. I declare that the research described in this thesis is unique and I have clearly mentioned the part that was conducted by our research collaborators. I also declare that all the text in this thesis has been written by me and the parts that have already appeared in publication have been suitably quoted.

Signature _____ Date _____

Acknowledgement

Firstly, I would like to express my deepest appreciation and profound gratitude to my respected supervisors, Dr Khondaker M Rahman and Professor David Thurston for their valued supervision and encouraging support throughout my research work.

I deeply appreciate the generous help and guidance of Dr Isabel Villanueva Margalef and Mr Rashedul Haque from the School of Pharmacy, UCL, during the course of my work.

I am highly grateful to Mrs Kazi Sharmin Nahar and Mohammad Kaisarul Islam of my group for their generous help and encouragement.

I would like to express my gratitude to Miss Laureen Sander and Sunil Lagh for helping me with the biological assay of the synthesised compounds.

I am thankful to all the members of the Gene Targeted Drug Design Research Group and Spirogen for their assistance and kindness.

Finally, I want to acknowledge the tremendous support I received during the course of my PhD from my family members particularly my husband Mr Mohammad Gias Uddin Khan, my mother Mrs Ayesha Begum, my father Mr Mohammad Abul Husain, my brother, sister, my son Zahin Aariz Khan and my daughters Zahia Aaima Khan and Zaina Aasia Khan.

Abstract

Guanine-rich nucleic acids can fold into distinctive four-stranded G-quadruplex structures which are found in telomeric DNA repeats, as well as in sequences in promoter and other regulatory regions of genes, especially those involved in cellular proliferation. Small molecules that can selectively bind and stabilize the G-quadruplex structure have become of significant interest to researchers and are gaining momentum as a possible new class of anticancer agents [1]. Using a distamycin scaffold as a starting point, we introduced biaryl building blocks in place of pyrroles to switch preference from duplex to quadruplex DNA. This alteration in shape ensures that the molecules have low affinity for duplex DNA while increasing their interaction with a G-quadruplex structure, since the ligands have similar dimensions. The structures of the biaryl polyamides previously reported by the Thurston group were tailored to enhance affinity for specific G-quadruplexes (*e.g.*, *c-kit1* vs *c-kit2* vs HT4) while retaining the quadruplex vs duplex selectivity. A 66 member focused second generation biaryl polyamide library was synthesized based on structural information obtained from the previously reported polyamide types. Assessment of the G-quadruplex interaction of the library members was initially carried out using a FRET-based melting assay. Compound KN-242 with hybrid benzofused and biaryl building blocks showed significant selective stabilization of human Telomeric G-quadruplex. At 1 μM concentration it stabilized human Telomeric G-quadruplex by 32 °C, while showing insignificant affinity for duplex DNA. FRET competition assays with C-kit quadruplexes and CT DNA further confirmed selective stabilization of telomeric quadruplexes. A short-term growth inhibitory experiment against six different cancer cell lines, MiaPaCa2, A549 MCF7, HeLa, U87MG, A431 and WI38 gave low micromolar IC_{50} values and between 5-8 fold selectivity for cancer cell lines compared with the non-cancerous WI 38 cell line. Therefore, given their low molecular weight, good water solubility and excellent cellular penetration properties, molecules of this type have the potential to be developed into either potential therapeutic agents or reagents that can probe DNA structure, and/or down-regulate individual signalling pathways in cells.

Abbreviations

ADME	Absorption, Distribution, Metabolism, Excretion
ADAR1	Adenosine Deaminase type I
AID	Activation Induced Cytosine Deaminase
A-T	Adenine-Thymine
APC	Adenomatous Polyposis Coli
BLM	Bloom's syndrome protein
C-G	Cytosine-Guanine
DCM	Dichloromethane
DIC	1,3-Diisopropylcarbodiimide
DMF	<i>N,N</i> -Dimethylformamide
DMSO	Dimethyl Sulfoxide
DNA	Deoxyribonucleic acid
DNA-PK	DNA -Dependent Protein Kinase
EB1	End-Binding protein 1
ES	Electrospray
EPM1	Myoclonus Epilepsy 1
FBX4	F-box Protein
FID	Fluorescent Intercalator Displacement
FRET	Fluorescence Resonance Energy Transfer
FXS	Fragile X syndrome
GIST	Gastrointestinal Stromal Tumor
GQN	G-quadruplex-specific Nuclease
HOBt	1-Hydroxybenzotriazole
hPot1	Human Pot1
hnRNP	Heterogeneous Nuclear RiboNucleoProtein
HPLC	High Performance Liquid Chromatography

HRMS	High Resolution Mass Spectrometry
HT	Human Telomere
IR	Infrared
LCMS	Liquid Chromatography coupled Mass Spectrometry
LFS	Li-Fraumeni syndrome
MS	Mass Spectrometry
mRNA	messenger RNA
NMR	Nuclear Magnetic Resonance
NSE	Nuclease-Sensitive Element
PDA	Photo Diode Array
POT1	Protection Of Telomeres 1
pRb	Retinoblastoma protein
QSAR	Quantitative Structure Activity relationship
Rb	Retinoblastoma
RT	Room temperature
RPA	Replication Protein A
RNP	Ribonucleo Protein
SC	Synaptonemal Complexes
SBMA	Spinal and Bulbar Muscular Atrophy
TANK 1	Tankyrase 1
TANK 2	tankyrase 2
TEBP	Telomere End-Binding Proteins
TTTA Box	Goldstein-Hogness Box
TBP	TATA Binding Protein
TER	Telomerase RNA
TERT	Telomerase Reverse Transcriptase
TFO's	Triplex Forming Oligonucleotides

THF	Tetrahydrofuran
TLC	Thin Layer Chromatography
Topo I	Human Topoisomerase I
TRAP	Telomerase Repeat Amplification Protocol Assay
TRF1	Telomeric Repeat binding Factor 1
TRF2	Telomeric Repeat binding Factor 2
TSS	Transcription Start Sites
UV	Ultra Violet
WRN	Werner's syndrome protein

Table of Contents

Plagiarism statement.....	2
Acknowledgement.....	3
Abstract.....	4
Abbreviations.....	5
 1.0 INTRODUCTION	 12
1.1 Cancer	12
1.2 Hallmarks of Cancer	12
1.3 Cancer Chemotherapy	13
1.4 DNA as a Target for Anticancer Therapy	14
1.5 DNA Structure	15
1.5.1 Double Helix DNA	16
1.5.2 Triplex DNA	17
1.5.3 Quadruplex DNA	19
1.5.4 i-Motif DNA	32
1.5.5 Z-DNA	34
1.6 DNA Replication and the End Replication Problem	35
1.7 Human Telomere	36
1.7.1 Telomeric Complex/ Shelterin complex	37
1.8 Telomerase	38
1.8.1 Components of human telomerase enzyme	40
1.8.2 Regulating Telomerase Access to Telomeres	42
1.9 Telomere Length Regulation by Alternative Mechanisms	44
1.10 Targeting Telomerase for Cancer Therapy	45
1.10.1 Inhibiting the Catalytic Activity of Telomerase	46

1.11 Targeting the telomere	47
1.12 Telomeric G-Quadruplex Structure	48
1.13 Non-Telomeric G-quadruplex DNA	51
1.13.1 c-kit	53
1.13.2 c-myc	56
1.13.3 G-quadruplex found in other human promoters	59
1.14 RNA G-quadruplex	60
1.14.1 RNA G-quadruplexes in 5'-UTRs of mRNAs	62
1.15 G-quadruplexes as a Potential Anticancer Drug Target	64
1.15.1 Common Features of G-quadruplex-interactive Compounds	66
1.15.2 Modes of Interaction of Ligands with G-quadruplex Structures	66
1.15.3 Structural types of G-quadruplex targeting ligands	68
1.15.4 Examples of some G-quadruplex Binding Ligands	79
1.16 The Aim of this Study	97
 CHAPTER TWO: EXPERIMENTAL TECHNIQUES FOR THE INVESTIGATION OF G-QUADRUPLEX/LIGAND INTERACTIONS	 98
 2.0 BIOPHYSICAL AND BIOLOGICAL TECHNIQUES FOR THE INVESTIGATION OF G-QUADRUPLEX LIGANDS	 98
2.1 Biophysical techniques	98
2.1.1 Optical spectroscopic methods	98
2.1.2 Circular Dichroism (CD) Spectroscopy	100
2.1.3 Molecular Fluorescence	102
2.1.4 Equilibrium Dialysis	111
2.1.5 Mass Spectrometry	112
2.1.6 Quantitative Analysis of Binding Events	113
2.1.7 Dimethylsulphate (DMS) Footprinting	115
2.1.8 X-Ray Diffraction and NMR Spectroscopy	116
2.1.9 Molecular Modelling	119

2.1.10	Polyacrylamide Gel Electrophoresis	119
2.1.11	Sedimentation Velocity Analysis and Sedimentation Equilibrium	120
2.1.12	Cross-Linking DNA and Topology	120
2.1.13	Other Methods	121
2.2	Biological Methods	121
2.2.1	Polymerase Chain Reaction (PCR)	121
2.2.2	Telomerase Repeat Amplification Protocol (TRAP)	122
2.2.3	Sulphorhodamine B Assay (SRB)	126
2.2.4	Long-term Population Doubling Studies	128
3.0	RESULTS AND DISCUSSION	130
3.1	Results and Discussion: Chemical	130
3.1.1	Aryl Polyamides as G-quadruplex Ligands	130
3.1.2	Overview of Design and Evaluation of Ligands	131
3.1.3	Design of Library Types	133
3.2	Results and Discussion: Biological	173
3.2.1	Biophysical Evaluation of the Biaryl Polyamide Series	173
3.2.2	Fluorescence Resonance Energy Transfer (FRET) Melting Assay	173
3.2.3	Biological Evaluation of the Synthesized Compounds	185
3.3	Structure Activity Relationship	201
3.3.1	R1.1 - The First Ring Moiety	207
3.3.2	R1.2 - The Terminal Contiguous Ring Moiety	210
3.3.3	R2 - The Benzofused Ring Moiety	210
3.3.4	Biological Evaluation of Type-3 Library Molecules.	211
4.0	EXPERIMENTAL-CHEMICAL	212
4.1.1	General Experimental (Chemistry)	212
4.1.2	General procedure for purification by 'Catch and Release' method	212
4.1.3	General Procedures	214
4.1.4	Type-1 Library synthesis	216
4.1.5	Type-2 Library synthesis	241

4.1.6	Type-2 Library synthesis	274
4.1.7	Type 3 Library synthesis	318
4.2	Experimental-Biophysical	388
4.2.1	Assays used for the biophysical evaluation of the ligands	388
4.3	Experimental-Biological	395
4.3.1	Assays for the biological evaluation of G-quadruplex ligands	395
4.3.2	Materials and methods	395
5.0	CONCLUSION AND FUTURE WORK	399
Reference.....		400
Appendix.....		420

Chapter One: Introduction

1.0 Introduction

1.1 Cancer

Cancer is a clinical condition which involves *unregulated cell growth* (abnormal cell division), intrusion (the invasion and resulting effects on neighbouring tissues), and occasionally *metastasis* (spreading of cancerous cells throughout the body by lymph or blood). Benign tumours are self-limited, and do not invade or undergo metastasis; therefore they are different from malignant cancers due to their self-contained nature.

Cancers are started in transformed cells, caused by abnormalities in the genetic material [1]. Carcinogens (radiation, chemicals, or other infectious agents that promote the formation of cancer) might initiate these abnormalities. Malignant tumours develop through a multistep process involving alterations of tumour-suppressor genes and other genes in cancer cells - namely, oncogenes and microRNA [2]. In most cases, more than one mutation must occur in order for cancer to develop.

Tumour cells can vary in sensitivity to different types of treatment such as chemotherapy and radiotherapy, as well as others, making it difficult to manage. This is why the initial stages of cancer development are important and are a pivotal point in developing rational treatments for cancer. As research is developing, it has become possible to target different types of cancer cells more specifically by targeted therapy where the drugs are acting directly on the identifiable molecular targets in tumours while minimizing healthy cell destruction.

1.2 Hallmarks of Cancer

Cancer research primarily targets mechanisms for governing the inter-conversion of healthy cells to malignant cells. To understand the complex and interrelated cancer development process, the mechanism was described as “six essential alterations in cell physiology that

collectively dictate malignant growth: self-sufficiency in growth signals, insensitivity to growth-inhibitory (antigrowth) signals, evasion of programmed cell death (apoptosis), limitless replicative potential, sustained angiogenesis, and tissue invasion and metastasis” (D. Hanahan & R. Weinberg) (**Figure 1.1 a**) [3]. Genome instability underlies these hallmarks that produce the genetic diversity, increasing acquisition and inflammation of these genes which in turn foster numerous hallmark functions. During the last decade, conceptual progress included two emerging hallmarks, in addition to the existing list (**Figure 1.1 b**). Tumours produce a different magnitude of complexities along with the cancer cells by creating a “tumour microenvironment”, which contributes to gaining hallmark traits through recruiting a group of ostensibly normal cells. As such, an understanding of the concept and its applicability will guide us in developing new strategies for treating cancer [4].

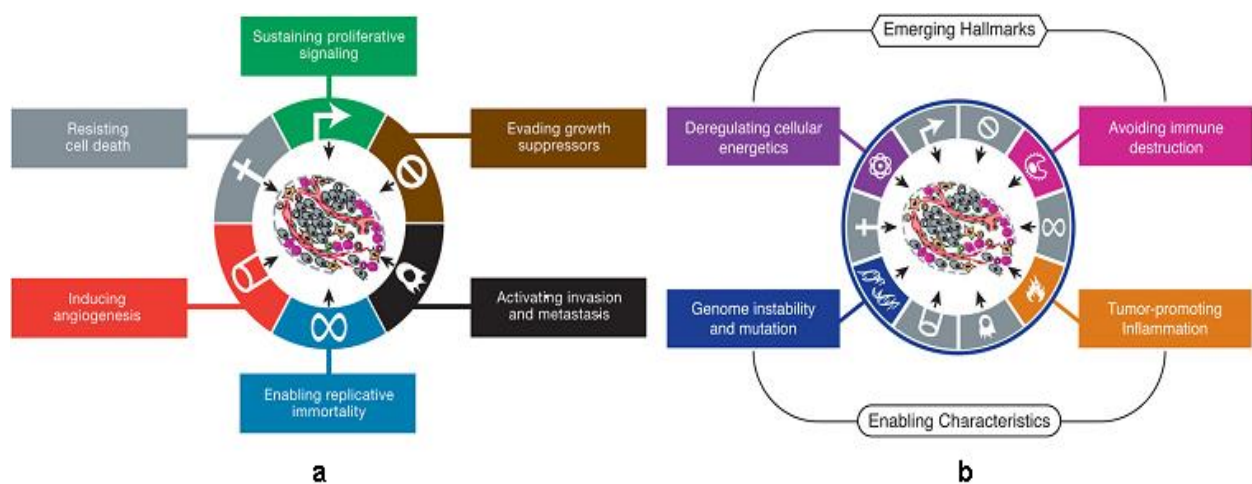


Figure 1.1: a) The Hallmarks of Cancer; b) Emerging Hallmarks and Enabling Characteristics taken from Hanahan and Weinberg, 2011 [4].

1.3 Cancer Chemotherapy

In 1940, nitrogen mustards and folic acid agonists were first used as chemotherapeutic agents for treating cancer. The new approach (termed “targeted therapy”) is now common, though many of the principles and limitations of chemotherapy are still applied in designing anticancer drug discovery programs.

Chemotherapy involves treatment with anticancer drugs to destroy cancerous cells by interfering with cell division during different stages. Chemotherapy generally targets rapidly dividing cells and is non-specific to cancer cells, although some degree of specificity might be achieved in cancerous cells, as the DNA damage response in cancer cells has been found to be different from that of healthy cells [5]. However, chemotherapy could harm healthy tissue, especially those with higher turnover rates (e.g. intestinal lining). To get the maximum result, more than one drug is often given in the form of "combination chemotherapy", which is the most common method in practice. Recently, numerous potential anticancer targets were identified, which resulted in a great expansion of the drug development process. At present, the number of clinically useful anticancer drugs is growing significantly; the main challenges are optimising their clinical use as well as successfully and rationally integrating them with existing anticancer therapies [5].

The increasing knowledge of the biochemical steps engaged in cancer is encouraging the development of new anticancer drugs that exploit the differences between cancer cells and normal cells. Studying the patterns of gene and protein expression enable the successful identification of enzymes, receptors and other molecular targets that are exclusively-expressed or over-expressed in cancer cells compared with normal cells.

1.4 DNA as a Target for Anticancer Therapy

Cancer brings changes to the DNA structure, causing an alteration of normal DNA regulation. Therefore, cancer cells do not respond to normal regulatory signals. DNA has been targeted for a long time for the invention of chemotherapeutic agents for inhibiting gene transcription, translation and other cellular processes - hence, anticancer drugs primarily work by binding to DNA. Cytotoxic agents target DNA non-specifically, and at present chemotherapeutics are designed to target DNA with high specificity. Currently, researchers are trying to develop new molecules that will target not only DNA but also their associated proteins and pathways more specifically.

1.5 DNA Structure

DNA has been known to be polymorphic prior to our understanding of the three-dimensional form of DNA, and it has been shown that it can adopt more than one form (**Figure 1.2**) [7,8]. Over 60 years ago, fibre diffraction studies by Maurice Wilkins and Rosalind Franklin demonstrated that the A-form diffraction pattern was produced by dried, oriented DNA fibres, whereas the same fibre produced a different pattern, called the B form, in a moist form. The B-DNA form (**Figure 1.2 a**) is the common double helical form, where the helical axis runs through the Watson-Crick base pairs [6]. Nucleic acid structures are also found to be present in a number of triple- and quadruple-stranded structures, as well as in left-handed forms (**Figure 1.2 c, f**). Quadruplex structures (**Figure 1.2 f**) based on G-quartets are reported to form at the guanine-rich segments of the telomere and centromere, while their complementary cytosine-rich sequences fold to form an intercalated tetramer referred to as the i-motif [7]. The G-quadruple structures are of great interest for structural biologists, as they have been found to deregulate the telomerase enzyme that favours the division of some tumours [8], hence causing telomeres to be a significant target in designing anticancer drugs. Moreover, the remainder of the DNA structures are reported to take numerous unusual conformations. Three strands with polypurine-polypyrimidine rich sequences in the eukaryotic genome have been found to form H-DNA (**Figure 1.2 e**), demonstrating an important part in DNA replication, metabolism and transcription. Oligonucleotides capable of forming triplexes were designed recently that act as "anti-gene" agents [8]. Therefore, uncommon DNA forms might have an important role in the basic cell regulation processes such as gene expression, chromosomal stability, cellular replication and programmed cell death, representing novel targets for structure, as well as sequence-specific drugs [7].

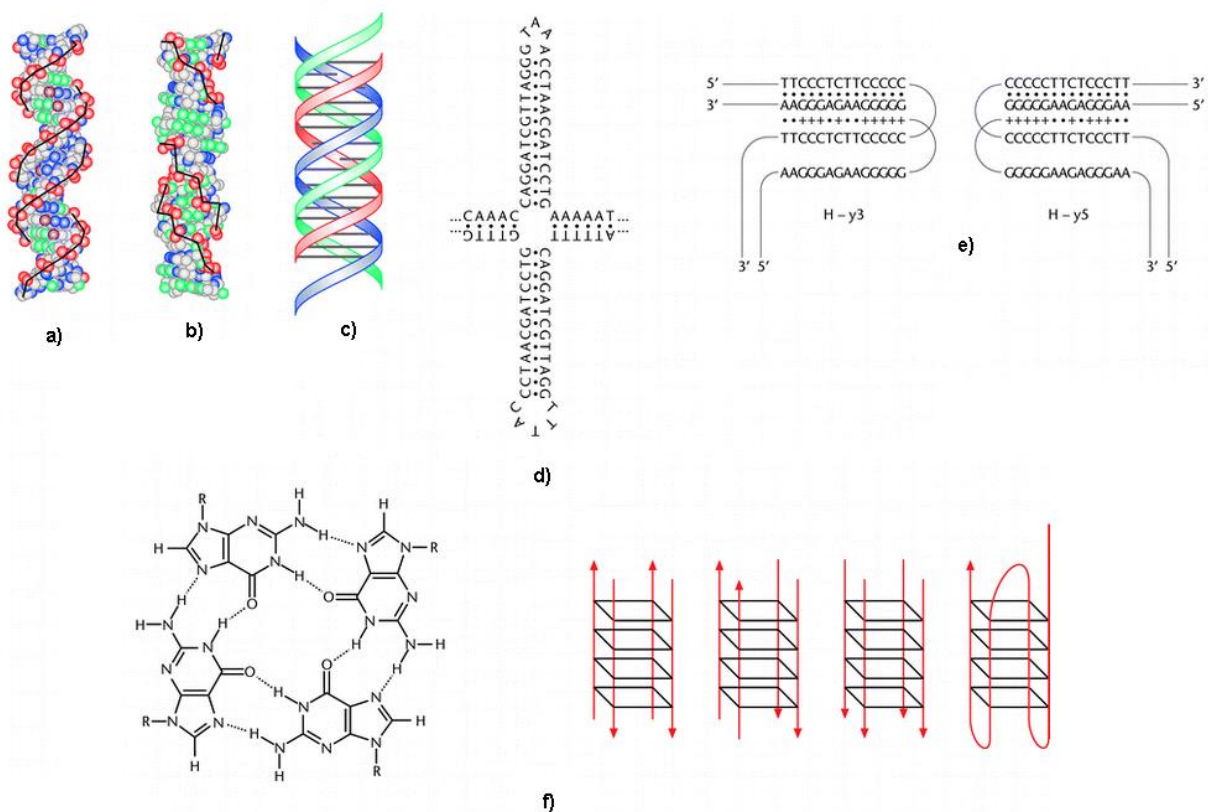


Figure 1.2: Various forms of DNA. (a) B-DNA form, (b) Z-DNA form, (c) triplex DNA form, (d) cruciform DNA, (e) H-DNA form, (f) G-quadruplex DNA with different topology [9].

1.5.1 Double Helix DNA

The double-helix model of the DNA structure (**Figure 1.3 a**) was first published in Nature by James D. Watson and Francis Crick in 1953 [10]. DNA is a long polymer of repeating nucleotide units of 22 to 26 Å wide, where each nucleotide is 3.3 Å (0.33 nm) long [11]. Alternating phosphate and sugar residues form the backbone of the DNA strand [12], where the sugar is 2-deoxyribose and joined with others via phosphodiester bonds formed by phosphate groups between the 3rd & 5th carbon of neighbouring sugar rings. In a double helix the ends of asymmetric antiparallel strands are termed as 5' ends with a terminal phosphate group and 3' ends with a terminal hydroxyl group. Four different bases {named cytosine (C), adenine (A), thymine (T) and guanine (G)} in DNA are linked to the sugar/phosphate backbone, completing the nucleotide structure (**Figure 1.3 b**). The DNA double helical structure is stabilized by two types of forces: the hydrogen bonds among the nucleotides and the base-stacking interactions between the aromatic nucleobases [13]. Conjugated π bonds of

nucleotide bases, in the aqueous environment of the cell, align themselves perpendicularly to the axis of the DNA structure, and thus minimize the interaction between the solvation shell and Gibbs free energy. All these hydrogen bonds acting internally and externally thus stabilize the DNA structure by bringing the two complementary strands together.

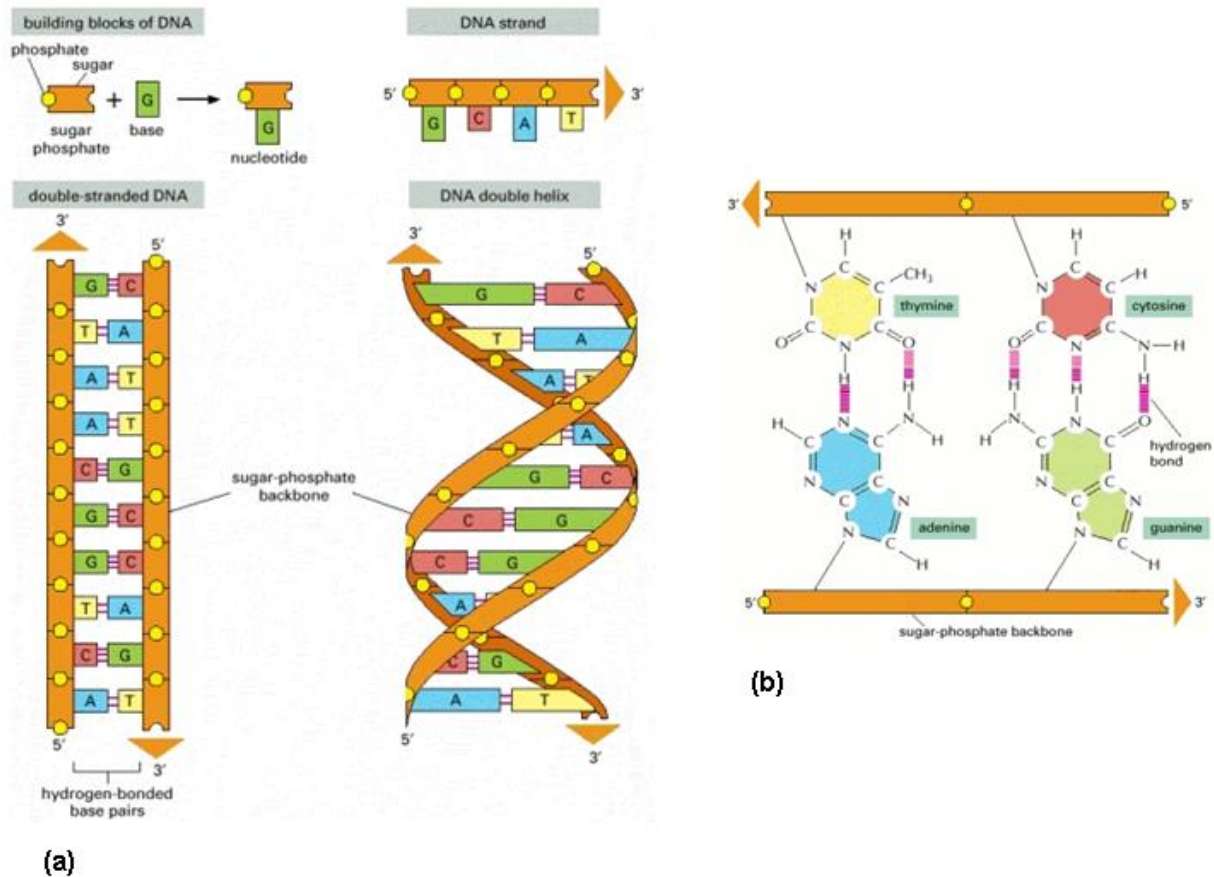


Figure 1.3: (a) DNA and its building blocks, (b) Complementary base pairs in the DNA double helix [14].

1.5.2 Triplex DNA

Nearly 56 years ago, intramolecular triple helical DNA and triplex DNA structures were first reported [15-18] and were found to form at polypurine-polypyrimidine (R.Y) tracts (**Figure 1.4 a**). A third strand binds the minor groove with the major groove using either Hoogsteen or reversed Hoogsteen hydrogen bonds with a duplex resulting in a triplex formation (**Figure 1.4 b, c**) under two conditions. Firstly, melting and refolding of the adjacent homopurine and homopyrimidine segments must occur in order to form intramolecular triplexes, and

secondly, the site-selective binding of the triplex-forming oligonucleotides (TFO's) like antigens with duplex DNA must also occur to form triplexes [19]. There are two basic forms of triplexes, termed R.R.Y and Y.R.Y: either one of these triplexes is formed depending on the overall proportion of base in the third strand, which can be either purine (R) rich or pyrimidine (Y) rich. Reaction conditions determine the formation of either of these triplexes: for example, an acidic pH favours the generation of Y.R.Y type triplexes, whereas for the formation of R.R.Y triplexes neutral pH and divalent metal cations are required, making it frequently available in normal physiological conditions [20]. R.R.Y type triplexes have been found to form rapidly as they can tolerate more versatile pairing schemes [21].

Triplex formation is highly affected by the location of the formation and cannot be formed in every DNA location because of its structure, charge and rigid nature. Additionally, the DNA sequence is another important factor for triplex formation which needs to be either mirror repeats or palindromes of homopurine-homopyrimidine [22]. Triplex formation is again dependent on the pH of the medium as the protonation or non-protonation of certain bases dictates the generation of triplex structures [23].

Triple helical DNA can be targeted selectively to control gene expression *in vivo*, which provides an opportunity to develop therapeutic agents such as anticancer and anti-viral drugs. The binding of oligonucleotides for triplex formation can be either in a parallel or an anti-parallel way. For the parallel binding motif, a low pH is required, allowing the protonation of cytosine, which is difficult under normal physiological conditions [24]. On the contrary, anti-parallel motif formation is insensitive to pH [19].

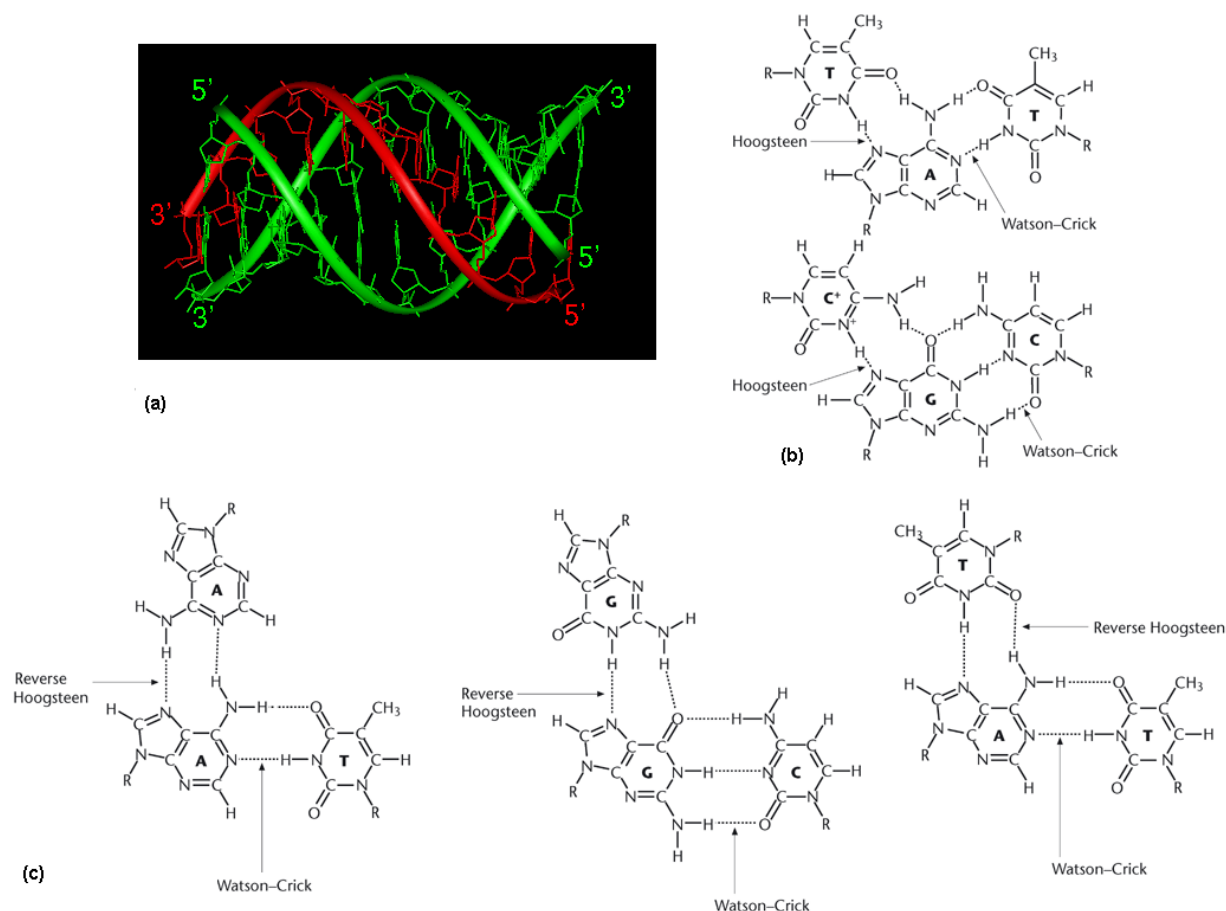


Figure 1.4: Diagram of triplex DNA (a) Triplex DNA structure, (b) Hoogsteen hydrogen bonding. (c) Reverse Hoogsteen hydrogen bonding [9].

1.5.3 Quadruplex DNA

The four-stranded nucleic acid structures were discovered in 1958 while studying the polyinosinic acid fibre. The X-ray diffraction pattern indicated the presence of parallel three- or fourfold polynucleotide strands [25], which later on were proven to be quadruple-stranded [15, 26]. After a few years, Gellert and his team studied the X-ray diffraction patterns of guanosine monophosphate gels and proposed the formation of a cyclic structure by four guanine moieties through hydrogen bonds [6]. Presently, scientists are analysing the existence and functional importance of these quadruple DNAs, referred to as G-quadruplex structures (**Figure 1.5**), forming from specific guanine-rich sequences. These G-quartet

structures are considered important for basic cellular activities and can be very important targets for treating various diseases such as cancer.

The G-quadruplex structures are generated by the folding of either a single polynucleotide molecule or by the association of two or four molecules. The guanine bases stack on each other in square planer geometry to form a tetrad structure (**Figure 1.6**), which is again stabilized through Hoogsteen hydrogen bond formation among the 4 guanine bases. These structures are reported to be found in telomeric regions, as well as in the promoters of certain genes like *c-myc*, *c-kit*, and *bcl-2* with different structural patterns: for example, telomeric DNA forms parallel or antiparallel/parallel mixed-type structures in the presence of K^+ ions, while in the presence of Na^+ cations antiparallel structures are formed. In *c-myc*, promoters with four-looped parallel G-quadruplex structures are found, while in *c-kit* promoters four connecting loops are found in three stacked G-tetrads [27].

Different biophysical experiments have identified around 375,000 potential G-tetrad-forming sequences in the human genome, although their existence has yet to be proven *in vivo* [29]. However, a multitude of indirect evidence indicates the presence of G-quadruplex structures at numerous places in the human genome and these are suggested to be involved in various cellular activities. For instance, a number of proteins isolated from yeast and ciliates showed selective binding ability to G-quadruplexes, as well as converting the duplex DNA to the quadruplex form in the presence of Na^+ and K^+ ions (~150 mM). These quadruple structures are found to control the expression of some genes that are involved in the process of carcinogenesis and in maintaining telomere organization [28]. Their capability to prevent telomeric elongation by inhibition of the enzyme telomerase, which is found to be over-expressed in malignant cells, has gained tremendous research interest [29].

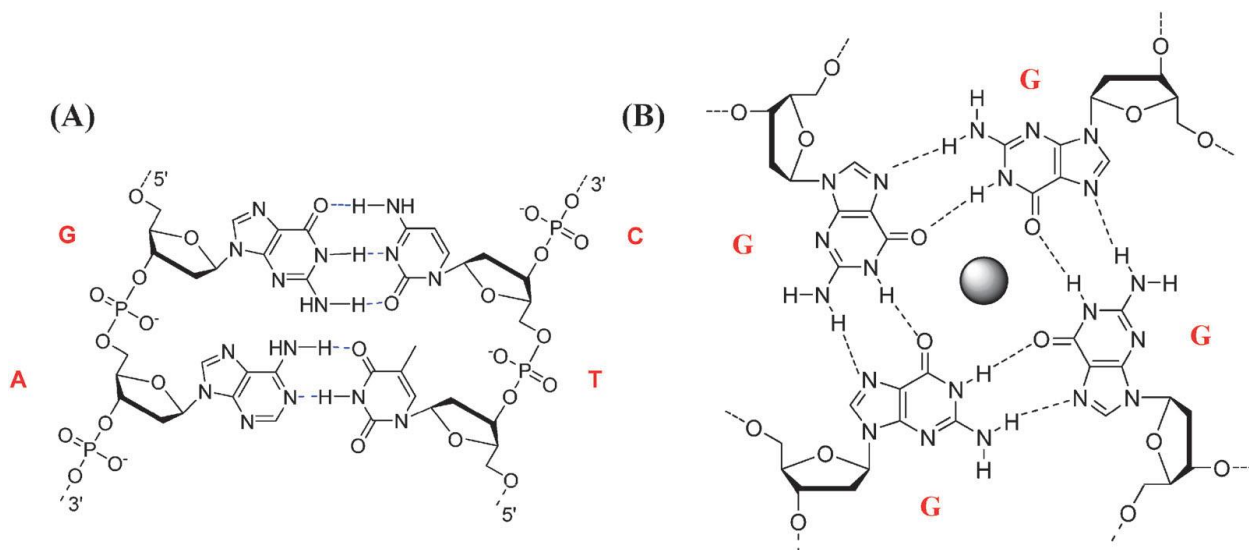


Figure 1.5: (A) Usual A-T and G-C coupling; (B) the G-quadruplex structure [28]

1.5.3.1 General Features of Quadruplex Topology and Structure

Guanine bases form the central part of G-quadruplexes where four guanine bases are organized in a rotationally symmetric way and form hydrogen bonds from N1–O6 and N2–N7 of the resultant square [30]. Quadruplexes are formed by the participation of 1, 2 or 4 different DNA/RNA strands, resulting in numerous different topologies that arise not only because of strand combinations that have different directions but also for different loop size as well as sequences (**Figure 1.8 c**). Possible **unimolecular** (i.e. intramolecular) (**Figure 1.8 e**) sequences can be represented as $G_m X_n G_m X_o X_p G_m$ (m = number of G residues, X_n , X_o & X_p = any arrangement of residues). The association of non-equal sequences can give rise to **bimolecular** (dimeric) (**Figure 1.8 e**) and **tetramolecular** (tetrameric) quadruplexes. Most of the bimolecular quadruplexes are produced through the binding of two identical sequences, $X_n G_m X_o G_m X_p$, (n & p may/may not be 0). Association of four $X_n G_m X_o$ or $G_m X_n G_m$ strands forms tetramolecular quadruplexes [31].

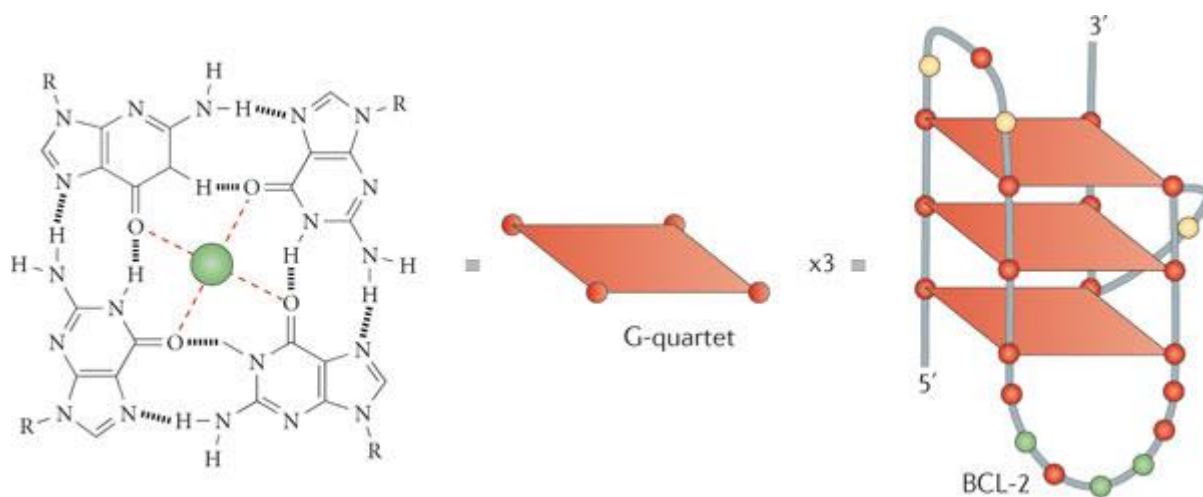


Figure 1.6: Example of G-quadruplex structure [29]

1.5.3.2 G-Quadruplex Stabilization

Factors that stabilize the quadruplex include the base stacking interaction, hydrogen bonds, electrostatic interactions and the hydration shell [32]. In the formation of G-quadruplex structures, base stacking only needs to accommodate the guanine bases. However, quadruplex structures become unstable even in the presence of these stabilizing factors, due to the arrangement of the central guanine O6 carbonyl groups of the G-quartet. The O6 atoms forming a square planar structure for each tetrad give a twist of 30° and a rise of 3.3 \AA between each tetrad step, generating a bipyramidal-antiprismatic arrangement for the eight O6 atoms (**Figure 1.7**). This arrangement of O6 carbonyl atoms forms negatively charged cavities between the G-tetrads that need to be neutralized by the coordination of cations. The overall stability of the finally folded quadruplex largely depends on the selection of a suitable cation, more specifically its size and charge.

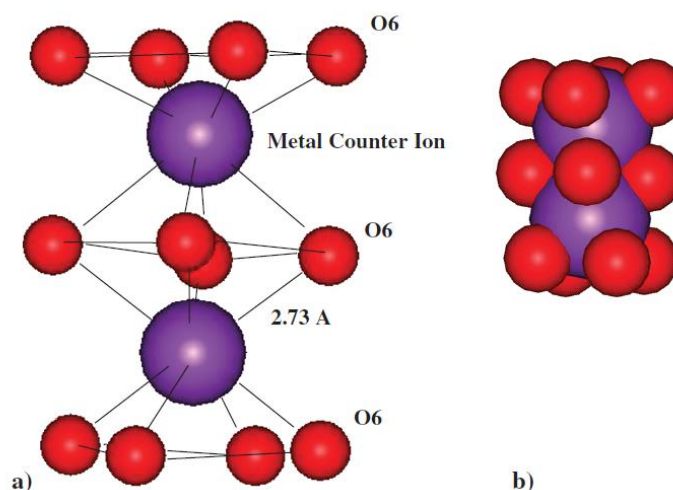


Figure 1.7: Counter ion coordination between tetrad bases shown with a twist between bases. (a) Potassium metal ion is shown coordinated between the eight carbonyl O6 with an average coordination distance of 2.73 Å°. (b) A space filling model with potassium counter ions [33].

1.5.3.3 Loop Structures of G-Quadruplexes

G-tetrad structures are differentiated depending on the strand polarities and the guanine strands connecting loop location. The loops can be divided into three families: propeller, lateral and diagonal (**Figure 1.8 d**). The bases in the loops can also interact with the G-tetrads.

1.5.3.3.1 Propeller Loops

Adjacent parallel strands are linked by a joining loop where the bottom G-quartet is joined with the top G-quartet forming **propeller** loops (**Figure 1.8 D**), sometimes also known as strand-reversal loops. Human telomeric DNA sequences form quadruplexes of this type in crystal structure and solution [34], and more recently this feature has been reported in a number of non-telomeric quadruplexes [35]. When any one of the four strands is in an anti-parallel direction, the G-tetrad structure is called anti-parallel.

1.5.3.3.2 Lateral Loops

The first type of antiparallel loop, **lateral** or edge-wise loops (**Figure 1.8 D**), joins the neighbouring G-strands where two of these loops are present either on the same faces or on the opposite faces of a G-quadruplex structure, representing head-to-head or head-to-tail connections, respectively, in bimolecular G-quadruplex structures. As an example, this type of loop was found in asymmetric quadruplexes for the sequence d(TG4T2G4T) [36], as well as in the bimolecular quadruplex with a sequence of d(GGGCT4GGGC).

1.5.3.3.3 Diagonal Loops

The **diagonal** loop (**Figure 1.8 D**) is another form of anti-parallel loop that connects opposite G-strands, where the adjacent strands have to be of alternating directions between parallel and anti-parallel. This type of loop has been reported to be found in the telomeric region of *Oxytricha nova* with a sequence of d(G4T4G4) [31].

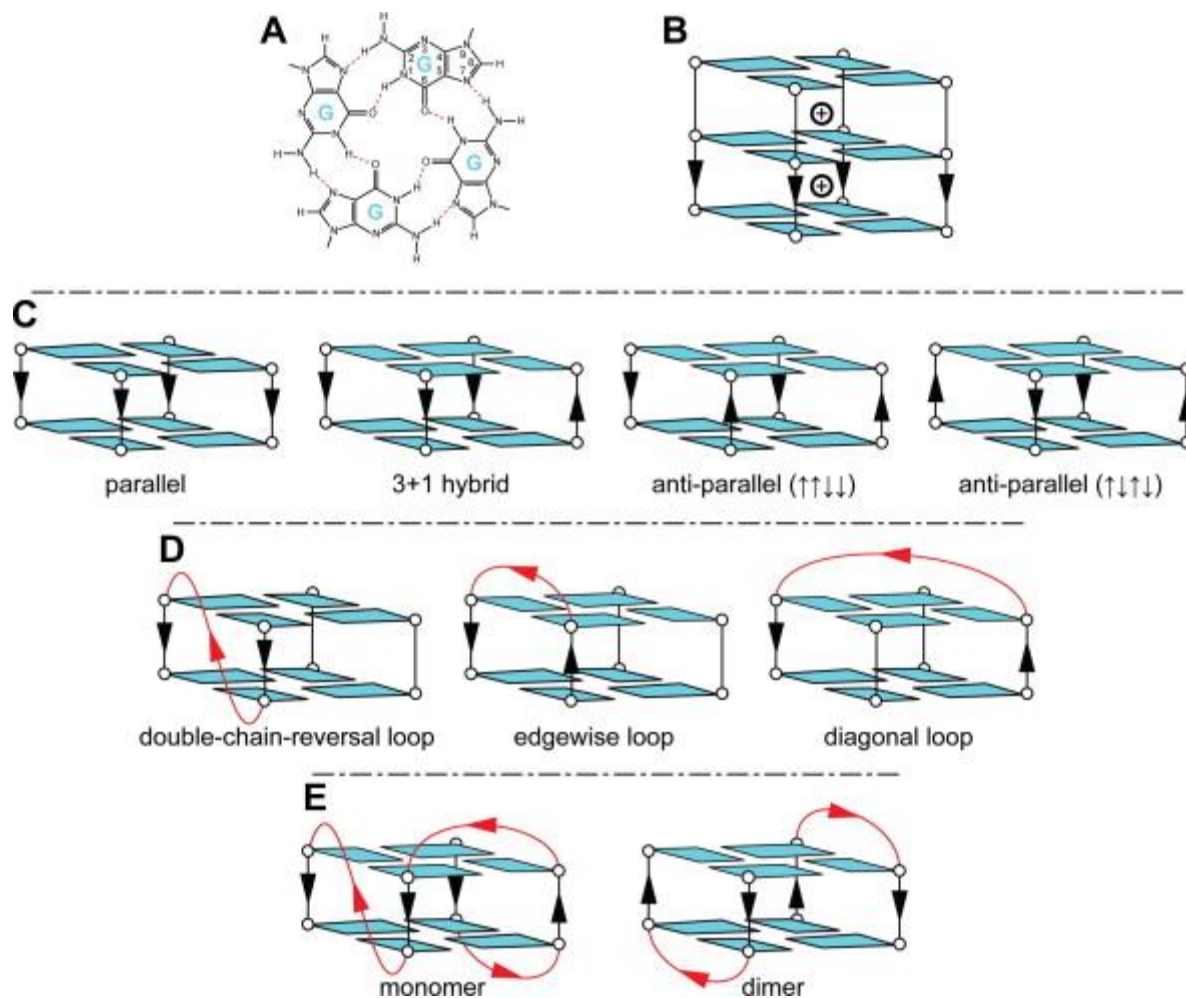


Figure 1.8: (A) G-quadruplex structure. (B) G-quadruplex structure with cation coordination sites. (C) Classification of G-quadruplex structure based on strand polarity. (D) Three principal forms of loop. (E) Monomeric intramolecular and dimeric intermolecular G-quadruplex structures [37].

1.5.3.4 Glycosidic Bond in Quadruplex

The different strand directionality of the G-quartet structures is related to the conformational shape of the *syn* (1.1) or *anti* (1.2) (Figure 1.9) glycosidic bonds formed between the guanine base and the sugar. Bases are in anti-conformation when all of the four strands are in the parallel direction. If any one of the strands is in the anti-parallel direction (Figure 1.10) then the bases have to be in the *syn* (1.1) orientation to form the hydrogen bonds correctly, which

effects the direction of the backbone in relation to the G-tetrads, therefore resulting in grooves of various sizes. Depending on the topology and loop nature, grooves can be of various dimensions. The groove is of medium size when successive guanines are both *anti* (1.2) or both *syn* (1.1). When the first base is *anti* (1.2) and second base is *syn* (1.1), the groove is wider. The groove is narrower when the first is *syn* (1.1) and the second *anti* (1.2) [30]. The complexity of the groove depends on the type of connecting loop: in the case of lateral or diagonal loops the groove structure is simple, whereas in the case of propeller loops the groove structure is complex.

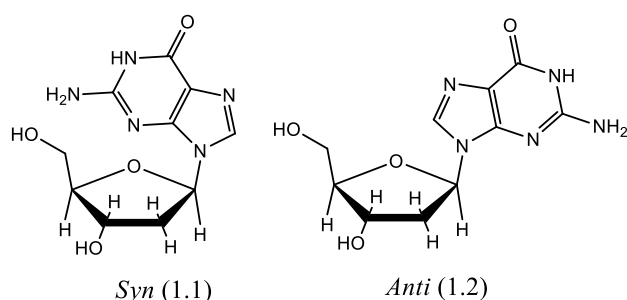


Figure 1.9: Glycosidic bonds within a G-quadruplex can rotate to form two preferred conformations, *syn* (1.1) and *anti* (1.2) [30]

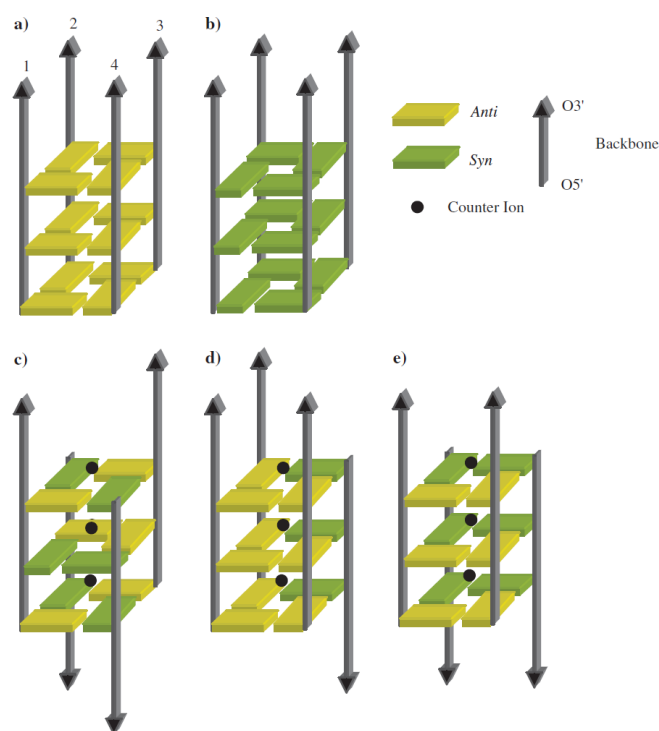


Figure 1.10: Schematic diagram showing the potential strand polarity and related glycosidic bonds for intermolecular quadruplexes. a) Parallel with all *anti* glycosidic bonds. b) Parallel with all *syn* glycosidic bond. c-e) Alternating strand arrangements with the corresponding mixed *syn anti* relationships [33].

1.5.3.5 Evidence for the Presence of G-Quadruplex Structures in the Biological System

Recently accumulated data reveal the existence of numerous putative G-quadruplexes forming guanine clusters in the evolutionarily distant genomes of prokaryotes [38] and humans [39] (**Figure 1.11**). A computational search of human genes for guanine-rich, potential G-quadruplex-forming sequences has identified 226,157 such sites [39], whereas analysis of >61,000 open reading frames of 18 prokaryotes' genomes detected a statistically disproportionate incidence of tetraplex-forming sequences in the gene promoters [38]. Further analysis of nearly 17,000 human genes showed that gene function is correlated with the potential quadruplex-forming sequences. It was found that some classes of genes, such as tumour-suppressor genes, possess low tetraplex-forming potential, whereas others, like proto-oncogenes, have a very high potential to fold into tetraplex structures due to the presence of unique genomic sequences. Since quadruplex-forming sequences are relatively short and quadruplexes are likely to be transiently formed, the detection of these regions in genomic

DNA is similar to a search for a needle in a haystack. However, quadruplex-recognizing specific antibodies, dye molecules and direct electron microscopy analysis provided rather convincing evidence for the relevance of these DNA structures in the genomes of several organisms [40].

For the first time, telomeric DNA was reported with the capability of forming G-quadruplex structures in biological systems. Several organisms containing single-stranded telomeric terminal sequences were found to form an association of G–G paired hairpin type structures [41], which, later on, was described in *Tetrahymena* telomeric DNA [42]. Williamson, for the first time, reported the important role of monovalent cations in forming and stabilizing the G-quadruplex structures and suggested that the cations placed themselves in the cavity generated by the guanines of each tetrad [43]. *Stylonychia lemnae* telomeric DNA was used to establish the biological existence of the quadruplexes, where particular antibodies were used against the formed parallel- and antiparallel-quadruplex structures of the ciliate [44]. Recently, it has also been shown that the control of *in vivo* G-quadruplex formation depends on the telomere end-binding proteins TEBP α and TEBP β through using the same antibody in ciliates, and during replication, phosphorylation of TEBP β is required for resolving the quadruplex structures. *In vivo* G-quartet formation was further shown by the binding and detection of the radio-labelled ligand 360A (2,6-*N,N'*-methylquinolinio-3-yl-pyridine dicarboxamide) or the fluorescent ligand BMVC (3,6-bis(1-methyl-4-vinylpyridinium) carbazole diiodide). Along with the increasing evidence for the existence of human telomeric quadruplex structures, there is growing evidence for the biological existence of these quadruplexes in the non-coding regions of genes and particularly in the gene promoter sites. Recently, quadruplex-forming sequences were found to be near the transcription start sites (TSS) of promoter regions, where there is a strong relation between nuclease-hypersensitive elements and quadruplex-forming sequences [45]. Researchers have suggested that the denaturation or unwinding of duplex DNA favours the formation of a quadruplex, which happens during the transcription, replication and recombination processes [46].

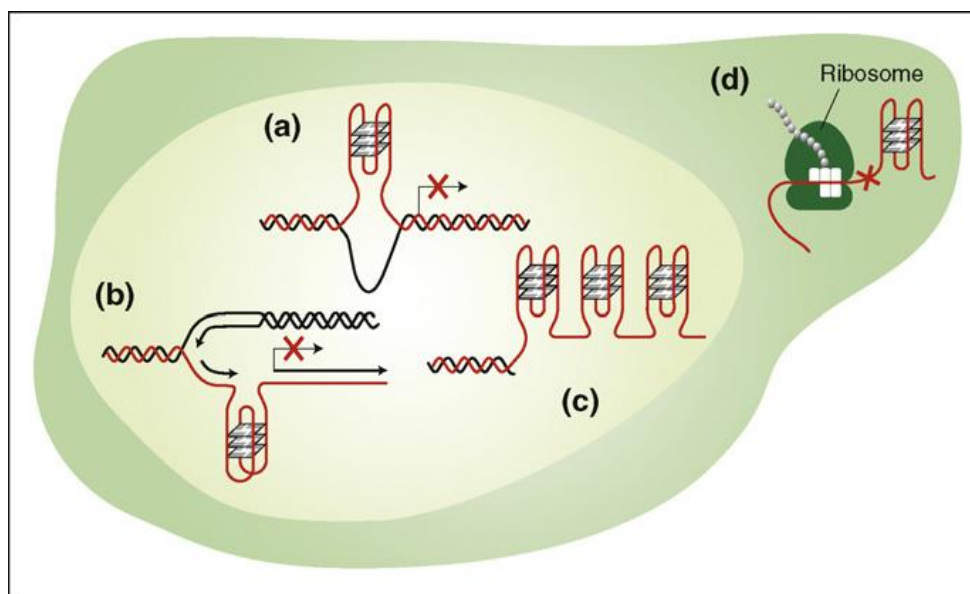


Figure 1.11: Probable locations of the G-quadruplex structures within cells. In nucleus (a) during replication (b) transient single stranded form of DNA. (c) Telomeric single stranded G-rich overhangs. (d) G-quadruplexes in mRNA. Red crosses indicate possible blockage of the replication, transcription and translation process by G-quadruplexes [47].

1.5.3.6 The Proposed Biological role of Quadruplex DNA

1.5.3.6.1 Regulation of Gene Transcription

A significant amount of data supports the proposed role of quadruplex DNA structures in regulating gene transcription [38, 48]. Researchers have identified quadruplex-forming guanine-rich sequences in the regulatory regions of various genes by focusing on particular genes which can readily form different types of tetrahelices *in vitro*. In some cases, additional evidence was provided by the selective interaction of specific transcription proteins within the tetrahelix domains. In most cases, the quadruplex-generating sequences were found in gene promoter or enhancer regions, and the assumed negative or positive effects of such structures on transcription are mostly based on either indirect or *in vitro* accumulated results. However, all the evidence supports the idea that the quadruplex DNA structures serve as regulatory elements and control gene expression either by attracting or dispelling transcription factors [40].

One prominent example of the regulation of gene transcription by quadruplex structures is *c-myc* (**Figure 1.12**). In one early report, it was shown that *c-myc* contains a guanine-rich sequence near the control region located at -142 to -115 bp of the promoter, which can fold to form an intramolecular quadruplex structure [49]. Previously, it was assumed that the quadruplex structure may act to promote transcription by attracting the nuclease hypersensitive binding proteins hnRNPs A1 and K and CNBP, but recent results indicate that it is likely to repress rather than stimulate transcription. Among the two intramolecular G-tetrads formed by the *c-myc* control sequence [50, 51], only the chair-form one was found to be biologically relevant.

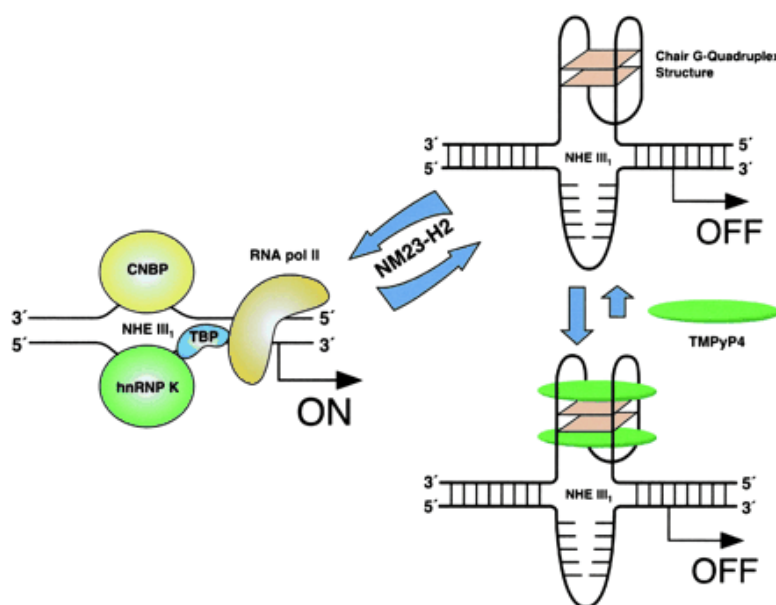


Figure 1.12: Schematic diagram demonstrating the activation as well as the repression process of gene transcription including the part of NM23-H2 in converting guanine-rich single-stranded DNA into quadruplex DNA structures. The binding of TMPyP4 (**1.32**) stabilizes the G-quadruplex structure and inhibits the gene transcription [50].

A G→A point mutation in HeLa S3 cells increases the basal transcription of *c-myc* by 3-fold due to the lack of the formation of this tetraplex structure. On the contrary, the expression of *c-myc* was found to be diminished by stabilization of the tetrad structure with the cationic porphyrin TMPyP4 (**1.32**) (**Figure 1.12**) [50]. Therefore, after analysing these data, it can be proposed that the quadruplex domain in the *c-myc* control region acts to suppress

transcription. Moreover, some other ligands that bind and stabilize telomeric quadruplex DNA inhibiting telomerase activity were found to suppress the *in vitro* transcription of *c-myc* as well [52].

1.5.3.6.2 Telomere Metabolism

Telomeres are DNA-protein complexes found at the end of linear eukaryotic chromosomes that protect the chromosome from degradation by fusion. The single-stranded guanine-rich telomeric DNA overhang folds back to form a specialized tertiary structure known as the G-quadruplex structure. The length of the telomere is maintained by extending the protruding 3' guanine-rich strand by the ribonucleoprotein enzyme telomerase. Effects of the folding of telomeric DNA of *Oxytricha nova* to its role as primer for the elongation of the telomere by the telomerase enzyme was reported in an early study and was demonstrated that its extension by telomerase was blocked by the formation of a quadruplex structure (**Figure 1.13 a**) [53], suggesting that the interconversion of the telomeric DNA into the G-quartet structure may result in the delayed elongation of the guanine strand by telomerase.

A huge number of significant investigations support the hypothesis that the formation of stable quadruplex structures at the telomeric ends act as negative controls and block their extension by telomerase [54]. More directly, several laboratories have reported the stabilization of the G-quadruplex structures of telomeric DNA through using various groups of drugs which inhibited telomeric elongation by telomerase (**Figure 1.13 b**). They demonstrated that the drugs that can bind and stabilize the G-quadruplex structures of telomeric sequences can also block the *in vitro* action of the telomerase, as well as serve to inhibit telomere elongation *in vivo* and the proliferation of cancer cells [55-57]. In addition to its inhibitory effect on telomeric elongation by telomerase, the unimolecular tetrad structure was found to diminish the efficiency of the assembly of telomeric complexes by hindering the formation of some telomeric nucleoprotein complexes, including the proteins TRF2 and pot1 [58].

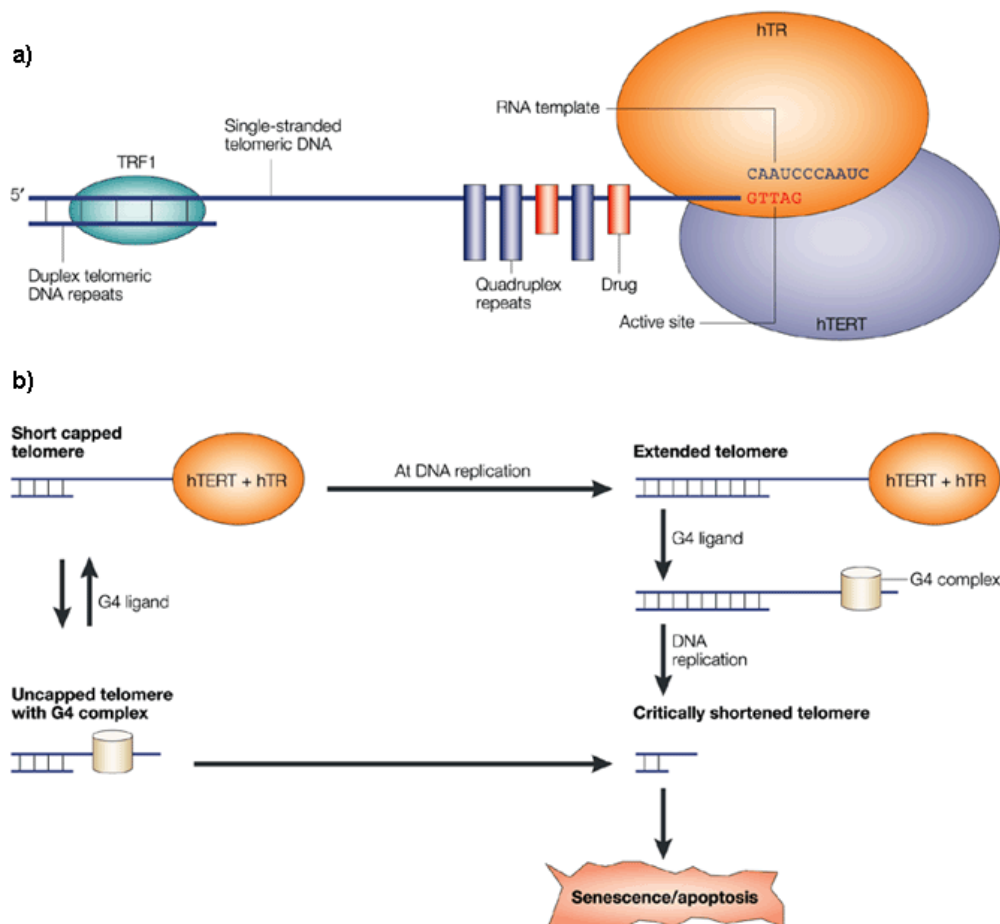


Figure 1.13: Telomere length regulation a) Inhibition of the telomerase enzyme by G-quadruplex formation at 3' end, which was further stabilized by ligand interaction inhibiting further telomere elongation. b) Schematic diagram showing the effects of inhibition of telomere elongation [59].

1.5.4 i-Motif DNA

The i-motif (**Figure 1.14**) is a tertiary DNA structure generated by intercalating two parallel duplex structures in a head-to-tail fashion, where the strands are connected together through hemiprotonated C.C⁺ pairs. This structure can be generated by the association of a single, two or four strands containing four, two or one cytidine repeats, respectively. The centromeric and telomeric C-rich repeats can fold to form an intramolecular i-motif structure [60, 61].

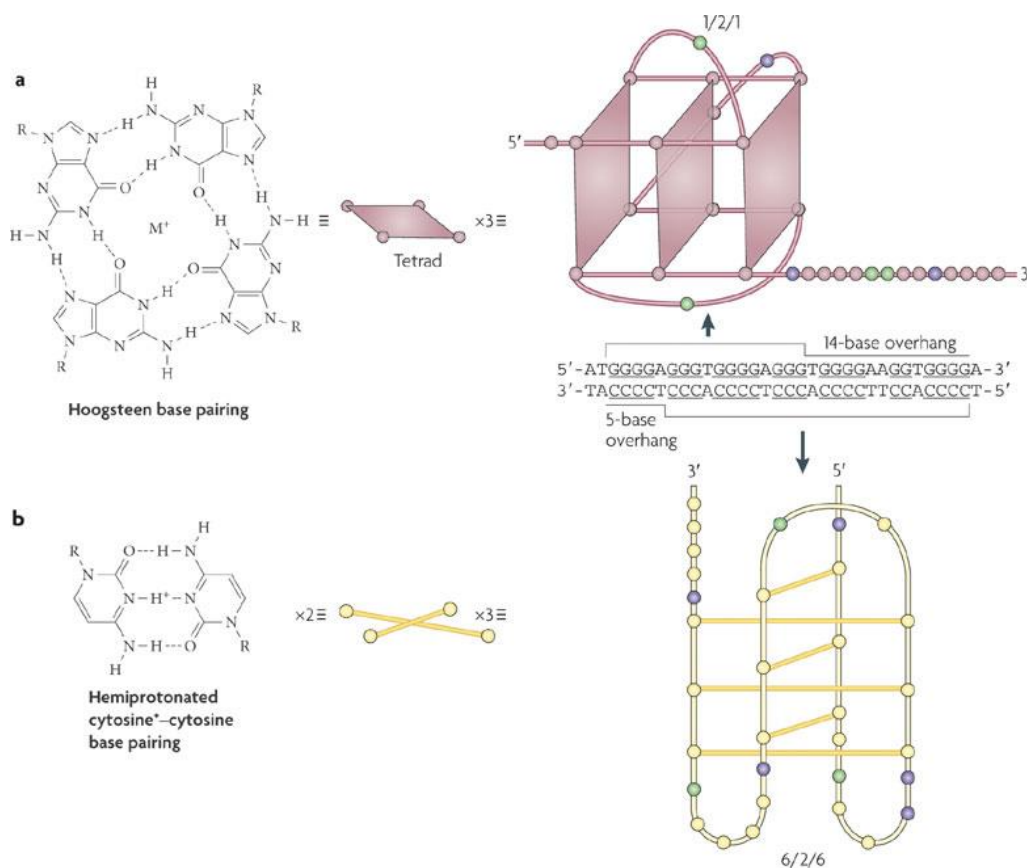


Figure 1.14: Schematic diagram of the quadruplex and i-motif a) Intramolecular G-quadruplex structure with a 1/2/1 loop pattern. b) An intramolecular i-motif with a 6/2/6 loop pattern [62].

Although the G-quadruplex structures have been studied extensively with respect to their loop structures and folding patterns, as well as their interactions with small ligands or DNA-binding proteins, comparatively few investigations have been carried out on the i-motif structures. A slightly acidic pH favours and guides the interconversion of the C-rich single-stranded DNA to the i-motif and forms an antiparallel structure [60]. The pH-dependent structure is found to be considerably affected by the cytosine base numbers, environmental condition and length of the loops [63]. There are diverse potential i-motif structures with changed intercalation and looping topologies [64]. It is well known that >40% of all genes contain C-rich sequences in or near the regulatory regions including the oncogenes [65].

1.5.5 Z-DNA

A different type of B-DNA double helical structure was revealed in 1979 during an investigation into the DNA hexamer crystal structure of d(CGCGCG) where the two strands were found to be connected by Watson-Crick base pairing in an antiparallel direction, but the helix was left handed [66]. Due to the unusual zig-zag backbone, the structure was termed as Z-DNA (**Figure 1.15 a**). The base pairs were flipped upside down because of the rotating cytidine moieties and introduced a zig-zag shape in the backbone, leading to the conversion of B-DNA to Z-DNA. Additionally, the guanine residues rotated to the *syn* form from an *anti*-conformation (**Figure 1.15 b**). On the contrary, the mononucleotide repeat observed in the B-DNA had a dinucleotide repeat as the bases alternate in *syn*- and *anti*-conformations when moved along the Z-DNA sugar-phosphate chains. Alternate purine and pyrimidine moieties with d(CG) sequences readily form the Z-DNA because pyrimidine's preferred *anti*-conformation [67] requires less energy to form Z-DNA.

Although it is difficult to explain *in vivo* the presence of alternative forms of DNA, as well as reveal their biological role, considerable progress has been made for Z-DNA. A number of investigations support the existence of Z-DNA in prokaryotic cells, whereas it is complex for eukaryotic cells as the negatively supercoiled DNA is organised into nucleosomes [68].

The *C-myc* gene, when studied using a computer program that scanned the nucleotide sequence and calculated the required energy for flipping the various sequences from B-DNA to Z-DNA, was demonstrated to contain three regions with high propensity to form Z-DNA [69]. In 1992 Schroth and co-workers carried out an extensive compilation and almost 137 genes were scanned upstream and downstream to determine the most probable position for Z-DNA-generating elements. The isolation and characterization of Z-DNA-selective proteins can be a way for determining Z-DNA's role in the biological system [70].

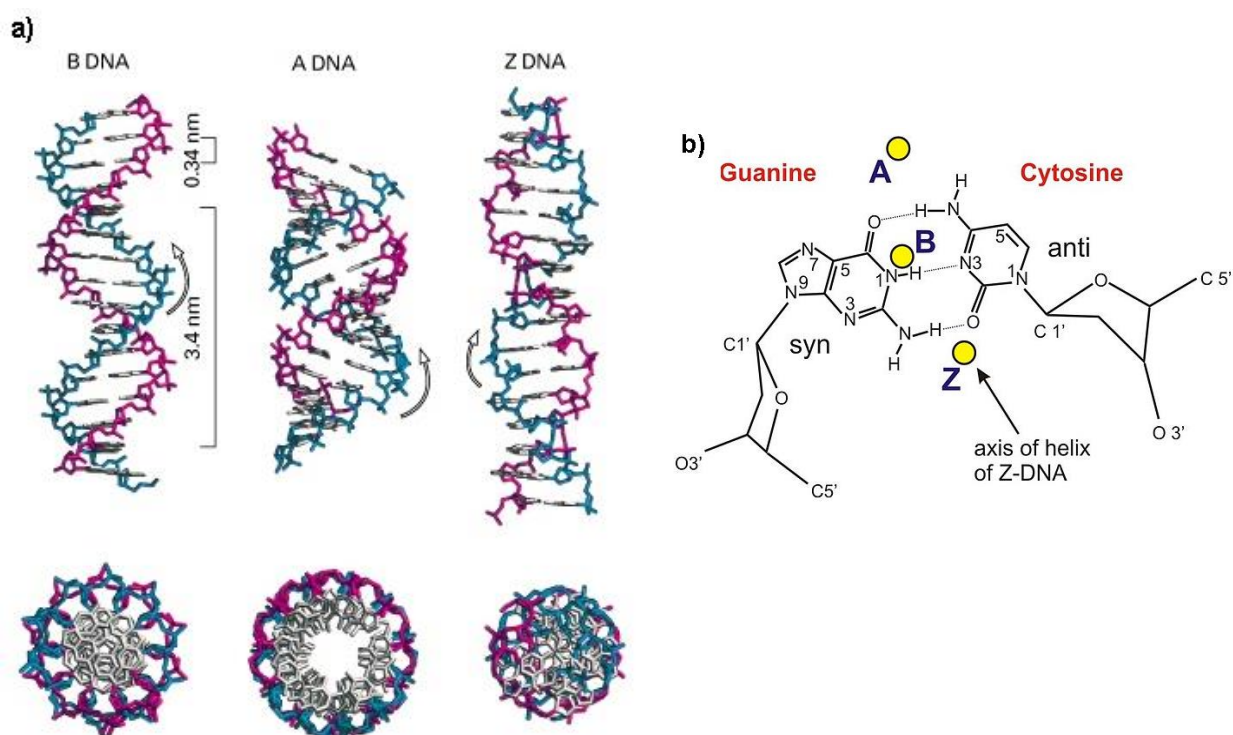


Figure 1.15: a) Various forms of double helix DNA b) The helix axis of A-, B-, and Z-DNA.

1.6 DNA Replication and the End Replication Problem

With the complementary structure of genomic DNA solved, the first mechanisms of its semi-conservative replication (**Figure 1.16**) were proposed [71]. The semi-conservative replication is catalyzed by DNA polymerases in a 5' to 3' direction. This results in the continuous replication of one strand in the replication fork occurring unhindered, termed the 'leading strand', while the other 'lagging strand' requires significant RNA priming to allow the discontinuous synthesis of discrete Okazaki fragments, which are subsequently joined into continuous DNA. However, DNA is unable to replace the distal 5'-RNA primer on the lagging strand, which once digested results in an 8-12 nucleotide shortening of the 5'-DNA strand, affording the 3'-telomeric overhang [72, 73]. It has, however, subsequently been observed that the length of the 3'-overhang is greater than that predicted by the 'end-replication' model, suggesting that a level of 5'-exonuclease processing is prevalent in the generation of the ~100-200 nucleotide overhang, which often terminates in 5'-CTAACC [74, 75], and hence the 3'-overhang has a highly conserved part in the function of chromosomes.

Telomeric DNA is, therefore, shortened by ~50-200 nucleotides per replication cycle [76], suggesting that telomere attrition is linked to cellular ageing acting as a ‘counting’ mechanism to account for the limited replicative potential of normal human cells prior to the onset of senescence [77].

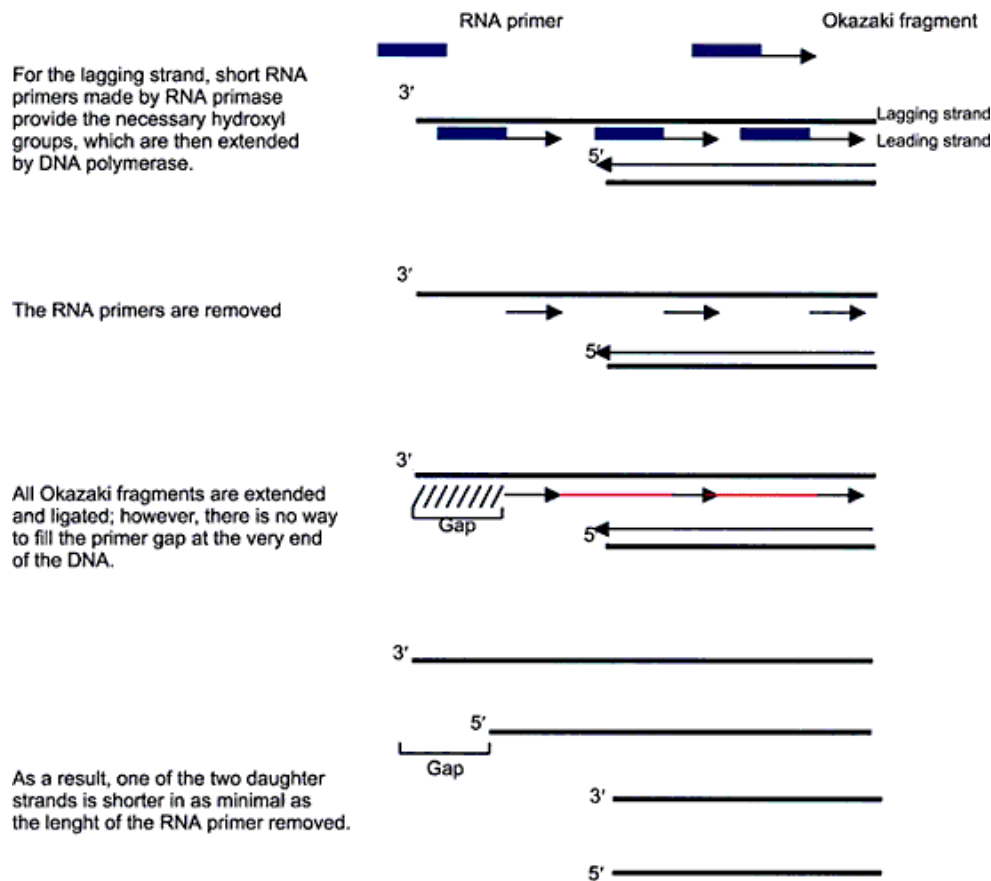


Figure 1.16: Telomere shortening during DNA replication.[78]

1.7 Human Telomere

Telomeres are protein-DNA complexes (**Figure 1.17**) present at the end of chromosomes and are responsible for genome stability. Human telomeric DNA consists of tandem repeats [79, 80] of TTAGGG sequences with several kilobase pairs stretching outwards. During DNA replication, telomeres are gradually shortened, leading to a critical threshold when DNA replication is halted (replicative senescence). Human telomeric DNA forms t-loops (lasso-type structures) and the 3′ single-strand end invades the double-stranded telomeric DNA repeat part [81]. The Shelterin complex (protein factors bound with telomeric DNA) regulates

telomere length and protects the chromosome end from DNA damage, recombination, unregulated nucleolytic attack and non-homologous end-joining [82].

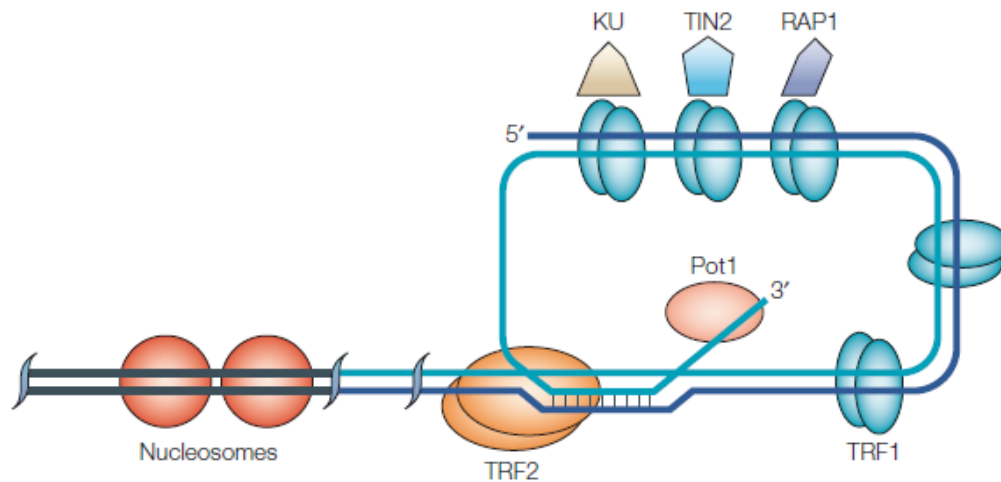


Figure 1.17: Schematic diagram of the t-loop structure of the human telomere. Major telomere binding proteins are demonstrated here such as Pot1; TRF; TIN2; RAP1.[59]

1.7.1 Telomeric Complex/ Shelterin complex

Previously, mammalian telomeres were considered to be linear (**Figure 1.18 a**); however, recent research has demonstrated that telomeric ends contain 2 loops composing a duplex structure. According to this model, the T-loop is formed through the fold-back of the telomere into itself (**Figure 1.18 b**), whereas a D-loop is generated by the binding of the 3' G-strand overhang with the double-stranded telomere repeat sequence of the 5'-end. The formation of these two structures hides the telomere overhang and protects the telomere from destruction.

Researchers have demonstrated that for the integrity and function of the telomere, three factors are essential:

- A minimum length of the TTAGGG repeating sequence
- Overhang integrity and
- Telomere-binding proteins regulation [83].

The Shelterin complex is a complex structure that brings together three telomeric DNA binding factors called TRF1, TRF2 and POT1, although most of the complex contains six basic elements: TRF1, TRF2, POT1, TIN2, TPP1 and RAP1 (**Figure 1.18 c**). The TIN2 subunit binds simultaneously to TRF1, TRF2 and TPP1, whereas TPP1 joins POT1 with TIN2. Lastly, RAP1 is associated with TRF2. Along with this 6-member complex, Shelterin (**Figure 1.18 d, e**) has also been reported to be found as sub-complexes lacking either TRF1 or TRF2/RAP1. Although the role of these subunits is yet to be identified, the function of TRF1, TRF2 and POT1 is well known [84].

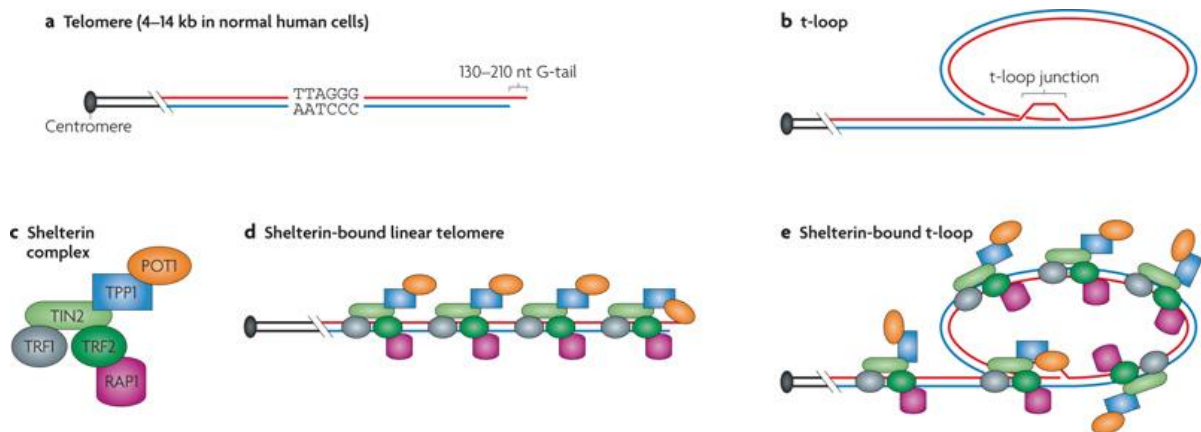


Figure 1.18: Schematic diagram of the Shelterin complex **a)** Vertebrate telomere containing repetitive DNA sequence (5'-TTAGGG-3')_n. **b)** Formation of t-loop. **c)** Six-subunits of shelterin complex. **d,e)** Formation of Shelterin complex by binding of six sub-units.[85]

1.8 Telomerase

For chromosomal stability, a balance between DNA loss and gain is required at the end of the telomere and this balance is maintained by the repeat addition of nucleotides by a reverse transcriptase enzyme called telomerase [86]. The telomerase enzyme helps in maintaining sufficient telomeric length in various cells such as in human stem cells, reproductive cells and cancer cells through the addition of TTAGGG repeats, using its own RNA as the template for reverse transcription. Almost all human tumour cells have been found to exhibit telomerase activity, but not in neighbouring normal cells. Telomere length maintenance is essential for

infinite tumour cell proliferation, for avoiding the normal cellular senescence process and to become immortal. These cells gain immortality either through activation of telomerase enzyme, or through an alternative mechanism that maintains the telomere length. This makes telomerase a significant target for developing novel anti-cancer therapeutic agents [87].

The telomere becomes short after avoiding the cell-cycle arrest checkpoint pathway. The extremely short telomere is considered as the double strand break and initiates the DNA damage response pathway by activating proteins such as Ku, Mrt-2/Rad17 and ATM. These proteins cause the homologous recombination/non-homologous end-joining of the chromosome. Cells which contain abnormal chromosomes enter into a crisis or the mortality M2 stage and start the apoptosis process. In the case of tumour cells, the bypass of these stages results in shorter telomeres, triggering the activation of the telomerase enzyme (**Figure 1.19**), which maintains a definite telomere length. However, in the case of telomerase inactivity, human tumour cells are capable of maintaining their length through alternative mechanisms. The stability of the telomere length makes the cell immortal, as these cells can avoid the crisis, M1 and M2 phase of the usual cell death process and can divide indefinitely [88].

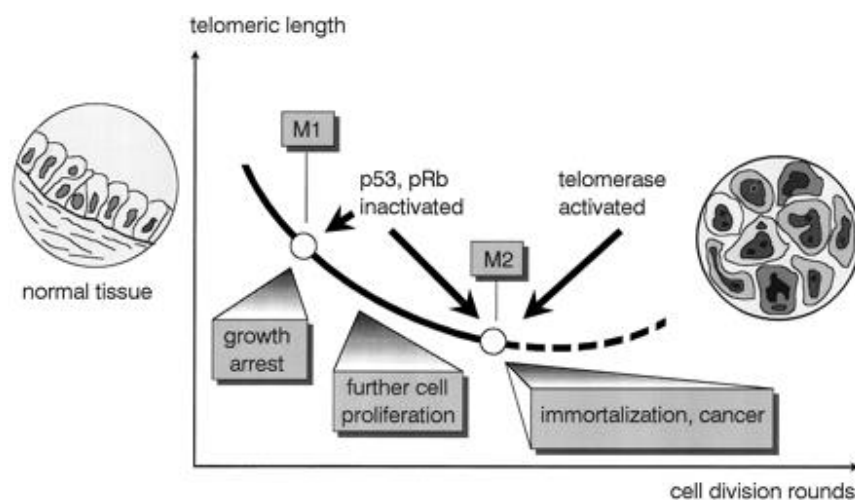


Figure 1.19: Schematic diagram demonstrating the process of cellular senescence and immortalization [89].

1.8.1 Components of human telomerase enzyme

The telomerase enzyme includes two essential components (**Figure 1.20**):

- hTR or hTERC:- Functional RNA component
- hTERT:- Catalytic protein

Two essential components constitute the telomerase enzyme. Either hTR or hTERC is the functional RNA component that acts as the template for synthesizing telomeric DNA. hTERT is the catalytic protein with reverse transcriptase activity [90]. In addition to the template region, telomerase RNA (TER) contains various functionally essential secondary structural elements, which are involved in protein binding, template restriction and catalytic functions. Along with the reverse transcriptase domain, telomerase reverse transcriptase (TERT) contains the telomerase-specific part required for TER and DNA substrate binding, as well as for telomerase function. The core parts of the enzyme are TER and TERT, which are capable enough to provide *in vitro* functional activity of the enzyme. For *in vivo* activity several auxiliary proteins are required, some of which are included in the holoenzyme [91].

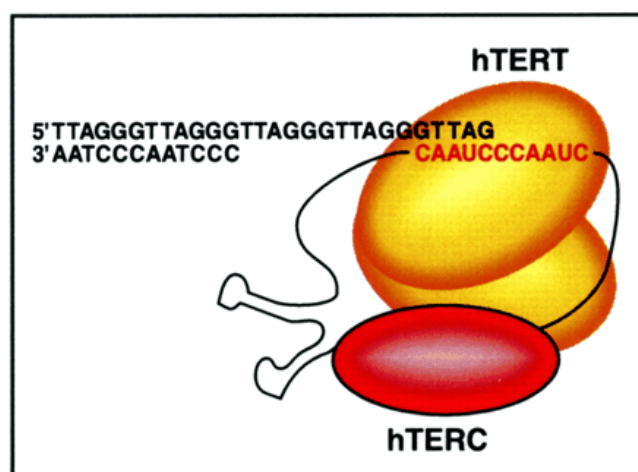


Figure 1.20: Schematic diagram of the telomerase enzyme showing its two subunits [90]

Among these two components, the hTR component is generously expressed in all tissues, even without telomerase enzymatic activity, whereas it is found to be five times more concentrated in malignant cells than normal cells. On the contrary, the hTERT moiety is

found to express at less than 1 to 5 copies per cell, which again is dependent on the cellular telomerase enzymatic activity. In normal cells hTERT expression is usually down-regulated, which up-regulates into immortal cells, making hTERT as the primary determinant for the activity of the enzyme [92]. Because of some baffling factors such as low cellular concentration and difficulties in the isolation process in soluble form in measurable quantities, structural information about TERT, TER, and other telomerase proteins only became available in recent years [91].

1.8.1.1 RNA Subunit (hTR) of Telomerase

Human telomerase is a long 451 nucleotide RNA (hTR) containing an eleven nucleotide templating region (5'-CUAACCCUAAC-3') found near the 5' terminal and provides a template region for telomere synthesis. RNA polymerase II, in humans, helps the transcription of hTR at the 3' end for producing a mature transcript of 451 nts [93, 94]. At the 5' end, it lays the template for reverse transcription for synthesizing d(GGTAG) and the alignment domain (italicized) [92, 94]. It is suggested that at the 3' terminal of the DNA, the alignment domain hybridizes and places the telomere for synthesizing the telomeric repeats [94]. In this way, it can be said that telomerase RNA plays two roles: provides a binding site for RNP proteins, as well as providing a template region which can be copied by TERT in telomere DNA sequences [95].

These RNAs were discovered in a number of phylogenetically different species, including 2 yeasts, 35 vertebrates and 24 ciliated protozoa (**Figure 1.21**). Even though these telomerase RNAs have different sizes and fundamental structures, all of them contain a pseudoknot domain that is similar to the template structure found in ciliate telomerase RNAs, consisting of a pseudoknot structure as well as a 3'-terminal hairpin structure containing 148–209 nt, as well as being relatively small [95]. In active telomerase, the structurally conserved domains demonstrate some particular functions. It has been found that for enzymatic activity CR4/CR5 and pseudoknot motifs are essential [94]. *In vitro* studies indicated that in the presence of the protein component, these two motifs can reconstitute telomerase activity [96].

Other studies have shown that the hTERT-binding site containing nucleotide 33–147 and 163–330 are important for telomerase enzymatic activity [97].

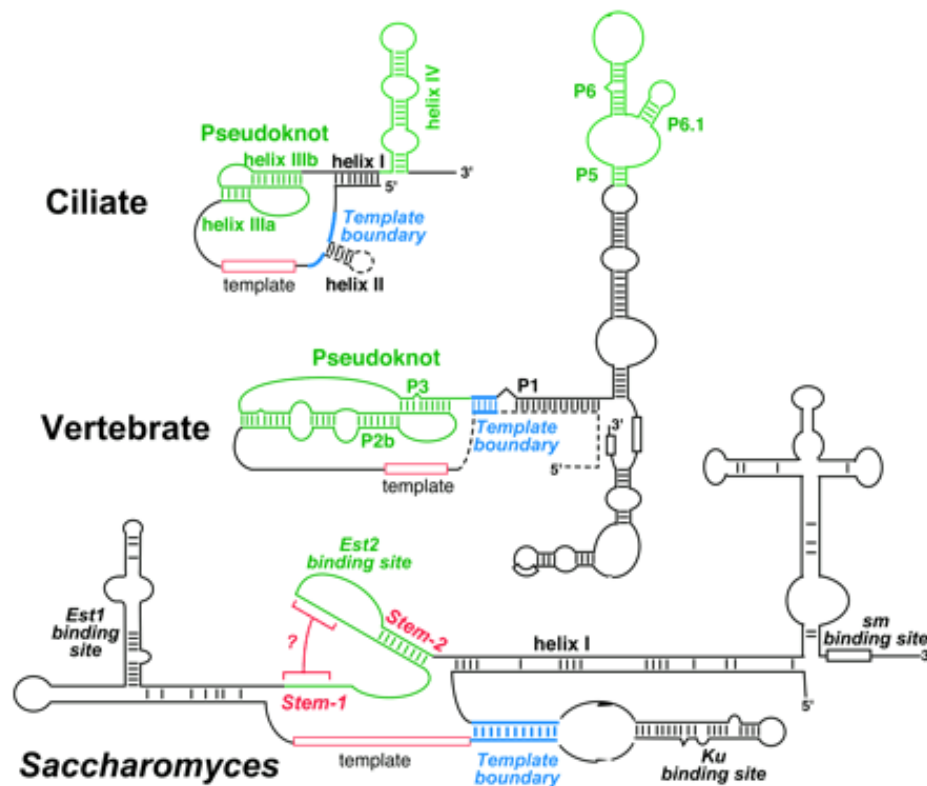


Figure 1.21: Schematic diagram representing the secondary structures of ciliate, vertebrate, and yeast (*Saccharomyces*) telomerase RNAs. Green: conserved regions; Dashed lines: these parts are not present in all species; Red: template region; Blue: template boundary; Red brackets: putative stem-1 of *Saccharomyces* RNA [98].

1.8.2 Regulating Telomerase Access to Telomeres

The human telomeric complex helps the cells to differentiate telomeres from degraded DNAs and protects the telomere from degradation and fusion. Additionally, the complex structure can sense as well as control telomere homeostasis through controlling telomerase enzyme accessibility. This DNA-protein complex of telomeres is assumed to convert stochastically between the capped and uncapped status (**Figure 1.22**) [99].

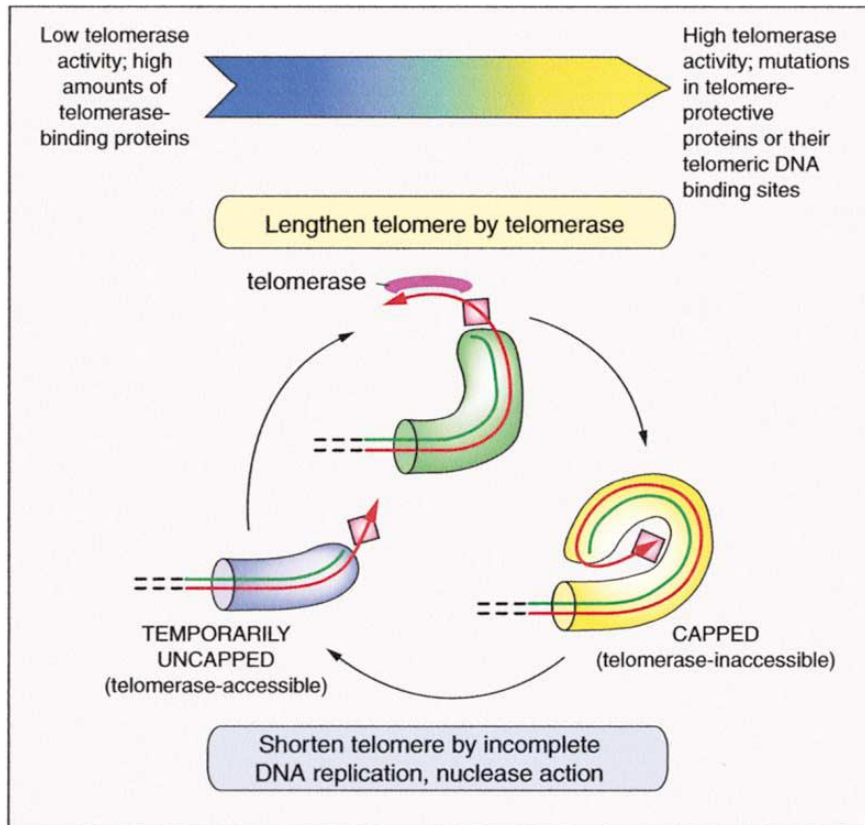


Figure 1.22: Changes accompanying the cycle of capping (telomerase-inaccessible state) and temporary uncapping (telomerase accessible state) of telomeres in dividing cells with telomerase [100].

Current studies show that the accessibility of telomerase can be regulated by positive or negative ways by telomere binding proteins [101]. The first detected telomeric proteins, TRF1 and TRF2, act as negative regulators by forming a t-loop with the duplex telomeric DNA. In telomerase-positive cells, telomere elongation is inhibited by the overexpression of either TRF1 or TRF2 [102]. Recent research has demonstrated that TRF1 and TRF2 controls the telomere length by interacting with the DNA damage repair complex. The TRF1-related protein TIN2 and tankyrase also showed negative regulation in maintaining telomere length. It has currently been found that the TRF1/Pin2-interacting protein PinX1 acts as a potent telomerase inhibitor by interacting directly with hTERT [103].

1.9 Telomere Length Regulation by Alternative Mechanisms

Several different human cell lines and tumours can maintain the telomere length by alternative mechanisms in spite of lacking the telomerase enzyme. These processes are termed as alternative lengthening of telomeres (ALT) [104]. ALT can occur in common malignancies such as breast cancers. However, this mechanism is most frequently found in the tumours of mesenchymal origin, as these cells seem to have a propensity to activate the ALT mechanism [85]. It has been observed that ALT-positive cells contain telomeres of various length in the nucleus and in the ALT-associated PML bodies (APB) [105, 106]. Although there is little information about the exact mechanism, two have been proposed [85]:

- **Unequal T-SCE model (Figure 1.23 a):** The telomere length is maintained by an exchange of an unequal telomere sister chromatid exchange (T-SCEs) process from one daughter cell to another, which allows that cell to divide indefinitely and leaves the other daughter cell with a short telomere length and reduced dividing capability.
- **Homologous recombination-dependent DNA replication model (Figure 1.23 b):** According to this model, the telomere becomes elongated by synthesizing new telomeric DNA through the recombination-mediated process using the existing telomere sequence from the neighbouring telomere as template.

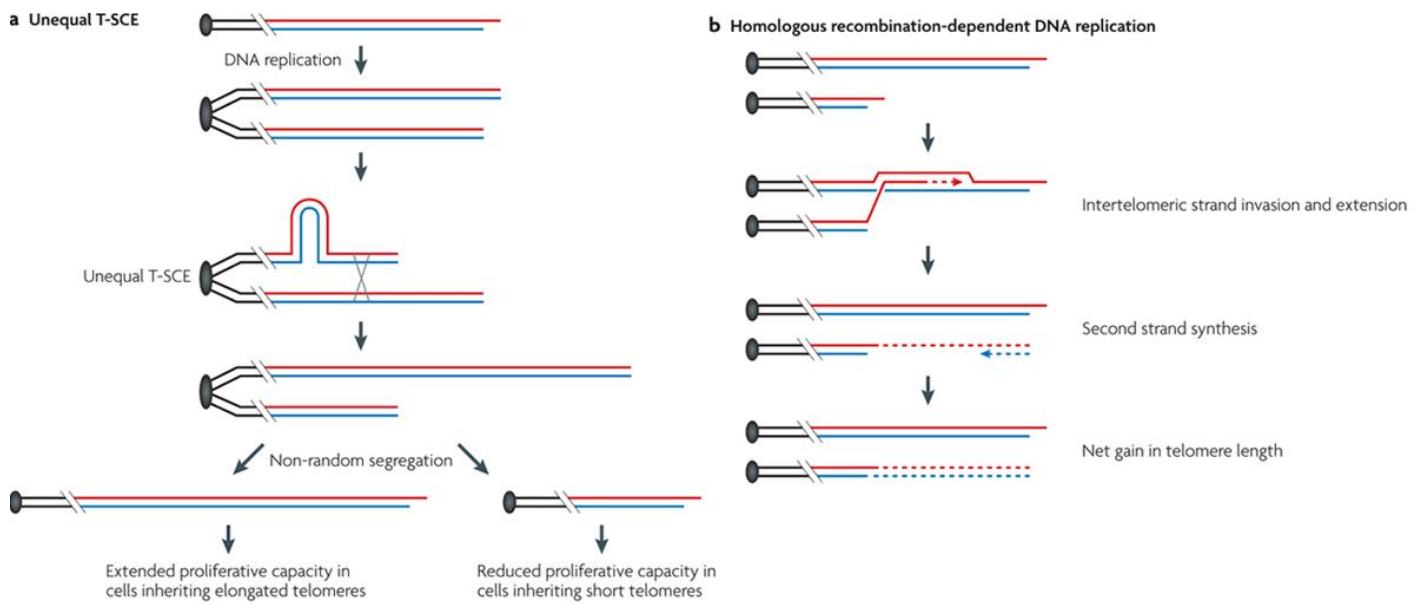


Figure 1.23: Schematic diagram of a) Unequal T-SCE model. b) Homologous recombination-dependent DNA replication model [85].

Increasing evidence indicates that, in mammalian cells, telomere length can be influenced by several factors without remarkable changes in telomerase activity. Proteins involved in homologous recombination (HR), like Rad54, can act as factors in ALT. Moreover, Rad51D, a Rad51 paralog essential for normal gene recombination, has also been found to be needed for maintaining telomere length as well as for telomere capping [107].

1.10 Targeting Telomerase for Cancer Therapy

Substantial research indicates that the telomeric length maintenance provides immortality to cancer cells. It has been observed that almost 90% of cancer cells have short telomeres and high telomerase activity. In contrast, the apoptotic process is induced with a shortening of the telomere due to the loss of telomeric sequences. Therefore, the telomerase enzyme and the telomere can be potential targets for developing anticancer drugs [88].

1.10.1 Inhibiting the Catalytic Activity of Telomerase

During early tumourigenesis, the reactivation of telomerase and creating a balance in maintaining telomeric length are principal steps. Based on the discussion above, it looks very reasonable that the telomerase enzyme or the proteins associated with telomere/telomerase complex can be targeted by small molecules which can inhibit malignant conversion and/or tumour development. The inhibition of the telomerase enzyme may produce site selective, novel anticancer drugs with wide spectrum (**Figure 1.24**). There are numerous possibilities of developing inhibitors that will act on the telomere/telomerase complex and a variety of ways are presently either under advanced preclinical investigations or in early clinical trials.

Approaches include:

- Inhibiting telomerase activity through telomerase inhibitor agents leading to accelerated senescence and cell death.
- Eliminating telomerase-expressing cells by immune effectors.
- Disrupting telomere function by expressing mutant telomerase RNA templates that induce cell death [88].

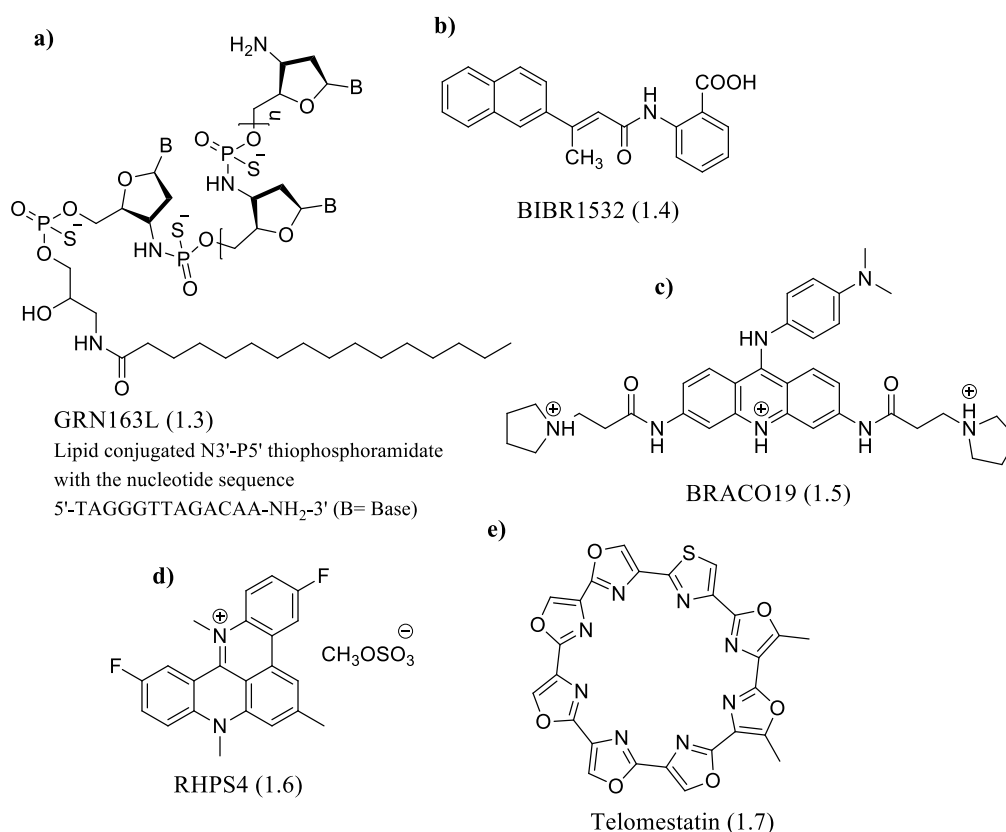


Figure 1.24: Structures of several telomerase inhibitors. (a) GRN163L (1.3), (b) BIBR1532 (1.4), (c) BRACO19 (1.5), (d) RHPS4 (1.6) and (e) telomestatin (1.7) [54]

1.11 Targeting the telomere

Recently, experimental studies have indicated that telomere uncapping leads to rapid cell killing (**Figure 1.25 b**). The uncapping of chromosomal DNA can take place due to damage signals near the telomeric overhang and the analogous lagging strand, which can result in either rapid apoptosis or genomic instability. Additionally, static telomere conditions due to telomere-related senescence and premature senescence can also reduce the lag time to a greater extent, compared with telomere shortening by the telomerase enzyme inhibition alone. Thus, ligands that focus telomeres directly or uncap it can be more efficient monotherapeutic agents that might act more rapidly when compared with ‘pure’ enzyme inhibitors (**Figure 1.25 a**). Both the shortening and uncapping of the telomeres are effectively accomplished by telomere targeting agents (TTA), which also inhibit telomerase activity. Molecules, targeting particularly the telomeric repeat sequences, are defined as G-quadruplex

ligands. These include pentacyclic RHPS4 (**1.6**), trisubstituted BRACO19 (**1.5**), acridines, ethidium derivatives and cationic porphyrins TMPyP4 (**1.32**), as well as the natural product telomestatin (**1.7**) [54].

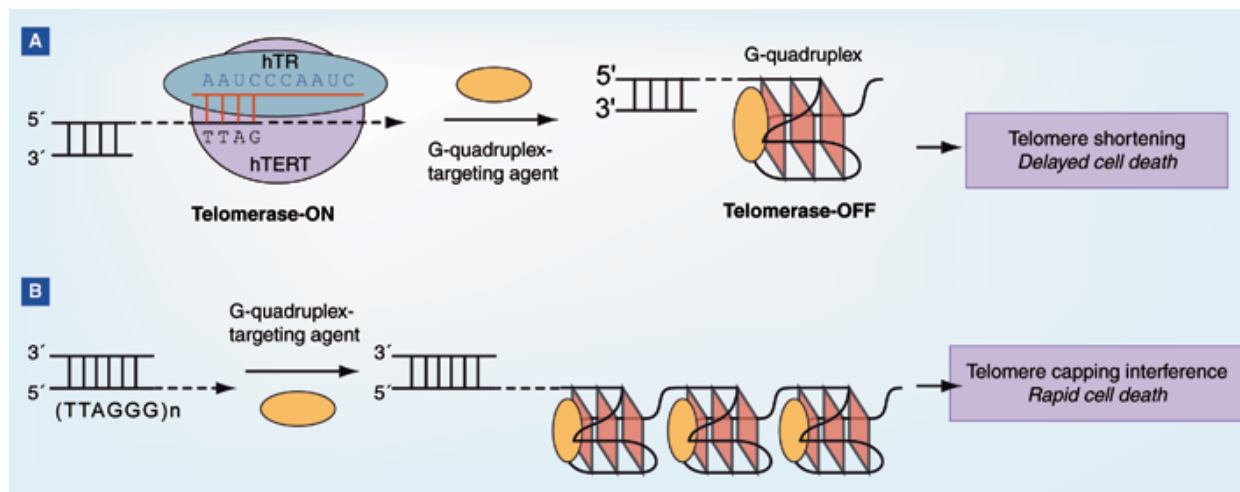


Figure 1.25: Comparative demonstration of the telomerase inhibition with direct telomere targeting. (A) Telomerase inhibition by G-quadruplex-ligands. (B) Inhibition of telomere capping by G-quadruplex-ligands [45]

1.12 Telomeric G-Quadruplex Structure

For targeting the formation of telomeric G-quadruplexes (**Figure 1.26 a**) clinically, it is necessary to understand further the structural features of human telomere *in vivo*. In recent years, much effort has been expanded to investigate further this sequence and this has been recently reviewed.

The NMR analysis of a natural sequence with 22-mer (four TTAGGG repeats) demonstrated antiparallel topology in a Na⁺ ion solution containing a diagonal and two lateral loops [108], while the crystal structure of this showed parallel topology containing three strand-reversal loops in K⁺ solution. NMR and X-ray crystallographic analysis of d(T₂AG₃)₂T showed bi-

molecular parallel topology in K^+ solution [109]. The NMR study also revealed an anti-parallel structure in equilibrium with the parallel structure (**Figure 1.26 b**).

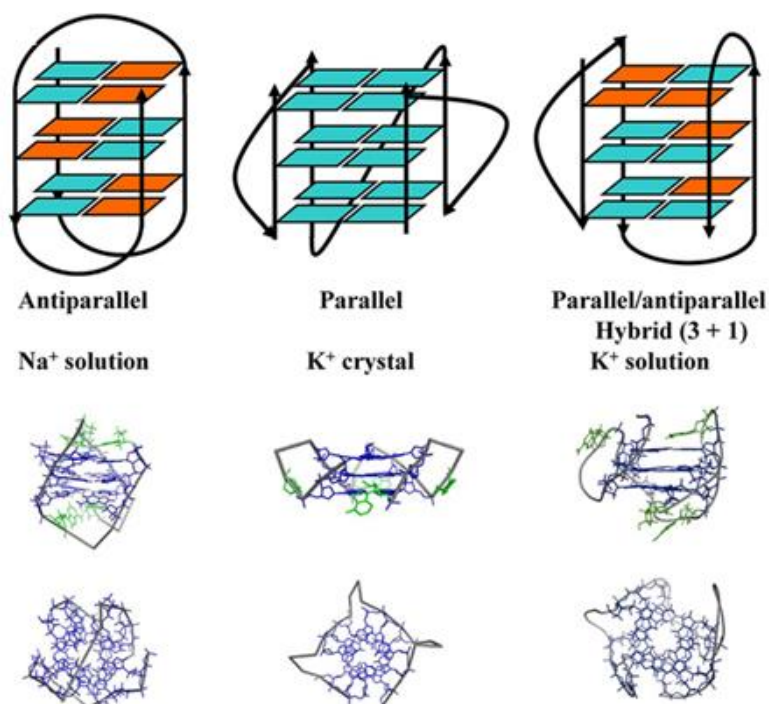


Figure 1.26: The structures of the intramolecular quadruplex in a Na^+ solution, and the crystal and solution structure in K^+ [56, 110].

Other variations in the telomeric sequence have shown different structures as determined by NMR. Some of these have resulted from the modification of the sequence in order to solve the structure. The wide varieties of topologies (**Figure 1.27**) published for sequences close to the human telomere sequence show the dynamic and heterogeneous nature of the human telomere quadruplex structure.

More recently, many of the structures published have shown a (3+1) topology (**Figure 1.27 c**). The (3+1) quadruplex topology covers those distinctive patterns of (3+1) *syn* (**1.1**) and *anti* (**1.2**) glycosidic angles at each G-quartet [111].

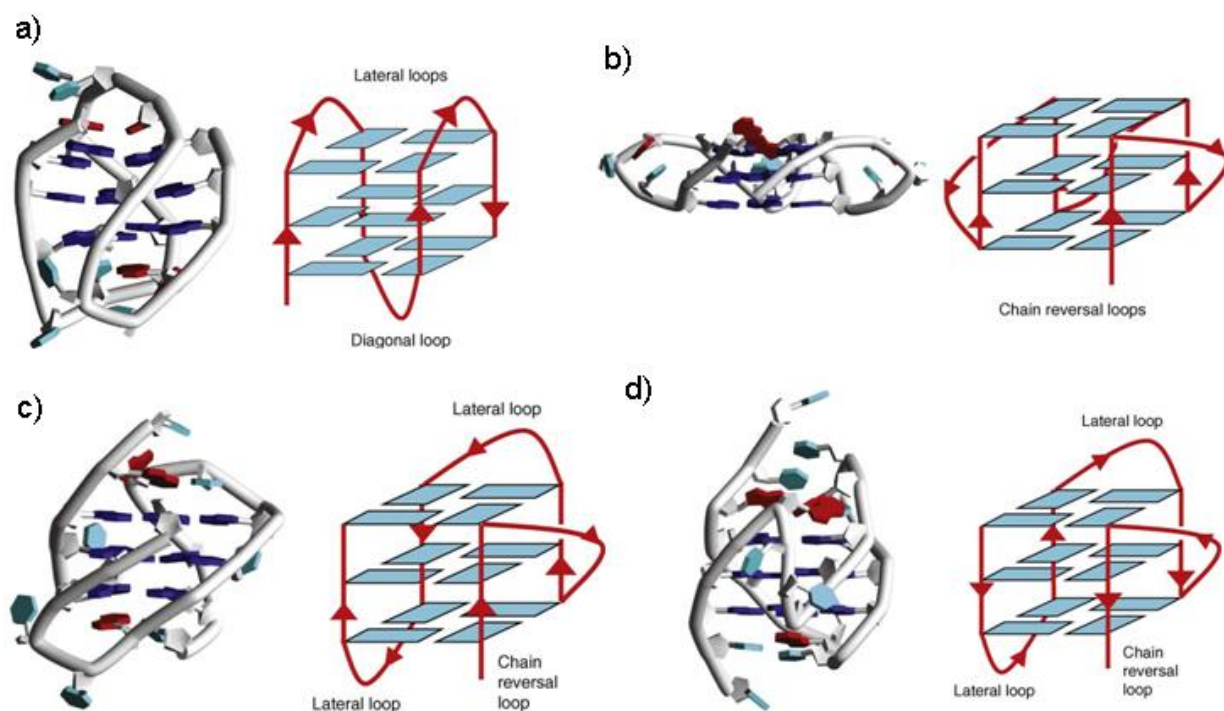


Figure 1.27: Diagrams of different human telomeric intramolecular quadruplex structures. (a) Antiparallel topology in Na^+ solution. (b) Parallel topology of crystal structure in K^+ . (c) (3 + 1) Hybrid topology (form 1) of human telomeric quadruplex in K^+ . (d) (3 + 1) Hybrid topology (form 2) [112].

A second form of the (3+1) structure (**Figure 1.27 d**) results from the two lateral loops and one side chain reversal loop. This form has mainly been seen in structures where the 3' end of the flanking sequence has been altered to include TT. One such structure is that of the NMR structure of the sequence $\text{d}(\text{TAG}_3(\text{T}_2\text{AG}_3)_3\text{TT})$ in a K^+ ion solution[113] in which these two forms have been found to exist in equilibrium (**Figure 1.28**).

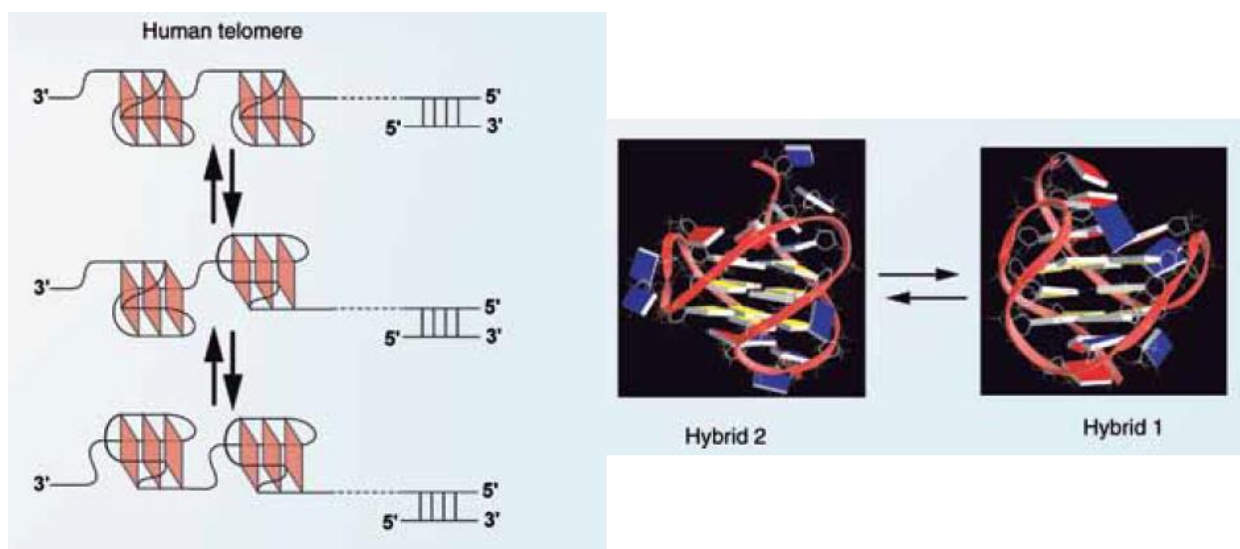


Figure 1.28: Schematic diagram of hybrid form of telomeric quadruplexes demonstrating equilibrium between the two forms in a K^+ ion solution [45].

The importance of flanking sequences in all of these structures has been recently reported and it is suggested that these sequences have a large influence on the topological structure, as well as on the structural stability [112].

1.13 Non-Telomeric G-quadruplex DNA

Recent studies have proposed that G-quadruplex structures might have various important roles *in vivo*. Much effort has been expended in finding the location of other putative quadruplex forming sequences within the human gene that have been found, not only in human telomeres but also in various genomic loci, with potential roles in oncogene regulation by using bioinformatics for human and other genome sequences (**Table 1.1**) [39, 114]. In 2005, two surveys of the genome by Huppert & co-workers and Todd *et al.* estimated that there could be, in principle, approximately 376,000 putative quadruplex-generating sequences present in the human gene. Higher than average numbers of putative quadruplex generating sequences were found in the promoter regions, suggesting that they might have a potential role in regulating expression of the gene (**Figure 1.30**) [39, 114]. Hence, various G-

quadruplex-forming DNA sequences are located in the promoter regions of oncogenes like *VEGF*, *c-myc*, *bcl-2*, *Rb*, *HIF- α* , *k-ras* and *c-kit* genes, amongst others (**Figure 1.29**) [30, 31, 112]. Of particular interest to this work are the two quadruplexes found in *c-kit* and to a lesser extent the *c-myc* G-quadruplex.

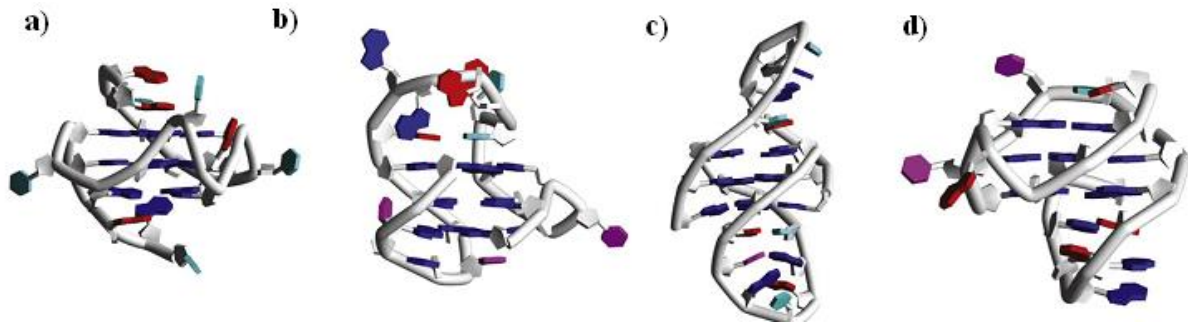


Figure 1.29: Structures of genomic and related quadruplexes. Quadruplex formed within (a) the *cmyc* promoter sequence, (b) the *bcl2* promoter sequence, (c) bimolecular quadruplex with extended hairpin loop, (d) *c-kit* 22-mer quadruplex [112].

Table 1.1: Nucleotide sequences present in cancer-related genes that can form quadruplex structures [31].

<i>Gene</i>	<i>Sequence</i>	
<i>c-myc</i>	<i>Pu27</i>	<i>TTATGGGGAGGGTGGGGAGGGTGGGGAAGG</i>
	<i>Myc-2345</i>	<i>TGAGGGTGGGGAGGGTGGGGAA</i>
	<i>Myc-1245</i>	<i>TGGGGAGGGTTTTAGGGTGGGGA</i>
	<i>Myc-22</i>	<i>TGAGGGTGGGTAGGGTGGGTAA</i>
	<i>Pu241</i>	<i>TGAGGGTGGIGAGGGTGGGGAAGG</i>
<i>c-kit</i>	<i>c-kit1</i>	<i>CAGAGGGAGGGCGCTGGGAGGAGGGGCTG</i>
	<i>c-kit2</i>	<i>CCCCGGGCGGGCGCGAGGGGAGGGGAGGC</i>
<i>VEGF</i>		<i>CCCGGGGCGGGCCGGGGGCGGGGTCCCGGCGGGGCGGAG</i>
<i>HIF-α</i>		<i>GCGAGGGCGGGGGAGAGGGGAGGGGCGCG</i>
<i>bcl-2</i>		<i>GTCGGGGCGAGGGCGGGGGAAGGAGGGCGCGGGCGGGGA</i>
<i>k-ras</i>		<i>GGGAGGGAGGGAAGGAGGGAGGGAGGGA</i>
<i>Rb</i>		<i>CGGGGGGTTTTGGGCGGC</i>

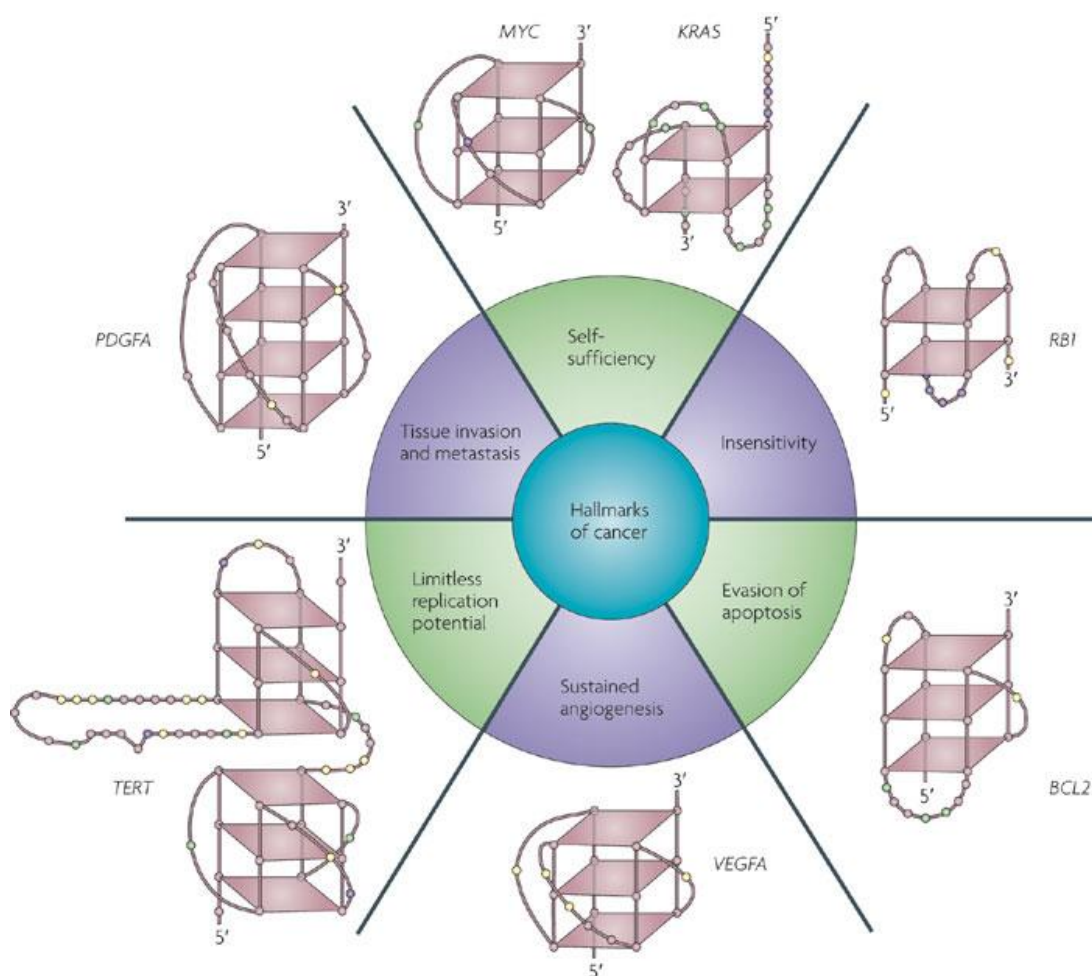


Figure 1.30: The association of the quadruplex generating sequences found in promoter of oncogenes and proto-oncogenes with the six hallmarks of cancer [62].

1.13.1 c-kit

The *c-kit* proto-oncogene is expressed into melanocytes, mast cells and hematopoietic stem cells encoding 145–160 kDa tyrosine kinase receptors and has a function in cell survival, proliferation, and differentiation. Over-expression and/or mutation of the oncogene may be the cause of several types of cancer such as gastrointestinal stromal tumours (GIST), leukaemia, seminomas, pancreatic cancers and melanoma [115]. Therefore, the tyrosine kinase part of *c-kit* is a significant target for treating GIST.

The human *c-kit* promoter region has been found to form two different quadruplex structures: *c-kit1* d(AGGGAGGGCGCTGGGAGGAGGG)[116] and *c-kit2* d(CGGGCGGGCGCGAGGGGAGGGG)[117], which have been proved by biophysical and 1-D NMR studies [118] and have currently been solved by NMR spectroscopy in a K^+ solution [119] (**Figure 1.31**). *c-kit1* has a unique G-quadruplex-forming topology where 18 of the 22 nucleotides have a tertiary structure. Four loops are present there; two single-nucleotide double-chain-reversal loops, a two-residue loop and a five-residue d(AGGAG) stem-loop that collectively form the complex tertiary quadruplex structure usually not present in other simple quadruplexes like the parallel and antiparallel topology of the human telomere. However, it might be possible to target the *c-kit1* quadruplex for designing selective small ligands because of the presence of two well-described clefts, stabilization of which will down-regulate the *c-kit* expression. The simulation and modelling study summarized that *c-kit* may also be found in a few locations of the human gene; however, the probability of playing an important role with these in gene expression is quite low, and this again proves the exceptionality of this structure and its appropriateness for designing drugs [118, 120]. This unique structure and G-quadruplex-forming sequence may challenge the initial thoughts on what constitutes a possible quadruplex-forming sequence.

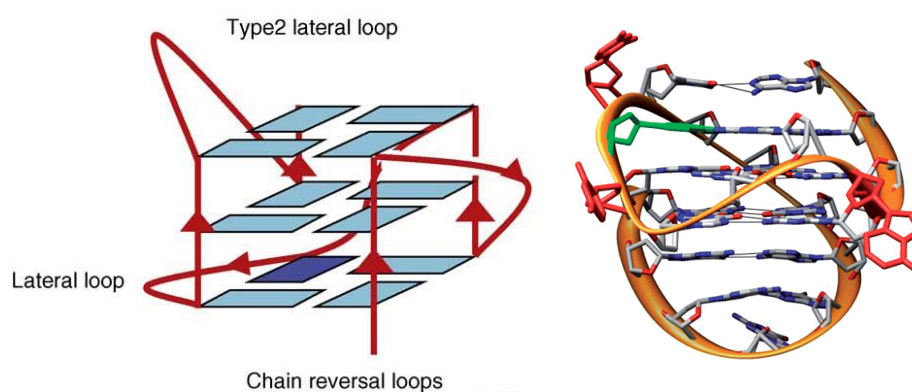
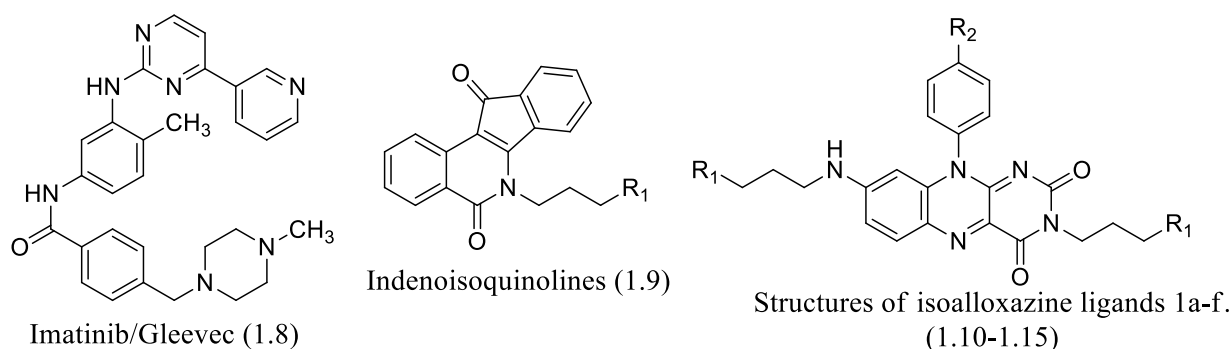


Figure 1.31: NMR structures of the *c-kit* quadruplex [112, 118].

The NMR investigations of the *c-kit2* wild type (wt) sequence by Hsu *et al.* [120] revealed the presence of two dynamically different but structurally close populations, suggesting that the sequence is structurally heterogeneous. This was evident due to the presence of extra sets of resonances in the imino proton area of the NMR spectra. In the presence of K^+ , the modified sequence was shown to adopt parallel propeller topology, including one long loop.

The *c-kit2* sequence has also been shown to have multiple conformations by FRET, CD and NMR, which show both parallel and antiparallel conformations which are dependent on the K^+ concentration [120]. It has been hypothesized by Hsu and co-workers that the one long loop region present in the *c-kit2* sequence allows greater conformational heterogeneity [120].

The *c-kit* quadruplex-forming sequences may be an attractive target for ligand design (**Figure 1.32**). Gleevec (imatinib mesylate) (**1.8**), a small molecule inhibitor of *c-kit*, has been found to be effective for treating gastrointestinal stromal tumours (GIST)[121]. 3,8,10-Trisubstituted isoalloxazines (**1.10-1.15**) are found to bind selectively to *c-kit* promoter quadruplexes and inhibit *c-kit* expression [122]. In one recent study indenoisoquinolines (**1.9**) have been found to inhibit cell growth in the GIST cell line (GIST882) by inhibiting both *c-kit* transcription and KIT oncoprotein levels [123]. Recently, two novel ligands benzo[*a*]phenoxazines (**1.16**) have been identified to reduce *c-kit* expression in gastric cancer cells by reducing the transcription of the gene, as well as a demonstrated selectivity for *c-kit* G-quadruplex over duplex DNA [115].



Ligand	1a (1.10)	1b (1.11)	1c (1.12)	1d (1.13)	1e (1.14)	1f (1.15)
R1						
R2				-F		-OMe

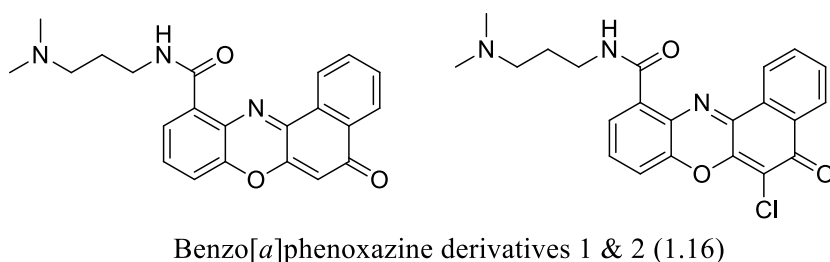


Figure 1.32: Structures of some *c-kit* promoter quadruplex binding ligands [115, 121-123].

The various putative G-quadruplex-forming sequences that were recently identified represent further interesting targets for drug discovery. However, the huge number of potential G-quadruplex-generating sequences also highlights an important issue; G-quadruplex ligands must be selective for a particular target, as there is a possibility for them to interact with a large variety of G-quadruplex targets *in vivo*.

1.13.2 c-myc

c-myc is an important oncoprotein and transcription factor that is essential for controlling cell growth and the determination of cell fate, including the induction of apoptosis. Overexpression and/or mutation of this oncoprotein cause a large number of human

malignancies like cervical, colon, breast, and prostate. P1 and P2 are important promoters of the *c-myc* gene (**Figure 1.33 a**); however, 80–90% of its transcriptional activities are regulated by the nuclease hypersensitivity element III1 (NHE III1) (27-base-pair) of the *c-myc* promoter [45].

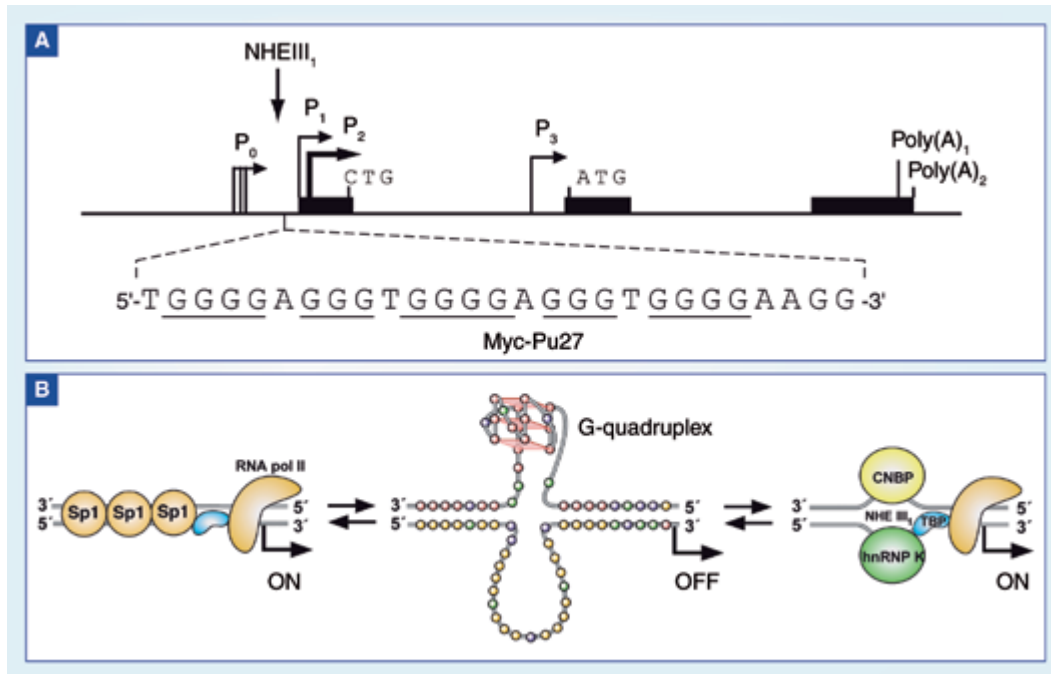


Figure 1.33: (A) The human *c-MYC* gene promoter structure. (B) The functional role of NHE III1 structure in transcriptional activation or silencing [45].

The nuclease hypersensitivity element (NHE) III is a 27-bp sequence located -142 to -115 bp upstream from the P1 promoter (5'-TGGGGAGGGTGGGGAGGGTGGGGAAGG-3')[50]. *c-myc*, containing G-rich sequences, is capable of forming multiple quadruplexes because of the negative superhelicity produced during the transcription process and then stabilized by monovalent cations, such as K⁺ and Na⁺ [124]. Two NMR structures Myc-2345 and Myc-1245 were identified for *c-myc* in a K⁺ ion solution, where each of them contained four G-tracts and formed stable parallel intramolecular quadruplex structures in solution (**Figure 1.34**). The G-tracts are joined through propeller loops and all the guanine bases are in an *anti* (1.2) conformation [51]. The first and third loops in both structures are single-nucleotide propeller loops, whereas the central loop in myc-2345 is a GA propeller loop, but that in

myc-1245 is a large six-base TTTTGA loop that destabilizes myc-1245 by 16°C compared with that of the myc-2345 sequence. The Pu241 consisting of five G-tracts shows unique features in the NMR structure. The 3' terminal G in the last G-tract of P241 folds-back to form the G-tetrad and establish an adjacent G-A-G hydrogen-bonded triad, which is placed above this G-tetrad as a planar platform-like diagonal loop[30].

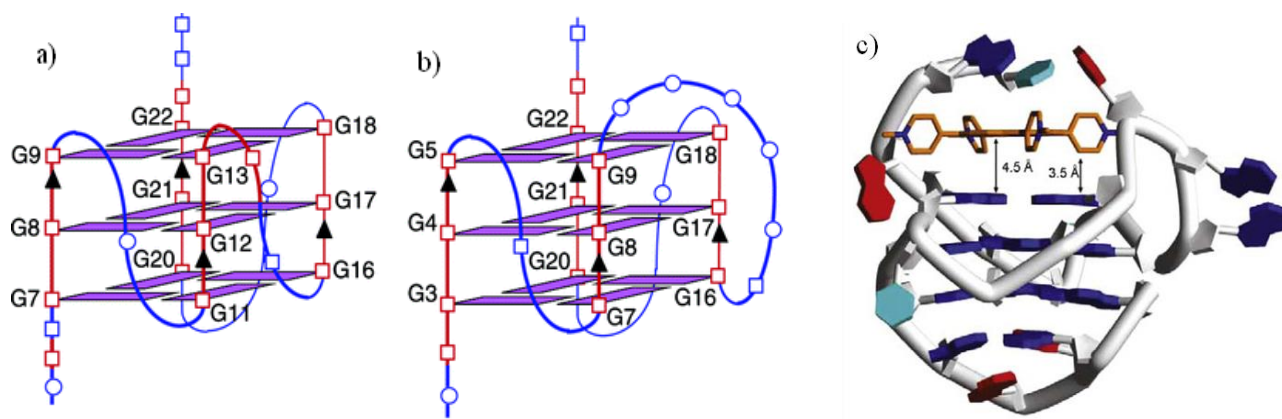


Figure 1.34: Propeller type parallel-strand NMR structures from sequences a) Myc-2345 and b) Myc-1245. c) A view of the *c-myc* complex with TMPyP4 (1.35), showing relevant ligand-G-quartet distances [51, 112].

In vivo footprinting methods have shown that the silenced form and the transcriptionally active form of the *c-myc* promoter NHEIII1 are quite different [125]. Recently, it has been found that NHEIII1 acts as a silencer element for *c-myc* transcription and quadruplex generation in the promoter region, and is critically important for the transcriptional activity of *c-myc* [50]. Small molecules with binding and stabilizing abilities of this G-quadruplex are found to reduce the expression and transcription of *c-myc* and are anti-tumorigenic. Some of the reported ligands that stabilize *c-myc* G-quadruplex include quindoline derivatives, cationic porphyrins, and platinum complexes (**Figure 1.35**). The aromatic moieties of these molecules have shown to π -stack onto the terminal G-tetrad of the quadruplex, giving extra stabilization. Their side chains either contain a positive charge or can become protonated with biological pH help in forming electrostatic bonds with negatively charged phosphate residues of grooves [126].

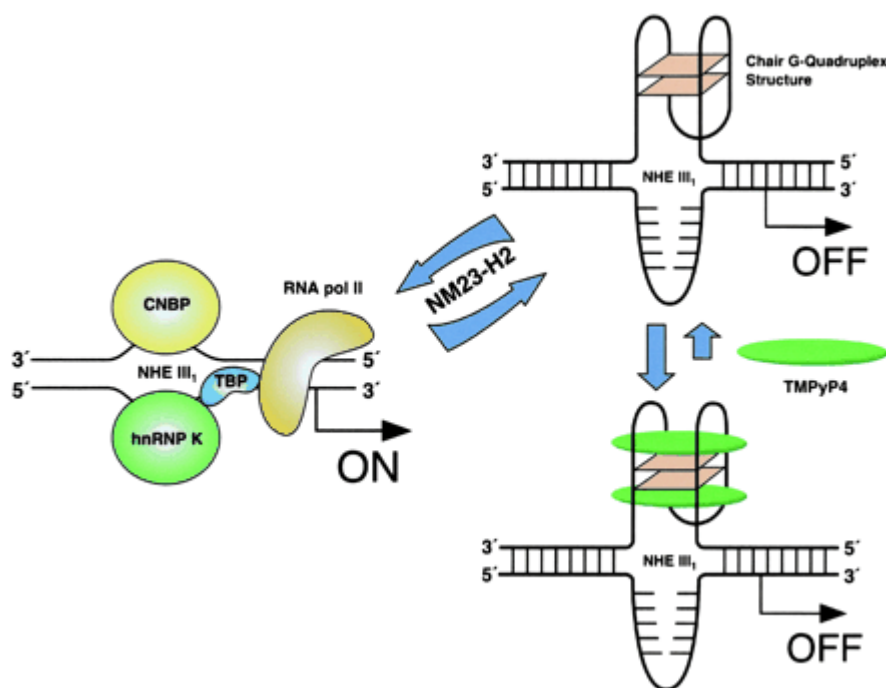


Figure 1.35: Schematic diagram representing the regulation of the *c-myc* gene transcription through TMPyP4 (1.35) binding [50].

1.13.3 G-quadruplex found in other human promoters

Promoter regions of some other human oncogenes like *RET*, *HIF-1 α* , *VEGF*, *PDGF-A*, *KRAS*, *c-MYB* and *bcl-2* are also reported to contain quadruplex forming sequence in their regulatory element and are also found to form intramolecular quadruplexes. The *HIF-1 α* , *VEGF*, *KRAS*, and *RET* promoter region quadruplexes were suggested to form parallel quadruplexes [45] that were characterized by biophysical analyses like chemical footprinting and CD methods [118]. The G-quadruplexes of *PDGF-A*, with four G-tetrads, were found to form a mixed parallel-stranded structure. The *bcl-2* oncogene product inhibits cell apoptosis, overexpression of which is related to a number of human tumours, such as B and T-cell lymphomas, cervical colorectal, breast, lung and prostate carcinomas. The principal promoter P1 of this gene, located within the nuclease hypersensitive site, is rich in guanine, and a 39-bp GC-rich region near the 5'-end of the P1 promoter plays the principal role in regulating the transcription of the *bcl-2* gene [127]. This 39-mer G-rich strand has six guanine repeats that are separated by one or more bases, which are capable of forming various intramolecular quadruplex structures [45]. NMR studies of the mixed parallel/anti-parallel *bcl-2*

unimolecular quadruplex showed that it contains two lateral loops and one propeller loop. Putative quadruplex-forming sequences have also been reported to be found in the *k-ras* and neuroblastoma oncogenes [128].

1.14 RNA G-quadruplex

In 1990, G-quadruplexes were found in biologically relevant RNA from *Escherichia coli* 5S RNA, which contained a 19-nt oligonucleotide with the sequence UG₄U, and was identified to form an extremely stable tetrameric aggregate in a K⁺ solution *in vitro* [129]. Later on, biophysical analysis of the UG₄U motif led to the proposal that the quadruplex structure contains four G- and one U-quartet, all in parallel directions. Some other studies linked the G-quadruplex structures of RNA in viruses like HIV and the Herpes simplex virus with the processing and translational control in human transcripts. TERRA (telomeric repeat containing RNA) (**Figure 1.36**), a ~100 to 9000 nt sequence rich in guanine, derived from the transcription of a C-rich human telomere strand by RNA polymerase II, is another mentionable example which represents the importance of the RNA G-quadruplex. TERRA transcripts are found to be involved in chromatin remodelling, as well as in regulating telomerase activity [130]. In addition to TERRA, RNA G-quadruplex structures are found at the 5' end of human telomerase RNA (hTR) [131].

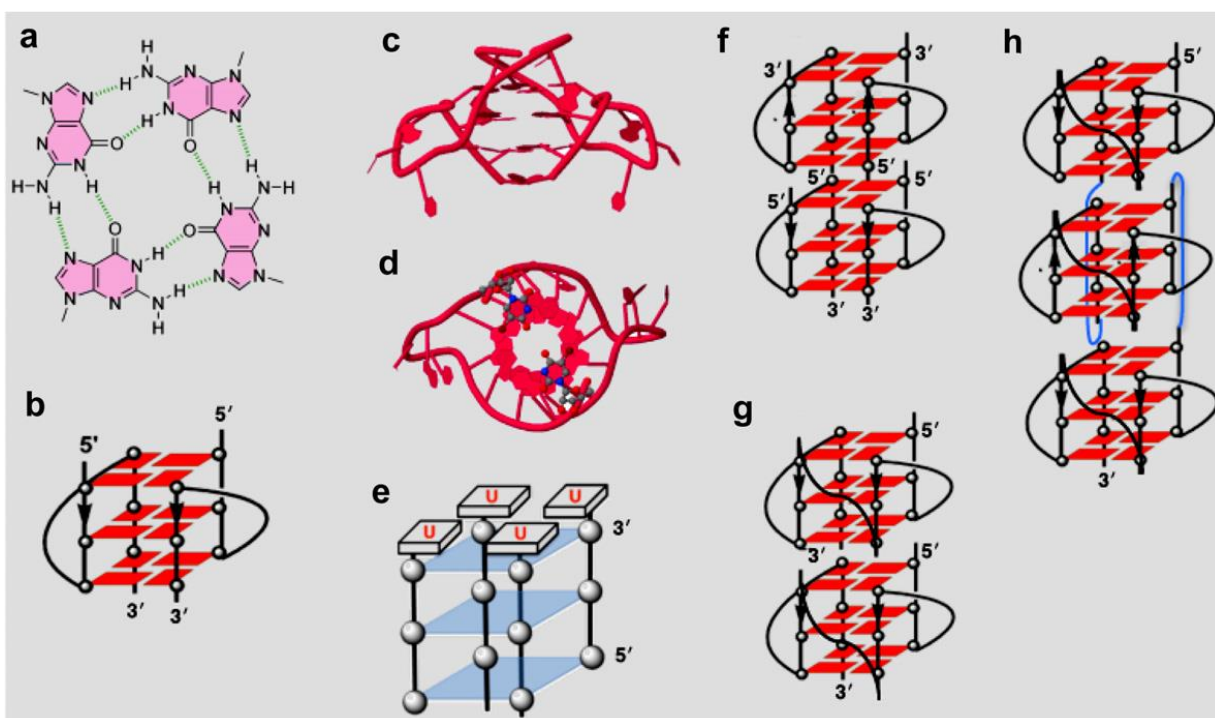


Figure 1.36: Different topologies of TERRA RNA G-quadruplexes. (a) A planer quadruplex structure formed by hydrogen bonding. (b) A bimolecular G-quadruplex with parallel topology in human telomeric RNA r(UAGGGUUAAGGGU) in Na⁺ solution, (c) in a K⁺ solution and (d) in a K⁺-stabilized crystal. (e) Parallel topology of human telomeric RNA r(UAGGGU) G-quadruplex in K⁺ and Na⁺. (f) Two parallel G-quadruplex sub units assembling through 5'-5' stacking and (g) through 5'-3' stacking. (h) G-quadruplexes arranged in long human telomeric RNA sequences by alternate stacking [110].

Various biophysical studies have proved that the G-quadruplex structures formed from RNA sequences are more stable than their DNA counterparts, and structural explanations have been provided by X-ray crystallographic analysis of human telomeric RNA and DNA intramolecular quadruplexes [130]. In RNA G-quadruplexes, the hydroxyl groups of ribose C2' take part to form a hydrogen bond network through interactions with the backbone phosphate and oxygen atoms, sugar oxygen O4' and the H-bond acceptor N2 groups of quartet-forming guanines (**Figure 1.37**). Compared with their DNA counterparts, these structures are more stable because of these additional interactions, which not only reduce the entropy of the involved water molecules but also decrease the free energy required for the

formation of the RNA G-quadruplex. Furthermore, intramolecular DNA tetrads are very polymorphic [8, 31], whereas intramolecular RNA G-tetrads prefer to adopt a parallel conformation [132-136]. Moreover, in the transcriptome, the concentration of RNA quadruplexes might be much more compared with the DNA quadruplexes in genes, due to the absence of complementary strands that can compete with the folding into the quadruplex structure [137].

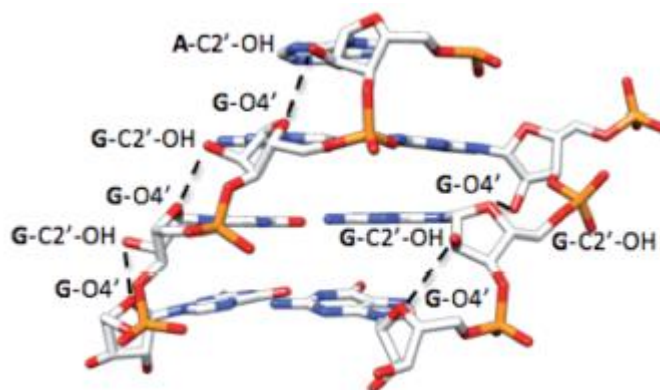


Figure 1.37: Schematic representation of the intermolecular hydrogen bond formation in RNA G-quadruplexes [130].

1.14.1 RNA G-quadruplexes in 5'-UTRs of mRNAs

Transcribed RNA molecules are less constrained than the genomic DNA that can fold to form various intramolecular structures rapidly, which dictate the function and the fate of RNA. One specific example is the generation of secondary and tertiary structures within the 5' untranslated regions (UTRs) of mRNAs that function in regulating post-transcriptional gene expression [130]. Along with the general purine/pyrimidine base pairs, different non-covalent interactions, including G-quadruplex generation, are found to exist in 5'-UTRs. Recent computational analysis of all 5'-UTRs of the human transcriptome has found ~3000 5'-UTRs containing one or more RNA putative quadruplex-forming sequences (PQS), including several other proto-oncogenes, which allows us to assume that these quadruplexes have a potential role in regulating mRNA translation (**Figure 1.38**) [138].

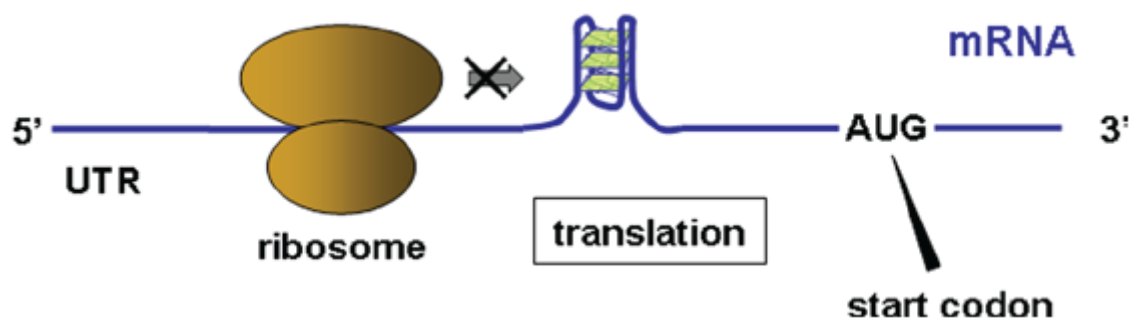


Figure 1.38: G-quadruplexes in the coding strand are transferred to the mRNA and inhibit translation [139].

mRNA G-quartets were identified to regulate translation into the NRAS proto-oncogene, *bcl-2*, the human Zic-1 zinc-finger protein, and the MT3 matrix metalloproteinase [139]. The human NRAS proto-oncogene contains an RNA G-quartet within 5'-UTR of the mRNA that inhibits translation (**Figure 1.39**), inferred from the fact that its deletion increased the translation efficiency by 3.7-fold [138]. A growing number of studies suggests the existence of the RNA G-quadruplex in many mRNAs that might be involved in regulating gene translation at various levels, including genes of clinical importance for human diseases. Stabilization of this RNA G-quadruplex with numerous small molecule ligands, such as RR82 (**1.17**), RR110 (**1.18**), 360A (**1.19**), PhenDC3 (**1.20**) and PhenDC6 (**1.21**) (**Figure 1.40**), can inhibit the translation of RNA, including the NRAS-UTR containing mRNA [130].

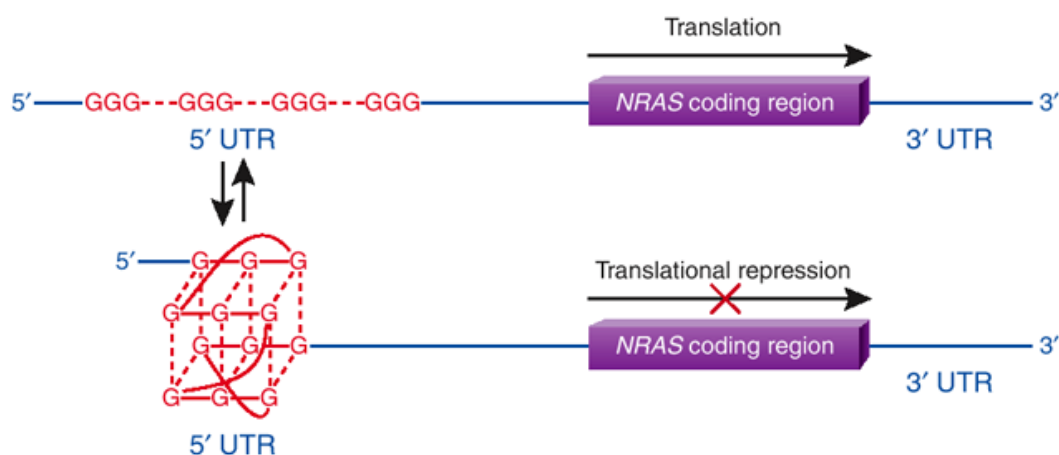


Figure 1.39: 5'-UTR G-quadruplex structure of the NRAS mRNA that acts as a translational repressor [137]

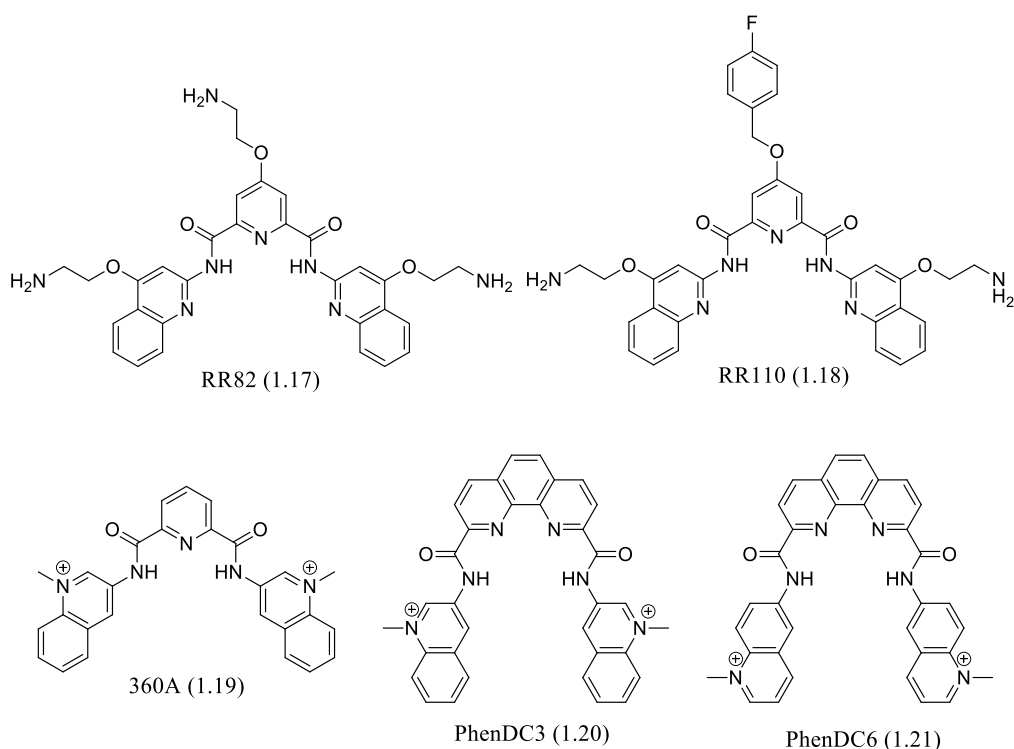


Figure 1.40: Chemical structures of some RNA G-quadruplex-binding molecules that inhibit the translation of RNA [130]

1.15 G-quadruplexes as a Potential Anticancer Drug Target

Growing knowledge about the biological importance of DNA and RNA G-quadruplex structures (**Figure 1.41**) has instigated interest into the research and development of G-quadruplex-binding ligands. Drugs targeting the secondary and tertiary structure of either DNA or RNA represent a new approach to the design and development of anticancer drugs; the possibilities to target G-quadruplexes for therapeutic purposes were first reported by Sun *et al.* in 1997 [140]. This group proposed that quadruplex-stabilizing agents are capable of inhibiting the telomerase enzyme that is excessively expressed and activated in most of the malignant cells. Subsequently, PIPER (**1.40**), the perylene derivative, was discovered to facilitate G-quadruplex formation [141], which blocked the Sgs1-derived G-quadruplex unwinding [142] and paved the way for the development of G-quadruplex-binding agents. After that, numerous categories of small molecules containing diverse chemical features with enhanced selectivity and binding affinity were discovered and developed; the search for additional active molecules is ongoing. Various methods, including *in silico*, conventional

screening methods and rational structure-based drug design, are involved in the search for better molecules [59], and the structural data of the quadruplexes and quadruplex-ligand interactions are playing important roles in designing and developing G-quadruplex-binding molecules. G-quadruplex ligands can selectively bind and stabilize various forms of quadruplexes that showed related biological activity. For example, telomestatin (**1.7**) was reported as a potent telomerase inhibitor through the formation and stabilization of the basket-type telomeric quadruplex [143, 144]. Quarfloxacin[®] (**1.103**) has shown promising *in vivo* G-quadruplex binding activity against different types of tumours and is undergoing Phase II clinical trials. Again, some other G-quadruplex-interactive molecules with relatively low cytotoxicity have become prospective anticancer agents. In fact, G-quadruplex-targeting molecules themselves have played an immense role in understanding G-quadruplexes as therapeutic targets.

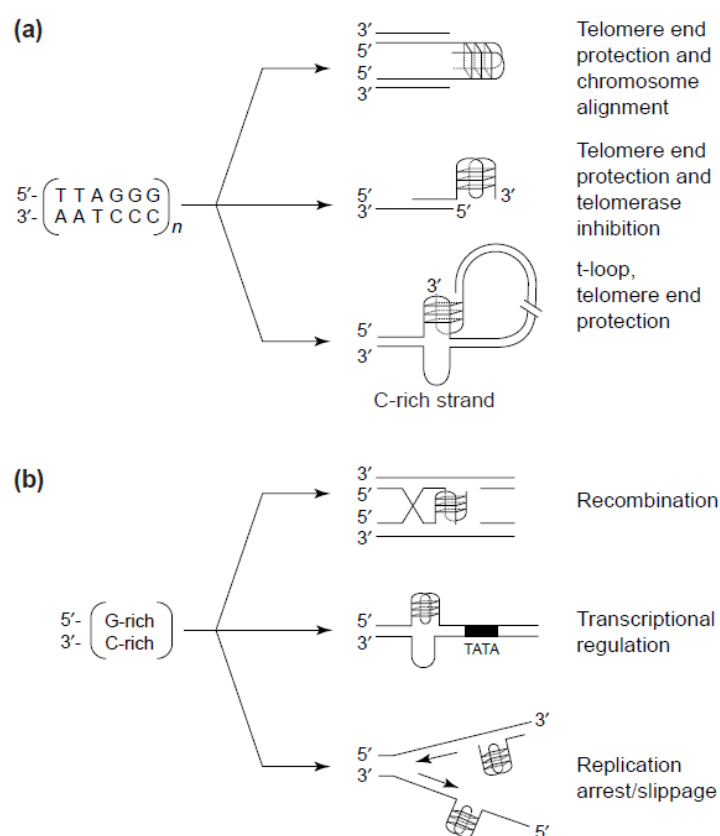


Figure 1.41: G-quadruplex formation during normal cellular events. (a) Protection of the telomere by quadruplex formation and the inhibition of the telomerase enzyme. (b) In non-

telomeric regions, G-quadruplex structures are formed transiently from ds DNA for participating in cellular events [145].

1.15.1 Common Features of G-quadruplex-interactive Compounds

Analysis of the ligands demonstrated several clear requirements for ligand-G-quadruplex DNA SAR. Hence, maximal DNA G-quadruplex binding agents require:

- A large planar aromatic core for optimal π - π stacking interactions that is larger than that required for duplex DNA interactions to be able to afford G-quadruplex DNA selectivity. Optimal ligand dimensions will approach $\sim 11 \times 11 \text{ \AA}$ for the planar aromatic core, consistent with the dimensions of a G-quartet. The introduction of heteroaromatic electron-deficient rings may enhance the strength of π - π stacking interactions.
- Cationic charge in order to afford water solubility of the large hydrophobic aromatic core and allow an electrostatic interaction with the DNA phosphate backbone. Cationic charge exists in three current forms: the *in situ* protonation of tertiary amine groups, N-methylation and metal ion coordination. Natural products and their analogues are uncharged, with no loss of potency.

Hence, these two simple SAR criteria need to be considered and optimized when designing and developing novel G-quadruplex-targeting ligands.

1.15.2 Modes of Interaction of Ligands with G-quadruplex Structures

Various types of compounds, such as cationic porphyrin (TMPyP4, **1.32**), acridine (BSU6039), polycyclic acridine (RHPS4, **1.6**) and *N,N'*-bis-[2-(1-piperidino)ethyl]-3,4,9,10-perylenetetracarboxylic diimide (PIPER, **1.40**) were found to interact with G-quadruplexes with more specificity [146]. The specific geometry of the G-quadruplexes facilitates ligand

recognition through various types of binding modes, similar to that of double-stranded DNA intercalators. Three basic types of binding modes (**Figure 1.42**) are:

- **External Stacking:** The stacking of ligands on the outer part of the G-tetrads are much more energetically favourable and the most probable binding mode (**Figure 1.42 a**). Drugs, such as RHPS4 (**1.6**) [147] and BSU6039 [148], in their NMR studies, have been reported to show stacking interactions with the quadruplexes (**Figure 1.43**).

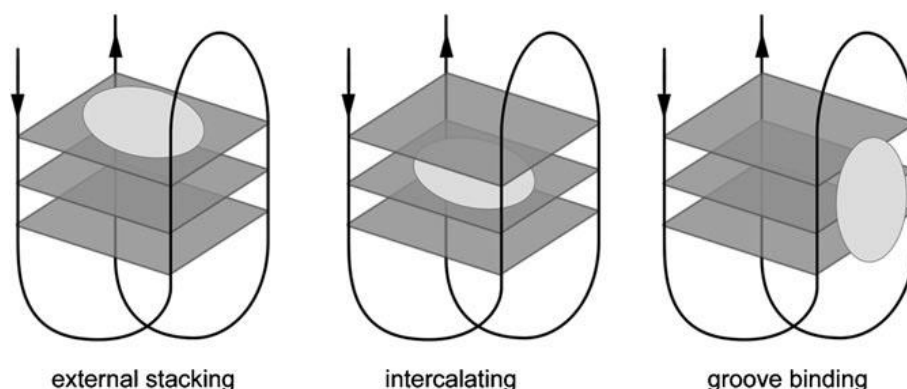


Figure 1.42: Schematic diagram representing various binding modes of ligands with G-quadruplexes through a) external stacking, b) intercalating, and c) the groove binding mode [146].

- **Intercalating:** G-quadruplex structures are very stable and rigid; therefore, any distortion of the integrity of these structures involves high energy. These features of quadruplex structures make it almost impossible for the ligands to show intercalator binding (**Figure 1.42 b**).
- **Loops and grooves binding:** Several ligands have been found to bind with grooves and loops of quadruplex structures instead of π stacking interactions with the DNA bases - an example would be peptide-hemicyanine conjugates (**Figure 1.42 c**) [149].

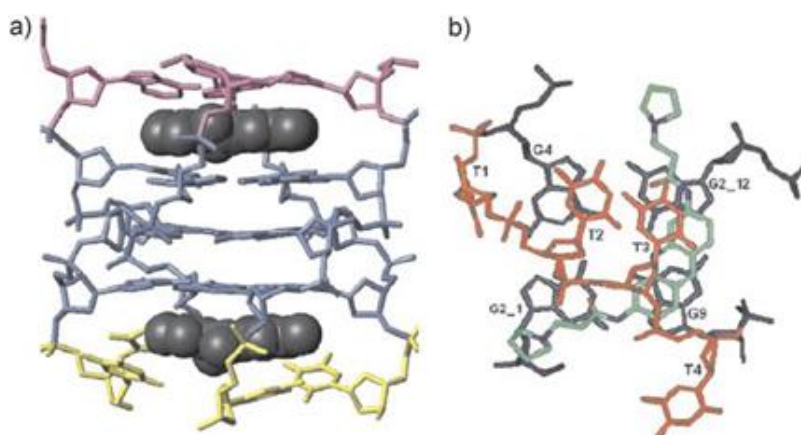


Figure 1.43: a) 2:1 RHPS4–d (TTAGGGT)₄ complex demonstrating the intercalation of the RHPS4 (**1.6**) with the AGGGT core. b) A stacking interaction of BSU6039 (cyan) onto the neighbouring G-quartet (blue) [147, 148].

1.15.3 Structural types of G-quadruplex targeting ligands

Zahler in 1991 demonstrated that K^+ ion-stabilized quadruplexes are capable of inhibiting telomerase activity [53]. Since then, G-tetrad structures have been targeted for telomerase inhibition. There are numerous research groups who are working in this field and are searching for small organic molecules capable of binding and stabilizing G-quadruplexes. Therefore, these ligands can inhibit either telomerase enzyme activity or G-quadruplex-related gene expression. Even though some potential and promising molecules have been discovered as lead compounds through structure-based design and organic synthesis, a potent quadruplex-binding drug is yet to be discovered. Common structural types of G-quadruplex binding ligands are named below, with general structures:

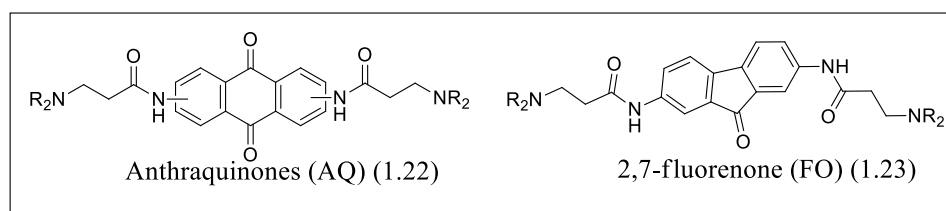
- **Anthraquinones and related inhibitors**

The symmetric molecule 2,6-disubstituted aminoalkylamido anthraquinone BSU-1051 (**1.22**) (**Figure 1.44 a**) is the first such quadruplex-interactive ligand with telomerase inhibitory activity [140]. The cytotoxic effect of the AQ series has been reduced by designing a series of 2,7-fluorenone (2,7-FO) (**1.23**) (**Figure 1.44 a**) derivatives to prevent redox cycling by removing one of the quinone carbonyl moieties [150].

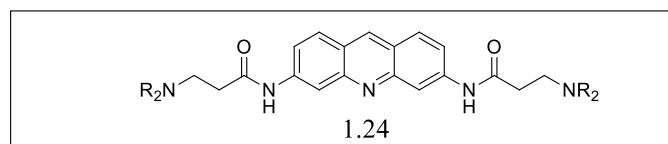
- **Acridine analogues**

Rational drug design and molecular modelling led to the development of 3,6-substituted acridines (**1.24**) (**Figure 1.44 b**). The nitrogen atom of the central ring of the chromophore is protonated at a physiological pH, which increases electron deficiency within the chromophore, resulting in quadruplex binding. It was also assumed that the pseudo-cationic nitrogen atom would increase water solubility compared with the anthraquinone ligands [151].

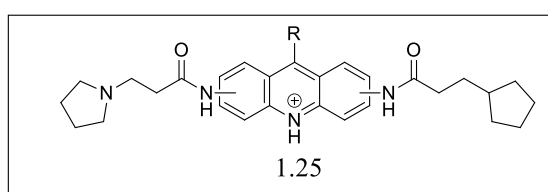
A series of 3,6,9-trisubstituted acridines (**1.25**) (**Figure 1.44 c**) were rationally designed and synthesized [152] and showed better binding affinity for the quadruplexes due to their structural features. A pentacyclic acridine, 3,11-difluoro-6,8,13-trimethyl(8H)-quino [4,3,2-*kl*]acridinium methylsulfate (RHPS4, **1.6**, **Figure 1.44 d**), was also found to be a potent telomerase inhibitor [146].



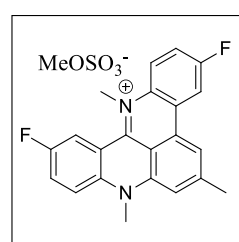
a) Anthraquinone regioisomers and 2,7-fluorenones



b) 3,6-bisamidoacridines



c) 3,6,9-trisamidoacridines



d) RHPS4 (1.6)

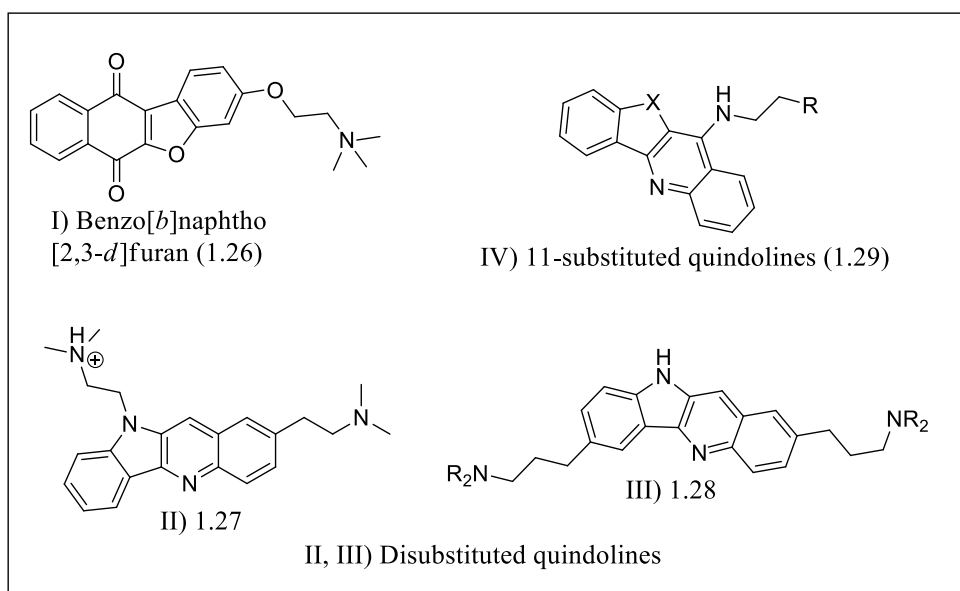
Figure 1.44: The general structure of G-quadruplex ligands; a) Anthraquinone regioisomers (1.22) and 2,7-fluorenones (1.23), b) 3,6-bisamidoacridines (1.24), c) 3,6,9-trisamidoacridines (1.25), d) RHPS4 (1.6) [146].

- **Quindoline analogues**

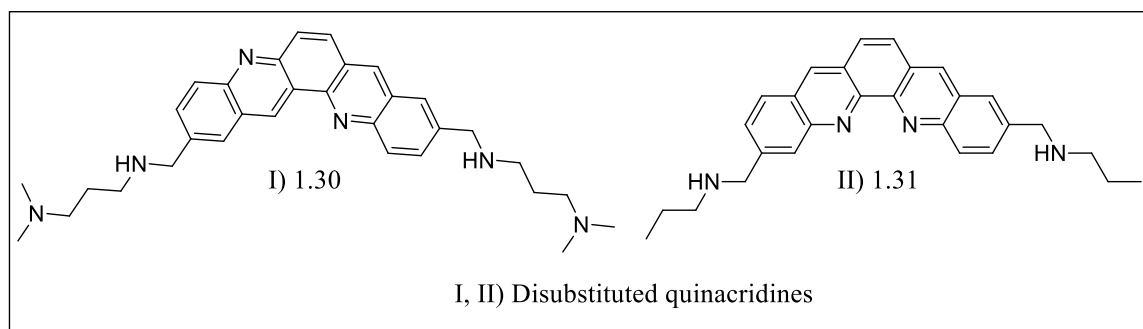
Four aromatic rings containing tetracyclic chromophore ligands, consisting of a fused five-membered ring in the middle, have been developed, which give the molecules a crescent shape. De-substituted derivatives of the natural product quindoline (1.27, 1.28) (**Figure 1.45 a II, a III**) showed more modest activity than the mono substituted benzo[*b*]naphtho [2,3-*d*]furan (1.26) (**Figure 1.45 a I**) [153-155]. Interestingly, 11 substituted quindolines (1.29) (**Figure 1.45 a IV**) showed better telomerase inhibitory activity than the de-substituted ones, which might be due to the pyridine nitrogen atom of quindoline [156, 157].

- **Quinacridine analogues**

FRET assay has shown that the pentacyclic dibenzophenanthroline and quinacridine (**1.30**, **1.31**) (**Figure 1.45 b I, b II**) derivatives are capable of stabilizing G-quadruplex structures. The aromatic rings in the chromophore are fused in a linear fashion, giving it a crescent shape.



a) Quindoline analogues



b) Quinacridine analogues

Figure 1.45: The structure of G-quadruplex ligands; a) Quindoline analogues, b) Quinacridine analogues [146].

- **Cationic porphyrins and related analogues**

- **Cationic porphyrins**

The Porphyrin analogues were found to interact with the quadruplex structures, probably because of the planer geometry of the aromatic rings (TMPyP4, **1.32**, TMPyP2, **1.33**) (**Figure 1.46 a, b**).

- **Pentacationic manganese (III) porphyrin**

A porphyrin analogue, pentacationic manganese (III) porphyrin (**1.34**) (**Figure 1.46 c**) with one central aromatic core and four cationic arms, showed much more selectivity towards the quadruplex structure than the duplex DNA, with a selectivity factor of nearly 10000-fold [158].

- **Expanded porphyrin**

A core-modified expanded porphyrin analogue, 5,10,15,20-[tetra(*N*-methyl-3-pyridyl)]-26,28-diselenasapphyrin chloride (Se2SAP, **1.35**, **Figure 1.46 d**), has been developed, synthesized [159] and identified to bind to *c-myc* quadruplexes more selectively than duplex DNA, as well as other G-quadruplexes.

- **Porphyrazines**

By substituting the four benzene moieties in the macrocycle periphery of the porphyrin, new non-symmetrical phthalocyanine azo analogues (tetrapyridinoporphyrazines) have been devised and synthesized. These molecules are different from the porphyrin cores by having individual pyrrole units linked by nitrogen atoms in the meso positions. The pyridyl groups of the 3,4-tetrapyridinoporphyrazine (3,4-TPyPz, **1.36**, **Figure 1.46 e**) compounds can be methylated to give 3,4-tetramethylpyridinium porphyrazines (3,4-TMPyPz, **1.37**, **Figure 1.46 f**). Both 3,4-TMPyPz (**1.37**) and 3,4-TMPyPz zinc(II) (**1.38**) (**Figure 1.46 g**) showed strong and selective binding affinity towards human telomeric G-quadruplex DNA [160]. Octacationic quaternary ammonium zinc phthalocyanine (ZnPc, **1.39**, **Figure 1.46 h**) is another porphyrazine analogue that displayed strong inhibitory activity against telomerase [161].

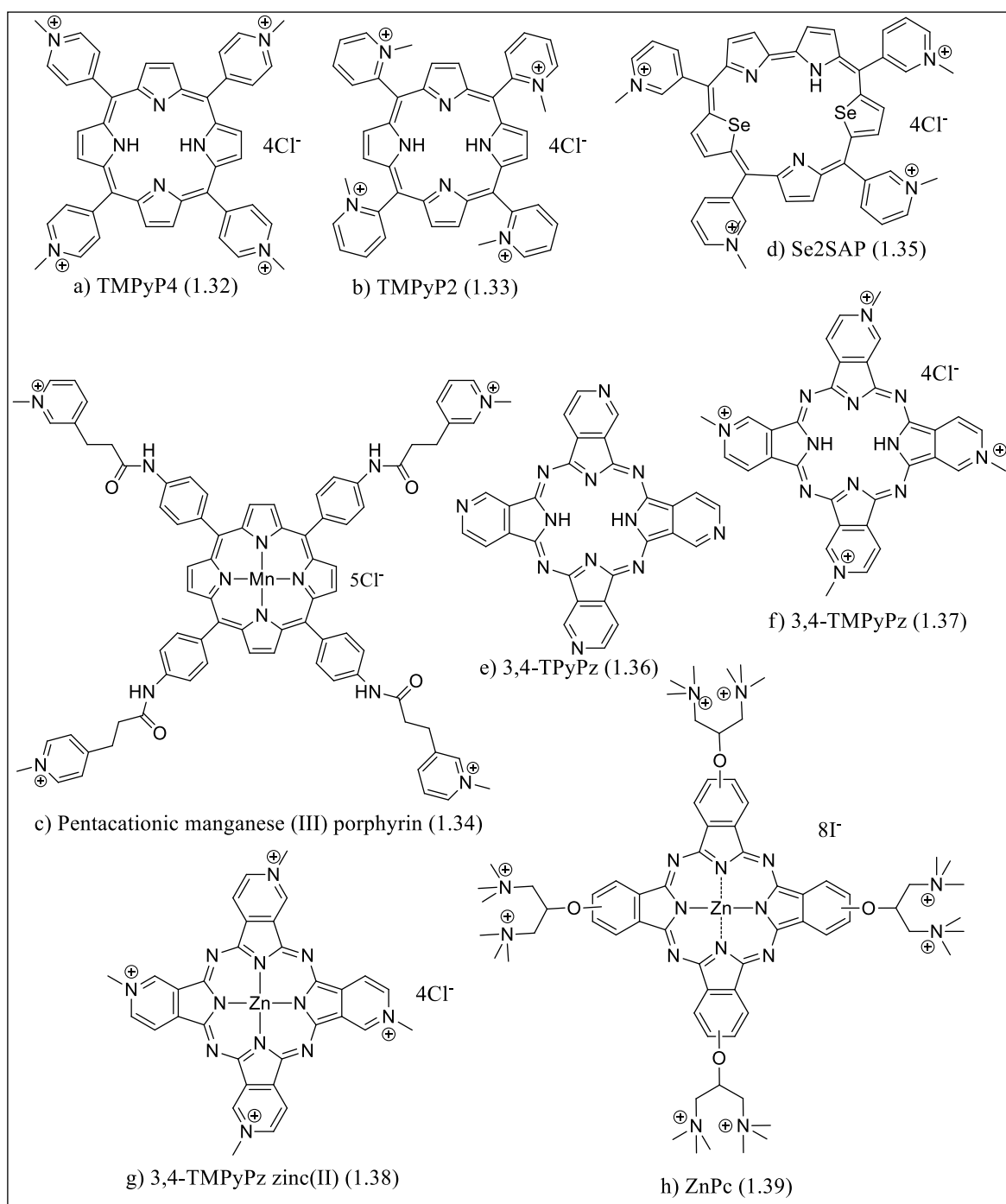


Figure 1.46: The structure of cationic porphyrins; a) TMPyP4 (1.32), b) TMPyP2 (1.33), c) Pentacationic manganese (III) porphyrin (1.34), d) Se2SAP (1.35), e) 3,4-TPyPz (1.36), f) 3,4-TMPyPz (1.37), g) 3,4-TMPyPz zinc(II) (1.38), h) ZnPc (1.39).

- **Perylene derivatives**

The polycyclic compound *N,N'*-bis[-(1-piperidino)-ethyl]-3,4,9,10-perylenetetracarboxylic diimide (PIPER, **1.40**, **Figure 1.47 a**) was identified to be suitable for quadruplex binding by use of the DOCK programme and found to bind to quadruplexes more specifically than duplex DNA.

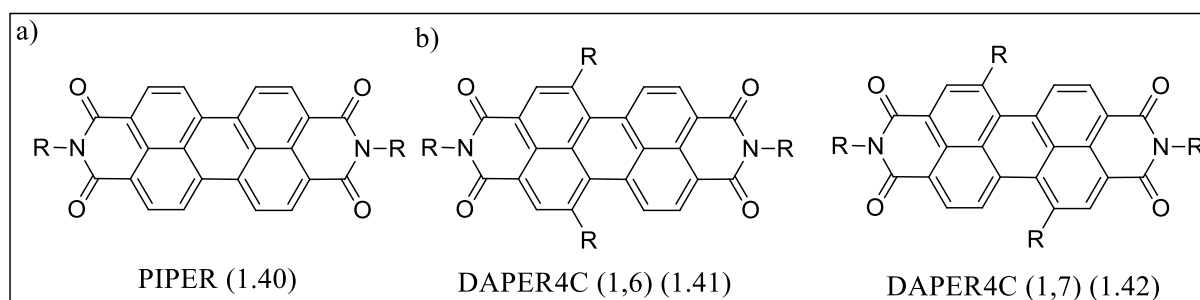


Figure 1.47: The structure of some perylene derivatives; a) Two side chains, b) Four side chains.

- **Natural Products**

Another group of molecules that has been investigated as G-quadruplex binders are natural compounds and their synthetic analogues, including distamycin [162], berberine and berberine derivatives [163-165], and the capping of binding platforms with neomycin.

➤ **Telomestatin and its derivatives**

Telomestatin (SOT-095, **1.7**), one of the most potent *in vitro* telomerase inhibitors, was extracted from a marine actinomycete *Streptomyces anulatus* 3533-SV4. The compound contains seven oxazole rings and one thiazoline ring [146]. Telomestatin derivatives such as macrocyclic hexaoxazole HXDV and bistrioxazole acetate have been reported to be synthesized [166, 167]. HXDV (**1.43**) (**Figure 1.48 a I**) binds to quadruplex DNA (through a non-intercalative “terminal capping” mode) preferentially than to duplex or triplex DNA. Bistrioxazole acetates (**1.44**) (**Figure 1.48 a II**) were designed based on the telomestatin

structure, and contain a macrocyclic bisamide structure, one of which demonstrated telomerase inhibitory activity with a $^{tel}IC_{50}$ value of 2 μ m.

➤ Berberine derivatives

Although the antimicrobial activity of the alkaloid berberine (**1.45**) (**Figure 1.48 b I**), isolated from Chinese herbs, was known for a long time, its telomerase inhibitory activity was first reported in 1999 [165]. Later on, 13 substituted berberine analogues (**1.46**) (**Figure 1.48 b II**) were reported with telomerase inhibiting activity through telomeric G-quadruplex binding [164]. Recently, 9 substituted derivatives of berberine (**1.47**) (**Figure 1.48 b III**) have been found to induce antiparallel quadruplex formation, with stabilization either in the presence or absence of metal cations and with a stronger binding affinity than berberine. Their higher inhibitory activity against telomerase might be because of the inclusion of methylene units and an amino group at the 9 position [168].

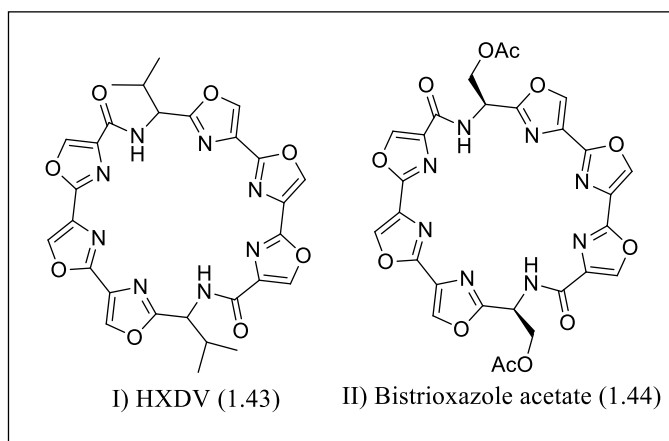
➤ Quinoanthroxazine derivatives

Although fluoroquinolones like norfloxacin are widely used for their antimicrobial activity, some tetracyclic quinolone derivatives showed strong anticancer activity through interactions with topoisomerase II. Fluoroquinoanthroxazines (FQA, **1.48**, **Figure 1.48 c**) are fluoroquinolone derivatives with extended aromatic rings and have shown binding affinities for G-quadruplex DNA by stacking interactions, which might be because of their extended phenoxazine ring [146].

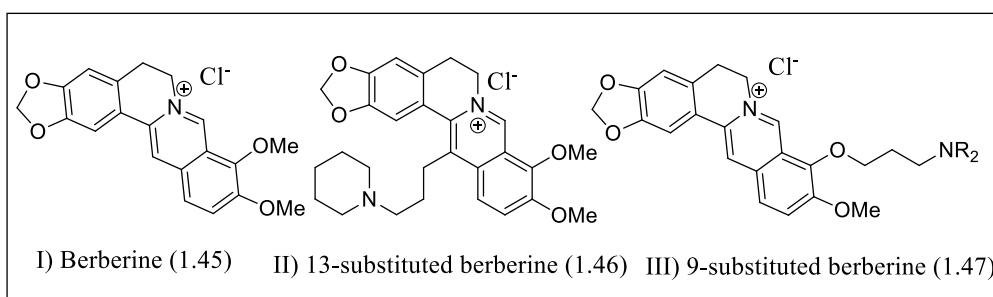
• Bisquinolinium compounds

Bisquinoline-substituted triazines (**Figure 1.49a**), such as 115405 (**1.51**) and 12459 (**1.49**), can inhibit the human telomerase enzyme at nanomolar concentrations [169]. Another class of bisquinoline analogues (**Figure 1.49 a**), such as 307A (**1.50**) and 360A (**1.52**), were synthesized by joining two quinolinium moieties with a 2,6-pyridodicarboxamide unit. The central pyridodicarboxamide unit can give the ligand a crescent shape through the generation

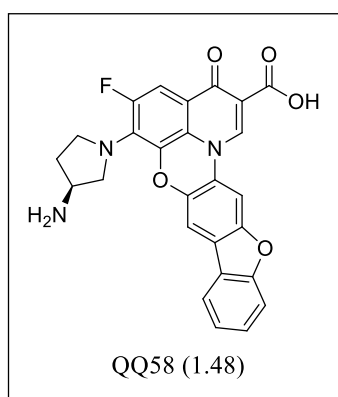
of *syn-syn* conformations, by forming internal H-bonds, which favour G-quartet overlaps. Based on this, compounds have been reported in which pyridine cores have been replaced by bipyridine and phenanthroline (**1.53**, **1.54**) units (**Figure 1.49 b**), which increased the aromaticity of the central core without disrupting the hydrogen bonding capability [170].



a) Structures of telomestatins



b) Structures of berberine derivatives



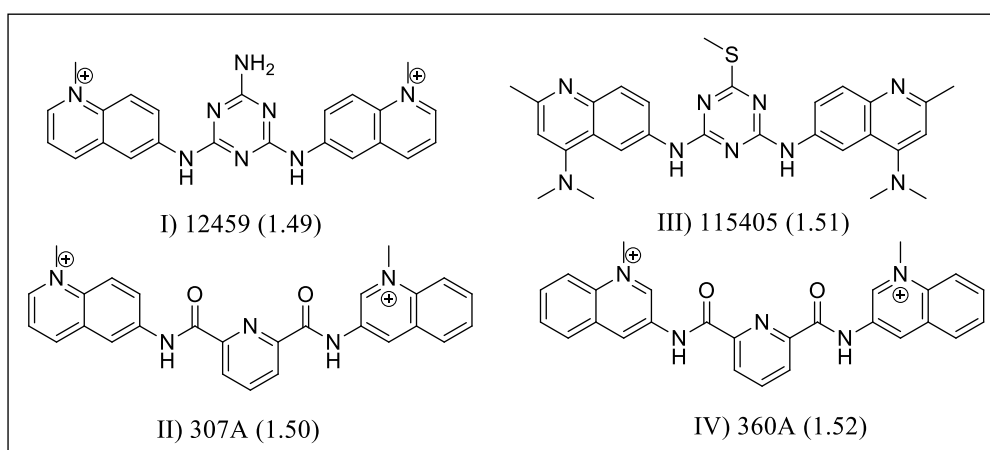
c) Structures of fluoroquinoanthroxazine (FQA)

Figure 1.48: Structure of some natural quadruplex binding ligands; a) telomestatins (**1.43**, **1.44**), b) berberine derivatives (**1.45-1.47**), c) fluoroquinoanthroxazines (FQAs) (**1.48**).

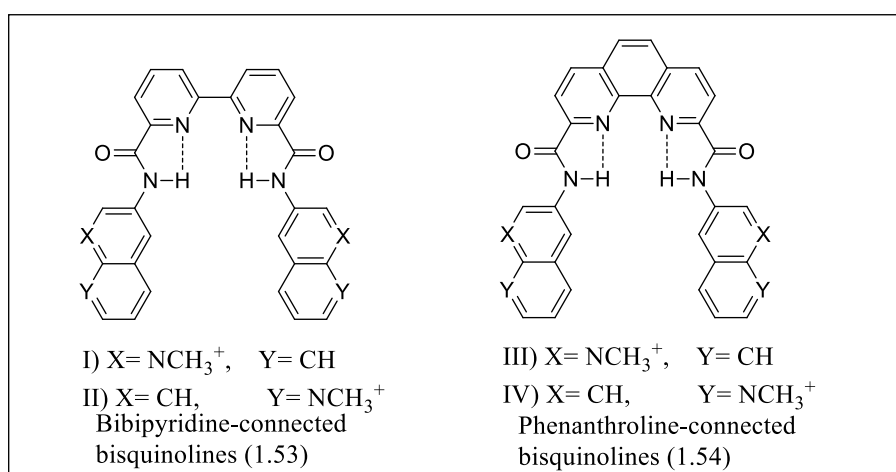
- **Biaryl polyamides**

Based on the distamycin scaffold, in 2009 Rahman and co-workers reported a series of new biaryl polyamides (**Figure 1.49 c**) with significant selectivity for quadruplexes over duplex DNA and modest selectivity for different quadruplex types [171]. The pyrroles of distamycin were replaced with biaryl building blocks in order to switch binding preferences for quadruplex over duplex DNA. The design of the new polyamide constructs positioned the biaryl units at either end of the polyamide core, in order to gain ligand diversity. The introduction of a biaryl unit significantly altered the classical crescent-shaped structure of the molecules, forcing them to adopt a U-shaped scaffold instead. This alteration in shape ensured that the molecules had a lower binding affinity for duplex DNA, while increasing their interaction with a G-quadruplex structure, since the ligands have similar dimensions. In contrast to previous attempts to produce quadruplex-selective distamycin analogs [172], these biaryl polyamides offer synthetic versatility and significant quadruplex selectivity. They consist of two different structural motifs: Motif-1 (**1.55**), containing one biaryl unit; and Motif-2 (**1.56**), which has dimers of biaryl units (**Figure 1.49 c**).

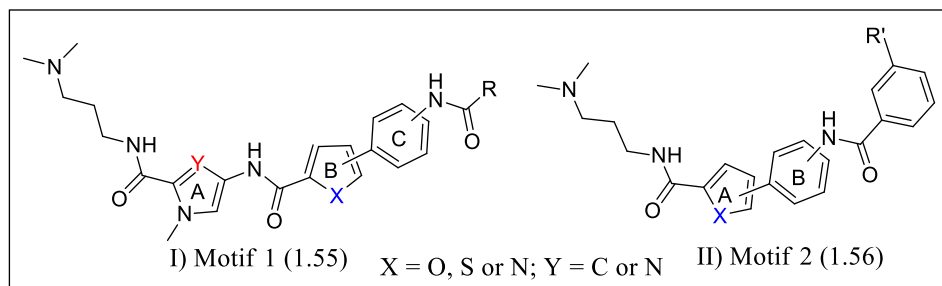
Therefore, given their low molecular weight, good water solubility and excellent cellular penetration properties, molecules of this type have the potential to be developed into reagents that can probe DNA structure, and/or down-regulate individual signalling pathways in cells without the need for microinjection, transfection or electroporation (as is the case with antisense- and RNAi-type agents).



a) Bisquinoline derivatives



b) Connected bisquinolines



c) Biaryl polyamides

Figure 1.49: The structure of a) Bisquinoline derivatives, b) Connected bisquinolines, and c) Biaryl polyamides.

1.15.4 Examples of some G-quadruplex Binding Ligands

Many chemotherapeutic agents (like cisplatin, mitomycin C, chloroethyl nitrosoureas, and daunomycin) show non-specific interactions with DNA. Therefore, it has become important to develop small drug-like molecules with selective binding affinity for specific secondary and tertiary structures in DNA, as well as having site-specific effects, while minimizing side effects. Because of recent developments in G-quadruplex research, detailed information about their structures, thermodynamic stabilities and potential biological activities are available, which makes these structures an interesting target for developing cancer-specific drugs. An increasing number of research groups are now working on targeting these G-quadruplex structures by developing G4 binding ligands for inhibiting cancer development, depending on two mechanisms (**Figure 1.50**). Firstly, over-expression of oncogenes (*c-Myc*, *c-kit*, *KRAS*, etc.) may be repressed by deactivating their promoters. The second approach involves the inhibition of the telomerase enzyme that catalyses the synthesis of the 3'-overhang of telomeric DNA [173].

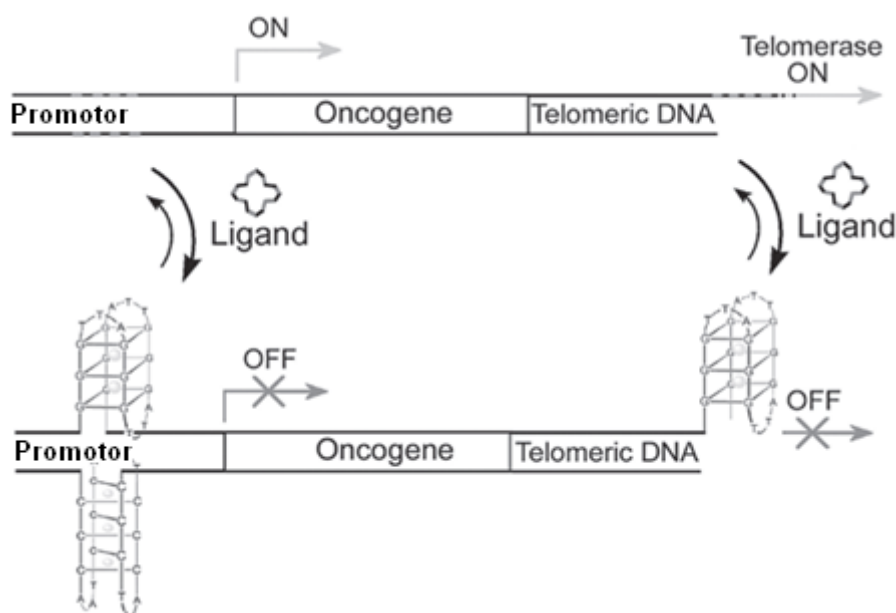


Figure 1.50: Ligand-mediated G-quadruplex stabilization may regulate gene expression and/or telomerase inhibition [173].

For the first time, the duplex DNA intercalating agent ethidium was reported to stabilize the G-quartet structure generated by d(TTTTGGGG) in a Na⁺ ion solution [174]. This apparently showed a strong binding between the G-tetrad stacks, through intercalation. It was suggested that this inhibits the telomerase enzyme, although no further attempts were made to prove this. However, recent studies of ethidium binding for different quadruplexes demonstrated a weak quadruplex affinity, while also observing a 12-fold greater affinity for duplex and triplex DNA [175].

Anthraquinones (**1.57**) and 3,6-disubstituted acridines (**1.61**) were the first reported telomerase inhibitors. After that, trisubstituted acridines, porphyrins, and triazines were synthesised for increased potency [176]. A significantly important molecule of this series is BRACO-19 (**1.5**), a 3,6,9-trisubstituted acridine that was developed and analysed by Neidle *et al.* [177]. Furthermore, 9-[4-(dimethylamino)phenylamino]-3,6-bis(3-pyrrolidinopropionamido)-acridine inhibited tumour growth both in *in vitro* and in *in vivo* analysis at less than 1 μ M concentrations [173]. The inhibitors interact with quadruplexes by π - π stacking and stabilize the quadruplex structures by the electrostatic interaction between the positively charged side chains of inhibitors and negatively charged phosphate DNA backbone, resulting in telomere complex disruption. BRACO-19 (**1.5**) has produced some potentially interesting results, demonstrating telomerase inhibition as well as telomere dysfunction, leading to apoptosis [178]. Another molecule, BRACO-20 (**1.60**), has 30-fold higher affinities for quadruplexes than duplex DNA. Additionally, BRACO-20 (**1.60**) showed telomerase inhibition potential, with an EC₅₀ value of 0.06 μ M [179]. Although BRACO-19 (**1.5**) stabilized the quadruplex structure effectively, its affinity for duplex DNA (ΔT_m =14.5 °C at 1 μ M)[180] is comparatively higher than many other ligands, which was a major drawback for the progression of the compound towards clinical trials.

Another important family of G-quadruplex-binding ligands is based on the porphyrin scaffold, with the original agent TMPyP4 (**1.32**). TMPyP4 (**1.32**) inhibits both telomerase (IC₅₀ \approx 0.7–10 μ M) and Taq DNA polymerase (IC₅₀ \approx 2 μ M). The process of inhibition of telomerase by TMPyP4 (**1.32**) depends on the chemical groups present at the *meso* positions.

Substitution by pyridinium only at the *meso* positions was successful in enhancing activity, while the other substituents showed no enhancement of activity. However, the structure–activity relationship analysis demonstrated that, for better porphyrin-DNA binding, two forces - base stacking and electrostatic interactions - are important. Although TMPyP4 (**1.32**) demonstrated some good antitumor activity *in vivo*, it has poor DNA specificity and high toxicity. Thus, TMPyP4 (**1.32**), which binds to every type of DNA with nearly similar affinities ($K_d \approx 200$ nM), might not be considered as a structure-specific ligand [173].

Natural compounds such as berberine (**1.45**, **1.58**) and telomestatin (**1.7**) were reported to inhibit telomerase. Telomestatin, (**1.7**) obtained from *Streptomyces anulatus* 3533-SV4, demonstrated telomerase inhibitory activity at a 5 nM concentration. Structural analysis of telomestatin (**1.7**) revealed the presence of macrocyclic linkages of two methyloxazoles, five oxazoles and one thiazoline ring, which helped in the total synthesis of the ligand. Telomestatin (**1.7**) reduced cell growth *in vitro* as well as *in vivo* in a number of human tumours, such as multiple myeloma, neuroblastomas and leukaemia. Berberine (**1.45**, **1.58**) is an antibiotic alkaloid which showed anticancer activity by down-regulating telomerase activity through G-quadruplex binding [181].

Perylenedicarboximides [182] have been found to initiate G-quadruplex structure formation and inhibit telomerase according to the side chain basicity and length. The first reported molecule of this series was PIPER (**1.40**), and recently a new series of highly water soluble perylenes has been reported, such as DAPER4C (1, 6) (**1.41**) and coronene (CORON) (**1.63**) analogues with 3/4 side chains containing different basic moieties. Compared with previous perylene analogues, all of them showed evidence of improved interactions with quadruplexes, as well as telomerase inhibition [176].

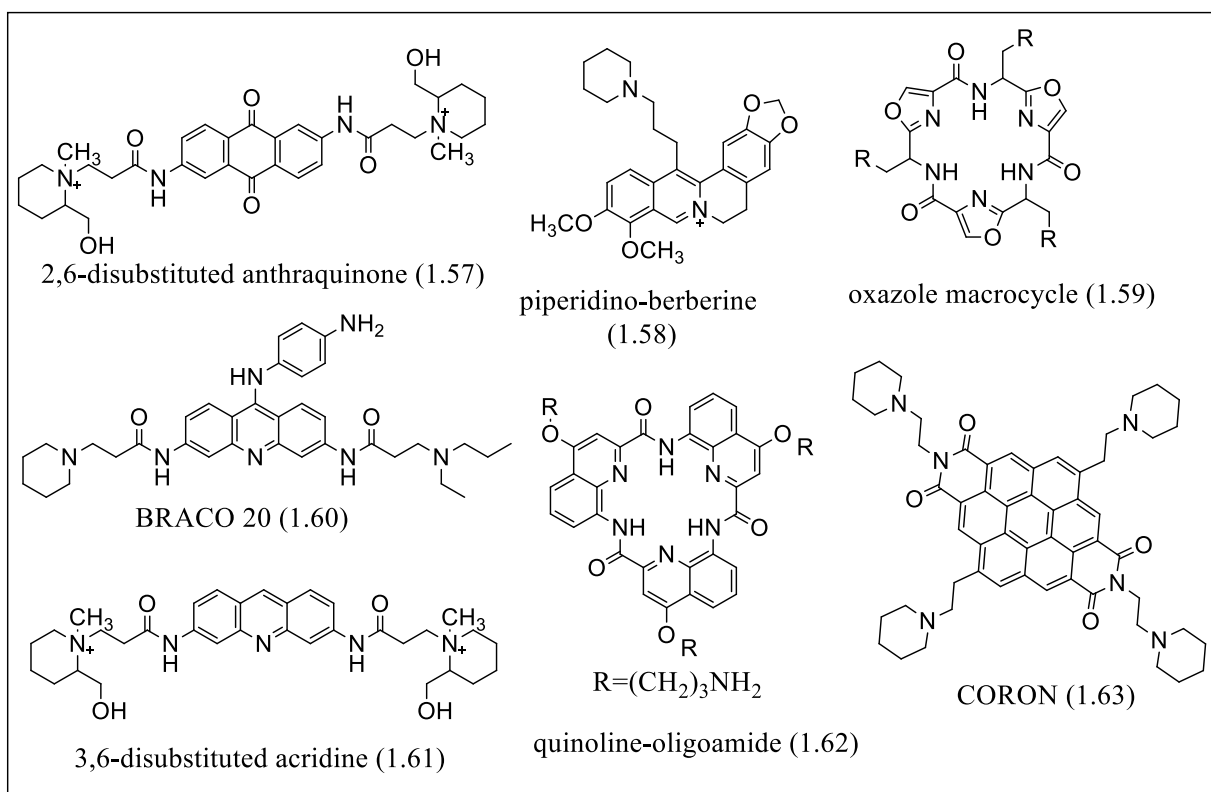


Figure 1.51: Examples of some known G-quadruplex ligands [176, 179].

The success of telomestatin (**1.7**) as a quadruplex-binding agent encouraged the synthesis of several macrocycles containing quinacridine (**1.30**, **1.31**), oxazole (**1.59**) and quinoline (**1.62**) moieties that were studied as G-quadruplex-binding ligands. Recently, macrocyclic hexa-oxazoles, which have structural similarities to telomestatin, have been synthesized using a similar strategy that combined a planar macrocyclic hexa-oxazole pharmacophore with basic side chains. These molecules demonstrated excellent G-quadruplex specificities and act as potent telomerase inhibitors in both cell-free and cell-based assay systems [183].

G-quadruplexes contain planer, square-like, electron-rich π -surfaces that can act as molecular recognition targets. Fujita and co-workers have utilized this feature of the quadruplex structure for designing supramolecular structures (**Figure 1.52**) known as the platinum “square” complexes. A platinum molecular square [Pt(en)(4,4'-dipyridyl)] (**1.64**) has been reported to be an excellent G4 binding and telomerase inhibiting agent. According to molecular modelling studies, the binding affinity of these ligands arises from the square

arrangement of the four bipyridyl ligands and the highly electropositive nature of the overall complex, as well as hydrogen bonding interactions between the ethylenediamine ligands and the phosphates of the DNA backbone [184].

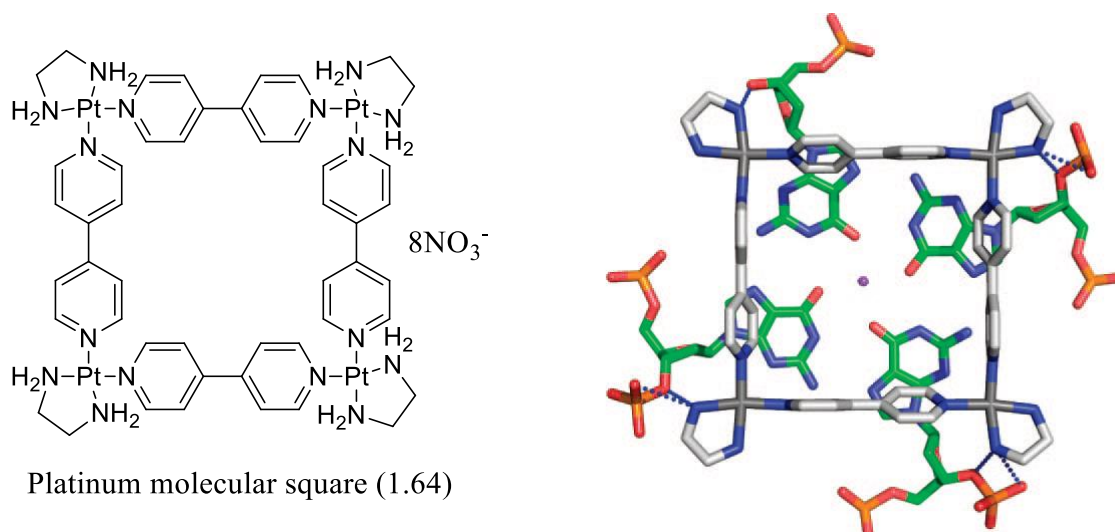


Figure 1.52: Left: Structure of the platinum molecular square. Right: G-quadruplex and the platinum molecule complex [184].

The metallo-supramolecular cylinders $[M_2L_3](PF_6)_4$ and $[M_2L_3]Cl_4$ ($M=Ni$ or Fe) (**1.65**) were found to discriminate between DNA duplex and G-quadruplex DNA. The chiral compound has a bi-metallo triple helicate structure, and two pairs of enantiomers M and P (**Figure 1.53**), each of which has a hydrophobic surface and a size (length ~ 18 Å, diameter ~ 8 Å) compatible with G-quartets (length ~ 14 Å, width ~ 11 Å). The P-enantiomer demonstrated a strong binding affinity for G4s over duplexes [185].

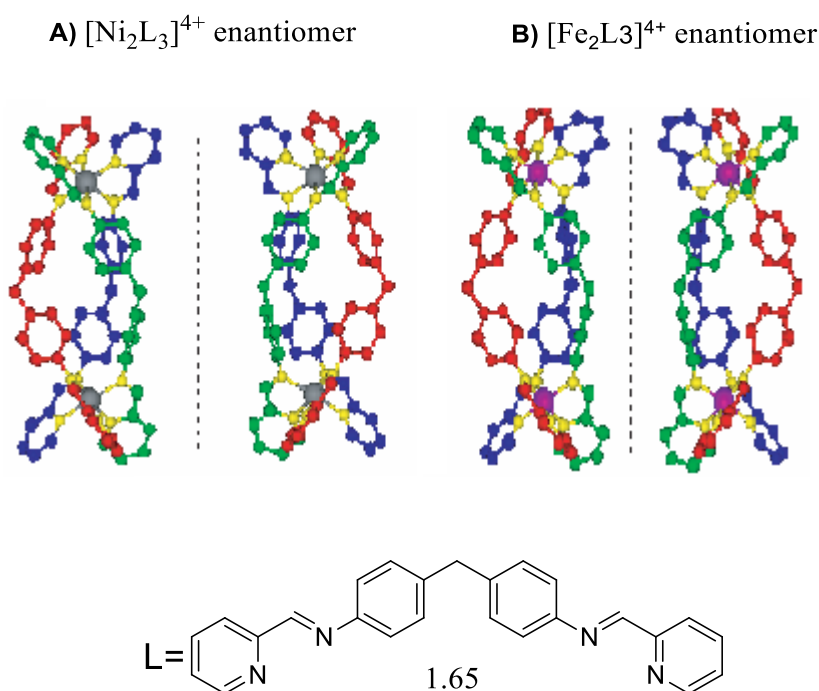


Figure 1.53: (A) Structures of the M (left) and P-enantiomer (right) of $[\text{Ni}_2\text{L}_3]^{4+}$ cation. (B) Structures of the M (left) and P-enantiomer (right) of $[\text{Fe}_2\text{L}_3]^{4+}$ cation [185].

A family of urea-based non-polycyclic aromatic ligands with alkylaminoanilino side chains has been developed and synthesized as G4 binding ligands. These molecules showed binding potential for particular quadruplexes and significant selectivity over duplex DNA. Initial biological studies showed cancer cell selectivity for some of the ligands as well [186].

Several 4,5-bis(dialkylaminoalkyl)-substituted acridines (**1.66**) were synthesized from acridine, and their G4-stabilizing potentials were evaluated using various biophysical methods. Among the 4,5-disubstituted molecules, the dimethylaminopropyl substituted acridine derivative showed significant sub-micromolar TRAP inhibitory activity ($\text{IC}_{50} = 0.15 \mu\text{M}$) [187].

The naphthalene diimide derivative **1.67** showed high potency against primary tumour GIST cell lines. Human gastrointestinal stromal tumours (GIST) usually occur because of mutations in the tyrosine kinase receptor of the proto-oncogene kit. Reoccurrence of tumour regrowth

happens with imatinib treatment because of the development of resistant mutants in its target kinase domain of kit. A naphthalene diimide analogue (**1.67**) was used to target kit genes directly in GIST therapy through kit quadruplex stabilization, and hence kinase resistance may be circumvented [188].

Based on the distamycin scaffold, a new class of biaryl polyamides (**1.55** and **1.56**) has been reported recently by Rahman *et al.*, which has shown high selectivity for the G-quartet, as well as having showed potent cytotoxic effects in various cancer cell lines. Their U-shaped planer form facilitates more in binding the surface area of the quadruplexes than the grooves of double-stranded DNA. These ligands showed potent growth inhibitory activity against human colorectal carcinoma (HT29) and human lung carcinoma (A549) lines [189].

Derivatives of 1,3-substituted symmetrical phenylene bisbenzimidazole systems demonstrated prominent effects on quadruplex stability, depending on the types of substitution on aromatic skeletons. Two isomeric bisbenzimidazole-based compounds, *p*-Phenbbim (**1.69**) and *m*-Phenbbim (**1.68**), were designed and synthesized, both of which stabilized the quadruplex structures. The G4 binding ability of these compounds depended on the shape of the molecules. As an example, the linear isomer was found to stabilize the Na⁺-induced intramolecular quadruplex, while the V-shaped isomer showed structural transition above a particular ligand concentration level, with a higher binding affinity for the G-quadruplex [190].

Bis-phenanthroline (bis-Phen) ligands (**1.70**) containing two Phen moieties covalently linked through an amine or thioether bond have been found to recognize different G-4 structures. The transition metal ions Mn²⁺, Ni²⁺, Cu²⁺, and the biologically relevant Mg²⁺ and Zn²⁺, efficiently form 1:1 bis-Phen complexes with a large planar structure capable of recognizing the G4 structures. These complexes induce quadruplex formation from linear G-rich sequences, and are also effective telomerase inhibitors, with the Ni(II) complexes being effective in the sub-micromolar range [191].

It has also been found that some phthalocyanines bind to G4 structures with a high affinity and selectivity due to the presence of a large π planar structure and bulky cationic groups. Water-soluble octacationic zinc phthalocyanine (ZnPc) (**1.41**) has been found to be an excellent G4 stabilizer and telomerase inhibitor [161]. Although cationic ligands have a great advantage in terms of cell permeability, it may not be possible to fully eliminate the electrostatic interaction between the cationic groups and dsDNA of cell nuclei; this can be solved by making the ligand non-ionic or anionic. Telomestatin, a non-ionic ligand, can bind to telomeric G-quadruplex structures with high selectivity, but has less solubility. On the other hand, only a few anionic molecules were analysed for their binding ability to G-quadruplexes and subsequent telomerase inhibitory effects. However, one anionic copper phthalocyanine (Cu-APC) (**1.71**), containing four sulfonic groups, has been shown to bind to telomere G-quadruplexes with high selectivity [192].

More recently, a pair of furan-based cyclic homo-oligopeptides (**1.72**) has been reported to specifically target G-quadruplexes. These ligands induced G4 formation effectively in a 22-mer c-MYC DNA sequence and also stabilized that structure. It has a high affinity for quadruplex structures without showing any affinity for duplex DNA, demonstrating selectivity for G-quadruplex structures. Moreover, these ligands caused apoptosis in HeLa cells by down-regulating up to 90% of the *c-MYC* transcripts. Therefore, these molecules provide suitable scaffolds for developing quadruplex binding agents [193].

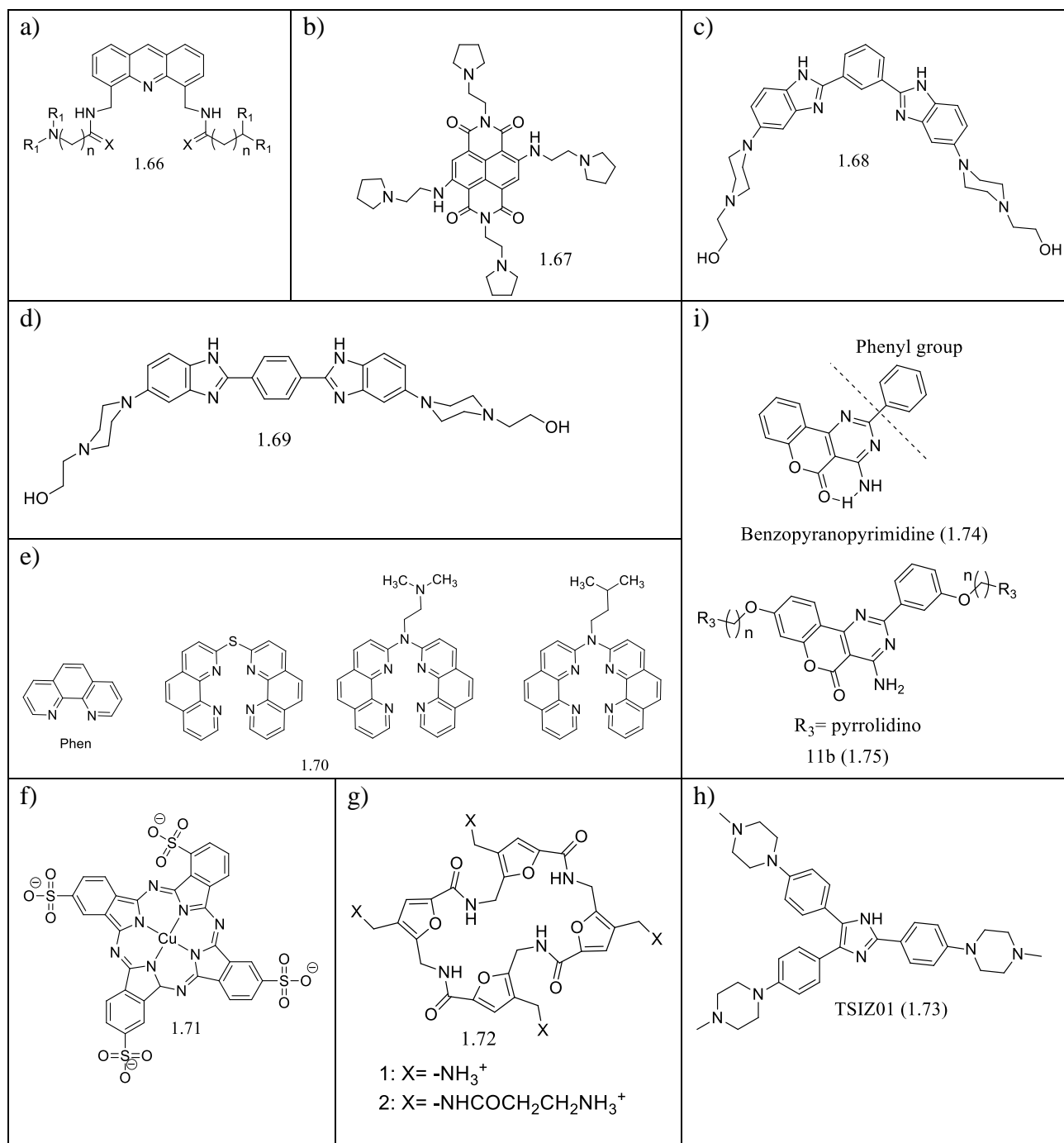


Figure 1.54: The structure of a) some 4,5-bis(dialkylaminoalkyl)-substituted acridines (**1.66**), b) naphthalene diimide derivatives (**1.67**), c) *m*-Phenbbim (**1.68**), d) *p*-Phenbbim (**1.69**), e) bis-phenanthroline ligands (**1.70**), f) anionic copper phthalocyanine (Cu-APC) (**1.71**), g) furan-based cyclic homooligopeptides, ligand 1 and ligand 2 (**1.72**), h) TSIZ01 (**1.73**), i) PBPPs scaffold (**1.74**) and the promising compound 11b (**1.75**) [161, 187-195].

Recently, an acridine based triaryl-substituted imidazole derivative TSIZ01 (**1.73**) has been reported as a new potential quadruplex binding and stabilizing ligand. TSIZ01 (**1.73**) exhibited a high level of selectivity for telomeric quadruplexes (F21T) rather than duplex DNA (F10T). According to the FRET melting assay, TSIZ01 (**1.73**) stabilized the human telomeric G-quadruplex (F21T) effectively with a ΔT_m value of 23.5 °C at 1 μ M concentration compared with the duplex hairpin DNA (ΔT_m = 2.7 °C at 1 μ M). When the concentration of the compound was raised to 3 μ M, it stabilized the quadruplex more, with an increase in the melting temperature (ΔT_m) to 32 °C. Moreover, the quadruplex selectivity of the compound was further established through FRET-based competition assays, which showed that the thermal stabilization of F21T by the compound was still retained even with the addition of a 15-fold excess of duplex DNA competitors. Again, TSIZ01 (**1.73**) has a higher binding affinity towards the quadruplex DNA with an equilibrium binding constant (K_A) value of $2.19 \times 10^6 \text{ M}^{-1}$, which is 8.7-fold higher than that of duplex DNA ($K_A = 2.51 \times 10^5 \text{ M}^{-1}$). All these studies established that TSIZ01 (**1.73**), with good stability, has good selectivity for telomeric G-quadruplex DNA, along with potent binding and stabilizing activity [194].

A series of 2-phenyl-benzopyranopyrimidine (PBPP) derivatives with alkylamino side chains was reported for the first time as a new class of highly selective G-quadruplex ligand. In addition to the rotatable C-C single bond between the benzopyranopyrimidine moiety (**1.74**) and the phenyl group, which allows various conformation, the PBPP structure forms an intramolecular hydrogen bond, improving the planarity of the molecule due to enhancing the π -delocalization. The cationic amino side chains enhanced the G-quadruplex binding potency through an interaction with the grooves and loops of G4 structures, as well as its aqueous solubility. All the results obtained from the biophysical analyses demonstrated that de-substituted PBPP derivatives have a stronger G-4 binding affinity and stabilizing potential, as well as more selectivity over duplex DNA than the mono-substituted derivatives. Furthermore, compound 11b (**1.75**) (ΔT_m = 16.5 °C and K_D = 4.5 for telomeric G-quadruplex, and ΔT_m = 0.4 °C for duplex DNA) was identified as the most promising telomerase inhibitor within this series [195].

Depending on bis(phenylenethynyl) amides (1 and 2) (**1.76**, **1.77**), two novel G-quadruplex ligands 1,2,3-triazole-linked diethynylpyridine amides (3a-c) (**1.78**, **1.79**, **1.80**) and trisubstituted diethynyl-pyridine amides (4a,b) (**1.81**, **1.82**) have been reported by Dash and co-workers to exhibit enhanced binding potential to both G4s and specificity promoter G-quadruplexes, compared with the first generation of diaryl-ethynyl amides. The parent molecules contain *N,N*-dimethyl-propylamine side chains and are conformationally flexible due to free rotation around the triple bond. The best first generation molecule, 2 (**1.77**), was modified to generate 1,4-triazole-linked amides (**1.78**, **1.79**, **1.80**) and trisubstituted amides (**1.81**, **1.82**) in order to get an improved binding ability as well as differential recognition of these molecules towards various classes of G-quadruplex sequences. Compared with other molecules, 3a (**1.78**) and 4a (**1.81**) were found to have greater selectivity for the G-quadruplex than the duplex DNA. Among the bis-triazole ligand series, 3a (**1.78**), having primary amino groups, showed the highest degree of stabilization, with ΔT_m values of 17.1, 11.8, 20.0, 16.5 and 0.7 °C for *k-ras*, *c-myc*, *c-kit1*, *c-kit2* quadruplexes and duplex DNA, respectively, at a 1 μ M ligand concentration, whereas the trisubstituted ligand with *N,N*-dimethylamino side chains, 4a (**1.81**), showed the best G-quadruplex stabilization potential in this series, showing nearly the highest measurable ΔT_m values for *c-myc* and *c-kit2* quadruplexes by Förster Resonance Energy Transfer (ΔT_m = 17.0 and 21.8 °C at 1 μ M, respectively). Ligand 4a (**1.81**) also exhibited stronger stabilization for *k-ras* (ΔT_m = 33.0 °C) and *c-kit1* (ΔT_m = 31.3 °C) quadruplexes at a 1 μ M concentration [196].

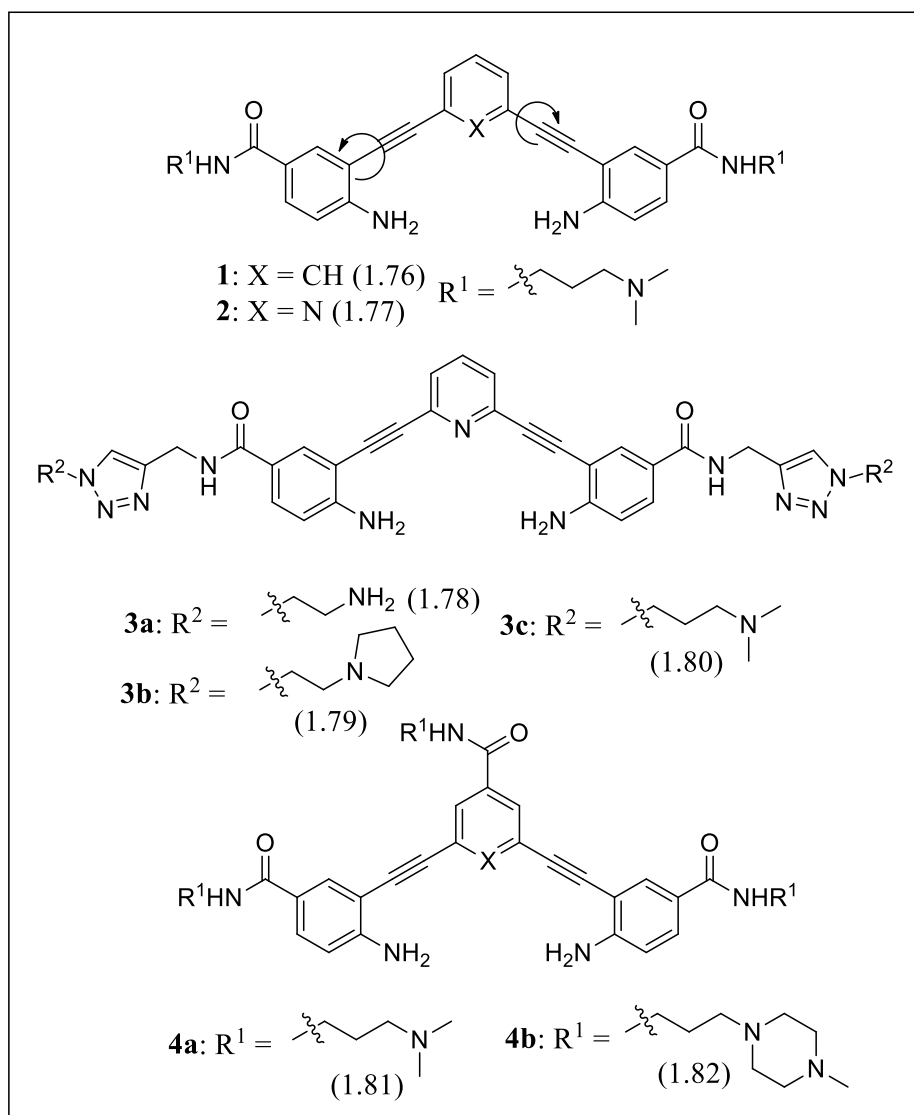


Figure 1.55: Structure of bis(phenylenethynyl) amides (**1** and **2**) (**1.76**, **1.77**), diethynylpyridine amides (**3a-c**) (**1.78**, **1.79**, **1.80**) and trisubstituted diethynyl-pyridine amides (**4a,b**) (**1.81**, **1.82**) [196].

Cell based assay and biophysical analysis have shown that two benzo [*a*] phenoxazine (BPO) derivatives (BPO-1, BPO-2) (**1.83**, **1.84**) bind to the G-quartet sequences of the gastric carcinoma cell (HGC-27) *c-KIT* promoter with a high affinity, and reduce the transcription of the luciferase reporter, as well as down-regulate endogenous *c-KIT* expression. Both of them contain an *N*-(3-dimethylaminopropyl) amino carbonyl side chain at the 11 position of the BPO moiety. These ligands have a stronger affinity for *c-kit2*, having K_d values of 1.0 ± 0.3 and 1.1 ± 0.3 μM for BPO-1 (**1.83**) and BPO-2 (**1.84**), respectively, than *c-kit1* ($K_d = 9.6 \pm 4$

μM for **1** and $8.3 \pm 0.1 \mu\text{M}$ for **2**), resulting in a 9.6- and 7.5-fold preference for binding *c-kit2* over *c-kit1*, for **1** and **2**, respectively. BPO-1 (**1. 83**) showed a 10-fold higher K_d value for double-stranded DNA binding compared with *c-kit2* ($K_d = 9.8 \pm 1.7 \mu\text{M}$), whereas no binding of BPO-2 (**1. 84**) with dsDNA was detected. These data are easily comparable with the previously reported *c-kit* binding ligands such as trisubstituted isoalloxazines (K_d ranging from 2.8-9.7 μM), triarylpyridines (K_d ranging from 0.2-25 μM) and oxazole-based peptide macrocycles (K_d ranging from 4-31 μM). Again, BPO-2 (**1. 84**) was found to reduce the *KIT* mRNA expression in the range of 2.6-3.5-fold, whereas BPO-1 (**1. 83**) showed a time-dependent response with a maximum reduction of 2.9 fold at 24 h, compared with the control. Moreover, these compounds have a good aqueous solubility, less cytotoxic effects and easy synthetic routes [197].

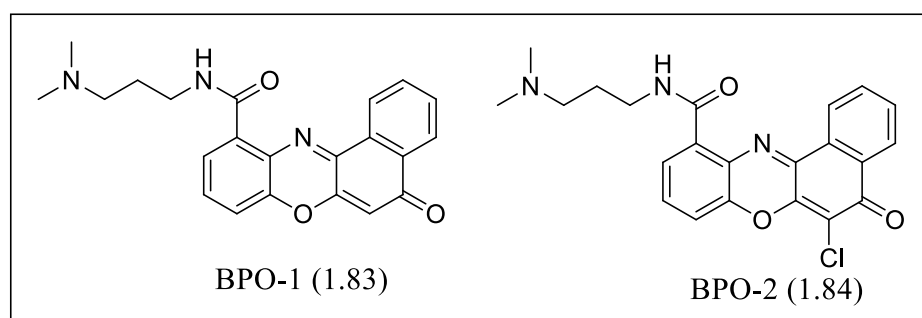


Figure 1.56: Structure of BPO-1 (**1. 83**) and BPO-2 (**1. 84**) [197].

A series of novel quinoline-benzo-[5,6]- dihydroisoquinolium (QBDI) compounds (3a, 3f, 3g, and 3j) (**1.85, 1.86, 1.87, 1.88**), derivatives of the natural alkaloid berberine, showed an enhanced binding affinity and selectivity for the tetrad structures of *c-myc* and illustrated good inhibition of the *c-myc* transcription into tumour cells but not into normal cells. These compounds contained a hexacyclic ring system, having one additional pyridine ring and amino acid on the barberine scaffold, expanding the aromatic planer surface of barberine (**1.45**), resulting in enhanced quadruplex-stabilization ability and binding selectivity. The compounds demonstrated an effective stabilization of *c-myc* quadruplexes, with ΔT_m values ranging from 20 to 29 $^{\circ}\text{C}$, whereas the compound 3j (**1.88**) had the highest ΔT_m value of 29 $^{\circ}\text{C}$ and derivative 3a had a value of 20 $^{\circ}\text{C}$, both of which were higher compared with the

reference compound barberine (**1.45**) ($\Delta T_m = 1\text{ }^\circ\text{C}$). Furthermore, FRET-based competition assays of these derivatives proved their selectivity towards G-quadruplexes over duplex DNA. Subsequent bioassays indicated that **3j** (**1.88**) down-regulated *c-myc* transcription and inhibited lymphoma cell growth, but did slightly affect the healthy cell [198].

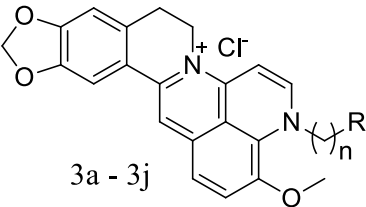
 <p>3a - 3j</p>	Compound	n	R
	3a (1.85)	2	N(CH ₃) ₂
	3f (1.86)	3	N(CH ₃) ₂
	3g (1.87)	3	morpholyl
	3j (1.88)	6	NH ₂

Figure 1.57: The structure of QBDI compounds [198].

From *Clausena harmandiana* and *C. excavata*, several carbazole alkaloids have been isolated and reported to have significant cytotoxic activity against cancer cell lines. Recently, 3,6-bis(1-methyl-4-vinylpyridinium) carbazole diiodide (BMVC) (**1.89**), a carbazole derivative, has shown good G-quadruplex stabilization with a ΔT_m of $13\text{ }^\circ\text{C}$, as well as showing telomerase inhibitory activity. Based on this carbazole chromophore, a series of 1,8-dipyrazolcarbazole (DPC) derivatives (6a–6d, 7a–7d) (**1.90**, **1.91**) have been designed, which contained two pyrazole groups to have better π - π stacking interactions with the G-quadruplex. These molecules form intramolecular hydrogen bonds, improving molecular planarity through increased π -delocalization and the cationic side chains, which could interact with the grooves and loops of the G-quadruplex; this may be effective for selective binding with the G-quadruplex, as well as its aqueous solubility. These molecules have been reported to interact more selectively with *c-myc* G-quadruplexes than telomeric G-quadruplex structures, and RT-PCR analysis has proven that, from this series, 7b can down-regulate *c-myc* expression in the Ramos cell line, but not in the CA46 cell line with the NHE III₁ element removed [126].

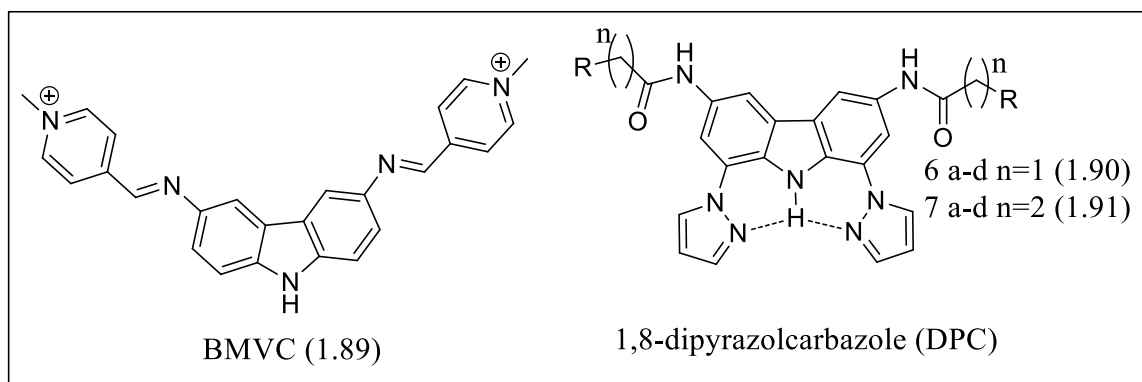
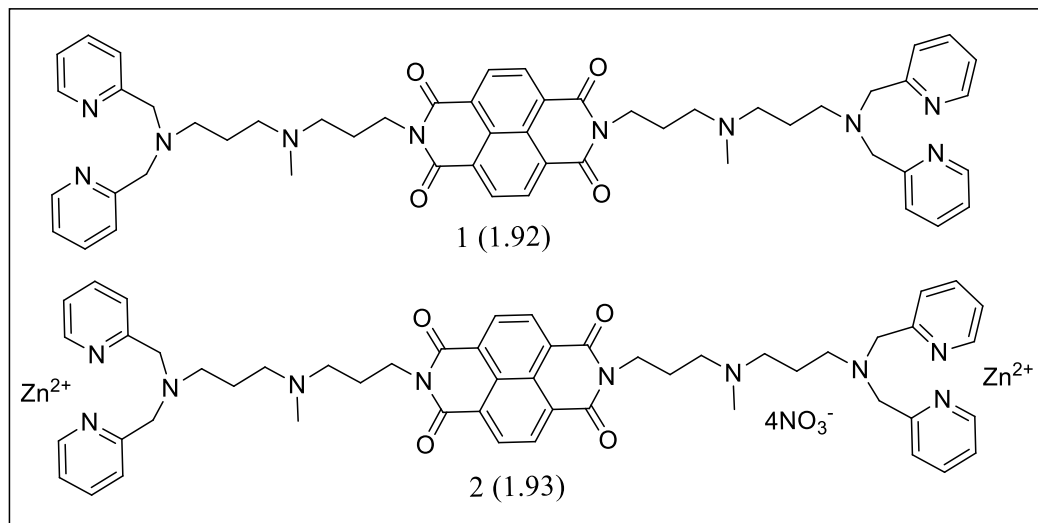


Figure 1.58: The structures of BMVC (**1.89**) and DPC derivatives (**1.90**, **1.91**) [126].

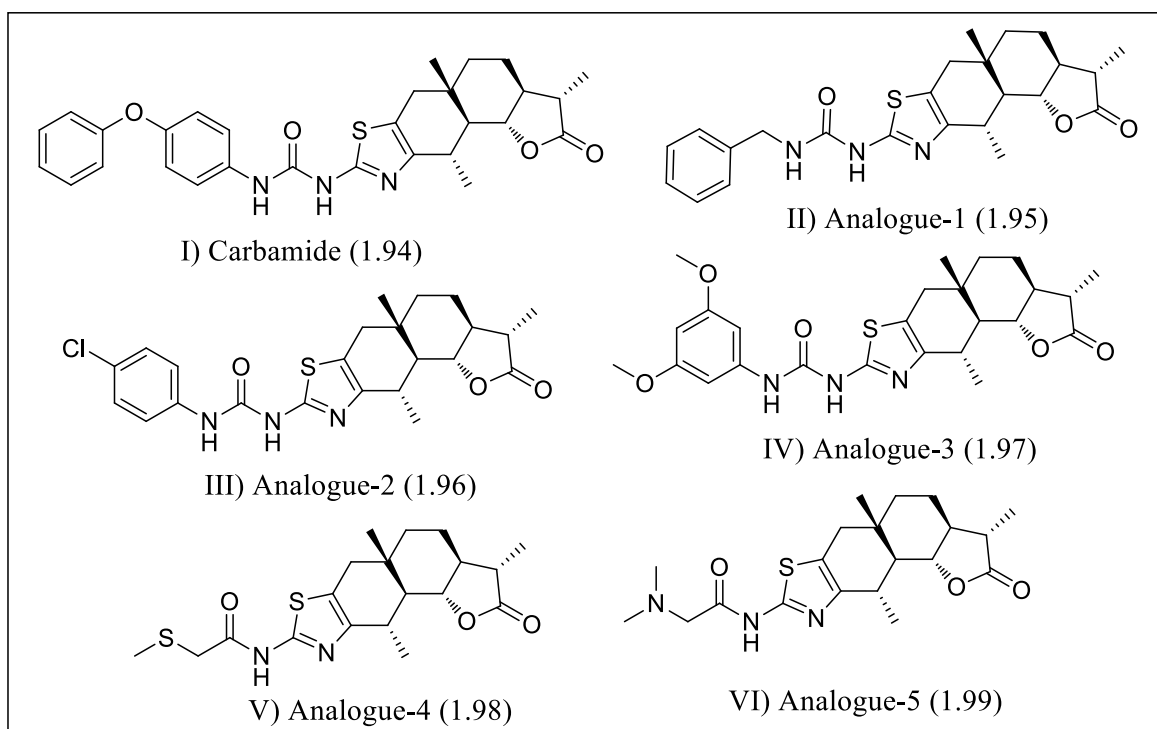
Recently two naphthalene derivatives, *N,N'*-bis[3-[3-(2,2'-dipicolyl)methylaminopropyl]-methylaminopropyl]naphthalene-1,4,5,8-tetracarboxylic acid diimide (**1**) (**1.92**) and its zinc complex (**2**) (**1.93**) have been analysed against two telomere sequences, [TAGGG(TTAGGG)₃] and [AGGG(TTAGGG)₃]. Various biophysical analyses have proven that these ligands have higher binding affinities for hybrid-type quadruplex structures formed in a K⁺ ion solution. Moreover, analogue **2** (**1.93**) showed a higher binding affinity towards the investigated oligonucleotides over compound **1** (**1.92**), suggesting that the Zn₂⁺ complex of the naphthalenediimide derivative facilitated additional electrostatic or coordination interactions between positively charged zinc ions and the negatively charged G4 DNA [199].

High-throughput virtual screening has been used recently to identify the natural product carbamide (**1.94**), which stabilized the *c-myc* G-quadruplex. This compound contains the sesquiterpene lactone skeleton, where a diphenyl ether unit and a tetracyclic moiety are linked through urea moieties. These classes of molecules were known for their anti-inflammatory activity, but biological analysis of the carbamide against the *c-myc* G-quadruplex showed transcriptional inhibition of the *c-myc* gene by inhibiting the Taq polymerase-mediated DNA extension and stabilizing the *c-myc* promoter G-quadruplex activity. Some other analogues (analogues 1- 5) (**1.95-1.99**) were designed and synthesized to establish the SAR of the molecule. Analogues 1 (**1.95**) and 3 (**1.97**) showed moderate activity, whereas analogue 2 (**1.96**) showed lower activity compared with carbamide.

Furthermore, analogues 4 (**1.98**) and 5 (**1.99**) showed no activity against the *c-myc* G-quadruplex [200].



a) Naphthalenediimide derivative



b) Carbamide and its analogues

Figure 1.59: The structure of a) Naphthalenediimide derivative, b) Carbamide (**1.94**) and its analogues [199, 200].

The new Ru(II) complex $[Ru(bpy)_2L](ClO_4)_2$ ($bpy = 2,2'$ -bipyridine, $L = 1,10$ -phenanthrolineselenazole) (**1.100**) was reported to bind selectively and change the steric

configuration of the G-quadruplex DNA of the 5'-AG₃(T₂AG₃)₃-3' sequence. Furthermore, this complex was found to inhibit telomerase by stabilizing the quadruplex by 11 °C [201].

Rahman and co-workers have reported, for the first time, the quadruplex binding and stabilizing ability of a prenylated dioxopiperazine alkaloid, Cristatin A (1a/b) (**1.101**, **1.102**). This molecule, previously known as an immunosuppressive agent, represents a novel series of G-quadruplex binding ligands and stabilized human telomeric G-quartet with ~10 times more selectivity than the duplex DNA. Moreover, it has the capability to differentiate between various G-4 structures. More importantly, this molecule contains more drug-like features compared with previously reported compounds, and represents a new scaffold for further exploration [202].

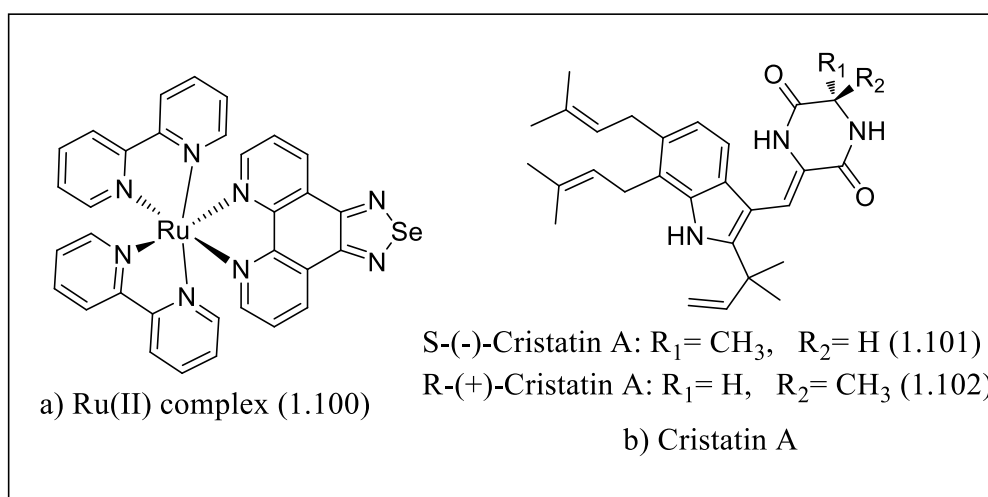
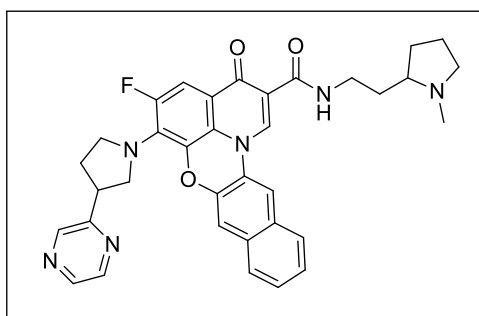


Figure 1.60: Structure of a) Ru(II) complex (**1.100**), b) Cristatin A (**1.101**, **1.102**) [201, 202].

The G-quadruplex binding capability and selectivity for the quadruplexes over duplex DNA is insufficient for the ligands to be therapeutically effective. The ligand needs to have the ability to discriminate between different quadruplex structures and should bind to one topology in the presence of others, which might be very challenging, as there are very few recognition points for discriminating between different G-quadruplex structures. Although various target sites like loops and grooves along with the quartet structure were considered before developing ligands, very few successes have been achieved till now [203].

1.15.4.1 Quarfloxin

Laurence Hurley and his group designed quarfloxin (**1.103**) (**Figure 1.61**) from the G-quadruplex-interactive fluoroquinolones and it is the first drug currently in Phase II clinical trials for treating neuroendocrine tumours as a single agent therapy. Quarfloxin (**1.103**), because of its wide therapeutic window and *in vivo* efficacy against a wide variety of tumours, is going to be in additional Phase II trials [204]. Quarfloxin (**1.103**) has been found to be highly selective towards ribosomal DNA (rDNA) over duplex DNA (400-fold selectivity) and selectively enters the nucleolus in cancer cells, resulting in a low level of toxicity [205]. Moreover, quarfloxin (**1.103**) has shown higher selectivity for the quadruplexes in *c-myc* promoters than other quadruplex structures, as well as duplex or single-stranded DNA. Quarfloxin (**1.103**) lacks topoisomerase-II and -I poisoning activities and has shown potent and tumour-selective activity both *in vitro* and *in vivo*.



Quarfloxin (1.103)

Figure 1.61: The structure of Quarfloxin (**1.103**) [45].

1.16 The Aim of this Study

The overall goal of the project is to exploit the recent structural information on human telomeric DNA (in particular *c-myc* and *c-kit* quadruplexes) to guide the rational design of quadruplex-specific small molecule ligands. Based on the promising quadruplex-selectivity observed for the reported biaryl polyamides [189], the main objective is to synthesize libraries of novel ligands based on this template that have enhanced the selectivity and binding affinity for quadruplex versus duplex DNA, and selectivity for quadruplexes of different types within specific oncogene sequences, in order to gain an understanding of structure-activity relationships for molecules of this type.

The specific objectives are as follows:

- To synthesise novel G-quadruplex targeting ligands using a variety of chemical approaches.
- To evaluate the new molecules using FRET-based DNA thermal denaturation assays (including duplex competition), CD and surface plasmon resonance (Quantity binding affinities and kinetics) for determining their affinity and selectivity for a particular quadruplex, such as the parallel G-quadruplexes found within the *c-kit* and *c-myc* oncogene promoters.
- To evaluate the novel ligands for cytotoxicity in short and long term assays in tumour cell lines.
- The subsequent use of the results to compare the newly synthesized ligands with those previously synthesized to obtain structure activity relationships (SARs). SARs should contribute to a greater understanding of how small molecules of this type interact with G-quadruplex structures.

Chapter Two: Experimental techniques for the investigation of G-quadruplex/ligand interactions

2.0 Biophysical and Biological Techniques for the Investigation of G-quadruplex Ligands

2.1 Biophysical techniques

A large number of methods are available to study the interaction between natural and synthetic ligands and the G-quadruplex structures. Some of the methods are very simple, employed for analysing properties like ligand affinity and selectivity, while some others are sophisticated and complex, analysing kinetics, thermodynamics, stoichiometry and conformational data for establishing structure activity relationships. The main focus of designing quadruplex ligands is the selectivity of the ligand towards quadruplexes over duplex DNA; hence the analysing methods used should be able to detect and investigate the selectivity of the ligands for various types of quadruplex structures and other secondary structures, as well as their binding modes. Each method has its own advantages and disadvantages; therefore, to get complete information about G-quadruplex/ligand interactions, more than one method is usually used. Here, some of the common methods are discussed.

2.1.1 Optical spectroscopic methods

Optical spectroscopic methods were used for recognizing double-stranded DNA previously, but, at present, these methods have been adapted for analysing quadruplex nucleic acids. Among other methods, C (UV-Vis), circular dichroism (CD) and fluorescence spectroscopy are preferred, as these methods are rapid, need small sample amounts and are non-destructive, as well as these instruments being routinely available in laboratories. Generally, melting temperatures are measured, which provides information about the stabilization or destabilization of the quadruplex structure by the ligand under investigation. Besides, these methods also provide useful information about the quadruplex DNA/ligand interactions.

2.1.1.1 UV-visible (UV-Vis) Spectroscopy

The UV-visible (UV-Vis) spectroscopic method is probably the simplest and the most commonly used method to obtain information about the stability of the G-quadruplex structure and its interaction with the ligands.

Generally, ligands show an absorption band that can be clearly observed in the visible range. Therefore, by analysing the shift of position of the maxima for this band for the unbound and bound ligand in solution, it is possible to investigate the interaction of the ligand with the DNA, and the magnitude of this shifting gives an idea about the strength of the interaction. Similar analysis can be performed with quadruplex/ligand interactions. Additionally, with the qualitative information, quantitative information such as stoichiometries and binding constants can be determined by performing titration of the DNA with the ligands and *vice versa*. There are various examples (**Figure 2.1**) which utilize this method to study quadruplex/ligand interactions [206].

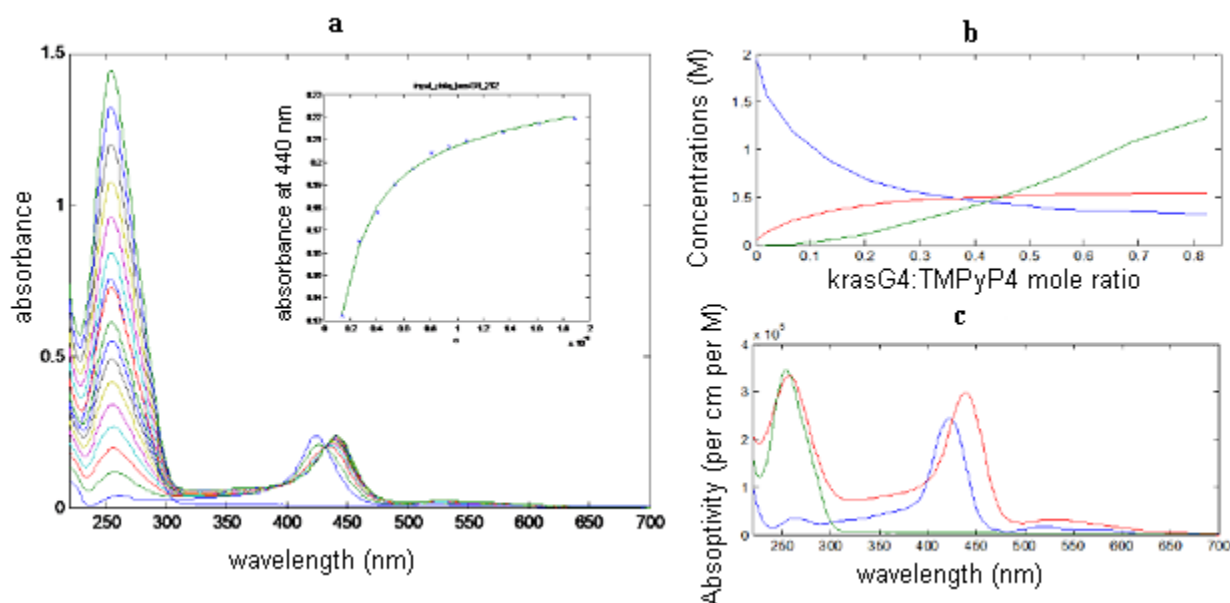


Figure 2.1: An example of the titration of a ligand with a G-quadruplex structure monitored by UV-visible molecular absorption. a) Experimental data obtained upon the titration of TMPyP4 (**1.32**) porphyrin with *k-ras*, inset: fit of the experimental data to the proposed model at 445 nm, b) distribution diagram and c) spectra of the recovered species using multivariate analysis [206].

Thermodynamic parameters of the G-quadruplex/ligand interactions can be calculated from UV-monitored melting experiments where the melting temperature and the thermodynamic parameters are determined from the change in absorbance as a function of temperature. Due to π -stacking of the bases in duplex DNA, the UV absorption of nucleic acid is usually greatly reduced from 260 nm, which is again recovered upon thermal denaturation. This simple denaturation experiment by heating is commonly performed to investigate the stabilization and destabilization of double-stranded DNA by the ligands. This same method can be used for quadruplex DNA, but the absorbance is measured at 295 nm instead of 265 nm, where it shows maximum absorbance. At this wavelength, the transition is inverted compared with the classical duplex melting profile. This is a simple method, since sample preparation is easy and requires small sample amounts. The association of ligands with the G-quadruplex structure increases the melting temperature, and G-quartet dissociation leads to a decrease in absorbance [28]. UV spectroscopy has been used for the kinetic investigation of various G-quadruplex structures and the binding of ligands to G-quadruplex structures.

2.1.2 Circular Dichroism (CD) Spectroscopy

The CD spectroscopy method has become one of the most essential techniques for studying the G-quadruplex structure and G-quadruplex/ligand interactions. It measures the conformational changes in the DNA structure that are induced by modification of the environment, such as temperature, the nature and/or concentration of counterions, pH or the addition of crowding agents, in addition to chemical modifications. Titrations of quadruplexes with the quadruplex-binding ligands induce changes in the conformation of the quadruplex structure, which can be correlated with the characteristics of the ligands under investigation.

CD measures the differences in the way that a sample interacts with the left handed and right handed polarised light. Chiral molecules act differently with the left handed and right handed polarised light, leading to a change in the absorbance spectrum. The conformation of the quadruplex structures can be roughly determined from the position and magnitude of CD bands by comparison with those of known structures in solution. A positive band in the CD

spectrum at 260 nm is assigned to a parallel quadruplex structure, such as the four stranded intermolecular quadruplexes formed by the sequence d(TTGGGGT), while a positive band at 290 nm and a negative band at 260 nm is considered for antiparallel conformation, which was formed by dimers of the thrombin binding aptamer sequence d(GGTTGGTGTGGTTGG) or d(GGGGTTTTGGGG) [207]. These reference sequences were assessed by CD by Bolton and co-workers in 2007 [207], and the results are shown in **Figure 2.2**.

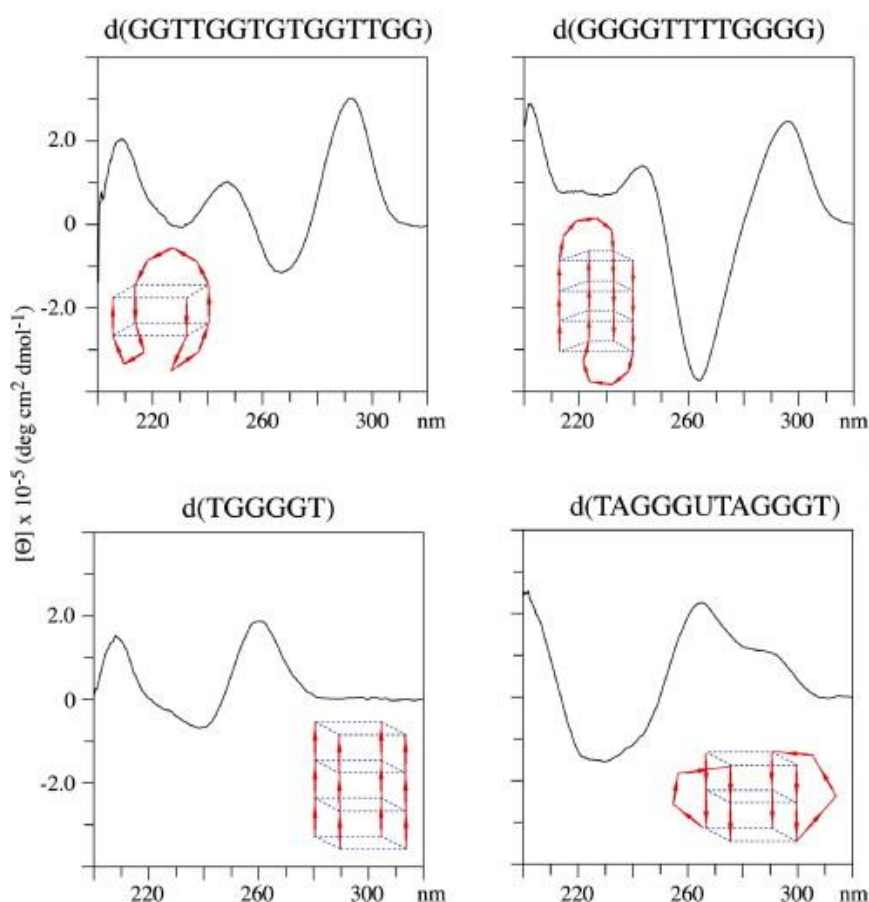


Figure 2.2: The CD spectra of the four reference quadruplex DNAs [207].

CD spectroscopy can be used for monitoring the thermal unfolding of the quadruplex structures by plotting the measured ellipticity at the wavelength corresponding to the maximum of a positive band (around 260 nm for parallel structures or 288 nm for antiparallel structures) versus temperature [206]. Furthermore, CD can be used to study the G-quadruplex/ligand interactions, as well as binding sites that are present on the ligands [208].

2.1.3 Molecular Fluorescence

Other than molecular absorption and CD spectroscopy, molecular fluorescence is probably one of the most commonly used techniques for studying G-quadruplex/ligand interactions. This technique is highly sensitive, has a wide concentration range and is more selective than the other methods. For studying G-quadruplex/ligand interactions, several approaches of molecular fluorescence are used.

2.1.3.1 Fluorescence Spectroscopy

The fluorescence spectroscopic method is used to study the folding pattern of the quadruplex structures. In this dye–quencher pairings method (**Figure 2.3**), synthetic oligonucleotides containing a fluorophore dye, such as fluorescein at one end and a fluorescence quencher like dabcyI or methyl red at the other end, are used. Folding of the oligonucleotide in a preferred configuration brings the dye and quencher group close to each other, resulting in quenching of the fluorescence. Separation of the groups, due to the melting of the oligonucleotide at increased temperatures, increases the fluorescence signal. This technique is routinely used to compare the stability of different DNA quadruplexes [209].

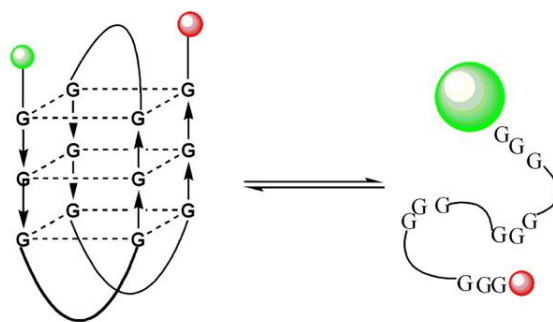


Figure 2.3: A typical fluorescence melting profile. Schematic representation of the melting of a quadruplex-forming oligonucleotide that has been labelled with a fluorophore (green) and quencher (red) [209].

2.1.3.2 Fluorescence Resonance Energy Transfer (FRET) assay

Fluorescence Resonance Energy Transfer (or FRET) is a physical phenomenon first described over 50 years ago and is widely used today in biomedical research and drug discovery. FRET is dependent on the transfer of energy from a donor molecule to an acceptor molecule in a non-radioactive way, which is based on the distance between the donor and acceptor. As it is sensitive to distance, FRET has been used to investigate molecular interactions. The donor molecule is the dye or chromophore that initially absorbs the energy; the acceptor is the chromophore to which the energy is subsequently transferred. This resonance interaction occurs over greater than interatomic distances, without conversion to thermal energy, and without any molecular collision. The transfer of energy leads to a reduction in the donor's fluorescence intensity and excited state lifetime, and an increase in the acceptor's emission intensity. A pair of molecules that interact in such a manner that FRET occurs is often referred to as a donor/acceptor pair.

For efficient FRET to occur, the donor and acceptor molecules must be in close proximity to one another and typically in a 10-100Å range, as well as the condition that the absorption or excitation spectrum of the acceptor must overlap with the fluorescence emission spectrum of the donor (**Figure 2.4 b**). The degree to which they overlap is referred to as the spectral overlap integral (J). The donor and acceptor transition dipole orientations must be approximately parallel. If the donor-acceptor pairs are compatible, the most critical element necessary for FRET to occur is the close proximity of the pairs. Förster demonstrated that the efficiency of the process (E) depends on the inverse sixth-distance between the donor and acceptor (**Equation 2.1**) [210].

$$E = R_o^6 / (R_o^6 + r^6) \quad \begin{array}{l} R_o = \text{Förster distance} \\ r = \text{Actual distance between donor and acceptor} \end{array}$$

Equation 2.1: Equation for FRET efficiency.

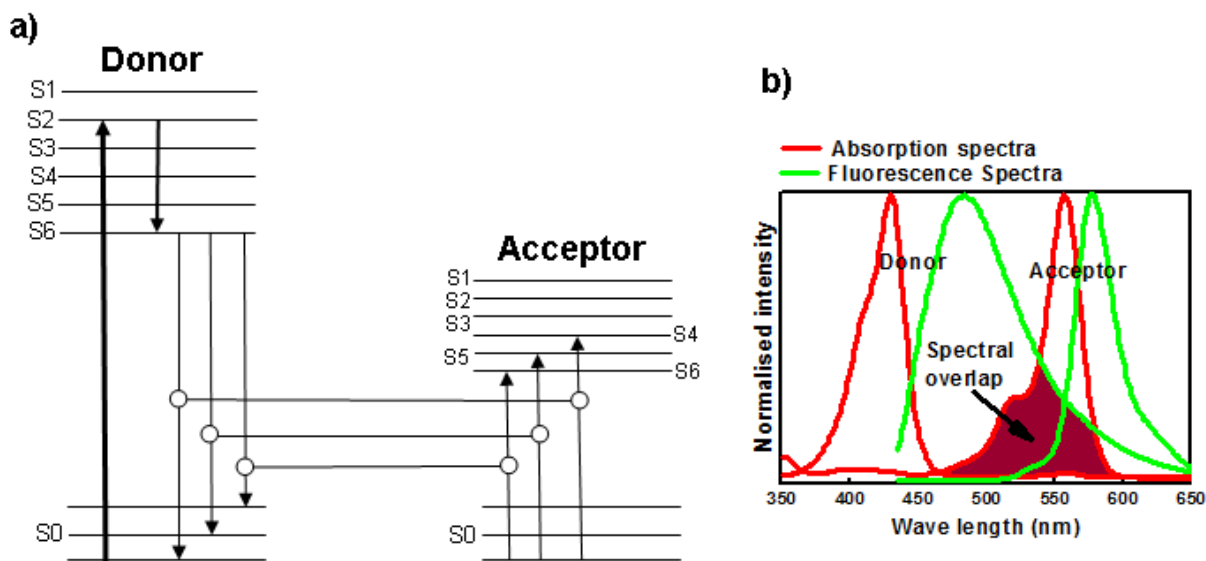


Figure 2.4: a) Jablonski diagram illustrating the FRET process, b) Absorption and fluorescence spectra of an ideal donor-acceptor pair. The brown coloured region is the spectral overlap between the fluorescence spectrum of donor and the absorption spectrum of the acceptor.

Usually, the donor and acceptor molecules are different, and either by the appearance of acceptor fluorescence or by quenching of fluorescence of the donor can FRET be detected. A fluorescent molecule is always chosen as the donor moiety. With appropriate excitation, electrons from the donor moiety jump from the ground state (S_0) to a higher vibrational level and within picoseconds these electrons come back to the lowest vibrational levels (S_1), which eventually decay back to the ground state (S_0) by emitting a photon of light. When conditions for FRET to occur are met, decay as donor fluorescence and energy transfer to the acceptor will compete for the decay of excitation energy. With resonance energy transfer, the energy (rather than the photon) is transferred to the acceptor molecule, whose electrons in turn become excited, as described for the donor molecule. The subsequent return to the ground state emits a photon (**Figure 2.4 a**).

The ‘FRET melting assay’ utilizes this basic principle where the increase in temperature leads to the denaturing or melting of the macromolecule, causing the distance between the

probes to increase, leading to an increase in fluorescent energy. The technique has been found to be very useful to investigate various types of nucleic acid structures [211]; however, availability of suitable labelled substrates limits its use in biological systems. However, this is not a problem for studying quadruplex DNA stability, as synthetic DNA is usually used for all analysis relating to G-quadruplex formation and labelled oligonucleotides can be obtained easily [209].

Mergny and co-workers first used this FRET technique in 2001 for investigating the G-quartet structures [212]. A synthetic oligonucleotide containing a FRET pair on both the 5' and 3' end of a suitable Förster diameter was used, which, upon folding, brought the donor and acceptor moieties close to each other for efficient FRET to occur (**Figure 2.5 a**). Sometimes, energy can be transferred to the acceptor from the donor by collision due to the close proximity of the moieties, resulting from the generation of a G-quadruplex structure [209]. The unfolding of the oligonucleotide results in a loss of FRET, as the donor-acceptor pair is too far apart to transfer any energy (**Figure 2.5 b**). The melting of G-quadruplex-ligand structure can be monitored by carefully choosing the pair so that they provide different fluorescence absorbance/emission spectra for folded and unfolded structures.

To conduct the FRET melting assay in our research, we selected the fluorescent dye 'fluorescein' (FAM, **2.1**) at the 5' end as donor and 'tetramethylrhodamine' (TAMRA, **2.2**) (**Figure 2.6**) at the 3' end as an acceptor dye and a single stranded guanine rich nucleotide chain containing 21-bases as our quadruplex-forming oligonucleotide (QFO). Using the FRET system distance between the donor (FAM, **2.1**) and the acceptor (TAMRA, **2.2**), moieties can be measured in terms of the fluorescence of the donor (FAM, **2.1**). At low temperatures, the oligonucleotide is folded to form a quadruplex structure, which brings the probes within the Förster radius (R_0), resulting in the quenching of the emission radiation of FAM (**2.1**) by TAMRA (**2.2**). An increase in temperature toward the melting point of the oligonucleotide leads to the unfolding of the oligonucleotide, causing the fluorophores to be separated sufficiently for the FRET efficiency to be significantly diminished (**Figure 2.5 b**). Stabilization of the quadruplex structure upon addition of the ligand results in an increase in the melting temperature of the ligand-bound oligonucleotide. The magnitude of the change in

melting temperature gives an idea about the binding efficiency of the ligand to the quadruplex structure.

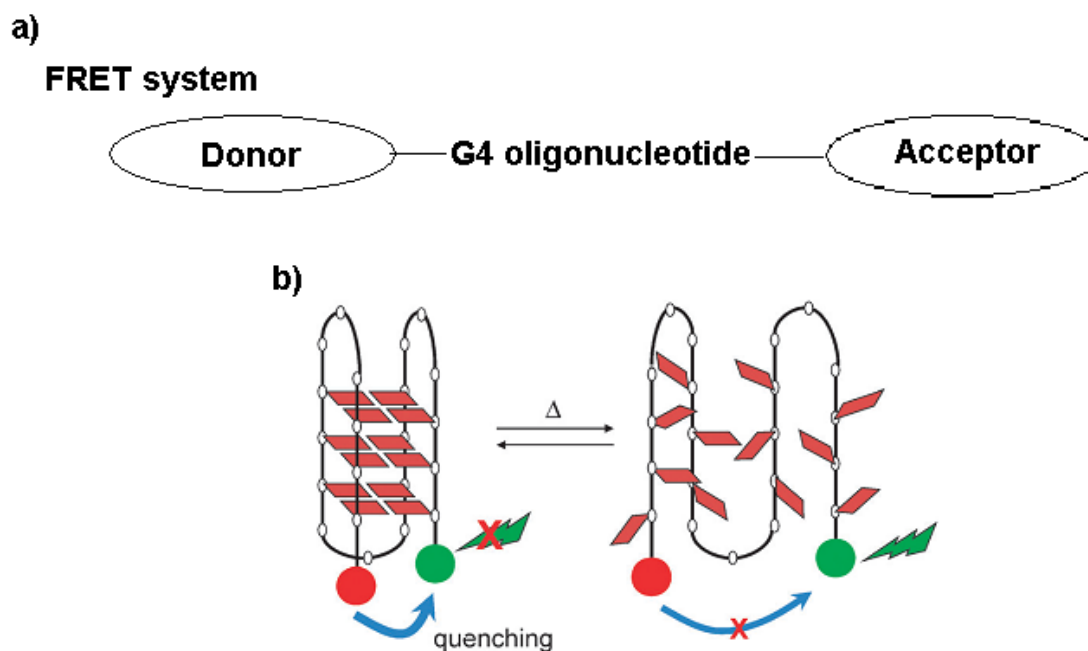


Figure 2.5: a) The structure of the dual probe labelled QFO, b) Schematic representation of FRET-based melting temperature experiments [28].

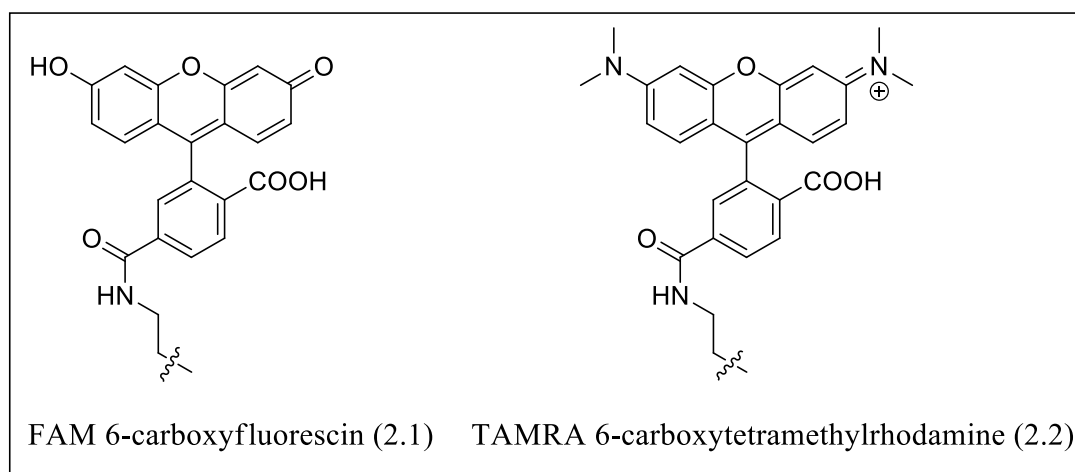


Figure 2.6: The structure of FAM (2.1) and TAMARA (2.2).

The FRET technique allows analysis to be conducted in a variety of ionic conditions; it is a simple, rapid, convenient and cost-effective method and can easily be adapted for 96-well plate high-throughput screening. For this reason, it has been adopted by various groups, and a

large number of molecules with diverse structural features have been screened by using this technique. However, this method has some disadvantages. Sometimes, it can give false positives due to the quenching of the donor emission by the planer chromophore present in the ligands, and sometimes it can produce false negatives because of the folding of the QFO with the ligands in such a way that the distance between the donor and acceptor prevent efficient FRET to occur. To avoid the problem of false positives, the absorbance for the ligands should be checked beforehand, to make sure that they do not absorb at the same wavelength as the acceptor. The DNA bases, especially guanine, can also cause the quenching of the donor emission; hence, it should be separated from the donor moiety.

Competitive FRET-melting Assay

The selectivity of the ligands towards a G-quadruplex structure is considered as an important point during designing G-quadruplex-interactive agents, and can be determined by using FRET melting experiments where duplex, triplex and other quadruplex-forming sequences can be used as a competitor (**Figure 2.7**). Every compound should be tested against one or more suitable competitors, as the duplex and other competitor sequences are present in extremely high concentrations compared with G-quadruplex-forming sequences in the biological media. Hence, G-quadruplex-interactive ligands have to be highly selective in order to interact with particular quadruplex structures in an environment rich in duplexes and other competitors. The competitive FRET melting assay is thus an effective and efficient method for assessing the selectivity of ligands with a wide variety of duplex sequences.

Competitors that can trap a drug lower the stabilization potential of the quadruplex. The drug should be challenged by a number of competitors that should follow the criteria stated below:

- The competitor should have no effect on the melting temperature of the labelled oligonucleotide in the absence of the quadruplex-interactive ligands. The competitor should not be complementary to the oligonucleotide (at least, not of the fluorescent part).

- The competitor's stability should be significantly higher than that of the fluorescent quadruplex under the experimental conditions. If it melts before the quadruplex structure, the unfolded, single-stranded competitor will no longer be able to bear its binding capability [213].

Calf thymus DNA (CTDNA) is DNA that contains a wide variety of oligonucleotides of various lengths. Because of this, it is a good competitor DNA, allowing competition from a variety of sequences, creating a more accurate simulation of the *in vivo* conditions. The melting temperature measured by UV was found to be 81 °C and preliminary FRET control experiments showed no effect on the melting temperature of the labelled G-quadruplex DNA.

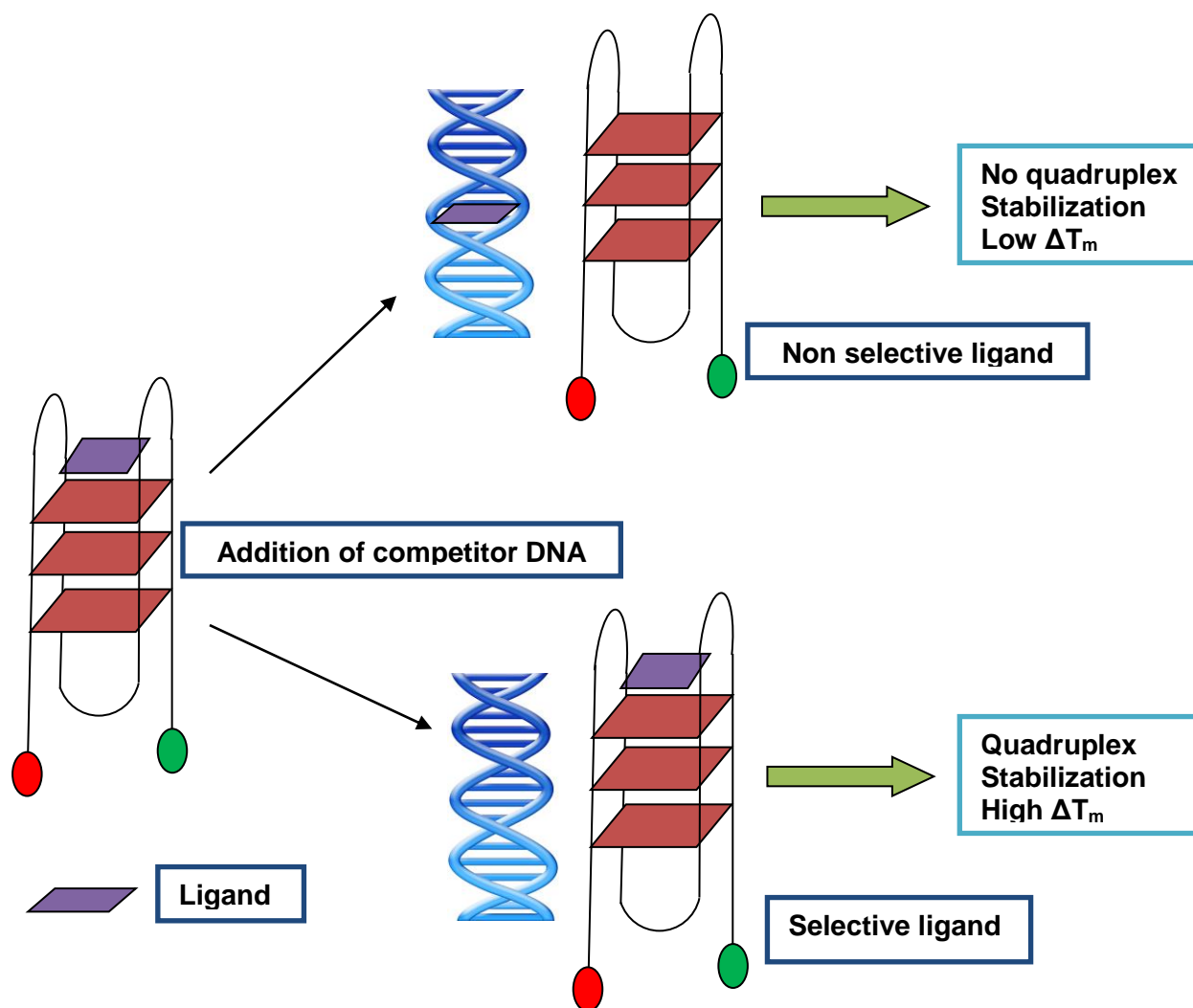


Figure 2.7: Competitive FRET assay. The addition of competitor to a selective ligand/G-quadruplex will result in no change in ΔT_m . The addition of competitor to a non-selective ligand/G-quadruplex will result in the transfer of the ligand to the competitor sequence and thus lowering the stabilization of the G-quadruplex and decreasing the ΔT_m .

2.1.3.3 Fluorescent Intercalator Displacement (FID) Assay

Rapid and automated methods were needed to be developed for screening and comparing the properties of the huge number of emerging G-quadruplex-interactive ligands over the last few years. In 2006 Monchaud and his group developed the fluorescent intercalator displacement assay (G4-FID) for investigating the binding affinity and selectivity of G-quadruplex binding ligands, which is based on the displacement of thiazole orange (TO, **2.4**) from the quadruplex-forming sequence by the ligands (**Figure 2.8**) [214]. Before that, FID was

routinely used to investigate the binding affinity, sequence selectivity and binding stoichiometry for duplex DNA binding agents [215]. This method is dependent on the change in fluorescence of the intercalating agents, such as ethidium bromide (**2.3**) or thiazole orange (**2.4**) (**Figure 2.9**), when bound to DNA. On binding to DNA, the fluorescence property of the intercalator agent is enhanced, which is then decreased when it is displaced by a DNA binding ligand. The same principle is used for the assay of G-quadruplex/ligand interactions, where the change in fluorescence of the thiazole orange (**2.4**) is measured upon the addition of G-quadruplex-binding ligands. The technique is non-destructive, simple, fast and can be carried out with a small sample amount. Adaptation to a 96-well format is possible, allowing the technique to be cost effective.

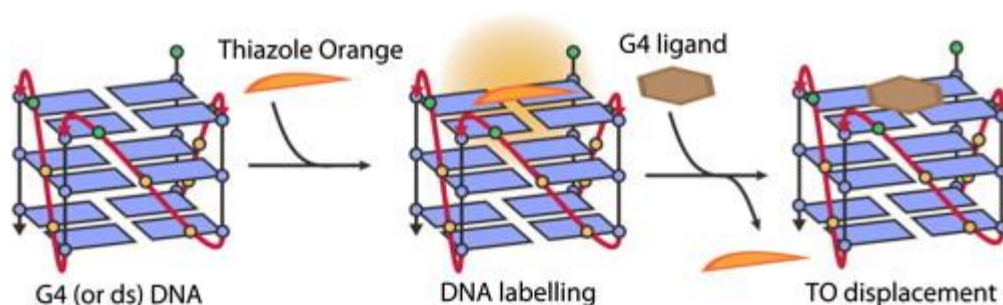


Figure 2.8: Schematic representation of the two main steps of the G4-FID assay, i.e., (a) labelling of the DNA matrices (quadruplex or duplex DNA) by Thiazole Orange (TO) (**2.4**) and (b) displacing the fluorescent probe from the DNA matrices by a small molecule candidate [216].

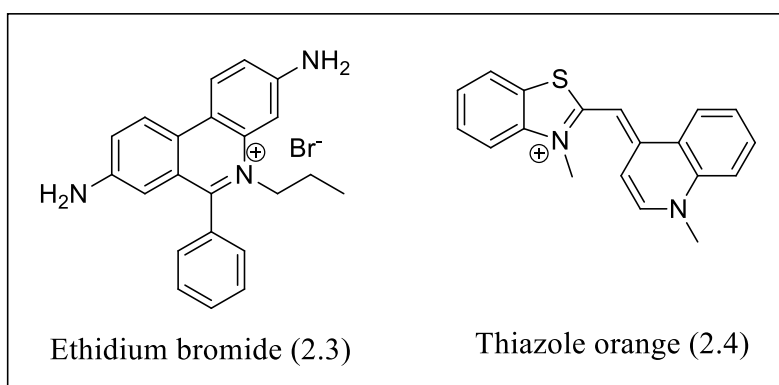


Figure 2.9: The structure of ethidium bromide (**2.3**) and thiazole orange (**2.4**).

Several assumptions must be appropriately considered during the use of the FID technique. One important assumption involves the binding sites; it is assumed that the ligand and TO (2.4) will bind at the same site, and thus the ligand displaces TO (2.4). However, it is possible that the binding site may be different for the ligand and TO (2.4) and the ligand will not displace TO (2.4). The stoichiometry of the ligand quadruplex is also unknown, and may be different to that of TO (2.4).

Secondly, the equilibrium and kinetics of binding of the ligand and TO (2.4) will be affected by the concentration of ligand and TO (2.4) in solution. If the concentration of TO (2.4) is kept constant every time, then it will not affect the comparison between ligands; however, it is important to check the conditions before comparing results with ligands assessed with a different TO (2.4) concentration.

2.1.4 Equilibrium Dialysis

The equilibrium dialysis method, first introduced in 1975 to investigate the interaction of small organic molecules with double stranded DNA [217], has been adapted to study ligand recognition by triplex and quadruplex nucleic acids [218]. This is a simple method used to investigate ligand binding and determine preferential nucleic acid confirmations for nucleic acid recognition. Dialysis is a physical process involving the diffusion of one or more solutes through a semi-permeable membrane - the flow of molecules will depend on the relationship between their size and the membrane pore size. In this process, nucleic acids of different confirmations are placed in dialysis tubes that permit the diffusion of small organic molecules while still retaining the nucleic acids. These tubes are emerged in a solution containing the drug solution and the ligands are allowed to pass through the semi-permeable membrane of the dialysis tube (**Figure 2.10**). Thus, some ligands will interact with the oligonucleotides, while the others will remain free in the solution. At equilibrium conditions, the concentration of free ligands will be the same in both compartments, although the ligand concentration will be higher in the oligonucleotide-containing chamber as it contains ligand both in bound and unbound form and will be dependent on the affinity of the ligand toward various types of oligonucleotides present in the dialysis tubes. Measurement of the concentration of the

unbound ligand and the bound ligand in both chambers allows the investigation of equilibrium-binding constants and ligand sequence selectivity. As, in this test, the ligand is in close contact with either various sequences of nucleic acids or various forms of quadruplex structures, the concentration of the ligand may vary in the dialysis chamber depending on the sequence affinity of the ligand.

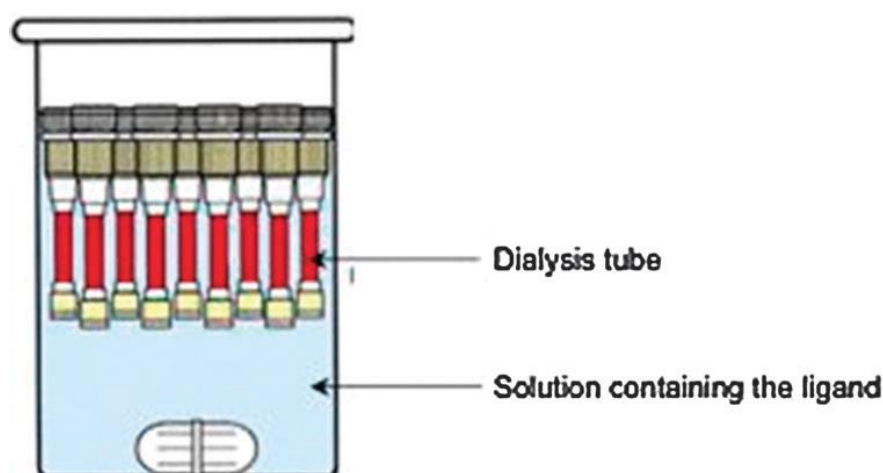


Figure 2.10: Experimental device used for equilibrium dialysis [28].

2.1.5 Mass Spectrometry

Mass spectroscopy has been adopted to study the interactions between nucleic acids and ligands. Although there are several mass spectroscopic techniques available, the electrospray ionization (ESI) technique is used widely because of its soft ionization [206, 219]. In ESI techniques, the mass of both the G-quadruplex and the G-quadruplex/ligand complex can be determined easily, since the non-covalent bond between the ligand and the quadruplex remains unchanged, due to minimum fragmentation when the biomolecules are sprayed to the mass spectrometer [219]. In the ESI-MS technique, the sample is transferred in the gaseous phase, but the qualitative result is similar to that in solution. Here, the MS gives individual signals for each different species with different masses detected and is a very straightforward method for determining the stoichiometry of the complexes. The ESI-MS technique can be used to obtain the number of DNA strands involved, the number of bound cations (if present) and the number of bound ligands.

2.1.6 Quantitative Analysis of Binding Events

Thermodynamic and kinetic parameters are very important for understanding the driving force for ligand/quadruplex complex formation. Isothermal titration calorimetry (ITC) and surface plasmon resonance (SPR) have been found to be useful in recent years to investigate these parameters of quadruplex/ligand interactions.

2.1.6.1 Isothermal Titration Calorimetry (ITC)

Isothermal titration calorimetry (ITC) is a biophysical method used to measure thermodynamic parameters directly, including the binding affinity constant (K_A), changes in enthalpy (ΔH), and entropy (ΔS), as well as the binding stoichiometry between the ligands and the G-quadruplex structure in solution [220]. Previously, the ITC technique was used for studying duplex DNA/ligand interactions [221], but recently it has been used for quadruplex/ligand interactions [222]. From measurements of small changes in temperature, Gibbs energy changes (ΔG) and entropy changes (ΔS) can be calculated according to the equation 2.2:

$$\Delta G = -RT \ln K = \Delta H - T \Delta S$$

ΔG = Gibbs energy change
 R = Gas constant
 T = Absolute temperature
 ΔH = Enthalpy change
 ΔS = Entropy change

Equation 2.2: Equation for calculating Gibbs energy changes.

In order to determine these thermodynamic parameters, the ligands are usually titrated into the oligonucleotide solution and the heat response is recorded. These heat values are usually corrected for the heat of ligand dilution. The representation of the heat values as a function of the molar ratio between the ligand and the G-quadruplex is known as the binding isotherm. Finally, fitting the binding isotherms to the proposed model allows the thermodynamic parameters to be obtained [206].

This method is fast and highly informative, without the need of any chemical tag or having to immobilize the DNA or ligands, and can be controlled entirely by computer. However, a large amount of DNA and ligands are required, and it is not possible to adapt this into a high throughput setup.

2.1.6.2 Surface Plasmon Resonance (SPR)

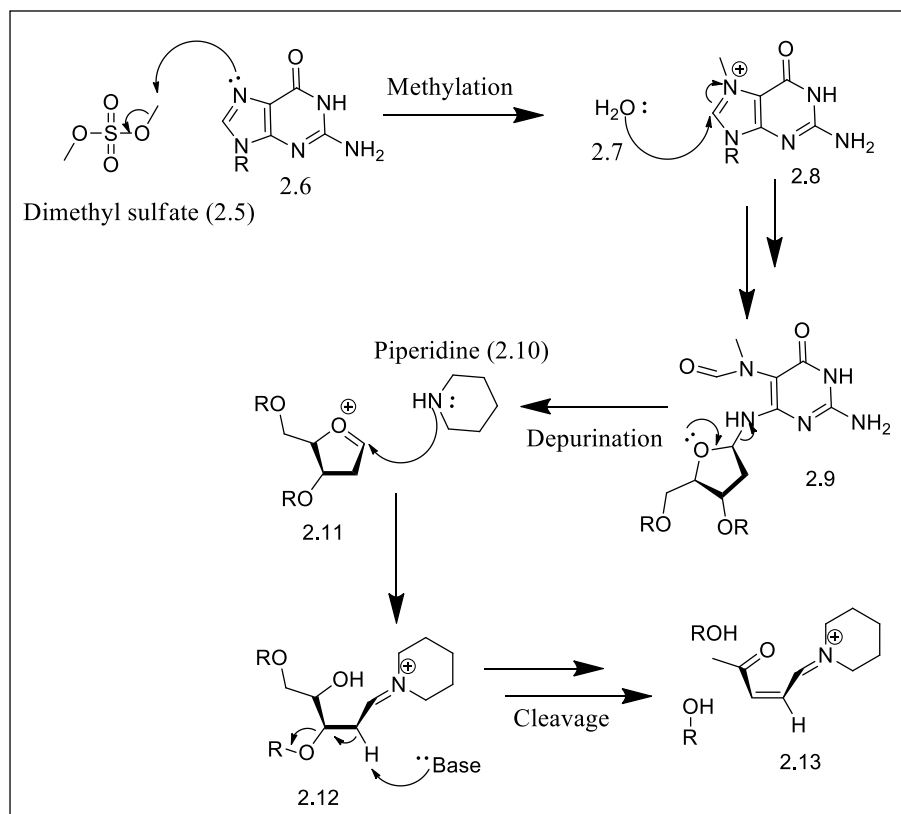
The surface plasmon resonance (SPR) technique provides quantitative information about the affinity between the ligand and the DNA, and can be used to determine the stoichiometry, strength and kinetics of the interactions [223, 224]. SPR is an optical technique utilising the reduction in intensity of circular polarized light that is reflected from the surface of a thin metal film-coated glass prism. Surface plasmons of the metal are excited by the minima in a reflected light density occurring at a specific angle. The created evanescent electromagnetic field spreads from the surface into the surrounding medium for a short distance (~200 nm). The angle at which the resonance occurs becomes a function of the refractive index of the medium in the vicinity of the surface. By recording the variation in value of this angle, the SPR can detect interactions involving free species in solution and one that is covalently bound to the surface [28].

In order to study the binding interactions of small organic molecules with proteins, different types of quadruplex-forming oligonucleotides have been immobilized on the surface of the sensor chips where the sequence of the oligonucleotides depends on the purpose of the study. Usually, intramolecular quadruplexes are used for the study, since the intermolecular quadruplexes dissociate during the regeneration step. Various ways such as forming amide, disulfide or thioether bonds are used to attach oligonucleotides covalently onto the surface. In most of the studies, biotin-functionalized oligonucleotides are applied for attachment onto streptavidin-coated surfaces. This prevents the non-specific binding of ligands with streptavidin, resulting in a more rapid and effective method for SPR studies. The SPR technique is however still challenging for a number of reasons:

- SPR sensors predominantly require aqueous solvents, which becomes problematic for the solubility of the aromatic G-quadruplex-binding compounds used in the study.
- The non-specific binding of the compounds to sensor chips is another problem.
- Ligands can bind on the surface of the plastic parts of the instrument, resulting in fewer ligands reaching the surface [225].

2.1.7 Dimethylsulphate (DMS) Footprinting

Dimethylsulphate (DMS) footprinting is one of the earliest methods used to determine particular features of the quadruplex, which was part of the Maxam and Gilbert protocol for DNA sequencing. The methylation of the N₇ position of guanine by DMS (**2.5**) leads to facile depurination (**Scheme 2.1**). The addition of piperidine (**2.10**) to the solution leads to cleavage at the now abasic site, and gel electrophoresis allows the visualization of the length of the cleaved fragments, resulting in a ladder with peaks corresponding to every guanine in a sequence. When the N₇ is hydrogen bonded, as in a G-quadruplex, it is protected from methylation, resulting in little or no cleavage at the guanines involved in the formation of the G-quadruplex [30].



Scheme 2.1: A schematic diagram of the DMS footprinting method.

2.1.8 X-Ray Diffraction and NMR Spectroscopy

All the techniques described above provide information about the recognition of a G-quadruplex structure by small organic molecules. It is possible to obtain the stabilization potential, selectivity, affinity constants, and the stoichiometry of the formed complex, but not the structural information. Structural information can be very important to investigate the process involved in recognition of G-quadruplex structures by small organic molecules at the molecular level, and these data can be utilized for the further improvement of the existing ligands. The X-Ray diffraction and NMR spectroscopy techniques provide structural information about the interactions of ligands with the G-quadruplex, and various reports have been published providing the structural information of a number of G-quadruplex/ligand interactions.

Table 2.1: An example of some solved structures of complexes formed between quadruplexes and small organic molecules [28].

Ligand	Method	G-quadruplex sequence	PDB
BRACO19	X Ray	d[TAGGGTTAGGGT] ₂	3CE5
Distamycin A	NMR	d[TGGGGT] ₄	2JT7
TMPyP4	X-Ray	d[TAGGGTTAGGG] ₂	2HR
TMPyP4	NMR	d(TGAGGGTGGIGAGGGTGGGGAAGG)	2A5R
RHPS4	NMR	d[TTAGGGT] ₄	1NZM

2.1.8.1 X-Ray Diffraction Spectroscopy

X-Ray crystallography provides information at the atomic level during structure determination and is able to identify various topologies of the quadruplex structure. A solid crystal structure is formed from the complex formed between the ligand and the quadruplex structure, and thus reflects the state of matter in a condensed state. Analysis of the crystal structures of quadruplex and quadruplex/ligand complex provide information about the binding site and the mode of interaction of the ligand with the quadruplex [148]. Moreover, visualization of hydrogen bonds involved in the stabilization of the complexes is possible with X-ray crystallography. X-Ray crystallography has been widely used to design rationally more quadruplex-selective drugs by modifying the chain used for the substitution of aromatic rings [226]. Furthermore, it has been used to distinguish differences between the DNA and RNA quadruplex structures and suggested that it is possible to design ligands that can discriminate between DNA and RNA quadruplexes [227].

Although X-ray crystallography is the most precise method for obtaining structural information, the process is extremely time-consuming and needs expertise. It is very difficult to grow perfect crystals, and many different conditions have to be considered before growing crystal structures. Additionally, once a crystal is obtained it is very difficult and time-consuming to mount the crystal. Furthermore, it may not be perfect. If more than one phase is present, there may be more than one set of refraction patterns, which makes analysis very

difficult. Complex and expensive machinery is also required to generate the X-rays and measure the diffraction pattern.

2.1.8.2 Nuclear Magnetic Resonance (NMR) Spectroscopy

Nuclear magnetic resonance (NMR) has become an essential tool for investigating nucleic acids that provides structural information of a complex at an atomic level. NMR provides the most complete structural data on interactions involved in the recognition process in solution and it has been successfully used to study ligand/G4 interactions. NMR is mainly used to determine the correlations between signals due to ligands and those attributable to nucleic acid, in order to determine the contact area. The use of NOESY is essential in this context [28].

For G-quadruplex structures, characteristic NMR signals have been found in regions of amino and imino protons between 8 and 13 ppm, approximately, considering a typical proton spectrum [228]. Intermolecular G-quadruplexes have shown better resolved signals in the NMR spectrum than that of an intramolecular structure. Higher-dimensional NMR techniques allow more than one species in equilibrium to be detected and determine their relative populations.

The NMR technique can be coupled with other methods to obtain more precise information about the G-quadruplex/ligand interaction. For example, by using an NMR titration experiment, the stoichiometry and binding mode of the complex can be determined [229]. Again, Trotta and collaborators coupled NMR with molecular modelling techniques to investigate the interaction of six potential quadruplex-binding ligands with a quadruplex-forming oligonucleotide [230]. Sometimes, researchers combined the use of two different NMR methods; first, the NMR titration method for identifying and confirming the G-quadruplex/ligand interaction, and secondly to calculate the structure of the complex. Several examples are available in the literature [206].

Structure determination by NMR depends on sequence-forming stable species in solution. The presence of various topologies of quadruplex structures in solution limits the use of this process [228]. The use of modified or mutated sequences of the original quadruplex that will form only a single species in solution can help to overcome this problem.

2.1.9 Molecular Modelling

2.1.9.1 Molecular Modelling to Aid NMR

NMR spectroscopy and molecular modelling are closely related. The distance restraints obtained from NOE connectivities are utilized for structure calculation and refinement, and molecular modelling is used to propose the 3D solution structure.

2.1.9.2 Stability and Thermodynamics of G-quadruplex/ligand Complexes

In order to investigate structure, dynamics, surface properties and the thermodynamics of quadruplex and quadruplex/ligand interactions, molecular modelling and molecular dynamics methods are now used routinely. These methods have been used to understand and improve the recognition of quadruplexes by small organic molecules. In order to design more selective and potent G-quadruplex binders, models have been used as a starting point. Molecular dynamic simulation studies can also be used to investigate complexes between the quadruplex and ligand in order to complement experimental data lacking atomic resolution.

In the computational studies, the first step involves the manual docking of the ligand under investigation onto a quadruplex, and it is imperative that one must carefully consider whether the chosen binding site is in agreement with known data about this ligand.

2.1.10 Polyacrylamide Gel Electrophoresis

Based on size and charge, DNA molecules can be separated by gel electrophoresis experiments by using an electric field. In an electrophoresis chamber, usually agarose or

polyacrylamide gel is placed and connected to a power source. Smaller molecules move faster than the larger molecules through the gel when an electric current is applied. In the case of the study of drug-DNA interactions, the distance moved by the free G-quadruplex structure and the bound structure may be different. By using the spectroscopic methods, such as molecular fluorescence or UV-visible absorption, the molecules, with a required previous staining step, can be detected [206].

Under strict conditions, folded motifs can be identified quickly against unfolded single-stranded DNA. With careful consideration about the speed (voltage) of the run and the stability of the quadruplex, additional analysis of possible structures can be made. Quadruplex stability can be sensitive to temperature and buffering conditions used during the experiment. The DNA can be visualized by using radioactive labels, EtBr staining or other dyes [33].

2.1.11 Sedimentation Velocity Analysis and Sedimentation Equilibrium

Buoyant density, sedimentation coefficients and the molecular weights of DNA and quadruplexes can be determined by using density gradient ultra-centrifugation. Hydrodynamic properties, such as translational diffusion, sedimentation coefficients (*S*) and correlation times of the DNA structures, can be calculated through bead modelling on atomic-level model structures. Hydrodynamic properties have been used in conjunction with the program HYDROPRO [231] to help differentiate between known or inferred structural conformations measured by analytical ultra-centrifugation.

2.1.12 Cross-Linking DNA and Topology

Adjacent guanine nucleotides have been identified successfully through the cross-linking of DNA bases by using di-functional platinum complexes, and so provide distance constraints for the construction of G-quadruplex-folded motifs [232]. Compounds suitable for cross-linking, such as *cis*- and *trans*-Pt(NH₃)₂ or *cis*- and *trans*-diamminediaquaplatinum(II), are able to link covalently the N₇ of purine bases together. If the N₇ of guanines are involved in

G-tetrad formation, they will not be able to cross-link. Adenine-containing sequences can participate in forming additional cross-linking, but efficiency will be reduced by 10 times, since they are less nucleophilic. Once the products are formed, the folded structures can be investigated by either mass spectrometry or by 3'-exonuclease digestion and subsequent analysis by gel electrophoresis.

2.1.13 Other Methods

In addition to the principal methods, there are numerous biophysical techniques available that have been used to investigate the quadruplex structures and G-quadruplex/ligand interactions. These include viscometry titrations, DNA footprinting, Raman spectrometry, nuclease sensitivity, photocrosslinking, infrared spectroscopy and high performance liquid chromatography-photodiode array (HPLC-PDA).

2.2 Biological Methods

G-quadruplex/ligand interactions have also been studied by using a number of biochemical methods. Some of these are briefly described here.

2.2.1 Polymerase Chain Reaction (PCR)

Most of the methods used for investigating G-quadruplex/ligand interactions are based on the polymerase chain reaction or PCR, and one of the most widely used methods is the PCR stop assay method, which studies the interference of ligands with polymerase activity to obtain more information about the ligand stabilization of the G-quadruplex [233]. If the quadruplex structure is stabilized by the investigated ligand, bands of paused polymerase activity near the guanine rich portion are observed on the electrophoresis assays on the PCR products, and the inhibition of polymerase activity is proportional to the intensity of the paused bands. A large number of molecules have been investigated by using this method to analyse their interaction with G-quadruplex and many reports are available [52, 198, 206, 234].

2.2.2 Telomerase Repeat Amplification Protocol (TRAP)

The telomerase repeat amplification protocol (TRAP) assay has been widely used to investigate telomerase activity in cell extracts, as well as the telomerase inhibitory property of small molecules [235, 236]. The telomerase enzyme is found to over-express in 85% of cancer cells and is rarely found in other somatic cells. Hence, the TRAP assay has been used in the detection of telomerase activity in numerous human malignancies as a diagnostic tool in the early diagnosis of malignancy, as a potential prognostic indicator and as a means to identify telomerase inhibitors [237]. The recent development of G-quadruplex ligands as potential telomerase inhibitors prompted the utilization of the TRAP assay for evaluating the efficacy of the G-quadruplex/ligand complex against telomerase activity.

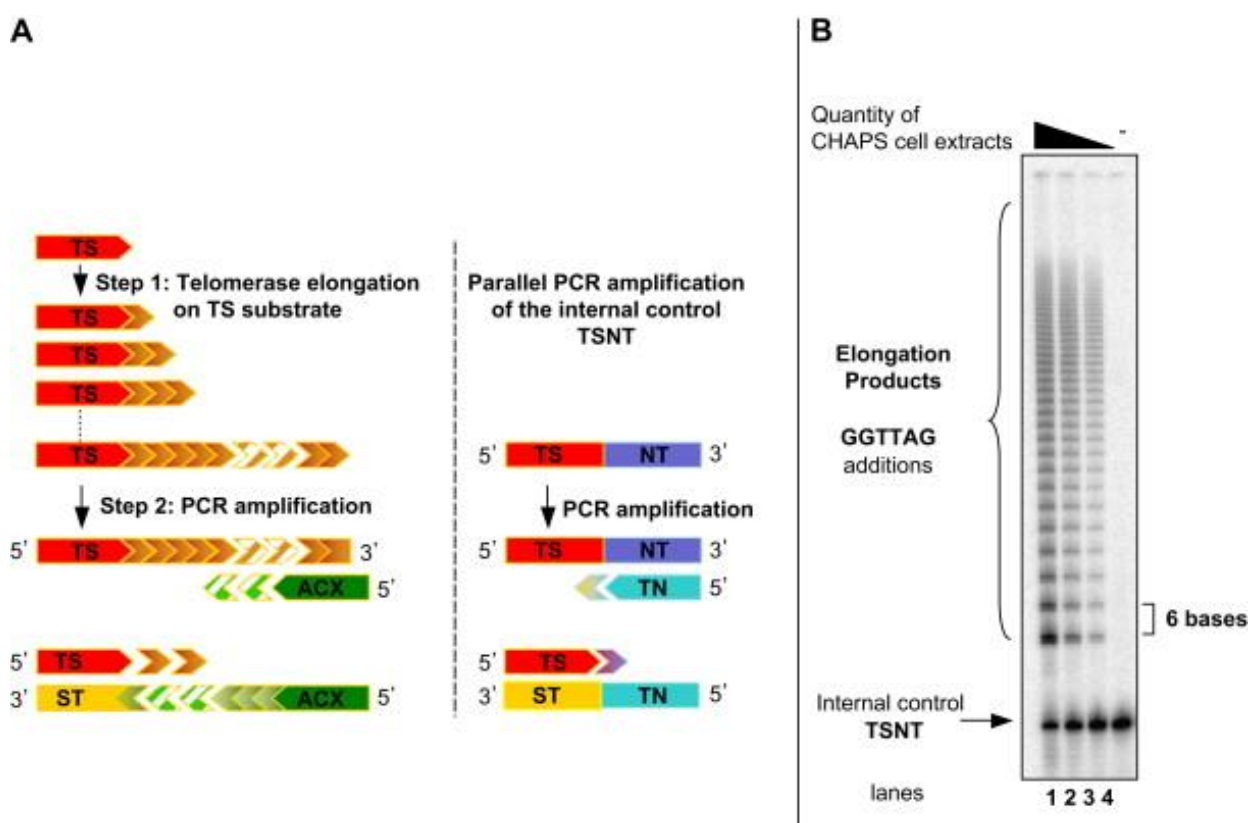


Figure 2.11: The steps of the Telomeric Repeat Amplification Protocol (TRAP) assay [238]

The *in vitro* TRAP assay uses a telomeric substrate (TS) primer that is elongated by telomerase. The elongated TS primers are then specifically amplified via PCR and the use of a reverse primer, ACX. Through comparing the extent of primer elongation of treated, positive (untreated) and negative (no telomerase) protein extracts, the *in vitro* telomerase-inhibiting properties of G-quadruplex ligands can be determined. TRAP products are

visualized as ladders, with bands corresponding to elongated TRAP products. Ladder length is indicative of telomerase activity. The traditional TRAP assay is conducted in two stages (**Figure 2.11**):

- The telomerase enzyme extends the primer when it is incubated with the TS primer in buffer conditions suitable for primer elongation. After the addition of four repeats, the DNA sequence becomes capable of folding into a G-quadruplex structure, resulting in the inhibition of telomerase activity by preventing its access to the TS (**Figure 2.12**). Upon ligand-induced quadruplex stabilization, the substrate single-stranded DNA is sequestered, inhibiting telomerase's ability to add further hexanucleotide repeats, resulting in short products. In the absence of quadruplex-stabilizing ligands, the quadruplex structure becomes unstable, and the telomerase enzyme is free to further extend the primer, leading to longer products.

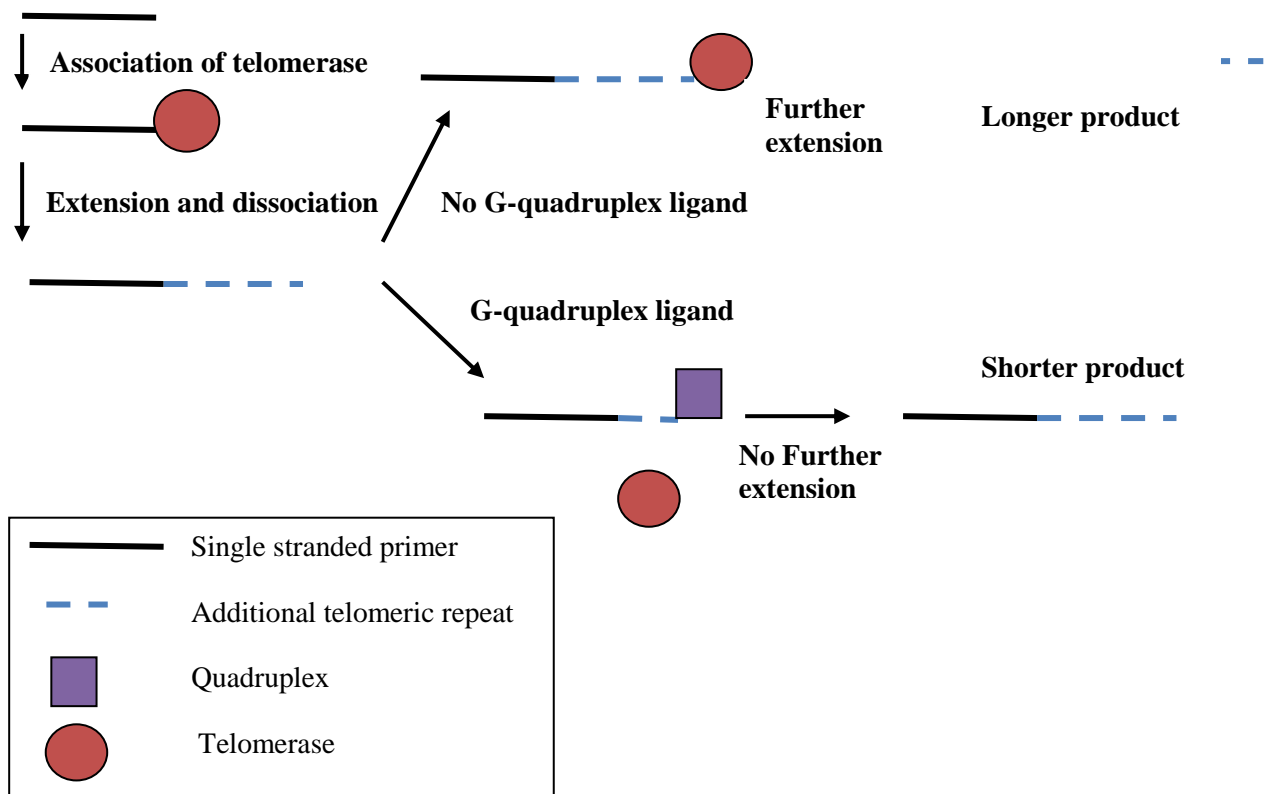


Figure 2.12: The TRAP assay in the presence of G-quadruplex-binding ligands.

- The second stage uses PCR to amplify the elongated TRAP products to enable visualization and semi-quantification. PCR is a well-known technique used to amplify a small section of a particular DNA sequence. The reaction involves the template sequence to be amplified, using DNA polymerase and primers. The telomerase products from step 1 serve as templates for the PCR amplification. The primer utilizes a CX reverse primer (5'-GCG CGG [CTTACC]₃ CTA ACC-3') and TS as a forward primer (5'-AAT CCG TCG AGC AGA GTT-3'), and *Taq*-polymerase is used. Traditional TRAP additionally utilizes a standard internal control (S-IC). This S-IC is not elongated, and is used to guard against false-positive results, arising through quadruplex ligands inhibiting the PCR-stage of TRAP, resulting in differential amplification of TRAP products from positive control (untreated) and treated ligand-containing samples.
- The length of the telomere extension fragments can then be measured by gel electrophoresis.

Although this two-stage TRAP assay was widely used in the assessment of G-quadruplex ligands as telomerase inhibitors [235], its validity was questioned upon the discovery that ligand-induced G-quadruplexes inhibit *Taq* polymerase [239]. This differential amplification of TRAP products demonstrated false-positive results, and a suitably-modified TRAP assay was consequently developed [240].

2.2.2.1 TRAP-LIG Modified TRAP Assay

De Cian and co-workers demonstrated that the TRAP assay is not appropriate for determining telomerase inhibitory activity by quadruplex ligands. They suggested that these molecules might interfere with the PCR of a sequence that is capable of forming G-quadruplexes but nonetheless leaves the internal control unaffected. Moreover, the presence of some ligands in the PCR steps inhibits *Taq*-polymerase [239]. To avoid this problem, in some laboratories the compounds were first screened for *Taq*-polymerase inhibition, and then preceded for the TRAP assay at a concentration where *Taq*-polymerase inhibition does not occur [241].

Reed *et al.* reported a modification of the TRAP assay protocol known as the TRAP–LIG modified TRAP assay that overcame the problem of inhibiting *Taq*-polymerase. In this process, bound ligands are removed before the PCR amplification step, which eliminates the possibilities of both PCR inhibition and the inhibition of *Taq* polymerase activity because of the presence of ligand-ligand complexes in the extended products and ligand–quadruplex complexes and unbound ligands, respectively. This new procedure, TRAP–LIG, has been tested and the results have been found to be reliable and reproducible for investigating telomerase inhibition, and can be made without a separate *Taq* polymerase assay [240].

The TRAP–LIG assay is a three-step process (**Figure 2.13**), following a similar protocol for the direct assay, except for the introduction of an intermediate aqueous washing and freeze-drying step prior to PCR amplification step. Hence the steps are:

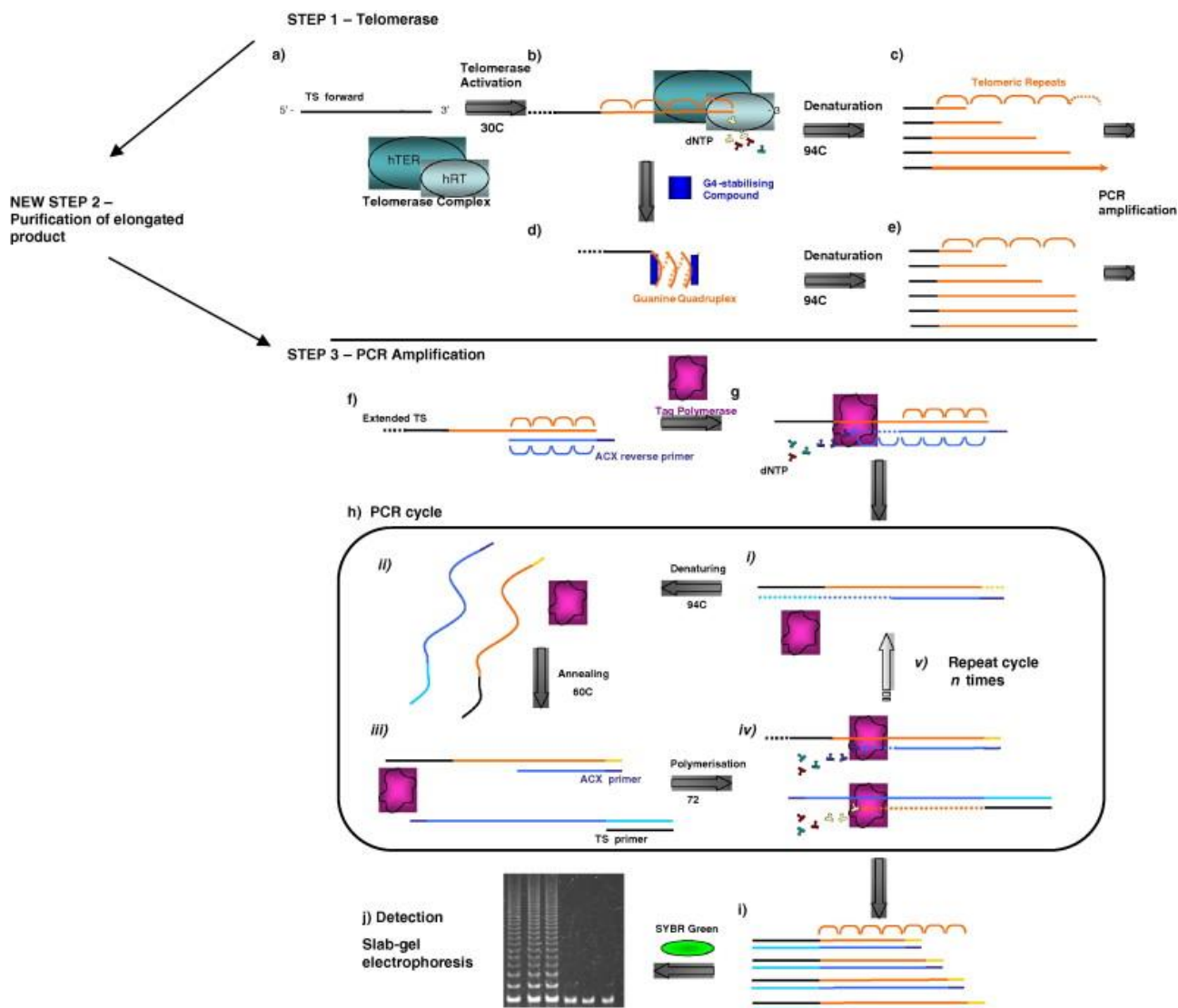


Figure 2.13: A schematic diagram of the steps involved in the TRAP–LIG assay [240]

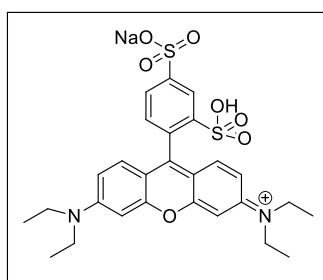
1. Initial elongation of a primer sequence by telomerase in the presence of a ligand.
2. Removal of all bound ligands by aqueous washing.
3. PCR amplification of the pure extended products of telomerase elongation [240].

2.2.3 Sulforhodamine B Assay (SRB)

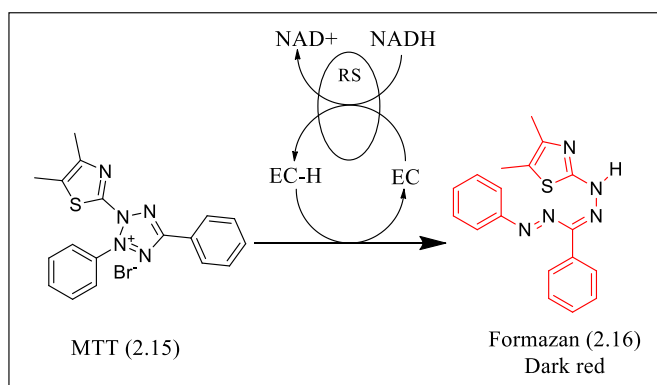
Short-term potent cell growth inhibition is a usual pre-requisite for anti-cancer drugs. As such, there are several assays to determine the toxic/growth-inhibitory effects of ligands in

the high-throughput fashion required by drug discovery groups. The two most common assays are the 3-(4,5-dimethylthiazol-2-yl)-2,5-diphenyltetrazolium bromide (MTT, **2.15**) assay and the sulforhodamine-B (SRB, **2.14**) assay (**Figure 2.14 a, b**).

In vitro cytotoxicity screening is mostly performed using the sulforhodamine B (SRB, **2.14**) assay, developed in 1990 [242]. This assay depends on the ability of SRB (**2.14**) to bind to protein components of cells that have been fixed to tissue-culture plates by trichloroacetic acid (TCA). The bright-pink aminoxanthene dye SRB (**2.14**), containing two sulfonic groups, can under mild acidic conditions bind to the basic amino-acid residues which again dissociate under basic conditions. The amount of extracted dye from stained cells is directly proportional to the mass of cell, since SRB (**2.14**) binds in a stoichiometric ratio [243].



a) Sulforhodamine B (SRB) (**2.14**)



b) Formation of formazan (**2.16**) from MTT (**2.15**)

Figure 2.14: a) The structure of sulforhodamine-B (SRB, **2.14**); b) A schematic diagram for the formation of formazan (**2.16**).

The effectiveness of the SRB (**2.14**) assay is often compared with another method using the tetrazolium dye 3-(4,5-dimethylthiazol-2-yl)-2,5-diphenyltetrazolium bromide or MTT (**2.15**). MTT (**2.15**) can be reduced by formed NADH from metabolic active cells, resulting in

a purple-coloured formazan (**2.16**) (**Figure 2.14 b**), which can be detected by a photometer. As most of the NADH is formed in the mitochondria, 1-methoxy-phenazine methosulphate is needed as an electron-carrier to transfer the reduction equivalents from the mitochondrial matrix into the medium. Because of the nature of its mechanism of action, the MTT (**2.15**) assay can only detect viable cells, whereas the SRB (**2.14**) method cannot differentiate between viable and dead cells. Several studies have proven that the result obtained by the SRB (**2.14**) assay correlated well with those of the MTT (**2.15**) assay, although the IC₅₀ values obtained by the SRB (**2.14**) assay were slightly higher. The SRB (**2.14**) assay, however, has several advantages over the MTT (**2.15**) assay. For example, some compounds can directly interfere with MTT's (**2.15**) reduction without effecting cell viability, while SRB (**2.14**) staining is rarely affected by this type of interference. Again, SRB (**2.14**) staining is not dependent on the cell's metabolic activity; therefore, optimization of the assay conditions for specific cell lines is easier than for the MTT (**2.15**) assay [243].

The SRB (**2.14**) assay has been optimized and adopted as the routine method by the NCI for drug discovery programs. Therefore, it has led the SRB (**2.14**) assay to become the chosen assay over tetrazolium-based assays.

2.2.4 Long-term Population Doubling Studies

Short-term cell growth inhibition investigations such as the SRB (**2.14**) assay provide insight on whether compounds are biologically active. However, they provide no information in determining the mechanism of action of the compound, such as molecular targeting, cytostatic or cytotoxic (necrotic or apoptotic) mechanisms. The mechanism of action of a compound is a useful preliminary tool in assessing whether a compound presents a viable therapeutic window and is important for pre-clinical evaluation.

There are two methods to elucidate the mechanism of action of G-quadruplex ligands; i) long-term sub-cytotoxic concentrations or ii) short-term post-cytotoxic concentrations. Two different methods are needed due to the fact that some cellular responses are rapid (DNA-

damage response/apoptotic factors), whereas some are significantly slower (telomere-dysfunction induced Ubiquitin-mediated telomerase degradation). Cells are counted weekly and are re-seeded at a given concentration. Population doublings (P_d) can be calculated from the following formula (**Equation 2.3**), and the drug is added twice weekly.

$$P_d = \log(N_f/N_0)/\log 2$$

N_0 = No of cells seeded
 N_f = No of cells counted on day 7

Equation 2.3: The formula for calculating population doublings (P_d) from cell count.

The cumulative number of population doublings is plotted against time. The data represent the extent of the proliferative/replicative capacity of viable cells in the presence of drugs (**Figure 2.15**).

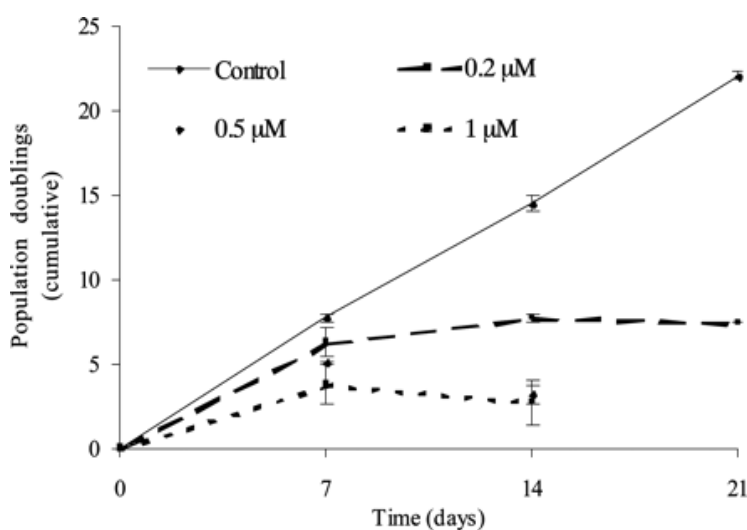


Figure 2.15: The effect of RHPS4 (**1.6**) on the long-term proliferation of MCF-7 cells where a cessation of growth on day 14 at 0.5 and 1 μ M and reduction in proliferative capacity/population doubling at 0.2 μ M RHPS4 (**1.6**) was found [244].

Chapter Three: Results and Discussion

3.0 Results and Discussion

3.1 Results and Discussion: Chemical

3.1.1 Aryl Polyamides as G-quadruplex Ligands

N-Methyl pyrrole/imidazole-based polyamides have long been recognized for their ability to bind to the minor groove of duplex DNA and studies have proved that pyrrole-imidazole polyamides can be cell-permeable and can inhibit the transcription of specific genes[245]. With the realisation that small quadruplex-binding ligands could function as transcriptional repressors of c-myc *via* stabilization of upstream proximal G-quadruplex structures [50], G-quadruplex anti-cancer drug discovery has progressed into developing DNA-binding agents with selectivity and high-affinity towards telomeric and non-telomeric G-quadruplexes.

Dervan and co-workers originally showed how distamycin-like polyamides containing *N*-methylpyrroles and *N*-methylimidazole amino acids bind to the minor groove of duplex DNA at AT-rich regions and demonstrated this to be an important probe for protein interactions with double-stranded DNA [246, 247]. Dervan and co-workers further showed that covalently linked polyamides with multiple pyrrole or imidazole moieties along a γ -aminobutyric acid chain form specific and high affinity DNA-binding agents. Subsequently, further studies have demonstrated that distamycin and distamycin-derivatives can also inhibit protein interactions with G-quadruplex DNA by stacking on the planar end-terminal G-tetrad of G-quadruplexes in 2:1 (ligand:G-tetrad) stoichiometry and contacting the flanking bases. These findings proved distamycin's importance as a probe of G-quadruplex DNA-protein interactions [247].

Polyamides containing more than five heterocyclic rings usually display reduced duplex affinity, which is a desirable characteristic for a G-quadruplex ligand owing to the relatively unknown degree and direction of bending in DNA (helical phasing) [248]. Polyamide quadruplex ligands are therefore usually elongated and contain several heterocyclic-rings in linear and/or branched form, providing a basis for ligand-tetrad stacking interactions. This correlation was demonstrated by Neidle and co-workers as an increase in heterocyclic groups resulted in an increased affinity and selectivity for G-quadruplex DNA over duplex DNA which is suggested to be consistent with a mixed groove/G-quartet stacking binding mode [172]. Unexpectedly, however, Neidle and co-workers observed longer-length polyamides

having greater quadruplex stabilization suggesting potential interactions with quadruplex grooves, as opposed to the commonly observed end-stacking paradigm.

Two distinct binding modes of distamycin with protein-G-quadruplex have been proposed which can be distinguished by sensitivity to distamycin and include

- (i) distamycin molecules bind as dimers in two of the four grooves of a quadruplex, and
- (ii) two molecules of distamycin A extend over each of the two G-tetrad planes in a 4 : 1 binding mode [172].

Isothermal titration calorimetry (ITC) can be utilized to assess such stereochemical/stoichiometric interactions to characterize the energetics of ligand-quadruplex interactions [249]. ITC showed the polyamide based Dist-A compound (**Figure 3.1**) bound with a 4:1 complex suggesting Dist-A formed dimers bound simultaneously to two opposite grooves of the quadruplex [222]. Although clearly not all polyamide-based compounds will bind in this manner, it provides evidence to suggest polyamide compounds can intercalate with the grooves of quadruplexes.

It is feasible therefore to assume that aryl polyamide based ligands may either stack onto the end-planar G-tetrad surfaces (commonly seen for most G-quadruplex ligands) or intercalate with quadruplex grooves (seen with Dist-A), although the former is still most likely due to the complex steric-hindrane observed in quadruplex grooves.

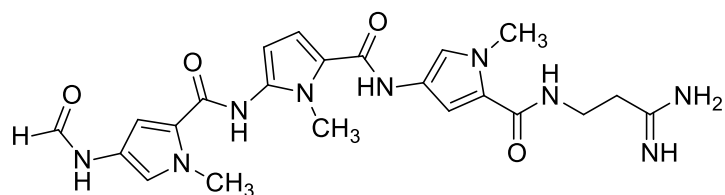


Figure 3.1: Structure of distamycin A.

3.1.2 Overview of Design and Evaluation of Ligands

There is a growing interest in small molecules that can bind selectively and stabilize G-quadruplex DNAs due to their potential as transcription/translation regulators and selective telomere targeting agents, which represent a new class of therapeutic agent. Most quadruplex-binding ligands studied to date contain functionalized polycyclic aromatic

systems such as acridines, anthraquinones, indoloquinolines and porphyrins.[189] A few of these have been shown to produce quadruplex-related biological effects, even though their physicochemical features are conventionally non-drug-like. Due to their distinctive structural features, it is possible to target particular G-quadruplex nucleic acid structures selectively without binding to the more-abundant duplex DNA. A common approach to G-quadruplex ligand design is the use of relatively large aromatic groups to interact with terminal G-quartets through π - π interactions (end-stacking), explaining why the majority of quadruplex-binding molecules studied to date are based on functionalized polycyclic aromatic systems. The first small molecule reported to bind to G-quadruplex DNA was an anthraquinone derivative [179]. Following this, molecules containing similar structural motifs such as fluorenones and acridines were developed.

Recently, Rahman and co-workers reported a series of novel biaryl polyamides with significant selectivity towards G-quadruplex compared with duplex DNA, and modest selectivity between different quadruplex types [[189]. Using a distamycin scaffold as a starting point, biaryl building blocks were introduced in place of pyrroles to switch preference from duplex to quadruplex DNA. Introduction of the biaryl unit significantly altered the classical crescent-shaped structure of the molecules, forcing them to adopt a U-shaped scaffold instead. This alteration in shape ensures that the molecules have low affinity for duplex DNA while increasing their interaction with a G-quadruplex structure, since the ligands have similar dimensions (**Figure 3.3**). In contrast to previous attempts to produce quadruplex-selective distamycin analogues [172], these biaryl polyamides offer synthetic versatility and significant quadruplex selectivity. They consist of two different structural motifs: Motif-1 containing one biaryl unit, and Motif-2 which are dimers of biaryl units (**Figure 3.2**).

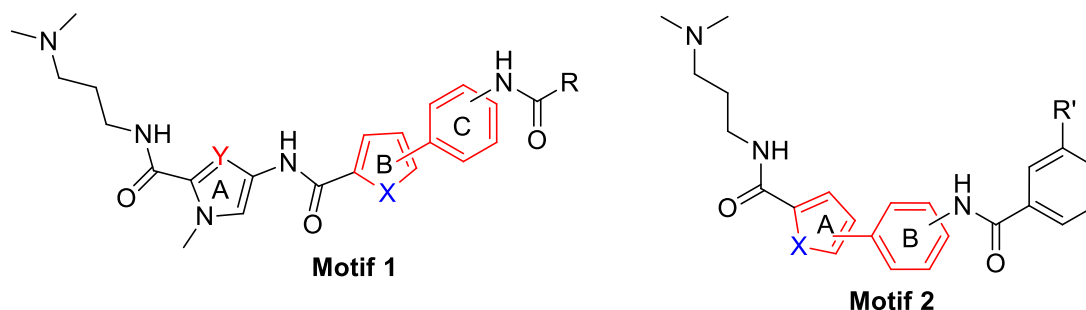


Figure 3.2: Structural motifs of the biaryl polyamides (X = O, S or N; Y = C or N).

Preliminary data suggested that it is possible to tailor the structure of these molecules to enhance affinity for specific G-quadruplexes (*e.g.*, c-kit1 vs c-kit2 vs HT4). The ligands proposed in this project were designed based on the concept of systematically lengthening and modifying the first-generation molecules while maintaining quadruplex contour in order to enhance (i) stacking interactions and (ii) non-bonded interactions with loops and grooves in the various quadruplex structures. This was done by introducing additional rings, heteroatoms in existing rings and additional functional groups to enhance hydrogen bonding opportunities and thus selectivity between different quadruplex structures.

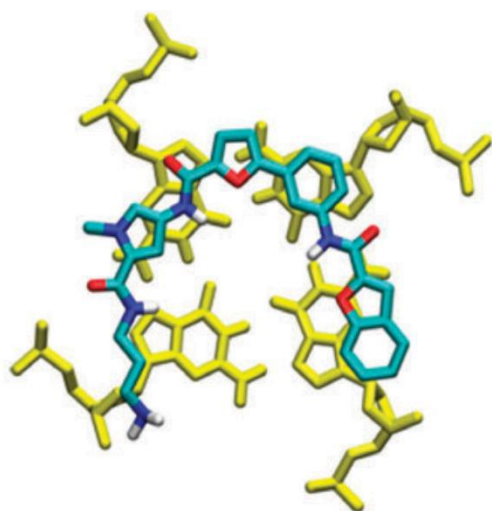


Figure 3.3: Model of the biaryl-polyamide compound overlapping the planar terminal G-tetrad of the human intramolecular telomeric quadruplex [189].

To achieve the goal of this project, libraries of compounds were synthesized and were screened by using various biophysical and biological techniques. After synthesis of the first library of molecules, the compounds were screened through a FRET based melting assay to identify a lead molecule with the highest degree of G-quadruplex stabilization and greater affinity towards the G-quadruplex over duplex DNA. These molecules were further analysed against several cancer cell lines and a normal cell line to determine their cytotoxicity. Other biophysical techniques such as CD-spectroscopy were applied to ensure the efficacy of the selected lead molecules. The lead molecules were then modified at various points to improve the G-quadruplex stabilization potential, binding affinity and selectivity of the molecules, which were then subjected to further analysis by biophysical and biological techniques.

3.1.3 Design of Library Types

Three different types of solution phase libraries, Type-1, Type-2 and Type-3, were planned on the basis of the structure of the building blocks in the target molecules. All the molecules in these libraries contain varying numbers of aromatic rings and various points of modification (**Figure 3.4**).

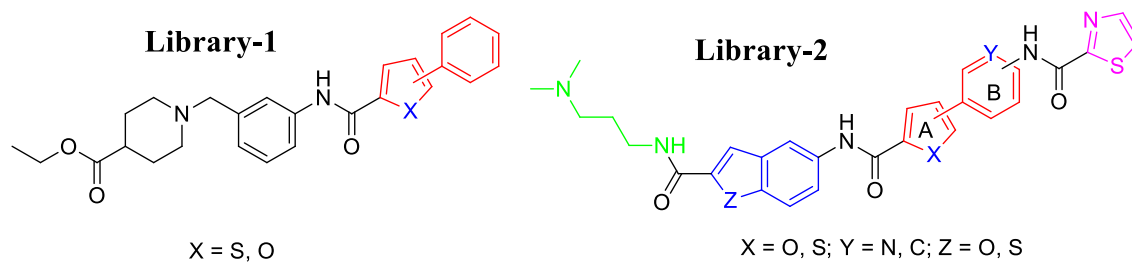


Figure 3.4: Structural motifs of the Type-1 and Type-2 library.

3.1.3.1 Type-1 Library

The Type-1 library molecules (**Figure 3.5**) are based on a non-variable core (black, pink circle) and two variable cores R1 (red) and R2 (blue). These molecules contain two building blocks which are connected together by an amide linkage where the non-variable core contains a tertiary amine group which facilitates purification by use of an SCX-2 cartridge. SCX cartridges are loaded with modified silica containing a sulfonic acid group which acts as a cation exchange resin and exchanges its acid group with the basic functional groups of the product. Therefore, the products with basic groups are kept bound inside the cartridge while impurities come out of the cartridge. Washing the column with ammonia methanol then releases the bound product from the silica. Of the two building blocks, one is a biaryl unit, which contains one five membered (R1) and one six membered ring (R2). The biaryl part of these molecules contains either a furan or a thiophene ring (**Figure 3.6**) joined to π -electron rich aryl groups (**Figure 3.7**) in either the 2/5 or 2/4 positions with the expectation of increasing affinity for G-quartets through additional π - π interactions (end-stacking). A 2/5 or 2/4 substituent ensures different shape characteristics which can potentially affect the way the molecules can interact with the terminal quartet of the G-quadruplex. The molecular weight of members of the proposed library varies from 473 to 555. Twenty-one molecules containing the Type-1 structural motif were synthesized. Depending on the arrangement of the building blocks, Type-1 had the following structural types depending on which boronic acid was used.

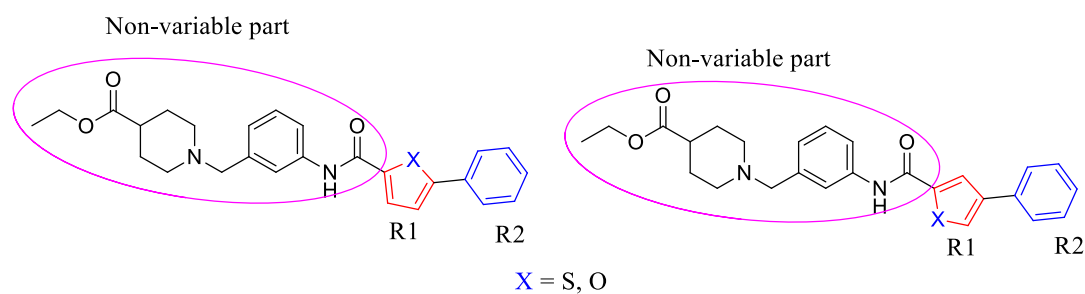


Figure 3.5: Structural types of library-1.

3.1.3.1.1 Synthesis of Type-1 Library

A linear synthetic approach was adopted for synthesis of the Type-1 library (**Scheme 3.2**). Starting from the ethyl 1-(3-aminobenzyl)piperidine-4-carboxylate building block, which was purchased from a commercial source, the compounds were synthesized in two steps. Every molecule in this library contains a tertiary nitrogen in the ring which offered the advantage of SCX cartridge purification after each step.

The first step involved amide coupling between the amine and three different bromo heterocyclic acids in a parallel fashion. 2.0-2.5 equivalents of HOBt were used to activate the carboxylic acids, and 1.75-2.0 equivalents of DIC were used as a coupling reagent depending on the substrate.

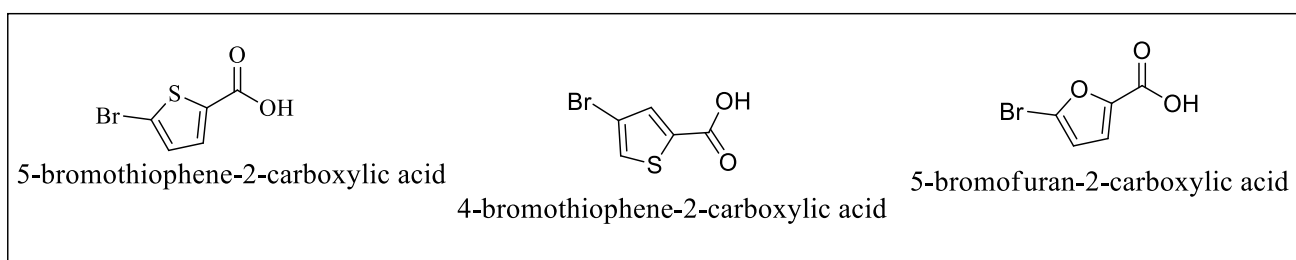
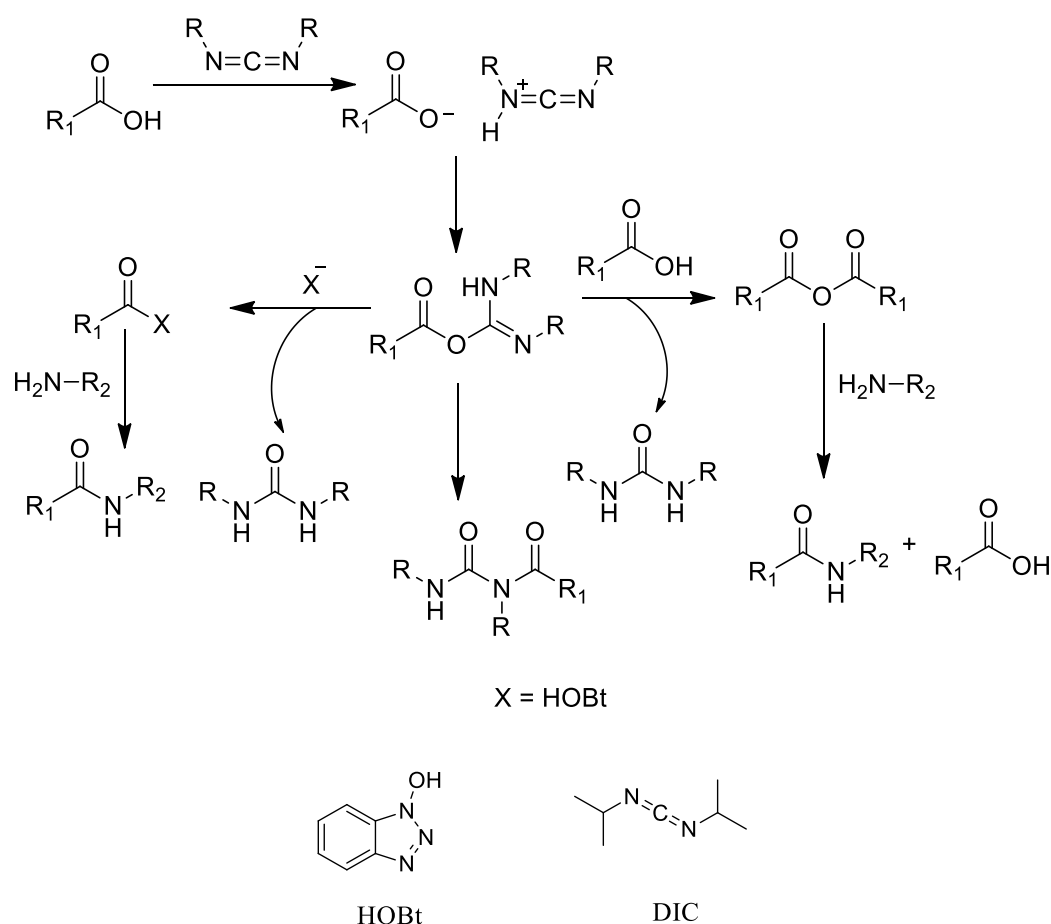


Figure 3.6: Bromo heterocyclic acids used to synthesize the Type-1 and Type-2 libraries.

HOBt reacts with activated acyl groups (e.g. carboxylic acid + DCC/DIC) to form intermediates referred to as activated esters. DIC (*N,N'*-diisopropylcarbodiimide) activates the carboxylic acids towards amide formation. In the amide coupling reactions most often carbodiimides are used as the dehydrating agents which activate the acid group and help the amide bond formation in the presence of additives like *N*-hydroxybenzotriazole or *N*-

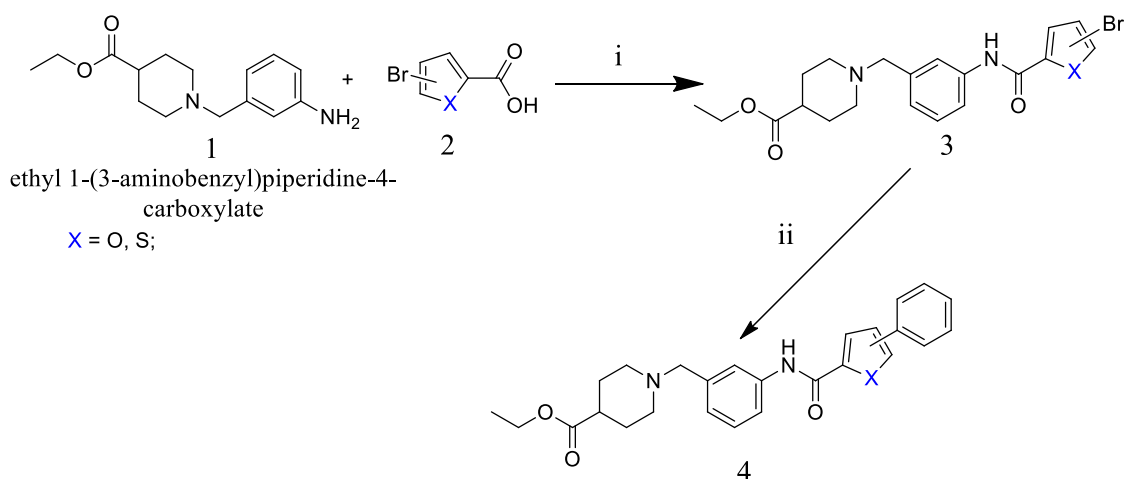
hydroxysuccinimide. Dicyclohexylcarbodiimide (DCC), *N,N'*-diisopropylcarbodiimide (DIC), and EDCI are some commonly used carbodiimides. Among these we chose DIC as it has several advantages over the others like that it is a liquid and easy to use. Additionally, the by-product, *N,N'*-diisopropylurea, is soluble in organic solvents and easily removed by extraction. Moreover, this is less likely to cause allergic reaction compared with DCC. The lone pair electron on the nitrogen of the carbodiimide makes it a nucleophile, which takes the acidic proton and becomes an electrophile leaving a nucleophilic carboxylate group. The positively charged nitrogen atom then attracts the N=C bonding electron to complete its lone pair and the carbon atom forms a bond with the carboxylate. This complex is further activated by HOBt as the hydroxyl oxygen of HOBt forms a bond with the carbonyl carbon of the carboxylate through its lone pair electron, while releasing the corresponding urea based on the carbodiimide used. The activated acid then reacts with the amine forming the amide bond releasing the HOBt (**Scheme 3.1**).



Scheme 3.1: General overview of amide coupling using DIC and HOBt.

The reaction mixture here was allowed to stir overnight. After 16 hours, the reaction mixture was passed through a SCX-2 cartridge (with a sorbent mass 10 times that of the product mass). SCX-2 cartridges are packed with silica-based sulfonic acid cationic exchange resins. Due to the presence of tertiary nitrogen in the starting material, all of these compounds were retained in the cartridge. The cartridges were then washed with DCM (3x) and DMF (3x) twice and finally MeOH (2x) to remove impurities and excess reagents. The trapped compounds were released from the cartridge using 5-10 ml of 2M NH₃ in MeOH and the solvent evaporated *in vacuo*. This trap and release method was highly effective in this case.

The *O*-acylisourea can react with an additional carboxylic acid to give an acid anhydride, which can react further to give the desired amide. An unwanted reaction pathway involves the rearrangement of the *O*-acylisourea to the stable *N*-acylurea. The use of solvents with low dielectric constants, such as dichloromethane and chloroform, can minimize this side reaction. In the case of the synthesis of Type-1 library members, dichloromethane was used as the solvent.



Reagents and conditions

i) DIC/HOBt, DCM, RT, 16 h ii) Boronic acid K₂CO₃, Pd(PPh₃)₄, EtOH: Toluene: Water-9:3:1, MW, 8-10 minutes

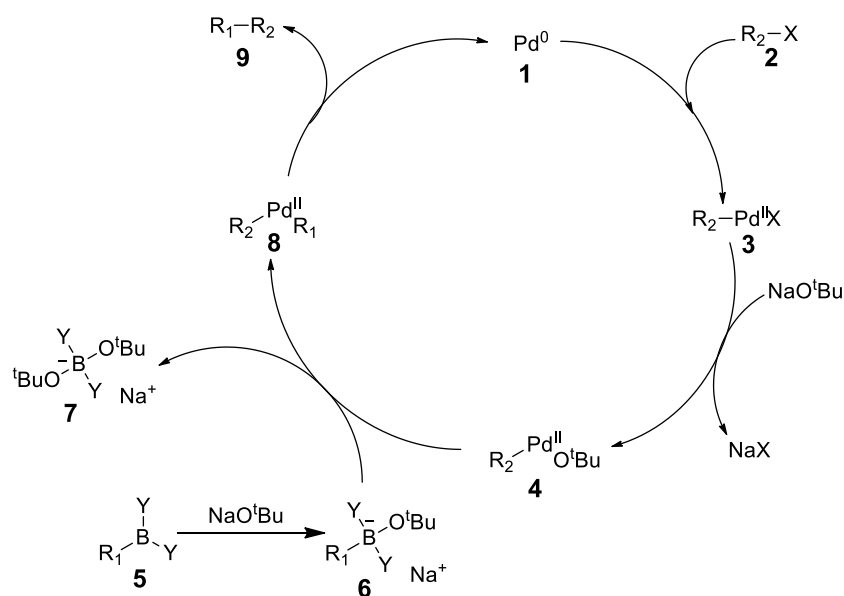
Scheme 3.2: General scheme for the synthesis of Type-1 library molecules.

The next step in the synthetic route was the cross coupling reaction to attach an aryl moiety directly to the terminal five-membered heterocyclic ring of intermediate **3** using a C-C bond formation reaction. A Suzuki cross-coupling reaction under microwave conditions was selected for its convenience and high yield in similar reactions. The Suzuki cross-coupling reaction is an extremely versatile reaction for generating carbon-carbon bonds. It involves

reaction of an aryl- or vinyl-boronic acid with an aryl-, vinyl- or an alkyl-halide catalyzed by palladium. It is widely used to synthesize poly-olefins, styrenes and substituted biphenyls. The reaction also works with pseudohalides, such as triflates (OTf), to replace halides, and also with boron-esters instead of boronic acids with a relative reactivity of $R_2-I > R_2-OTf > R_2-Br \gg R_2-Cl$.

First published in 1979 by Akira Suzuki, the Suzuki reaction relies on a palladium catalyst such as tetrakis(triphenylphosphine)palladium(0) to effect part of the transformation. The palladium catalyst (more strictly a pre-catalyst) is 4-coordinate, and usually involves phosphine supporting groups, as shown below (**Scheme 3.3**)

The mechanism of the Suzuki reaction (**Scheme 3.3**) is best viewed from the perspective of the palladium catalyst. The first step is oxidative addition of palladium to the halide **2** to form the organopalladium species **3**. Reaction with base gives intermediate **4**, which *via* transmetalation with the boronate complex **6** forms the organopalladium species **8**. Reductive elimination of the desired product **9** restores the original palladium catalyst **1**.



Scheme 3.3: The Suzuki cross-coupling catalytic cycle

The reaction conditions, solvents and microwave heating time were optimized through small scale trial reactions. Finally a combination of EtOH, toluene and water (9:3:1) was used as

the reaction solvent with 1.2 equivalents of boronic acid and 3.0 equivalents of K_2CO_3 as base. A 0.1 equivalent of tetrakis(triphenylphosphine)palladium, $Pd(PPh_3)_4$ was used as the catalyst. Microwave heating time was varied from 8-10 minutes.

For this Type-1 library three commercially available bromo heterocyclic acids (**Figure 3.6**) and seven different boronic acids (**Figure 3.7**) were used to obtain the final 21 compounds.

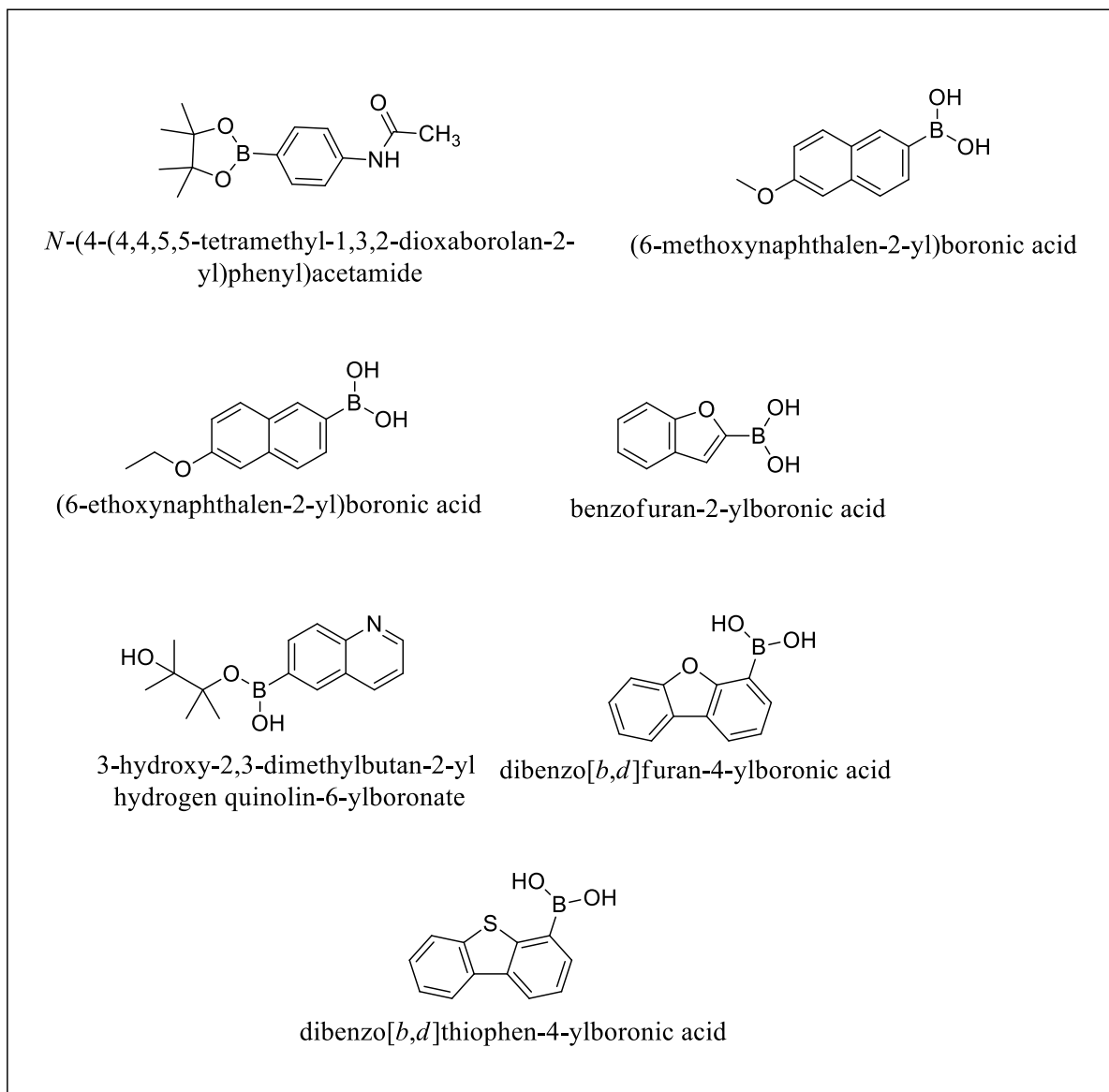


Figure 3.7: List of boronic acids used in the synthesis of Type-1 library molecules.

3.1.3.1.2 Structures of 21 Member Type-1 Library

The structures of the synthesized library compounds (**Table 3.1**) are listed below:

Table 3.1: Structures of 21 member Type-1 library.

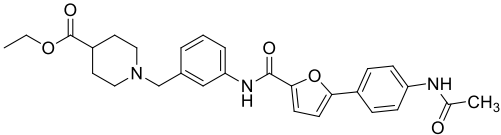
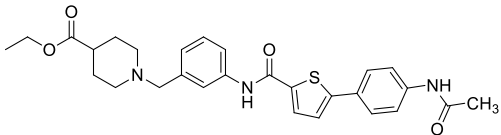
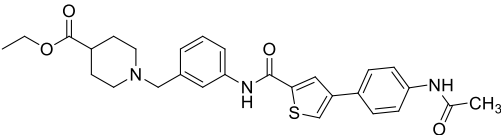
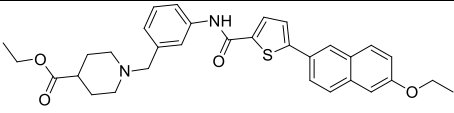
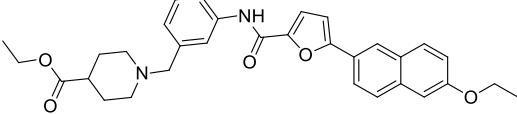
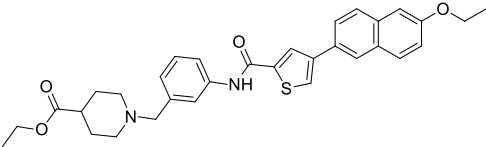
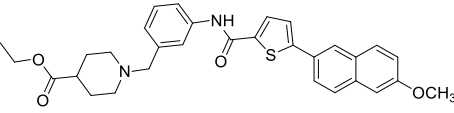
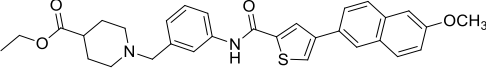
Code No.	Structure	Molecular Weight
KN-39 (4.9)		491.11
KN-40 (4.10)		507.38
KN-41 (4.11)		507.15
KN-45 (4.13)		543.00
KN-46 (4.14)		527.10
KN-47 (4.15)		543.05
KN-48 (4.17)		529.96
KN-49 (4.18)		528.94

Table 3.1: Structure of 21 member Type-1 Library (continued).

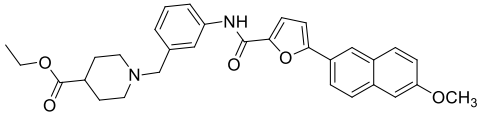
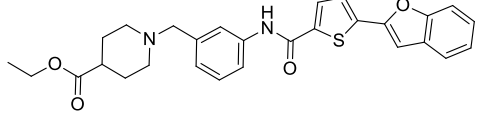
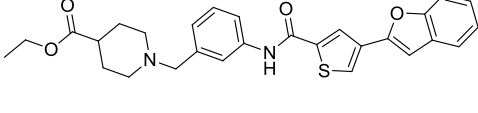
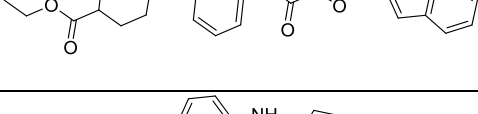
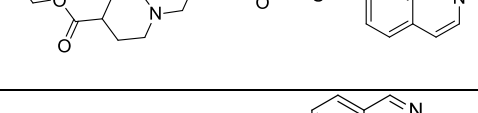
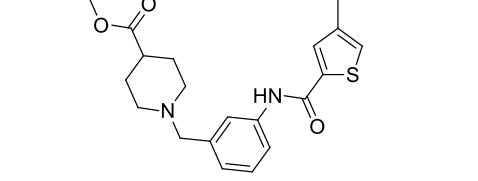
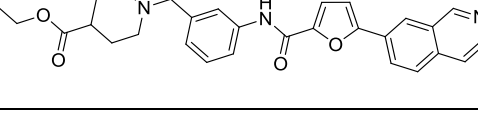
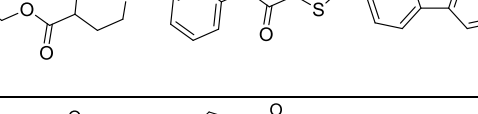
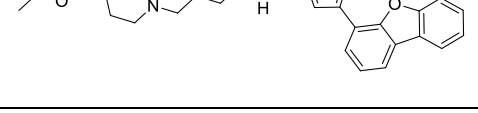
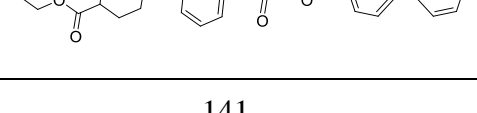
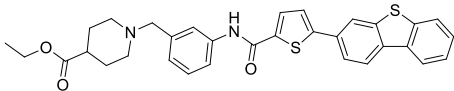
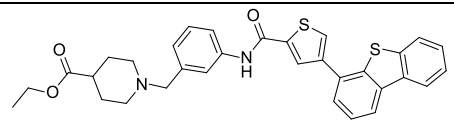
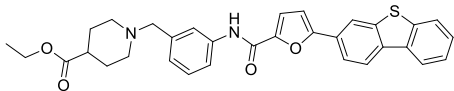
Code No.	Structure	Molecular Weight
KN-50 (4.19)		512.99
KN-51 (4.21)		489.17
KN-52 (4.22)		490.14
KN-53 (4.23)		473.13
KN-54 (4.25)		499.85
KN-55 (4.26)		499.92
KN-56 (4.27)		483.88
KN-57 (4.29)		539.09
KN-58 (4.30)		539.09
KN-59 (4.31)		523.12

Table 3.1: Structure of 21 member Type-1 Library (continued).

Code No.	Structure	Molecular Weight
KN-60 (4.33)		554.99
KN-61 (4.34)		554.99
KN-62 (4.35)		539.05

3.1.3.1.3 Purification of Type-1 Library Members

All compounds were purified by passing through sulphonic acid based Isolute™ SCX-2 cartridges, which were washed with DCM (3x) and DMF (3x) twice, and finally MeOH (2x) to remove impurities and excess reagents. The products were released from the cartridges using 2M NH₃ in MeOH, and concentrated *in vacuo* to obtain the final products. Product purity was in the range of 90-95% through this catch and release method, which required no further purification.

3.1.3.1.4 Characterization of Type-1 Library Molecules

The synthesized molecules were analysed using LCMS to ascertain their purity (**Table 3.2**). High resolution mass spectrometry (HRMS), and IR and NMR spectroscopic techniques (See experimental section for detail) were used to confirm their structures.

Table 3.2: LCMS and HRMS data of the Type-1 Library molecules.

Code No.	Mass obtained by LCMS	Mass obtained by HRMS
KN-39 (4.9)	491.11	490.2342
KN-40 (4.10)	507.08	506.2114
KN-41 (4.11)	507.15	506.2114
KN-45 (4.13)	543.00	543.2316
KN-46 (4.14)	527.10	527.2554
KN-47 (4.15)	543.05	543.2318
KN-48 (4.17)	529.96	529.2158
KN-49 (4.18)	528.94	529.2151
KN-50 (4.19)	512.99	513.2415
KN-51 (4.21)	489.17	489.1844
KN-52 (4.22)	490.14	489.1826
KN-53 (4.23)	473.13	473.2070
KN-54 (4.25)	499.85	500.2032
KN-55 (4.26)	499.92	500.2029
KN-56 (4.27)	483.88	484.2251
KN-57 (4.29)	539.09	539.2015
KN-58 (4.30)	539.09	539.2015
KN-59 (4.31)	523.12	523.2250
KN-60 (4.33)	554.99	555.1767
KN-61 (4.34)	554.99	555.1775
KN-62 (4.35)	539.05	539.2028

3.1.3.2 Type-2 Library

Type-2 library molecules contain four variable cores R1 (tail part, pink circle), R2 (heterocyclic part, green), R3 (biaryl moiety, red) and R4 (capping acid, blue), which are connected by amide linkages (**Figure 3.8**). Initially the tail portion of the molecules was kept fixed and the R2, R3 and R4 portions of the molecule were changed randomly depending on the commercially available building blocks, and 12 molecules were synthesized. These were subjected to initial screening by FRET based melting assay to identify their G-quadruplex binding potential. Two of the molecules (KN-88 and KN-119) were found to be highly effective in stabilizing G-quadruplex and showed high selectivity towards G-quadruplex over duplex DNA (**Table 3.11 and AP1**). These molecules were further analysed for their cytotoxic activity against various cancer and healthy cell lines and found to be cytotoxic against the cancer cell lines at nanomolar concentrations (**Table 3.15, 3.16**). These two molecules were considered as the lead molecules and were modified further at various positions and are grouped as Type-3 molecules.

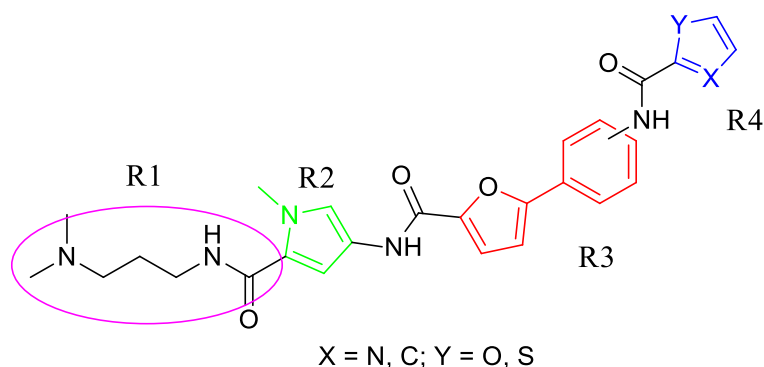


Figure 3.8: Example of Type-2 library molecules.

3.1.3.2.1 Type-2 Library

The 12 membered Type-2 library compounds (**Figure 3.9**) contain three building blocks where two of the building blocks contain biaryl units and the third is either a benzofused ring or a five membered heterocyclic ring. All three building blocks are connected by an amide linkage. These molecules contain three variable cores R2 (pink), R3 (red) and R4 (blue). R2 contains either a five membered heterocyclic ring or a benzofused ring, R3 is a biaryl unit that was synthesized in house and contains a variable five membered heterocyclic ring and

finally, R4, the capping acid, containing various aromatic rings. In some of the compounds there is a $-\text{CH}_2-$ group between the terminal biaryl building block located in the capping acid, which increases the length of the molecule, with the expectation that this will cover an extended length of the quadruplex. In each case the molecules contain an *N,N'*-dimethylaminopropyl amine tail, which facilitates purification. The molecules in this library are again divided into three sub types depending on the synthetic route. The molecular weight of the compounds varies from 503 to 715. Depending on the synthetic procedure these molecules are sub-divided into three classes.

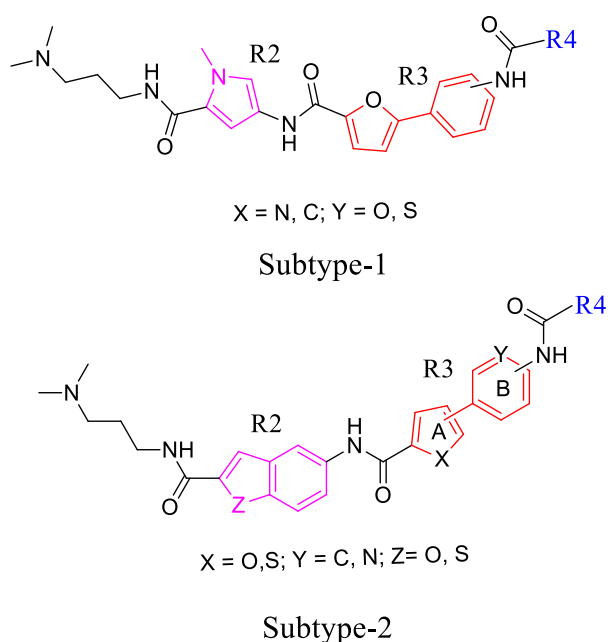


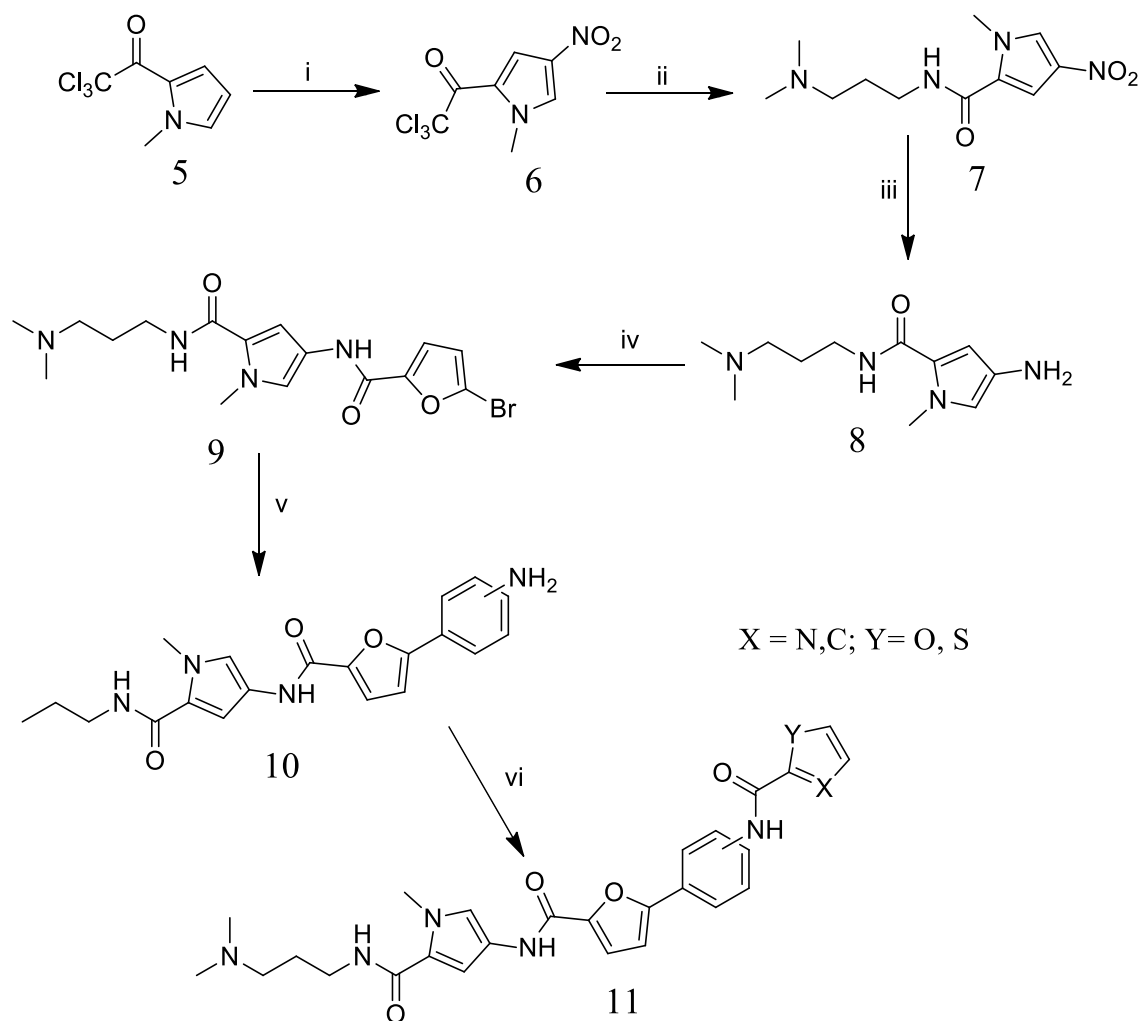
Figure 3.9: Structural types of library-2.

3.1.3.2.1.1 Design of Sub Type-1 Molecules

All three molecules of this type contain the non-variable *N,N'*-dimethylaminopropyl tail that is connected to a pyrrole at position 2 of the five membered ring. This pyrrole forms an amide bond with 5-bromoheterocyclic acid through its amine present at position 5. The bromoheterocyclic acid used here contains a five membered ring, which is furan in this case. The 5th position of furan is again linked with a benzene ring through a C-C bond where the benzene is connected to the final capping acid at different positions.

3.1.3.2.1.2 Synthesis of Sub Type-1 Molecules

A linear synthetic approach was adopted to obtain the amine building blocks for the synthesis of three compounds of this library. The first involved nitration of 2,2,2-trichloro-1-(1-methyl-1*H*-pyrrol-2-yl)ethanone **5** (**Scheme 3.4**) using concentrated HNO₃ acid and acetic anhydride. The reaction was conducted at -5 °C and the nitric acid was added very slowly over a period of 1 hour. The reaction was very vigorous but efficient. Then the tail was added through the coupling of *N,N'*-dimethylaminopropyl amine in THF at room temperature to obtain intermediate **7**. This reaction proceeded smoothly without any coupling reagent because of the presence of the terminal chlorides. The nitro group of intermediate **7** was reduced using hydrogen in the presence of a 0.1 equivalent of Pd/C catalysts using a hydrogenator. Ethanol was used as a solvent in this reaction step. The next step was addition of 5-bromo furan-2-carboxylic to intermediate **8**. DIC and HOBt were used as the coupling reagents, which followed the same mechanism previously mentioned (**Scheme 3.1**). The reaction proceeded smoothly with a yield greater than 80%.



Reagent and Conditions

i) Conc. HNO_3 , Acetic anhydride, -5°C , 3 h ii) N,N' -dimethylaminopropylamine, THF, RT, 3 h iii) H_2 , Pd/C, 45 psi, RT, 16 h iv) Bromo Heterocyclic acid, DIC, HOBt, DCM, RT, 16 h v) Boronic acid, $\text{Pd}(\text{PPh}_3)_4$, K_2CO_3 , Ethanol:Toluene:Water- 9:3:1, MW, 10-12 minutes vi) Heterocyclic carboxylic acid, DIC, HOBt, DIC/DMF, RT, 3 h

Scheme 3.4: General scheme for the synthesis of Sub Type-1 library compounds of library-2.

The Suzuki coupling reaction was carried out to obtain the intermediate **10** from the bromo heterocyclic intermediate. The reaction was completed within 10-12 minutes. Two boronic acids, 4-(4,4,5,5-tetramethyl-1,3,2-dioxaborolan-2-yl)aniline and (3-aminophenyl)boronic acid (**Figure 3.10**) were used to obtain two different intermediate amines. The final step involved coupling the heterocyclic carboxylic acid. The reactions were carried out in dichloromethane except for cases where the heterocyclic acid was not soluble in DCM. In those circumstances DMF was used as the reaction solvent.

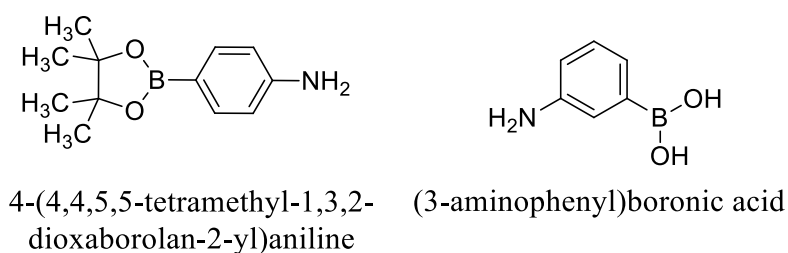


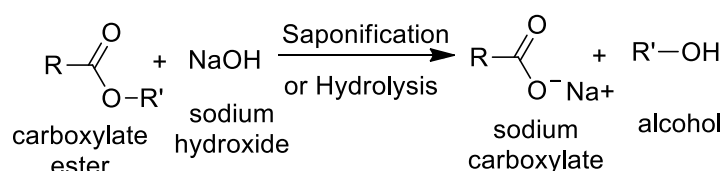
Figure 3.10: Boronic acids used for the synthesis of Sub Type-1 and Sub Type-3 library members.

3.1.3.2.1.3 Design of Sub Type-2 Molecules

Sub Type-2 molecules contain a benzofused heterocyclic moiety in R2, which is similarly connected to the tail *N,N'*-dimethylaminopropyl through an amide linkage at position 2 of R2. The heterocyclic ring of R2 here is furan in most cases, but also contains thiophene in some cases. The R2 moiety is then linked with the R3 by an amide bond. R3 is variable and contains either furan or a thiophene ring. The five membered ring of R3 forms a direct C-C bond either at position 4 or at 5 with boronic acids depending on the bromoheterocyclic acid used for synthesizing the R3 part of the molecules. The boronic acid part of R3 contains a six membered ring that forms an amide linkage with R4.

3.1.3.2.1.4 Synthesis of Sub Type-2 Molecules

In the first step of the synthesis of Sub Type -2 (**Scheme 3.6**), bromo heterocyclic acid was added to the commercially available starting material, methyl 5-aminobenzo[*b*]thiophene-2-carboxylate **12**, in the presence of DIC and HOBt. Reaction was complete after 16 hours, which was followed by purification by silica gel column chromatography. 100% DCM was used as the solvent to elute the compounds. This was an efficient method as 95% pure product was obtained in high yield (75-84%). The intermediate (**13**) was then hydrolysed in the presence of a 0.5 M solution of NaOH in dioxane at room temperature. Esters can undergo hydrolysis under acid or basic conditions. Under basic conditions, hydroxide acts as a nucleophile, while an alkoxide is the leaving group (**Scheme 3.5**). Progress of the reaction was monitored by TLC. The reaction was complete within 30 minutes, and aqueous work up was carried out to obtain the intermediate **14**, which was used for the next step.



Scheme 3.5: General scheme for ester hydrolysis.

The tail (*N,N*-dimethylaminopropyl amine) was then added by DIC/HOBt-mediated coupling which was followed by Suzuki coupling reaction in the presence of palladium catalyst. Three boronic acids (**Figure 3.11**) were used in the Suzuki coupling step to obtain three intermediate amines. The last step involved formation of an amide bond between intermediate **16** and two different acids (**Figure 3.12**) in DMF with DIC/HOBt used as the coupling reagent. Initially these reactions were incomplete, even after 16-24 hours. However, trial and error on some small scale reactions showed that addition of 2.0 equivalents of acid allowed the reactions to proceed smoothly to completion within 3 hours.

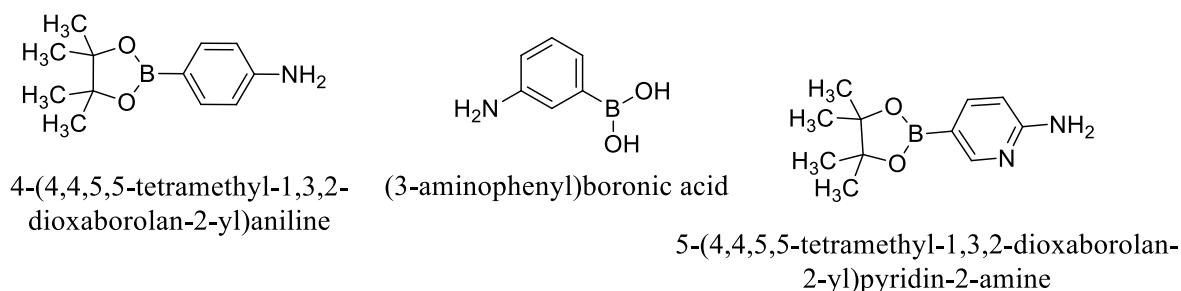


Figure 3.11: Boronic acids used for the synthesis of Sub Type-2 and Sub Type 3 library members.

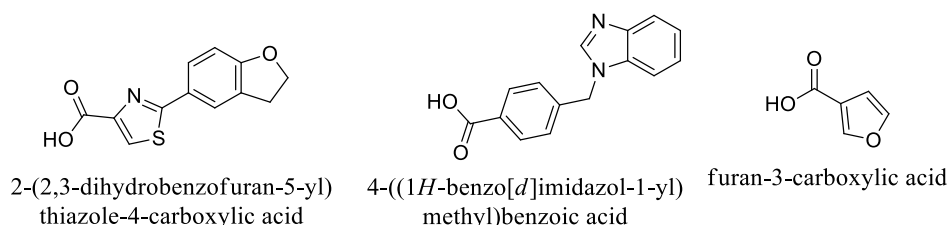
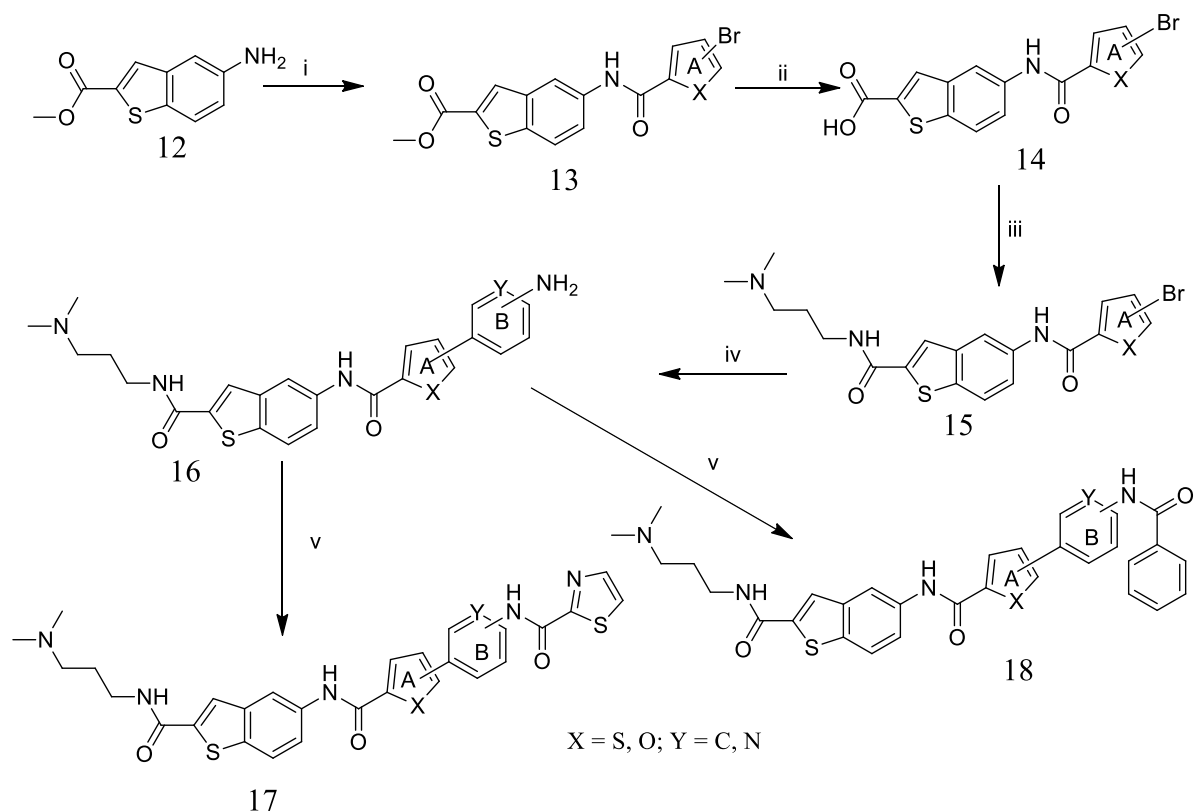


Figure 3.12: Heterocyclic acids used for the synthesis of Type-2A library members.



Reagent and Conditions

i) Bromo Heterocyclic acid, DIC, HOBt, DCM, RT, 16 h ii) 0.5 M NaOH, 1,4-dioxane, RT, 30 minutes iii) *N,N'*-dimethylaminopropylamine, DIC, HOBt, DCM RT, 2 h iv) Boronic acid, Pd(PPh₃)₄, K₂CO₃, Ethanol:Toluene:Water 9:3:1, MW, 20 minutes v) Heterocyclic carboxylic acid, DIC, HOBt, DMF, RT, 3 h

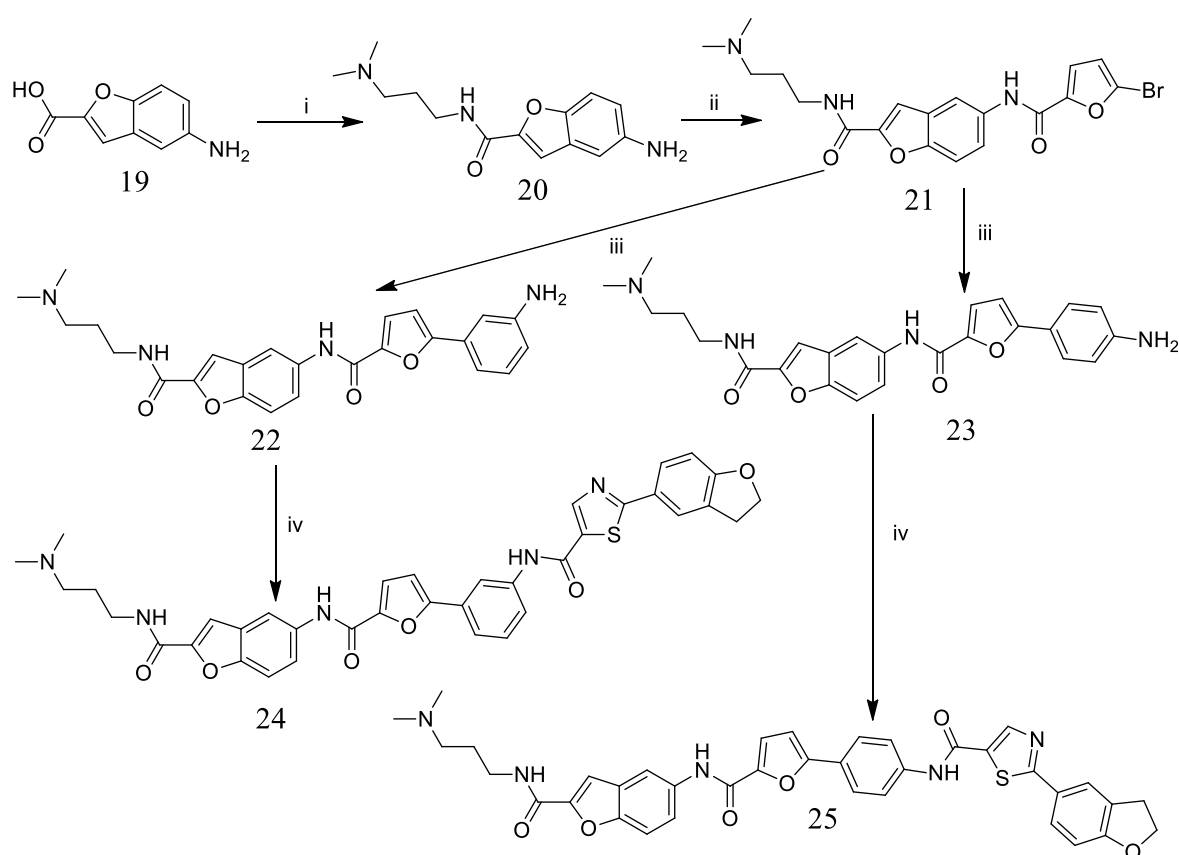
Scheme 3.6: General scheme for the synthesis of Sub Type-2 library compounds of library-2.

3.1.3.2.1.5 Design of Sub Type-3 Molecules

This group of molecules contains benzofuran as R2 in every case, which is connected to the tail at position 2 and the bromo furan moiety at position 5 through the amide bond. Either the furan or R3 forms a direct C-C bond with two different boronic acids where the amino group on the boronic acid moiety is at positions 3 and 4. This positioning of the amino groups on the R3 moiety helps in attaining slightly different shape characteristics of the synthesized molecules. Finally, the capping part was added to complete the synthesis of the molecules. In both cases, they have the same capping acid.

3.1.3.2.1.6 Synthesis of Sub Type 3 Molecules

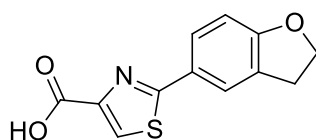
This library contains two compounds and these were synthesised from a commercially available molecule, 5-aminobenzofuran-2-carboxylic acid, containing both amine and acid groups. The tail *N,N'*-dimethylaminopropyl amine, was first added by amide coupling. This reaction was fast and complete within 2 hours to afford intermediate **20** (Scheme 3.7). 5-Bromofuroic acid was then coupled in the presence of DIC/HOBt. Suzuki coupling was carried out with two boronic acids (Figure 3.11) to give intermediates **22** and **23**. Both of these reacted with a heterocyclic acid (Figure 3.13) in DIC/HOBt to afford two final compounds.



Reagent and Conditions

i) *N,N'*-dimethylaminopropylamine, DIC, HOBt, DCM, RT, 2 h ii) 5-Bromo furan carboxylic acid, DIC, HOBt, DCM, RT, 16 h iii) Boronic acid, Pd(PPh₃)₄, K₂CO₃, Ethanol:Toluene:Water- 9:3:1, MW, 20 minutes iv) Heterocyclic carboxylic acid, DIC, HOBt, DMF, RT, 3 h

Scheme 3.7: General scheme for the synthesis of Sub Type-3 library compounds of library-2A.



2-(2,3-dihydrobenzofuran-5-yl)
thiazole-4-carboxylic acid

Figure 3.13: Heterocyclic acid used for the synthesis of Sub Type-3 molecules.

3.1.3.2.1.7 Purification of Type-2 Library Members

After completion of the reaction, the mixtures were initially passed through SCX-2 (silica based sulphonic acid) cartridges to catch the basic compounds. The cartridge was washed with DCM (2X), DMF (2X) and methanol (2X) and then eluted with 2M NH_3 in methanol. This ensured removal of impurities and excess reagents. TLC and LCMS analysis showed that 4 of the 14 compounds were more than 95% pure and did not require further purification. Other molecules showed minor to moderate impurities by TLC. These were purified using flash chromatography on silica gel employing a 18:1:1 ratio of DCM:2 molar NH_3 :methanol:methanol as the mobile phase. This provided pure compounds in 65-70% yield.

3.1.3.2.1.8 Structure of Type-2 Library Members

Structures of the synthesized molecules of this group are listed below (**Table 3.3**).

Table 3.3: Structures of 12 member Type-2 library.

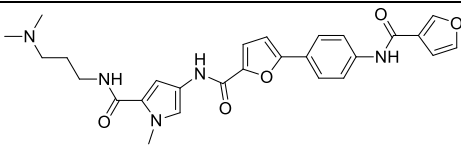
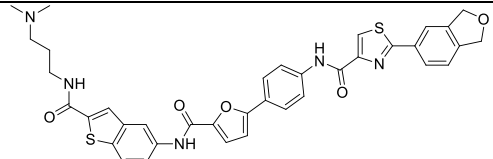
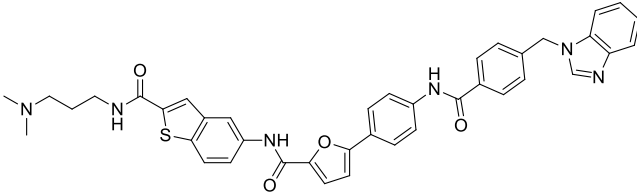
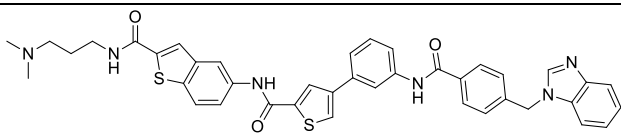
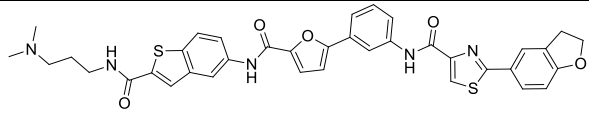
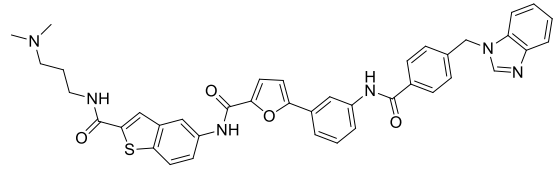
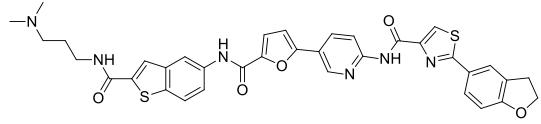
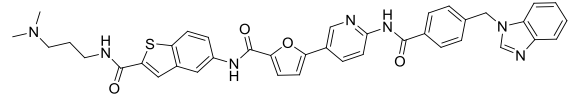
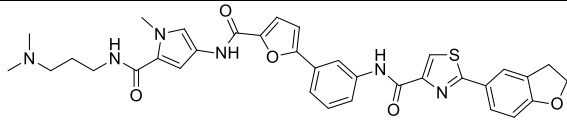
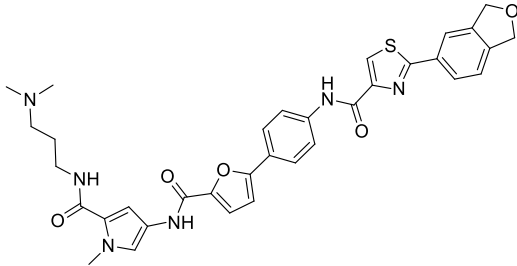
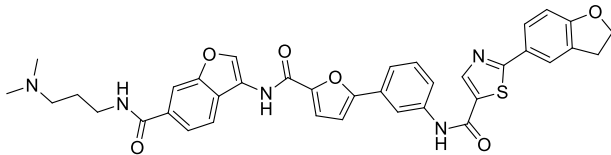
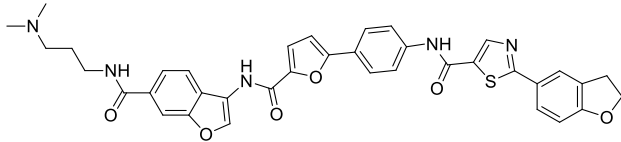
Code No.	Structure	Molecular Weight
KN-24 (4.52)		504.02
KN-78 (4.72)		692.55
KN-79 (4.74)		697.81
KN-83 (4.75)		713.39
KN-88 (4.76)		692.72
KN-89 (4.77)		697.57
KN-90 (4.78)		693.30
KN-91 (4.79)		698.53

Table 3.3: Structures of 12 member Type-2 library (continued).

Code No.	Structure	Molecular Weight
KN-110 (4.54)		639.33
KN-112 (4.55)		639.32
KN-119 (4.80)		676.13
KN-120 (4.81)		676.21

3.1.3.2.1.9 Characterization of 12 Member Type 2-A Library

Synthesised library compounds were analysed using LCMS (**Table 3.4**), IR and NMR to ascertain their purity and elucidate their structures (detail in experimental chapter). High resolution mass spectrometry (HRMS) (**Table 3.4**) was used to confirm their accurate mass.

Table 3.4: Type-2 library molecules with HRMS values found in LCMS analysis.

Code No.	Mass obtained by LCMS	Mass obtained by HRMS
KN-24 (4.52)	504.02	504.2261
KN-78 (4.72)	692.55	692.1985
KN-79 (4.74)	697.41	nt
KN-83 (4.75)	713.39	nt
KN-88 (4.76)	692.72	692.2009
KN-89 (4.77)	697.57	697.2620
KN-90 (4.78)	693.30	693.1954
KN-91 (4.79)	698.53	698.2559
KN-110 (4.54)	639.21	639.2424
KN-112 (4.55)	639.52	639.2390
KN-119 (4.80)	679.22	679.2230
KN-120 (4.81)	679.75	679.2230

nt: Not tested

3.1.3.2.2 Optimization of KN-88 and KN-119

Type-1 and Type-2 library molecules were analysed using various biophysical and biological tests, such as FRET melting assay, TRAP analysis, SRB assay, and modified TRAP, to identify the best molecules among the groups. In FRET analysis two molecules, KN-88 and KN-119, showed the highest degree of quadruplex stabilization with 21.20 and 19.00 °ΔT_m stabilization (**Table 3.11**), respectively, while showing no binding affinity for the control duplex DNA at 1μm concentration. These two molecules also showed some stabilization of other quadruplex sequences like Ckit-1(**Table 3.12**) and Ckit-2 (**Table 3.13**). In SRB assay these two molecules demonstrated significant efficacy with IC₅₀ values of 1.4μm and 0.2μm

for the pancreatic cancer cell line (**Table 3.16**), while the IC_{50} for the normal cell line was over 25.0 μ m. Considering and comparing the results obtained from the biophysical and biological assays these two molecules, KN-88 and KN-119, were considered as the lead compounds for further optimization. Again, of these two, KN-119 demonstrated a better combination of biophysical and biological results which made it the main lead molecule. The following library type compounds were then synthesized optimizing the various modification points of KN-119.

3.1.3.2.3 Type-3 Library

Following from the initial screening data of the synthesized molecules, two lead compounds, KN-88 and KN-119, were selected for further modifications. A type-2B library of 34 compounds was synthesized by modifying the structures of KN-88 and KN-119, which contain one non-variable biaryl core R3 (black) and three variable cores R1 (tail, pink), R2 (heterocyclic moiety, red) and R4 (capping acid, blue) (**Figure 3.14**). Depending on the type of modification, type-2B molecules were again classified into three groups termed as type-3A, type-3B and type-3C.

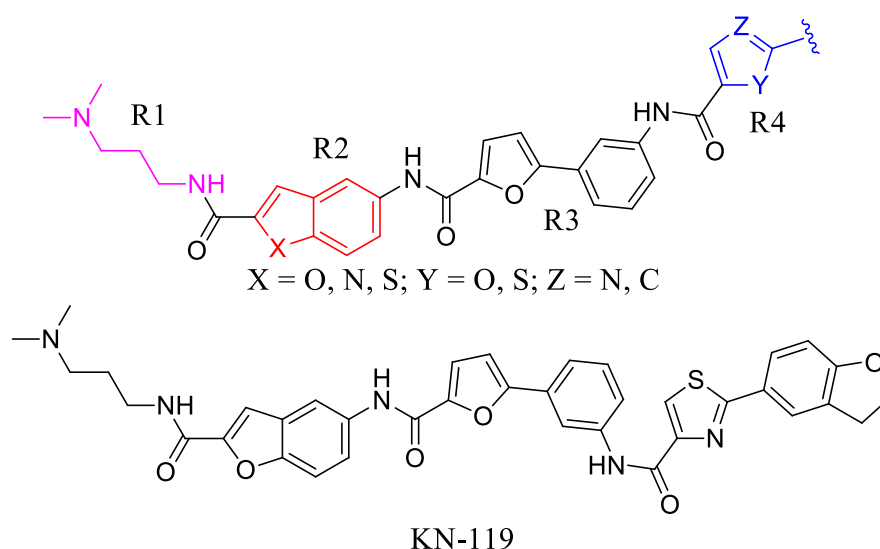


Figure 3.14: Structure of Type-2B molecules.

3.1.3.2.3.1 Type-3A Library Molecules

3.1.3.2.3.1.1 Design of Type-3A Library Molecules

Type-3A library molecules were synthesized by modification of the lead compound KN-119 containing only one variable core R2 (red) (**Figure 3.15**). The rest of the structures were kept the same for all the compounds of this library. The R2 core contains a benzofused heterocyclic ring where the heterocyclic five membered ring bears various heteroatoms such as oxygen, nitrogen and sulphur at various positions (**Figure 3.16**). The tail *N,N'*-dimethylaminopropyl facilitated purification of these compounds using a SCX-2 cartridge. The molecular weight of the molecules from this group varies from 674.77 to 755.86.

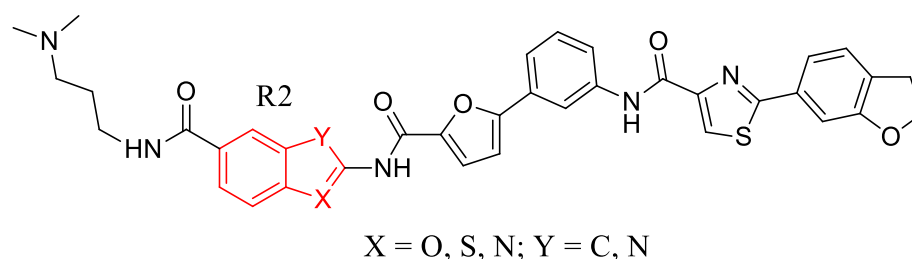


Figure 3.15: Structure of Type-3A molecules.

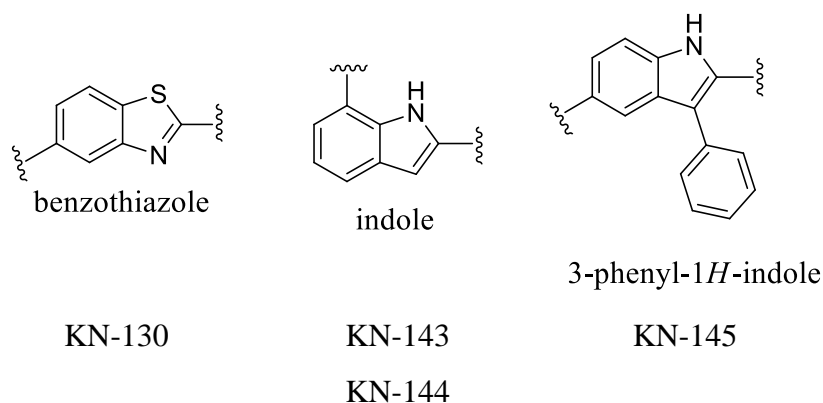
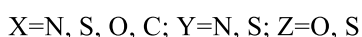
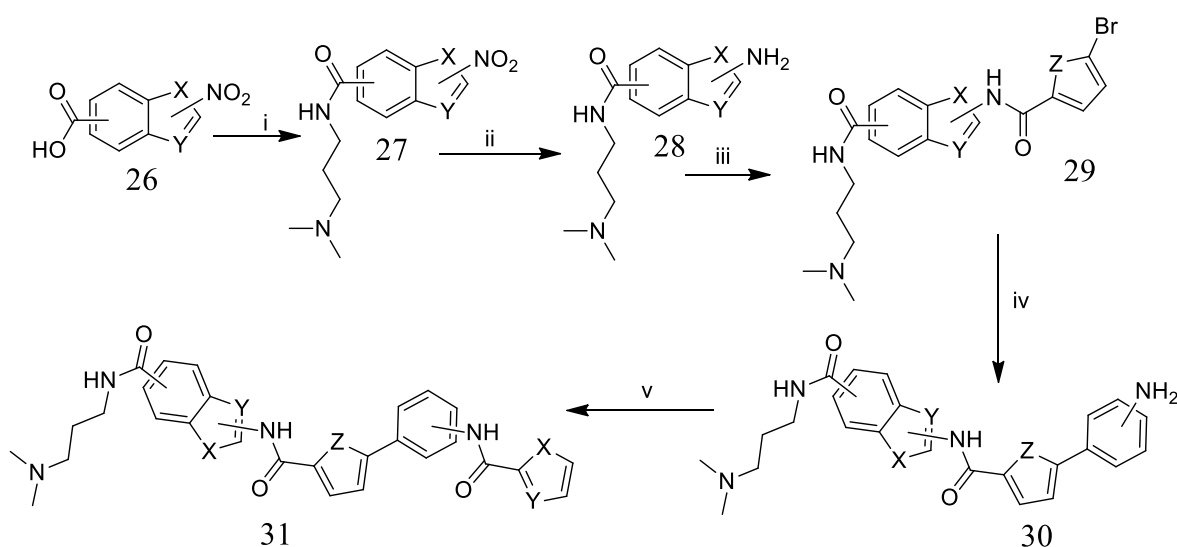


Figure 3.16: The structural variations of R2 with their linking positions. The numbers below these structures/names are the ligands in which these groups are present.

3.1.3.2.3.1.2 Synthesis of Type-3A Library Molecules

Synthesis of molecules of this group started with the commercially available starting material containing an acid and a nitro group **26** (**Scheme-3.8**). In the first step an amide coupling reaction was made between the acid **26** and the tail *N,N'*-dimethylpropylamine in the presence of DIC/HOBt to obtain intermediate product **27**. Either DCM or DMF was used as solvent depending on the solubility of the acid. The reaction was carried out at room temperature and

after 1-2 hours was found to be complete, as monitored by LCMS and TLC. Hydrogenation was then conducted to obtain product **28** from **27** in the presence of palladium on activated carbon and hydrogen gas, which reduced the nitro group to the amine. The product **29** was obtained by a DIC/HOBt mediated amide coupling reaction between **28** and bromo heterocyclic acid, which was subsequently subjected to Suzuki coupling in the presence of boronic acid, catalyst $\text{Pd}(\text{PPh}_3)_4$ and K_2CO_3 to obtain product **30**. Finally a further amide coupling reaction was carried out between **30** and the heterocyclic capping acid to obtain the final product **31** in the presence of DIC/HOBt.



Reagent and Conditions

i) *N,N*-dimethylaminopropylamine, DIC, HOBt, DCM/DMF, RT, 2 h ii) H_2 , Pd/C, 45 psi, RT, 16 h
 iii) 5-Bromo Heterocyclic acid, DIC, HOBt, DCM/DMF, RT, 3-16 h iv) Boronic acid, $\text{Pd}(\text{PPh}_3)_4$, K_2CO_3 , Ethanol:Toluene:Water-9:3:1, MW, 20 minutes
 v) Heterocyclic carboxylic acid, DIC, HOBt, DMF/DCM, RT, 3 h to over night

Scheme 3.8: General scheme for the synthesis of Type-3A library compounds.

3.1.3.2.3.1.3 Purification of Type-3A Library Compounds

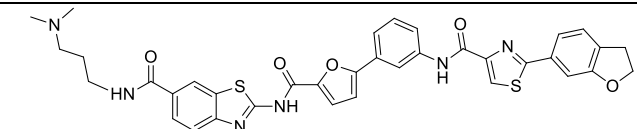
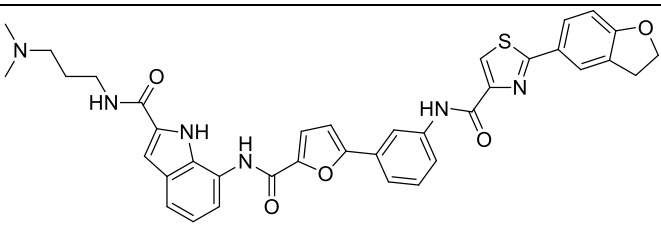
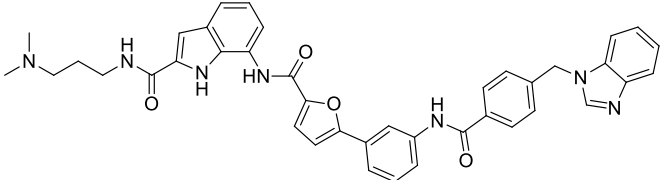
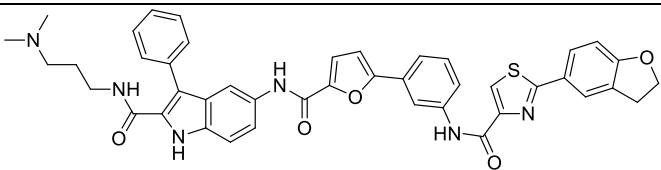
After completion of the reaction, the mixtures were initially passed through SCX-2 (silica based sulphonic acid) cartridges to catch basic compounds. Before pouring the reaction mixture in the SCX-2 cartridge, the cartridge was activated with DCM (2X) and methanol (2X). The reaction mixture was allowed to pass through the cartridge under gravity and then

washed with DCM (2X), DMF (2X) and methanol (2X) and the product was eluted with 2M NH₃ in methanol. This ensured removal of impurities and excess reagents. TLC and LCMS analysis showed that 5 of the 6 compounds were more than 95% pure and did not require further purification. KN-136 showed minor impurities by TLC. This compound was purified using flash chromatography on silica gel employing a 18:1:1 ratio of DCM:2M NH₃/methanol:methanol as the mobile phase. This provided the pure compounds in 45-85% yield after purification.

3.1.3.2.3.1.4 Structure of Type-3A Library Molecules

Structures of the synthesized molecules are listed below (**Table 3.5**).

Table 3.5: Structure of 4 member Type-3A library molecules.

Code No.	Structure	Molecular Weight
KN-130 (4.99)		692.81
KN-143 (4.100)		674.77
KN-144 (4.101)		679.77
KN-145 (4.102)		750.86

3.1.3.2.3.1.5 Characterization of Type-3A Library Molecules

The synthesised library compounds were analysed using LCMS (**Table 3.6**), IR and NMR to ascertain their purity and elucidate their structures (detail in experimental chapter). High resolution mass spectrometry (HRMS) was used to confirm their accurate mass (**Table 3.6**).

Table 3.6: HRMS and LCMS values of Type-3A library molecules.

Code No.	Mass obtained by LCMS	Mass obtained by HRMS
KN-130 (4.99)	692.55	693.1954
KN-143 (4.100)	675.30	675.2422
KN-144 (4.101)	679.74	680.2996
KN-145 (4.102)	751.25	751.2708

3.1.3.2.3.2 Type-3B Library

3.1.3.2.3.2.1 Design of Type-3B library

A 13 membered library of Type-3B compounds (**Figure 3.17**) was synthesized by modifying the final capping acid (R4) of the lead molecule KN-119. These compounds contain three non-variable cores R1 (tail), R2 (benzofused heterocyclic ring) and R3 (biaryl unit) and one variable core R4 (capping acid, red and blue, black circle). The variable core R4 has another biaryl linkage between the five membered heterocyclic ring (red) (**Figure 3.18**) and the six membered ring (blue), which is either benzofused or a six membered heterocyclic ring (**Figure 3.19**). Four molecules (KN-149, KN-150, KN-158, and KN-164) contain a methyl side chain on the five membered heterocyclic ring. All of these compounds contain the tail *N,N'*-dimethylaminopropyl which facilitates purification using an SCX-2 cartridge. The molecular weight of the molecules from this group varies from 649.72 to 703.19. Depending on the synthetic procedure these compounds can be subdivided into two groups as shown below.

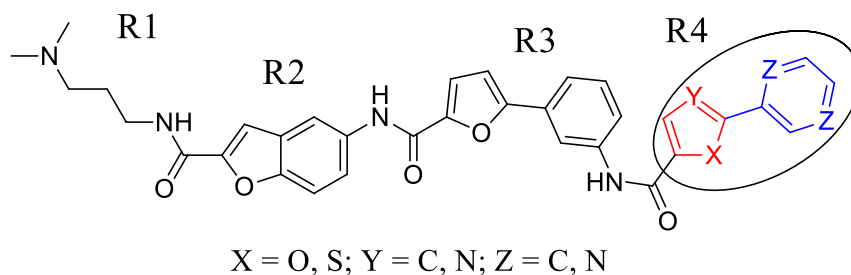


Figure 3.17: Structure of Type-3B molecules.

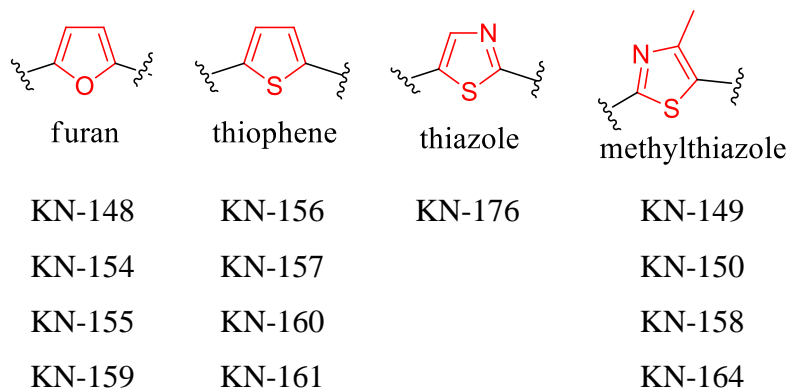


Figure 3.18: The structural variations of the five membered heterocyclic ring of R4 with linking positions. The numbers below these structures/names are the ligands in which these groups are present.

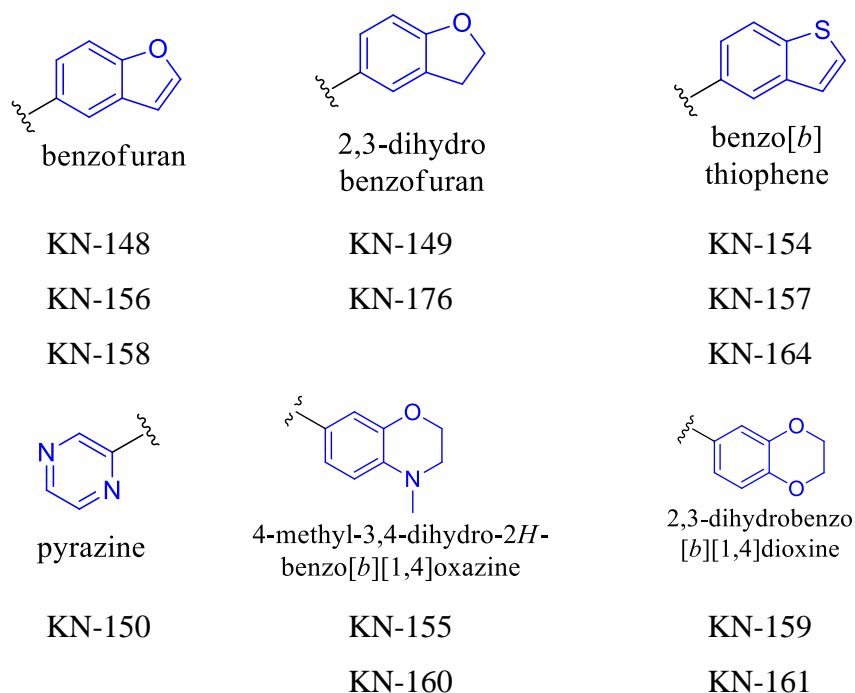
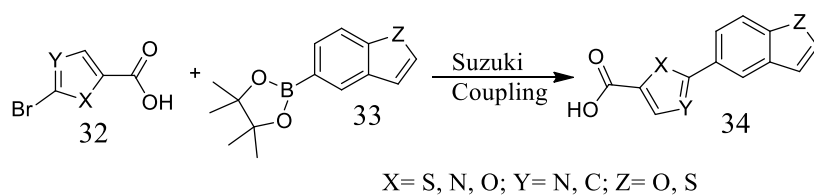


Figure 3.19: The structural variations of the six membered moieties of R4 with linking positions. The numbers below these structures/names are the ligands in which these groups are present.

3.1.3.2.3.2.2 Synthesis of Subtype-1 Molecules of Type-3B Library

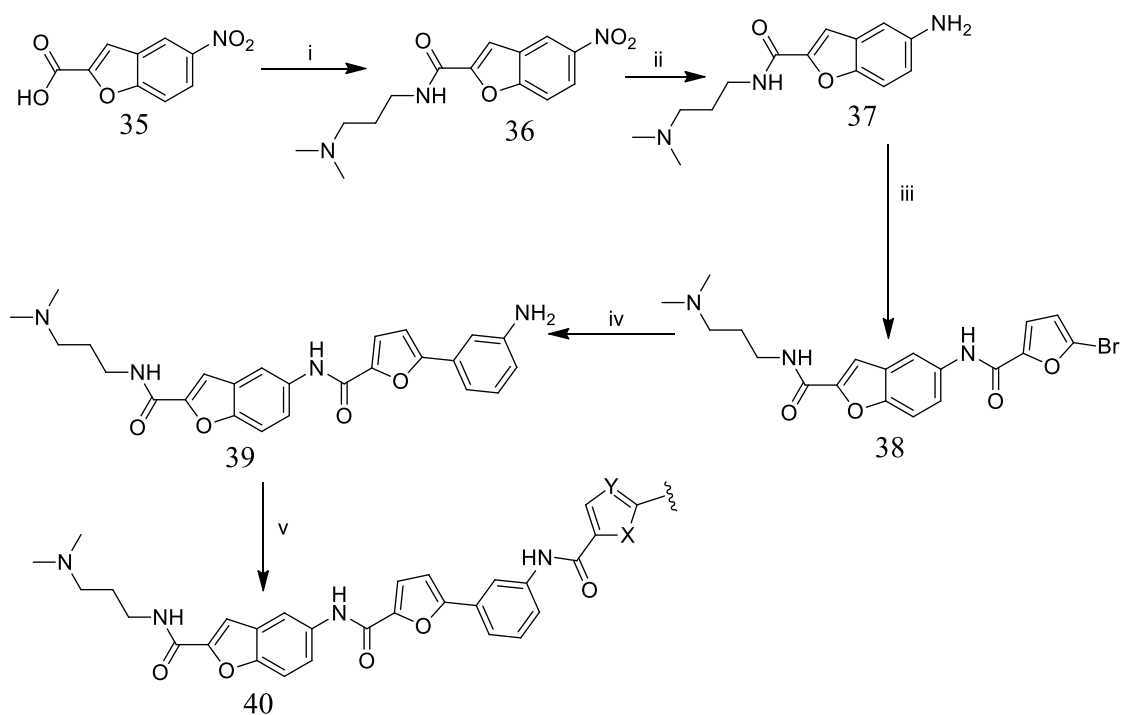
Synthesis of subtype-1 molecules of the Type-3B library (**Scheme 3.10**) started with the commercially available starting material 5-nitrobenzofuran-2-carboxylic acid (**35**) and the tail *N,N'*-dimethylaminopropyl. The amide coupling reaction between these starting materials in the presence of DIC/HOBt generated product **36** which, upon hydrogenation in the presence of Pd on activated carbon, produced **37**. Again, a typical amide coupling reaction was conducted between **37** and bromofuroic acid to obtain product **38**. Upon Suzuki coupling, product **39** was obtained from **38** which was subjected to amide coupling with the final capping acids. The final capping acids were either collected from an available commercial source or were synthesized in house by conducting a Suzuki coupling reaction between a bromo-heterocyclic acid **32** and a boronic acid **33** (**Scheme 3.9**).



Reaction conditions

Boronic acid, Pd(PPh₃)₄, K₂CO₃, Ethanol:Toluene:Water-9:3:1, MW, 20 minutes

Scheme 3.9: General scheme for the synthesis of biaryl capping acids in house.



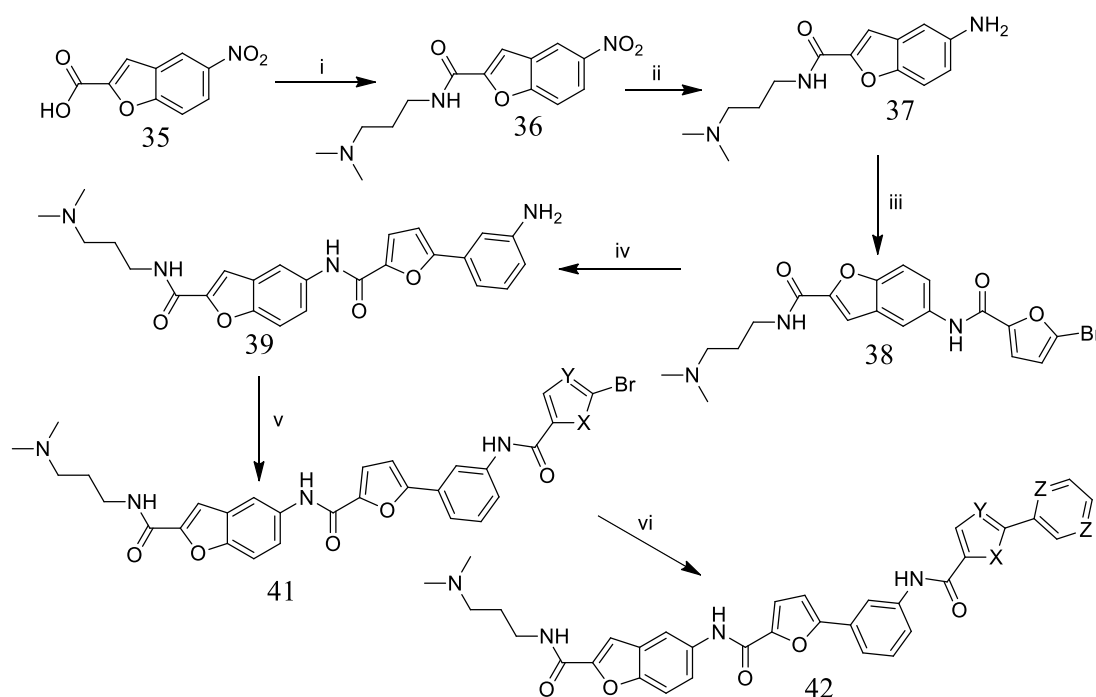
Reagent and Conditions

i) *N,N*-dimethylaminopropylamine, DIC, HOBt, DCM/DMF, RT, 2 h ii) H₂, Pd/C, 45 psi, RT, 16 h
 iii) 5-bromo Heterocyclic acid, DIC, HOBt, DCM/DMF, RT, 3-16 h iv) Boronic acid, Pd(PPh₃)₄, K₂CO₃, Ethanol:Toluene:Water-9:3:1, Microwave, 20 minutes v) Heterocyclic carboxylic acid, DIC, HOBt, DMF/DCM, RT, 3 h to over night

Scheme 3.10: General scheme for the synthesis of Sub type-1 molecules of Type-3B library.

3.1.3.2.3.2.3 Synthesis of Subtype-2 Molecules of Type-3B Library

Subtype-2 molecules of this library were synthesized following a procedure analogous to that employed for subtype-1 molecules, except for the final two steps (**Scheme 3.11**). Here, an amide coupling reaction was carried out between product **39** and various five membered bromo-heterocyclic acids in the presence of DIC and HOBt producing **41**. Then, a Suzuki coupling reaction was conducted to obtain the final product **42** and different commercially available boronic acids in the presence of the catalyst *tetrakis* triphenyl phosphine palladium and a base K_2CO_3 .



Reagent and Conditions

- i) *N,N'*-dimethylaminopropylamine, DIC, HOBt, DCM/DMF, RT, 2 h ii) H_2 , Pd/C, 45 psi, RT, 16 h
iii) 5-bromo Heterocyclic acid, DIC, HOBt, DCM/DMF, RT, 3-16 h iv) Boronic acid, $Pd(PPh_3)_4$, K_2CO_3 , Ethanol:Toluene:Water-9:3:1, MW, 20 minutes v) Heterocyclic carboxylic acid, DIC, HOBt, DMF/DCM, RT, 3 h to over night vi) Boronic acid, $Pd(PPh_3)_4$, K_2CO_3 , Ethanol:Toluene:Water-9:3:1, MW, 20-30 minutes

Scheme 3.11: General scheme for the synthesis of Sub Type-2 molecules of Type-3B library.

3.1.3.2.3.2.4 Purification of Type-3B Library Compounds

As all the molecules in this Type-3B library contained the *N,N'*-dimethylaminopropyl tail, they could be purified easily using SCX-2 cartridge methodology. A similar catch and release method as that described previously was used for purifying the compounds in this series.

TLC and LCMS analysis showed that all compounds were more than 95% pure and did not require further purification. This provided pure compounds in 45-75% yield.

3.1.3.2.3.2.5 Structure of 12 Member Type-3B Library

The structures of the synthesized molecules are listed below (**Table 3.7**).

Table 3.7: Structure of 12 Member Type-3B Library molecules.

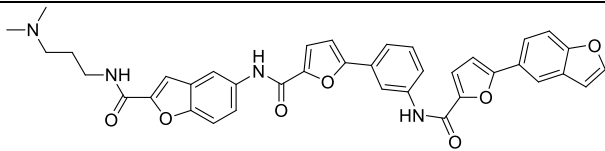
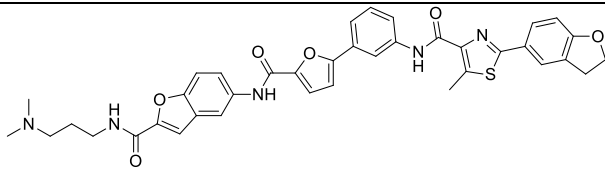
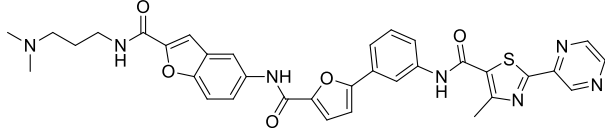
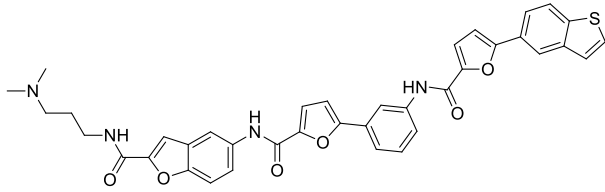
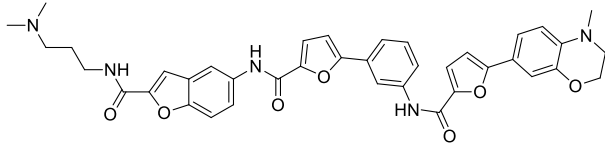
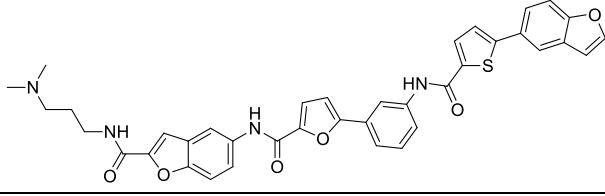
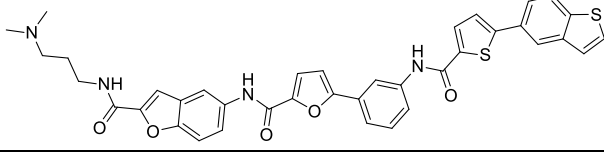
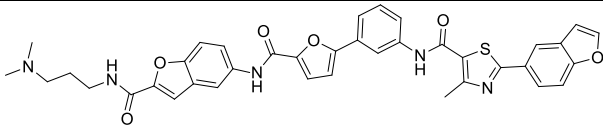
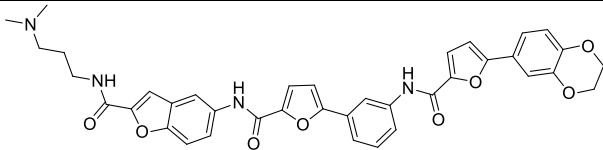
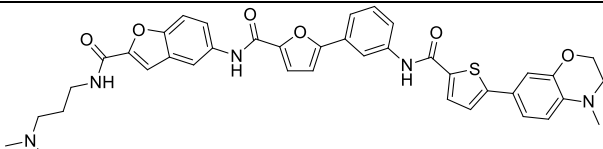
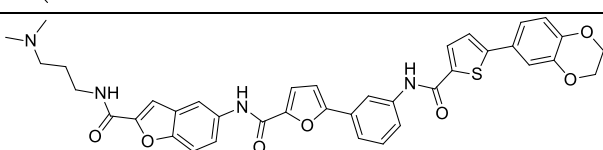
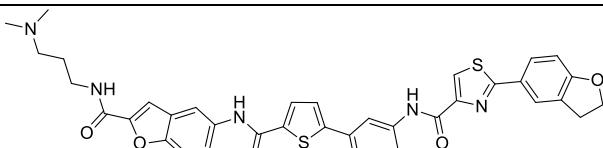
Code No.	Structure	Molecular Weight
KN-148 (4.112)		656.68
KN-149 (4.114)		689.78
KN-150 (4.116)		649.72
KN-154 (4.123)		672.75
KN-155 (4.125)		687.74
KN-156 (4.129)		672.75
KN-157 (4.130)		688.81

Table 3.7: Structure of 12 Member Type-3B Library molecules (continued).

Code No.	Structure	Molecular Weight
KN-158 (4.133)		687.76
KN-159 (4.127)		674.70
KN-160 (4.131)		703.81
KN-161 (4.132)		690.76
KN-176 (4.117)		691.82

3.1.3.2.3.2.6 Characterization of Type-3B Library Molecules

The synthesised library compounds were analysed using LCMS (**Table 3.8**), IR and NMR to ascertain their purity and elucidate their structures (detail in experimental chapter). High resolution mass spectrometry (HRMS) was used to confirm their accurate mass (**Table 3.8**).

Table 3.8: Type-3B Library molecules with HRMS and LCMS values.

Code No.	Mass obtained by LCMS	Mass obtained by HRMS
KN-148 (4.112)	656.87	657.2337
KN-149 (4.114)	690.93	690.2399
KN-150 (4.116)	649.61	650.2171
KN-154 (4.123)	672.61	673.2125
KN-155 (4.125)	688.22	688.2739
KN-156 (4.129)	673.20	673.2122
KN-157 (4.130)	689.14	689.1873
KN-158 (4.133)	687.59	688.2205
KN-159 (4.127)	675.04	675.2450
KN-160 (4.131)	704.13	704.2563
KN-161 (4.132)	690.98	691.2228
KN-176 (4.117)	691.58	692.2034

3.1.3.2.3.3 Type-3C Library

3.1.3.2.3.3.1 Design of Type-3C library

A 15 membered library of Type-3C was synthesized by modifying the R1 (tail, red) moiety of the lead molecule KN-119 (**Figure 3.20**). These compounds carry one variable part R1 and three non variable cores R2 (benzofused heterocyclic moiety), R3 (biaryl), and R4 (capping acid). The tail moiety contains various types of aromatic and heterocyclic rings (**Figure 3.21**), which are connected by an amide linkage with the R2 core and are separated by one or more carbon linkers. For one molecule of this group, the synthesis was started from an ester rather than an acid which was hydrolysed in the next step to obtain the free acid group. As these molecules do not have the typical tail of the others, the purification process varied, but most of the compounds were purified by use of an SCX-2 cartridge by the catch and release method. The molecular weight of these molecules varied from 687.76 to 777.86.

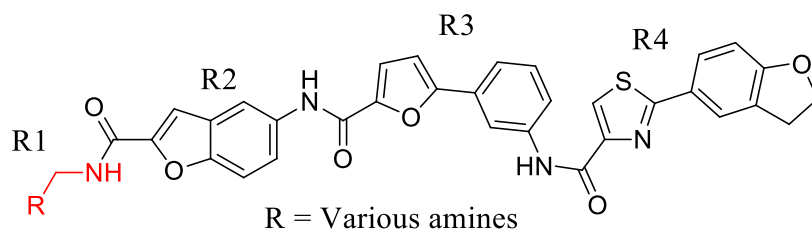


Figure 3.20: Structure of Type-3C molecules.

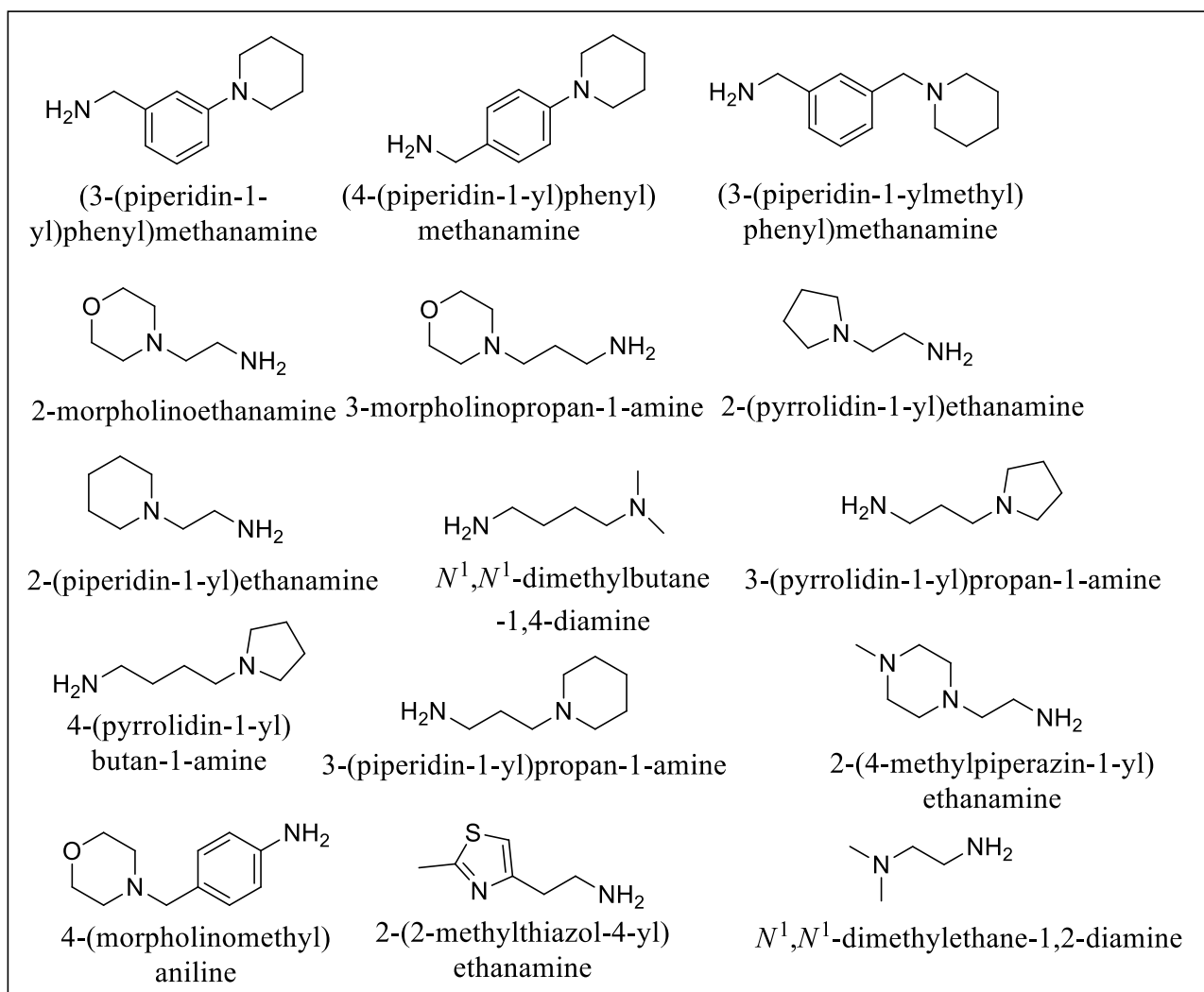
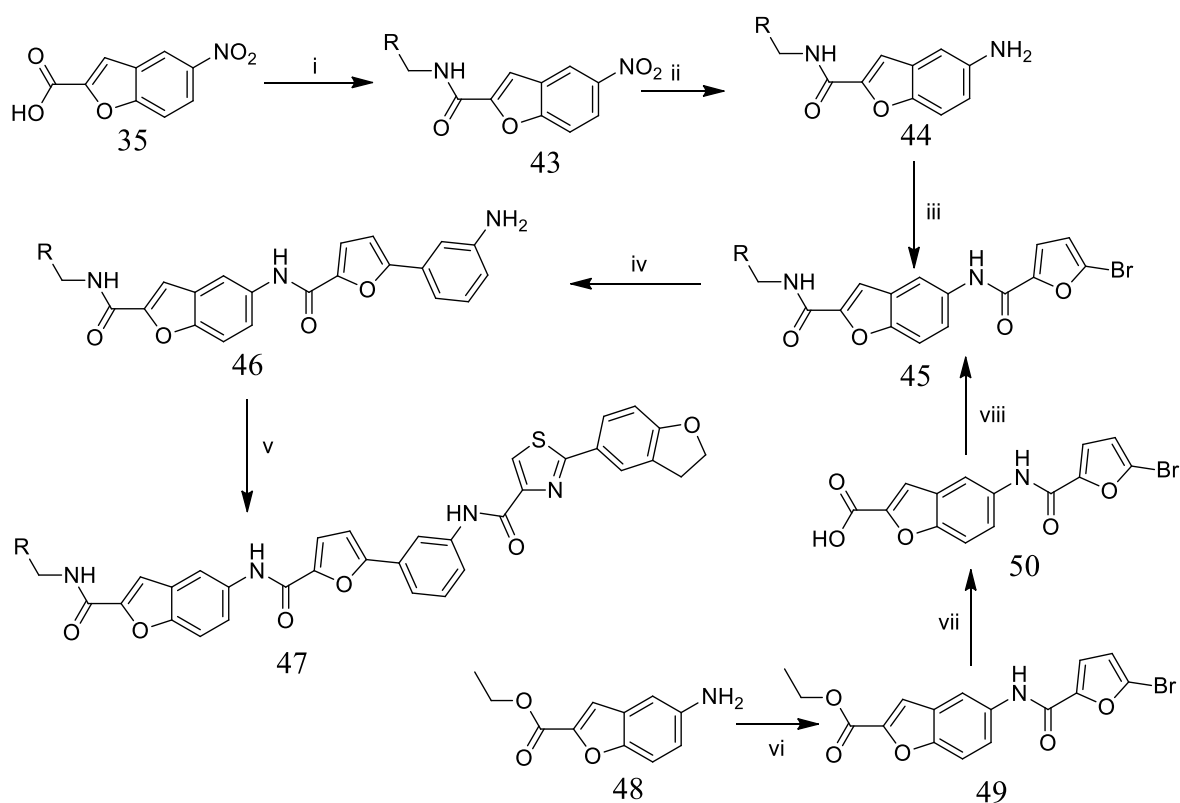


Figure 3.21: Amines used in the synthesis of Type-3C molecules.

3.1.3.2.3.2 Synthesis of Type-3C Library Molecules

Product **43** was synthesized from the commercially available starting material 5-nitrobenzofuran-2-carboxylic acid, **35** and various amines by the DIC/HOBt mediated amide

coupling reaction. As solvent, either DCM or DMF was used depending on the solubility of the corresponding starting materials. After purification, **43** was subjected to hydrogenation to convert the nitro group into an amine by following the method described earlier. The hydrogenated product **44** was then used for the next amide coupling reaction with bromofuroic acid to obtain product **45**. Suzuki coupling between **45** and 3-aminophenyl boronic acid created the biaryl linkage and the product **46** was subjected to final amide coupling with the heterocyclic acid to obtain the desired compound **47**. One of the molecules was synthesized by starting from the ester **48**, which formed an amide bond with bromofuroic acid first to form **49**. After purification, product **49** was subjected to hydrolysis, which freed the acid group for a further amide coupling reaction with the amine to form product **45**. (Scheme 3.12)



Reagent and Conditions

- i) Amine, DIC, HOBt, DCM/DMF, RT, 1-3 h ii) H₂, Pd/C, 45 psi, RT, 1.5 h
 iii) 5-bromofuroic acid, DIC, HOBt, DCM/DMF, RT, 3-16 h iv) 3-aminophenyl boronic acid, Pd(PPh₃)₄, K₂CO₃, Ethanol:Toluene:Water-9:3:1, MW, 15-30 minutes v) 2-(2,3-dihydrobenzofuran-5-yl)thiazole-4-carboxylic acid, DIC, HOBt, DMF/DCM, RT, 3 h to over night
 vi) 5-bromofuroic acid, DIC, HOBt, DCM/DMF, RT, 3 h vii) 1,4-dioxane:0.5M NaOH- 1:1, 3 h viii) Amine, DIC, HOBt, DCM/DMF, RT, 1-3 h

Scheme 3.12: General scheme for the synthesis of Sub type-1 molecules of Type-3C library.

3.1.3.2.3.3.3 Purification of Type-3C Library Compounds

Although some of the molecules from this group do not contain the *N,N*-dimethylaminopropyl tail, which facilitates the purification step, most of these compounds were purified using the SCX-2 cartridge methodology. A similar catch and release method as that described above was followed for purifying these molecules. TLC and LCMS analysis showed that all compounds were 85-95% pure with some purified further using conventional silica column chromatography. Other compounds were purified using flash chromatography and solvent of various composition and gradients was used depending on the nature of the compounds. Solvent mixtures for flash chromatography were selected from TLC results with various solvent mixtures. This provided pure compounds in 50-95% yield.

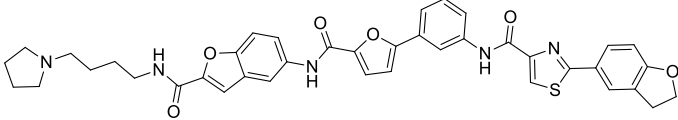
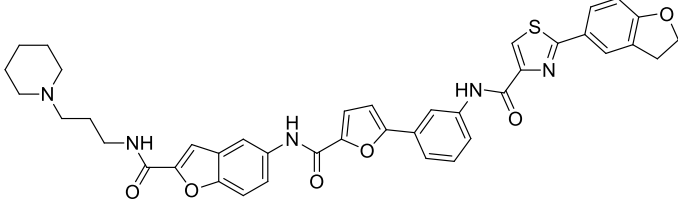
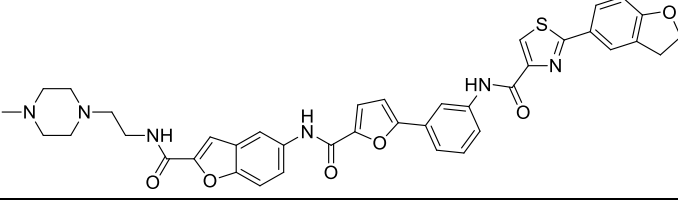
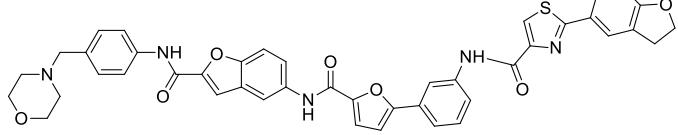
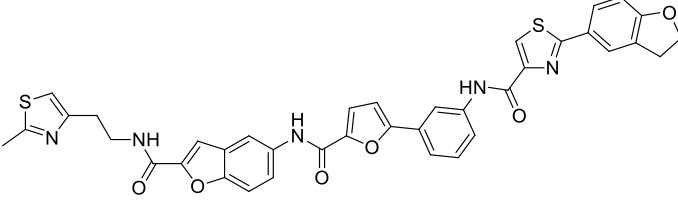
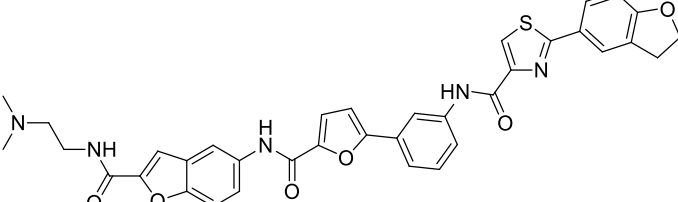
3.1.3.2.3.3.4 Structure of 14 Member Type-3C Library

Structures of the synthesized molecules are listed below (Table 3.9).

Table 3.9: Structures of Type-3C library molecules.

Code No.	Structure	Molecular Weight
KN-200 (4.210)		763.86
KN-202 (4.211)		763.86
KN-207 (4.212)		777.89
KN-212 (4.213)		701.79
KN-217 (4.214)		687.76
KN-222 (4.215)		703.76
KN-232 (4.217)		689.78
KN-237 (4.218)		701.79

Table 3.9: Structures of Type-3C library molecules (continued).

Code No.	Structure	Molecular Weight
KN-242 (4.219)		715.82
KN-247 (4.220)		715.25
KN-252 (4.221)		716.80
KN-257 (4.222)		765.83
KN-267 (4.223)		715.80
KN-272 (4.224)		661.73

3.1.3.2.3.3.5 Characterization of 14 Member Type-3C Library

The synthesised library compounds were analysed using LCMS (**Table 3.10**), IR and NMR to ascertain their purity and elucidate their structures (detail in experimental chapter). High resolution mass spectrometry (HRMS) was used to confirm their accurate mass (**Table 3.10**).

Table 3.10: Type-3C library with HRMS and LCMS values.

Code No.	Mass obtained by LCMS	Mass obtained by HRMS
KN-200 (4.210)	764.64	764.2539
KN-202 (4.211)	763.95	764.2536
KN-207 (4.212)	778.03	778.2693
KN-212 (4.213)	702.14	702.2375
KN-217 (4.214)	688.19	688.2223
KN-222 (4.215)	704.33	704.2179
KN-232 (4.217)	690.83	690.2371
KN-237 (4.218)	702.27	702.2373
KN-242 (4.219)	716.86	716.2528
KN-247 (4.220)	716.90	716.2526
KN-252 (4.221)	717.64	717.2483
KN-257 (4.222)	766.42	766.2313
KN-267 (4.223)	716.36	716.1622
KN-272 (4.224)	662.28	662.2063

3.2 Results and Discussion: Biological

FRET analyses of all synthesized molecules were carried out by me. FRET analysis and other biological analysis of some of the synthesized molecules was carried out by Sunil Lagh of the UCL School of Pharmacy

3.2.1 Biophysical Evaluation of the Biaryl Polyamide Series

3.2.2 Fluorescence Resonance Energy Transfer (FRET) Melting Assay

The binding and stabilizing potential of all the synthesized biaryl polyamide ligands were investigated against a series of oligonucleotide sequences like the F21T, Duplex, ckit1, ckit2, cmcy, DRH, and CDRH.

The FRET data (**Table 3.11**) demonstrated that some molecules, such as KN-88, KN-119, and KN-242, have a significant level of G-quadruplex stabilizing ability against the F21T sequence with ΔT_m values ranging from 22 °C to 34 °C, while a few molecules have moderate stabilizing potential (9-19 ΔT_m °C). Several other compounds showed mild G-

quadruplex stabilizing ability (2-7 ΔT_m °C) against the F21T sequence. The rest of the series have low to zero stabilizing ability. On the contrary, the biaryl polyamide molecules demonstrated negligible binding potential towards the duplex DNA (**Appendix, Table AP1**). Again, these molecules showed no stabilization of the DRH sequence (**Appendix, Table AP4**) while a few of the compounds showed low binding affinity towards the CDRH sequence (**Appendix, Table AP5**) having a ΔT_m value near 3 °C. Only, KN-148 had mild activity (7 ΔT_m °C) against cmyc (**Table 3.14**), whereas a few of the other molecules showed low to zero stabilization potential. KN-242 demonstrated good stabilization of both ckit1 (**Table 3.11**) and ckit2 (**Table 3.12**) with ΔT_m values of 16 °C and 13 °C, respectively. Along with KN-242, KN-148, KN-247 and KN-252 showed significant stabilization of the ckit2 sequence where the highest stabilization was achieved by KN-148 (13 ΔT_m °C).

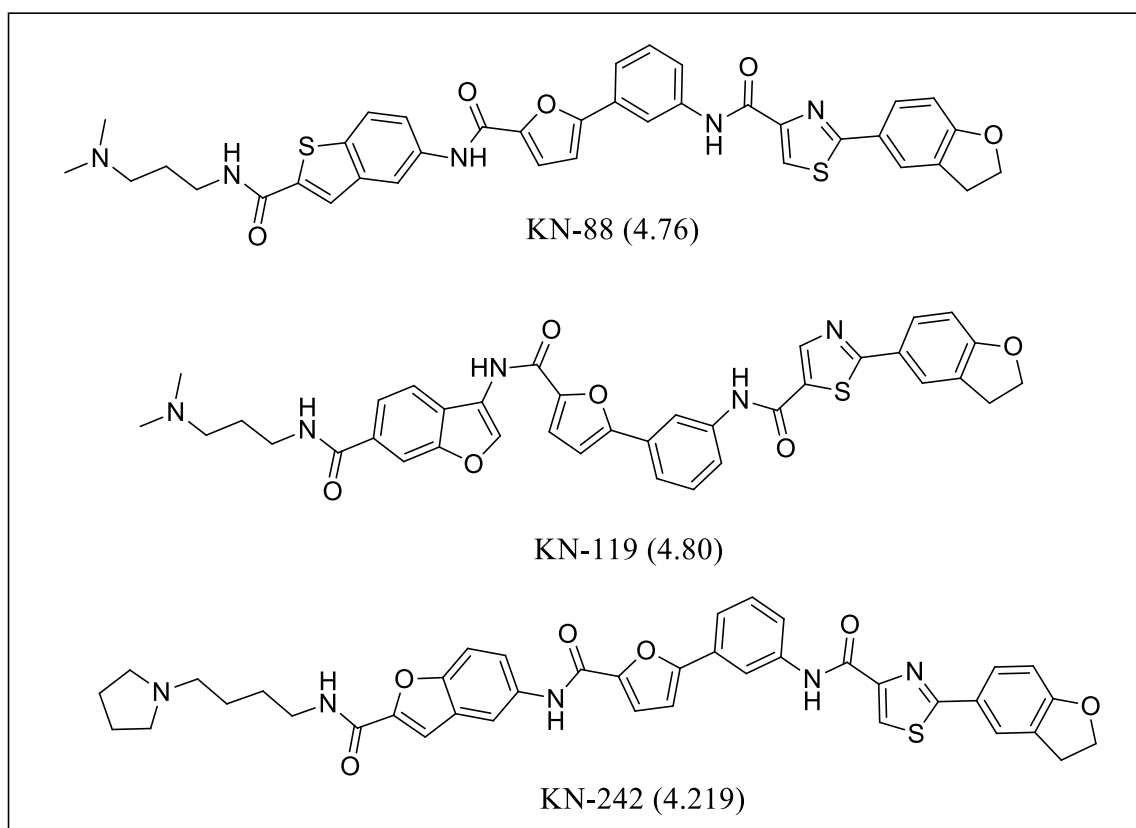


Figure 3.22: Structure of lead molecules and the most active molecule after lead optimization.

Among the analysed molecules, FRET data demonstrates that KN-232, KN-237, KN-242, and KN-247 [$c=1\ \mu\text{M}$] showed significantly high G-quadruplex stabilizing potential for F21T with a ΔT_m of 22-34 °C (**Table 3.11**). KN-242 and KN-247 showed the highest level of G-quadruplex stabilization with ΔT_m values of 34.43 °C (standard deviation ± 0.21) and 28.53 °C (standard deviation ± 1.32), respectively at 1 μM . This level of stabilization is significantly higher than the conventional G-quadruplex binding ligands such as BRACO-19, telomestatin and the recently developed acridone and naphthalene diimide (ND) G-quadruplex targeting agents showing ΔT_m s of 20-30 °C [250, 251]. One recently developed G-quadruplex binding ligand from an acridine based triaryl-substituted imidazole derivative, TSIZ01 (**1.82**), showed G-quadruplex stabilization of 32 °C at 3 μM and 23.5 °C at 1 μM concentration for F21T [311]. Again, KN-88, KN-119, KN-148, KN-158, KN-212 and KN-217 showed a moderate level of G-quadruplex stabilization potential with ΔT_m values ranging from 14 °C to 21 °C at 1 μM concentration against F21T, while KN-252 (ΔT_m 12.40 °C), KN-227 (ΔT_m 9.38 °C), KN-161 (ΔT_m 7.03 °C) and KN-207 (ΔT_m 6.95 °C) showed mild activity. Moreover, the biaryl-polyamides have better selectivity towards the G-quadruplex DNA over duplex DNA as these molecules showed negligible stabilization of duplex DNA compared with their acridone and ND derivatives. The $[\Delta T_m]_{\text{Quadruplex}}: [\Delta T_m]_{\text{Duplex}}$ ratio for the aryl-polyamides is extremely high (<300), whereas this ratio for the acridone/ND is relatively low ($\sim 3-10$). Therefore, in contrast with current G-quadruplex ligands in the literature, the greater degree of stabilization, as well as the extremely high level of selectivity of the synthesized biaryl polyamide ligands towards the F21T over the duplex DNA makes the aryl polyamide series a candidate for further investigations.

Table 3.11: ΔT_m values for F21T at 5 μm , 2 μm , and 1 μm concentrations with standard deviations.

ΔT_m values for F21T				
Code	MW	5 μm	2 μm	1 μm
KN-24 (4.52)	504.02	6.90 ± 0.20	2.43 ± 0.69	0.53 ± 0.10
KN-39 (4.9)	491.11	4.93 ± 0.00	2.20 ± 0.06	0.43 ± 0.12
KN-40 (4.10)	507.38	0.00 ± 0.06	0.00 ± 0.12	0.00 ± 0.00
KN-41(4.11)	507.15	0.07 ± 0.10	0.00 ± 0.05	0.00 ± 0.12
KN-45 (4.13)	543.00	0.27 ± 0.05	0.00 ± 0.12	0.00 ± 0.05
KN-46 (4.14)	527.10	4.77 ± 0.11	3.00 ± 0.12	0.23 ± 0.17
KN-47 (4.15)	543.05	1.77 ± 0.17	1.00 ± 0.05	0.17 ± 0.12
KN-48 (4.17)	529.96	0.33 ± 0.05	0.13 ± 0.10	0.10 ± 0.11
KN-49 (4.18)	528.94	1.07 ± 0.12	0.63 ± 0.17	0.33 ± 0.05
KN-50 (4.19)	512.99	0.63 ± 0.05	1.60 ± 0.05	1.10 ± 0.12
KN-51 (4.21)	489.17	1.90 ± 0.05	1.20 ± 0.12	0.73 ± 0.11
KN-52 (4.22)	490.14	1.97 ± 0.17	1.70 ± 0.05	0.97 ± 0.05
KN-53 (4.23)	473.13	0.70 ± 0.11	0.43 ± 0.12	0.57 ± 0.11
KN-54 (4.25)	499.85	0.83 ± 0.12	0.67 ± 0.06	0.63 ± 0.06
KN-55 (4.26)	499.92	1.43 ± 0.06	1.33 ± 0.10	0.70 ± 0.13
KN-56 (4.27)	483.88	0.77 ± 0.10	0.47 ± 0.06	0.00 ± 0.12
KN-57 (4.29)	539.09	1.17 ± 0.12	0.33 ± 0.00	0.00 ± 0.11
KN-58 (4.30)	539.09	1.00 ± 0.12	0.20 ± 0.00	0.00 ± 0.10
KN-59 (4.31)	523.12	0.00 ± 0.06	0.00 ± 0.10	0.00 ± 0.17
KN-60 (4.33)	554.99	0.03 ± 0.00	0.00 ± 0.06	0.00 ± 0.00

Table 3.11: ΔT_m values for F21T at 5 μm , 2 μm , and 1 μm concentrations with standard deviations (continued).

ΔT_m values for F21T				
Code	MW	5 μm	2 μm	1 μm
KN-61 (4.34)	554.99	0.60 ± 0.10	0.37 ± 0.17	0.07 ± 0.12
KN-62 (4.35)	539.05	2.93 ± 0.06	1.40 ± 0.2	1.00 ± 0.00
KN-78 (4.72)	692.55	1.27 ± 0.12	0.60 ± 0.11	0.47 ± 0.05
KN-79 (4.74)	697.81	3.40 ± 0.10	1.83 ± 0.17	0.50 ± 0.10
KN-83 (4.75)	713.39	6.50 ± 0.28	3.73 ± 0.37	1.73 ± 0.11
KN-88 (4.76)	692.72	36.37 ± 0.51	32.77 ± 1.09	21.20 ± 0.74
KN-89 (4.77)	697.57	18.50 ± 0.39	7.67 ± 0.20	3.13 ± 0.14
KN-90 (4.78)	693.30	0.87 ± 0.12	0.53 ± 0.00	0.23 ± 0.11
KN-91 (4.79)	698.53	0.93 ± 0.17	0.60 ± 0.22	0.03 ± 0.17
KN-110 (4.54)	639.33	4.00 ± 0.17	7.83 ± 0.12	2.07 ± 0.12
KN-112 (4.55)	639.32	1.463 ± 0.00	0.835 ± 0.05	0.632 ± 0.10
KN-119 (4.80)	676.13	22.18 ± 0.05	20.18 ± 0.10	19.00 ± 0.00
KN-120 (4.81)	676.21	6.15 ± 0.17	4.85 ± 0.34	2.95 ± 0.36
KN-130 (4.99)	692.81	22.48 ± 0.35	8.55 ± 1.00	3.85 ± 0.30
KN-143 (4.100)	674.77	21.51 ± 0.20	9.51 ± 1.16	5.01 ± 0.81
KN-144 (4.101)	679.77	20.38 ± 0.30	9.31 ± 0.05	5.78 ± 0.45
KN-145 (4.102)	750.86	25.51 ± 1.41	16.11 ± 0.64	10.15 ± 0.17
KN-148 (4.112)	656.68	17.38 ± 0.11	17.55 ± 0.25	15.45 ± 0.21
KN-149 (4.114)	689.78	7.45 ± 0.36	3.01 ± 0.55	1.85 ± 0.20

Table 3.11: ΔT_m values for F21T at 5 μm , 2 μm , and 1 μm concentrations with standard deviations (continued).

ΔT_m values for F21T				
Code	MW	5 μm	2 μm	1 μm
KN-150 (4.116)	649.72	2.50 ± 0.32	1.13 ± 0.45	0.96 ± 0.17
KN-154 (4.123)	672.75	5.50 ± 1.18	2.70 ± 0.32	2.26 ± 0.17
KN-155 (4.125)	687.74	11.53 ± 2.31	2.00 ± 0.58	0.76 ± 0.20
KN-156 (4.129)	672.75	1.93 ± 0.40	1.46 ± 0.34	0.56 ± 0.20
KN-157 (4.130)	688.81	1.86 ± 0.50	1.00 ± 0.05	0.80 ± 0.11
KN-158 (4.133)	687.76	21.53 ± 0.41	20.60 ± 0.29	18.00 ± 0.31
KN-159 (4.127)	674.71	28.80 ± 2.10	6.56 ± 0.28	2.23 ± 0.23
KN-160 (4.131)	703.81	11.96 ± 0.36	6.23 ± 1.00	2.63 ± 0.75
KN-161 (4.132)	690.76	19.26 ± 0.10	11.2 ± 0.15	7.03 ± 0.63
KN-176 (4.117)	691.82	8.11 ± 0.07	5.36 ± 0.20	3.77 ± 0.46
KN-200 (4.210)	763.86	1.18 ± 0.10	0.88 ± 0.10	0.22 ± 0.55
KN-202 (4.211)	763.86	2.45 ± 0.21	1.35 ± 0.15	1.05 ± 0.06
KN-207 (4.212)	777.89	-2.32 ± 0.10	10.48 ± 0.36	6.95 ± 0.06
KN-212 (4.213)	701.79	23.02 ± 0.38	18.28 ± 0.50	14.98 ± 0.20
KN-217 (4.214)	687.76	27.12 ± 0.25	21.02 ± 0.06	16.15 ± 0.55
KN-222 (4.215)	703.76	12.85 ± 0.12	8.95 ± 0.23	7.25 ± 0.25
KN-232 (4.217)	689.78	42.38 ± 0.35	34.46 ± 3.98	22.38 ± 2.61
KN-237 (4.218)	701.79	40.96 ± 1.20	29.73 ± 2.12	22.03 ± 1.83
KN-242 (4.219)	715.82	41.78 ± 0.92	40.53 ± 1.11	34.43 ± 0.21
KN-247 (4.220)	715.25	40.03 ± 0.40	35.03 ± 3.53	28.53 ± 1.32

Table 3.11: ΔT_m values for F21T at 5 μm , 2 μm , and 1 μm concentrations with standard deviations (continued).

ΔT_m values for F21T				
Code	MW	5 μm	2 μm	1 μm
KN-252 (4.221)	716.80	40.46 ± 1.10	31.66 ± 4.66	12.40 ± 0.15
KN-257 (4.222)	765.83	-0.53 ± 2.36	0.10 ± 0.05	0.86 ± 0.47
KN-267 (4.223)	715.80	-0.70 ± 1.61	1.23 ± 0.86	1.90 ± 3.11
KN-272 (4.224)	661.73	37.80 ± 3.23	9.967 ± 0.93	4.58 ± 0.21

cKit-1 (**Table 3.12** and **AP2**) and c-Kit-2 (**Table 3.13** and **AP3**) sequences are non-telomeric sequences with G-quadruplex forming potential. Among the analysed molecules, only KN-242 showed good stabilization ability against both sequences with ΔT_m values of 16.550 °C and 12.733 °C, respectively at a 1 μm concentration. However, KN-148, KN-242, KN-247 and KN-252 showed a significant level of cKit-2 stabilization having a ΔT_m value of 10-13 °C. KN-88 and KN-119 [$c=1 \mu\text{m}$], with good F21T stabilization potential, however, demonstrated low stabilization, with ΔT_{ms} of ~5-6 °C and ~3-4 °C for cKit-1 and cKit-2, respectively. On the contrary, the ND derivative compound 1, Braco-19 and TMPyP4 (**1.32**) [$c=0.5 \mu\text{m}$] showed significant stabilization, with ΔT_{ms} of ~18-29 °C and ~6-12 °C for cKit-1 and cKit-2, respectively [252].

Table 3.12: ΔT_m values for C-Kit1 at 5 μm , 2 μm , and 1 μm concentrations with standard deviations.

ΔT_m values for C-kit1				
Code	MW	5 μm	2 μm	1 μm
KN-39 (4.9)	491.11	2.75 ± 0.12	2.36 ± 0.20	2.23 ± 0.17
KN-78 (4.72)	692.55	1.78 ± 0.05	2.38 ± 0.12	1.19 ± 0.62
KN-88 (4.76)	692.72	3.80 ± 0.00	20.37 ± 0.12	6.24 ± 0.20
KN-89 (4.77)	697.57	3.86 ± 0.12	0.73 ± 0.05	2.11 ± 0.70
KN-119 (4.80)	676.13	10.028 ± 0.52	8.02 ± 0.14	5.50 ± 0.09
KN-120 (4.81)	676.21	4.48 ± 0.50	2.28 ± 0.32	2.51 ± 0.52
KN-130 (4.99)	692.81	4.91 ± 0.28	1.38 ± 0.21	1.25 ± 0.21
KN-143 (4.100)	674.77	14.46 ± 0.63	5.22 ± 0.42	1.88 ± 0.45
KN-144 (4.101)	679.77	2.72 ± 0.00	4.48 ± 0.96	2.98 ± 0.61
KN-145 (4.102)	750.86	24.91 ± 0.36	10.11 ± 2.40	6.48 ± 0.47
KN-148 (4.112)	656.68	4.03 ± 0.12	2.95 ± 0.10	2.01 ± 0.00
KN-149 (4.114)	689.78	3.05 ± 0.46	2.01 ± 0.28	1.05 ± 0.38
KN-150 (4.116)	649.72	4.88 ± 0.46	2.82 ± 0.17	2.31 ± 0.69
KN-154 (4.123)	672.75	13.91 ± 0.10	1.95 ± 0.20	2.08 ± 0.55
KN-155 (4.125)	687.74	10.81 ± 0.49	3.55 ± 0.40	1.48 ± 0.40
KN-156 (4.129)	672.75	2.08 ± 0.85	0.71 ± 0.11	1.51 ± 0.92
KN-159 (4.127)	674.70	29.31 ± 0.45	12.4 ± 2.75	7.38 ± 0.42
KN-160 (4.131)	703.81	14.25 ± 1.45	7.71 ± 1.04	5.25 ± 0.46

Table 3.12: ΔT_m values for C-Kit1 at 5 μm , 2 μm , and 1 μm concentrations with standard deviations (continued).

ΔT_m values for C-kit1				
Code	MW	5 μm	2 μm	1 μm
KN-161 (4.132)	690.76	43.93 ± 0.63	7.85 ± 1.30	4.85 ± 0.90
KN-176 (4.117)	691.82	12.43 ± 0.77	5.01 ± 0.30	4.38 ± 0.00
KN-212 (4.213)	701.79	4.81 ± 0.23	3.29 ± 0.52	2.01 ± 0.11
KN-217 (4.214)	687.76	3.12 ± 0.51	2.10 ± 0.29	1.140 ± 0.10
KN-232 (4.217)	689.78	36.81 ± 1.55	11.81 ± 3.89	4.35 ± 0.61
KN-237 (4.218)	701.79	35.68 ± 2.34	12.18 ± 0.20	5.25 ± 1.11
KN-242 (4.219)	715.82	41.58 ± 0.90	27.51 ± 1.27	16.55 ± 3.42
KN-247 (4.220)	715.25	39.85 ± 0.30	16.5 ± 3.44	3.05 ± 3.40
KN-252 (4.221)	716.80	35.75 ± 3.57	16.81 ± 1.80	4.78 ± 0.35
KN-267 (4.223)	715.80	2.31 ± 0.20	0.48 ± 0.30	1.18 ± 0.81
KN-272 (4.224)	661.73	28.95 ± 1.72	8.41 ± 2.65	3.58 ± 1.10

Table 3.13: ΔT_m values for C-kit2 at 5 μm , 2 μm , and 1 μm concentrations with standard deviations.

ΔT_m values for C-kit2				
Code	MW	5 μm	2 μm	1 μm
KN-88 (4.76)	692.72	22.66 ± 0.40	7.67 ± 0.53	3.00 ± 0.21
KN-89 (4.77)	697.57	7.78 ± 0.02	8.31 ± 0.83	6.40 ± 0.00
KN-90 (4.78)	693.30	2.53 ± 0.16	2.58 ± 0.20	2.37 ± 0.30
KN-119 (4.80)	676.13	8.33 ± 0.07	6.03 ± 0.23	4.30 ± 0.10
KN-120 (4.81)	676.21	9.03 ± 1.22	5.12 ± 0.23	2.69 ± 0.08
KN-130 (4.99)	692.81	13.38 ± 0.71	6.29 ± 0.11	2.93 ± 0.82
KN-150 (4.116)	649.72	3.18 ± 0.71	1.15 ± 0.10	1.03 ± 0.10
KN-154 (4.123)	672.75	11.75 ± 0.58	9.02 ± 0.66	7.02 ± 0.05
KN-155 (4.125)	687.74	15.01 ± 0.20	10.29 ± 0.23	4.61 ± 0.12
KN-159 (4.127)	674.70	26.21 ± 0.66	13.76 ± 0.28	5.42 ± 0.53
KN-160 (4.131)	703.81	11.85 ± 0.88	6.03 ± 0.09	3.62 ± 0.12
KN-161 (4.132)	690.76	18.53 ± 0.90	10.42 ± 0.19	6.92 ± 0.28
KN-176 (4.117)	691.82	-7.86 ± 1.01	3.02 ± 0.24	1.05 ± 0.29
KN-207 (4.212)	777.89	9.33 ± 0.40	6.13 ± 0.61	3.67 ± 0.25
KN-212 (4.213)	701.79	17.50 ± 1.15	7.87 ± 0.12	3.87 ± 0.25
KN-217 (4.214)	687.76	18.43 ± 0.64	8.53 ± 0.95	5.30 ± 0.36
KN-222 (4.215)	703.76	11.53 ± 0.50	6.90 ± 0.53	4.63 ± 0.47
KN-232 (4.217)	689.78	23.46 ± 1.38	11.46 ± 1.57	4.63 ± 0.90
KN-237 (4.218)	701.79	23.83 ± 1.30	11.63 ± 2.09	5.46 ± 1.79
KN-242 (4.219)	715.82	17.83 ± 2.91	17.67 ± 0.77	12.73 ± 0.75

Table 3.13: ΔT_m values for C-kit2 at 5 μm , 2 μm , and 1 μm concentrations with standard deviations (continued).

ΔT_m values for C-kit2				
Code	MW	5 μm	2 μm	1 μm
KN-247 (4.220)	715.25	20.46 ± 0.85	16.33 ± 0.36	11.80 ± 1.38
KN-252 (4.221)	716.80	24.60 ± 0.11	15.10 ± 0.56	10.67 ± 1.41
KN-257 (4.222)	765.83	2.73 ± 0.96	1.30 ± 0.53	1.20 ± 0.03
KN-267 (4.223)	715.80	1.67 ± 0.97	2.30 ± 0.66	1.97 ± 0.15
KN-272 (4.224)	661.73	19.87 ± 1.68	10.27 ± 1.15	6.13 ± 0.26

The compounds were investigated against c-Myc (**Table 3.14**), DNA/RNA hybrid duplex (DRH) (**Appendix, Table AP4**) sequence, and cDRH sequence (**Appendix, Table AP5**) (control DNA hairpin sequence, where U of DRH sequence was replaced with T). No significant stabilization was observed against any of the sequences. Only, KN-148 demonstrated a very mild level of stabilization against the C-myc sequence with a ΔT_m of 6.933 $^{\circ}\text{C}$ at 1 μm concentration.

Table 3.14: ΔT_m values for C-myc at 5 μm , 2 μm , and 1 μm concentrations with standard deviations.

ΔT_m values for C-myc				
Code	MW	5 μm	2 μm	1 μm
KN-45 (4.13)	543.00	0.36 ± 0.40	1.57 ± 0.02	1.40 ± 0.57
KN-46 (4.14)	527.10	0.30 ± 1.79	1.70 ± 0.39	2.133 ± 0.64
KN-47 (4.15)	543.05	0.60 ± 0.31	1.23 ± 0.59	1.37 ± 0.08
KN-48 (4.17)	529.96	1.23 ± 0.48	-0.60 ± 2.66	1.27 ± 0.44
KN-56 (4.27)	483.88	-0.13 ± 0.08	0.60 ± 0.25	1.00 ± 0.13
KN-88 (4.76)	692.72	5.50 ± 0.20	2.87 ± 0.13	2.43 ± 0.15
KN-91 (4.79)	698.53	1.33 ± 0.13	1.07 ± 0.15	1.37 ± 0.28
KN-119 (4.80)	676.13	9.33 ± 0.70	4.66 ± 0.15	3.03 ± 0.58
KN-120 (4.81)	676.21	3.13 ± 0.15	2.67 ± 0.11	2.200 ± 0.10
KN-130 (4.99)	692.81	5.70 ± 0.10	3.17 ± 0.08	2.43 ± 0.15
KN-143 (4.100)	674.77	6.73 ± 0.28	2.67 ± 0.08	2.27 ± 0.05
KN-144 (4.101)	679.77	8.67 ± 1.60	1.67 ± 0.36	2.23 ± 0.15
KN-145 (4.102)	750.86	10.40 ± 0.00	4.63 ± 0.15	3.50 ± 0.00
KN-148 (4.112)	656.68	10.30 ± 0.00	10.30 ± 0.00	6.93 ± 0.22
KN-149 (4.114)	689.78	2.30 ± 0.00	2.07 ± 0.71	2.20 ± 0.10
KN-150 (4.116)	649.72	4.60 ± 0.25	2.60 ± 0.17	2.03 ± 0.89
KN-200 (4.210)	763.86	2.03 ± 0.13	2.00 ± 0.10	2.00 ± 0.10
KN-202 (4.211)	763.86	1.87 ± 0.08	1.50 ± 1.05	2.33 ± 0.21
KN-207 (4.212)	777.89	3.10 ± 0.10	2.43 ± 0.15	2.67 ± 0.28
KN-212 (4.213)	701.79	9.67 ± 0.15	4.20 ± 0.40	2.60 ± 0.10

Table 3.14: ΔT_m values for C-myc at 5 μm , 2 μm , and 1 μm concentrations with standard deviations (continued).

ΔT_m values for C-myc				
Code	MW	5 μm	2 μm	1 μm
KN-217 (4.214)	687.76	10.30 ± 0.00	4.50 ± 0.17	2.73 ± 0.08
KN-222 (4.215)	703.76	4.87 ± 0.08	2.83 ± 0.13	2.87 ± 0.08
KN-232 (4.217)	689.78	15.77 ± 1.41	3.70 ± 3.35	1.80 ± 0.05
KN-242 (4.219)	715.82	8.53 ± 0.11	9.63 ± 1.78	2.80 ± 1.10
KN-247 (4.220)	715.25	13.70 ± 0.35	9.57 ± 0.51	3.33 ± 1.13
KN-252 (4.221)	716.80	17.26 ± 0.15	7.67 ± 0.94	2.67 ± 1.19

3.2.3 Biological Evaluation of the Synthesized Compounds

Based on the FRET results of the synthesized molecules, Type-1 and Type-2 compounds were analysed for their biological activity in collaboration with Professor Neidle's group at the School of Pharmacy, UCL using several biological assays such as:

- Telomere repeat amplification protocol assay (TRAP)
- Sulforhodamine B assay (SRB)
- Population doubling assay
- Modified TRAP assay
- B-galactosidase senescence studies
- hTERT expression, and
- k-Ras expression.

Type-3 molecules could not be analyzed using these assays because of lack of facilities as the group moved from the School of Pharmacy, UCL, to King's College London.

3.2.3.1 Telomere Repeat Amplification Protocol Assay (TRAP)

Some biaryl polyamides were selected for further biophysical analysis to establish their G-quadruplex binding ability depending on the initial result obtained from FRET melting assay. KN-88 and KN-119 showed good quadruplex stabilization and selectivity for quadruplex over duplex DNA, as well as demonstrating significant result in cell culture assays. Therefore, these compounds were selected as lead molecules for the further design of new compounds. Telomerase inhibiting activity of these ligands was assessed along with a few other biaryl polyamides in order to compare their activities.

Telomerase inhibition can be identified by stabilization of the TS oligonucleotide. The aryl polyamide series, at 25 μM concentrations, was subjected to *in vitro* biophysical assessment to investigate their telomerase inhibition and their activity was compared with that of the known telomerase inhibitors Braco19 and Telomestatin with TRAP EC_{50} values of 6.3 μM and 0.4 μM , respectively.

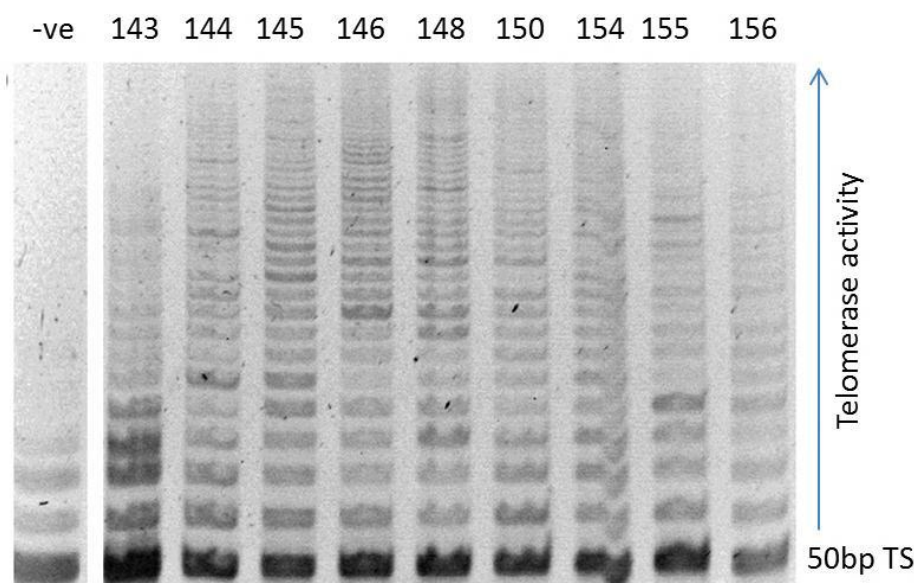


Figure 3.23: Biophysical TRAP-LIG assay denaturing gel. The effect of the aryl polyamide series [$c=25 \mu\text{M}$] on telomerase activity. Lane description: -ve; no telomerase, 2-10 indicative of ligands KN-143 to KN-156.

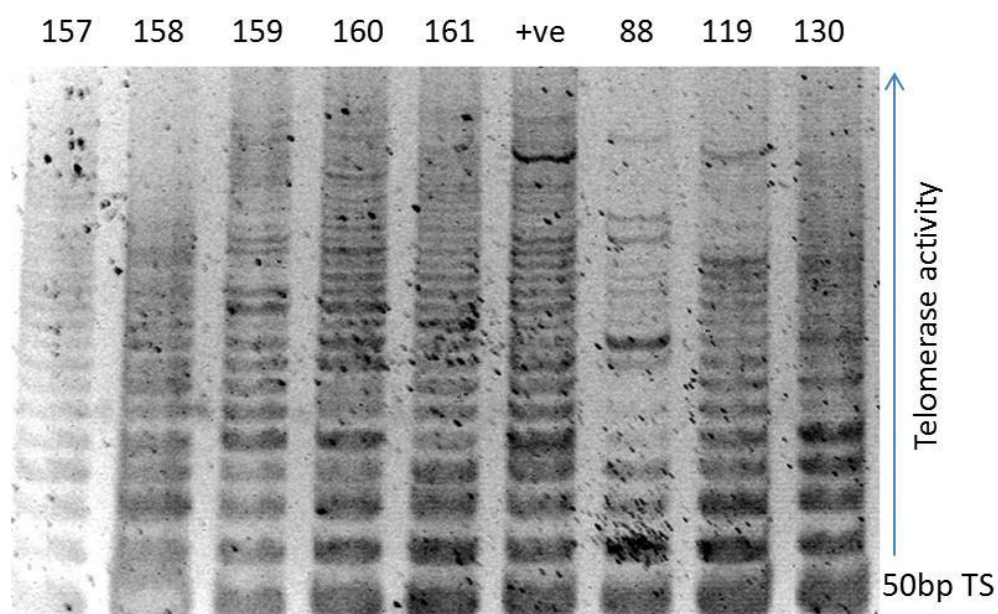


Figure 3.24: Biophysical TRAP-LIG assay denaturing gel. The effect of the aryl polyamide series [c=25 μ m] on telomerase activity. Lane description: +ve; telomerase positive extract, all other lanes as stated.

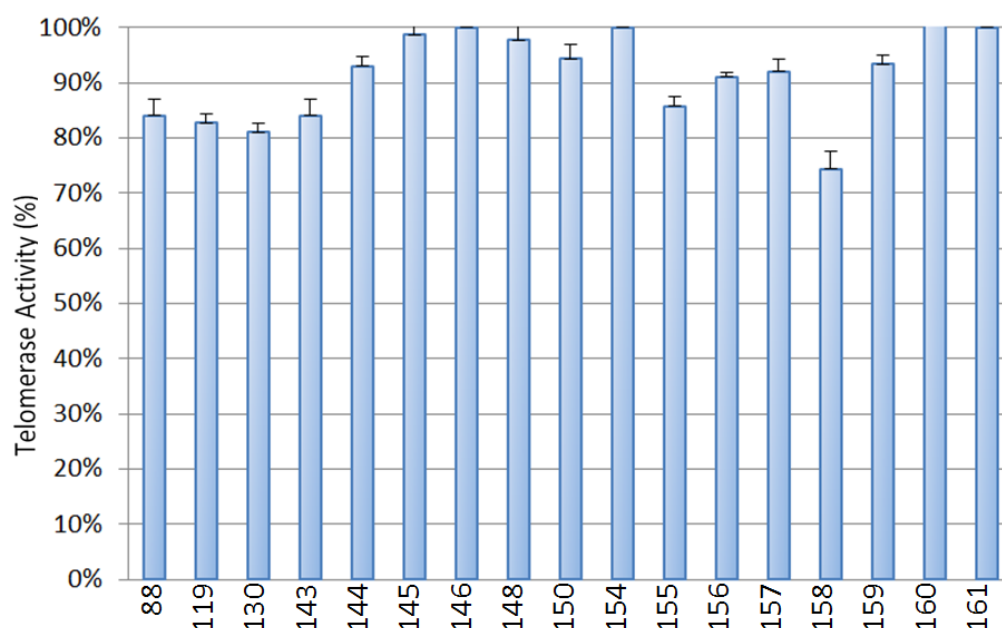


Figure 3.25: Quantified biophysical TRAP-LIG-assay. Number of bands and integrated lane intensity were measured, quantified and normalized with respect to the controls.

Generally, no significant telomerase inhibition was observed (as measured by the number and integrated intensity of TRAP artefacts) throughout the series at relatively high ligand concentration (25 μM), when compared with the known G-quadruplex ligands, Braco19, TMPyP4 and Telomestatin, with TRAP EC_{50} values of 6.3 μM , 8.9 μM , and 0.6 μM respectively [240]. However, compound KN-158 showed relatively significant telomerase inhibition ($\sim 30\%$), whereas compounds KN-88, KN-119, KN-130 and KN-143 showed moderate telomerase inhibition ($\sim 20\%$). Hence, no further dose-response investigations were required because of this low inhibition. To establish structure activity relationships, higher concentrations (commonly up to 100 μM) could be used, but biophysical data may not be translated biologically as these high concentrations effect solubility.

Additionally, these ligands are poorly soluble in diethylpyrocarbonate (DEPC) H_2O at 1mM concentration and some of these ligands are not entirely in solution at these concentrations. In particular, KN-156 and KN-157 were poorly soluble in 1mM DEPC H_2O . For studying structure-activity relationships it could be mentioned that KN-88, KN-119, KN-130, KN-143 and KN-158 show some anti-telomerase activity.

Although a TRAP EC_{50} [$c=25 \mu\text{M}$] could not be evaluated for any ligands from the aryl-polyamide series, some structure-activity relationships could be determined. The ligands (KN-88, KN-119, KN-130 and KN-143) containing the terminal **R1** [2-(2,3-dihydrobenzofuran-5-yl)-4-methylthiazole] group (Figure) demonstrate some ($\sim 20\%$) biophysical telomerase inhibition, whereas the terminal **R1** [2-(benzofuran-5-yl)-4,5-dimethylthiazole] motif containing ligand KN-158 demonstrated the most significant (30%) biophysical telomerase inhibition.

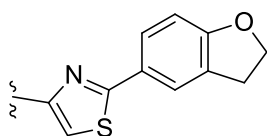


Figure 3.26: 2-(2,3-Dihydrobenzofuran-5-yl)thiazole R1 motif seen on ligands KN-88, KN-119, KN-130 and KN-143.

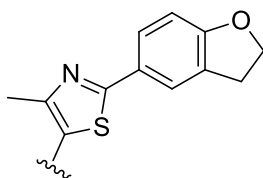


Figure 3.27: 2-(2,3-Dihydrobenzofuran-5-yl)-4-methylthiazole R1 motif seen on ligand KN-158.

The subtle structural difference between the two moieties seems to be due to the addition of a methyl group on the thiazole, i.e. the 4-methylthiazole to a 4,5-dimethylthiazole. Another ligand, KN-164, which is a derivative of KN-158 showed no significant telomerase inhibition. The end-terminal of compounds KN-158 and KN-164 alternate between the aryl rings 2,3- dihydrofuran (KN-158) and 2,3-dihydrothiophene (KN-164) that are contiguous with a benzene ring.

3.2.3.2 Surforhodamine B Assay (SRB)

The biaryl polyamide ligands were screened against various cancer cell lines, as well as a normal cell line, to evaluate their short-term (96 h) growth-inhibitory effect using the SRB assay (**Table 3.15**). After analysing the results, two ligands, KN-88 and KN-119, were identified as the lead-compounds and were screened against a wide range of cancer cell lines (**Table 3.16**).

Table 3.15: IC₅₀ values determined by the SRB assay evaluating the biaryl polyamide series. 25 µm was the highest concentration used, since several compounds presented solubility issues at higher concentrations.

KN Ligands	MCF7		A549		MIA-Paca-2		WI38	
	IC ₅₀ (µm)	SE	IC ₅₀ (µm)	SE	IC ₅₀ (µm)	SE	IC ₅₀ (µm)	SE
KN-143 (4.100)	1.8	0.4	2.4	0.2	1.4	0.1	22.1	1.1
KN-144 (4.101)	6.6	0.7	7.0	0.3	1.1	0.4	>25	n/a
KN-145 (4.102)	1.7	0.3	3.1	0.6	2.1	0.2	19.2	2.1
KN-146 (4.103)	4.3	1.1	5.4	0.7	1.8	0.1	>25	n/a
KN-148 (4.112)	2.5	0.4	3.2	0.6	2.3	0.1	21.1	1.9
KN-149 (4.114)	5.3	1.5	8.2	0.9	2.0	0.1	>25	n/a
KN-150 (4.116)	1.2	0.2	3.2	0.6	1.1	0.2	16.5	1.5
KN-154 (4.123)	2.6	0.6	5.0	0.3	2.4	0.1	15.3	2.1
KN-155 (4.125)	2.3	0.4	3.2	0.4	1.6	0.2	19.1	1.5
KN-156 (4.129)	2.1	0.5	2.4	0.4	1.9	0.1	17.5	1.1
KN-157 (4.130)	2.5	0.4	3.7	0.6	1.0	0.2	12.1	0.9
KN-158 (4.133)	3.7	0.3	5.7	0.5	3.9	0.3	>25	n/a
KN-159 (4.127)	3.2	0.6	7.1	0.7	1.9	0.1	10.9	0.9
KN-160 (4.131)	2.7	0.1	3.6	0.2	2.9	0.2	20.1	0.6

Table 3.15: IC₅₀ values determined by the SRB assay evaluating the biaryl polyamide series. 25 µm was the highest concentration used, since several compounds presented solubility issues at higher concentrations (continued).

KN Ligands	MCF7		A549		MIA-Paca-2		WI38	
	IC ₅₀ (µm)	SE	IC ₅₀ (µm)	SE	IC ₅₀ (µm)	SE	IC ₅₀ (µm)	SE
KN-161 (4.132)	5.4	1.9	5.9	0.3	3.2	0.1	>25	n/a
KN-88 (4.76)	2.3	0.2	3.1	0.2	0.7	0.1	15.5	1.1
KN-119 (4.80)	2.7	0.2	3.0	0.2	0.3	0.1	>25	n/a
KN-130 (4.99)	1.3	0.1	4.7	0.3	3.1	0.1	>25	n/a

Table 3.16: IC₅₀ values determined by the SRB assay evaluating KN-88, KN-119 and KN-130. 25 µm was the highest concentration used, since several compounds presented solubility issues at higher concentrations.

KN Ligands	RCC4		HPAC		PC3	
	IC ₅₀ (µm)	SE	IC ₅₀ (µm)	SE	IC ₅₀ (µm)	SE
KN-88 (4.76)	n/a	n/a	1.4	0.1	2.5	0.2
KN-119 (4.80)	n/a	n/a	0.2	0.1	1.7	0.2
KN-130 (4.99)	8.3	0.2	n/a	n/a	n/a	n/a

The biaryl polyamide ligands were found to be active (IC₅₀<5 µm) against the tumourigenic cell lines A549, MCF7 and MIA-PaCa-2. Among these molecules, two of the ligands, KN-88 and KN-119, were identified as the lead-compounds and were subject to further investigation in HPAC and PC3 cell-lines. Consequently, KN-119 was considered to be the lead compound. The IC₅₀ values for KN-119 in A549 and MCF7 (2.7 and 3 µm respectively) have been found to be comparable with the lead compound from the acridine series, BRACO-19 (2.5 and 2.4 µm respectively).

Moreover, KN-119 demonstrated no cell growth inhibition at 25 μm with WI38 fibroblast cells. Hence, the therapeutic index, defined by the ratio $\text{IC}_{50}^{\text{[WI38]}}:\text{IC}_{50}^{\text{[MIA-PaCa-2]}}$, exceeds 83 for KN-119. Up to 100 μm drug concentrations should be used to determine the definite therapeutic index. However, the biological relevance of using such high drug concentrations in monolayer cell culture studies is controversial as growth inhibition at high concentrations could be attributed to a large number of factors including unknown solubility compared with effective inhibition of the molecular target.

These polyamide ligands demonstrated an ordered and consistent activity throughout the tumourigenic cell-lines such as MCF7 (breast), A549 (lung) and MIA-PaCa-2 (pancreatic) cell lines, with the highest activity against (measured by IC_{50}) MIA-PaCa-2 ($\sim 1\text{--}2\ \mu\text{m}$), MCF7 ($\sim 2\text{--}4\ \mu\text{m}$) and A549 ($\sim 3\text{--}5\ \mu\text{m}$), which might be due to the subtle changes in structure. However, the selective toxicity seen towards MIA-PaCa-2 cells is significant. KN-88 and KN-119, which were considered as the lead-compounds with IC_{50} values of 0.7 and 0.3 μm , respectively, were subsequently screened against an additional pancreatic cell-line, HPAC, in order to confirm their selective toxicity towards pancreatic cell-lines (as opposed to a MIA-PaCa-2 specific trait). KN-88 and KN-119 produced IC_{50} values of 1.4 and 0.2 μm respectively. As KN-88 did not demonstrate the same degree of selective toxicity for HPAC, KN-119 was chosen as the lead compound to study against MIA-PaCa-2 cells as it showed consistent toxicity against the screened pancreatic cell lines. The degree of toxicity in KN-119 in A549, MCF7, MIA-PaCa-2 and WI38 (2.7, 3.0, 0.3 and $>25\ \mu\text{m}$, respectively) produced a therapeutic index (defined by $\text{IC}_{50}^{\text{[healthy cells]}}:\text{IC}_{50}^{\text{[cancer cell]}}$) of >9 , >8 , >83 for A549, MCF7 and MIA-PaCa-2, respectively.

In 2009, our group reported the first generation of biaryl polyamides [189]. Among the reported molecules, ligand-2 demonstrated IC_{50} values in A549, MCF7 and WI38 of 2.1, 2.0 and 9.2 μm respectively, which clearly implies that the second generation molecules are significantly more consistent and potent than the first-generation biaryl polyamides. Additionally, the therapeutic indexes of ligand-2 are 4.3 and 4.6 in A549 and MCF7 respectively. Hence, the potency and the significantly larger therapeutic index of KN-119 suggested that KN-119 has increased selectivity for cancerous cells. Generally, this can be extrapolated to all ligands reported in this thesis, which are selective for tumourigenic cells over healthy cells, a trait which the first-generation ligands do not entirely demonstrate.

Tetrasubstituted naphthalene diimide ligand, ND-2, is currently the most potent G-quadruplex ligand against MIA-PaCa-2 cells with IC_{50} values of 0.07 μM and 5.5 μM in MIA-PaCa-2 and WI38, respectively [250], and a therapeutic index of ~ 780 . The ND ligands are the result of successive generations of drug-development and are not selective towards pancreatic cancers over other cancer cells. Hence, these polyamide ligands might be an alternative choice as a potent G-quadruplex-ligand.

Pancreatic tumours are k-Ras dependent and the selective toxicity of KN-119 towards MIA-PaCa-2 (8-10 folds more potent for MIA-PaCa-2 than MCF7 and A549) suggested that KN-119 could function as a transcriptional repressor of k-Ras. So, studies investigating the effect of KN-119 on k-Ras expression were conducted and are discussed later.

3.2.3.3 Population Doubling Studies

KN-119 showed a dose-dependent effect on MIA-PaCa-2 cells when subjected to long-term population doubling studies and were analyzed following treatment profile **iii** IC_{50} , $0.5 \times IC_{50}$ and $0.2 \times IC_{50}$ [0.3, 0.15, 0.06 μM]

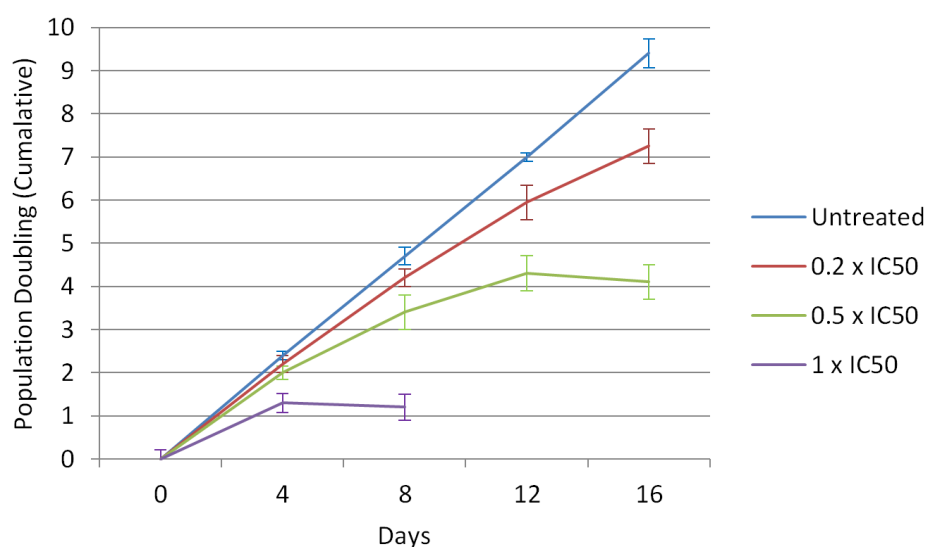


Figure 3.28: The 16-day effect of KN-119 on population doublings in MIA-PaCa-2 cells. The cumulative number of population doublings was determined every 4 days. Each data-point is the mean of two-differential seeding densities, each performed on three independent investigations.

There was no significant growth inhibition at 4-days in MIA-PaCa-2 cultures in 0.5 x IC₅₀ or 0.2 x IC₅₀ cultures. The cell-count for the 1 x IC₅₀ culture represented 50% of the control, in line with the SRB data. At 8-days, increasing numbers of non-adherent cells made the cultures look unhealthy in 0.2 x IC₅₀ and 0.2 x IC₅₀ cultures and was subsequently discontinued as the required number of cells for re-seeding could not be obtained from the IC₅₀ culture. At 12-days, 0.2 x IC₅₀ and 0.2 x IC₅₀ cultures looked increasingly non-adherent, while moderate growth inhibition was observed at 16-days, although the required number of cells for re-seeding could not be obtained from the 0.2 x IC₅₀ culture.

KN-119 inhibited cell proliferation (with reference to the number of cells) in long-term population doubling studies at 0.2 and 0.5 x IC₅₀ doses for up to 12-days, where a decreased rate of cell proliferation suggested that, KN-119 may influence senescence factors at sub-cytotoxic concentrations. Up to 40-days treatments at 0.1 x IC₅₀ should be conducted to investigate this completely. Senescence would be indicated by a decreased rate of proliferation, but crucially not a decrease in the number of cells seeded to the number of viable cells at the end of treatment.

The number of adherent cells decreased at 0.5 x IC₅₀ between days 12 and 16 (10,000 viable cells seeded, but only ~8,700 viable cells remained – data not shown) resulting in discontinuation of the investigation for this condition, due to lack of cells, and required re-seeding. A cytotoxic mechanism however, refers to the decrease in the number of cells, while a cytostatic mechanism would theoretically maintain a minimum of ~10,000 cells in culture. Again, a reduction in cell number was also seen at 1 x IC₅₀, between 4-8 days, although this was expected at cytotoxic concentrations. To confirm completely the mechanism of action of ligand KN-119 being entirely cytotoxic, the β -galactosidase assay should be conducted to identify the presence of senescence biomarkers in KN-119-treated MIA-PaCa-2 cells.

3.2.3.4 Modified Biological TRAP

The basic mechanism of action of the G-quadruplex ligands can be investigated by *in vivo*/biological-TRAP, which assumes that the ligands permeate cell-walls, enter the nuclei, displace POT1 and subsequently hTERT leading to its degradation via proteolytic-ubiquitin systems [178].

Although, KN-158 was marginally more potent than KN-119 and KN-88 in the *in vitro*/biophysical telomerase inhibition assay, and KN-88 showed better stabilizing effect against the F21T sequence in the biophysical FRET studies, only KN-119 was assessed *in vivo* using treatment profiles **i** and **ii**, as described in **4.3.2.3**, because of its better activity against pancreatic cancer cell lines. Moreover, KN-119 stabilized the F21T sequence in FRET, which suggested that KN-119 could function as a telomerase inhibitor and KN-119 [c=25 μ m] demonstrated ~20% telomerase inhibition in the *in vitro* modified-TRAP.

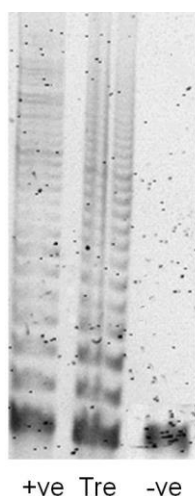


Figure 3.29: Biological modified TRAP assay (The effect of 0.2 μ m KN-119 (0.6 x IC₅₀) on telomerase activity in Mia-PaCa-2 cells after 7-days [treatment profile **i**]).

The results from the treatment profiles **i** and **ii** of the modified-TRAP assay for KN-119 failed to establish a biologically-relevant concentration with an effective EC₅₀ for telomerase inhibition (Figures **3.31** and **3.32**, respectively). *In vivo* modified TRAP suggested some inhibition (~30%) at 0.3 μ m for 5-days, but MIA-PaCa-2 cells in culture were increasingly non-adherent and no IC₅₀ could be established. The effect of unhealthy cells/degree of confluency on telomerase activity is unknown and could be responsible for this observed telomerase inhibition. Therefore, for compound KN-119, no clear correlation could be established between FRET and *in vivo* modified TRAP.

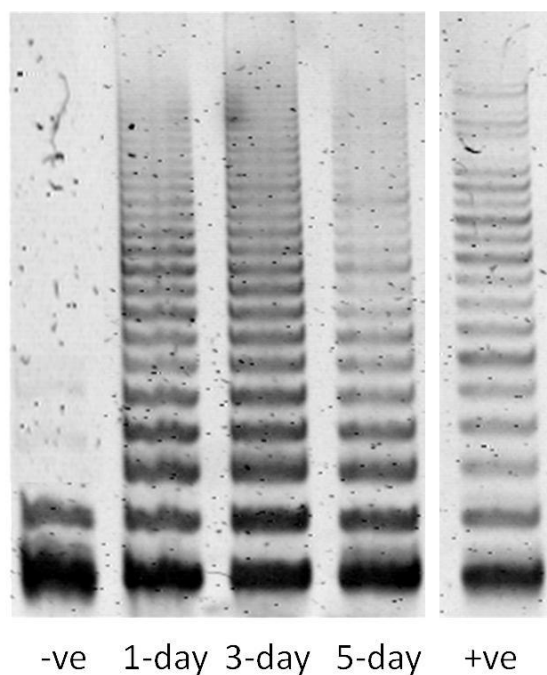


Figure 3.30: Biological TRAP-LIG assay denaturing gel. The effect of 0.3 μm KN-119 on telomerase activity in Mia-PaCa-2 cells after 1-, 3-, and 5-days [treatment profile ii].

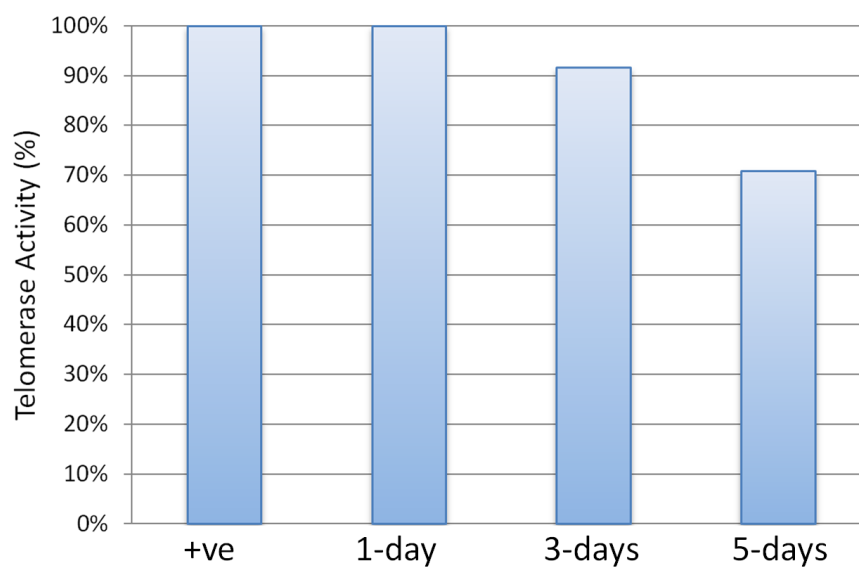


Figure 3.31: Quantified biological TRAP-LIG-assay. Number of bands and integrated lane intensity were measured, quantified and normalized with respect to the controls. +ve control indicative of telomerase positive MIA-PaCa-2 extract.

3.2.3.5 β -Galactosidase Senescence Studies

β -Galactosidase is a known biomarker for the senescent cell phenotype (flattened/enlarged cells expressing β -galactosidase) [251]. A senescent cell phenotype has been observed upon treatment with the G-quadruplex ligands quinolone and quindolone derivatives causing telomere dysfunction [156, 169]. A senescence detection kit (Cell Signaling Technology, USA) is readily available commercially which can detect β -galactosidase expression. This kit employs a chemically modified galactoside, X-Gal. Upon exposure to β -galactosidase-positive senescent cells, X-Gal is cleaved by β -galactosidase to form a blue/green precipitate within cells, which can be monitored and quantified by microscopy.

Senescence, as indicated by β -galactosidase activity, was measured at two stages in the long-term treatment experiment, as described in 4.3.2.3 treatment profile **iii**. The degree of senescence in MIA-PaCa-2 cells using the lead-compound KN-119 was quantified (**Table 3.13**). The number of senescent cells was determined at two time-points, 8 and 16-days.

Table 3.17: The long-term senescent effect of KN-119 on MIA-PaCa-2 cells. The values indicated are the percentage of cells demonstrating β -galactosidase activity.

KN-119 treatment	% senescent cells after treatment	
	8 days	16 days
Control	1.8 \pm 0.1	2.1 \pm 0.1
0.2 x IC ₅₀	6.4 \pm 2.1	9.1 \pm 2.1
0.5 x IC ₅₀	14 \pm 2.5	17 \pm 2.5

KN-119 has moderate β -galactosidase activity in MIA-PaCa-2 cultures compared with BRACO-19. BRACO-19, on 7-28 day long-term studies with 2 μ m in DU145 cultures (96 h IC₅₀ of 22.3 μ m) demonstrated significant β -galactosidase activity after 7 and 14 days (~40-50% β -gal positive cells) [253]. Each ligand demonstrates a significant difference in its degree of toxicity, which is attributed to different mechanisms of action. However, it is noted that KN-119 does not up-regulate β -galactosidase expression significantly (14-17%) at discontinued time-points. Nonetheless, when combined with the population doubling study, which demonstrated reduced cell-number, it can be suggested that KN-119 operates via a predominantly cytotoxic rather than cytostatic-dependent mechanism. To confirm this

definitively, a protein expression investigation of senescent factors p16 and p21 should be conducted.

3.2.3.6 hTERT Expression

A decrease in telomerase activity and hTERT protein expression levels were measured by the modified-TRAP assay in the *in vivo* hTERT inhibition assay. Dislocation of hTERT from telomere causes displacement of the enzyme from the substrate resulting in telomerase inhibition. The presence of two non-telomeric PQS within the promoter of hTERT [254] suggests that G-quadruplex ligands may act as transcriptional repressors of hTERT. However, neither TRAP nor protein expression studies can elucidate whether G-quadruplex ligands transcriptionally repress hTERT or promote hTERT displacement and degradation at the telomere.

In the modified-TRAP and protein-expression assays, telomerase inhibition is evaluated by the decrease in hTERT, and hTERT displacement is observed by confocal microscopy, which shows reduced co-localization of hTERT to the telomere. β -Actin was used as a control to investigate the effect of the biaryl polyamide ligands on hTERT levels. To ensure reproducibility, protein was extracted on three-independent occasions, as outlined in 4.3.2.3 treatment profiles **i** and **ii**.

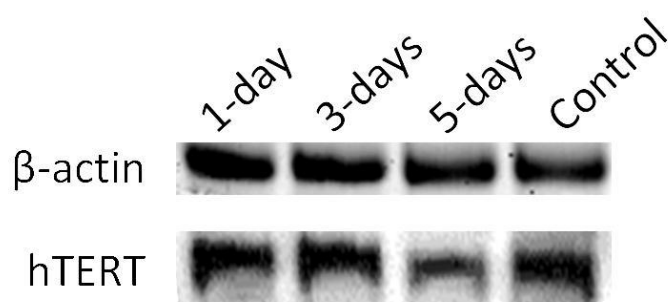


Figure 3.32: The effect of 0.3 μ m KN-119 on hTERT after 1, 3 and 5-days in MIA-PaCa-2 cells (Treatment profile **ii** as described in 4.3.2.3).

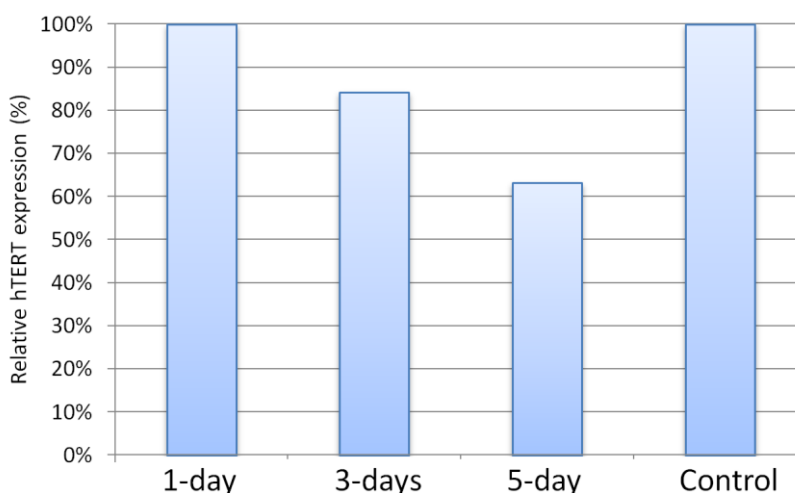


Figure 3.33 Quantified gel showing the effect of 0.3 μm KN-119 on hTERT after 1, 3 and 5-days in MIA-PaCa-2 cells. Quantitative figure indicative of two full-repeats, i.e. lysates obtained from two different MIA-PaCa-2 treatment cultures. Control indicative of untreated MIA-PaCa-2 extract.

In accordance with the TRAP data, the hTERT expression results suggest that at cytotoxic conditions KN-119 reduces both hTERT levels and activity. However, as the IC_{50} value cannot be established under these cytotoxic conditions (treatment profile **ii** as described in **4.3.2.3**), it can be assumed that the cytotoxic mechanism of KN-119 is not entirely dependent on hTERT-inhibition.

On day-5, for KN-119, TRAP exhibited ~30% inhibition and hTERT expression was down-regulated by ~40% while ND2 at 0.5 x IC_{50} reported ~50% telomerase inhibition (EC_{50}) in MCF7 cells after 7-days of treatment [250]. Similar findings from two distinct assay reports suggest a valid result; however, the cells used for protein extracts (extracted from three-independent investigations) appeared unhealthy after 5-days treatment. Hence, in order to have a valid result, long-term (40-day) sub-cytotoxic concentrations of KN-119 treatments should be conducted, along with the short-term (1-day) post-cytotoxic concentrations.

Since, KN-119 demonstrated no telomerase inhibition in MIA-PaCa-2 cells at 0.6 x IC_{50} for 5-days and 1 x IC_{50} was unable to produce an EC_{50} after 5-days of treatment, it is unlikely that 0.5 x IC_{50} for 7-days will result in an EC_{50} . Although no EC_{50} was established and further treatment profiles are required to consolidate the result, coupling the data-sets from hTERT

protein expression analysis, *in vivo* and *in vitro* modified-TRAP, it is likely that KN-119 is not a significant hTERT inhibitor.

3.2.3.7 k-Ras Expression

The biaryl-polyamide ligands demonstrated different degrees of selective toxicity towards the k-Ras-dependent pancreatic cell lines MIA-PaCa-2 and HPAC. However, the overall activity of KN-119 against the pancreatic cell line made it a suitable candidate for assessing its effect on k-Ras expression. Treatment profiles **i** and **ii**, as described in 4.3.2.3, were conducted in order to investigate k-Ras inhibition.

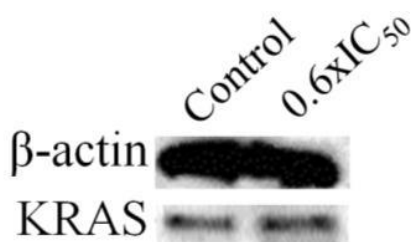


Figure 3.34: The effect of 0.2 μM KN-119 on k-Ras after 7-days in MIA-PaCa-2 cells. (Treatment profile **i** as described in 4.3.2.3).

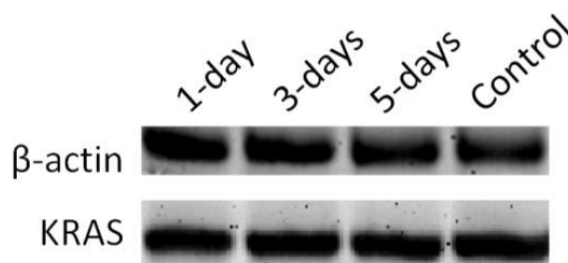


Figure 3.35: The effect of 0.3 μM KN-119 on k-Ras after 1, 3 and 5-days in MIA-PaCa-2 cells. (Treatment profile **ii** as described in 4.3.2.3).

The results from both treatment profiles the sub-cytotoxic long-term (7-day) culture (**Figure 3.34**) and the cytotoxic dose over 3-time points (**Figure 3.35**) that demonstrated no inhibition of k-Ras expression suggesting that KN-119 does not function as a transcriptional repressor of k-Ras and does not act *via* a k-Ras dependent pathway. Cytotoxic short-term treatment profiles (3x, 5x and 10x reported IC_{50} values for varied time points (12 h to 3-day) should be

tried instead of the sub-cytotoxic long-term treatment profiles in order to explore the result, which might not be feasible due to toxicity of the compound.

Considering the lag time required for cell membrane permeation, nuclei-entry and transcription-translation events, acute (12 h) high-dose treatments, however, are still unlikely to demonstrate a change in k-Ras expression and it can be concluded that KN-119 does not inhibit k-Ras expression.

3.3 Structure Activity Relationship

The structure activity relationship analysis was made by assessing three series-wide investigations as follows,

- i) ΔT_m °C from FRET
- ii) TRAP and Biophysical modified-TRAP
- iii) IC_{50} values from SRB assays

The following methods were adopted for structure-function analysis:

- i) From each investigation the strongest/weakest ligands were identified.
- ii) Consistency in activity of the ligands was identified by comparing the strongest/weakest ligands from FRET and modified-TRAP assays.
- iii) Consistency in activity of the ligands was identified by comparing the strongest/weakest ligands for SRB assay.
- iv) Comparison of ligands from part ii) and part iii) led to identification of consistently strong/weak ligands from all four investigations.

The structure activity relationship analysis was made in two segments. Firstly, the molecules were analysed based on their FRET data and it was tried to establish a relationship between the changes in activity of the molecules with subtle modifications within the structure of the molecules. The other way of investigation was based on the hypothesis that ligands with significant FRET ΔT_m °C values for F21T are more likely to function as telomerase inhibitors in the biophysical modified-TRAP, as well as could be co-related with the results from SRB

assays. All of the synthesized biaryl polyamide ligands could not be investigated using all the biophysical and biological assays such as TRAP, SRB, PD, and other assays mentioned earlier because of lack of facilities; however, a partial SAR could be established. Although this method is simplistic and bound to have several caveats, it is based on a grouping of biophysical and biologically-relevant investigations.

Initial modification of the biaryl polyamides developed by Rahman and co-workers showed some degree of G-quadruplex stabilization with better G-quadruplex selectivity over duplex DNA [172]. To develop molecules with better binding affinity and selectivity, some modification in motifs 1 and 2 of the first generation ligands was conducted. Library-1 second generation molecules contain only one non-variable core (blue circle), such as motif 1, whereas in library-2 ligands, a benzofused (purple circle) moiety was introduced after the tail moiety, which also contains a variable capping moiety (orange circle).

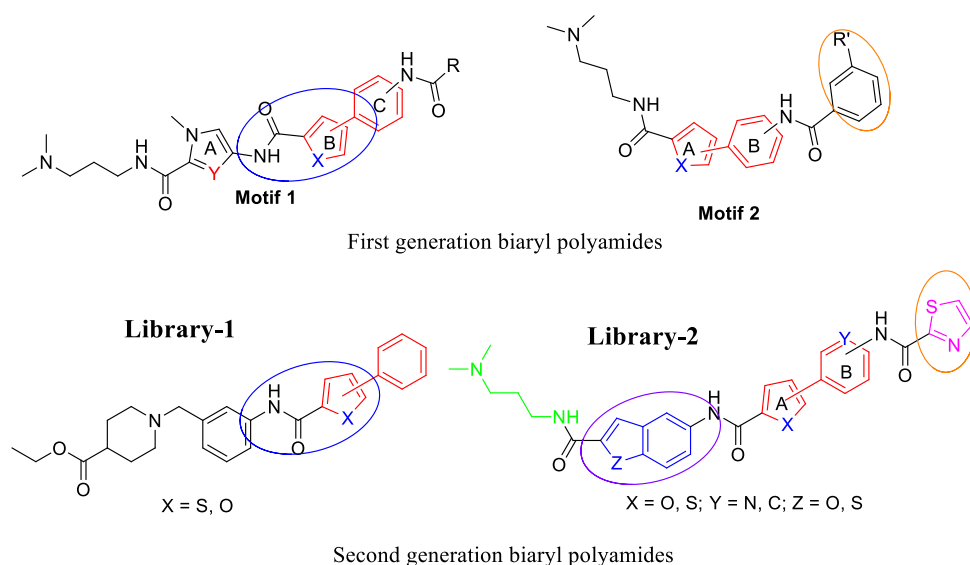


Figure 3.36: Comparison of first and second generation ligand structures.

The FRET data for the library-1 ligands against all investigated sequences showed complete loss in binding affinity. For molecules containing similar central cores, loss in activity may be attributed to the changes in the tail and capping moieties. However, the π -electron rich central core helps the molecules in π - π stacking with the G-quartet. The molecular modelling of the first generation biaryl ligands showed that the central core facilitates the U-shape formation of the molecules resulting in better selectivity towards the G-quadruplex over duplex DNA.

As with the previous results for the library-2 ligands, KN-88 and KN-119 demonstrated better G-quadruplex stabilization potential and selectivity than the first generation ligands. These molecules contain similar structural features analogous to the first generation motif 2 ligands, with the exception of the benzofused moiety. The presence of the tail moiety for other library-2 molecules did not show any significant effects. Hence, the enhancement in activity in the FRET assay might be due to the presence of the benzofused moiety. Although, KN-88 and KN-119 have a similar tail, central core and final capping moieties, KN-88 containing the benzothiophene ring showed better stabilization of the F21T sequence than KN-119 with the benzofuran ring. The subtle change from furan to thiophene in the benzofused ring resulted in an increased binding affinity of 2.20 °C.

KN-119 demonstrated consistently good results in other biophysical and biological analyses. Therefore, depending on the initial screening results some of the other second generation biaryl polyamides were designed based on KN-119 as the lead compound. Three points of modification of ligand KN-119 were selected and the resulting molecules were analysed by FRET melting assay. In these series, no significant stabilization of F21T was observed due to the change in the benzofused moiety (R2) where the highest level of F21T stabilization was observed with the modification of the tail motif (R1). KN-148 and KN-158, formed by modification of the final capping acid (R4), demonstrated significant binding affinity towards the human telomeric G-quadruplex DNA. Again, with these two molecules, the minor change in the structure of R4 from furan to 4-methylthiazole resulted in enhancement in the stabilization potential. Interestingly, the G-quadruplex stabilization ability of the ligands increased with increasing carbon number in the tail R1, as is evident from the FRET data for KN-212, KN-217, KN-232, KN-237, KN-242 and KN-247 (**Table 3.18**) (**Figure 3.37**). Although, KN-119 and KN-232 have similar structure, elongation of the tail molecule R1 by only one carbon in KN-232 caused an increase in FRET ΔT_m value by 3 °C over KN-119. Although, both molecules have similar structure, the binding ability of KN-247 was almost double that of its analogue KN-212, which is because of the extra carbon present in the tail of KN-247. A similar pattern was observed in the case of molecules KN-217, KN-237 and KN-242. However, the highest degree of stabilization was found with KN-242 with a pyrrolidine unit and a 4 carbon tail instead of the *N,N*-dimethyl propylamine tail of KN-119. Again, the stabilization ability of the ligand fell slightly when the tail contained the methylpiperazine

ring used in KN-252. Therefore, it can be suggested that for good G-quadruplex stabilization four carbons should be present in the tail.

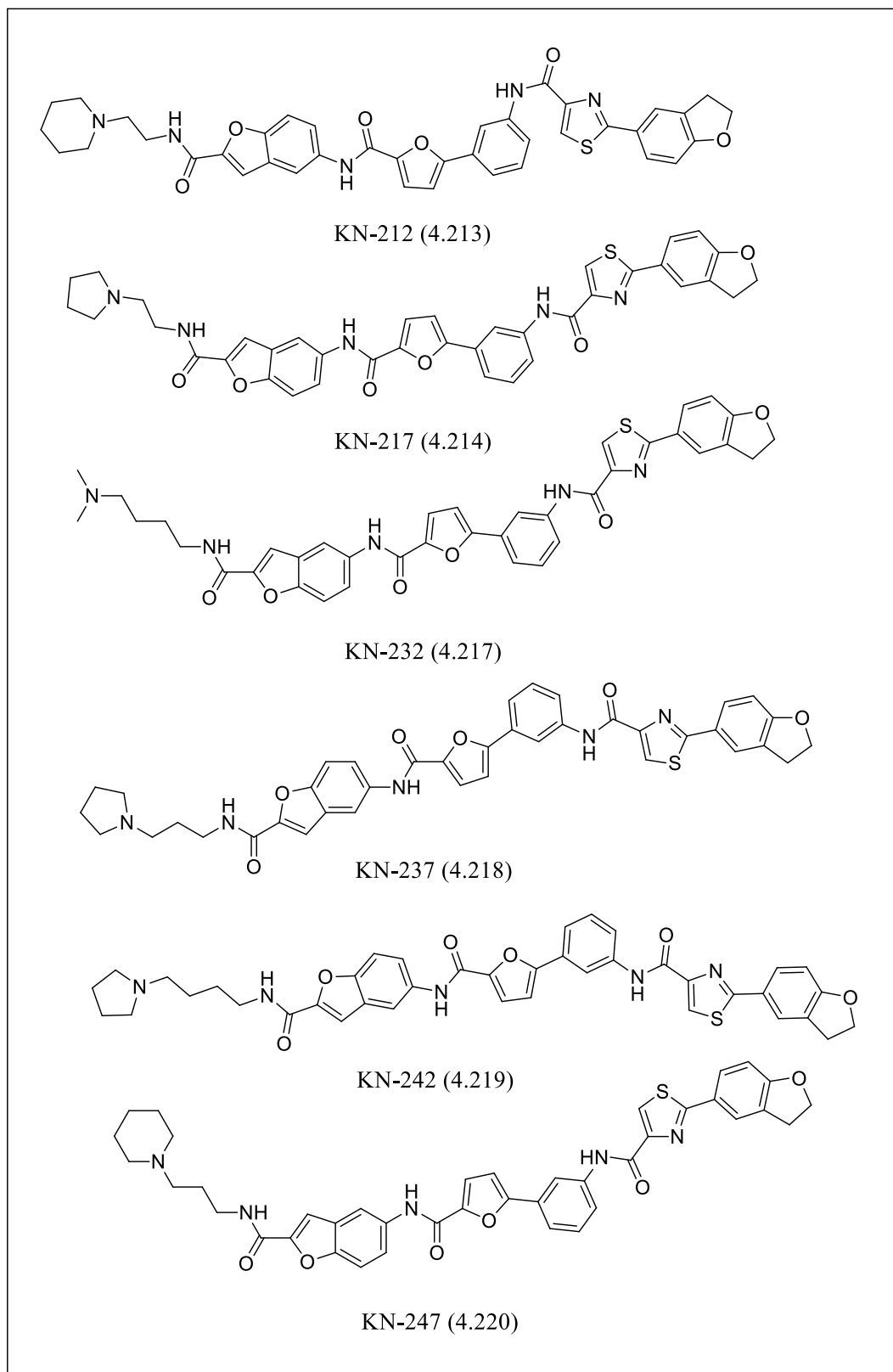


Figure 3.37: Structure of the active molecules.

Table 3.18: Structure-function analysis of the aryl polyamide series. The table shows the FRET ΔT_m values for F21T of the stronger ligands with structural variations.

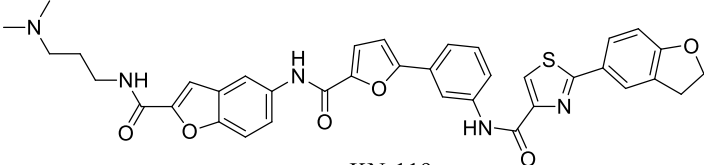
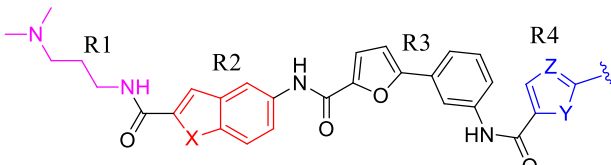
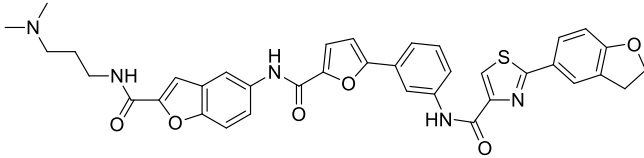
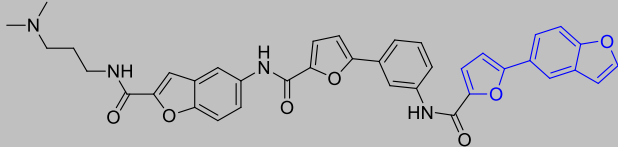
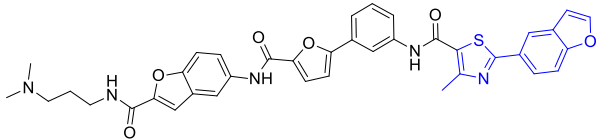
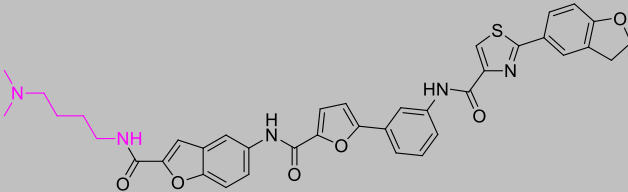
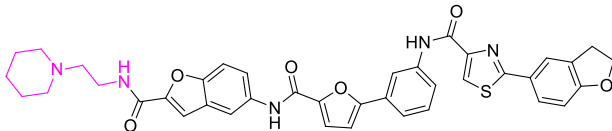
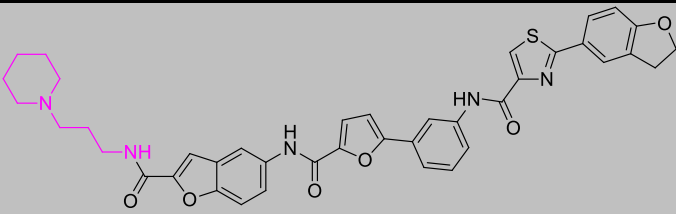
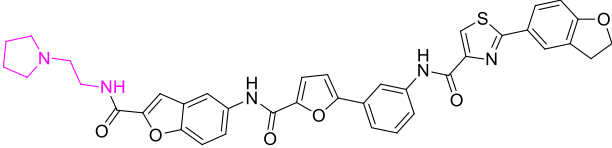
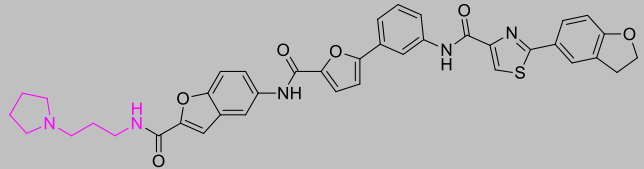
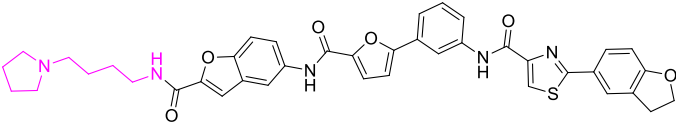
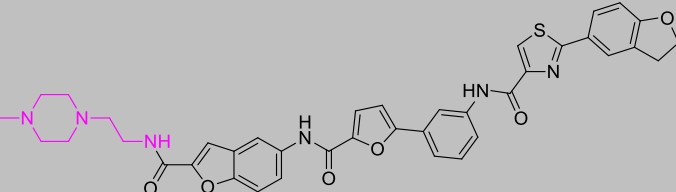
<div>  <p>KN-119</p> </div> <div>  <p>X = O, N, S; Y = O, S; Z = N, C</p> </div> <p>Structural modification of KN-119</p>		
Code KN	Ligand Structure	FRET ΔT_m F21T
119		19.00
148		15.45
158		18.00
232		22.38
212		14.98

Table 3.18: Structure-function analysis of the aryl polyamide series. The table shows the FRET ΔT_m values for F21T of the stronger ligands with structural variations (continued).

Code KN	Ligand Structure	FRET ΔT_m F21T
247		28.53
217		16.15
237		22.03
242		34.43
252		12.40

Analysis of the FRET data presented some promising G-quadruplex binding ligands which further correlated with the available biophysical and biological data. Although all the compounds were not screened through TRAP and SRB assays, we tried to establish a combined SAR between the molecules and their activity from the available data.

It is evident that KN-88, KN-119 and KN-148 are consistently good ligands in the SRB, TRAP and FRET assays. However, despite this, KN-158 showed good biophysical properties in TRAP and FRET, but displaying poor biological properties in the SRB assay. In contrast,

KN-150, with moderate biophysical properties in TRAP and FRET, demonstrated good biological properties via SRB analyses of the data. Although KN-159 and KN-144 showed some (~5%) telomerase inhibition in TRAP, they seemed to be the poorest ligands collectively in terms of analysis of the SRB and FRET data. Ligand KN-149, similar to KN-144, produced the poorest data in terms of SRB analysis.

3.3.1 R1.1 - The First Ring Moiety

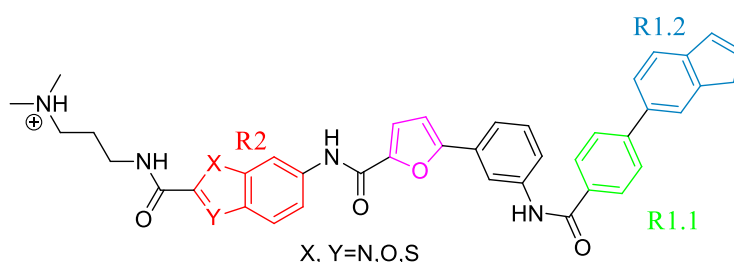


Figure 3.38: Structural illustration of biaryl-polyamide core. The non-variable core (black) shows the centrally situated furan (purple), the R2 group (red), R1.1 group (green) and R1.2 group (blue). (Illustration is for the purpose of identifying variable regions).

The thiazole ring in this position has been found to be important for activity of the compounds. The ligands KN-88 and KN-119 showed better results in the SRB assay although their TRAP data are not significant. Again, the thiazole ring containing ligand KN-143 and KN-145 at this position show good SRB data (although both show an IC₅₀ in WI38 cells of ~20 μ m and no significant toxic selectivity towards MIA-PaCa-2). The consistently good SRB-data from ligands containing the thiazole moiety suggest next-generation ligands should maintain the *thiazole* group at **R1.1** (Figure 3.38).

The 2-methylthiazole moiety containing derivatives KN-130, KN-149, KN-150 and KN-158 demonstrated varied results. Although, KN-158 showed good ΔT_m values in FRET and modified-TRAP, it presents relatively-poor SRB data. KN-130 and KN-149 showed poor results in FRET and SRB while KN-130 demonstrated mild telomerase inhibition (~20%). Again, moderate FRET activity was found for the ligand KN-150, which showed relatively better results in the SRB assays (although giving an IC₅₀ in WI38 cells of ~17 μ m and no significant toxic selectivity towards MIA-PaCa-2). Due to such variation in results it can be suggested that the 2-methylthiazole moiety may not be a crucial moiety. Among the furan ring containing derivatives only KN-148 showed a good level of activity in FRET, while the

other ligands, KN-154, KN-155 and KN-159 are poor in FRET. On the contrary, KN-154, KN-155 and KN-159 showed moderate activity in SRB and TRAP assays, but KN-148 had poor activity. This suggests that the efficacy of KN-148 is not dependent on the furan moiety but on either its **R1.2** terminal contiguous ring system or **R2**-moiety (**Table 3.19**).

As only two ligands KN-144 and KN-146 contain a *benzene* ring, hence it is difficult to assess the relative effect of it. Although, KN-144 shows some toxic selectivity towards MIA-Pa-Ca-2 cells, both ligands gave relatively poor results in the SRB, FRET and modified-TRAP assays. Little structure-function analysis can be performed because of the lack of ligands with the benzene ring in this position.

Thiophene ring containing ligands KN-156, KN-157, KN-160 and KN-161 showed varied results for different assays. All have identical R2-ring systems, along with the similar R1.1 moiety. SRB-assay demonstrates that KN-156 and KN-157 are good, while KN-160 and KN-161 are poor. FRET data show KN-156, KN-157 and KN-160 are poor while KN-161 is moderate. TRAP data show KN-156 to be moderate, KN-157 to have little effect while KN-160 and KN-161 have no effect. Such variation in results leads to the assumption that the thiophene moiety may only be poignant alongside the correct terminal contiguous ring system.

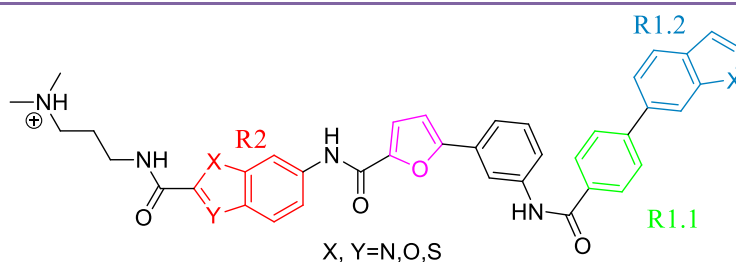
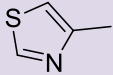
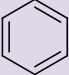
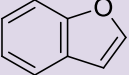
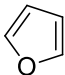
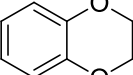
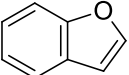
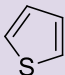
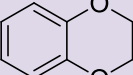
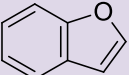


Table 3.19: Structure-function analysis of the aryl polyamide series. The table shows the stronger (top) and poorer (bottom) ligands and their variable motifs. FRET (ΔT_m F21T), %-inhibition of hTERT in the biophysical-TRAP [c=25 μ m] and IC₅₀ [MIA-PaCa-2] data are shown.

Table 3.19: Structure-function analysis of the aryl polyamide series. The table shows the stronger (top) and poorer (bottom) ligands and their variable motifs. FRET (ΔT_m F21T), %-inhibition of hTERT in the biophysical-TRAP [$c=25 \mu\text{m}$] and IC_{50} [MIA-PaCa-2] data are shown (continued).

Ligand	R1.1	R1.2 ring-system	R2 ring-system	FRET ΔT_m F21T	TRAP % [$c=25 \mu\text{m}$]	SRB IC_{50} [MIA-PaCa-2]
149				1.85	n/a	2
159				2.33	8	1.9
161				7.03	0	3.2

3.3.2 R1.2 - The Terminal Contiguous Ring Moiety

Different classes of ring-systems in the derivatives make it difficult to conduct a structure-function relationship analysis. However, interestingly, ligands with the 2,3-di-hydro-benzofuran ring system (KN-88, KN-119, KN-130, KN-143) are the most potent in SRB-assays. Amongst these molecules, the most potent ligand contains thiazole as opposed to furan as the **R1.1** first-ring group (**Figure 3.38**).

3.3.3 R2 - The Benzofused Ring Moiety

1*H*-indole (KN-143) and 3-phenyl-1*H*-indole (KN-145) R2-based ring systems containing ligands are potent in SRB-assays, though KN-145 showed better FRET data towards F21T. This could not be fully attributed to the change of the R2 ring to 3-phenyl-1*H*-indole from 1*H*-indole as TRAP data for KN-145 are negligible, whereas KN-143 showed moderate activity.

The R2-ring systems of KN-88, KN-119 and KN-130 contain benzothiophene, benzofuran and benzothiazole, respectively. SRB data for KN-130 show poorer degree of potency (apart from

in MCF7 cells) than KN-88 and KN-119. This suggests that the benzothiopene and benzothiazole terminal contiguous-ring moieties (single-substituted azoles as opposed to disubstituted azoles) have better degree of potency and selectivity for MIA-Pa-Ca-2 cells (**Table 3.19**).

It was understandable that lack of TRAP and SRB data for all synthesized biaryl polyamide ligands made it impossible to establish a complete structure activity relationship. However, analysis of FRET data for F21T gives some idea about the standard structural features that are necessary for optimum G-quadruplex stabilization and better selectivity.

3.3.4 Biological Evaluation of Type-3 Library Molecules.

New generation biaryl polyamides were designed and synthesized depending on the reported first generation biaryl polyamides by Rahman and co-workers. Initial synthesis and screening of Type-1 and Type-2 molecules by FRET provided two lead molecules KN-88 and KN-119. Among these two lead molecules, KN-119 showed better activity against two different types of pancreatic cancer cell line, which made it the first choice for further modification. Modification of the lead molecule, KN-119, resulted in Type-3 library molecules which were initially analysed by FRET melting assay. FRET data of those molecules demonstrated significant increase in G-quadruplex binding ability by 17 °C for KN-242 compared with KN-119. From assessment of the first type molecules it was evident that there is a correlation between the biophysical and biological activities as KN-119 showed good activities in both types of assay (please see **Table 3.11** and **section 3.2**). The biological analyses were not conducted because of lack of facilities as the group moved from the School of Pharmacy, UCL to King's College London. However, it can be assumed that their biological activity and their selectivity may increase correlating their increased biophysical activity.

Chapter Four: Experimental

4.0 Experimental-Chemical

4.1.1 General Experimental (Chemistry)

All reagents and solvents used were supplied from the commercial suppliers Sigma-Aldrich and Fluka. Reactions requiring anhydrous conditions were conducted in glassware, which had been oven-dried overnight and used the following day. All reactions were monitored by analytical thin-layer chromatography (TLC) performed using the indicated solvent on E. Merck silica gel 60 F₂₅₄ plates (0.25 mm). TLC plates were visualized using UV light (254 or 360 nm) and /or by staining the plates with either a cerium sulphate-ammonium molybdate solution or basic KMnO₄ followed by heating. A LCMS machine (liquid chromatography coupled with mass spectrometry) was also used to monitor the progress of the compounds. Solvents were removed using a rotary evaporator at or below 40 °C and the compounds further dried using low pressure vacuum pumps. Purification of the compounds was achieved by column chromatography using Merck Flash Silica Gel 60 (230-400 mesh). ¹H and ¹³C NMR spectra were recorded on either Bruker Avance 400 MHz or Bruker Avance 500 MHz spectrometers. Chemical shifts (δ H) are quoted in ppm (parts per million) and referenced to either the CDCl₃ residual chloroform signal (¹H δ = 7.26, ¹³C δ = 77.2) or the *d*₆-DMSO residual dimethyl-sulfoxide signal (¹H δ = 2.54, ¹³C δ = 40.45) or MeOD residual methanol signal (¹H δ = 3.31, ¹³C δ = 49.00). Multiplicities in the ¹H NMR spectra are quoted as: s = singlet, d = doublet, t = triplet, q = quartet, m = multiplet, dd = double doublet, ddd = double double doublet, dt = double triplet, td = triple doublet. The code (0) in the ¹³C NMR spectra denotes the presence of a quaternary carbon. High resolution mass spectra (HRMS) were obtained on a Thermo Navigator mass spectrometer coupled with a LC using electrospray ionisation (ES) and time-of-flight (TOF) mass spectrometry. Infrared spectra were recorded on a Perkin Elmer spectrum 1000 instrument.

4.1.2 General procedure for purification by 'Catch and Release' method

The sulphonic acid based SCX-2 resin cartridges were purchased from Biotage Synthesis (Virginia, USA) with different sorbent capacities (500 mg, 1 gm, 2 gm, 5 gm and 10 gm). The cartridges contained propylsulfonic acid functionalized silica. The strong cation

exchange sorbent is a very good choice for basic drug extraction. The cartridges were first activated by an initial wash with 2 column volumes of DCM and 2 column volumes of methanol. The reaction mixtures were then poured onto the cartridge (sorbent mass should be 10 times that of the calculated mass of the product) and the solvent was allowed to pass through the cartridges under gravity. The cartridges were washed with DCM (3X), DMF (3X) and methanol (1X) and the cycle was repeated three times to remove the impurities under vacuum to accelerate the elution. Products were released from the cartridge using 2M NH_3 in MeOH and concentrated *in vacuo*.

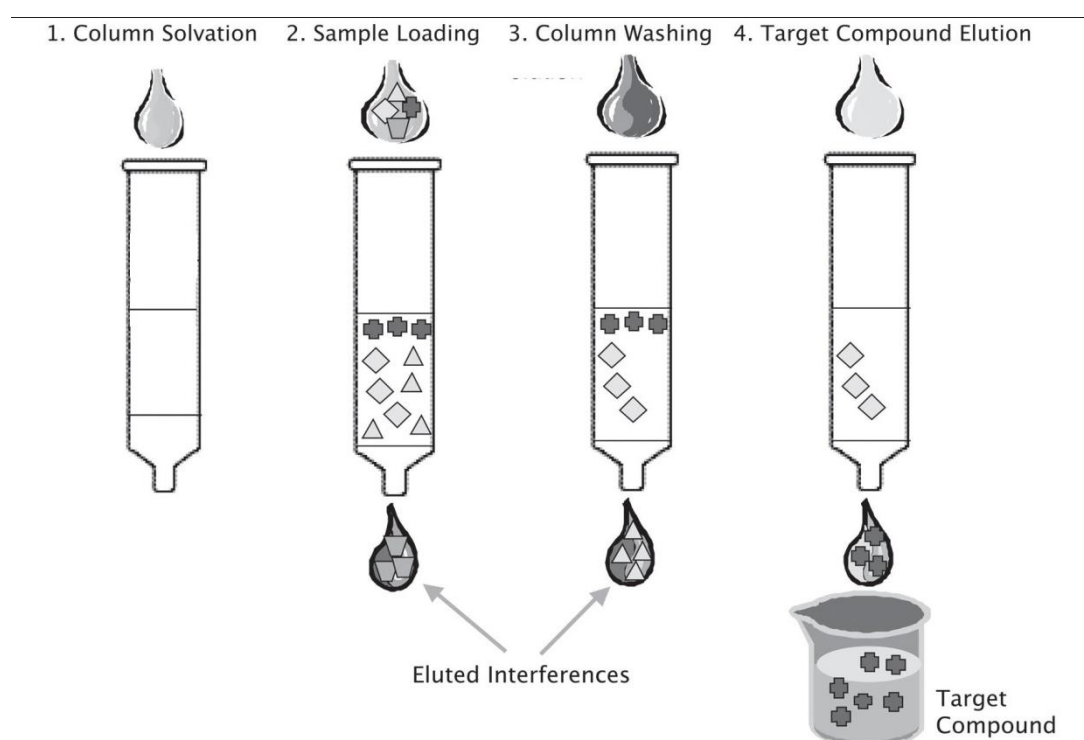


Figure 4.1: Purification procedure by 'Catch and Release' method.

4.1.3 General Procedures

4.1.3.1 Method A: Amide coupling between heterocyclic amine and heterocyclic base using HOBt and DIC

The acid (from 1.0 to 2.5 eq.) was dissolved in DCM/DMF (5-50 ml, depending on the amount of acid and solubility) in a round bottom flask/ Green House Parallel Synthesizer vial fitted with a magnetic stirrer. DIC (1.75 eq.) and HOBt (2.0 eq.) were added to the stirred solution at room temperature and the mixture was allowed to stir for between 45 minutes to 6 hours depending on the reactivity of the acid. The amine (1.0 eq.) was added after the initial activation step and the reaction mixture was allowed to stir until the reaction was deemed complete by TLC or LCMS. The reaction mixture was purified either by applying to a conditioned cartridge and the coupled product released by the 'Catch and Release' method described above or by using conventional column chromatography.

4.1.3.2 Method B: Standard hydrogenation procedure

The starting material was dissolved in either ethyl acetate or ethanol (maximum 150 ml) and a slurry of 10% Pd/C (10% w/w compared to the starting material) in the same solvent was added. The mixture was hydrogenated in a Parr hydrogenator at 45 psi until the H₂ uptake ceased. The progress of the reaction was monitored by either TLC or LCMS and the reaction mixture was filtered through a layer of celite and the residue washed with either ethyl acetate or ethanol. The solvent was removed under vacuum using a rotary evaporator to give the reduced product.

4.1.3.3 Method C: Microwave assisted Suzuki coupling between heterocyclic bromide and different boronic acids

The heterocyclic bromide (1.0 eq.), the boronic acid (1.2-1.5 eq.), K₂CO₃ (3.0 eq.) and *tetrakis* Pd(PPh₃)₄ (0.1 eq.) were added to an EmrysTM Process microwave vial containing a magnetic stirrer under nitrogen. An appropriate amount (5 ml for every 125 mg of substrate) of solvent mixture (Ethanol/Toluene/Water – 9:3:1) was added to the microwave vial under nitrogen and the vial was sealed with a ResealTM septum. The suspension was then irradiated

at microwave wavelengths and kept at 100 °C for 5-30 minutes depending on the substrate. The progress of the reaction was monitored by LCMS. For heterocyclic products containing the *N,N*-dimethylaminopropyl tail, the reaction mixtures were applied to a SCX-2 cartridge and purified by the 'Catch and Release' method described earlier. For products without a tail the reaction mixture was filtered through a celite layer and the residue washed with ethyl acetate. The solvent was removed under vacuum and the crude products were further purified using flash chromatography to give the pure product.

4.1.3.4 Method D: Hydrolysis of aromatic methyl ester

A 0.5 M aqueous solution of NaOH was added to a solution of the methyl ester in dioxane (1 ml for every 25 mg of ester). The reaction mixture was allowed to stir for 1.0-6.0 hours at which point TLC showed completion of the reaction. Excess dioxane was evaporated under vacuum and the residue was dissolved in water. The aqueous layer was acidified with 1M citric acid solution. The product was extracted with ethyl acetate and the organic layer was sequentially washed with water and brine, and finally dried over MgSO₄. The excess solvent was removed under vacuum and the product dried in a vacuum oven.

4.1.3.5 Method E: Nitration

Fuming nitric acid (37.5 ml) was added drop wise over a period of 1 hour to a mechanically stirred solution of the substrate (1.0 eq.) in acetic anhydride (475 ml), which was kept at -5 °C using an acetone/dry ice bath. After complete addition the temperature of the reaction mixture was gradually raised to 10 °C over a period of 3 hours, with continuous stirring. The reaction mixture was again cooled to -30 °C using an acetone/dry ice bath and diluted with 500 ml of isopropanol; the resulting precipitate was dried in a vacuum.

4.1.3.6 Method F: Procedure for disposing Pd/C waste

A Pd/C catalyst was used for the hydrogenation reaction. The catalyst was adsorbed on the celite bed over a filter paper after finishing the reaction. A slurry of celite was prepared using

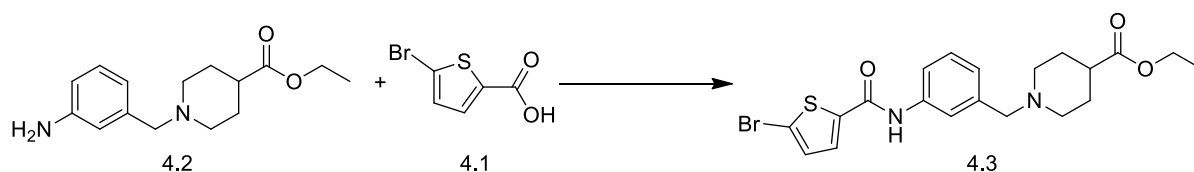
ethanol, which was passed under vacuum over several layers of filter paper to prepare the celite bed. The reaction mixture was poured over the bed after completion of the reaction, which trapped the Pd/C catalyst. The celite bed was then disposed of according to the standard procedure of the university in a separate container specified for Pd/C waste.

4.1.4 Type-1 Library synthesis

Procedure for the synthesis of ethyl 1-(3-(5-bromothiophene-2-carboxamido)benzyl)piperidine-4-carboxylate (4.3). (Amide coupling).

2.0 eq of HOBt (32 mg) and 1.75 eq. of DIC (145 μ l) were added to a solution of **4.2** (270 mg) in DCM (10 ml). After 30 minutes, 1.30 eq. of **4.1** (277 mg) was added and the reaction mixture was allowed to stir overnight. After 16 hours the reaction mixture was passed through a SCX-2 cartridge (5.0 gm) and the cartridge was washed with DCM (3x), DMF (3x) twice and finally MeOH (2x). The product **4.3** was released from the cartridge using 5.0 ml 2M NH_3 in MeOH and concentrated *in vacuo* to obtain 460.0 mg light brown, oily mass.

Ethyl 1-(3-(5-bromothiophene-2-carboxamido)benzyl)piperidine-4-carboxylate (4.3):

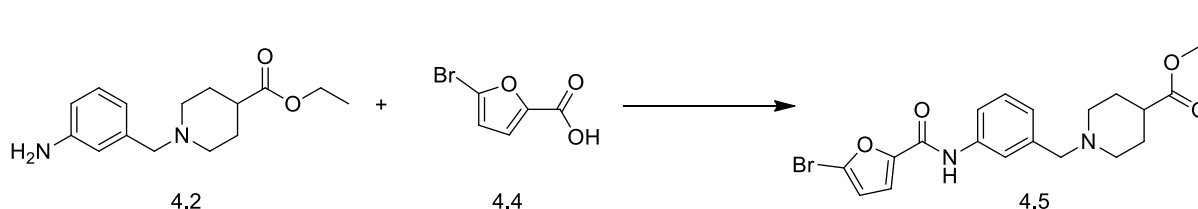


Light brown, oily mass. IR (FTIR, $\nu_{\text{max}}/\text{cm}^{-1}$) 635.14, 692.83, 775.02, 860.27, 1024.69, 1046.66, 1094.97, 1129.45, 1167.22, 1249.40, 1323.56, 1362.67, 1439.07, 1487.34, 1553.13, 1613.41, 1724.62, 2967.27, 3339.66; ^1H NMR (400 MHz, CDCl_3 , TMS); δ 1.12 (d, $J=6.4$ Hz, 3H), 1.22 – 1.24 (m, 2H), 1.80 – 1.85 (m, 2H), 2.02 (t, $J=10.0$ Hz, 2H), 2.26 – 2.29 (m, 1H), 2.86 – 2.88 (m, 2H), 3.54 (s, 2H), 4.14 (q, $J=6.8$ Hz, 2H), 6.85 (d, $J=3.79$ Hz, 1H), 7.06 (d, $J=4.0$ Hz, 1H), 7.28 (d, $J=7.6$ Hz, 1H), 7.42 (d, $J=4.0$ Hz, 1H), 7.47 (s, 1H), 7.61 (dd, $J=8.4$, 7.2 Hz, 1H), 7.98 – 7.99 (m, 1H); ^{13}C NMR (100 MHz, CDCl_3); δ 14.3, 29.05, 29.5, 41.1, 53.00, 61.5, 63.34, 64.7, 120.1, 121.06, 124.2, 124.5, 128.50, 132.15, 134.32, 135.6, 138.2, 139.62, 140.1, 161.1, 175.8; m/z (+EI) calc. For $\text{C}_{20}\text{H}_{23}\text{BrN}_2\text{O}_3\text{S}$ (M^+) 451.38, found 452.83 ($\text{M}+\text{H}$) $^+$; Yield: 95%.

Procedure for the synthesis of ethyl 1-(3-(5-bromofuran-2-carboxamido)benzyl)piperidine-4-carboxylate (4.5)

2.0 eq of HOBT (31 mg) and 1.75 eq. of DIC (141 μ l) were added to a solution of **4.2** (262 mg) in DCM (10 ml). After 30 minutes, 1.30 eq. of **4.4** (253 mg) was added and the reaction mixture was allowed to stir for 3 hours. After 3 hours the reaction mixture was passed through a SCX-2 cartridge (5.0 gm), which was washed with DCM (3x), DMF (3x) twice and finally MeOH (2x). The product **4.5** was released from the cartridge using 5.0 ml 2M NH_3 in MeOH and concentrated *in vacuo* to obtain 234.0 mg light brown solid.

Ethyl 1-(3-(5-bromofuran-2-carboxamido)benzyl)piperidine-4-carboxylate (4.5):



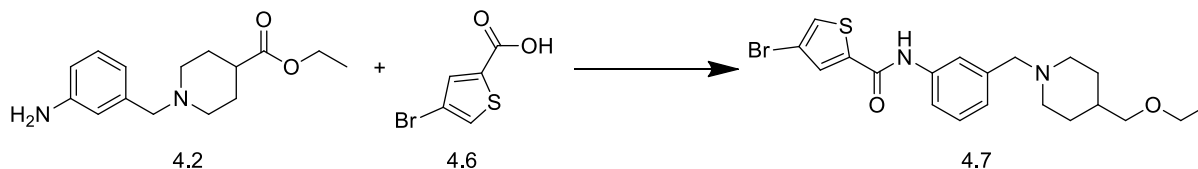
Light brown solid. IR (FTIR, $\nu_{\text{max}}/\text{cm}^{-1}$) 635.14, 692.83, 775.02, 860.27, 1024.69, 1046.66, 1094.97, 1129.45, 1167.22, 1249.40, 1323.56, 1362.67, 1439.07, 1487.34, 1553.13, 1613.41, 1724.62, 2967.27, 3339.66; ^1H NMR (400 MHz, CDCl_3 , TMS); δ 1.22 (t, $J=4.0$ Hz, 3H), 1.8 – 1.82 (m, 2H), 1.93 – 1.94 (m, 2H), 2.14 – 2.18 (m, 2H), 2.30 – 2.33 (m, 1H), 2.95 – 2.97 (m, 2H), 3.48 (s, 1H), 3.56 (s, 2H), 4.11 (q, $J=7.2$ Hz, 2H), 6.80 (d, $J=3.79$ Hz, 1H), 7.10 (d, $J=7.2$ Hz, 1H), 7.19 (d, $J=3.6$ Hz, 1H), 7.3 (t, $J=7.61$ Hz, 1H), 7.51 (s, 1H), 7.67 (dd, $J=1.2$, 6.8 Hz, 1H); ^{13}C NMR (100 MHz, CDCl_3); δ 14.24, 28.25, 29.5, 41.1, 53.00, 60.31, 63.11, 64.7, 113.69, 117.47, 120.58, 122.50, 124.50, 128.04, 134.32, 135.7, 137.24, 147.29, 161.24, 175.88; m/z (+EI) calc. For $\text{C}_{20}\text{H}_{23}\text{BrN}_2\text{O}_4$ (M^+) 435.31, found 436.94 ($\text{M}+\text{H}$) $^+$; Yield: 90%.

Procedure for the synthesis of ethyl 1-(3-(4-bromothiophene-2-carboxamido)benzyl)piperidine-4-carboxylate (4.7):

2.0 eq of HOBT (31 mg) and 1.75 eq. of DIC (141 μ l) were added to a solution of **4.2** (250 mg) in DCM (10 ml). After 30 minutes, 1.30 eq. of **4.6** (256 mg) was added and the reaction mixture was allowed to stir for 3 hours. After 3 hours the reaction mixture was passed through an SCX-2 cartridge (5.0 gm) and the cartridge washed with DCM (3x), DMF (3x)

twice and finally MeOH (2x). The product **4.7** was released from the cartridge using 5.0 ml 2M NH₃ in MeOH and concentrated *in vacuo*. 245.0 mg light brown, oily mass was obtained.

Ethyl 1-(3-(4-bromothiophene-2-carboxamido)benzyl)piperidine-4-carboxylate (4.7):



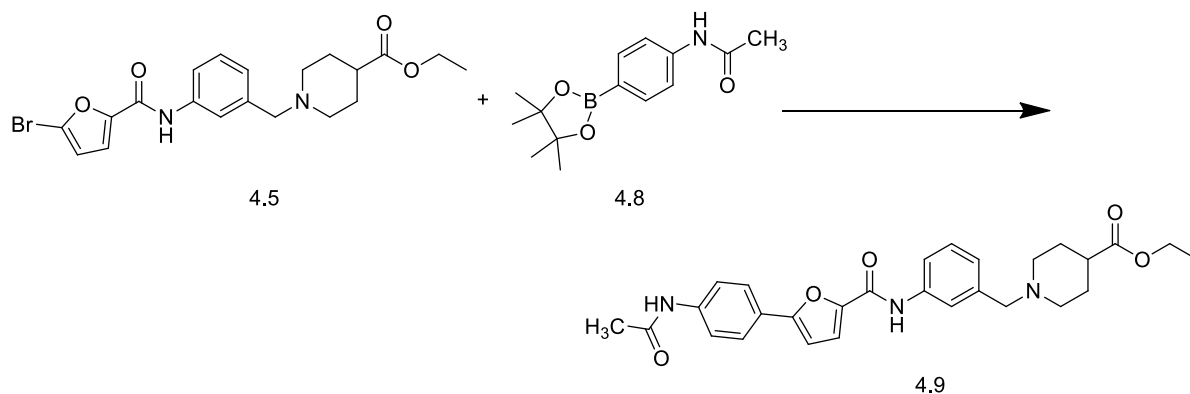
Light brown, oily mass. IR (FTIR, $\nu_{\text{max}}/\text{cm}^{-1}$) 635.14, 692.83, 775.02, 860.27, 1024.69, 1046.66, 1094.97, 1129.45, 1167.22, 1249.40, 1323.56, 1362.67, 1439.07, 1487.34, 1553.13, 1613.41, 1724.62, 2967.27, 3339.66; ¹H NMR (400 MHz, CDCl₃, TMS); δ 1.22 – 1.24 (m, 3H), 1.78 – 1.82 (m, 2H), 1.86 – 1.89 (m, 2H), 2.27 – 2.31 (m, 1H), 2.88 – 2.89 (m, 2H), 2.956 (s, 1H), 3.50 (d, $J=8.4$ Hz, 2H), 4.14 (q, $J=7.2$ Hz, 2H), 7.09 (d, $J=7.6$ Hz, 1H), 7.21 – 7.25 (m, 1 H), 7.30 (t, $J=8.0$ Hz, 1H), 7.43 (d, $J=1.2$ Hz, 1H), 7.50 (s, 1H), 7.62 – 7.63 (m, 1H), 8.14 (s, 1H); ¹³C NMR (100 MHz, CDCl₃); δ 14.24, 28.21, 29.5, 41.1, 52.94, 60.35, 62.99, 64.2, 110.78, 120.1, 121.1, 125.36, 129.07, 132.5, 133.6, 135.5, 136.07, 139.23, 161.8, 175.24; m/z (+EI) calc. For C₂₀H₂₃BrN₂O₃S (M⁺) 451.38, found 452.53 (M+H)⁺; Yield: 98%.

Procedure for the synthesis of ethyl 1-(3-(5-(4-acetamidophenyl)furan-2-carboxamido)benzyl)piperidine-4-carboxylate (4.9) using ethyl 1-(3-(5-bromofuran-2-carboxamido)benzyl)piperidine-4-carboxylate (4.5) *N*-(4-(4,4,5,5-tetramethyl-1,3,2-dioxaborolan-2-yl)phenyl)acetamide (4.8). (Suzuki coupling).

A catalytic amount of tetrakis(triphenylphosphine)palladium, Pd(PPh₃)₄ (0.1 eq., 9 mg) was added to a solution of **4.5** (1.0 eq., 34 mg) and **4.8** (1.2 eq., 25 mg) in a 9:3:1 combination of EtOH, toluene and water in the presence of K₂CO₃ (3.0 eq., 32 mg) in a 10 ml microwave vial containing a magnetic stirrer. The reaction vessel was flushed with nitrogen during each addition. The reaction mixture was sealed in an inert nitrogen environment and heated with microwave radiation in an EMRYSTM Optimizer Microwave Station (Personal Chemistry) at 100 °C for 8 minutes. After LCMS analysis revealed complete reaction, the cooled reaction mixture was passed through an IsoluteTM SCX-2 cartridge (2.0 gm) and washed with DCM (3x), DMF (3x) twice and finally MeOH (2x). The product **4.9** was released from the

cartridge using 5.0 ml 2M NH₃ in MeOH and concentrated *in vacuo* to obtain 31 mg of a light cream, oily mass.

Ethyl 1-(3-(5-(4-acetamidophenyl)furan-2-carboxamido)benzyl)piperidine-4-carboxylate (4.9):



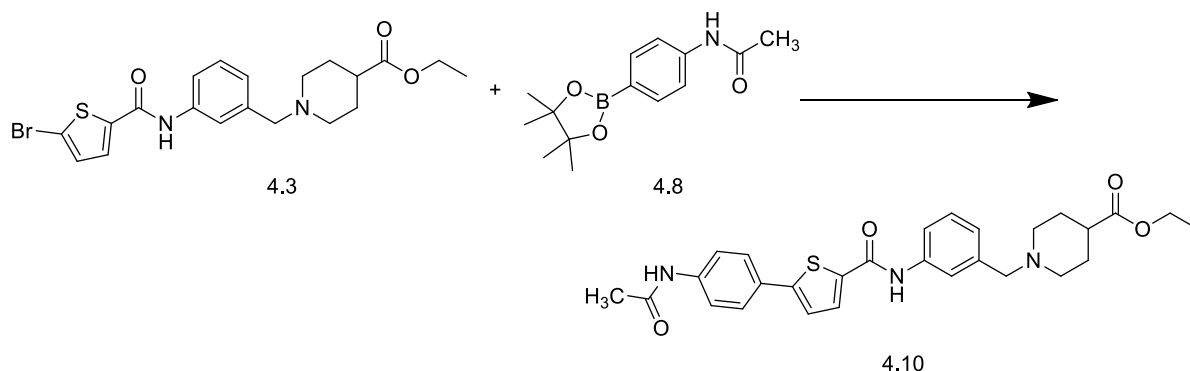
Light cream, oily mass. IR (FTIR, $\nu_{\text{max}}/\text{cm}^{-1}$) 695.36, 723.20, 777.41, 968.33, 1254.62, 1301.51, 1395.69, 1463.43, 1519.13, 1660.07, 1725.58, 2361.96, 2947.66, 3262.19; ¹H NMR (400 MHz, CDCl₃, TMS); δ 1.25 (t, $J=7.07$ Hz, 3H), 1.81 – 1.83 (m, 2H), 1.89 – 1.92 (m, 2H), 2.06 – 2.08 (m, 2H), 2.26 (s, 3H), 2.89 (s, 2H), 2.96 (s, 1H), 3.51 (s, 2H), 4.13 (q, $J=7.24$ Hz, 2H), 6.80 (d, $J=3.79$ Hz, 1H), 7.12 (d, $J=7.58$ Hz, 1H), 7.31 – 7.33 (m, 2H), 7.48 – 7.51 (m, 1H), 7.55 – 7.57 (m, 1H), 7.66 – 7.67 (m, 1H), 7.72 – 7.75 (m, 1H), 8.03 (d, $J=2.27$ Hz, 1H), 8.06 (d, $J=2.53$ Hz, 1H), 8.11 (s, 1H), 8.18 (s, 1H); ¹³C NMR (100 MHz, CDCl₃); δ 14.24, 24.82, 28.25, 53.00, 60.31, 63.11, 76.72, 77.04, 77.36, 108.06, 113.69, 117.47, 119.01, 120.58, 125.50, 128.50, 129.04, 132.03, 132.05, 132.15, 134.32, 137.24, 139.62, 144.22, 147.29, 151.24, 155.88, 175.4; m/z (+EI) calc. For C₂₈H₃₁N₃O₅ (M⁺) 489.56, found 491.11 (M+H)⁺; Yield: 90%.

Procedure for the synthesis of ethyl 1-(3-(5-(4-acetamidophenyl)thiophene-2-carboxamido)benzyl)piperidine-4-carboxylate (4.10)

A catalytic amount of tetrakis(triphenylphosphine)palladium, Pd(PPh₃)₄ (0.1 eq., 33 mg) was added to a solution of **4.3** (1.0 eq., 129 mg) and **4.8** (1.2 eq., 90 mg) in a 9:3:1 combination of EtOH, toluene and water in the presence of K₂CO₃ (3.0 eq., 118 mg) in a 10 ml microwave vial containing a magnetic stirrer. The reaction vessel was flushed with nitrogen during each addition. The reaction mixture was sealed in an inert nitrogen environment and heated with microwave radiation in an EMRYSTM Optimizer Microwave Station (Personal Chemistry) at

100 °C for 10 minutes. After LCMS analysis revealed complete reaction the cooled reaction mixture was passed through an Isolute™ SCX-2 cartridge (2.0 gm) and washed with DCM (3x), DMF (3x) twice and finally MeOH (2x). The product **4.10** was released from the cartridge using 5.0 ml 2M NH₃ in MeOH and concentrated *in vacuo*. 120 mg light cream oil was obtained as product.

Ethyl 1-(3-(5-(4-acetamidophenyl)thiophene-2-carboxamido)benzyl)piperidine-4-carboxylate (4.10):



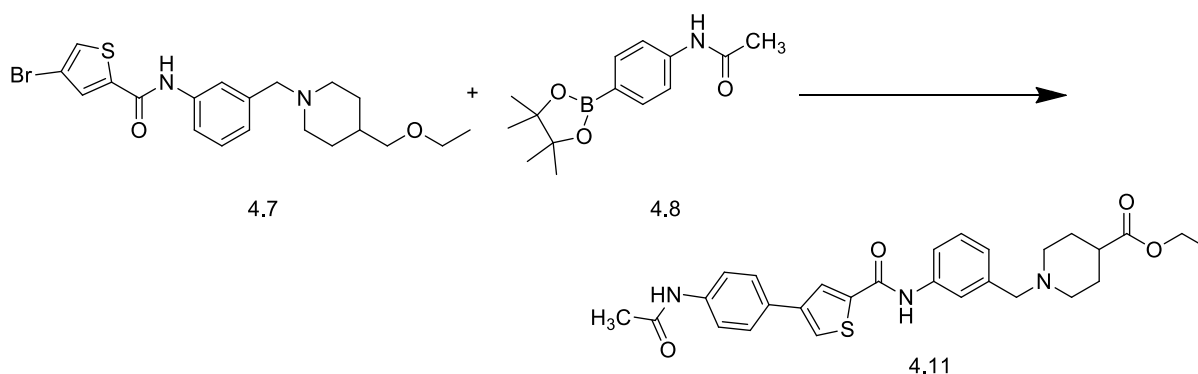
Cream oil. IR (FTIR, $\nu_{\text{max}}/\text{cm}^{-1}$) 630.87, 734.65, 797.03, 1047.27, 1259.00, 1301.51, 1388.22, 1443.02, 1541.85, 1595.69, 1637.12, 2335.36, 2361.75, 2919.25; ¹H NMR (400 MHz, CDCl₃, TMS); δ 1.24 (t, $J=7.07$ Hz, 3H), 1.62 (br. s., 4H), 1.83 – 1.85 (m, 2H), 1.92 – 1.95 (m, 2H), 2.19 (s, 1H), 2.25 (s, 3H), 3.54 (s, 2H), 4.14 (q, $J=7.07$ Hz, 2H), 7.13 (d, $J=7.58$ Hz, 1H), 7.31 (d, $J=4.04$ Hz, 1H), 7.35 – 7.38 (m, 1H), 7.54 (d, $J=5.05$ Hz, 1H), 7.61 (d, $J=3.79$ Hz, 1H), 7.647 (d, $J=7.33$ Hz, 1H), 7.94 (dd, $J=8.59, 2.5$ Hz, 1H), 7.97 (s, 1H), 8.28 (d, $J=8.84$ Hz, 1H), 8.57 (d, $J=2.27$ Hz, 1H); ¹³C NMR (100 MHz, CDCl₃); δ 14.3, 24.50, 29.05, 29.8, 41.1, 53.00, 53.3, 61.5, 63.34, 119.7, 120.1, 121.06, 124.4, 127.7, 127.9, 128.50, 129.04, 132.15, 134.32, 137.24, 138.2, 139.62, 145.7, 148.5, 151.24, 155.88, 168.9, 175.3; m/z (+EI) calc. For C₂₈H₃₁N₃O₄S (M⁺) 505.63, found 507.38 (M+H)⁺; Yield: 93%.

Procedure for the synthesis of ethyl 1-(3-(4-(4-acetamidophenyl)thiophene-2-carboxamido)benzyl)piperidine-4-carboxylate (4.11)

A catalytic amount of tetrakis(triphenylphosphine)palladium, Pd(PPh₃)₄ (0.1 eq., 22 mg) was added to a solution of **4.7** (1.0 eq., 85 mg) and **4.8** (1.2 eq., 59 mg) in a 9:3:1 combination of EtOH, toluene and water in the presence of K₂CO₃ (3.0 eq., 78 mg) in a 10 ml microwave vial containing a magnetic stirrer. The reaction vessel was flushed with nitrogen during each addition. The reaction mixture was sealed in an inert nitrogen environment and heated with microwave radiation in an EMRYS™ Optimizer Microwave Station (Personal Chemistry) at

100 °C for 10 minutes. After LCMS analysis revealed complete reaction the cooled reaction mixture was passed through an Isolute™ SCX-2 cartridge (2.0 gm) and washed with DCM (3x), DMF (3x) twice and finally MeOH (2x). The product **4.11** was released from the cartridge using 5.0 ml 2M NH₃ in MeOH and concentrated *in vacuo*. 77 mg light creamy, oily mass was obtained as product.

Ethyl 1-(3-(4-(4-acetamidophenyl)thiophene-2-carboxamido)benzyl)piperidine-4-carboxylate (4.11):



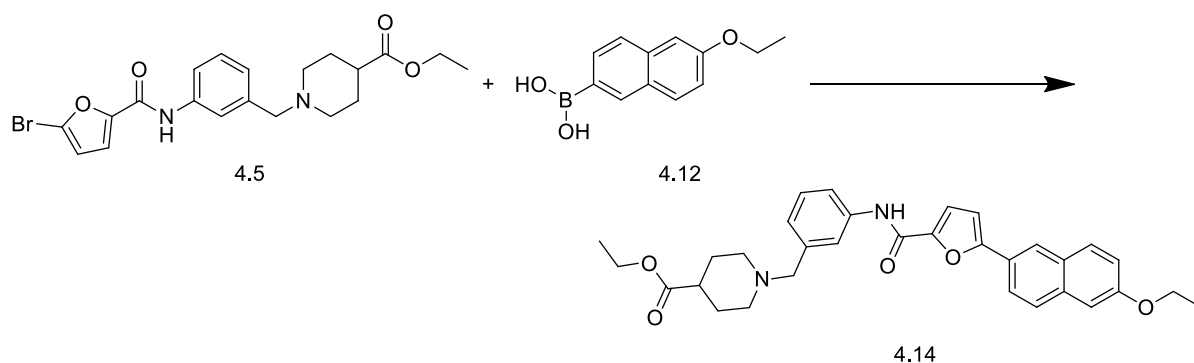
Light cream, oily mass IR (FTIR, $\nu_{\text{max}}/\text{cm}^{-1}$) 630.99, 785.77, 1186.34, 1258.67, 1307.74, 1520.78, 1648.70, 1718.45, 2359.48, 2630.49, 3090.43; ¹H NMR (400 MHz, CDCl₃, TMS); δ 1.25 – 1.27 (m, 3H), 1.79 – 1.82 (m, 2H), 1.88 – 1.92 (m, 2H), 2.07 – 2.11 (m, 1H), 2.24 (s, 3H), 2.88 – 2.90 (m, 2H), 3.51 (s, 2H), 4.13 (q, $J=7.07$ Hz, 2H), 7.12 (d, $J=7.83$ Hz, 1H), 7.33 (t, $J=7.96$ Hz, 1H), 7.54 (s, 1H), 7.65 (d, $J=1.52$ Hz, 1H), 7.67 (d, $J=1.52$ Hz, 1H), 7.86 (s, 1H), 7.89 – 7.90 (m, 2H), 7.92 (d, $J=2.27$ Hz, 1H), 8.04 (s, 1H), 8.27 (d, $J=8.59$ Hz, 1H), 8.53 (d, $J=1.77$ Hz, 1H); ¹³C NMR (100 MHz, CDCl₃); δ 14.24, 24.82, 28.21, 29.4, 29.7, 41.7, 52.94, 60.35, 62.99, 113.78, 119.13, 120.1, 121.5, 1221.1, 125.36, 126.82, 127.08, 128.9, 129.07, 132.5, 136.07, 139.23, 145.37, 151.3, 159.56, 161.8, 168.4, 175.24; m/z (+EI) calc. For C₂₈H₃₁N₃O₄S (M+) 505.63, found 507.15 (M+H)⁺; Yield: 80%.

Procedure for the synthesis of ethyl 1-(3-(5-(6-ethoxynaphthalen-2-yl)thiophene-2-carboxamido)benzyl)piperidine-4-carboxylate (4.13)

A catalytic amount of tetrakis(triphenylphosphine)palladium, Pd(PPh₃)₄ (0.1 eq., 22 mg) was added to a solution of **4.3** (1.0 eq., 60 mg) and **4.12** (1.2 eq., 34 mg) in a 9:3:1 combination of EtOH, toluene and water in the presence of K₂CO₃ (3.0 eq., 55 mg) in a 10 ml microwave vial containing a magnetic stirrer. The reaction vessel was flushed with nitrogen during each addition. The reaction mixture was sealed in an inert nitrogen environment and heated with

EtOH, toluene and water in the presence of K₂CO₃ (3.0 eq., 57 mg) in a 10 ml microwave vial containing a magnetic stirrer. The reaction vessel was flushed with nitrogen during each addition. The reaction mixture was sealed in an inert nitrogen environment and heated with microwave radiation in an EMRYSTM Optimizer Microwave Station (Personal Chemistry) at 100 °C for 8 minutes. After LCMS analysis revealed complete reaction the cooled reaction mixture was passed through an IsoluteTM SCX-2 cartridge (2.0 gm) and washed with DCM (3x), DMF (3x) twice and finally MeOH (2x). The product **4.14** was released from the cartridge using 5.0 ml 2M NH₃ in MeOH and concentrated *in vacuo*. 48 mg light cream, oily mass was obtained as product.

Ethyl 1-(3-(5-(6-ethoxynaphthalen-2-yl)furan-2-carboxamido)benzyl)piperidine-4-carboxylate (4.14):

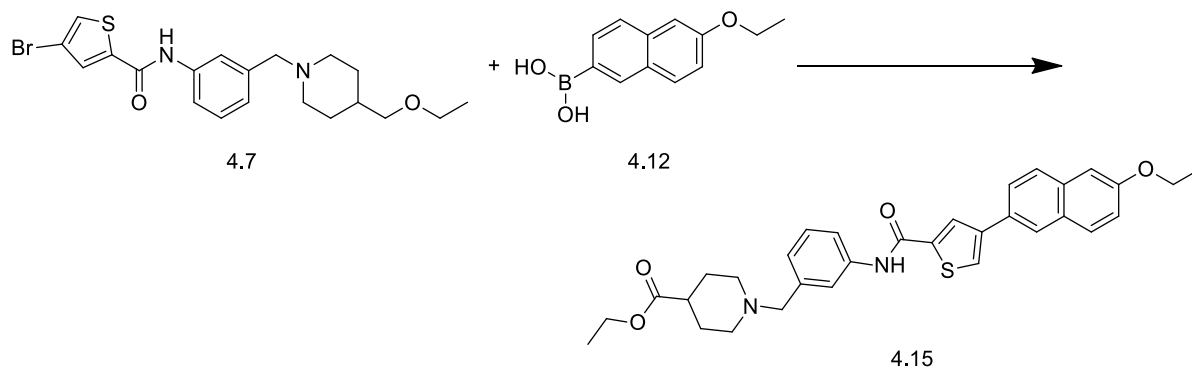


Light cream oily mass. IR (FTIR, $\nu_{\text{max}}/\text{cm}^{-1}$) 630.53, 664.57, 785.97, 1204.42, 1444.64, 1545.38, 1648.70, 1726.19, 1736.53, 2087.85, 2186.04, 2516.79, 3085.27, 3348.83; ¹H NMR (400 MHz, CDCl₃, TMS); δ 1.25 – 1.27 (m, 3H), 1.52 (t, $J=6.95$ Hz, 3H), 1.82 – 1.85 (m, 2H), 1.91 – 1.93 (m, 2H), 2.30 – 2.33 (m, 1H), 2.89 – 2.91 (m, 2H), 3.53 (s, 2H), 4.16 – 4.18 (m, 4 H), 6.86 (d, $J=3.54$ Hz, 1H), 7.13 (d, $J=7.83$ Hz, 1H), 7.16 (d, $J=2.53$ Hz, 1H), 7.23 (dd, $J=9.09$, 2.5 Hz, 1H), 7.36 (d, $J=4.0$ Hz, 1H), 7.37 (d, $J=2.50$ Hz, 1H), 7.48 (dd, $J=7.58$, 3.03Hz, 1H), 7.58 (d, $J=1.52$ Hz, 1H), 7.68 – 7.70 (m, 2H), 7.77 (dd, $J=7.96$, 1.3 Hz, 1H), 7.86 (d, $J=9.09$ Hz, 1H), 7.79 (s, 1H), 8.15 (s, 1H), 8.18 (s, 1H); ¹³C NMR (100 MHz, CDCl₃); δ 14.1, 14.8, 28.27, 29.5, 41.1, 52.95, 60.26, 63.56, 64.2, 64.7, 106.51, 108.88, 108.98, 120.45, 121.7, 121.9, 123.27, 124.47, 125.88, 127.57, 128.55, 130.7, 129.72, 132.12, 135.6, 137.19, 141.2, 146.70, 150.20, 157.64, 162.82, 175.00; m/z (+EI) calc. For C₃₂H₃₄N₂O₅ (M⁺) 526.62, found 527.10 (M+H)⁺; Yield: 80%.

Procedure for the synthesis of ethyl 1-(3-(4-(6-ethoxynaphthalen-2-yl)thiophene-2-carboxamido)benzyl)piperidine-4-carboxylate (4.15)

A catalytic amount of tetrakis(triphenylphosphine)palladium, Pd(PPh₃)₄ (0.1 eq., 22 mg) was added to a solution of **4.7** (1.0 eq., 60 mg) and **4.12** (1.2 eq., 34 mg) in a 9:3:1 combination of EtOH, toluene and water in the presence of K₂CO₃ (3.0 eq., 55 mg) in a 10 ml microwave vial containing a magnetic stirrer. The reaction vessel was flushed with nitrogen during each addition. The reaction mixture was sealed in an inert nitrogen environment and heated with microwave radiation in an EMRYSTM Optimizer Microwave Station (Personal Chemistry) at 100 °C for 8 minutes. After LCMS analysis revealed complete reaction the cooled reaction mixture was passed through an IsoluteTM SCX-2 cartridge (2.0 gm) and washed with DCM (3x), DMF (3x) twice and finally MeOH (2x). The product **4.15** was released from the cartridge using 5.0 ml 2M NH₃ in MeOH and concentrated *in vacuo*. 53 mg light cream, oily mass was obtained as product.

Ethyl 1-(3-(4-(6-ethoxynaphthalen-2-yl)thiophene-2-carboxamido)benzyl)piperidine-4-carboxylate (4.15):



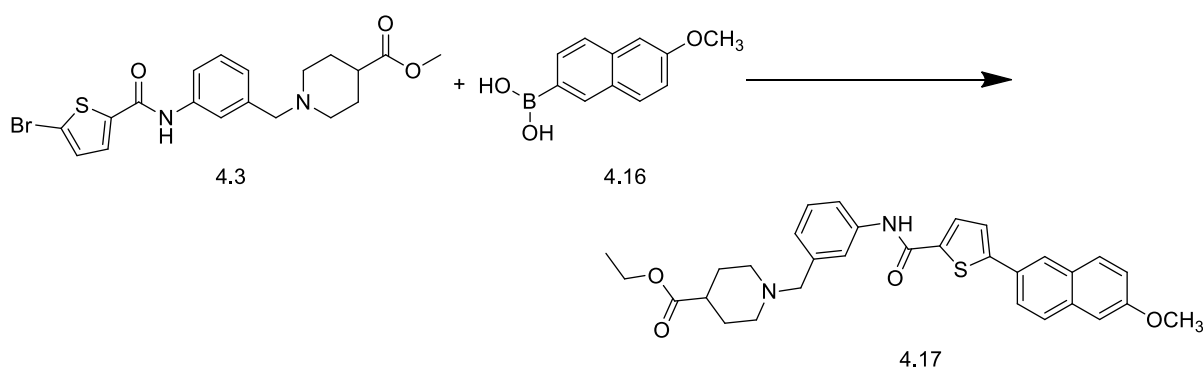
Light cream, oily mass. IR (FTIR, $\nu_{\text{max}}/\text{cm}^{-1}$) 628.65, 666.05, 735.62, 902.94, 1218.19, 1363.71, 1434.28, 1713.28, 1736.53, 2335.91, 2969.45, 3452.19; ¹H NMR (400 MHz, CDCl₃, TMS); δ 1.24 (m, 3H), 1.51 (t, $J=7.07$ Hz, 3H), 1.81 (m, 2H), 1.91 (m, 2H), 2.07 (m, 2H), 2.30 (m, 1H), 2.89 (m, 2H), 3.52 (s, 1H), 4.14 (q, $J=8.0$ Hz, 2H), 4.19 (q, $J=8.0$ Hz, 2H), 7.12 (d, $J=7.33$ Hz, 1H), 7.15 (d, $J=2.27$ Hz, 1H), 7.20 (dd, $J=2.5, 8.84$ Hz, 1H), 7.34 (t, $J=7.83$ Hz, 1H), 7.55 (s, 1H), 7.68 (m, 1H), 7.71 (d, $J=1.78$ Hz, 1H), 7.72 (d, $J=1.52$ Hz, 1H), 7.78 (s, 1H), 7.80 (s, 1H), 8.00 (d, $J=1.77$ Hz, 1H), 8.02 (d, $J=1.52$ Hz, 1H); ¹³C NMR (100 MHz, CDCl₃); δ 14.3, 14.6, 29.27, 29.5, 41.1, 53.5, 53.95, 61.26, 64.2, 64.7, 107.51, 118.88, 120.45, 121.0, 123.27, 124.88, 125.6, 127.57, 128.55, 128.96, 129.51, 129.72, 130.12, 134.6,

135.19, 135.6, 137.70, 144.3, 154.20, 157.64, 161.82, 173.00; m/z (+EI) calc. For $C_{32}H_{34}N_2O_4S$ (M^+) 542.69, found 543.05 ($M+H$)⁺; Yield: 89%.

Procedure for the synthesis of ethyl 1-(3-(5-(6-methoxynaphthalen-2-yl)thiophene-2-carboxamido)benzyl)piperidine-4-carboxylate (4.17)

A catalytic amount of tetrakis(triphenylphosphine)palladium, $Pd(PPh_3)_4$ (0.1 eq., 22 mg) was added to a solution of **4.3** (1.0 eq., 60 mg) and **4.16** (1.2 eq., 28 mg) in a 9:3:1 combination of EtOH, toluene and water in the presence of K_2CO_3 (3.0 eq., 55 mg) in a 10 ml microwave vial containing a magnetic stirrer. The reaction vessel was flushed with nitrogen during each addition. The reaction mixture was sealed in an inert nitrogen environment and heated with microwave radiation in an EMRYSTM Optimizer Microwave Station (Personal Chemistry) at 100 °C for 8 minutes. After LCMS analysis revealed complete reaction the cooled reaction mixture was passed through an IsoluteTM SCX-2 cartridge (2.0 gm) and washed with DCM (3x), DMF (3x) twice and finally MeOH (2x). The product **4.17** was released from the cartridge using 5.0 ml 2M NH_3 in MeOH and concentrated *in vacuo*. 55 mg colourless oily mass was obtained as product.

Ethyl 1-(3-(5-(6-methoxynaphthalen-2-yl)thiophene-2-carboxamido)benzyl)piperidine-4-carboxylate (4.17):



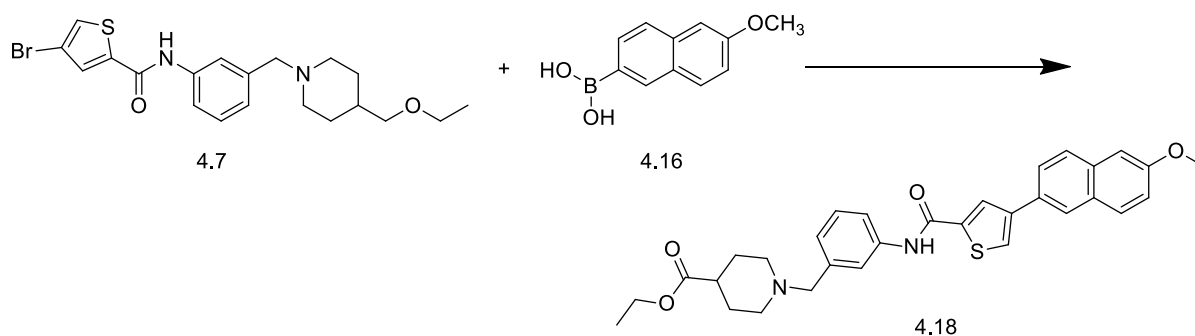
Colourless oily mass. IR (FTIR, ν_{max}/cm^{-1}) 629.97, 785.97, 1028.78, 1121.77, 1369.74, 1444.64, 1604.79, 1728.78, 1969.00, 2041.34, 2337.0, 2361.75, 2630.49, 3271.31; 1H NMR (400 MHz, $CDCl_3$, TMS); δ 1.25 – 1.27 (m, 3H), 1.78 – 1.81 (m, 2H), 1.86 (br s, 2H), 2.01 – 2.05 (m, 2H), 2.27 – 2.30 (m, 1H), 2.86 – 2.88 (m, 2H), 3.50 (s, 2H), 3.94 (s, 3H), 4.13 – 4.15 (m, 2H), 7.10 (d, $J=8.08$ Hz, 1H), 7.14 (d, $J=3.79$ Hz, 1H), 7.19 (dd, $J=7.58, 3.03$ Hz, 1H), 7.31 (t, $J=7.83$ Hz, 1H), 7.39 (d, $J=7.7$ Hz, 1H), 7.54 (s, 1H), 7.66 – 7.88 (m, 2H), 7.70 – 7.72 (m, 1H), 7.76 (s, 1H), 7.79 (s, 1H), 7.90 (s, 1H), 8.04 (s, 1H); ^{13}C NMR (100 MHz, $CDCl_3$); δ 13.86, 29.9, 30.58, 40.83, 52.61, 52.63, 55.02, 59.92, 62.94, 105.43, 119.10, 119.36, 120.5,

121.2, 122.96, 124.19, 124.52, 128.11, 128.27, 129.17, 129.41, 131.77, 134.19, 135.6, 135.9, 139.25, 139.29, 149.77, 157.94, 161.7, 174.93; m/z (+EI) calc. For $C_{31}H_{32}N_2O_4S$ (M+) 528.66, found 529.96 (M+H)⁺; Yield: 91%.

Procedure for the synthesis of ethyl 1-(3-(4-(6-methoxynaphthalen-2-yl)thiophene-2-carboxamido)benzyl)piperidine-4-carboxylate (4.18)

A catalytic amount of tetrakis(triphenylphosphine)palladium, $Pd(PPh_3)_4$ (0.1 eq., 22 mg) was added to a solution of **4.7** (1.0 eq., 60 mg) and **4.16** (1.2 eq., 28 mg) in a 9:3:1 combination of EtOH, toluene and water in the presence of K_2CO_3 (3.0 eq., 55 mg) in a 10 ml microwave vial containing a magnetic stirrer. The reaction vessel was flushed with nitrogen during each addition. The reaction mixture was sealed in an inert nitrogen environment and heated with microwave radiation in an EMRYSTM Optimizer Microwave Station (Personal Chemistry) at 100 °C for 8 minutes. After LCMS analysis revealed complete reaction the cooled reaction mixture was passed through an IsoluteTM SCX-2 cartridge (2.0 gm) and washed with DCM (3x), DMF (3x) twice and finally MeOH (2x). The product **4.18** was released from the cartridge using 5.0 ml 2M NH_3 in MeOH and concentrated *in vacuo*. 60 mg yellow, oily mass was obtained as product.

Ethyl 1-(3-(4-(6-methoxynaphthalen-2-yl)thiophene-2-carboxamido)benzyl)piperidine-4-carboxylate (4.18):



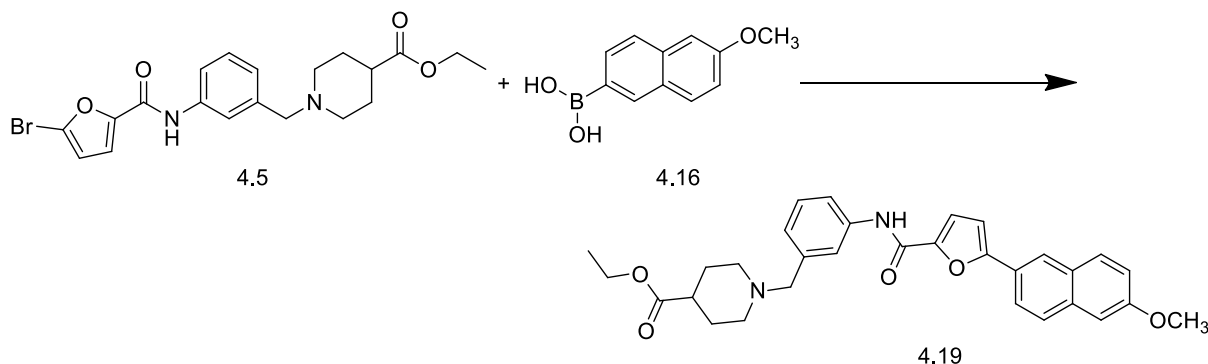
Yellow, oily mass. IR (FTIR, ν_{max}/cm^{-1}) 630.39, 775.64, 853.12, 1027.97, 1231.81, 1266.42, 1318.08, 1442.13, 1487.18, 1549.29, 1607.18, 1727.33, 2067.18, 2358.87, 2852.71, 2927.43, 3271.31; 1H NMR (400 MHz, $CDCl_3$, TMS); δ 1.23 – 1.25 (m, 3H), 1.76 – 1.78 (m, 2H), 1.86 – 1.89 (m, 2H), 2.02 (t, $J=10.99$ Hz, 2H) 2.27 – 2.31 (m, 1H), 2.86 (d, $J=11.12$ Hz, 2H), 3.47 (s, 2H), 3.92 (s, 3H), 4.13 (q, $J=10.99$ Hz, 2H), 7.09 (d, $J=7.33$ Hz, 1H), 7.13 (s, 1H), 7.16 (dd, $J=1.8, 8.97$ Hz, 1H), 7.31 – 7.33 (m, 1H), 7.44– 7.45 (m, 1H), 7.57 (s, 1H), 7.68 – 7.70 (m, 2H), 7.74 – 7.77 (m, 2H), 7.95 (s, 1H), 8.07 (s, 1H); ^{13}C NMR (100 MHz, $CDCl_3$); δ 14.47, 29.5, 31.20, 41.43, 53.19, 53.5, 55.59, 60.55, 63.29, 105.94, 119.34, 120.98, 122.3, 226

124.4, 125.04, 127.73, 128.06, 128.6, 129.17, 129.26, 129.84, 130.37, 134.19, 134.8, 135.6, 135.7, 140.29, 141.0, 143.31, 158.17, 175.59; m/z (+EI) calc. For $C_{31}H_{32}N_2O_4S$ (M+) 528.66, found 528.94 (M+H)⁺; Yield: 98%.

Procedure for the synthesis of ethyl 1-(3-(5-(6-methoxynaphthalen-2-yl)furan-2-carboxamido)benzyl)piperidine-4-carboxylate (4.19)

A catalytic amount of tetrakis(triphenylphosphine)palladium, $Pd(PPh_3)_4$ (0.1 eq.) was added to a solution of **4.5** (1.0 eq., 50 mg) and **4.16** (1.2 eq., 29 mg) in a 9:3:1 combination of EtOH, toluene and water in the presence of K_2CO_3 (3.0 eq.) in a 10 ml microwave vial containing a magnetic stirrer. The reaction vessel was flushed with nitrogen during each addition. The reaction mixture was sealed in an inert nitrogen environment and heated with microwave radiation in an EMRYSTM Optimizer Microwave Station (Personal Chemistry) at 100 °C for 8 minutes. After LCMS analysis revealed complete reaction the cooled reaction mixture was passed through an IsoluteTM SCX-2 cartridge (1.0 gm) and washed with DCM (3x), DMF (3x) twice and finally MeOH (2x). The product **4.19** was released from the cartridge using 5.0 ml 2M NH_3 in MeOH and concentrated *in vacuo*. 43 mg cream, oily mass was obtained as product.

Ethyl 1-(3-(5-(6-methoxynaphthalen-2-yl)furan-2-carboxamido)benzyl)piperidine-4-carboxylate (4.19):



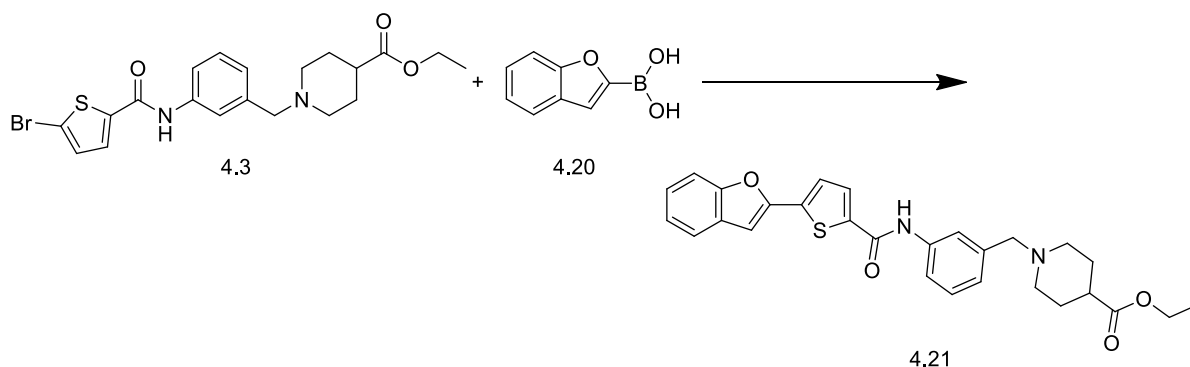
Cream oily mass. IR (FTIR, ν_{max}/cm^{-1}) 629.60, 690.40, 783.39, 1026.19, 1205.50, 1367.15, 1547.97, 1659.04, 1737.23, 1938.00, 2360.90, 2925.06, 3266.14, 3400.15; 1H NMR (400 MHz, $CDCl_3$, TMS); δ 1.24 (t, $J=7.20$ Hz, 3H), 1.79 – 1.80 (m, 2H), 1.89 – 1.91 (m, 2H), 2.05 (t, $J=11.12$ Hz, 2H), 2.29 – 2.32 (m, 1H), 2.91 – 2.93 (m, 2H), 3.51 (s, 2H), 3.94 (s, 3H), 4.12 (q, $J=7.16$ Hz, 2H), 6.84 (d, $J=3.54$ Hz, 1H), 7.10 (d, $J=7.58$ Hz, 1H), 7.15 (d, $J=2.27$ Hz, 1H), 7.20 (dd, $J=2.5, 8.84$ Hz, 1H), 7.34 – 7.35 (m, 2H), 7.58 (s, 1H), 7.75 (d, $J=7.58$

Hz, 1H), 7.78 – 7.80 (m, 2H), 7.82 (d, $J=8.84$ Hz, 1H), 8.16 (s, 1H), 8.23 (s, 1H); ^{13}C NMR (100 MHz, CDCl_3); δ 14.15, 28.19, 30.86, 41.12, 52.93, 53.3, 55.30, 60.20, 63.10, 105.85, 107.46, 117.57, 118.92, 119.66, 120.48, 122.85, 123.40, 124.67, 125.23, 127.45, 128.63, 128.89, 129.78, 134.56, 137.44, 139.45, 146.61, 156.15, 158.34, 175.17, 206.98; m/z (+EI) calc. For $\text{C}_{31}\text{H}_{32}\text{N}_2\text{O}_5$ (M^+) 512.60, found 512.99 ($\text{M}+\text{H}$) $^+$; Yield: 87%.

Procedure for the synthesis of ethyl 1-(3-(5-(benzofuran-2-yl)thiophene-2-carboxamido)benzyl)piperidine-4-carboxylate (4.21)

A catalytic amount of tetrakis(triphenylphosphine)palladium, $\text{Pd}(\text{PPh}_3)_4$ (0.1 eq.) was added to a solution of **4.3** (1.0 eq., 50 mg) and **4.20** (1.2 eq., 22 mg) in a 9:3:1 combination of EtOH, toluene and water in the presence of K_2CO_3 (3.0 eq.) in a 10 ml microwave vial containing a magnetic stirrer. The reaction vessel was flushed with nitrogen during each addition. The reaction mixture was sealed in an inert nitrogen environment and heated with microwave radiation in an EMRYSTM Optimizer Microwave Station (Personal Chemistry) at 100 °C for 8 minutes. After LCMS analysis revealed complete reaction the cooled reaction mixture was passed through an IsoluteTM SCX-2 cartridge (1.0 gm) and washed with DCM (3x), DMF (3x) twice and finally MeOH (2x). The product **4.21** was released from the cartridge using 5.0 ml 2M NH_3 in MeOH and concentrated *in vacuo*. 45 mg colourless oil was obtained as product.

Ethyl 1-(3-(5-(benzofuran-2-yl)thiophene-2-carboxamido)benzyl)piperidine-4-carboxylate (4.21):



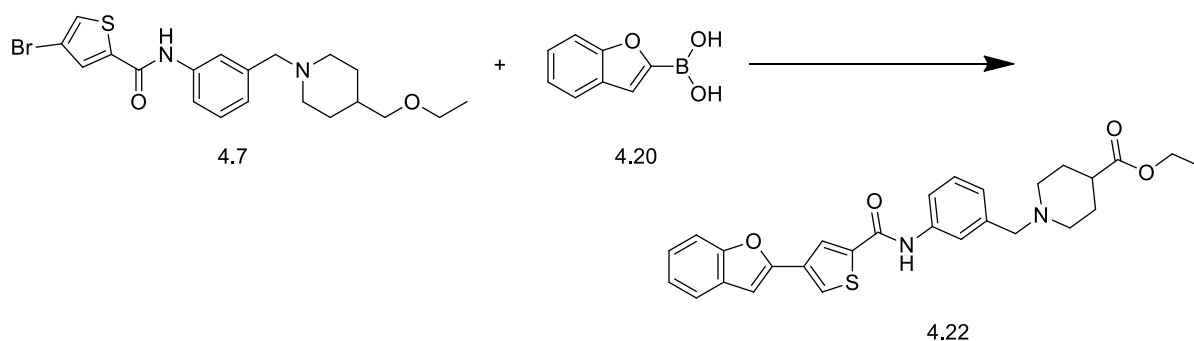
Colourless oil. IR (FTIR, $\nu_{\text{max}}/\text{cm}^{-1}$) 629.25, 734.68, 1047.89, 1090.77, 1221.36, 1267.75, 1360.93, 1440.10, 1547.68, 1609.96, 1658.17, 1710.70, 2180.87, 2360.43, 2928.69; ^1H NMR (400 MHz, CDCl_3 , TMS); δ 1.24 (t, $J=7.07$ Hz, 3H), 1.76 – 1.78 (m, 2H), 1.87 – 1.89 (m, 2H), 2.00 – 2.02 (m, 2H), 2.26 – 2.29 (m, 1H), 2.85 (d, $J=11.6$ Hz, 2H), 2.95 (s, 1H), 3.47 (s, 2H), 4.13 – 4.15 (m, 2H), 6.99 (s, 1H), 7.08 – 7.11 (m, 1H), 7.24 (t, $J=7.45$ Hz, 1H), 7.31

(d, $J=3.79$ Hz, 1H), 7.50 (d, $J=8.34$ Hz, 1H), 7.56 – 7.55 (m, 2H), 7.64 (d, $J=8.34$ Hz, 1H), 7.67 – 7.69 (m, 1H), 8.02 (s, 1H); ^{13}C NMR (100 MHz, CDCl_3); δ 14.16, 28.23, 29.3, 41.11, 52.92, 53.7, 60.21, 62.97, 103.12, 111.18, 120.66, 120.9, 121.12, 123.36, 124.56, 128.45, 129.01, 129.4, 135.95, 135.98, 137.05, 138.05, 138.87, 139.50, 150.01, 154.74, 175.27, 175.28; m/z (+EI) calc. For $\text{C}_{28}\text{H}_{28}\text{N}_2\text{O}_4\text{S}$ (M^+) 488.60, found 489.17 ($\text{M}+\text{H}$) $^+$; Yield: 90%.

Procedure for the synthesis of ethyl 1-(3-(4-(benzofuran-2-yl)thiophene-2-carboxamido)benzyl)piperidine-4-carboxylate (4.22)

A catalytic amount of tetrakis(triphenylphosphine)palladium, $\text{Pd}(\text{PPh}_3)_4$ (0.1 eq.) was added to a solution of **4.7** (1.0 eq., 50 mg) and **4.20** (1.2 eq., 22 mg) in a 9:3:1 combination of EtOH, toluene and water in the presence of K_2CO_3 (3.0 eq.) in a 10 ml microwave vial containing a magnetic stirrer. The reaction vessel was flushed with nitrogen during each addition. The reaction mixture was sealed in an inert nitrogen environment and heated with microwave radiation in an EMRYSTM Optimizer Microwave Station (Personal Chemistry) at 100 °C for 8 minutes. After LCMS analysis revealed complete reaction the cooled reaction mixture was passed through an IsoluteTM SCX-2 cartridge (1.0 gm) and washed with DCM (3x), DMF (3x) twice and finally MeOH (2x). The product **4.22** was released from the cartridge using 5.0 ml 2M NH_3 in MeOH and concentrated *in vacuo*. 50 mg colourless oil was obtained as product.

Ethyl 1-(3-(4-(benzofuran-2-yl)thiophene-2-carboxamido)benzyl)piperidine-4-carboxylate (4.22):



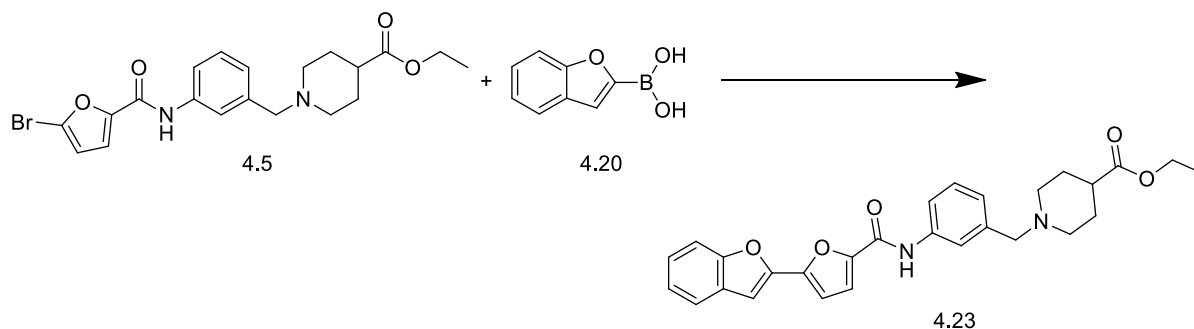
Colourless, oily mass. IR (FTIR, $\nu_{\text{max}}/\text{cm}^{-1}$) 629.20, 698.15, 734.74, 1090.77, 1221.72, 1362.08, 1439.71, 1550.55, 1656.45, 1708.11, 1969.00, 2041.34, 2335.91, 2919.89, 3394.18; ^1H NMR (400 MHz, CDCl_3 , TMS); δ 1.24 (t, $J=7.07$ Hz, 3H), 1.78 – 1.80 (m, 2H), 1.87 – 1.89 (m, 2H), 2.03 (td, $J=2.15, 4.0, 11.31$ Hz, 2H), 2.28 – 2.31 (m, 1H), 2.88 – 2.90 (m, 2H), 3.48 (s, 2H), 4.13 (q, $J=7.07$ Hz, 2H), 6.87 (s, 1H), 7.10 (d, $J=7.58$ Hz, 1H), 7.25 (dd, $J=0.9$,

7.5 Hz, 1H), 7.29 – 7.30 (m, 1H), 7.31 – 7.33 (m, 1H), 7.49 (d, $J=8.08$ Hz, 1H), 7.56 – 7.57 (m, 2H), 7.66 (d, $J=8.08$ Hz, 1H), 7.86 (d, $J=1.01$ Hz, 1H), 8.03 – 8.05 (m, 1H), 8.24 (s, 1H); ^{13}C NMR (100 MHz, CDCl_3); δ 14.16, 29.5, 29.7, 41.11, 52.92, 53.5, 60.21, 62.97, 103.12, 111.5, 120.1, 120.9, 121.12, 123.36, 124.7, 128.5, 129.3, 129.6, 135.4, 135.7, 135.98, 140.05, 141.2, 144.9, 154.74, 156.5, 164.27, 175.28; m/z (+EI) calc. For $\text{C}_{28}\text{H}_{28}\text{N}_2\text{O}_4\text{S}$ (M^+) 488.60, found 490.14 ($\text{M}+\text{H}$) $^+$; Yield: 92%.

Procedure for the synthesis of ethyl 1-(3-(5-(benzofuran-2-yl)furan-2-carboxamido)benzyl)piperidine-4-carboxylate (4.23)

A catalytic amount of tetrakis(triphenylphosphine)palladium, $\text{Pd}(\text{PPh}_3)_4$ (0.1 eq.) was added to a solution of **4.5** (1.0 eq., 50 mg) and **4.20** (1.2 eq., 22 mg) in a 9:3:1 combination of EtOH, toluene and water in the presence of K_2CO_3 (3.0 eq.) in a 10 ml microwave vial containing a magnetic stirrer. The reaction vessel was flushed with nitrogen during each addition. The reaction mixture was sealed in an inert nitrogen environment and heated with microwave radiation in an EMRYSTM Optimizer Microwave Station (Personal Chemistry) at 100 °C for 8 minutes. After LCMS analysis revealed complete reaction the cooled reaction mixture was passed through an IsoluteTM SCX-2 cartridge (1.0 gm) and washed with DCM (3x) and DMF (3x) twice and finally MeOH (2x). The product **4.23** was released from the cartridge using 5.0 ml 2M NH_3 in MeOH and concentrated *in vacuo*. 38 mg light cream, oily mass was obtained as product.

Ethyl 1-(3-(5-(benzofuran-2-yl)furan-2-carboxamido)benzyl)piperidine-4-carboxylate (4.23):



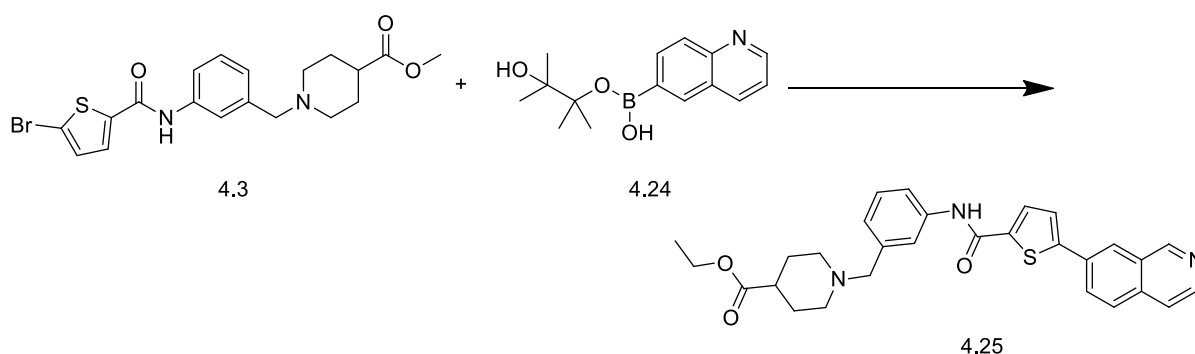
Light cream, oily mass. IR (FTIR, $\nu_{\text{max}}/\text{cm}^{-1}$) 629.68, 701.06, 736.90, 1093.35, 1170.84, 1221.26, 1266.40, 1362.54, 1443.09, 1487.98, 1573.19, 1667.61, 1710.43, 1974.16, 2358.14, 2916.46, 3436.69; ^1H NMR (400 MHz, CDCl_3 , TMS); δ 1.25 (t, $J=7.07$ Hz, 3H), 1.81 – 1.83 (m, 2H), 1.89 – 1.91 (m, 2H), 2.06 – 2.08 (m, 2H), 2.29 – 2.33 (m, 1H), 2.88 – 2.91 (m, 2H), 3.51 (s, 2H), 4.13 (q, $J=7.16$ Hz, 2H), 6.92 (d, $J=3.54$ Hz, 1H), 7.11 (d, $J=7.83$ Hz, 1H), 7.14 – 7.16 (m, 1H), 7.30 – 7.32 (m, 1H), 7.33 – 7.34 (m, 1H), 7.35 (d, $J=3.8$ Hz, 1H), 7.48 – 7.51

(m, 1H), 7.53 (d, $J=1.01$ Hz, 1H), 7.57 (s, 1H), 7.63 – 7.64 (m, 1H), 7.67 – 7.69 (m, 1H), 7.74 (dd, $J=1.2, 8.08$ Hz, 1H); ^{13}C NMR (100 MHz, CDCl_3); δ 14.1, 29.5, 29.7, 41.11, 52.92, 53.3, 60.21, 62.97, 103.12, 108.5, 108.7, 111.5, 120.1, 120.9, 121.12, 123.36, 124.7, 128.5, 129.6, 135.4, 135.7, 135.98, 140.9, 146.9, 154.74, 156.5, 164.27, 175.28; m/z (+EI) calc. For $\text{C}_{28}\text{H}_{28}\text{N}_2\text{O}_5$ (M^+) 472.53, found 473.13 ($\text{M}+\text{H}$) $^+$; Yield: 75%.

Procedure for the synthesis of ethyl 1-(3-(5-(isoquinolin-7-yl)thiophene-2-carboxamido)benzyl)piperidine-4-carboxylate (4.25)

A catalytic amount of tetrakis(triphenylphosphine)palladium, $\text{Pd}(\text{PPh}_3)_4$ (0.1 eq.) was added to a solution of **4.3** (1.0 eq., 50 mg) and **4.24** (1.2 eq., 36 mg) in a 9:3:1 combination of EtOH, toluene and water in the presence of K_2CO_3 (3.0 eq.) in a 10 ml microwave vial containing a magnetic stirrer. The reaction vessel was flushed with nitrogen during each addition. The reaction mixture was sealed in an inert nitrogen environment and heated with microwave radiation in an EMRYSTM Optimizer Microwave Station (Personal Chemistry) at 100 °C for 8 minutes. After LCMS analysis revealed complete reaction the cooled reaction mixture was passed through an IsoluteTM SCX-2 cartridge (1.0 gm) and washed with DCM (3x), DMF (3x) twice and finally MeOH (2x). The product **4.25** was released from the cartridge using 5.0 ml 2M NH_3 in MeOH and concentrated *in vacuo*. 40 mg light cream, oily mass was obtained as product.

Ethyl 1-(3-(5-(isoquinolin-7-yl)thiophene-2-carboxamido)benzyl)piperidine-4-carboxylate (4.25):



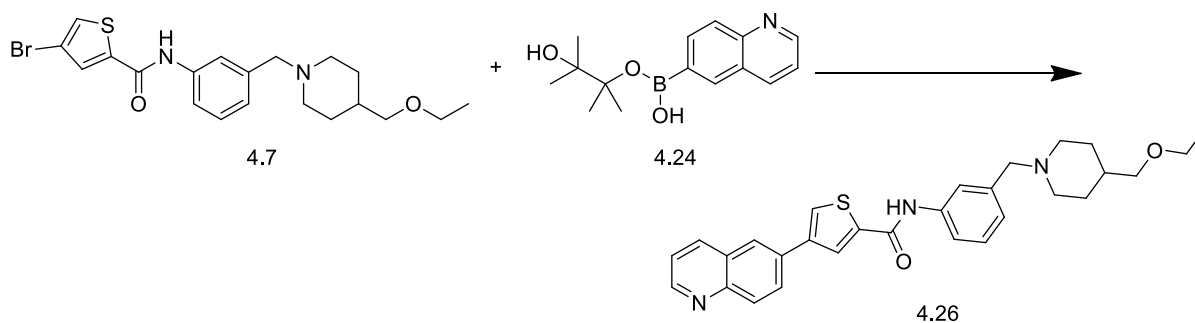
Light cream, oily mass. IR (FTIR, $\nu_{\text{max}}/\text{cm}^{-1}$) 629.54, 783.39, 1046.86, 1121.77, 1214.76, 1281.91, 1319.12, 1367.15, 1442.31, 1485.97, 1547.22, 1648.70, 1727.07, 2180.87, 2360.00, 2852.71, 2921.88, 3328.16; ^1H NMR (500 MHz, CDCl_3 , TMS); δ 1.25 (t, $J=7.09$ Hz, 3H), 1.79 – 1.81 (m, 2H), 1.88 – 1.90 (m, 2H), 2.05 – 2.08 (m, 2H), 2.29 – 2.31 (m, 1H), 2.87 – 2.89 (m, 2H), 3.49 (s, 2H), 4.13 (q, $J=7.15$ Hz, 2H), 7.10 (d, $J=7.57$ Hz, 1H), 7.31 (t, $J=7.88$ Hz, 1H), 7.44 – 7.45 (m, 1H), 7.55 (s, 1H), 7.67 (d, $J=4.10$ Hz, 2H), 7.99 – 8.01 (m, 2H),

8.06 (d, $J=2.21$ Hz, 1H), 8.14 (d, $J=8.83$ Hz, 1H), 8.18 (dd, $J=0.9, 8.83$ Hz, 1H), 8.92 (dd, $J=1.7, 4.26$ Hz, 1H); ^{13}C NMR (100 MHz, CDCl_3); δ 13.94, 28.02, 29.5, 40.91, 52.69, 53.5, 59.96, 62.72, 118.81, 120.36, 121.69, 124.23, 124.40, 125.05, 128.22, 128.71, 129.16, 130.18, 135.0, 135.8, 135.91, 136.4, 137.43, 138.57, 143.4, 148.39, 150.61, 159.44, 174.93; m/z (+EI) calc. For $\text{C}_{29}\text{H}_{29}\text{N}_3\text{O}_3\text{S}$ (M^+) 499.62, found 499.85 ($\text{M}+\text{H}$) $^+$; Yield: 79%.

Procedure for the synthesis of ethyl 1-(3-(4-(isoquinolin-5-yl)thiophene-2-carboxamido)benzyl)piperidine-4-carboxylate (4.26)

A catalytic amount of tetrakis(triphenylphosphine)palladium, $\text{Pd}(\text{PPh}_3)_4$ (0.1 eq.) was added to a solution of **4.7** (1.0 eq., 50 mg) and **4.24** (1.2 eq., 36 mg) in a 9:3:1 combination of EtOH, toluene and water in the presence of K_2CO_3 (3.0 eq.) in a 10 ml microwave vial containing a magnetic stirrer. The reaction vessel was flushed with nitrogen during each addition. The reaction mixture was sealed in an inert nitrogen environment and heated with microwave radiation in an EMRYSTM Optimizer Microwave Station (Personal Chemistry) at 100 °C for 8 minutes. After LCMS analysis revealed complete reaction the cooled reaction mixture was passed through an IsoluteTM SCX-2 cartridge (1.0 gm) and washed with DCM (3x) and DMF (3x) twice and finally MeOH (2x). The product **4.26** was released from the cartridge using 5.0 ml 2M NH_3 in MeOH and concentrated *in vacuo*. 48 mg light cream, oily mass was obtained as product.

Ethyl 1-(3-(4-(isoquinolin-5-yl)thiophene-2-carboxamido)benzyl)piperidine-4-carboxylate (4.26):



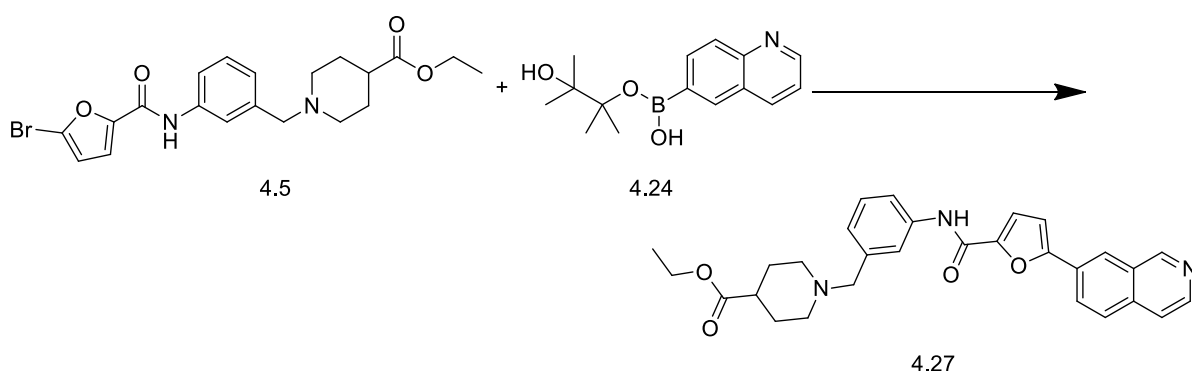
Light cream, oily mass. IR (FTIR, $\nu_{\text{max}}/\text{cm}^{-1}$) 628.41, 782.19, 835.05, 1046.86, 1222.55, 1318.08, 1364.57, 1440.50, 1485.97, 1550.87, 1651.29, 1711.71, 2041.34, 2361.75, 2916.48, 3395.34; ^1H NMR (500 MHz, CDCl_3 , TMS); δ 1.22 (t, $J=7.09$ Hz, 3H), 1.73 – 1.75 (m, 2H), 1.84 (dd, $J=3.15, 13.24$ Hz, 2H), 2.00 – 2.03 (m, 2H), 2.25 – 2.27 (m, 1H), 2.85 – 2.91 (m, 2H), 3.45 (s, 2H), 4.11 (q, $J=7.15$ Hz, 2H), 7.08 (d, $J=7.57$ Hz, 1H), 7.29 – 7.31 (m, 1H),

7.38 (dd, $J=4.1$, 8.20 Hz, 1H), 7.60 – 7.63 (m, 1H), 7.69 (dd, $J=1.58$, 7.88 Hz, 1H), 7.73 (d, $J=1.58$ Hz, 1H), 7.83 (dd, $J=2.22$, 8.83 Hz, 1H), 7.89 (d, $J=2.21$ Hz, 1H), 8.07 – 8.09 (m, 2H), 8.09 (d, $J=3.15$ Hz, 1H), 8.59 (s, 1H), 8.87 (dd, $J=1.7$, 4.26 Hz, 1H); ^{13}C NMR (100 MHz, CDCl_3); δ 14.42, 28.52, 29.3, 41.39, 53.15, 53.8, 60.48, 63.19, 119.41, 121.00, 121.94, 124.81, 125.54, 126.24, 127.71, 128.41, 128.73, 129.16, 130.32, 133.25, 136.35, 138.02, 139.94, 140.83, 142.26, 147.91, 150.71, 160.19, 175.47; m/z (+EI) calc. For $\text{C}_{29}\text{H}_{29}\text{N}_3\text{O}_3\text{S}$ (M^+) 499.62, found 499.92 ($\text{M}+\text{H}$) $^+$; Yield: 88%.

Procedure for the synthesis of ethyl 1-(3-(5-(isoquinolin-7-yl)furan-2-carboxamido)benzyl)piperidine-4-carboxylate (4.27)

A catalytic amount of tetrakis(triphenylphosphine)palladium, $\text{Pd}(\text{PPh}_3)_4$ (0.1 eq.) was added to a solution of **4.5** (1.0 eq., 50 mg) and **4.24** (1.2 eq., 38 mg) in a 9:3:1 combination of EtOH, toluene and water in the presence of K_2CO_3 (3.0 eq.) in a 10 ml microwave vial containing a magnetic stirrer. The reaction vessel was flushed with nitrogen during each addition. The reaction mixture was sealed in an inert nitrogen environment and heated with microwave radiation in an EMRYSTM Optimizer Microwave Station (Personal Chemistry) at 100 °C for 8 minutes. After LCMS analysis revealed complete reaction the cooled reaction mixture was passed through an IsoluteTM SCX-2 cartridge (1.0 gm) and washed with DCM (3x), DMF (3x) twice and finally MeOH (2x). The product **4.27** was released from the cartridge using 5.0 ml 2M NH_3 in MeOH and concentrated *in vacuo*. 40 mg cream oil was obtained as product.

Ethyl 1-(3-(5-(isoquinolin-7-yl)furan-2-carboxamido)benzyl)piperidine-4-carboxylate (4.27):



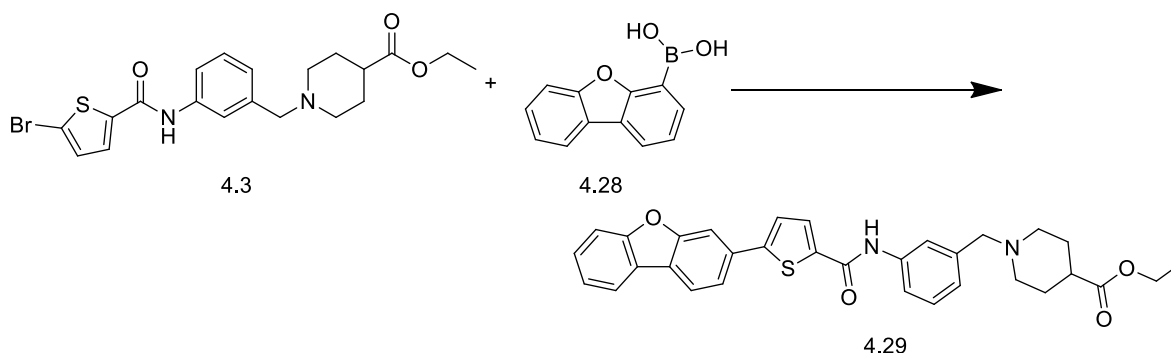
Cream oil. IR (FTIR, $\nu_{\text{max}}/\text{cm}^{-1}$) 629.72, 785.97, 1023.61, 1214.76, 1364.57, 1547.97, 1728.78, 1736.53, 1857.93, 1971.58, 2051.67, 2335.91, 2360.03, 2780.36, 3266.14; ^1H NMR (500 MHz, CDCl_3 , TMS); δ 1.25 – 1.27 (m, 3H), 1.79 – 1.81 (m, 2H), 1.90 – 1.93 (m, 2H),

2.06 – 2.09 (m, 2H), 2.30 – 2.31 (m, 1H), 2.88 – 2.92 (m, 2H), 3.52 (s, 2H), 4.13 (q, $J=7.07$ Hz, 2H), 6.95 (d, $J=3.78$ Hz, 1H), 7.12 (d, $J=7.88$ Hz, 1H), 7.34 (t, $J=7.88$ Hz, 1H), 7.38 (d, $J=3.47$ Hz, 1H), 7.47 – 7.49 (m, 1H), 7.58 – 7.61 (m, 1H), 7.67 (d, $J=4.10$ Hz, 1H), 7.77 (dd, $J=1.10$, 8.04 Hz, 1H), 8.06 (dd, $J=1.89$, 8.83 Hz, 1H), 8.17 (d, $J=8.83$ Hz, 1H), 8.22 (d, $J=1.89$ Hz, 1H), 8.25 (s, 1H), 8.94 (dd, $J=1.7$, 4.26 Hz, 1H); ^{13}C NMR (100 MHz, CDCl_3); δ 14.20, 28.29, 29.1, 41.40, 53.01, 53.3, 60.22, 63.11, 108.96, 117.48, 119.06, 120.55, 121.66, 122.01, 128.38, 129.17, 130.23, 130.42, 132.06, 135.6, 135.9, 140.1, 145.6, 147.59, 148.26, 150.66, 155.09, 155.97, 175.15; m/z (+EI) calc. For $\text{C}_{29}\text{H}_{29}\text{N}_3\text{O}_4$ (M^+) 483.56, found 483.88 ($\text{M}+\text{H}$) $^+$; Yield: 79%.

Procedure for the synthesis of ethyl 1-(3-(5-(dibenzo[*b,d*]furan-3-yl)thiophene-2-carboxamido)benzyl)piperidine-4-carboxylate (4.29)

A catalytic amount of tetrakis(triphenylphosphine)palladium, $\text{Pd}(\text{PPh}_3)_4$ (0.1 eq.) was added to a solution of **4.3** (1.0 eq., 65 mg) and **4.28** (1.2 eq., 36 mg) in a 9:3:1 combination of EtOH, toluene and water in the presence of K_2CO_3 (3.0 eq.) in a 10 ml microwave vial containing a magnetic stirrer. The reaction vessel was flushed with nitrogen during each addition. The reaction mixture was sealed in an inert nitrogen environment and heated with microwave radiation in an EMRYSTM Optimizer Microwave Station (Personal Chemistry) at 100 °C for 10 minutes. After LCMS analysis revealed complete reaction the cooled reaction mixture was passed through an IsoluteTM SCX-2 cartridge (1.0 gm) and washed with DCM (3x), DMF (3x) twice and finally MeOH (2x). The product **4.29** was released from the cartridge using 5.0 ml 2M NH_3 in MeOH and concentrated *in vacuo*. 57 mg light cream oil was obtained as product.

Ethyl 1-(3-(5-(dibenzo[*b,d*]furan-3-yl)thiophene-2-carboxamido)benzyl)piperidine-4-carboxylate (4.29):

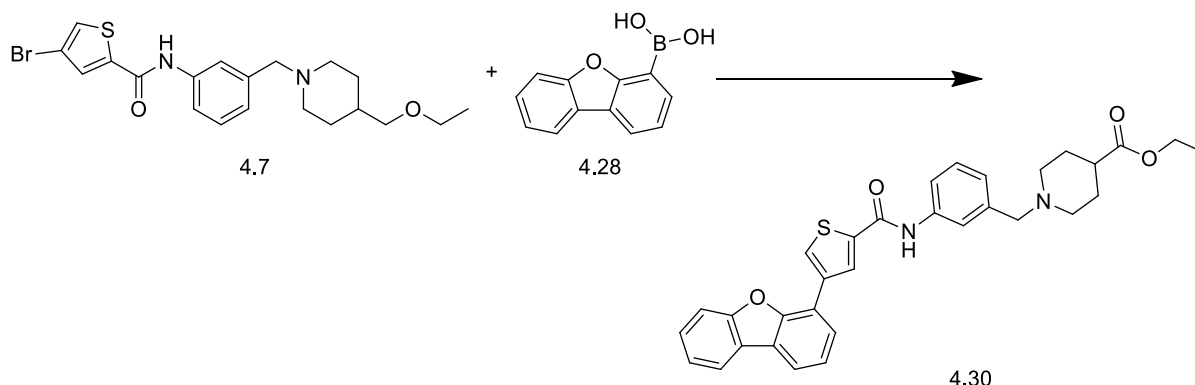


Light cream, oily mass. IR (FTIR, $\nu_{\text{max}}/\text{cm}^{-1}$) 628.20, 697.91, 734.33, 1047.87, 1119.28, 1188.78, 1220.47, 1263.69, 1316.68, 1360.45, 1418.81, 1443.78, 1487.80, 1546.74, 1657.75, 1710.70, 2925.50; ^1H NMR (500 MHz, CDCl_3 , TMS); δ 1.25 – 1.27 (m, 3H), 1.78 – 1.80 (m, 2H), 1.88 – 1.90 (m, 2H), 2.04 – 2.06 (m, 2H), 2.27 – 2.29 (m, 1H), 2.88 – 2.90 (m, 2H), 3.49 (s, 2H), 4.13 (q, $J=7.15$ Hz, 2H), 7.10 (d, $J=7.57$ Hz, 1H), 7.31 (t, $J=7.88$ Hz, 1H), 7.38 – 7.41 (m, 1H), 7.46 – 7.48 (m, 2H), 7.51 – 7.53 (m, 1H), 7.55 – 7.58 (m, 1H), 7.60 (s, 1H), 7.67 – 7.68 (m, 1H), 7.78 (d, $J=4.10$ Hz, 1H), 7.87 (d, $J=4.10$ Hz, 1H), 7.91 (dd, $J=1.2, 7.57$ Hz, 1H), 7.98 – 8.00 (m, 1H), 8.02 (s, 1H); ^{13}C NMR (100 MHz, CDCl_3); δ 14.18, 28.30, 29.3, 41.20, 52.94, 53.0, 60.20, 63.04, 111.5, 111.92, 113.0, 120.56, 120.77, 121.0, 123.15, 123.23, 125.14, 126.65, 128.43, 129.27, 132.03, 132.11, 135.7, 136.5, 137.2, 139.63, 140.1, 148.4, 150.0, 156.19, 161.9, 175.20; m/z (+EI) calc. For $\text{C}_{32}\text{H}_{30}\text{N}_2\text{O}_4\text{S}$ (M^+) 538.66, found 539.09 ($\text{M}+\text{H}$) $^+$; Yield: 73%.

Procedure for the synthesis of ethyl 1-(3-(4-(dibenzo[*b,d*]furan-4-yl)thiophene-2-carboxamido)benzyl)piperidine-4-carboxylate (4.30)

A catalytic amount of tetrakis(triphenylphosphine)palladium, $\text{Pd}(\text{PPh}_3)_4$ (0.1 eq.) was added to a solution of **4.7** (1.0 eq., 65 mg) and **4.28** (1.2 eq., 37 mg) in a 9:3:1 combination of EtOH, toluene and water in the presence of K_2CO_3 (3.0 eq.) in a 10 ml microwave vial containing a magnetic stirrer. The reaction vessel was flushed with nitrogen during each addition. The reaction mixture was sealed in an inert nitrogen environment and heated with microwave radiation in an EMRYSTM Optimizer Microwave Station (Personal Chemistry) at 100 °C for 10 minutes. After LCMS analysis revealed complete reaction the cooled reaction mixture was passed through an IsoluteTM SCX-2 cartridge (2.0 gm) and washed with DCM (3x) and DMF (3x) twice and finally MeOH (2x). The product **4.30** was released from the cartridge using 5.0 ml 2M NH_3 in MeOH and concentrated *in vacuo*. 61 mg light yellow oil was obtained as product.

Ethyl 1-(3-(4-(dibenzo[*b,d*]furan-4-yl)thiophene-2-carboxamido)benzyl)piperidine-4-carboxylate (4.30):



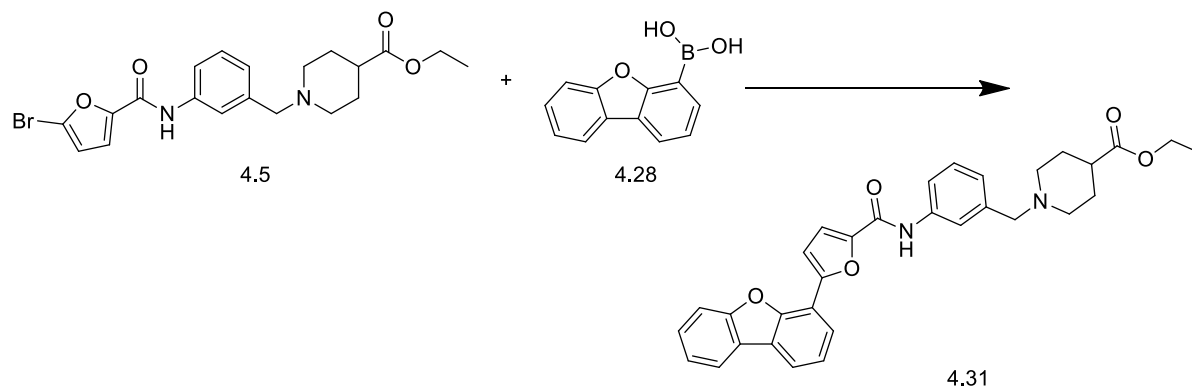
Light yellow oily mass. IR (FTIR, $\nu_{\text{max}}/\text{cm}^{-1}$) 629.82, 695.57, 751.96, 778.22, 1047.42, 1116.60, 1186.34, 1319.08, 1364.57, 1437.95, 1487.32, 1551.12, 1609.96, 1639.03, 1726.03, 2335.91, 2917.38, 3312.66; ^1H NMR (500 MHz, CDCl_3 , TMS); δ 1.23 – 1.25 (m, 3H), 1.77 – 1.79 (m, 2H), 1.86 – 1.89 (m, 2H), 2.01 – 2.03 (m, 2H), 2.26 – 2.27 (m, 1H), 2.86 – 2.90 (m, 2H), 3.45 (s, 2H), 4.11 (q, $J=7.25$ Hz, 2H), 7.08 (d, $J=7.57$ Hz, 1H), 7.30 – 7.32 (m, 1H), 7.34 (d, $J=7.57$ Hz, 1H), 7.37 – 7.38 (m, 1H), 7.41 – 7.43 (m, 1H), 7.49 – 7.52 (m, 1H), 7.62 – 7.63 (m, 1H), 7.65 – 7.67 (m, 1H), 7.68 – 7.70 (m, 1H), 7.86 (dd, $J=1.1, 7.72$ Hz, 1H), 7.95 – 7.97 (m, 1H), 8.22 (d, $J=1.26$ Hz, 1H), 8.32 (d, $J=1.26$ Hz, 1H), 8.46 (br.s, 1H); ^{13}C NMR (100 MHz, CDCl_3); δ 14.15, 28.23, 28.26, 41.17, 52.89, 53.4, 60.17, 62.98, 111.78, 113.5, 119.76, 120.68, 120.85, 121.1, 122.98, 123.14, 123.95, 125.10, 125.18, 127.37, 128.21, 128.81, 134.5, 135.6, 135.9, 137.32, 139.52, 139.58, 142.58, 152.82, 156.05, 175.19; m/z (+EI) calc. For $\text{C}_{32}\text{H}_{30}\text{N}_2\text{O}_4\text{S}$ (M^+) 538.66, found 539.09 ($\text{M}+\text{H}$) $^+$; Yield: 79%.

Procedure for the synthesis of ethyl 1-(3-(5-(dibenzo[*b,d*]furan-3-yl)furan-2-carboxamido)benzyl)piperidine-4-carboxylate (4.31)

A catalytic amount of tetrakis(triphenylphosphine)palladium, $\text{Pd}(\text{PPh}_3)_4$ (0.1 eq.) was added to a solution of **4.5** (1.0 eq., 40 mg) and **4.28** (1.2 eq., 23 mg) in a 9:3:1 combination of EtOH, toluene and water in the presence of K_2CO_3 (3.0 eq.) in a 10 ml microwave vial containing a magnetic stirrer. The reaction vessel was flushed with nitrogen during each addition. The reaction mixture was sealed in an inert nitrogen environment and heated with microwave radiation in an EMRYSTM Optimizer Microwave Station (Personal Chemistry) at 100 °C for 10 minutes. After LCMS analysis revealed complete reaction the cooled reaction mixture was passed through an IsoluteTM SCX-2 cartridge (1.0 gm) and washed with DCM (3x), DMF (3x) twice and finally MeOH (2x). The product **4.31** was released from the

cartridge using 5.0 ml 2M NH₃ in MeOH and concentrated *in vacuo*. 39 mg colourless oil was obtained as product.

Ethyl 1-(3-(5-(dibenzo[*b,d*]furan-3-yl)furan-2-carboxamido)benzyl)piperidine-4-carboxylate (4.31):



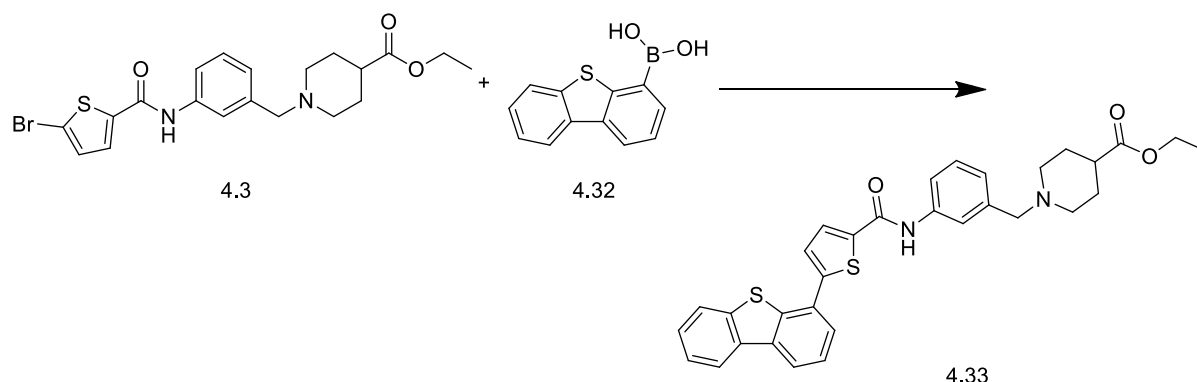
Colourless oily mass. IR (FTIR, $\nu_{\text{max}}/\text{cm}^{-1}$) 630.79, 696.25, 723.98, 754.16, 796.15, 844.04, 1025.47, 1119.81, 1183.76, 1219.81, 1262.45, 1319.31, 1363.24, 1447.97, 1487.79, 1546.45, 1610.05, 1665.82, 1711.68, 2341.08, 2926.67; ¹H NMR (500 MHz, CDCl₃, TMS); δ 1.08 (t, $J=7.09$ Hz, 3H), 1.64 – 1.65 (m, 2H), 1.73 – 1.76 (m, 2H), 1.90 – 1.92 (m, 2H), 2.13 – 2.16 (m, 1H), 2.71 – 2.73 (m, 2H), 3.36 (s, 2H), 3.96 (q, $J=6.94$ Hz, 2H), 6.95 (d, $J=7.57$ Hz, 1H), 7.18 (t, $J=7.72$ Hz, 1H), 7.23 (td, $J=0.05$, 7.41, 7.41 Hz, 1H), 7.28 – 7.30 (m, 1H), 7.30 – 7.31 (m, 1H), 7.34 – 7.36 (m, 1H), 7.37 – 7.40 (m, 1H), 7.43 – 7.45 (m, 1H), 7.48 – 7.49 (m, 1H), 7.50 – 7.52 (m, 1H), 7.58 (dt, $J=1.06$, 7.96 Hz, 1H), 7.79 (dd, $J=1.2$, 4.41 Hz, 1H), 7.81 (d, $J=0.95$ Hz, 1H), 8.11 (s, 1H); ¹³C NMR (100 MHz, CDCl₃); δ 14.19, 28.28, 29.0, 41.19, 52.97, 53.1, 60.20, 63.08, 108.9, 111.83, 112.25, 114.72, 120.51, 120.77, 120.78, 122.79, 123.05, 125.24, 128.42, 128.51, 128.96, 132.03, 132.11, 134.3, 137.49, 141.0, 146.73, 151.16, 156.11, 157.0, 162.0, 175.14; m/z (+EI) calc. For C₃₂H₃₀N₂O₅ (M⁺) 522.59, found 523.12 (M+H)⁺; Yield: 81%.

Procedure for the synthesis of ethyl 1-(3-(5-(dibenzo[*b,d*]thiophen-3-yl)thiophene-2-carboxamido)benzyl)piperidine-4-carboxylate (4.33)

A catalytic amount of tetrakis(triphenylphosphine)palladium, Pd(PPh₃)₄ (0.1 eq.) was added to a solution of **4.3** (1.0 eq., 42 mg) and **4.32** (1.2 eq., 25 mg) in a 9:3:1 combination of EtOH, toluene and water in the presence of K₂CO₃ (3.0 eq.) in a 10 ml microwave vial containing a magnetic stirrer. The reaction vessel was flushed with nitrogen during each addition. The reaction mixture was sealed in an inert nitrogen environment and heated with microwave radiation in an EMRYSTM Optimizer Microwave Station (Personal Chemistry) at

100 °C for 8 minutes. After LCMS analysis revealed complete reaction the cooled reaction mixture was passed through an Isolute™ SCX-2 cartridge (1.0 gm) and washed with DCM (3x), DMF (3x) twice and finally MeOH (2x). The product **4.33** was released from the cartridge using 5.0 ml 2M NH₃ in MeOH and concentrated *in vacuo*. 38 mg yellowish, oily mass was obtained as product.

Ethyl 1-(3-(5-(dibenzo[*b,d*]thiophen-3-yl)thiophene-2-carboxamido)benzyl)piperidine-4-carboxylate (4.33**):**



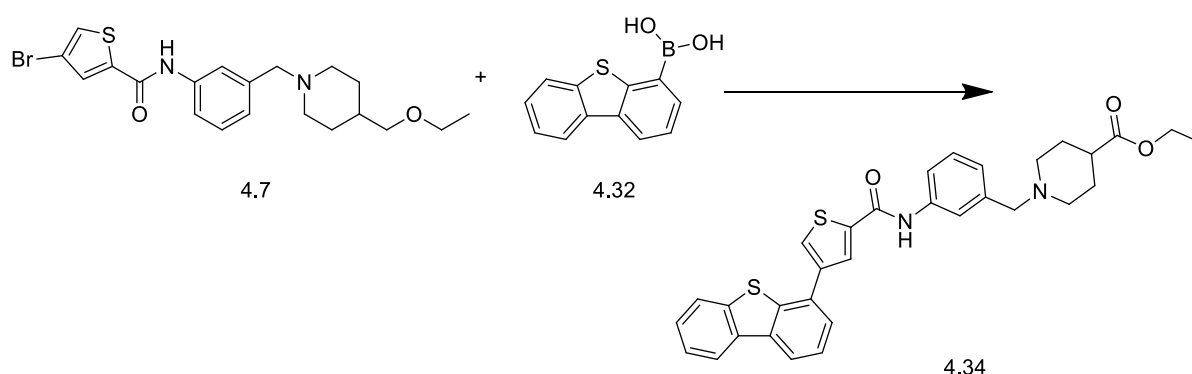
Yellowish, oily mass. IR (FTIR, $\nu_{\text{max}}/\text{cm}^{-1}$) 629.52, 695.89, 734.83, 755.36, 1047.64, 1092.50, 1221.45, 1320.93, 1362.01, 1438.37, 1487.72, 1547.68, 1651.16, 1710.70, 2341.08, 2935.40, 3418.26; ¹H NMR (500 MHz, CDCl₃, TMS); δ 1.24 (t, *J*=7.09 Hz, 3H), 1.79 – 1.81 (m, 2H), 1.86 (d, *J*=12.30 Hz, 2H), 2.03 (t, *J*=10.88 Hz, 2H), 2.27 – 2.30 (m, 1H), 2.88 – 2.91 (m, 2H), 3.48 (s, 2H), 4.13 (q, *J*=6.73 Hz, 2H), 7.10 (d, *J*=7.57 Hz, 1H), 7.30 (t, *J*=7.88 Hz, 1H), 7.49 – 7.51 (m, 2H), 7.52 (d, *J*=7.57 Hz, 1H), 7.59 (d, *J*=4.73 Hz, 2H), 7.67 (t, *J*=6.62 Hz, 2H), 7.77 (d, *J*=3.78 Hz, 1H), 7.87 (dd, *J*=3.3, 5.20 Hz, 1H), 8.15 (d, *J*=8.20 Hz, 1H), 8.18 – 8.19 (m, 1H); ¹³C NMR (100 MHz, CDCl₃); δ 14.21, 28.33, 29.5, 41.23, 52.97, 53.0, 60.23, 63.05, 120.75, 121.64, 121.79, 122.66, 123.05, 123.2, 124.74, 125.08, 126.08, 127.19, 128.47, 129.19, 132.06, 135.04, 135.7, 135.9, 137.69, 138.74, 139.72, 141.0, 147.64, 148.2, 161.8, 175.24; *m/z* (+EI) calc. For C₃₂H₃₀N₂O₃S₂ (M⁺) 554.72, found 554.99 (M+H)⁺; Yield: 91%.

Procedure for the synthesis of ethyl 1-(3-(4-(dibenzo[*b,d*]thiophen-4-yl)thiophene-2-carboxamido)benzyl)piperidine-4-carboxylate (4.34**)**

A catalytic amount of tetrakis(triphenylphosphine)palladium, Pd(PPh₃)₄ (0.1 eq.) was added to a solution of **4.7** (1.0 eq., 54 mg) and **4.32** (1.2 eq., 33 mg) in a 9:3:1 combination of EtOH, toluene and water in the presence of K₂CO₃ (3.0 eq.) in a 10 ml microwave vial containing a magnetic stirrer. The reaction vessel was flushed with nitrogen during each

addition. The reaction mixture was sealed in an inert nitrogen environment and heated with microwave radiation in an EMRYS™ Optimizer Microwave Station (Personal Chemistry) at 100 °C for 8 minutes. After LCMS analysis revealed complete reaction the cooled reaction mixture was passed through an Isolute™ SCX-2 cartridge (1.0 gm) and washed with DCM (3x), DMF (3x) twice and finally MeOH (2x). The product **4.34** was released from the cartridge using 5.0 ml 2M NH₃ in MeOH and concentrated *in vacuo*. 46 mg cream oily mass was obtained as product.

Ethyl 1-(3-(4-(dibenzo[*b,d*]thiophen-4-yl)thiophene-2-carboxamido)benzyl)piperidine-4-carboxylate (4.34**):**



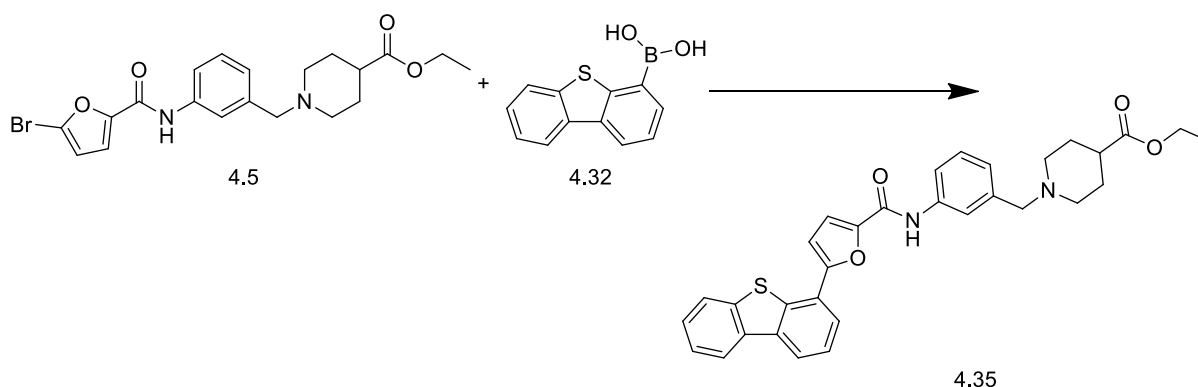
Cream oily mass. IR (FTIR, $\nu_{\text{max}}/\text{cm}^{-1}$) 624.90, 694.64, 722.06, 752.39, 869.93, 1047.62, 1118.85, 1178.28, 1256.08, 1317.77, 1364.88, 1437.69, 1485.98, 1549.53, 1609.82, 1654.66, 1725.49, 2341.08, 2801.03, 2931.90, 3059.43, 3260.98; ¹H NMR (500 MHz, CDCl₃, TMS); δ 1.23 (t, *J*=7.09 Hz, 3H), 1.75 – 1.79 (m, 2H), 1.85 – 1.88 (m, 2H), 2.00 – 2.02 (m, 2H), 2.25 – 2.26 (m, 1H), 2.86 – 2.89 (m, 2H), 3.45 (s, 2H), 4.11 (q, *J*=6.94 Hz, 2H), 7.08 (d, *J*=7.57 Hz, 1H), 7.28 – 7.30 (m, 1H), 7.39 – 7.41 (m, 1H), 7.47 – 7.48 (m, 1H), 7.48 – 7.49 (m, 1H), 7.49 – 7.51 (m, 1H), 7.52 – 7.53 (m, 1H), 7.60 – 7.63 (m, 2H), 7.66 (dd, *J*=1.2, 7.88 Hz, 1H), 7.83 – 7.85 (m, 1H), 7.89 (d, *J*=1.58 Hz, 1H), 8.11 (d, *J*=1.26 Hz, 1H), 8.16 – 8.18 (m, 1H); ¹³C NMR (100 MHz, CDCl₃); δ 14.15, 28.27, 28.29, 41.18, 52.89, 53.0, 60.18, 62.99, 119.09, 120.76, 121.64, 121.72, 122.63, 122.8, 123.05, 123.2, 124.4, 124.59, 125.01, 125.18, 126.30, 128.36, 129.19, 135.58, 135.6, 135.8, 137.91, 139.15, 140.26, 144.1, 162.48, 175.20; *m/z* (+EI) calc. For C₃₂H₃₀N₂O₃S₂ (M⁺) 554.72, found 554.99 (M+H)⁺; Yield: 70%.

Procedure for the synthesis of ethyl 1-(3-(5-(dibenzo[*b,d*]thiophen-3-yl)furan-2-carboxamido)benzyl)piperidine-4-carboxylate (4.35**)**

A catalytic amount of tetrakis(triphenylphosphine)palladium, Pd(PPh₃)₄ (0.1 eq.) was added to a solution of **4.5** (1.0 eq., 37 mg) and **4.32** (1.2 eq., 23 mg) in a 9:3:1 combination of

EtOH, toluene and water in the presence of K_2CO_3 (3.0 eq.) in a 10 ml microwave vial containing a magnetic stirrer. The reaction vessel was flushed with nitrogen during each addition. The reaction mixture was sealed in an inert nitrogen environment and heated with microwave radiation in an EMRYSTM Optimizer Microwave Station (Personal Chemistry) at 100 °C for 8 minutes. After LCMS analysis revealed complete reaction the cooled reaction mixture was passed through an IsoluteTM SCX-2 cartridge (1.0 gm) and washed with DCM (3x), DMF (3x) twice and finally MeOH (2x). The product **4.35** was released from the cartridge using 5.0 ml 2M NH_3 in MeOH and concentrated *in vacuo*. 46 mg colourless oil was obtained as product.

Ethyl 1-(3-(5-(dibenzo[*b,d*]thiophen-3-yl)furan-2-carboxamido)benzyl)piperidine-4-carboxylate (4.35):



Colourless oil. IR (FTIR, ν_{max}/cm^{-1}) 631.34, 695.57, 721.40, 754.98, 791.40, 1025.78, 1048.11, 1119.96, 1182.94, 1322.61, 1439.86, 1487.65, 1542.18, 1591.88, 1609.94, 1666.13, 1726.87, 2363.64, 2852.71, 2916.88, 3307.49; 1H NMR (500 MHz, $CDCl_3$, TMS); δ 1.24 (t, $J=m$, 3H), 1.81 – 1.83 (m, 2H), 1.91 – 1.95 (m, 2H), 2.08 (d, $J=10.40$ Hz, 2H), 2.30 – 2.31 (m, 1H), 2.90 – 2.93 (m, 2H), 3.53 (s, 2H), 4.13 (q, $J=7.25$ Hz, 2H), 7.04 (d, $J=3.78$ Hz, 1H), 7.14 (d, $J=7.57$ Hz, 1H), 7.36 (t, $J=7.72$ Hz, 1H), 7.40 – 7.43 (m, 1H), 7.51 (d, $J=1.89$ Hz, 1H), 7.52 – 7.54 (m, 1H), 7.54 – 7.58 (m, 1H), 7.67 – 7.68 (m, 1H), 7.70 – 7.72 (m, 1H), 7.90 – 7.93 (m, 2H), 8.16 – 8.18 (m, 2H), 8.38 (s, 1H); ^{13}C NMR (100 MHz, $CDCl_3$); δ 14.18, 28.5, 29.5, 41.20, 52.97, 53.6, 60.17, 63.07, 108.9, 109.76, 120.52, 121.67, 121.77, 122.50, 122.70, 123.7, 124.51, 124.79, 124.81, 127.31, 128.41, 128.50, 131.86, 132.10, 134.88, 135.09, 135.5, 139.77, 146.96, 155.95, 162.5, 175.12; m/z (+EI) calc. For $C_{32}H_{30}N_2O_4S$ (M^+) 538.66, found 539.05 ($M+H$)⁺; Yield: 100%.

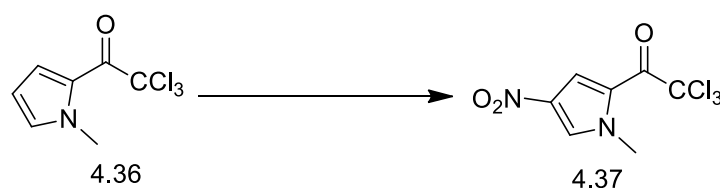
4.1.5 Type-2 Library synthesis

4.1.5.1 Sub type 1 Library synthesis

General procedure for the synthesis of 2,2,2-trichloro-1-(1-methyl-4-nitro-1*H*-pyrrol-2-yl) ethanone (4.37).

Fuming nitric acid (37.5 ml) was added drop wise over a period of 1 hour to a mechanically stirred solution of 2,2,2-trichloro-1-(1-methyl-1*H*-pyrrol-2-yl) ethanone (1.0 eq., 100 gm) (4.36) in acetic anhydride (475 ml), which was kept at -5 °C using an acetone/dry ice bath. After the addition was complete, the temperature of the reaction mixture was gradually raised to 10 °C over a period of 3 hours with continuous stirring. The reaction mixture was again cooled to -30 °C using an acetone/dry ice bath and diluted with 500 ml of isopropanol. The resulting precipitate was collected using a Buchner flask and dried in a vacuum. 710 mg yellow crystalline powder was obtained.

2,2,2-Trichloro-1-(1-methyl-4-nitro-1*H*-pyrrol-2-yl) ethanone (4.37):

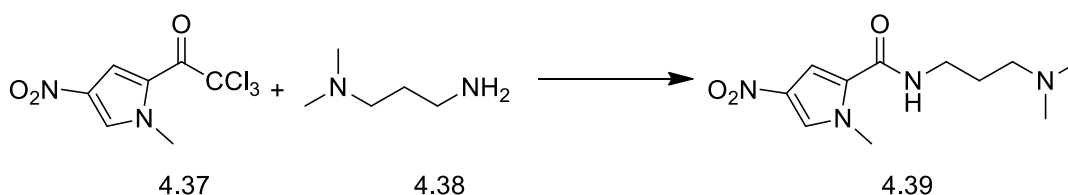


Yellow crystalline powder. IR (FTIR, $\nu_{\text{max}}/\text{cm}^{-1}$) 630.76, 688.78, 714.79, 749.37, 814.51, 853.33, 1111.00, 1183.53, 1225.52, 1406.45, 1426.38, 1494.51, 1514.83, 1691.56, 3139.95; ¹H NMR (400 MHz, CDCl₃, TMS); δ 4.04 (s, 3H), 7.74 (s, 1H), 7.94 (s, 1H); ¹³C NMR (100 MHz, CDCl₃); δ 39.80, 94.83, 117.46, 121.47, 130.25, 135.3, 173.7; m/z (+EI) calc. For C₇H₅Cl₃N₂O₃ (M⁺) 271.49, found 271.23 (M+H)⁺; Yield: 71%.

General procedure for the synthesis of *N*-(3-(dimethylamino)propyl)-1-methyl-4-nitro-1*H*-pyrrole-2-carboxamide (4.39).

N,N-dimethylpropane-1,3-diamine (1 eq., 1.4 μ l) (4.38) was added to a mechanically stirred solution of 2,2,2-trichloro-1-(1-methyl-4-nitro-1*H*-pyrrol-2-yl)ethanone (1 eq., 3.0 gm) (4.37) in THF (50.0 ml). The reaction mixture was allowed to stir for 2 hours. After completion of the reaction the reaction mixture was evaporated and 2.43 gm cream crystalline product was obtained (4.39).

***N*-(3-(dimethylamino)propyl)-1-methyl-4-nitro-1*H*-pyrrole-2-carboxamide (4.39):**

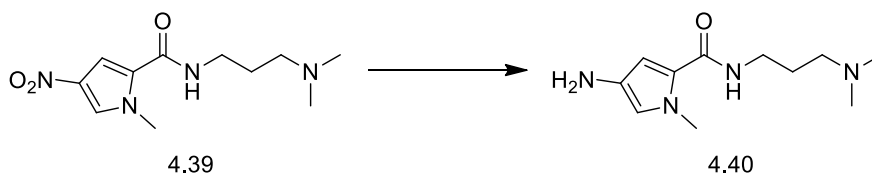


Cream crystalline solid. IR (FTIR, $\nu_{\text{max}}/\text{cm}^{-1}$) 789.72, 1138.06, 1211.26, 1301.51, 1414.54, 1469.90, 1498.81, 1590.13, 1658.18, 2163.56, 2823.99, 3126.84, 3385.19; ^1H NMR (400 MHz, CDCl_3 , TMS); δ 1.74 – 1.77 (m, 2H), 2.31 (s, 6H), 2.5 (t, $J=8.0$, Hz, 2H), 3.5 (q, $J=8.0$, 5.0, Hz, 2H), 4.0 (s, Hz, 3H), 6.20 (d, $J=2.0$, Hz, 1H), 7.51 (d, $J=2.0$, Hz, 1H), 8.66 (s, 1H); ^{13}C NMR (100 MHz, CDCl_3); δ 26.0, 35.5, 39.8, 47.0, 47.1, 58.6, 115.9, 127.99, 131.02, 134.7, 162.7; m/z (+EI) calc. For $\text{C}_{11}\text{H}_{18}\text{N}_4\text{O}_3$ (M^+) 254.29, found 254.95 ($\text{M}+\text{H}$) $^+$; Yield: 81%.

General procedure for the synthesis of 4-amino-*N*-(3-(dimethylamino)propyl)-1-methyl-1*H*-pyrrole-2-carboxamide (4.40).

N-(3-(Dimethylamino)propyl)-1-methyl-4-nitro-1*H*-pyrrole-2-carboxamide (1.0 eq., 500 mg) (4.39) was dissolved in the minimum amount of ethyl acetate (30 ml) and a catalytic amount of 10% Pd/C (40 mg) was added as a slurry in ethyl acetate. The reaction mixture was shaken overnight at 45 psi in a Parr hydrogenator. After completion of the reduction, the suspension was filtered with caution over celite using a Buchner flask (Procedure for Pd/C waste disposal in section 4.1.3.6) and the filtrate was concentrated to obtain 441 mg colourless oil.

4-Amino-*N*-(3-(dimethylamino)propyl)-1-methyl-1*H*-pyrrole-2-carboxamide (4.40):

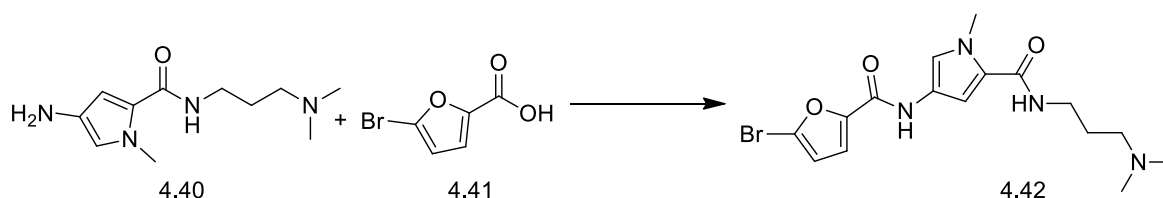


Colourless oil. IR (FTIR, $\nu_{\text{max}}/\text{cm}^{-1}$) 630.39, 1035.66, 1216.48, 1229.16, 1283.22, 1365.62, 1436.08, 1529.13, 1580.48, 1633.12, 1737.52, 2356.88, 2946.50, 3307.70; ^1H NMR (400 MHz, CDCl_3 , TMS); δ 1.74 – 1.77 (m, 2H), 2.31 (s, 6H), 2.5 (t, $J=8.0$, Hz, 2H), 3.5 (q, $J=8.0$, 5.0, Hz, 2H), 4.0 (s, Hz, 3H), 6.20 (d, $J=2.0$, Hz, 1H), 7.51 (d, $J=2.0$, Hz, 1H), 8.66 (s, 1H); ^{13}C NMR (100 MHz, CDCl_3); δ 25.7, 36.9, 39.6, 45.7, 59.3, 109.8, 129.1, 147.6, 158.6; m/z (+EI) calc. For $\text{C}_{11}\text{H}_{20}\text{N}_4\text{O}$ (M^+) 224.30, found 225.40 ($\text{M}+\text{H}$) $^+$; Yield: 100%.

General procedure for the synthesis of 4-(5-bromofuran-2-carboxamido)-N-(3-(dimethylamino)propyl)-1-methyl-1H-pyrrole-2-carboxamide (4.42). (Amide coupling).

2.0 eq of HOBT (535 mg) and 1.75 eq. of DIC (536.0 μ l) were added to a solution of **4.40** (1 eq., 444 mg) in DCM. After 30 minutes, 1.30 eq. (492 mg) of **4.41** was added and the reaction mixture was allowed to stir for 3 hours. After completion of the reaction, the mixture was passed through a SCX-2 cartridge (5.0 gm); the cartridge was washed with DCM (3x), DMF (3x) twice and finally MeOH (2x). The product **4.42** was released from the cartridge using 5.0 ml 2M NH₃ in MeOH and concentrated *in vacuo* to obtain a brown oily mass (337 mg).

4-(5-Bromofuran-2-carboxamido)-N-(3-(dimethylamino)propyl)-1-methyl-1H-pyrrole-2-carboxamide (4.42):

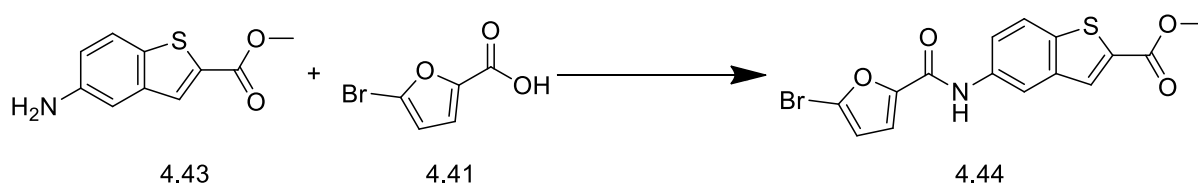


Brown oil. IR (FTIR, $\nu_{\text{max}}/\text{cm}^{-1}$) 636.44, 744.67, 924.48, 958.03, 1028.54, 1112.71, 1144.42, 1204.86, 1284.31, 1401.60, 1437.75, 1465.50, 1525.01, 1633.48, 2357.96, 2938.39, 3334.27; ¹H NMR (400 MHz, CDCl₃, TMS); δ 1.89 – 1.91 (m, 2H), 2.52 (s, 6H), 2.76 (t, $J=6.4$ Hz, 2H), 3.23 (s, 2H), 3.92 (s, Hz, 3H), 6.48 (d, $J=3.6$ Hz, 1H), 6.65 (d, $J=2.0$ Hz, 1H), 7.6 (dd, $J=1.6, 2.0$ Hz, 1H), 7.8 (dd, $J=1.6, 2.0$ Hz, 1H), 8.01 (s, 1H), 8.22 (s, 1H); ¹³C NMR (100 MHz, CDCl₃); δ 23.5, 34.7, 37.5, 40.1, 43.4, 57.1, 101.8, 112.4, 114.8, 116.6, 118.2, 122.1, 122.3, 147.4, 152.1, 159.5; m/z (+EI) calc. For C₁₆H₂₁BrN₄O₃ (M⁺) 397.27, found 399.29 (M+H)⁺; Yield: 76%.

Procedure for the synthesis of methyl 5-(5-bromofuran-2-carboxamido)benzo[*b*]thiophene-2-carboxylate (4.44)

2.0 eq of HOBT and 1.75 eq. of DIC (340.0 μ l) were added to a solution of **4.43** (1 eq., 500 mg) in DCM. After 30 minutes 1.20 eq. (553 mg) of **4.41** was added and the reaction mixture was allowed to stir for 3 hours. After completion of the reaction, the mixture was dried. It was then dissolved in a small amount of DCM and coated over silica. The final compound was purified using a silica column. Either 100% DCM or 100% CHCl₃ was used to purify and obtain compound **4.44**, which was dried *in vacuo*; 700 mg light yellow powder was obtained as the product.

Methyl 5-(5-bromofuran-2-carboxamido)benzo[*b*]thiophene-2-carboxylate (4.44):

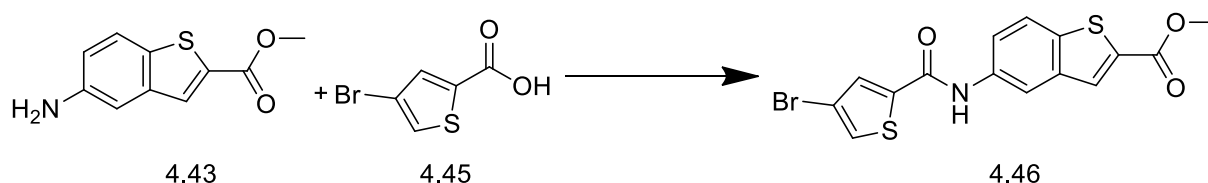


Light yellow powder. IR (FTIR, $\nu_{\text{max}}/\text{cm}^{-1}$) 629.77, 788.56, 1160.51, 1258.67, 1473.06, 1529.88, 1710.17, 1992.25, 2361.75, 2914.72; ^1H NMR (400 MHz, CDCl_3 , TMS); δ 3.97 (s, 3H), 6.55 (dd, $J=0.76, 3.54$ Hz, 1H), 7.14 (d, $J=2.27$ Hz, 1H), 7.24 (dd, $J=0.76, 3.54$ Hz, 1H), 7.86 – 7.89 (m, 1H), 8.05 (s, 1H), 8.09 (s, 1H), 8.38 (d, $J=2.02$ Hz, 1H); ^{13}C NMR (100 MHz, CDCl_3); δ 50.5, 112.0, 114.5, 115.3, 115.9, 117.0, 122.3, 123.03, 134.7, 138.5, 140.1, 141.2, 150.1, 162.2, 162.7; δ m/z (+EI) calc. For $\text{C}_{15}\text{H}_{10}\text{BrNO}_4\text{S}$ (M^+) 380.21, found 382.18 ($\text{M}+\text{H}^+$); Yield: 76%.

Procedure for the synthesis of methyl 5-(4-bromothiophene-2-carboxamido)benzo[*b*]thiophene-2-carboxylate (4.46)

2.0 eq of HOBT and 1.75 eq. of DIC (340.0 μl) were added to a solution of **4.43** (1 eq., 500 mg) in DCM. After 30 minutes, 1.20 eq. (599 mg) of **4.45** was added and the reaction mixture was allowed to stir for 3 hours. After completion of the reaction, the mixture was dried, the residue dissolved in a small amount of DCM and coated over silica. The final compound was purified using a silica column. Either 100% DCM or 100% CHCl_3 was used to purify compound **4.46**, which was dried *in vacuo*; 800 mg yellow powder was obtained as the product.

Methyl 5-(4-bromothiophene-2-carboxamido)benzo[*b*]thiophene-2-carboxylate (4.46):

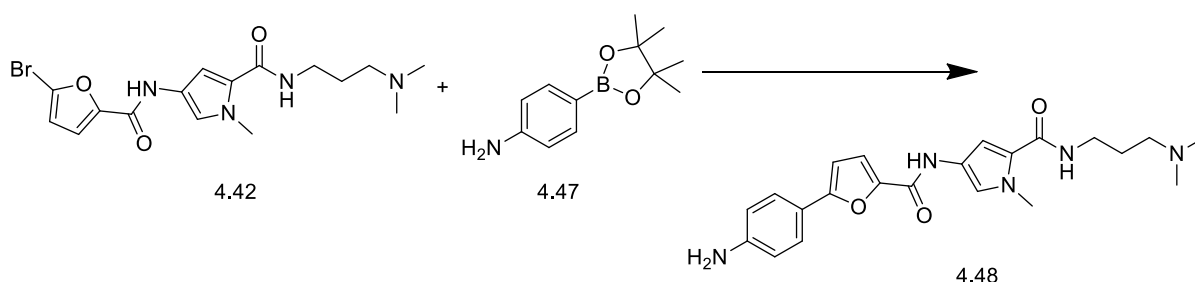


Yellow powder. IR (FTIR, $\nu_{\text{max}}/\text{cm}^{-1}$) 711.15, 821.39, 1076.07, 1151.87, 1254.73, 1429.80, 1519.51, 1580.92, 1667.63, 2364.00, 3101.02; ^1H NMR (400 MHz, CDCl_3 , TMS); δ 3.97 (s, 3H), 7.50 (d, $J=1.52$ Hz, 1H), 7.56 – 7.58 (m, 2H), 7.73 (br.s, 1H), 7.85 (d, $J=8.84$ Hz, 1H), 8.05 (s, 1H), 8.32 (d, $J=4.0$ Hz, 1H); ^{13}C NMR (100 MHz, CDCl_3); δ 51.2, 109.1, 115.2, 116.8, 117.0, 122.8, 130.7, 133.0, 135.1, 138.9, 139.2, 140.1, 141.6, 161.2, 162.03; m/z (+EI) calc. For $\text{C}_{15}\text{H}_{10}\text{BrNO}_3\text{S}_2$ (M^+) 396.28, found 397.88 ($\text{M}+\text{H}^+$); Yield: 84%.

General procedure for the synthesis of 4-(5-(4-aminophenyl)furan-2-carboxamido)-N-(3-(dimethylamino)propyl)-1-methyl-1H-pyrrole-2-carboxamide (4.48). (Suzuki coupling).

A catalytic amount of tetrakis(triphenylphosphine)palladium, Pd(PPh₃)₄ (0.1 eq., 54 mg) was added to a solution of **4.42** (1.0 eq., 187.0 mg) and **4.47** (1.2 eq., 124 mg) in a 9:3:1 combination of EtOH, toluene and water in the presence of K₂CO₃ (3.0 eq., 195 mg) in a 10 ml microwave vial containing a magnetic stirrer. The reaction vessel was flushed with nitrogen during each addition. The reaction mixture was sealed in an inert nitrogen environment and heated with microwave radiation in an EMRYS™ Optimizer Microwave Station (Personal Chemistry) at 100 °C for 15 minutes. After LCMS analysis revealed complete reaction the cooled reaction mixture was passed through an Isolute™ SCX-2 cartridge (2 gm) and washed with DCM (3x), DMF (3x) twice and finally MeOH (2x). The product **4.48** was released from the cartridge using 10.0 ml 2M NH₃ in MeOH and concentrated *in vacuo* to obtain a light cream oily mass (131 mg).

4-(5-(4-Aminophenyl)furan-2-carboxamido)-N-(3-(dimethylamino)propyl)-1-methyl-1H-pyrrole-2-carboxamide (4.48):

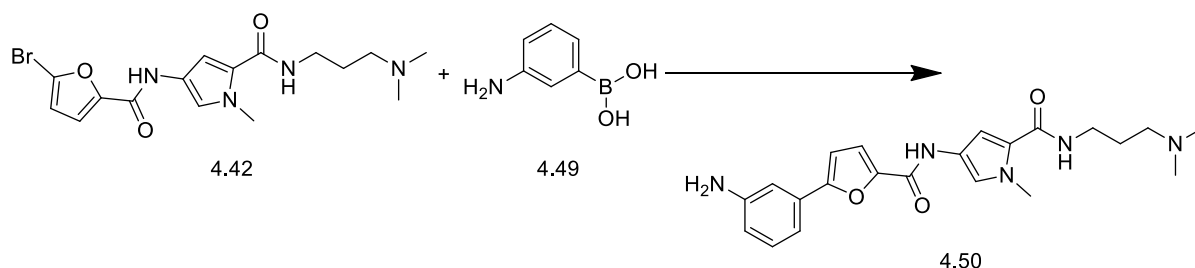


Cream oil. IR (FTIR, $\nu_{\text{max}}/\text{cm}^{-1}$) 634.44, 743.67, 804.16, 958.03, 1019.54, 1112.71, 1161.42, 1204.86, 1284.31, 1413.60, 1437.75, 1465.50, 1522.01, 1633.48, 1736.91, 2357.96, 2938.39, 3234.27; ¹H NMR (400 MHz, CDCl₃, TMS); δ 1.90 – 1.92 (m, 2H), 2.53 (s, 6H), 2.86 (t, $J=6.4$, Hz, 2H), 3.57 – 3.60 (m, 2H), 3.90 (s, Hz, 3H), 6.48 (d, $J=3.6$, Hz, 1H), 6.70 (d, $J=2.0$, Hz, 1H), 6.80 – 6.82 (m, 2H), 7.30 (d, $J=2.0$, Hz, 1H), 7.50 (d, $J=3.6$, Hz, 1H), 7.65 – 6.67 (m, 2H), 8.05 (s, 1H), 8.27 (s, 1H); ¹³C NMR (100 MHz, CDCl₃); δ 25.4, 35.9, 40.1, 45.7, 57.9, 108.9, 108.11, 115.1, 119.9, 120.5, 122.3, 123.7, 125.2, 126.0, 129.36, 135.2, 140.5, 144.6, 147.02, 150.1, 156.7, 160.0; m/z (+EI) calc. For C₂₂H₂₇N₅O₃ (M⁺) 409.48, found 410.31 (M+H)⁺; Yield: 70%.

Procedure for the synthesis of 4-(5-(3-aminophenyl)furan-2-carboxamido)-N-(3-(dimethylamino)propyl)-1-methyl-1H-pyrrole-2-carboxamide (4.50)

A catalytic amount of tetrakis(triphenylphosphine)palladium, Pd(PPh₃)₄ (0.1 eq., 54 mg) was added to a solution of **4.42** (1.0 eq., 150.0 mg) and **4.49** (1.2 eq., 100 mg) in a 9:3:1 combination of EtOH, toluene and water in the presence of K₂CO₃ (3.0 eq., 195 mg) in a 10 ml microwave vial containing a magnetic stirrer. The reaction vessel was flushed with nitrogen during each addition. The reaction mixture was sealed in an inert nitrogen environment and heated with microwave radiation in an EMRYSTM Optimizer Microwave Station (Personal Chemistry) at 100 °C for 15 minutes. After LCMS analysis revealed complete reaction the cooled reaction mixture was passed through an IsoluteTM SCX-2 cartridge (2 gm) and washed with DCM (3x), DMF (3x) twice and finally MeOH (2x). The product **4.48** was released from the cartridge using 10.0 ml 2M NH₃ in MeOH and concentrated *in vacuo* to obtain a brown oil (105 mg).

4-(5-(3-Aminophenyl)furan-2-carboxamido)-N-(3-(dimethylamino)propyl)-1-methyl-1H-pyrrole-2-carboxamide (4.50):



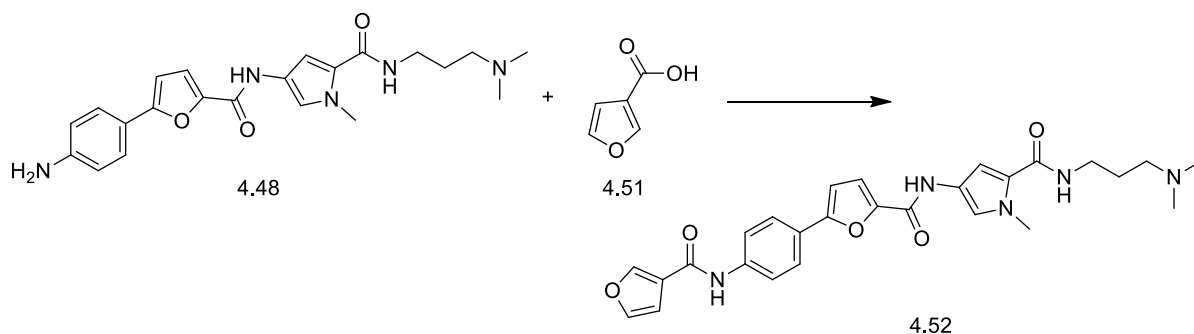
Brown oil. IR (FTIR, $\nu_{\text{max}}/\text{cm}^{-1}$) 691.72, 721.47, 779.20, 992.15, 1022.66, 1142.28, 1230.90, 1287.73, 1401.68, 1437.10, 1527.62, 1738.06, 2947.76, 3231.70; ¹H NMR (400 MHz, CDCl₃, TMS); δ 1.75 (dt, $J=6.28, 6.28, 12.44$ Hz, 2H), 2.33 – 2.36 (m, 6H), 2.47 (t, $J=6.32$ Hz, 2H), 3.48 – 3.50 (m, 2H), 3.80 (s, 1H), 3.96 (s, 3H), 6.58 (d, $J=1.77$ Hz, 1H), 6.70 (dd, $J=0.88, 7.71$ Hz, 1H), 6.72 (d, $J=3.54$ Hz, 1H), 7.06 (s, 1H), 7.14 (d, $J=8.08$ Hz, 1H), 7.20 (d, $J=1.52$ Hz, 1H), 7.23 (d, $J=8.08$ Hz, 1H), 7.25 (d, $J=3.54$ Hz, 1H), 7.51 – 7.53 (m, 1H), 7.68 – 7.70 (m, 1H), 7.94 (s, 1H); ¹³C NMR (100 MHz, CDCl₃); δ 25.56, 36.35, 40.81, 45.08, 47.1, 58.4, 108.2, 108.9, 109.49, 114.7, 115.41, 120.29, 120.8, 123.20, 129.4, 130.22, 131.0, 146.81, 150.0, 155.76, 160.5, 162.31; m/z (+EI) calc. For C₂₂H₂₇N₅O₃ (M⁺) 409.48, found 410.39 (M+H)⁺; Yield: 73%.

The following compounds (**4.52** to **4.55**) were synthesised adopting the amide coupling reaction from **4.48** and **4.50**.

Procedure for the synthesis of *N*-(3-(dimethylamino)propyl)-4-(5-(4-(furan-2-carboxamido)phenyl)furan-2-carboxamido)-1-methyl-1*H*-pyrrole-2-carboxamide (4.52**)**

2.0 eq of HOBT (46 mg) and 1.75 eq. of DIC (46 μ l) were added to a solution of **4.48** (1 eq., 70 mg) in DCM. After 30 minutes, 1.20 eq. (23 mg) of **4.51** was added and the reaction mixture was allowed to stir for 3 hours. The reaction mixture was initially purified using a SCX cartridge (2.0 gm). Final purification was achieved using a silica column and a DCM:MeOH:2MNH₃ solvent system. Various concentration gradients were used for releasing the impurities and the desired product **4.52**, which was dried *in vacuo*; 53 mg light brown oil was obtained as the product.

***N*-(3-(dimethylamino)propyl)-4-(5-(4-(furan-2-carboxamido)phenyl)furan-2-carboxamido)-1-methyl-1*H*-pyrrole-2-carboxamide (**4.52**):**

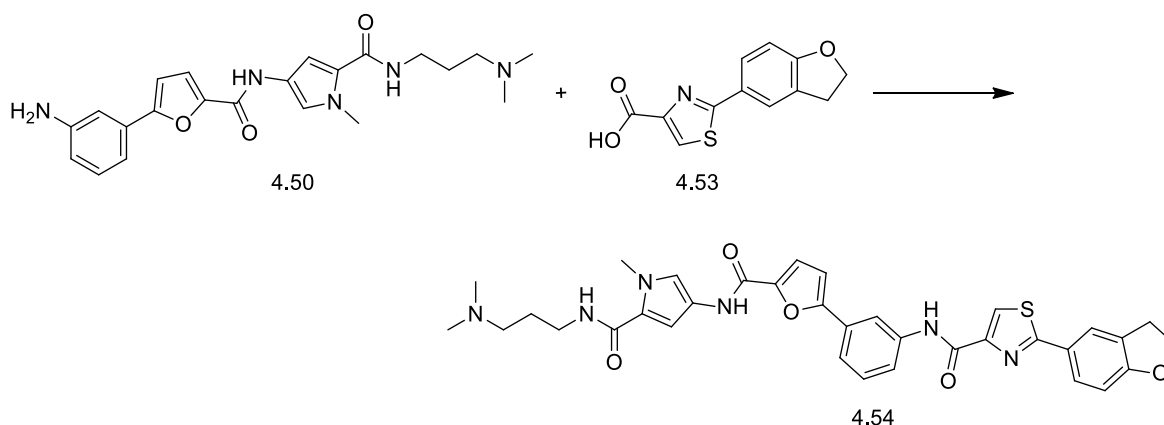


Light brown oil. IR (FTIR, $\nu_{\text{max}}/\text{cm}^{-1}$) 667.93, 739.40, 785.55, 804.16, 873.54, 971.00, 1019.28, 1161.79, 1279.29, 1328.22, 1413.69, 1435.76, 1483.73, 1522.50, 1596.01, 1633.62, 1736.91, 2357.91, 2939.40; ¹H NMR (400 MHz, CDCl₃, TMS); δ 1.73 – 1.75 (m, 2H), 2.30 (s, 6H), 2.46 (t, J =6.06 Hz, 2H), 3.47 – 3.50 (m, 2H), 3.94 (s, 3H), 6.70 (d, J =3.54 Hz, 1H), 6.81 (s, 1H), 7.24 (d, J =3.79 Hz, 1H), 7.42 (dd, J =4.29, 8.34 Hz, 1H), 7.49 (s, 1H), 7.57 (ddd, J =1.26, 7.01, 8.15 Hz, 1H), 7.68 (s, 1H), 7.74 (ddd, J =1.52, 6.95, 8.46 Hz, 1H), 7.84 – 7.86 (m, 1H), 8.12 (d, J =7.83 Hz, 1H), 8.18 (d, J =8.34 Hz, 1H), 8.29 (br.s, 1H), 8.94 (d, J =1.7 Hz, 1H); ¹³C NMR (100 MHz, CDCl₃); δ 25.41, 36.40, 40.12, 45.02, 47.0, 58.49, 106.76, 108.13, 108.17, 118.58, 119.96, 120.76, 122.61, 125.1, 125.3, 126.0, 126.23, 129.15, 131.0, 137.98, 145.08, 146.32, 150.09, 155.26, 160.49, 162.7, 164.7; m/z (+EI) calc. For C₂₇H₂₉N₅O₅ (M+) 503.55, found 504.02 (M+H)⁺; Yield: 76%.

Procedure for the synthesis of 2-(2,3-dihydrobenzofuran-5-yl)-N-(3-(5-((5-((3-(dimethylamino)propyl)carbamoyl)-1-methyl-1H-pyrrol-3-yl)carbamoyl)furan-2-yl)phenyl)thiazole-4-carboxamide (4.54)

2.0 eq of HOBT and 1.75 eq. of DIC were added to a solution of **4.50** (1 eq., 50 mg) in DCM. After 30 minutes, 2 eq. (60 mg) of **4.53** was added and the reaction mixture was allowed to stir for 3 hours. The reaction mixture was initially purified using a SCX cartridge (2.0 gm). Final purification was achieved using a silica column and a DCM:MeOH:2MNH₃ solvent system of various concentration gradients for releasing the impurities and the desired product **4.54**. This was dried *in vacuo* and 39 mg colourless oil was obtained as the product.

2-(2,3-Dihydrobenzofuran-5-yl)-N-(3-(5-((5-((3-(dimethylamino)propyl)carbamoyl)-1-methyl-1H-pyrrol-3-yl)carbamoyl)furan-2-yl)phenyl)thiazole-4-carboxamide (4.54):

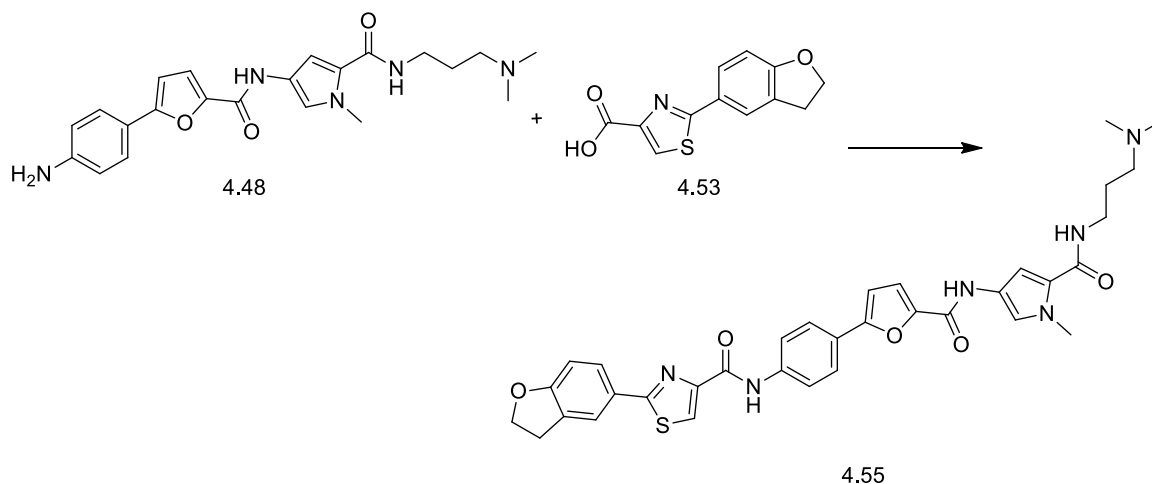


Colourless oil. IR (FTIR, $\nu_{\max}/\text{cm}^{-1}$) 640.06, 738.23, 866.73, 980.83, 1097.45, 1167.89, 1216.56, 1365.34, 1537.77, 1737.23, 2969.37, 3335.36; ¹H NMR (400 MHz, CDCl₃, TMS); δ 1.73 – 1.75 (m, 2H), 2.30 (s, 6H), 2.45 (t, $J=6.19$ Hz, 2H), 3.31 – 3.35 (m, 2H), 3.47 – 3.49 (m, 2H), 3.84 – 3.87 (m, 2H), 3.95 (s, 3H), 4.68 (t, $J=8.72$ Hz, 2H), 6.63 (d, $J=2.02$ Hz, 1H), 6.82 (d, $J=2.02$ Hz, 1H), 6.88 (d, $J=8.34$ Hz, 1H), 7.22 (d, $J=1.77$ Hz, 1H), 7.43 (t, $J=8.34$ Hz, 1H), 7.51 (dt, $J=1.2, 7.96$ Hz, 1H), 7.63 – 7.65 (m, 1H), 7.68 – 7.69 (m, 1H), 7.78 (dd, $J=1.7, 8.34$ Hz, 1H), 7.86 (d, $J=1.52$ Hz, 1H), 8.11 (s, 1H), 8.26 – 8.27 (m, 1H), 9.38 (s, 1H); ¹³C NMR (100 MHz, CDCl₃); δ 25.56, 28.95, 29.8, 36.35, 41.81, 45.08, 58.48, 79.0, 107.82, 108.2, 108.7, 109.49, 115.41, 119.63, 120.29, 120.8, 121.7, 122.56, 123.20, 125.15, 127.28, 128.00, 129.20, 129.4, 130.22, 130.8, 137.95, 146.81, 150.0, 154.76, 160.1, 162.31, 169.0, 184.4; m/z (+EI) calc. For C₃₄H₃₄N₆O₅S (M⁺) 638.74, found 639.33 (M+H)⁺; Yield: 78%.

Procedure for the synthesis of 2-(2,3-dihydrobenzofuran-5-yl)-N-(4-(5-((5-((3-(dimethylamino)propyl)carbamoyl)-1-methyl-1H-pyrrol-3-yl)carbamoyl)furan-2-yl)phenyl)thiazole-4-carboxamide (4.55)

2.0 eq of HOBT and 1.75 eq. of DIC were added to a solution of **4.48** (1 eq., 80 mg) in DCM. After 30 minutes, 2 eq. (97 mg) of **4.53** was added and the reaction mixture was allowed to stir for 3 hours. The reaction mixture was initially purified using a SCX cartridge (2.0 gm). Final purification was achieved using a silica column and a DCM:MeOH:2MNH₃ solvent system of various concentration gradients for releasing the impurities and the desired product **4.55**. This was dried *in vacuo* and 78 mg cream solid was obtained.

2-(2,3-Dihydrobenzofuran-5-yl)-N-(4-(5-((5-((3-(dimethylamino)propyl)carbamoyl)-1-methyl-1H-pyrrol-3-yl)carbamoyl)furan-2-yl)phenyl)thiazole-4-carboxamide (4.55):

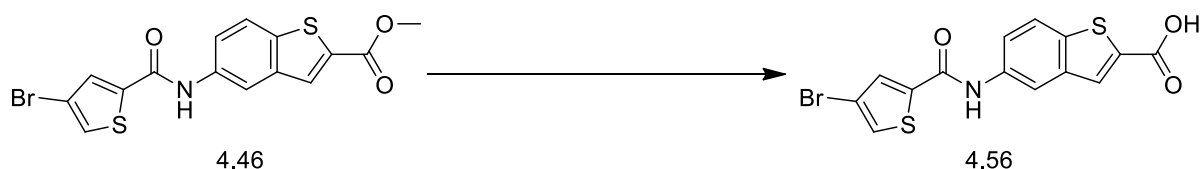


Cream solid. IR (FTIR, $\nu_{\text{max}}/\text{cm}^{-1}$) 635.73, 781.12, 981.00, 1027.27, 1142.76, 1240.76, 1279.65, 1415.36, 1466.26, 1530.61, 1592.28, 1638.34, 2945.61, 3345.31; ¹H NMR (400 MHz, CDCl₃, TMS); δ 1.74 – 1.79 (m, 2H), 2.32 (s, 6H), 2.47 (t, $J=6.15$ Hz, 2H), 3.32 (t, $J=8.67$ Hz, 2H), 3.47 – 3.49 (m, 2H), 3.96 (s, 3H), 4.69 (t, $J=8.67$ Hz, 2H), 6.61 (d, $J=1.89$ Hz, 1H), 6.73 (d, $J=3.47$ Hz, 1H), 6.88 (d, $J=8.15$ Hz, 1H), 7.23 (d, $J=1.89$ Hz, 1H), 7.26 (d, $J=3.47$ Hz, 1H), 7.75 – 7.78 (m, 2H), 7.78 (dd, $J=2.0, 8.35$ Hz, 1H), 7.84 – 7.85 (m, 1H), 7.85 – 7.90 (m, 2H), 8.09 (s, 1H), 8.12(s, 1H), 9.39 (s, 1H); ¹³C NMR (100 MHz, CDCl₃); δ 25.70, 29.09, 36.39, 39.15, 45.23, 47.1, 58.75, 79.1, 106.87, 109.60, 114.7, 116.62, 118.46, 119.74, 120.37, 122.59, 123.31, 125.15, 125.35, 125.48, 126.0, 127.39, 127.5, 129.4, 131.7, 138.02, 146.55, 149.99, 155.10, 161.41, 162.45, 162.7, 168.59, 206.42; m/z (+EI) calc. For C₃₄H₃₄N₆O₅S (M⁺) 638.74, found 639.32 (M+H)⁺; Yield: 70%.

General procedure for the synthesis of 5-(4-bromothiophene-2-carboxamido)benzo[*b*]thiophene-2-carboxylic acid (4.56) from methyl 5-(4-bromothiophene-2-carboxamido)benzo[*b*]thiophene-2-carboxylate (4.46) by hydrolysis:

A 0.5 M solution of NaOH (6.0 ml) was added to a solution of **4.46** (1 eq., 150 mg) in 6.0 ml dioxane at room temperature. The reaction mixture was allowed to stir for 2 hours at which point TLC showed completion of the reaction. Dioxane was evaporated under high vacuum and the residue was diluted with water. The resulting solution was acidified with 1.0 M citric acid solution followed by extraction with ethyl acetate (3 X 50 ml). The combined organic layer was washed with water (60X2 ml) and brine (60X2 ml), dried over MgSO₄ and finally concentrated using a rotary evaporator under reduced pressure to obtain 143 mg light green, oily product **4.56**.

5-(4-Bromothiophene-2-carboxamido)benzo[*b*]thiophene-2-carboxylic acid (4.56):

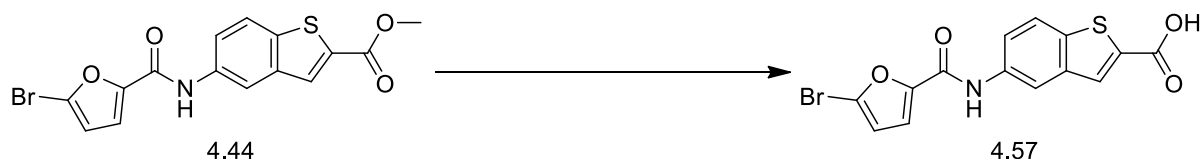


Light green oil. IR (FTIR, $\nu_{\text{max}}/\text{cm}^{-1}$) 629.01, 785.97, 1216.44, 1364.57, 1737.71, 2041.34, 2335.91, 2359.65, 2925.06, 3260.98, 3390.18; ¹H NMR (400 MHz, CDCl₃, TMS); δ 7.50 (d, *J*=1.6 Hz, 1H), 7.56 – 7.58 (m, 1H), 7.73 (d, *J*=1.6 Hz, 1H), 7.86 (d, *J*=8.0 Hz, 1H), 8.05 (s, 1H), 8.09 (s, 1H), 8.32 (d, *J*=2.0 Hz, 1H); ¹³C NMR (100 MHz, CDCl₃); δ 109.60, 115.6, 116.62, 118.46, 123.37, 131.7, 133.9, 135.2, 138.02, 139.1, 140.1, 141.55, 161.41, 162.45 *m/z* (+EI) calc. For C₁₄H₈BrNO₃S₂ (M⁺) 382.25, found 384.00 (M+H)⁺; Yield: 95%.

Procedure for the synthesis of 5-(5-bromofuran-2-carboxamido)benzo[*b*]thiophene-2-carboxylic acid (4.57)

A 0.5 M solution of NaOH (6.0 ml) was added to a solution of **4.46** (1 eq., 249 mg) in 6.0 ml dioxane at room temperature. The reaction mixture was allowed to stir for 2 hours at which point TLC showed completion of the reaction. Dioxane was evaporated under high vacuum and the residue was diluted with water. The resulting solution was acidified with 1.0 M citric acid solution followed by extraction with ethyl acetate (3 X 50 ml). The combined organic layer was washed with water (60X2 ml) and brine (60X2 ml), dried over MgSO₄ and finally concentrated using a rotary evaporator under reduced pressure to obtain 177 mg light yellow, oily product **4.57**.

5-(5-Bromofuran-2-carboxamido)benzo[*b*]thiophene-2-carboxylic acid (4.57):



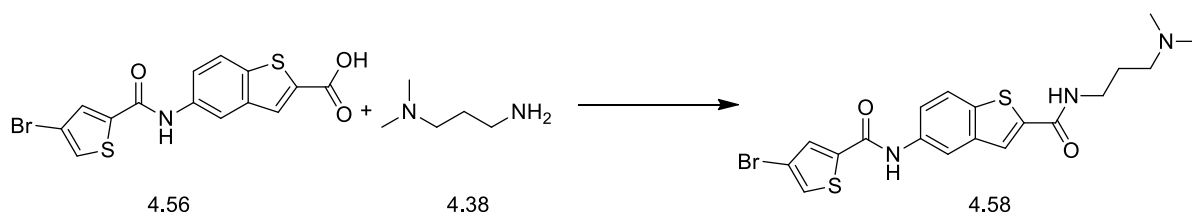
Light yellow oil. IR (FTIR, $\nu_{\text{max}}/\text{cm}^{-1}$) 615.89, 714.22, 798.11, 953.73, 1073.01, 1163.08, 1217.34, 1304.72, 1415.21, 1467.52, 1586.44, 1676.74, 1736.53, 2930.23, 2968.38; ^1H NMR (400 MHz, DMSO, TMS); δ 6.86 (d, $J=3.54$ Hz, 1H), 7.41 (d, $J=3.54$ Hz, 1H), 7.79 (dd, $J=2.0, 8.84$ Hz, 1H), 8.0 (d, $J=8.59$ Hz, 1H), 8.09 (s, 1H), 8.41 (d, $J=1.77$ Hz, 1H), 10.41 (s, 1H); ^{13}C NMR (100 MHz, DMSO); δ 110.7, 115.2, 115.7, 116.9, 118.2, 121.9, 123.0, 135.04, 139.5, 140.1, 142.0, 148.99, 161.8, 162.3; m/z (+EI) calc. For $\text{C}_{14}\text{H}_8\text{BrNO}_4\text{S}$ (M^+) 366.19, found 368.01 ($\text{M}+\text{H}$) $^+$; Yield: 74%.

Compounds **4.58** to **4.61** were synthesised by the amide coupling reaction from **4.56** and **4.57** using *N,N*-dimethylpropane-1,3-diamine (1 eq.) (**4.38** as the amine).

Procedure for the synthesis of 5-(4-bromothiophene-2-carboxamido)-*N*-(3-(dimethylamino)propyl)benzo[*b*]thiophene-2-carboxamide (4.58)

2.0 eq of HOBT (67 mg) and 1.75 eq. of DIC (67 μl) were added to a solution of **4.56** (1 eq., 150 mg) in DCM. After 30 minutes, 1.2 eq. (48 μl) of **4.38** was added and the reaction mixture was allowed to stir for 3 hours. Completion of the reaction was confirmed using LCMS and TLC. The reaction mixture was then purified using a SCX cartridge (2.0 gm), which was washed using DCM (3x), DMF (3x) twice and finally MeOH (2x). The product **4.58** was released from the cartridge using 10.0 ml 2M NH_3 in MeOH and concentrated *in vacuo* to obtain yellow oil (126 mg).

5-(4-Bromothiophene-2-carboxamido)-*N*-(3-(dimethylamino)propyl)benzo[*b*]thiophene-2-carboxamide (4.58):

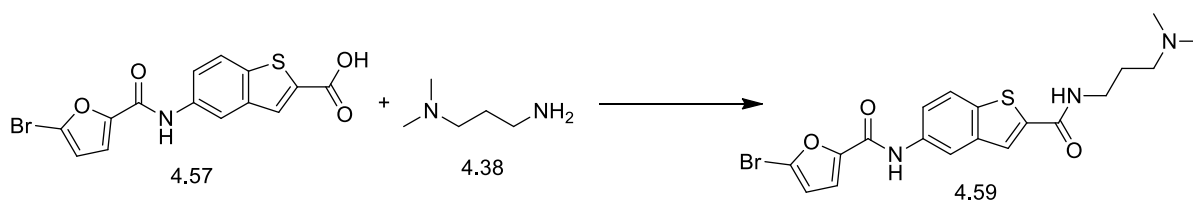


Yellow oil. IR (FTIR, $\nu_{\text{max}}/\text{cm}^{-1}$) 629.66, 674.90, 785.97, 1230.25, 1343.91, 1444.64, 1631.65, 1723.61, 1739.11, 2196.38, 2930.23, 3261.50; ^1H NMR (400 MHz, CDCl_3 , TMS); δ 1.78 – 1.79 (m, 2H), 2.26 (s, 3H), 2.36 (s, 3H), 2.40 (t, $J=8.0$, Hz, 2H), 3.59 – 3.62 (m, 2H), 7.21 – 7.23 (m, 1H), 7.47 (d, $J=3.0$, Hz, 1H), 7.55 (dd, $J=2.0$, 8.59 Hz, 1H), 7.70 (d, $J=3.0$ Hz, 1H), 7.79 (d, $J=8.84$ Hz, 1H), 8.31 (d, $J=2.02$ Hz, 1H), 8.51 (br.s, 1H), 8.98 (br.s, 1H); ^{13}C NMR (100 MHz, CDCl_3); δ 25.70, 39.15, 45.23, 47.0, 58.75, 109.60, 110.2, 116.62, 118.46, 120.37, 131.7, 133.9, 135.2, 138.02, 139.0, 141.1, 146.55, 161.41, 162.45; m/z (+EI) calc. For $\text{C}_{19}\text{H}_{20}\text{BrN}_3\text{O}_2\text{S}_2$ (M^+) 466.42, found 466.06 ($\text{M}+\text{H}$) $^+$; Yield 69%.

Procedure for the synthesis of 5-bromo-*N*-(2-((3-(dimethylamino)propyl)carbamoyl)benzo[*b*]thiophen-5-yl)furan-2-carboxamide (4.59)

2.0 eq of HOBT (83 mg) and 1.75 eq. of DIC (83 μl) were added to a solution of **4.57** (1 eq., 177 mg) in DCM. After 30 minutes, 1.2 eq. (59 μl) of **4.38** was added and the reaction mixture was allowed to stir for 3 hours. Completion of the reaction was confirmed using LCMS and TLC. The reaction mixture was then purified using a SCX cartridge (2.0 gm), which was washed using DCM (3x), DMF (3x) twice and finally MeOH (2x). The product **4.59** was released from the cartridge using 10.0 ml 2M NH_3 in MeOH and concentrated *in vacuo* to obtain colourless oil (129 mg).

5-Bromo-*N*-(2-((3-(dimethylamino)propyl)carbamoyl)benzo[*b*]thiophen-5-yl)furan-2-carboxamide (4.59):

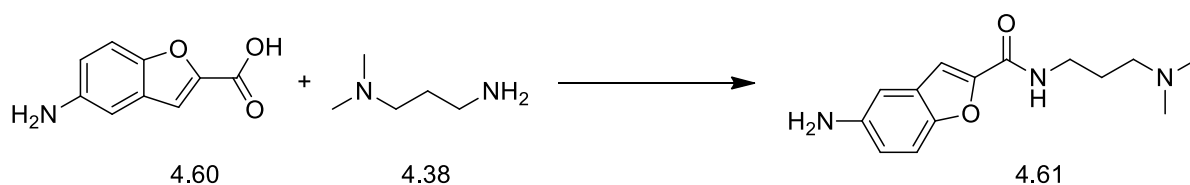


Colourless oil. IR (FTIR, $\nu_{\text{max}}/\text{cm}^{-1}$) 716.07, 742.51, 799.66, 924.57, 1035.56, 1098.33, 1167.83, 1229.76, 1304.84, 1445.18, 1464.00, 1527.30, 1553.13, 1617.66, 1737.39, 2967.50, 3339.26; ^1H NMR (400 MHz, DMSO, TMS); δ 1.67 – 1.69 (m, 2H), 2.14 (s, 6H), 2.25 – 2.27 (m, 2H), 3.63 – 3.65 (m, 2H), 6.86 (d, $J=3.79$ Hz, 1H), 6.96 – 6.98 (m, 1H), 7.42 (d, $J=3.54$ Hz, 1H), 7.75 – 7.77 (m, 1H), 7.97 – 8.00 (m, 1H), 8.02 (s, 1H), 8.35 (d, $J=2.02$ Hz, 1H), 8.78 (t, $J=5.43$ Hz, 1H); ^{13}C NMR (100 MHz, DMSO); δ 25.70, 39.15, 45.23, 47.1, 58.75, 112.7, 115.2, 116.62, 118.46, 120.0, 121.9, 123.0, 133.9, 139.2, 141.1, 146.05, 148.99, 161.8, 162.3; m/z (+EI) calc. For $\text{C}_{19}\text{H}_{20}\text{BrN}_3\text{O}_3\text{S}$ (M^+) 450.35, found 450.20 ($\text{M}+\text{H}$) $^+$; Yield: 73%.

Procedure for the synthesis of 5-amino-N-(3-(dimethylamino)propyl)benzofuran-2-carboxamide (4.61)

2.0 eq of HOBT and 1.75 eq. of DIC were added to a solution of **4.60** (1 eq., 100 mg) in DCM. After 30 minutes, 1.2 eq. (58 μ l) of **4.38** was added and the reaction mixture was allowed to stir for 3 hours. Completion of the reaction was confirmed using LCMS and TLC. The reaction mixture was then purified using a SCX cartridge (2.0 gm), which was washed using DCM (3x), DMF (3x) twice and finally MeOH (2x). The product **4.61** was released from the cartridge using 10.0 ml 2M NH_3 in MeOH and concentrated *in vacuo* to obtain light yellow oil (120 mg).

5-Amino-N-(3-(dimethylamino)propyl)benzofuran-2-carboxamide (4.61):



Light yellow oil. IR (FTIR, $\nu_{\text{max}}/\text{cm}^{-1}$) 739.34, 767.68, 820.64, 876.90, 942.88, 1022.41, 1047.88, 1151.02, 1233.66, 1292.49, 1365.79, 1477.38, 1540.42, 1702.25, 2360.07, 2974.76, 3278.68; ^1H NMR (400 MHz, DMSO, TMS); δ 1.68 – 1.70 (m, 2H), 2.24 (s, 6H), 2.36 – 3.39 (m, 2H), 3.31 – 3.32 (m, 2H), 7.77 (d, $J=2.27$ Hz, 1H), 8.02 (s, 1H), 8.14 (s, 1H), 8.20 (d, $J=2.02$ Hz, 1H), 8.67 (d, $J=5.68$ Hz, 1H); ^{13}C NMR (100 MHz, DMSO); δ 26.63, 38.60, 45.9, 47.1, 58.2, 110.60, 119.24, 123.97, 126.82, 127.5, 135.42, 146.79, 152.75, 159.91; m/z (+EI) calc. For $\text{C}_{14}\text{H}_{19}\text{N}_3\text{O}_2$ (M^+) 261.32, found 262.38 ($\text{M}+\text{H}$) $^+$; Yield: 81%.

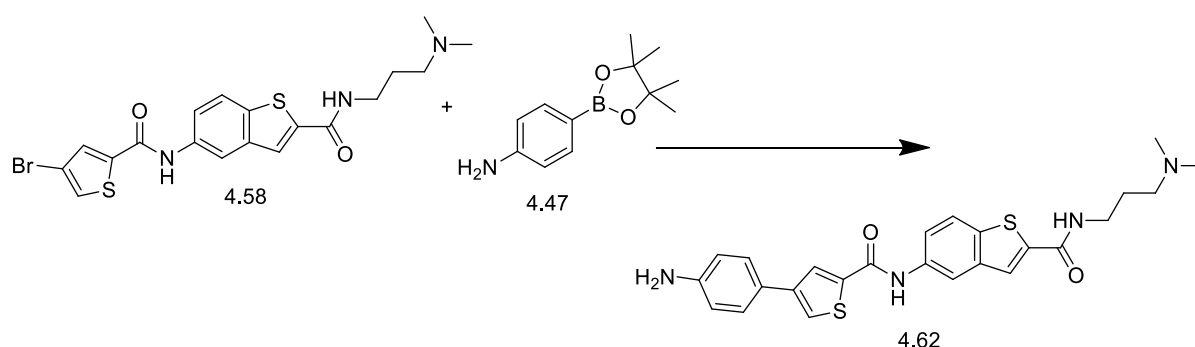
Suzuki coupling was used for the synthesis of compounds **4.62** to **4.70** following the usual procedure and conditions for the reaction.

Procedure for the synthesis of 5-(4-(4-aminophenyl)thiophene-2-carboxamido)-N-(3-(dimethylamino)propyl)benzo[b] thiophene-2-carboxamide (4.62)

A catalytic amount of tetrakis(triphenylphosphine)palladium, $\text{Pd}(\text{PPh}_3)_4$ (0.1 eq) was added to a solution of **4.58** (1.0 eq., 126 mg) and **4.47** (1.2 eq., 71 mg) in a 9:3:1 combination of EtOH, toluene and water in the presence of K_2CO_3 (3.0 eq) in a 10 ml microwave vial containing a magnetic stirrer. The reaction vessel was flushed with nitrogen during each addition. The reaction mixture was sealed in an inert nitrogen environment and heated with microwave radiation in an EMRYSTM Optimizer Microwave Station (Personal Chemistry) at

100 °C for 15 minutes. LCMS analysis showed that the reaction was not completed after 15 minutes and it was again microwaved for another 10 minutes and then for a final 5 minutes. After LCMS analysis revealed completion of the reaction, the cooled reaction mixture was passed through an Isolute™ SCX-2 cartridge (2 gm) and washed with DCM (3x), DMF (3x) twice and finally MeOH (2x). The product **4.62** was released from the cartridge using 10.0 ml 2M NH₃ in MeOH and concentrated *in vacuo* (121 mg).

5-(4-(4-Aminophenyl)thiophene-2-carboxamido)-N-(3-(dimethylamino)propyl)benzo[*b*]thiophene-2-carboxamide (4.62):



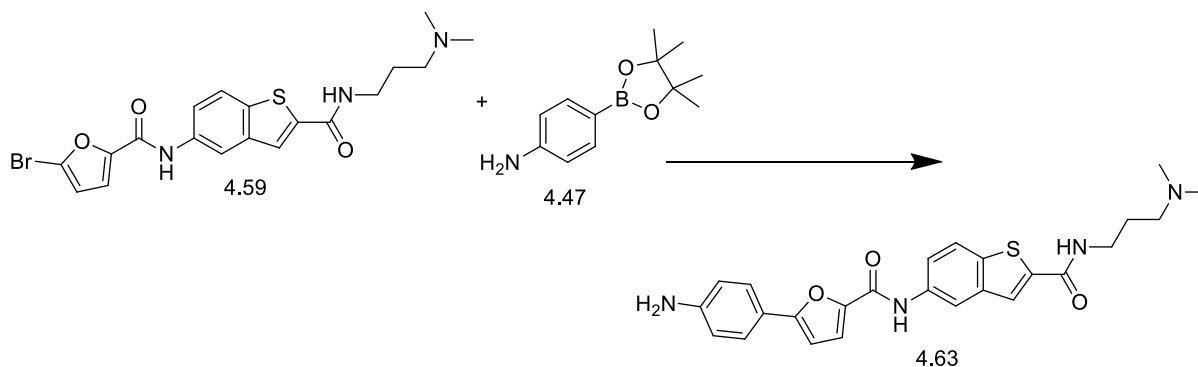
Colourless oil. IR (FTIR, $\nu_{\text{max}}/\text{cm}^{-1}$) 629.78, 785.97, 1116.60, 1230.25, 1511.80, 1630.62, 1736.53, 1873.43, 1969.00, 2175.71, 2334.48, 3266.14, 3333.33; ¹H NMR (400 MHz, DMSO, TMS); δ 1.68 – 1.69 (m, 2H), 2.16 (s, 6H), 2.29 (t, $J=7.07$ Hz, 2H), 3.30 – 3.32 (m, 2H), 6.41 – 6.43 (m, 1H), 6.45 – 6.48 (m, 1H), 6.64 (d, $J=8.59$ Hz, 2H), 7.43 (d, $J=8.59$ Hz, 2H), 7.75 (dd, $J=2.0, 8.84$ Hz, 1H), 7.85 (d, $J=1.26$ Hz, 1H), 7.99 (d, $J=8.84$ Hz, 1H), 8.02 (s, 1H), 8.32 (s, 1H), 8.38 (s, 1H), 8.79 (s, 1H), 10.37 (s, 1H); ¹³C NMR (100 MHz, DMSO); δ 26.70, 39.15, 46.23, 47.0, 58.75, 115.6, 116.62, 118.46, 119.34, 120.37, 123.0, 125.35, 127.39, 127.5, 129.4, 131.7, 133.9, 135.2, 138.02, 140.8, 141.2, 145.0, 146.55, 161.41, 162.45; m/z (+EI) calc. For C₂₅H₂₆N₄O₂S₂ (M⁺) 478.63, found 479.12 (M+H)⁺; Yield: 94%.

Procedure for the synthesis of 5-(4-aminophenyl)-N-(2-((3-(dimethylamino)propyl)carbamoyl)benzo[*b*]thiophen-5-yl)furan-2-carboxamide (4.63)

A catalytic amount of tetrakis(triphenylphosphine)palladium, Pd(PPh₃)₄ (0.1 eq) was added to a solution of **4.59** (1.0 eq., 105 mg) and **4.47** (1.2 eq., 72 mg) in a 9:3:1 combination of EtOH, toluene and water in the presence of K₂CO₃ (3.0 eq) in a 10 ml microwave vial containing a magnetic stirrer. The reaction vessel was flushed with nitrogen during each

addition. The reaction mixture was sealed in an inert nitrogen environment and heated with microwave radiation in an EMRYS™ Optimizer Microwave Station (Personal Chemistry) at 100 °C for 15 minutes. LCMS analysis showed that the reaction was not completed after 15 minutes and it was again microwaved for another 10 minutes and then for a final 5 minutes. After LCMS analysis revealed completion of the reaction, the cooled reaction mixture was passed through an Isolute™ SCX-2 cartridge (2 gm) and washed with DCM (3x), DMF (3x) twice and finally MeOH (2x). The product **4.63** was released from the cartridge using 10.0 ml 2M NH₃ in MeOH and concentrated *in vacuo* (79 mg).

5-(4-Aminophenyl)-N-(2-((3-(dimethylamino)propyl)carbamoyl)benzo[*b*]thiophen-5-yl)furan-2-carboxamide (4.63):



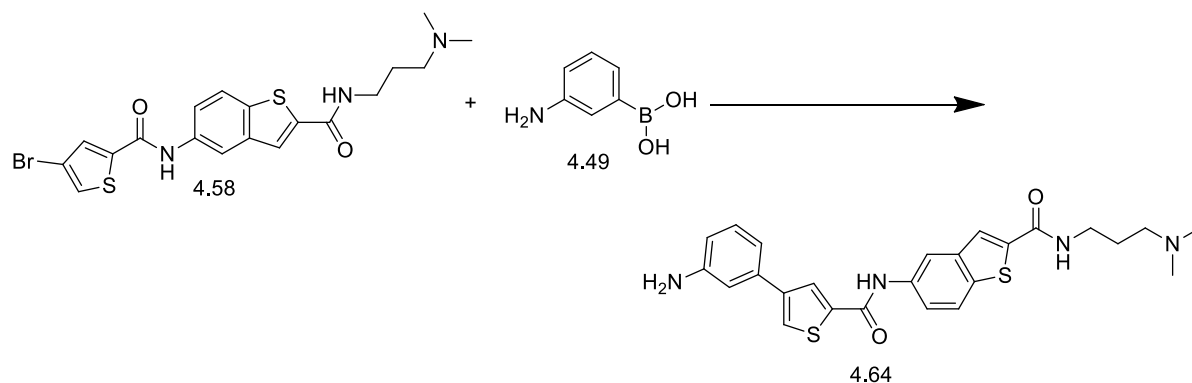
Colourless oil. IR (FTIR, $\nu_{\text{max}}/\text{cm}^{-1}$) 628.41, 720.28, 1120.85, 1177.78, 1302.75, 1444.86, 1483.39, 1538.39, 1610.21, 2821.70, 2967.27, 3336.67; ¹H NMR (400 MHz, DMSO, TMS); δ 1.67 – 1.69 (m, 2H), 2.14 (s, 6H), 2.25 – 2.28 (m, 2H), 3.04 – 3.07 (m, 2H), 6.41 – 6.42 (m, 2H), 6.86 (d, $J=3.79$ Hz, 1H), 7.42 (d, $J=3.79$ Hz, 1H), 7.75 – 7.77 (m, 1H), 7.97 – 8.00 (m, 1H), 8.0 – 8.01 (m, 2H), 8.02 (s, 1H), 8.35 (d, $J=2.02$ Hz, 1H), 8.78 (t, $J=5.43$ Hz, 1H), 10.41 (s, 1H); ¹³C NMR (100 MHz, DMSO); δ 26.70, 39.15, 46.23, 47.1, 58.75, 108.9, 109.3, 115.2, 115.6, 115.8, 116.62, 119.34, 120.37, 123.9, 125.35, 135.2, 138.02, 140.8, 141.2, 145.0, 146.3, 146.55, 156.0, 161.41, 162.45; m/z (+EI) calc. For C₂₅H₂₆N₄O₃S (M⁺) 462.56, found 463.23 (M+H)⁺; Yield: 73%.

Procedure for the synthesis of 5-(4-(3-aminophenyl)thiophene-2-carboxamido)-N-(3-(dimethylamino)propyl)benzo [b]thiophene-2-carboxamide (4.64)

A catalytic amount of tetrakis(triphenylphosphine)palladium, Pd(PPh₃)₄ (0.1 eq) was added to a solution of **4.58** (1.0 eq., 350 mg) and **4.49** (1.5 eq., 154 mg) in a 9:3:1 combination of

EtOH, toluene and water in the presence of K_2CO_3 (3.0 eq) in a 10 ml microwave vial containing a magnetic stirrer. The reaction vessel was flushed with nitrogen during each addition. The reaction mixture was sealed in an inert nitrogen environment and heated with microwave radiation in an EMRYSTM Optimizer Microwave Station (Personal Chemistry) at 100 °C for 20 minutes. LCMS analysis showed that the reaction was not completed after 20 minutes and it was again microwaved for another 10 minutes. After LCMS analysis revealed completion of the reaction, the cooled reaction mixture was passed through an IsoluteTM SCX-2 cartridge (5 gm) and washed with DCM (3x), DMF (3x) twice and finally MeOH (2x). The product **4.64** was released from the cartridge using 10.0 ml 2M NH_3 in MeOH and concentrated *in vacuo* (300 mg).

5-(4-(3-Aminophenyl)thiophene-2-carboxamido)-N-(3-(dimethylamino)propyl)benzo[b]thiophene-2-carboxamide (4.64):

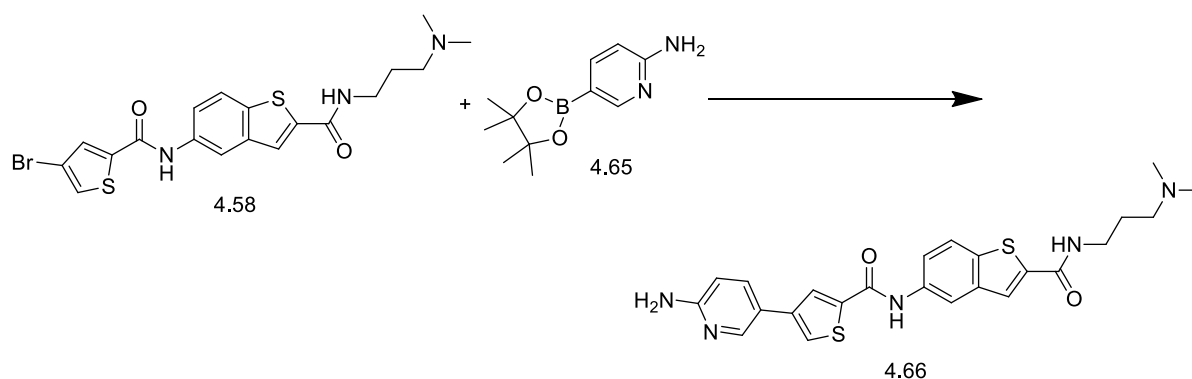


Colourless oily mass. IR (FTIR, ν_{max}/cm^{-1}) 664.84, 684.11, 719.47, 762.73, 816.52, 848.36, 893.97, 968.15, 1119.89, 1162.92, 1222.91, 1272.50, 1309.31, 1337.48, 1365.79, 1428.76, 1529.61, 1574.16, 1619.90, 1738.57, 2832.04, 3251.64; 1H NMR (400 MHz, $DMSO-d_6$, TMS); δ 1.71 – 1.73 (m, 2H), 2.18 (s, 6H), 2.32 (t, $J=7.07$ Hz, 2H), 3.39 – 3.42 (m, 2H), 6.59 – 6.60 (m, 2H), 6.95 – 6.97 (m, 1H), 6.98 – 7.00 (m, 2H), 7.11 (t, $J=8.0$ Hz, 1H), 7.57 – 7.59 (m, 1H), 7.64 – 7.65 (m, 1H), 7.65 – 7.68 (m, 1H), 7.72 (br.s, 1H), 7.98 – 8.00 (m, 1H), 8.02 (s, 1H), 8.39 – 8.41 (m, 1H), 10.44 (s, 1H); ^{13}C NMR (100 MHz, $DMSO-d_6$); δ 26.92, 39.72, 45.04, 47.1, 56.73, 111.27, 115.67, 116.3, 117.5, 119.92, 121.84, 122.92, 124.38, 129.45, 131.39, 134.97, 136.05, 139.50, 140.14, 142.86, 144.5, 147.50, 149.16, 159.93, 163.4; m/z (+EI) calc. For $C_{25}H_{26}N_4O_2S_2$ (M^+) 478.63, found 479.12 ($M+H$)⁺; Yield: 83%.

Procedure for the synthesis of 5-(4-(6-aminopyridin-3-yl)thiophene-2-carboxamido)-N-(3-(dimethylamino)propyl)benzo[*b*]thiophene-2-carboxamide (4.66)

A catalytic amount of tetrakis(triphenylphosphine)palladium, Pd(PPh₃)₄ (0.1 eq) was added to a solution of **4.58** (1.0 eq., 413 mg) and **4.65** (1.5 eq., 292 mg) in a 9:3:1 combination of EtOH, toluene and water in the presence of K₂CO₃ (3.0 eq) in a 10 ml microwave vial containing a magnetic stirrer. The reaction vessel was flushed with nitrogen during each addition. The reaction mixture was sealed in an inert nitrogen environment and heated with microwave radiation in an EMRYSTM Optimizer Microwave Station (Personal Chemistry) at 100 °C for 20 minutes. LCMS analysis showed that the reaction was not completed after 20 minutes and it was again microwaved for another 10 minutes. After LCMS analysis revealed completion of the reaction, the cooled reaction mixture was passed through an IsoluteTM SCX-2 cartridge (5 gm) and washed with DCM (3x), DMF (3x) twice and finally MeOH (2x). The product **4.66** was released from the cartridge using 10.0 ml 2M NH₃ in MeOH and concentrated *in vacuo* (374 mg).

5-(4-(6-Aminopyridin-3-yl)thiophene-2-carboxamido)-N-(3-(dimethylamino)propyl)benzo[*b*]thiophene-2-carboxamide (4.66):



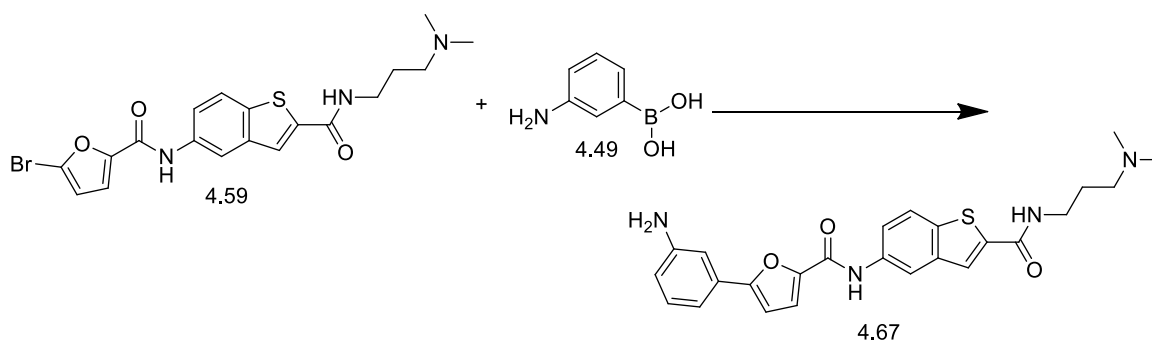
Light yellow oil. IR (FTIR, $\nu_{\text{max}}/\text{cm}^{-1}$) 630.82, 722.61, 777.76, 1119.83, 1168.50, 1360.87, 1436.62, 1501.95, 1553.57, 1626.46, 2362.18, 2969.51, 3332.28; ¹H NMR (400 MHz, DMSO-*d*₆, TMS); δ 1.68 (t, *J*=7.07 Hz, 2H), 2.16 (s, 6H), 2.30 (t, *J*=7.33Hz, 2H), 3.01 – 3.02 (m, 2H), 6.10 (s, 2H), 6.53 (dd, *J*=0.51, 8.59 Hz, 1H), 7.55 – 7.57 (m, 1H), 7.61 – 7.62 (m, 1H), 7.62 (d, *J*=1.52 Hz, 1H), 7.95 (d, *J*=1.52Hz, 1H), 7.99 (d, *J*=8.59 Hz, 1H), 8.02 (s, 1H), 8.35 – 8.36 (m, 1H), 8.37 (d, *J*=2.02Hz, 1H), 8.40 (d, *J*=1.26Hz, 1H), 10.36 (s, 1H); ¹³C NMR (100 MHz, DMSO-*d*₆); δ 26.46, 39.10, 45.14, 47.1, 56.97, 108.16, 115.73, 116.3, 121.84, 122.92, 125.73, 128.86, 132.42, 134.96, 135.63, 139.71, 140.46, 141.42, 142.74,

146.2, f4r159.35, 160.11, 161.02, 161.47; m/z (+EI) calc. For $C_{24}H_{25}N_5O_2S_2$ (M^+) 479.62, found 480.17 ($M+H$)⁺; Yield: 88%.

Procedure for the synthesis of 5-(3-aminophenyl)-*N*-(2-((3-(dimethylamino)propyl)carbamoyl)benzo[*b*]thiophen-5-yl)furan-2-carboxamide (4.67)

A catalytic amount of tetrakis(triphenylphosphine)palladium, $Pd(PPh_3)_4$ (0.1 eq) was added to a solution of **4.59** (1.0 eq., 280 mg) and **4.49** (1.5 eq., 128 mg) in a 9:3:1 combination of EtOH, toluene and water in the presence of K_2CO_3 (3.0 eq) in a 10 ml microwave vial containing a magnetic stirrer. The reaction vessel was flushed with nitrogen during each addition. The reaction mixture was sealed in an inert nitrogen environment and heated with microwave radiation in an EMRYSTM Optimizer Microwave Station (Personal Chemistry) at 100 °C for 20 minutes. LCMS analysis showed that the reaction was not completed after 20 minutes and it was microwaved for another 10 minutes. After LCMS analysis revealed completion of the reaction, the cooled reaction mixture was passed through an IsoluteTM SCX-2 cartridge (5 gm) and washed with DCM (3x), DMF (3x) twice and finally MeOH (2x). The product **4.67** was released from the cartridge using 10.0 ml 2M NH_3 in MeOH and concentrated *in vacuo* (230 mg).

5-(3-Aminophenyl)-*N*-(2-((3-(dimethylamino)propyl)carbamoyl)benzo[*b*]thiophen-5-yl)furan-2-carboxamide (4.67):



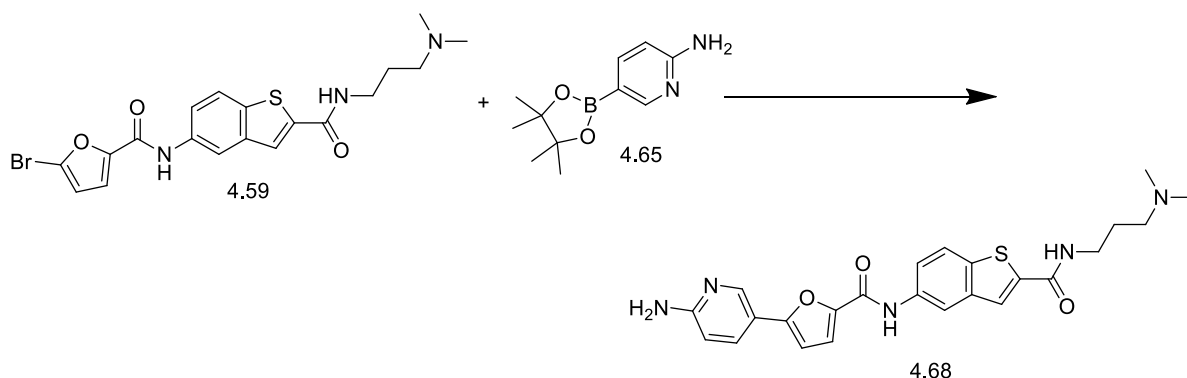
Colourless oil. IR (FTIR, ν_{max}/cm^{-1}) 690.56, 743.45, 768.52, 1018.27, 1120.38, 1179.90, 1225.59, 1298.48, 1439.92, 1522.89, 1576.95, 1614.31, 2339.42, 2360.70, 2945.12, 3339.84; 1H NMR (400 MHz, DMSO- d_6 , TMS); δ 1.67 – 1.69 (m, 2H), 2.14 (s, 6H), 2.28 – 2.30 (m, 2H), 3.39 – 3.41 (m, 2H), 6.60 – 6.63 (m, 2H), 6.97 – 7.00 (m, 2H), 7.02 – 7.03 (m, 1H), 7.10 – 7.11 (m, 1H), 7.11 (d, $J=1.52$ Hz, 1H), 7.43 (d, $J=3.79$ Hz, 1H), 7.63 (d, $J=1.52$ Hz, 1H), 7.78 (dd, $J=2.02, 8.84$ Hz, 1H), 7.98 (d, $J=8.84$ Hz, 1H), 8.02 (s, 1H), 8.38 (d, $J=2.01.77$ Hz, 1H), 10.28 (s, 1H); ^{13}C NMR (100 MHz, DMSO- d_6); δ 27.67, 39.72, 47.3, 49.50, 57.02,

103.81, 109.81, 112.66, 115.88, 117.02, 118.28, 120.13, 122.05, 123.03, 124.56, 129.96, 131.60, 131.70, 133.43, 135.63, 136.08, 147.70, 149.26, 156.52, 161.47; m/z (+EI) calc. For $C_{25}H_{26}N_4O_3$ (M^+) 462.56, found 463.30 ($M+H$)⁺; Yield: 80%.

Procedure for the synthesis of 5-(6-aminopyridin-3-yl)-*N*-(2-((3-(dimethylamino)propyl)carbamoyl)benzo[*b*]thiophen-5-yl)furan-2-carboxamide (4.68)

A catalytic amount of tetrakis(triphenylphosphine)palladium, $Pd(PPh_3)_4$ (0.1 eq) was added to a solution of **4.59** (1.0 eq., 131 mg) and **4.65** (1.5 eq., 96 mg) in a 9:3:1 combination of EtOH, toluene and water in the presence of K_2CO_3 (3.0 eq) in a 10 ml microwave vial containing a magnetic stirrer. The reaction vessel was flushed with nitrogen during each addition. The reaction mixture was sealed in an inert nitrogen environment and heated with microwave radiation in an EMRYSTM Optimizer Microwave Station (Personal Chemistry) at 100 °C for 20 minutes. LCMS analysis showed that the reaction was not completed after 20 minutes and it was microwaved for another 10 minutes. After LCMS analysis revealed completion of the reaction, the cooled reaction mixture was passed through an IsoluteTM SCX-2 cartridge (5 gm) and washed with DCM (3x) and DMF (3x) twice and finally MeOH (2x). The product **4.68** was released from the cartridge using 10.0 ml 2M NH_3 in MeOH and concentrated *in vacuo* (105 mg).

5-(6-Aminopyridin-3-yl)-*N*-(2-((3-(dimethylamino)propyl)carbamoyl)benzo[*b*]thiophen-5-yl)furan-2-carboxamide (4.68):



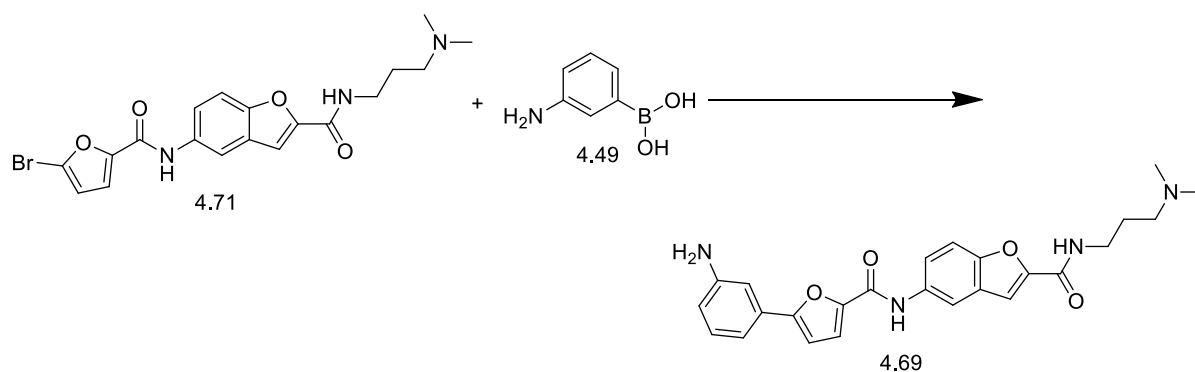
Yellow oil. IR (FTIR, ν_{max}/cm^{-1}) 691.10, 737.63, 1017.76, 1177.00, 1265.07, 1304.85, 1409.00, 1477.65, 1583.94, 1617.69, 2362.23, 3322.29; 1H NMR (400 MHz, DMSO- d_6 , TMS); δ 1.68 – 1.70 (m, 2H), 2.15 (s, 6H), 2.28 – 2.31 (m, 2H), 3.12 – 3.15 (m, 2H), 6.36 (s, 2H), 6.54 – 6.55 (m, 1H), 6.90 (d, $J=3.54$ Hz, 1H), 7.36 (d, $J=3.54$ Hz, 1H), 7.56 – 7.58 (m, 1H), 7.78 (dd, $J=2.0, 8.84$ Hz, 1H), 7.92 (dd, $J=2.40, 8.72$ Hz, 1H), 7.98 (d, $J=8.84$ Hz, 1H), 8.02 (s, 1H), 8.38 (d, $J=1.77$ Hz, 1H), 8.59 (d, $J=2.27$ Hz, 1H), 10.19 (s, 1H); ^{13}C NMR (100

MHz, DMSO- d_6); δ 27.67, 39.72, 47.1, 49.50, 57.02, 103.81, 109.81, 112.66, 115.88, 117.02, 118.28, 120.13, 122.05, 123.03, 129.96, 131.60, 131.70, 133.43, 135.63, 136.08, 147.70, 149.26, 156.52, 161.47; m/z (+EI) calc. For $C_{24}H_{25}N_5O_3S$ (M^+) 463.55, found 464.49 ($M+H$) $^+$; Yield: 78%.

Procedure for the synthesis of 3-(5-(3-aminophenyl)furan-2-carboxamido)-N-(3-(dimethylamino)propyl)benzofuran-6-carboxamide (4.69)

A catalytic amount of tetrakis(triphenylphosphine)palladium, $Pd(PPh_3)_4$ (0.1 eq) was added to a solution of **4.71** (1.0 eq., 61 mg) and **4.49** (1.2 eq., 23 mg) in a 9:3:1 combination of EtOH, toluene and water in the presence of K_2CO_3 (3.0 eq) in a 10 ml microwave vial containing a magnetic stirrer. The reaction vessel was flushed with nitrogen during each addition. The reaction mixture was sealed in an inert nitrogen environment and heated with microwave radiation in an EMRYSTM Optimizer Microwave Station (Personal Chemistry) at 100 °C for 20 minutes. LCMS analysis showed that the reaction was not completed after 20 minutes and it was microwaved for another 10 minutes. After LCMS analysis revealed completion of the reaction, the cooled reaction mixture was passed through an IsoluteTM SCX-2 cartridge (5 gm) and washed with DCM (3x), DMF (3x) twice and finally MeOH (2x). The product **4.69** was released from the cartridge using 10.0 ml 2M NH_3 in MeOH and concentrated *in vacuo* (54 mg).

3-(5-(3-Aminophenyl)furan-2-carboxamido)-N-(3-(dimethylamino)propyl)benzofuran-6-carboxamide (4.69):



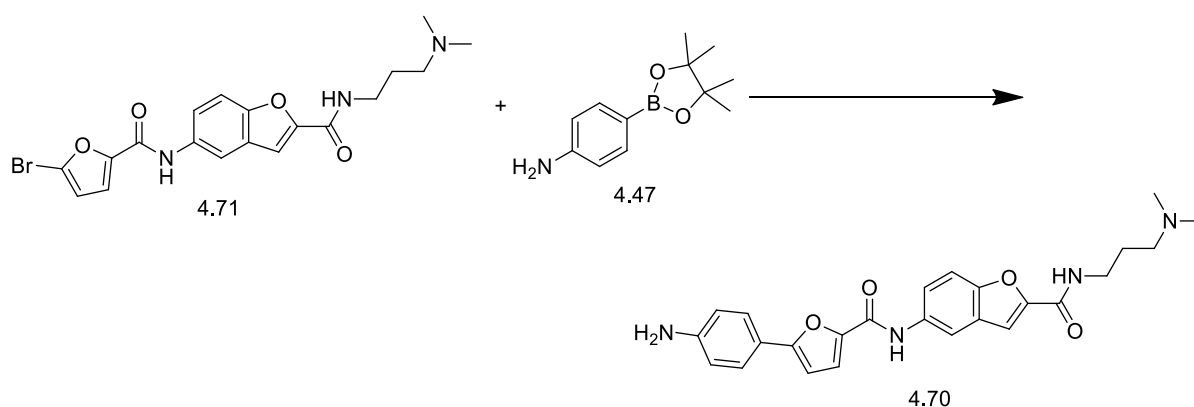
Light yellow oil. IR (FTIR, ν_{max}/cm^{-1}) 722.40, 785.89, 992.82, 1021.62, 1114.11, 1233.37, 1297.16, 1441.25, 1468.87, 1540.61, 1578.87, 1643.60, 3229.50, 3336.67; 1H NMR (400 MHz, DMSO- d_6 , TMS); δ 1.69 (t, $J=6.95$ Hz, 2H), 2.20 (s, 6H), 2.35 – 2.38 (m, 2H), 3.32 (s, 2H), 6.60 (d, $J=2.02$ Hz, 1H), 6.61 (dd, $J=1.26, 3.28$ Hz, 1H), 6.96 (d, $J=1.26$ Hz, 1H), 6.97 (d, $J=2.27$ Hz, 1H), 7.10 (d, $J=0.76$ Hz, 1H), 7.41 (d, $J=3.54$ Hz, 1H), 7.55 – 7.57 (m, 1H),

7.63 – 7.64 (m, 1H), 7.66 (s, 1H), 7.73 (s, 2H), 7.75 (d, $J=2.27$ Hz, 1H), 8.19 (d, $J=2.02$ Hz, 1H), 10.23 (s, 1H); ^{13}C NMR (100 MHz, DMSO- d_6); δ 26.62, 37.09, 44.81, 47.1, 56.60, 106.75, 109.11, 109.21, 114.36, 115.48, 119.72, 120.50, 121.65, 127.04, 127.51, 129.57, 131.19, 131.28, 145.99, 147.29, 148.83, 156.03, 157.70, 162.07, 167.77; m/z (+EI) calc. For $\text{C}_{25}\text{H}_{26}\text{N}_4\text{O}_4$ (M^+) 446.50, found 447.25 ($\text{M}+\text{H}$) $^+$; Yield: 86%.

Procedure for the synthesis of 3-(5-(4-aminophenyl)furan-2-carboxamido)-*N*-(3-(dimethylamino)propyl)benzofuran-6-carboxamide (4.70)

A catalytic amount of tetrakis(triphenylphosphine)palladium, $\text{Pd}(\text{PPh}_3)_4$ (0.1 eq) was added to a solution of **4.71** (1.0 eq., 54 mg) and **4.47** (1.2 eq., 33 mg) in a 9:3:1 combination of EtOH, toluene and water in the presence of K_2CO_3 (3.0 eq) in a 10 ml microwave vial containing a magnetic stirrer. The reaction vessel was flushed with nitrogen during each addition. The reaction mixture was sealed in an inert nitrogen environment and heated with microwave radiation in an EMRYSTM Optimizer Microwave Station (Personal Chemistry) at 100 °C for 20 minutes. LCMS analysis showed that the reaction was not completed after 20 minutes and it was microwaved for another 10 minutes. After LCMS analysis revealed completion of the reaction, the cooled reaction mixture was passed through an IsoluteTM SCX-2 cartridge (5 gm) and washed with DCM (3x), DMF (3x) twice and finally MeOH (2x). The product **4.70** was released from the cartridge using 10.0 ml 2M NH_3 in MeOH and concentrated *in vacuo* (42 mg).

3-(5-(4-Aminophenyl)furan-2-carboxamido)-*N*-(3-(dimethylamino)propyl)benzofuran-6-carboxamide (4.70):



Greenish yellow oil. IR (FTIR, $\nu_{\text{max}}/\text{cm}^{-1}$) 668.24, 802.47, 1021.34, 1177.83, 1203.07, 1234.29, 1297.91, 1434.74, 1469.38, 1548.02, 1608.16, 1644.05, 2359.97, 3237.45, 3336.06; ^1H NMR (400 MHz, DMSO- d_6 , TMS); δ 1.68 (t, $J=7.07$ Hz, 2H), 2.18 (s, 6H), 2.32 – 2.34

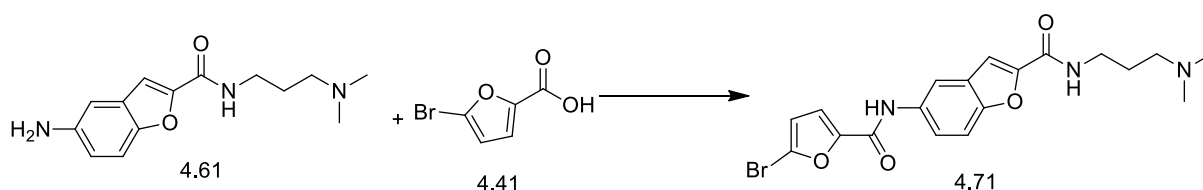
(m, 2H), 3.31 – 3.32 (m, 2H), 6.46 – 6.48 (m, 2H), 6.64 – 6.65 (m, 1H), 6.66 – 6.68 (m, 1H), 6.78 (d, $J=3.54$ Hz, 1H), 7.33 (d, $J=3.79$ Hz, 1H), 7.53 (d, $J=1.01$ Hz, 1H), 7.63 – 7.64 (m, 2H), 7.65 – 7.67 (m, 1H), 7.76 (dd, $J=2.1, 8.97$ Hz, 1H), 8.18 (d, $J=2.02$ Hz, 1H), 10.10 (s, 1H); ^{13}C NMR (100 MHz, DMSO- d_6); δ 26.85, 37.31, 45.05, 47.3, 56.82, 109.31, 111.57, 112.71, 115.18, 115.49, 117.01, 120.78, 121.3, 125.94, 127.22, 128.66, 128.74, 135.47, 140.1, 144.84, 148.56, 156.26, 157.00, 157.93, 167.7; m/z (+EI) calc. For $\text{C}_{25}\text{H}_{26}\text{N}_4\text{O}_4$ (M^+) 446.50, found 447.18 ($\text{M}+\text{H}$) $^+$; Yield: 78%.

The amide coupling reaction was carried out for the synthesis of compounds **4.71** to **4.81** following the usual procedure and conditions for the reaction.

Procedure for the synthesis of 5-(5-bromofuran-2-carboxamido)-*N*-(3-(dimethylamino)propyl)benzofuran-2-carboxamide (4.71)

2.0 eq of HOBT and 1.75 eq. of DIC were added to a solution of **4.61** (1 eq., 71 mg) in DCM. Then 1.2 eq. (62 mg) of **4.41** was added to the reaction mixture, which was allowed to stir for 3 hours. Completion of the reaction was confirmed using LCMS. The reaction mixture was then purified by SCX cartridge (2.0 gm), which was washed using DCM (3x), DMF (3x) twice and finally MeOH (2x). The product **4.71** was released from the cartridge using 10.0 ml 2M NH_3 in MeOH and concentrated *in vacuo* to obtain yellow oil (51 mg).

5-(5-Bromofuran-2-carboxamido)-*N*-(3-(dimethylamino)propyl)benzofuran-2-carboxamide (4.71):



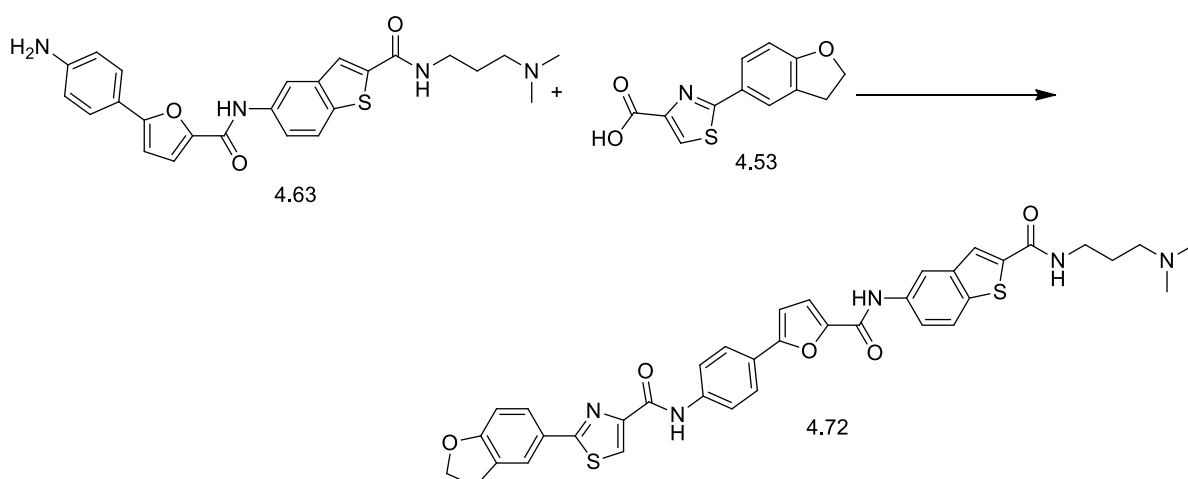
Yellowish oil. IR (FTIR, $\nu_{\text{max}}/\text{cm}^{-1}$) 739.32, 813.63, 963.39, 1028.10, 1179.59, 1235.62, 1283.62, 1343.33, 1457.14, 1537.87, 1566.39, 1590.85, 1651.30, 2819.67, 2944.27, 3319.83; ^1H NMR (400 MHz, DMSO- d_6 , TMS); δ 1.67 (t, $J=7.07$ Hz, 2H), 2.14 (s, 6H), 2.26 (t, $J=6.95$ Hz, 2H), 3.30 – 3.32 (m, 2H), 6.84 (d, $J=3.54$ Hz, 1H), 7.38 (d, $J=3.54$ Hz, 1H), 7.51 (d, $J=1.01$ Hz, 1H), 7.70 (d, $J=2.27$ Hz, 1H), 8.17 (d, $J=2.02$ Hz, 1H), 8.17 (d, $J=2.02$ Hz, 1H), 8.76 (d, $J=5.68$ Hz, 1H), 10.31 (s, 1H); ^{13}C NMR (100 MHz, DMSO- d_6); δ 27.13, 37.56, 45.33, 47.1, 57.09, 109.52, 111.89, 114.45, 117.24, 120.83, 125.44, 134.35, 146.9, 149.50,

150.22, 155.34, 158.09, 162.1, 167.0; m/z (+EI) calc. For $C_{19}H_{20}BrN_3O_4$ (M^+) 434.28, found 435.95 ($M+H$)⁺; Yield: 82%.

Procedure for the synthesis of 2-(1,3-dihydroisobenzofuran-5-yl)-N-(4-(5-((2-((3-(dimethylamino)propyl)carbamoyl)benzo[*b*]thiophen-5-yl)carbamoyl)furan-2-yl)phenyl)thiazole-4-carboxamide (4.72)

1 eq. of **4.63** (27 mg), 1.7 eq. of **4.53** (25 mg), 2 eq. HOBt and 1.75 eq. DIC were measured into a round bottom flask and dissolved in a minimum amount of DMF. The reaction mixture was allowed to stir for 3 hours at room temperature. After 3 hours the reaction mixture was checked by LCMS to identify completion of the reaction. LCMS analysis indicated completion of the reaction and the reaction mixture was poured onto an Isolute SCX (500 mg) column for purification. The cartridge was washed using DCM (3x), DMF (3x) twice and finally MeOH (2x). The product **4.72** was released from the cartridge using 10.0 ml 2M NH_3 in MeOH and concentrated *in vacuo*. Further purification was achieved using a silica column with DCM:MeOH:2M NH_3 (18:1:1) as the solvent system. 21 mg colourless oil was obtained as the final compound.

2-(1,3-Dihydroisobenzofuran-5-yl)-N-(4-(5-((2-((3-(dimethylamino)propyl)carbamoyl)benzo[*b*]thiophen-5-yl)carbamoyl)furan-2-yl)phenyl)thiazole-4-carboxamide (4.72):



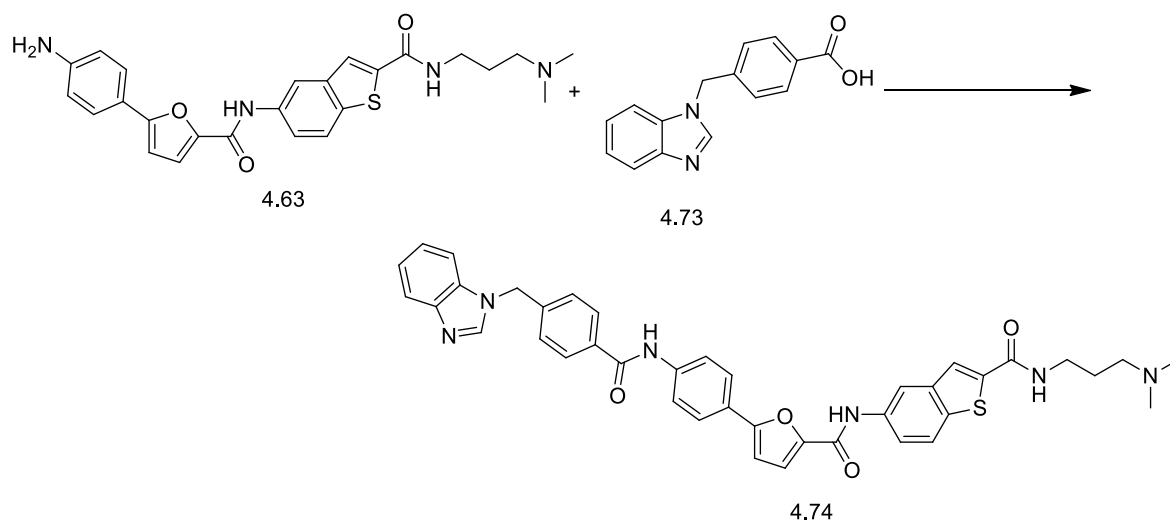
Colourless oil. IR (FTIR, ν_{max}/cm^{-1}) 640.14, 729.94, 798.27, 980.55, 1015.93, 1099.83, 1230.74, 1294.34, 1365.13, 1413.76, 1447.00, 1482.14, 1522.14, 1637.74, 2969.08, 3307.49; 1H NMR (400 MHz, $CDCl_3$, TMS); δ 1.80 – 1.82 (m, 2H), 2.37 (s, 6H), 2.57 – 2.60 (m, 2H), 3.33 (t, $J=8.59$ Hz, 2H), 3.60 – 3.62 (m, 2H), 4.69 – 4.71 (m, 2H), 6.78 (d, $J=3.54$ Hz, 1H),

6.89 (m, 1H), 7.36 (d, $J=3.54$ Hz, 1H), 7.59 (dd, $J=2.02, 8.84$ Hz, 1H), 7.69 (s, 1H), 7.79 – 7.82 (m, 2H), 7.84 (d, $J=8.84$ Hz, 1H), 7.86 – 7.88 (m, 2H), 8.02 (s, 1H), 8.13 – 8.15 (m, 1H), 8.27 (s, 1H), 8.40 (d, $J=2.02$ Hz, 1H), 8.85 (br.s, 1H), 9.41 – 9.42 (m, 1H), 10.37 (br.s, 1H); ^{13}C NMR (100 MHz, CDCl_3); δ 24.74, 36.48, 45.29, 47.1, 59.40, 71.96, 76.69, 107.32, 108.5, 109.83, 115.75, 117.79, 119.52, 119.97, 122.93, 123.09, 123.54, 124.56, 125.44, 125.47, 125.50, 125.57, 127.60, 128.7, 129.6, 134.66, 136.79, 138.38, 139.91, 141.1, 141.7, 146.4, 150.09, 156.26, 159.06, 162.63, 170.3; m/z (+EI) calc. For $\text{C}_{37}\text{H}_{33}\text{N}_5\text{O}_5\text{S}_2$ (M^+) 691.82, found 692.55 ($\text{M}+\text{H}$) $^+$; Yield: 76%.

Procedure for the synthesis of 5-(4-(4-((1H-benzo[d]imidazol-1-yl)methyl)benzamido)phenyl)-N-(2-((3-(dimethylamino)propyl)carbonyl)benzo[b]thiophen-5-yl)furan-2-carboxamide (4.74)

1 eq. of **4.63** (39 mg), 1.7 eq. of **4.73** (30 mg), 2 eq. HOBt and 1.75 eq. DIC were measured into a round bottom flask and dissolved in a minimum amount of DMF. The reaction mixture was allowed to stir for 3 hours at room temperature. After 3 hours the reaction mixture was checked by LCMS to identify completion of the reaction. LCMS analysis indicated completion of the reaction and the reaction mixture was poured onto an Isolute SCX (500 mg) column for purification. The cartridge was washed using DCM (3x), DMF (3x) twice and finally MeOH (2x). The product **4.74** was released from the cartridge using 10.0 ml 2M NH_3 in MeOH and concentrated *in vacuo*. Further purification was achieved using a silica column and DCM:MeOH:2M NH_3 (18:1:1) as the solvent system. 55 mg colourless, oily mass was obtained as the final compound.

5-(4-(4-((1*H*-benzo[*d*]imidazol-1-yl)methyl)benzamido)phenyl)-*N*-(2-((3-(dimethylamino)propyl)carbamoyl)benzo[*b*]thiophen-5-yl)furan-2-carboxamide (4.74):



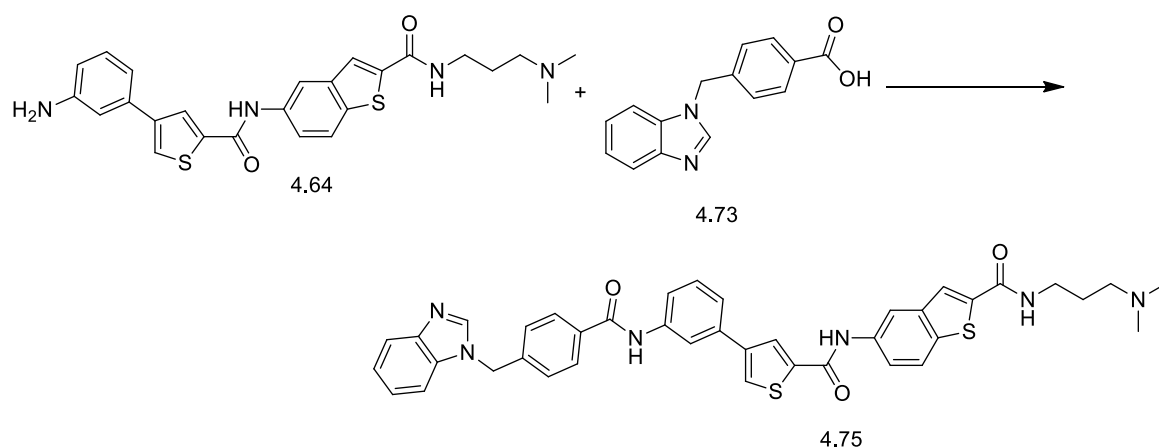
Colourless oily mass. IR (FTIR, $\nu_{\text{max}}/\text{cm}^{-1}$) 665.26, 736.90, 798.66, 831.62, 1019.70, 1097.66, 1217.81, 1260.68, 1286.13, 1324.16, 1445.96, 1491.83, 1541.96, 1645.86, 1737.17, 2359.90, 2922.19, 3339.00; ^1H NMR (400 MHz, DMSO- d_6 , TMS); δ 1.73 – 1.75 (m, 2H), 2.20 (s, 6H), 2.36 – 3.39 (m, 2H), 3.39 (s, 2H), 6.72 – 6.74 (m, 2H), 6.75 (d, $J=3.54$ Hz, 1H), 7.20 – 7.21 (m, 2H), 7.38 (d, $J=3.54$ Hz, 1H), 7.39 – 7.42 (m, 2H), 7.49 – 7.51 (m, 2H), 7.62 (dd, $J=2.0, 8.84$ Hz, 1H), 7.77 – 7.79 (m, 2H), 7.80 – 7.81 (m, 2H), 7.93 (d, $J=8.84$ Hz, 1H), 8.05 (s, 1H), 8.07 (s, 1H), 8.30 (s, 1H), 8.35 (d, $J=2.0$ Hz, 1H), 10.37 (br.s, 1H); ^{13}C NMR (100 MHz, DMSO- d_6); δ 25.74, 38.48, 47.29, 47.5, 51.0, 59.40, 108.1, 108.6, 115.0, 116.75, 118.79, 119.52, 119.97, 120.93, 123.09, 123.54, 125.50, 125.57, 127.60, 129.1, 131.7, 134.2, 134.66, 136.79, 140.91, 141.1, 143.0, 144.4, 146.7, 146.9, 147.8, 150.09, 156.26, 159.06, 161.3, 162.63, 164.1, 164.7, 170.3, 176.1; m/z (+EI) calc. For $\text{C}_{40}\text{H}_{36}\text{N}_6\text{O}_4\text{S}$ (M^+) 696.82, found 697.81 ($\text{M}+\text{H}$) $^+$; Yield: 93%.

Procedure for the synthesis of 5-(4-(3-(4-((1*H*-benzo[*d*]imidazol-1-yl)methyl)benzamido)phenyl)thiophene-2-carboxamido)-*N*-(3-(dimethylamino)propyl)benzo[*b*]thiophene-2-carboxamide (4.75)

1 eq. of **4.64** (77 mg), 1.4 eq. of **4.73** (57 mg), 2 eq. HOBT and 1.75 eq. DIC were measured into a round bottom flask and dissolved in a minimum amount of DMF. The reaction mixture was allowed to stir for 3 hours at room temperature. After 3 hours the reaction mixture was

checked by LCMS to identify completion of the reaction. LCMS analysis indicated the completion of the reaction and the reaction mixture was poured onto an Isolute SCX (500 mg) column for purification. The cartridge was washed using DCM (3x), DMF (3x) twice and finally MeOH (2x). The product **4.75** was released from the cartridge using 10.0 ml 2M NH₃ in MeOH and concentrated *in vacuo*. Further purification was achieved using a silica column and DCM:MeOH:2MNH₃ (18:1:1) as the solvent system. 70 mg colourless oil was obtained as the final compound.

5-(4-(3-(4-((1*H*-benzo[d]imidazol-1-yl)methyl)benzamido)phenyl)thiophene-2-carboxamido)-*N*-(3-(dimethylamino)propyl)benzo[*b*]thiophene-2-carboxamide (4.75):

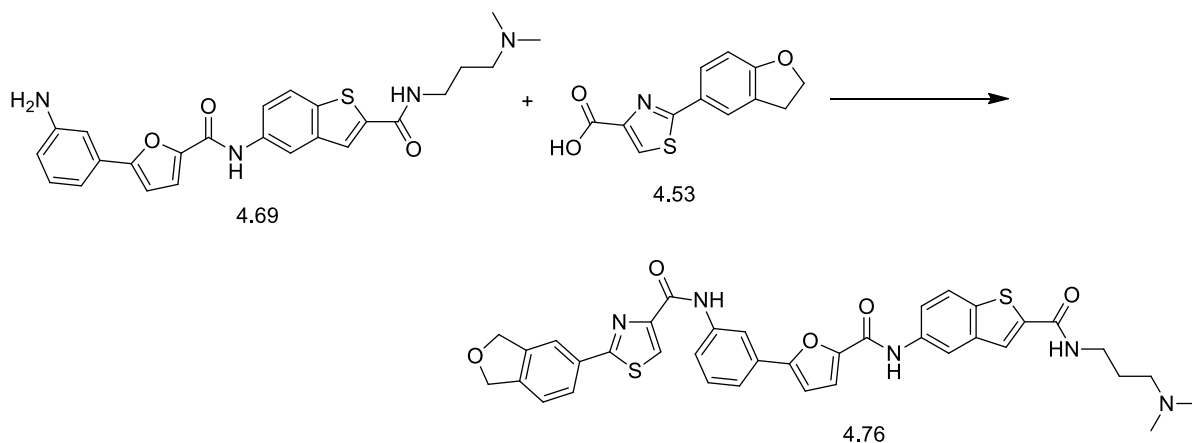


Colourless oil. IR (FTIR, $\nu_{\text{max}}/\text{cm}^{-1}$) 739.69, 888.50, 1110.67, 1180.04, 1260.22, 1286.33, 1434.06, 1494.42, 1538.07, 1613.68, 1644.08, 1714.53, 2358.40, 3073.17, 3303.99; ¹H NMR (400 MHz, DMSO-*d*₆, TMS); δ 1.68 – 1.70 (m, 2H), 2.16 (s, 6H), 2.31 – 2.34 (m, 2H), 3.39 (s, 2H), 5.56 (s, 2H), 7.19 – 7.21 (m, 1H), 7.22 – 7.25 (m, 2H), 7.29 – 7.31 (m, 1H), 7.35 (d, *J*=8.59 Hz, 1H), 7.41(d, *J*=3.79 Hz, 1H), 7.46 – 7.49 (m, 2H), 7.52 – 7.53 (m, 2H), 7.67 – 7.68 (m, 1H), 7.73 – 7.75 (m, 1H), 7.91 – 7.92 (m, 1H), 7.98 – 8.00 (m, 2H), 8.02 (s, 1H), 8.11 (d, *J*=1.5 Hz, 1H), 8.20 (s, 1H), 8.35 (s, 1H), 8.38 (s, 1H); ¹³C NMR (100 MHz, DMSO-*d*₆); δ 26.46, 39.10, 47.70, 47.9, 52.50, 56.97, 110.96, 111.06, 115.6, 116.0, 119.92, 119.94, 122.02, 122.82, 123.1, 123.7, 123.8, 126.97, 127.50, 127.65, 127.89, 128.24, 128.43, 128.47, 129.38, 129.96, 133.99, 136.4, 138.56, 140.1, 141.1, 142.73, 143.99, 144.71, 146.3, 161.3, 164.7, 165.37, 166.24, 206.82; *m/z* (+EI) calc. For C₄₀H₃₆N₆O₃S₂ (M⁺) 712.88, found 713.39 (M+H)⁺; Yield: 61%.

Procedure for the synthesis of 2-(2,3-dihydrobenzofuran-5-yl)-N-(3-(5-((2-((3-(dimethylamino)propyl)carbamoyl)benzo[*b*]thiophen-5-yl)carbamoyl)furan-2-yl)phenyl)thiazole-4-carboxamide (4.76)

1 eq. of **4.69** (111 mg), 1.4 eq. of **4.53** (80 mg), 2 eq. HOBT and 1.75 eq. DIC were measured into a round bottom flask and dissolved in a minimum amount of DMF. The reaction mixture was allowed to stir for 3 hours at room temperature. After 3 hours, the reaction mixture was checked by LCMS to identify completion of the reaction. LCMS analysis indicated the completion of the reaction and the reaction mixture was poured onto an Isolute SCX (500 mg) column for purification. The cartridge was washed using DCM (3x), DMF (3x) twice and finally MeOH (2x). The product **4.76** was released from the cartridge using 10.0 ml 2M NH₃ in MeOH and concentrated *in vacuo*. Further purification was achieved using a silica column and DCM:MeOH:2MNH₃ (18:1:1) as the solvent system. 77 mg cream powder was obtained as the final compound.

2-(2,3-Dihydrobenzofuran-5-yl)-N-(3-(5-((2-((3-(dimethylamino)propyl)carbamoyl)benzo[*b*]thiophen-5-yl)carbamoyl)furan-2-yl)phenyl)thiazole-4-carboxamide (4.76):



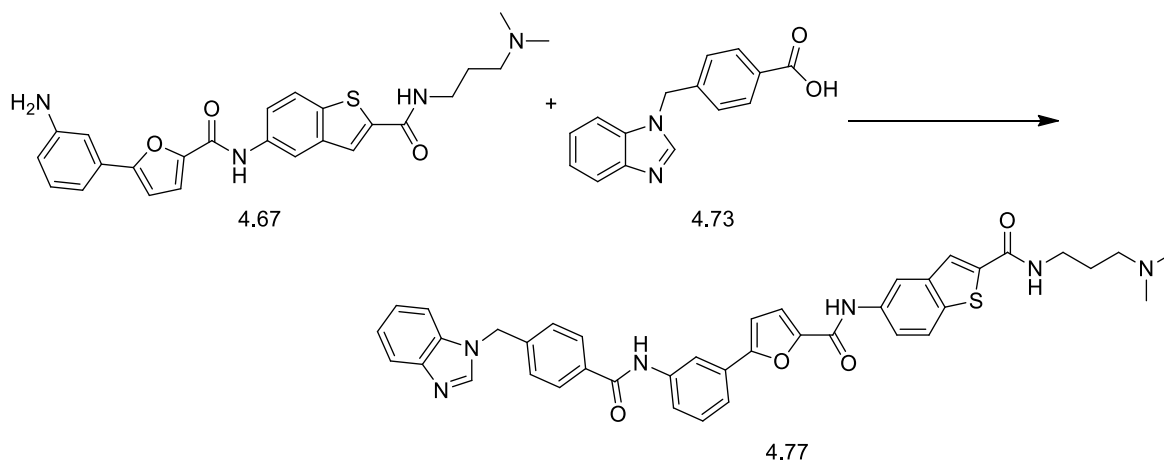
Cream powder. IR (FTIR, $\nu_{\text{max}}/\text{cm}^{-1}$) 633.40, 741.29, 787.78, 1019.08, 1110.19, 1228.04, 1304.55, 1422.99, 1447.00, 1535.35, 1586.59, 1651.93, 2357.64, 2951.21, 3115.85, 3348.21; ¹H NMR (400 MHz, CDCl₃, TMS); δ 1.78(t, *J*=5.68 Hz, 2H), 2.35 (s, 6H), 2.54 – 2.56 (m, 2H), 3.31 (t, *J*=8.72 Hz, 2H), 3.59 – 3.61 (m, 2H), 4.68 (t, *J*=8.72 Hz, 2H), 6.86 (d, *J*=3.79 Hz, 1H), 6.88 (d, *J*=8.34 Hz, 1H), 7.35 (d, *J*=3.54 Hz, 1H), 7.46 (t, *J*=7.83 Hz, 1H), 7.54 (dt, *J*=1.33, 7.54 Hz, 1H), 7.60 (dd, *J*=2.0, 8.84 Hz, 1H), 7.65 (s, 1H), 7.67 (ddd, *J*=1.01, 2.15, 7.96 Hz, 1H), 7.77 (d, *J*=2.02 Hz, 1H), 7.80 – 7.82 (m, 1H), 7.86 (d, *J*=1.26 Hz, 1H), 8.13 (s, 1H), 8.27 (t, *J*=1.77 Hz, 1H), 8.36 (s, 1H), 8.40 (d, *J*=2.02Hz, 1H), 8.85 (t, *J*=4.55 Hz, 1H),

9.38 (s, 1H); ^{13}C NMR (100 MHz, CDCl_3); δ 24.83, 29.31, 41.15, 47.1, 47.3, 59.70, 77.30, 108.38, 109.84, 115.91, 115.94, 117.60, 119.69, 120.28, 120.66, 122.91, 123.02, 123.55, 124.64, 125.54, 127.64, 128.35, 129.64, 130.38, 134.67, 136.82, 138.44, 139.89, 140.88, 146.91, 150.16, 155.60, 156.27, 159.24, 161.88, 162.68, 168.85; m/z (+EI) calc. For $\text{C}_{37}\text{H}_{33}\text{N}_5\text{O}_5\text{S}_2$ (M^+) 691.82, found 692.72 ($\text{M}+\text{H}$) $^+$; Yield: 69%.

Procedure for the synthesis of 5-(3-(4-((1H-benzo[d]imidazol-1-yl)methyl)benzamido)phenyl)-N-(2-((3-(dimethylamino)propyl)carbamoyl)benzo[b]thiophen-5-yl)furan-2-carboxamide (4.77)

1 eq. of **4.67** (97 mg), 1.4 eq. of **4.73** (74 mg), 2 eq. HOBT and 1.75 eq. DIC were measured into a round bottom flask and dissolved in a minimum amount of DMF. The reaction mixture was allowed to stir for 3 hours at room temperature. After 3 hours the reaction mixture was checked by LCMS to identify completion of the reaction. LCMS analysis indicated the completion of the reaction and the reaction mixture was poured onto an Isolute SCX (500 mg) column for purification. The cartridge was washed using DCM (3x), DMF (3x) twice and finally MeOH (2x). The product **4.77** was released from the cartridge using 10.0 ml 2M NH_3 in MeOH and concentrated *in vacuo*. Further purification was achieved using a silica column and DCM:MeOH:2M NH_3 (18:1:1) as the solvent system. 71 mg colourless oil was obtained as the final compound.

5-(3-(4-((1H-benzo[d]imidazol-1-yl)methyl)benzamido)phenyl)-N-(2-((3-(dimethylamino)propyl)carbamoyl)benzo[b]thiophen-5-yl)furan-2-carboxamide (4.77):



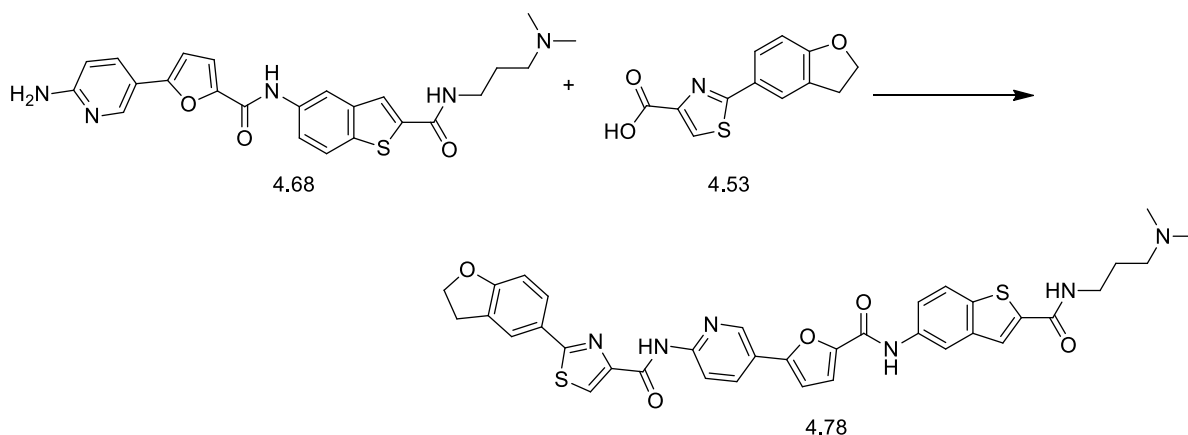
Colourless oil. IR (FTIR, $\nu_{\text{max}}/\text{cm}^{-1}$) 634.22, 686.48, 742.14, 783.28, 884.53, 967.28, 1030.00, 1221.88, 1264.20, 1288.49, 1365.41, 1439.46, 1497.81, 1525.18, 1547.87, 1584.65, 1641.64, 1708.81, 2358.16, 3310.12; ^1H NMR (400 MHz, CDCl_3 , TMS); δ 1.78 – 1.80 (m, 2H), 2.30

(s, 6H), 2.53 – 2.55 (m, 2H), 3.57 (dd, $J=5.43, 11.49$ Hz, 2H), 5.42 (s, 2H), 6.85 (d, $J=3.79$ Hz, 1H), 7.23 (d, $J=8.34$ Hz, 2H), 7.26 – 7.29 (m, 1H), 7.30 (d, $J=3.54$ Hz, 1H), 7.32 – 7.34 (m, 1H), 7.35 (d, $J=3.79$ Hz, 1H), 7.47 (d, $J=8.08$ Hz, 1H), 7.54 (d, $J=9.1$ Hz, 1H), 7.59 (d, $J=8.34$ Hz, 1H), 7.76 (d, $J=8.34$ Hz, 2H), 7.81 (d, $J=8.59$ Hz, 1H), 7.85 – 7.89 (m, 1H), 7.89 – 7.91 (m, 1H), 7.98 (s, 1H), 8.02 (s, 1H), 8.20 (s, 1H), 8.28 (s, 1H), 8.37 (s, 1H), 8.52 (br.s, 1H), ^{13}C NMR (100 MHz, CDCl_3); δ 24.83, 29.31, 41.15, 47.1, 47.6, 59.70, 77.30, 108.38, 108.5, 109.84, 110.0, 115.91, 115.94, 117.60, 119.69, 120.28, 120.66, 122.91, 123.02, 123.55, 124.64, 125.54, 127.64, 128.35, 129.64, 130.38, 134.67, 136.82, 138.44, 139.89, 140.88, 146.91, 150.16, 155.60, 156.27, 159.24, 161.88, 162.68, 164.8, 168.85; m/z (+EI) calc. For $\text{C}_{40}\text{H}_{36}\text{N}_6\text{O}_4\text{S}$ (M^+) 696.82, found 697.57 ($\text{M}+\text{H}$) $^+$; Yield: 73%.

Procedure for the synthesis of 2-(2,3-dihydrobenzofuran-5-yl)-N-(5-(5-((2-((3-(dimethylamino)propyl)carbamoyl)benzo[*b*]thiophen-5-yl)carbamoyl)furan-2-yl)pyridin-2-yl)thiazole-4-carboxamide (4.78)

1 eq. of **4.68** (32 mg), 1.4 eq. of **4.53** (24 mg), 2 eq. HOBt and 1.75 eq. DIC were measured into a round bottom flask and dissolved in a minimum amount of DMF. The reaction mixture was allowed to stir for 3 hours at room temperature. After 3 hours, the reaction mixture was checked by LCMS to identify completion of the reaction. LCMS analysis indicated the completion of the reaction and the reaction mixture was poured onto an Isolute SCX (500 mg) column for purification. The cartridge was washed using DCM (3x), DMF (3x) twice and finally MeOH (2x). The product **4.78** was released from the cartridge using 10.0 ml 2M NH_3 in MeOH and concentrated *in vacuo*. Further purification was achieved using a silica column and DCM:MeOH:2M NH_3 (18:1:1) as the solvent system. 24 mg colourless oil was obtained as the final compound.

2-(2,3-Dihydrobenzofuran-5-yl)-N-(5-(5-((2-((3-(dimethylamino)propyl)carbamoyl)benzo[*b*]thiophen-5-yl)carbamoyl)furan-2-yl)pyridin-2-yl)thiazole-4-carboxamide (4.78):



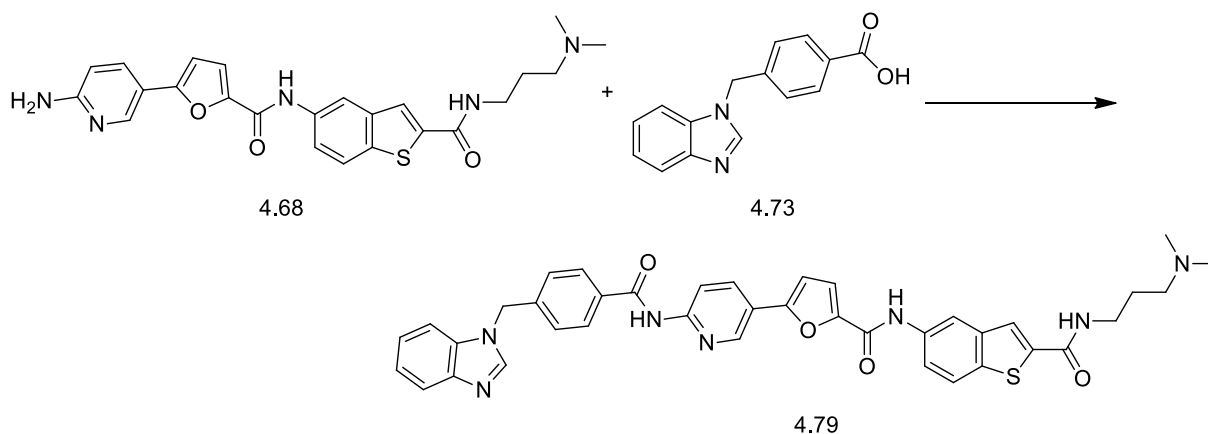
Colourless oil. IR (FTIR, $\nu_{\text{max}}/\text{cm}^{-1}$) 638.77, 792.06, 940.13, 982.64, 1016.05, 1101.08, 1230.41, 1295.44, 1397.26, 1444.25, 1485.48, 1520.17, 1583.94, 1611.27, 1647.72, 1741.86, 2362.36, 2933.66, 3115.85, 3341.46; ^1H NMR (400 MHz, CDCl_3 , TMS); δ 1.79 (t, $J=6.44$ Hz, 2H), 2.37 (s, 6H), 2.57 – 2.59 (m, 2H), 3.34 (t, $J=8.84$ Hz, 2H), 3.61 – 3.64 (m, 2H), 4.70 (t, $J=8.84$ Hz, 2H), 6.87 (d, $J=3.79$ Hz, 1H), 6.90 (d, $J=8.59$ Hz, 1H), 7.39 (d, $J=3.54$ Hz, 1H), 7.58 (dd, $J=2.1, 8.72$ Hz, 1H), 7.68 (s, 1H), 7.80 (d, $J=6.06$ Hz, 1H), 7.86 (d, $J=8.59$ Hz, 1H), 7.95 (s, 1H), 8.13 (dd, $J=2.4, 8.72$ Hz, 1H), 8.18 – 8.20 (m, 1H), 8.41 (d, $J=1.52$ Hz, 1H), 8.57 (d, $J=8.84$ Hz, 1H), 8.79 (d, $J=3.28$ Hz, 1H), 8.88 (br s, 1H), 10.0 (s, 1H); ^{13}C NMR (100 MHz, CDCl_3); δ 24.73, 39.31, 47.15, 47.2, 51.0, 59.0, 78.4, 108.38, 108.7, 110.84, 115.01, 116.94, 119.60, 120.67, 121.66, 122.81, 123.02, 123.55, 124.00, 125.54, 127.64, 128.35, 129.64, 130.38, 135.67, 136.22, 138.65, 139.89, 141.88, 146.91, 150.16, 155.60, 156.27, 161.88, 162.68, 168.85; m/z (+EI) calc. For $\text{C}_{36}\text{H}_{32}\text{N}_6\text{O}_5\text{S}_2$ (M^+) 692.81, found 693.30 ($\text{M}+\text{H}$) $^+$; Yield: 74%.

Procedure for the synthesis of 5-(6-(4-((1*H*-benzo[*d*]imidazol-1-yl)methyl)benzamido)pyridin-3-yl)-N-(2-((3-(dimethylamino)propyl)carbamoyl)benzo[*b*]thiophen-5-yl)furan-2-carboxamide (4.79)

1 eq. of **4.68** (46 mg), 1.4 eq. of **4.73** (35 mg), 2 eq. HOBt and 1.75 eq. DIC were measured into a round bottom flask and dissolved in a minimum amount of DMF. The reaction mixture was allowed to stir for 3 hours at room temperature. After 3 hours the reaction mixture was checked by LCMS to identify completion of the reaction. LCMS analysis indicated the completion of the reaction and the reaction mixture was poured onto an Isolute SCX (500 mg) column for purification. The cartridge was washed using DCM (3x), DMF (3x) twice

and finally MeOH (2x). The product **4.79** was released from the cartridge using 10.0 ml 2M NH₃ in MeOH and concentrated *in vacuo*. Further purification was achieved using a silica column and DCM:MeOH:2MNH₃ (18:1:1) as the solvent system. 34 mg colourless oil was obtained as the final compound.

5-(6-(4-((1*H*-benzo[d]imidazol-1-yl)methyl)benzamido)pyridin-3-yl)-*N*-(2-((3-(dimethylamino)propyl)carbamoyl)benzo[*b*]thiophen-5-yl)furan-2-carboxamide (4.79**):**



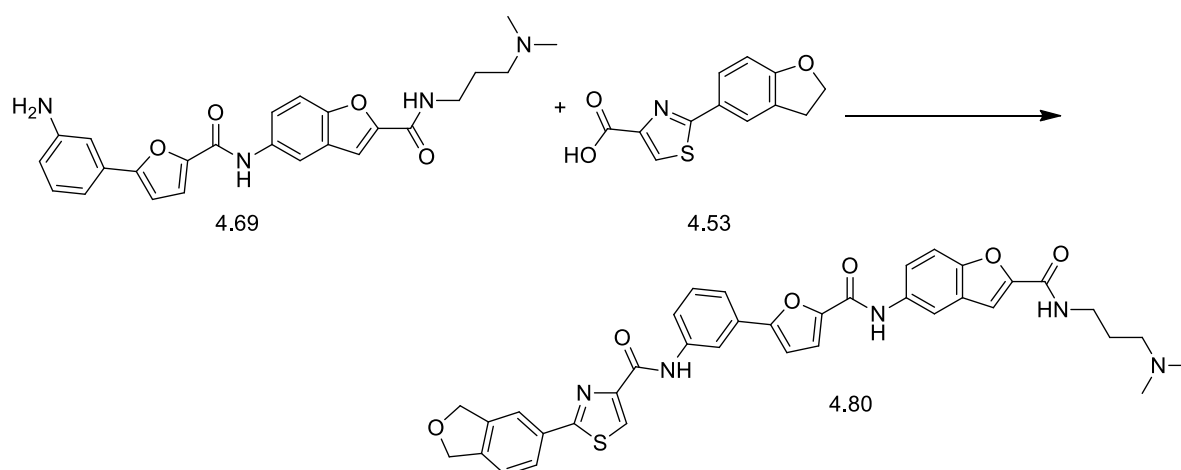
Colourless oil. IR (FTIR, $\nu_{\text{max}}/\text{cm}^{-1}$) 740.95, 795.26, 1039.37, 1213.44, 1365.59, 1445.88, 1494.87, 1538.39, 1633.71, 1737.22, 2361.96, 2969.45, 3018.29, 3341.46; ¹H NMR (400 MHz, CDCl₃, TMS); δ 1.80 – 1.82 (m, 2H), 2.39 (s, 6H), 2.59 – 2.62 (m, 2H), 3.60 – 3.62 (m, 2H), 5.49 (s, 2H), 6.86 (d, $J=3.54$ Hz, 1H), 7.01 – 7.02 (m, 1H), 7.17 – 7.19 (m, 1H), 7.32 – 7.35 (m, 2H), 7.35 – 7.37 (m, 1H), 7.38 (d, $J=3.54$ Hz, 1H), 7.56 – 7.60 (m, 2H), 7.70 (s, 1H), 7.86 – 7.89 (m, 2H), 7.93 – 7.95 (m, 2H), 8.02 (s, 1H), 8.11 – 8.13 (m, 1H), 8.16 (s, 1H), 8.39 (s, 1H), 8.59 (s, 1H), 8.74 (d, $J=2.3$ Hz, 1H); ¹³C NMR (100 MHz, CDCl₃); δ 25.83, 30.31, 41.11, 47.1, 47.4, 59.50, 109.38, 109.94, 110.1, 115.38, 115.94, 116.0, 117.10, 119.70, 120.35, 121.66, 122.34, 123.02, 123.75, 124.34, 125.84, 127.34, 129.35, 129.64, 130.38, 134.07, 136.45, 138.14, 139.69, 141.88, 143.3, 147.91, 150.16, 155.80, 156.48, 159.24, 161.18, 162.86, 168.85; m/z (+EI) calc. For C₃₉H₃₅N₇O₄S (M⁺) 697.80, found 698.53 (M+H)⁺; Yield: 73%.

Procedure for the synthesis of 2-(2,3-dihydrobenzofuran-5-yl)-*N*-(3-(5-((2-((3-(dimethylamino)propyl)carbamoyl)benzofuran-5-yl)carbamoyl)furan-2-yl)phenyl)thiazole-4-carboxamide (4.80**)**

1 eq. of **4.69** (66 mg), 1.5 eq. of **4.53** (55 mg), 2 eq. HOBT and 1.75 eq. DIC were measured into a round bottom flask and dissolved in a minimum amount of DMF. The reaction mixture

was allowed to stir for 3 hours at room temperature. After 3 hours the reaction mixture was checked by LCMS to identify completion of the reaction. LCMS analysis indicated the completion of the reaction and the reaction mixture was poured onto an Isolute SCX (500 mg) column for purification. The cartridge was washed using DCM (3x), DMF (3x) twice and finally MeOH (2x). The product **4.80** was released from the cartridge using 10.0 ml 2M NH₃ in MeOH and concentrated *in vacuo*. Further purification was achieved using a silica column and DCM:MeOH:2MNH₃ (18:1:1) as the solvent system. 50 mg colourless oil was obtained as the final compound.

2-(2,3-Dihydrobenzofuran-5-yl)-N-(3-(5-((2-((3-(dimethylamino)propyl)carbamoyl)benzofuran-5-yl)carbamoyl)furan-2-yl)phenyl)thiazole-4-carboxamide (4.80):

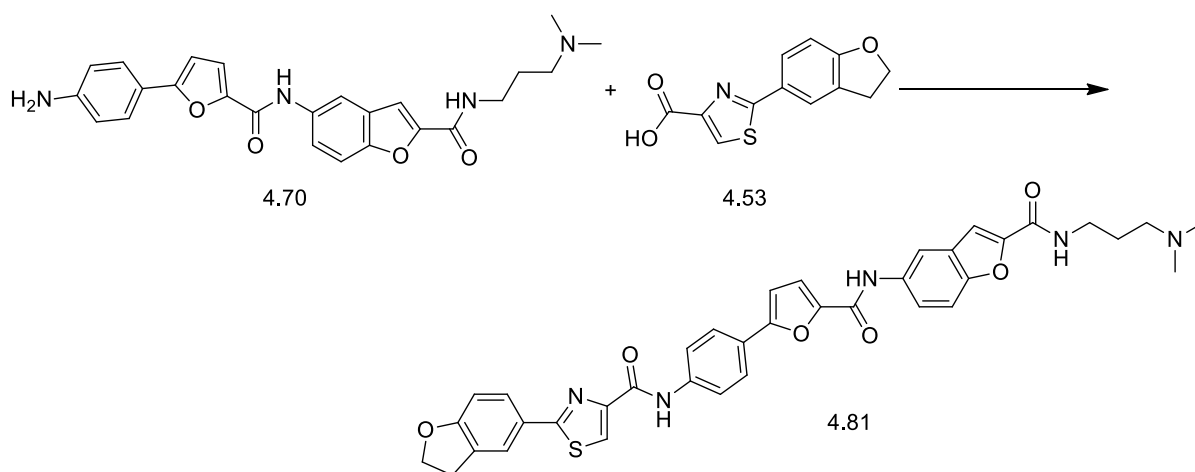


Colourless oil. IR (FTIR, $\nu_{\text{max}}/\text{cm}^{-1}$) 677.55, 778.73, 869.38, 938.77, 1000.0, 1102.16, 1231.56, 1302.04, 1465.30, 1537.96, 1555.10, 1587.75, 1644.23, 1738.77, 2967.21, 3284.85; ¹H NMR (400 MHz, DMSO-d₆, TMS); δ 1.67 – 1.69 (m, 2H), 2.14 (s, 6H), 2.27 (t, $J=7.07$ Hz, 2H), 3.30 – 3.32 (m, 4H), 4.64 (t, $J=8.72$ Hz, 2H), 6.92 (d, $J=8.34$ Hz, 1H), 7.15 (d, $J=3.54$ Hz, 1H), 7.48 (d, $J=3.54$ Hz, 1H), 7.51 – 7.53 (m, 1H), 7.54 (d, $J=0.76$ Hz, 1H), 7.66 (d, $J=9.09$ Hz, 1H), 7.77 (d, $J=2.02$ Hz, 1H), 7.93 – 7.94 (m, 1H), 7.96 – 7.98 (m, 1H), 8.07 – 8.09 (m, 1H), 8.20 (d, $J=2.02$ Hz, 1H), 8.32 (t, $J=1.89$ Hz, 1H), 8.38 (s, 1H), 8.78 (t, $J=5.68$ Hz, 1H), 10.33 (d, $J=2.53$ Hz, 1H); ¹³C NMR (100 MHz, DMSO-d₆); δ 26.93, 28.62, 37.37, 45.12, 47.5, 56.89, 77.5, 107.99, 109.32, 109.38, 114.12, 116.69, 116.81, 120.34, 120.84, 121.04, 123.72, 124.70, 125.20, 127.28, 127.41, 128.74, 129.33, 129.72, 134.32, 138.91, 146.77, 149.86, 150.03, 155.10, 156.16, 157.91, 159.21, 162.08, 162.28, 167.76, 170.1; m/z (+EI) calc. For C₃₇H₃₃N₅O₆S (M⁺) 675.75, found 676.13 (M+H)⁺; Yield: 75%.

Procedure for the synthesis of 2-(2,3-dihydrobenzofuran-5-yl)-N-(4-(5-((2-((3-(dimethylamino)propyl)carbamoyl)benzofuran-5-yl)carbamoyl)furan-2-yl)phenyl)thiazole-4-carboxamide (4.81)

1 eq. of **4.70** (76 mg), 1.5 eq. of **4.53** (63 mg), 2 eq. HOBT and 1.75 eq. DIC were measured into a round bottom flask and dissolved in a minimum amount of DMF. The reaction mixture was allowed to stir for 3 hours at room temperature. After 3 hours the reaction mixture was checked by LCMS to identify completion of the reaction. LCMS analysis indicated the completion of the reaction and the reaction mixture was poured onto an Isolute SCX (500 mg) column for purification. The cartridge was washed using DCM (3x), DMF (3x) twice and finally MeOH (2x). The product **4.81** was released from the cartridge using 10.0 ml 2M NH₃ in MeOH and concentrated *in vacuo*. Further purification was achieved using a silica column and DCM:MeOH:2MNH₃ (18:1:1) as the solvent system. 53 mg colourless oil was obtained as the final compound.

2-(2,3-Dihydrobenzofuran-5-yl)-N-(4-(5-((2-((3-(dimethylamino)propyl)carbamoyl)benzofuran-5-yl)carbamoyl)furan-2-yl)phenyl)thiazole-4-carboxamide (4.81):



Colourless oil. IR (FTIR, $\nu_{\text{max}}/\text{cm}^{-1}$) 730.61, 808.16, 1032.65, 1106.12, 1204.08, 1234.28, 1314.28, 1359.18, 1465.30, 1528.09, 1575.51, 1591.83, 1640.81, 1738.77, 2360.05, 3081.96, 3292.02; ¹H NMR (400 MHz, DMSO-d₆, TMS); δ 1.68 (t, $J=7.07$ Hz, 2H), 2.15 (s, 6H), 2.28 (t, $J=6.95$ Hz, 2H), 3.33 – 3.35 (m, 4H), 4.65 (t, $J=8.84$ Hz, 2H), 6.93 (d, $J=8.59$ Hz, 1H), 7.13 (d, $J=3.54$ Hz, 1H), 7.42 (d, $J=3.54$ Hz, 1H), 7.55 (d, $J=0.76$ Hz, 1H), 7.67 (d, $J=9.09$ Hz, 1H), 7.79 (dd, $J=2.1, 8.97$ Hz, 1H), 7.93 (dd, $J=2.0, 8.34$ Hz, 1H), 8.00 – 8.01 (m, 1H), 8.02 (s, 1H), 8.04 – 8.06 (m, 1H), 8.07 – 8.10 (m, 1H), 8.20 (d, $J=2.27$ Hz, 1H), 8.39 (s, 1H),

8.78 (t, $J=5.68$ Hz, 1H), 10.27 (s, 1H), 10.34 (s, 1H); ^{13}C NMR (100 MHz, DMSO- d_6); δ 26.92, 28.61, 37.36, 45.11, 47.4, 56.89, 71.75, 107.11, 109.29, 109.37, 114.18, 117.06, 120.51, 120.90, 123.73, 125.04, 125.18, 126.7, 127.25, 127.41, 128.72, 134.29, 137.5, 138.87, 146.32, 146.7, 149.88, 150.01, 155.19, 156.11, 156.8, 157.90, 159.14, 160.9, 162.07, 167.77, 169.39; m/z (+EI) calc. For $\text{C}_{37}\text{H}_{33}\text{N}_5\text{O}_6\text{S}$ (M^+) 675.75, found 676.21 ($\text{M}+\text{H}$) $^+$; Yield: 72%.

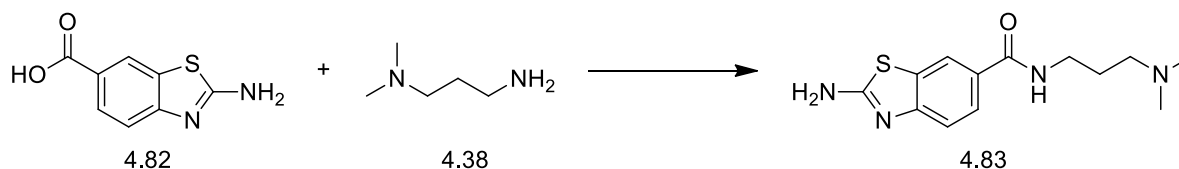
4.1.6 Type-2 Library synthesis

4.1.6.1 Sub type 2 Library synthesis

General procedure for the synthesis of 2-amino-*N*-(3-(dimethylamino)propyl)benzo[*d*]thiazole-6-carboxamide (4.83). (Amide coupling).

2.0 eq of HOBT (108 mg) and 1.75 eq. of DIC (108 μl) were added to a solution of **4.82** in DMF. After 30 minutes 1.0 eq. (50 μl) of **4.38** was added and the reaction mixture was allowed to stand for 3 hours. After completion the reaction mixture was passed through a SCX-2 cartridge (2.0 gm), which was washed with DCM (3x), DMF (3x) twice and finally MeOH (2x). The product **4.83** was released from the cartridge using 5.0 ml 2M NH_3 in MeOH and concentrated *in vacuo* to obtain a colourless oily mass (126.0 mg).

2-Amino-*N*-(3-(dimethylamino)propyl)benzo[*d*]thiazole-6-carboxamide (4.83)



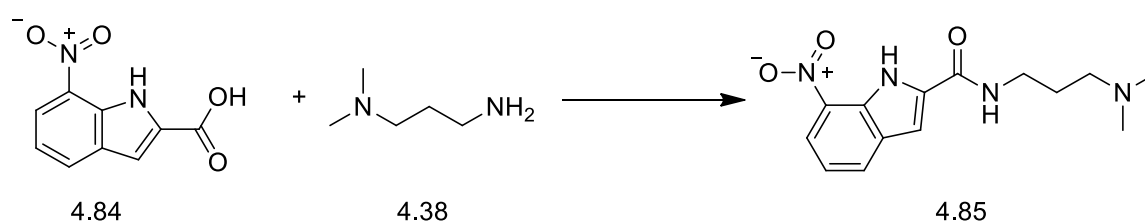
Colourless oil. IR (FTIR, $\nu_{\text{max}}/\text{cm}^{-1}$) 659.93, 692.43, 732.58, 828.26, 884.35, 915.91, 1024.61, 1098.55, 1125.22, 1284.94, 1308.01, 1459.16, 1524.72, 1628.24, 2775.91, 2932.94, 2976.39, 3073.91, 3276.48; ^1H NMR (400 MHz, DMSO- d_6 , TMS); δ 1.64 (quin, $J=7.14$ Hz, 2H), 2.12 (s, 6H), 2.22 - 2.28 (m, 2H), 3.24 - 3.28 (m, 2H), 5.74 (s, 2H), 7.33 (d, $J=8.34$ Hz, 1H), 7.71 (dd, $J=8.34$, 1.77 Hz, 1H), 8.14 (d, $J=1.77$ Hz, 1H); ^{13}C NMR (100 MHz, DMSO- d_6); δ 26.95, 37.54, 44.79, 44.94, 56.73, 121.03, 121.79, 124.67, 127.01, 130.55, 154.83, 165.58, 168.12; m/z (+EI) calc. For $\text{C}_{13}\text{H}_{18}\text{N}_4\text{OS}$ (M^+) 278.37, found 278.62 ($\text{M}+\text{H}$) $^+$; Yield: 97%.

The following compounds (**4.85** to **4.88**) were synthesised by the amide coupling reaction using *N,N*-dimethylpropane-1,3-diamine (1 eq.) (**4.38**) as the amine from **4.84** and **4.86**.

Procedure for the synthesis of *N*-(3-(dimethylamino)propyl)-7-nitro-1*H*-indole-2-carboxamide (4.85)

2.0 eq of HOBT (131 mg) and 1.75 eq. of DIC (120 μ l) were added to a solution of **4.84** (100 mg) in DMF. After 30 minutes 1.0 eq. (50 μ l) of **4.38** was added and the reaction mixture was allowed to stand for 3 hours. After completion, the reaction mixture was passed through a SCX-2 cartridge (2.0 gm), which was washed with DCM (3x), DMF (3x) twice and finally MeOH (2x). The product **4.85** was released from the cartridge using 5.0 ml 2M NH₃ in MeOH and concentrated *in vacuo* to obtain a dark brown oil (95 mg).

***N*-(3-(dimethylamino)propyl)-7-nitro-1*H*-indole-2-carboxamide (4.85):**

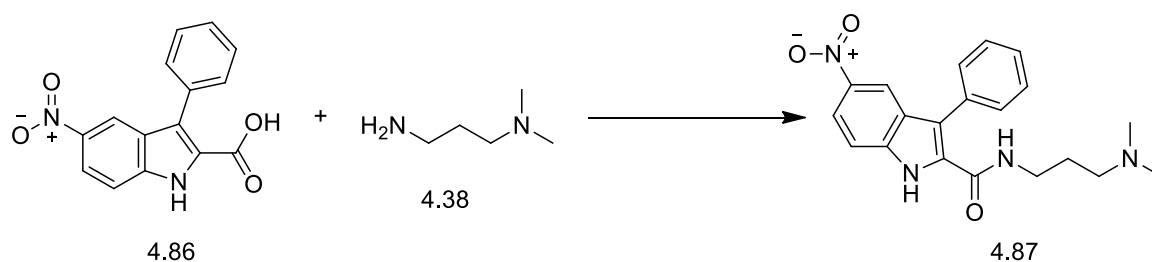


Dark brown oil. IR (FTIR, $\nu_{\text{max}}/\text{cm}^{-1}$) 632.65, 732.11, 831.16, 1037.47, 1098.41, 1156.32, 1222.05, 1291.79, 1403.50, 1483.21, 1560.37, 1636.15, 2818.52, 2976.72, 3281.36; ¹H NMR (400 MHz, DMSO-*d*₆, TMS); δ 2.08 - 2.11 (m, 2H), 2.14 (s, 6H), 2.27 (t, *J*=7.07 Hz, 2H), 3.30 - 3.37 (m, 2H), 7.32 (t, *J*=7.83 Hz, 1H), 7.36 (s, 1H), 8.19 (dd, *J*=7.83, 1.01 Hz, 1H), 8.22 (dd, *J*=8.08, 1.01 Hz, 1H); ¹³C NMR (100 MHz, DMSO-*d*₆); δ 27.01, 40.14, 44.97, 45.13, 56.71, 105.93, 111.65, 120.84, 128.61, 130.47, 130.96, 132.99, 134.81, 159.32; *m/z* (+EI) calc. For C₁₄H₁₈N₄O₃ (M⁺) 290.32, found 292.01 (M+H)⁺; Yield: 95%.

Procedure for the synthesis of *N*-(3-(dimethylamino)propyl)-5-nitro-3-phenyl-1*H*-indole-2-carboxamide (4.87)

2.0 eq of HOBT (96 mg) and 1.75 eq. of DIC (87 μ l) were added to a solution of **4.86** (100 mg) in DMF. After 30 minutes 1.0 eq. (36 μ l) of **4.38** was added and the reaction mixture was allowed to stand for 3 hours. After completion, the reaction mixture was passed through a SCX-2 cartridge (2.0 gm), which was washed with DCM (3x), DMF (3x) twice and finally MeOH (2x). The product **4.87** was released from the cartridge using 5.0 ml 2M NH₃ in MeOH and concentrated *in vacuo* to obtain a light brown powder (93 mg).

***N*-(3-(dimethylamino)propyl)-5-nitro-3-phenyl-1*H*-indole-2-carboxamide (4.87):**

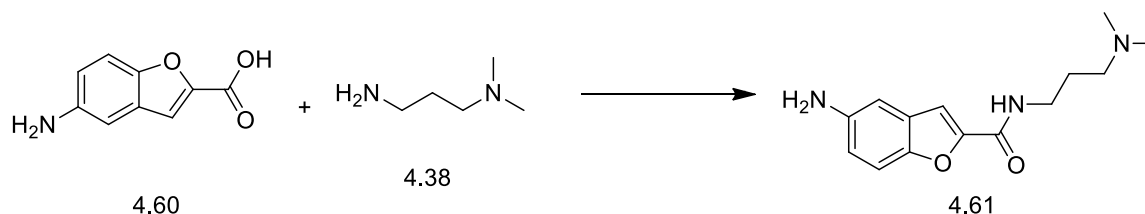


Light brown powder. IR (FTIR, $\nu_{\max}/\text{cm}^{-1}$) 626.07, 663.89, 718.36, 769.98, 839.66, 893.01, 1037.09, 1064.64, 1172.34, 1257.60, 1291.25, 1327.17, 1474.81, 1520.20, 1551.31, 1634.11, 2771.79, 2822.83, 3203.26; ^1H NMR (400 MHz, DMSO- d_6 , TMS); δ 1.49-1.56 (m, 2H), 2.03 (s, 6H), 2.10 (s, 2H), 3.20-3.26 (m, 2H), 7.43-7.47 (m, 1H), 7.54 (br s, 2H), 7.55 (br s, 2H), 7.63 (d, $J=9.09$ Hz, 1H), 8.11 (dd, $J=9.09$, 2.27 Hz, 1H), 8.36 (d, $J=2.02$ Hz, 1H); ^{13}C NMR (100 MHz, DMSO- d_6); δ 26.69, 40.35, 45.24, 46.3, 56.98, 113.21, 117.13, 118.66, 126.32, 127.65, 127.9, 128.98, 129.3, 129.5, 130.0, 132.47, 132.62, 138.71, 141.57, 161.06; m/z (+EI) calc. For $\text{C}_{20}\text{H}_{22}\text{N}_4\text{O}_3$ (M^+) 366.41, found 368.07 ($\text{M}+\text{H}^+$); Yield: 93%.

Procedure for the synthesis of 5-amino-*N*-(3-(dimethylamino)propyl)benzofuran-2-carboxamide (4.61)

2.0 eq of HOBT and 1.75 eq. of DIC were added to a solution of **4.60** (100 mg) in DMF. After 30 minutes 1.0 eq. (58 μl) of **4.38** was added and the reaction mixture was allowed to stand for 3 hours. After completion, the reaction mixture was passed through a SCX-2 cartridge (2.0 gm), which was washed with DCM (3x) and DMF (3x) twice and finally MeOH (2x). The product **4.61** was released from the cartridge using 5.0 ml 2M NH_3 in MeOH and concentrated *in vacuo* to obtain brown oil (100 mg).

5-amino-*N*-(3-(dimethylamino)propyl)benzofuran-2-carboxamide (4.61):



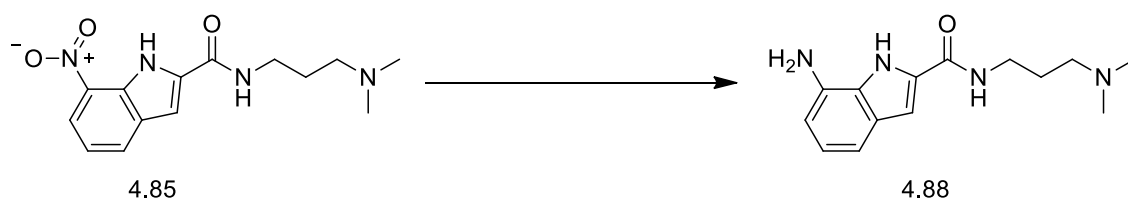
Brown oil. IR (FTIR, $\nu_{\max}/\text{cm}^{-1}$) 616.66, 657.70, 809.89, 842.95, 943.42, 1037.48, 1097.11, 1159.69, 1209.08, 1244.28, 1302.57, 1383.71, 1455.82, 1580.91, 1649.71, 2774.39, 2817.07, 2859.75, 2938.85, 3231.44, 3341.46; ^1H NMR (400 MHz, DMSO- d_6) δ 1.65 (t, $J=7.07$ Hz, 2H), 2.13 (s, 6H), 2.21 (t, $J=7.07$ Hz, 2H), 3.25 - 3.30 (m, 2H), 6.74 (dd, $J=8.84$, 2.27 Hz, 276

1H), 6.78 (d, $J=1.77$ Hz, 1H), 7.24 (d, $J=1.01$ Hz, 1H), 7.29 (d, $J=8.59$ Hz, 1H), 8.60 (t, $J=5.56$ Hz, 1H); ^{13}C NMR (100 MHz, DMSO- d_6) δ 26.98, 37.23, 45.12, 45.12, 56.89, 104.22, 108.60, 111.50, 115.48, 127.84, 145.14, 147.53, 149.12, 158.19; m/z (+EI) calc. For $\text{C}_{14}\text{H}_{19}\text{N}_3\text{O}_2$ (M+) 261.32, found 262.0 (M+H) $^+$; Yield: 68%.

General procedure for the synthesis of 7-amino-*N*-(3-(dimethylamino)propyl)-1*H*-indole-2-carboxamide (4.88) by hydrogenation.

N-(3-(dimethylamino)propyl)-7-nitro-1*H*-indole-2-carboxamide (1.0 eq., 200 mg) (**4.85**) was dissolved in a minimum amount of ethanol (30 ml) and a catalytic amount of 10% Pd/C (20 mg) was added as a slurry in ethyl acetate. The reaction mixture was shaken overnight at 45 psi in a Parr hydrogenator. After completion of the reduction, the suspension was filtered through a layer of celite, with caution, using a Buchner flask and the filtrate concentrated to obtain 150 mg colourless product (**4.88**).

7-Amino-*N*-(3-(dimethylamino)propyl)-1*H*-indole-2-carboxamide (4.88):



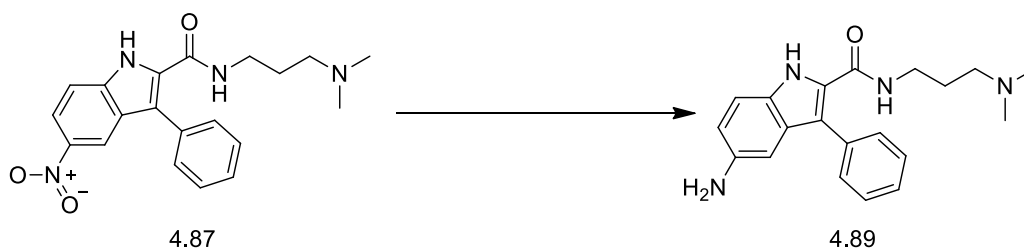
Colourless oil. IR (FTIR, $\nu_{\text{max}}/\text{cm}^{-1}$) 732.66, 781.76, 822.48, 882.42, 1048.76, 1094.60, 1229.15, 1256.07, 1290.85, 1380.02, 1421.18, 1556.24, 1622.31, 1737.52, 2856.85, 2969.34, 3271.90; ^1H NMR (400 MHz, DMSO- d_6) δ 1.63 - 1.73 (m, 2H), 2.12 - 2.20 (m, 6H), 2.30 (t, $J=7.20$ Hz, 2H), 3.27 - 3.35 (m, 2H), 6.35 (dd, $J=7.20$, 1.14 Hz, 1H), 6.73 - 6.78 (m, 1H), 6.78 - 6.83 (m, 1H), 6.96 (d, $J=2.02$ Hz, 1H), 8.43 (t, $J=5.68$ Hz, 1H), 11.19 (br. s., 1H); ^{13}C NMR (100 MHz, DMSO- d_6) δ 27.15, 37.20, 44.88, 45.07, 56.82, 102.40, 105.54, 109.00, 120.88, 126.03, 127.88, 130.75, 134.40, 161.19; m/z (+EI) calc. For $\text{C}_{14}\text{H}_{20}\text{N}_4\text{O}$ (M+) 260.16, found 262.00 (M+H) $^+$; Yield: 75%.

The same procedure was followed for the synthesis of **4.89**

Procedure for the synthesis of 5-amino-N-(3-(dimethylamino)propyl)-3-phenyl-1H-indole-2-carboxamide (4.89)

1.0 eq. (156 mg) **4.87** was dissolved in a minimum amount of ethanol (30 ml) and a catalytic amount of 10% Pd/C (16 mg) was added as a slurry in ethyl acetate. The reaction mixture was shaken for 2 hours at 45 psi in a Parr hydrogenator. After completion of the reduction the suspension was filtered through a layer of celite, with caution, using a Buchner flask and the filtrate was concentrated to obtain 140 mg colourless oil (**4.89**).

5-Amino-N-(3-(dimethylamino)propyl)-3-phenyl-1H-indole-2-carboxamide (4.89)



Colourless oil. IR (FTIR, $\nu_{\text{max}}/\text{cm}^{-1}$) 616.02, 633.72, 665.50, 757.87, 773.73, 801.97, 840.74, 1041.73, 1097.56, 1128.33, 1228.46, 1248.38, 1321.62, 1383.03, 1454.88, 1498.74, 1542.27, 1600.24, 1630.62, 2950.02, 3253.14, 3406.64; ^1H NMR (400 MHz, $\text{DMSO}-d_6$) δ 1.48 (t, $J=6.95$ Hz, 2H), 2.03 (s, 6H), 2.11 - 2.13 (m, 2H), 3.15 - 3.20 (m, 2H), 6.61 (d, $J=1.52$ Hz, 1H), 6.62 - 6.66 (m, 1H), 7.11 (t, $J=5.68$ Hz, 1H), 7.14 - 7.18 (m, 1H), 7.32 - 7.37 (m, 1H), 7.44 (d, $J=2.27$ Hz, 2H), 7.46 - 7.47 (m, 1H), 11.22 (s, 1H); ^{13}C NMR (100 MHz, $\text{DMSO}-d_6$) δ 26.56, 37.31, 45.00, 45.00, 56.76, 101.34, 112.36, 115.02, 115.29, 126.41, 127.85, 127.94, 128.38, 129.05, 129.90, 130.13, 130.63, 135.85, 142.37, 161.62; m/z (+EI) calc. For $\text{C}_{20}\text{H}_{24}\text{N}_4\text{O}$ (M^+) 336.43, found 336.86 ($\text{M}+\text{H}$) $^+$; Yield: 98%.

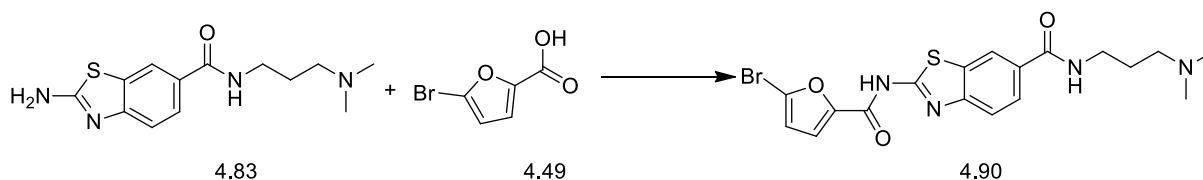
The following compounds (**4.90** to **4.95**) were synthesized following the same procedure for amide coupling.

Procedure for the synthesis of 2-(5-bromofuran-2-carboxamido)-N-(3-(dimethylamino)propyl)benzo[d]thiazole-6-carboxamide (4.90)

2.0 eq of HOBT and 1.75 eq. of DIC were added to a solution of **4.83** (98 mg) in DMF. After 30 minutes, 1.2 eq. (81 mg) of **4.49** was added and the reaction mixture was allowed to stand for 3 hours. After completion, the reaction mixture was passed through a SCX-2 cartridge (2.0 gm), which was washed with DCM (3x), DMF (3x) twice and finally MeOH (2x). The

product **4.90** was released from the cartridge using 5.0 ml 2M NH₃ in MeOH and concentrated *in vacuo* to obtain a dark brown, oily mass (116 mg).

2-(5-Bromofuran-2-carboxamido)-N-(3-(dimethylamino)propyl)benzo[d]thiazole-6-carboxamide (4.90):

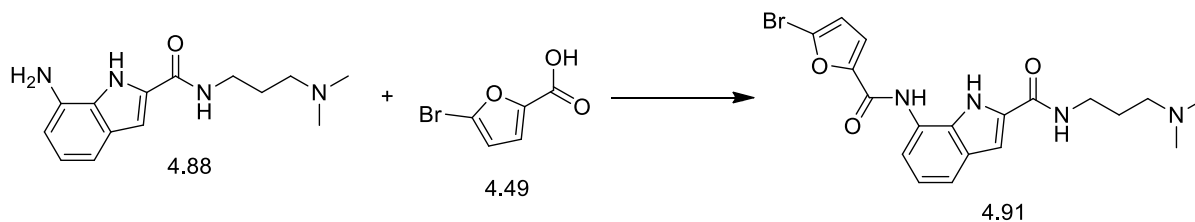


Dark brown, oily mass. IR (FTIR, $\nu_{\text{max}}/\text{cm}^{-1}$) 659.34, 765.92, 839.20, 922.33, 960.31, 1060.22, 1092.58, 1216.41, 1279.33, 1381.64, 1406.04, 1428.31, 1524.33, 1596.51, 1659.91, 1736.89, 2775.19, 2863.04, 2938.27, 3312.15; ¹H NMR (400 MHz, DMSO-*d*₆, TMS); δ 1.68 - 1.76 (m, 2H), 2.24 - 2.27 (m, 3H), 2.30 (s, 3H), 2.41 (t, *J*=7.20 Hz, 2H), 3.28 - 3.33 (m, 2H), 6.79 (d, *J*=3.54 Hz, 1H), 7.31 - 7.38 (m, 1H), 7.62 (d, *J*=8.34 Hz, 1H), 7.83 (dd, *J*=8.59, 1.77 Hz, 1H), 8.32 (d, *J*=1.52 Hz, 1H); ¹³C NMR (100 MHz, DMSO-*d*₆); δ 26.3, 36.8, 45.03, 45.85, 57.73, 110.8, 113.9, 120.0, 120.7, 121.9, 123.1, 128.9, 130.6, 145.7, 155.13, 163.82, 166.9, 175.32; *m/z* (+EI) calc. For C₁₈H₁₉BrN₄O₃S (M⁺) 451.34, found 452.58 (M+H)⁺; Yield: 73%.

Procedure for the synthesis of 7-(5-bromofuran-2-carboxamido)-N-(3-(dimethylamino)propyl)-1*H*-indole-2-carboxamide (4.91)

2.0 eq of HOBT and 1.75 eq. of DIC were added to a solution of **4.88** (135 mg) in DMF. After 30 minutes, 2.0 eq. (198 mg) of **4.49** was added and the reaction mixture allowed to stand for 3 hours. After completion, the reaction mixture was passed through a SCX-2 cartridge (2.0 gm), which was washed with DCM (3x), DMF (3x) twice and finally MeOH (2x). The product **4.91** was released from the cartridge using 5.0 ml 2M NH₃ in MeOH and concentrated *in vacuo* to obtain a dark brown oil (130 mg).

7-(5-Bromofuran-2-carboxamido)-N-(3-(dimethylamino)propyl)-1H-indole-2-carboxamide (4.91):

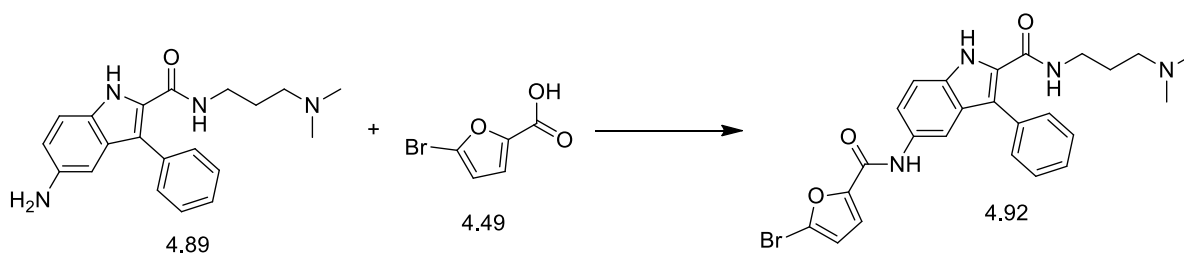


Dark brown oil. IR (FTIR, $\nu_{\text{max}}/\text{cm}^{-1}$) 661.40, 736.65, 783.32, 924.20, 953.68, 1010.79, 1097.99, 1174.27, 1256.67, 1285.10, 1384.52, 1432.87, 1464.95, 1537.21, 1631.97, 2774.39, 2817.07, 2859.75, 2935.48, 3283.45; ^1H NMR (400 MHz, $\text{DMSO}-d_6$, TMS); δ 1.68 (t, $J=7.07$ Hz, 2H), 2.15 (s, 6H), 2.29 (t, $J=7.07$ Hz, 2H), 3.34 (d, $J=6.82$ Hz, 2H), 6.87 (d, $J=3.79$ Hz, 1H), 7.05 (t, $J=7.83$ Hz, 1H), 7.14 (d, $J=2.02$ Hz, 1H), 7.42 (d, $J=3.54$ Hz, 1H), 7.46 (d, $J=7.83$ Hz, 1H), 7.70 (dd, $J=7.71, 0.88$ Hz, 1H), 7.95 (s, 1H), 10.11 (s, 1H), 11.57 (s, 1H); ^{13}C NMR (100 MHz, $\text{DMSO}-d_6$); δ 27.33, 37.47, 45.23, 45.29, 57.00, 114.05, 114.36, 115.62, 116.63, 117.45, 120.02, 123.18, 125.41, 128.99, 132.15, 149.65, 150.10, 161.02, 162.46; m/z (+EI) calc. For $\text{C}_{19}\text{H}_{21}\text{BrN}_4\text{O}_3$ (M^+) 433.30, found 434.59 ($\text{M}+\text{H}$) $^+$; Yield: 58%.

Procedure for the synthesis of 5-(5-bromofuran-2-carboxamido)-N-(3-(dimethylamino)propyl)-3-phenyl-1H-indole-2-carboxamide (4.92)

2.0 eq of HOBT and 1.75 eq. of DIC were added to a solution of **4.89** (140 mg) in DMF. After 30 minutes, 2.0 eq. (159 mg) of **4.49** was added and the reaction mixture was allowed to stand for 3 hours. After completion, the reaction mixture was passed through a SCX-2 cartridge (5.0 gm), which was washed with DCM (3x), DMF (3x) twice and finally MeOH (2x). The product **4.92** was released from the cartridge using 5.0 ml 2M NH_3 in MeOH and concentrated *in vacuo* to obtain a dark brown oil (129 mg).

5-(5-Bromofuran-2-carboxamido)-N-(3-(dimethylamino)propyl)-3-phenyl-1H-indole-2-carboxamide (4.92):

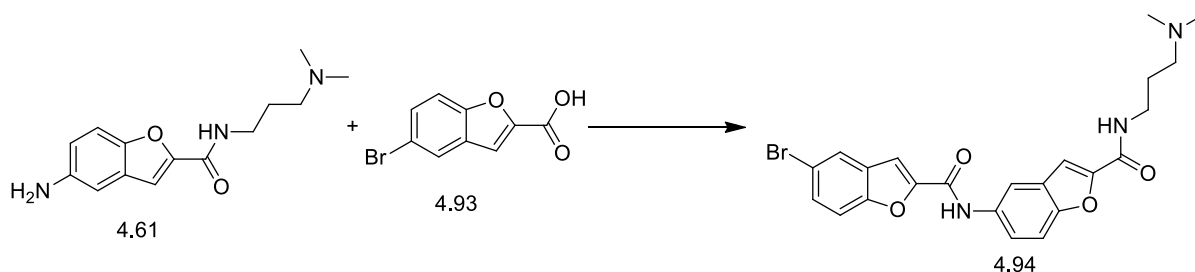


Brown oily mass. IR (FTIR, $\nu_{\text{max}}/\text{cm}^{-1}$) 619.84, 636.40, 663.05, 705.39, 727.16, 744.00, 762.96, 809.18, 883.86, 921.78, 945.20, 1018.25, 1037.90, 1100.26, 1199.68, 1246.29, 1272.54, 1304.51, 1338.43, 1386.13, 1424.24, 1474.28, 1540.25, 1590.25, 1638.61, 1737.52, 2779.91, 2947.48, 3244.75, 3419.67; ^1H NMR (400 MHz, $\text{DMSO}-d_6$, TMS); δ 1.50 (t, $J=6.95$ Hz, 2H), 2.04 (s, 6H), 2.08 - 2.13 (m, 2H), 3.19 - 3.23 (m, 2H), 6.80 (d, $J=3.79$ Hz, 1H), 7.31 (d, $J=3.54$ Hz, 1H), 7.33 (br. s., 1H), 7.43 (d, $J=9.09$ Hz, 1H), 7.49 (s, 2H), 7.50 (d, $J=1.52$ Hz, 1H), 7.60 (dd, $J=8.97, 1.89$ Hz, 1H), 7.89 (d, $J=1.77$ Hz, 1H), 7.95 (s, 1H), 10.09 (s, 1H), 11.68 (s, 1H); ^{13}C NMR (100 MHz, $\text{DMSO}-d_6$); δ 26.50, 35.73, 44.99, 45.03, 56.76, 111.28, 112.04, 114.08, 115.42, 116.41, 116.57, 118.53, 124.80, 126.61, 126.84, 128.56, 129.04, 129.89, 131.30, 132.39, 133.87, 149.61, 154.84, 161.41, 162.26; m/z (+EI) calc. For $\text{C}_{25}\text{H}_{25}\text{BrN}_4\text{O}_3$ (M^+) 509.39, found 510.61 ($\text{M}+\text{H}$) $^+$; Yield: 61%.

Procedure for the synthesis of 5-bromo-*N*-(2-((3-(dimethylamino)propyl)carbamoyl)benzofuran-5-yl)benzofuran-2-carboxamide (4.94)

2.0 eq of HOBT and 1.75 eq. of DIC were added to a solution of **4.61** (71 mg) in DMF. After 30 minutes, 2.0 eq. (131 mg) of **4.93** was added and the reaction mixture was allowed to stand for 3 hours. After completion, the reaction mixture was passed through a SCX-2 cartridge (2.0 gm), which was washed with DCM (3x), DMF (3x) twice and finally MeOH (2x). The product **4.94** was released from the cartridge using 5.0 ml 2M NH_3 in MeOH. Further purification of the product was achieved using a silica column and DCM:MeOH:2M NH_3 as solvent system; the polarity of the system was changed from 18:1:1 to 17:2:1 gradually until the product was obtained in pure form. It was then concentrated *in vacuo* to obtain a colourless powder (100 mg).

5-Bromo-*N*-(2-((3-(dimethylamino)propyl)carbamoyl)benzofuran-5-yl)benzofuran-2-carboxamide (4.94):



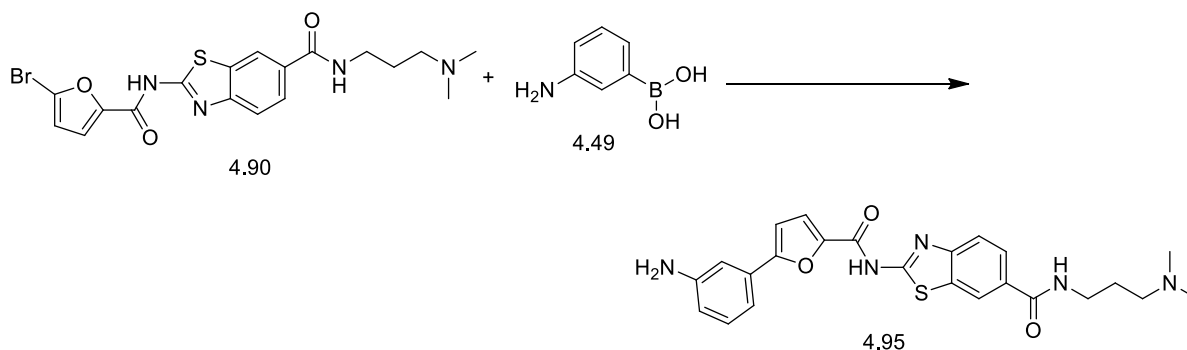
Colourless powder. IR (FTIR, $\nu_{\text{max}}/\text{cm}^{-1}$) 621.55, 669.97, 751.69, 803.47, 889.49, 941.00, 971.80, 1039.37, 1098.23, 1154.24, 1175.62, 1198.44, 1231.11, 1259.30, 1295.39, 1371.05, 1438.21, 1458.15, 1475.57, 1521.26, 1540.45, 1588.93, 1636.36, 1654.06, 1736.55, 2754.04,

2812.03, 2938.35, 3344.11; ^1H NMR (400 MHz, $\text{DMSO-}d_6$) δ 1.67 (t, $J=7.07$ Hz, 2H), 2.14 (s, 6H), 2.27 (t, $J=6.95$ Hz, 2H), 3.29 (br. s., 2H), 7.54 (d, $J=0.76$ Hz, 1H), 7.64 - 7.65 (m, 1H), 7.66 (d, $J=5.56$ Hz, 1H), 7.70 - 7.74 (m, 1H), 7.76 - 7.78 (m, 2H), 8.08 (d, $J=2.02$ Hz, 1H), 8.27 (d, $J=2.02$ Hz, 1H), 8.77 (t, $J=5.68$ Hz, 1H), 10.69 (s, 1H); ^{13}C NMR (100 MHz, $\text{DMSO-}d_6$) δ 26.92, 37.35, 45.11, 45.11, 56.87, 109.33, 109.88, 111.75, 113.80, 114.00, 116.03, 120.62, 125.28, 127.26, 129.32, 129.67, 134.09, 149.93, 150.06, 151.02, 153.23, 156.24, 157.85; m/z (+EI) calc. For $\text{C}_{23}\text{H}_{22}\text{BrN}_3\text{O}_4$ (M^+) 484.34, found 486.66 ($\text{M}+\text{H}$) $^+$; Yield: 76%.

General procedure for the synthesis of 2-(5-(3-aminophenyl)furan-2-carboxamido)-N-(3-(dimethylamino)propyl)benzo[d]thiazole-6-carboxamide (4.95) using 2-(5-bromofuran-2-carboxamido)-N-(3-(dimethylamino)propyl)benzo[d]thiazole-6-carboxamide (4.90) and (3-aminophenyl)boronic acid (4.49). (Suzuki coupling).

A catalytic amount of tetrakis(triphenylphosphine)palladium, $\text{Pd}(\text{PPh}_3)_4$ (0.1 eq., 28 mg) was added to a solution of **4.90** (1.0 eq., 108 mg) and **4.49** (1.2 eq., 39 mg) in a 9:3:1 combination of EtOH, toluene and water in the presence of K_2CO_3 (3.0 eq., 99 mg) in a 10 ml microwave vial containing a magnetic stirrer. The reaction vessel was flushed with nitrogen during each addition. The reaction mixture was sealed in an inert nitrogen environment and heated with microwave radiation in an EMRYSTM Optimizer Microwave Station (Personal Chemistry) at 100 °C for 82 minutes (20 minutes + 10 minutes + 20 minutes + 20 minutes + 12 minutes). After LCMS analysis revealed complete reaction, the cooled reaction mixture was passed through an IsoluteTM SCX-2 cartridge (2.0 gm) and washed with DCM (3x), DMF (3x) twice and finally MeOH (2x). The product was released from the cartridge using 5.0 ml 2M NH_3 in MeOH and concentrated *in vacuo* to obtain a crude product. This was further purified by flash chromatography using DCM/2M NH_3 in methanol/MeOH at a ratio 9:0.5:0.5 to obtain a light yellow powder of product **4.95** (87 mg).

2-(5-(3-Aminophenyl)furan-2-carboxamido)-N-(3-(dimethylamino)propyl)benzo[d]thiazole-6-carboxamide (4.95):



Light yellow powder. IR (FTIR, $\nu_{\text{max}}/\text{cm}^{-1}$) 616.20, 660.42, 693.22, 723.03, 768.10, 839.48, 1025.14, 1096.30, 1119.84, 1154.60, 1233.46, 1282.66, 1383.33, 1407.90, 1435.14, 1523.57, 1578.38, 1658.54, 1737.42, 2945.12, 3225.60, 3333.93; ^1H NMR (400 MHz, METHANOL- d_4 , TMS); δ 1.83 - 1.93 (m, 2H), 2.39 (s, 6H), 2.54 - 2.61 (m, 2H), 3.46 (t, $J=6.95$ Hz, 2H), 6.76 (d, $J=7.83$ Hz, 1H), 6.93 (d, $J=3.79$ Hz, 1H), 7.19 (t, $J=7.71$ Hz, 1H), 7.25 (d, $J=7.83$ Hz, 1H), 7.28 (d, $J=1.77$ Hz, 1H), 7.52 (d, $J=3.54$ Hz, 1H), 7.80 (d, $J=8.34$ Hz, 1H), 7.89 (dd, $J=8.34$, 1.77 Hz, 1H), 8.36 (d, $J=1.77$ Hz, 1H); ^{13}C NMR (100 MHz, METHANOL- d_4); δ 27.12, 36.39, 45.87, 46.18, 57.62, 107.35, 108.13, 113.93, 115.43, 118.27, 119.27, 120.10, 122.19, 129.86, 130.15, 130.63, 131.98, 145.6, 147.9, 155.16, 156.1, 160.3, 165.8, 175.3; m/z (+EI) calc. For $\text{C}_{24}\text{H}_{25}\text{N}_5\text{O}_3\text{S}$ (M^+) 463.55, found 463.80 ($\text{M}+\text{H}^+$); Yield: 81%.

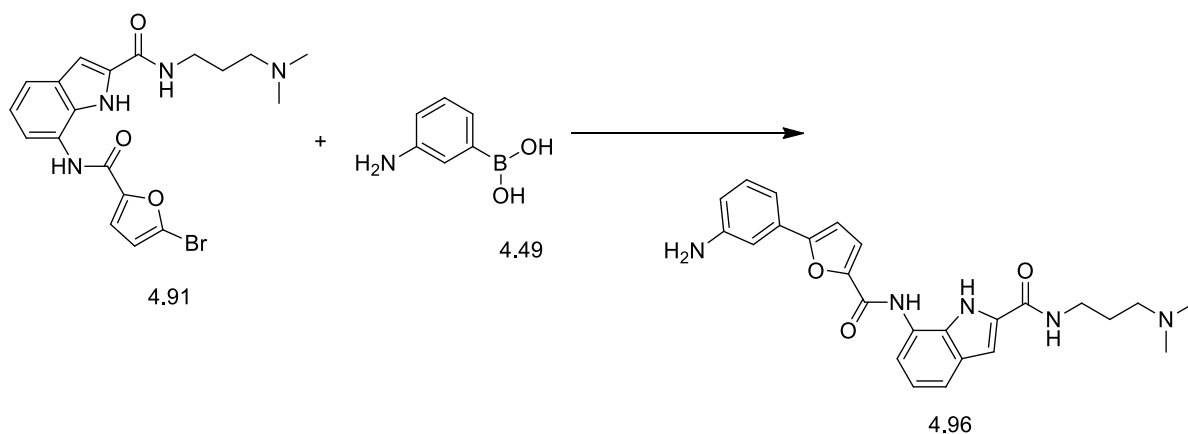
A similar procedure was followed for the following molecules, but the microwave irradiation time was 20 minutes.

Procedure for the synthesis of 7-(5-(3-aminophenyl)furan-2-carboxamido)-N-(3-(dimethylamino)propyl)-1H-indole-2-carboxamide (4.96)

A catalytic amount of tetrakis(triphenylphosphine)palladium, $\text{Pd}(\text{PPh}_3)_4$ (0.1 eq.) was added to a solution of **4.91** (1.0 eq., 130 mg) and **4.49** (2 eq., 82 mg) in a 9:3:1 combination of EtOH, toluene and water in the presence of K_2CO_3 (3.0 eq.) in a 10 ml microwave vial containing a magnetic stirrer. The reaction vessel was flushed with nitrogen during each addition. The reaction mixture was sealed in an inert nitrogen environment and heated with microwave radiation in an EMRYSTM Optimizer Microwave Station (Personal Chemistry) at 100 °C for 20 minutes. After LCMS analysis revealed complete reaction, the cooled reaction mixture was passed through an IsoluteTM SCX-2 cartridge (2.0 gm) and washed with DCM (3x), DMF (3x) twice and finally MeOH (2x). The product was released from the cartridge

using 5.0 ml 2M NH₃ in MeOH and concentrated *in vacuo* to obtain a crude product. The product was further purified by flash chromatography using DCM/2M NH₃ in methanol/MeOH at a ratio 9:0.5:0.5 to obtain product **4.96** (120 mg).

7-(5-(3-Aminophenyl)furan-2-carboxamido)-N-(3-(dimethylamino)propyl)-1H-indole-2-carboxamide (4.96):



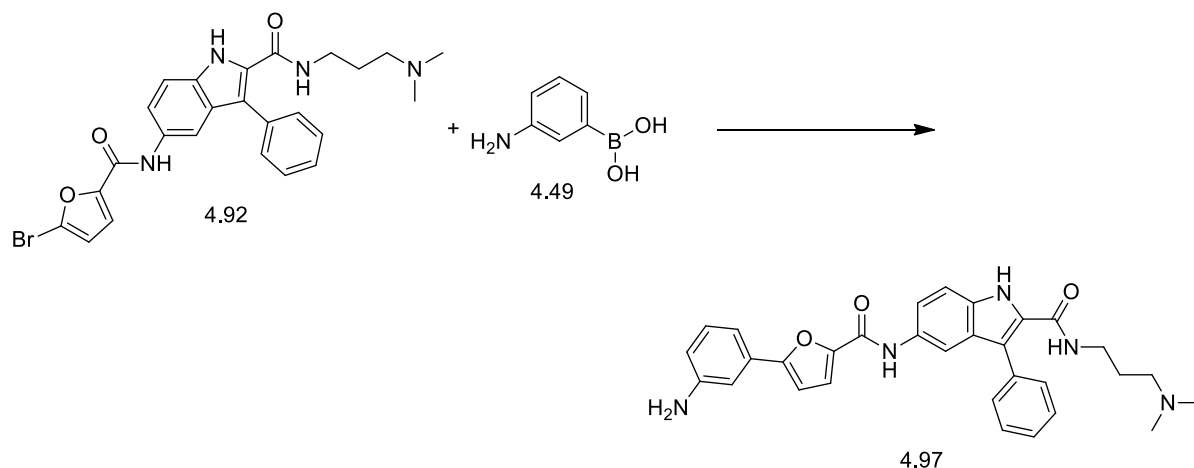
Dark brown oil. IR (FTIR, $\nu_{\text{max}}/\text{cm}^{-1}$) 636.44, 692.88, 723.99, 782.50, 1025.16, 1154.19, 1233.04, 1290.02, 1412.22, 1438.43, 1540.62, 1577.71, 1626.28, 2823.17, 2937.80, 3231.70, 3342.25; ¹H NMR (400 MHz, DMSO-*d*₆, TMS); δ 1.69 (quin, *J*=6.88 Hz, 2H), 2.15 (s, 6H), 2.29 (t, *J*=7.07 Hz, 2H), 3.33 (br. s., 2H), 6.57 - 6.60 (m, 1H), 6.95 - 6.96 (m, 1H), 6.97 - 6.99 (m, 1H), 7.00 (d, *J*=3.54 Hz, 1H), 7.04 - 7.07 (m, 1H), 7.08 - 7.10 (m, 1H), 7.10 - 7.11 (m, 1H), 7.13 (d, *J*=7.83 Hz, 1H), 7.15 (d, *J*=2.02 Hz, 1H), 7.47 (d, *J*=3.79 Hz, 1H), 7.70 - 7.73 (m, 1H), 7.73 (s, 1H), 10.06 (s, 1H), 11.59 (s, 1H); ¹³C NMR (100 MHz, DMSO-*d*₆); δ 26.96, 37.07, 44.91, 48.35, 56.61, 106.68, 109.14, 112.18, 114.31, 115.47, 116.66, 117.81, 119.73, 121.65, 123.14, 127.50, 128.56, 129.20, 129.62, 146.09, 147.29, 148.88, 155.99, 160.61, 162.06; *m/z* (+EI) calc. For C₂₅H₂₇N₅O₃ (M⁺) 445.51, found 445.61 (M+H)⁺; Yield: 90%.

Procedure for the synthesis of 5-(5-(3-aminophenyl)furan-2-carboxamido)-N-(3-(dimethylamino)propyl)-3-phenyl-1H-indole-2-carboxamide (4.97)

A catalytic amount of tetrakis(triphenylphosphine)palladium, Pd(PPh₃)₄ (0.1 eq.) was added to a solution of **4.92** (1.0 eq., 129 mg) and **4.49** (2 eq., 69 mg) in a 9:3:1 combination of EtOH, toluene and water in the presence of K₂CO₃ (3.0 eq.) in a 10 ml microwave vial containing a magnetic stirrer. The reaction vessel was flushed with nitrogen during each addition. The reaction mixture was sealed in an inert nitrogen environment and heated with microwave radiation in an EMRYSTM Optimizer Microwave Station (Personal Chemistry) at

100 °C for 20 minutes. After LCMS analysis revealed complete reaction, the cooled reaction mixture was passed through an Isolute™ SCX-2 cartridge (2.0 gm) and washed with DCM (3x), DMF (3x) twice and finally MeOH (2x). The product was released from the cartridge using 5.0 ml 2M NH₃ in MeOH and concentrated *in vacuo* to obtain a crude product. The product was further purified by flash chromatography using DCM/2M NH₃ in methanol/MeOH at a ratio 9:0.5:0.5 to obtain product **4.97** (125 mg).

5-(5-(3-Aminophenyl)furan-2-carboxamido)-N-(3-(dimethylamino)propyl)-3-phenyl-1H-indole-2-carboxamide (4.97):

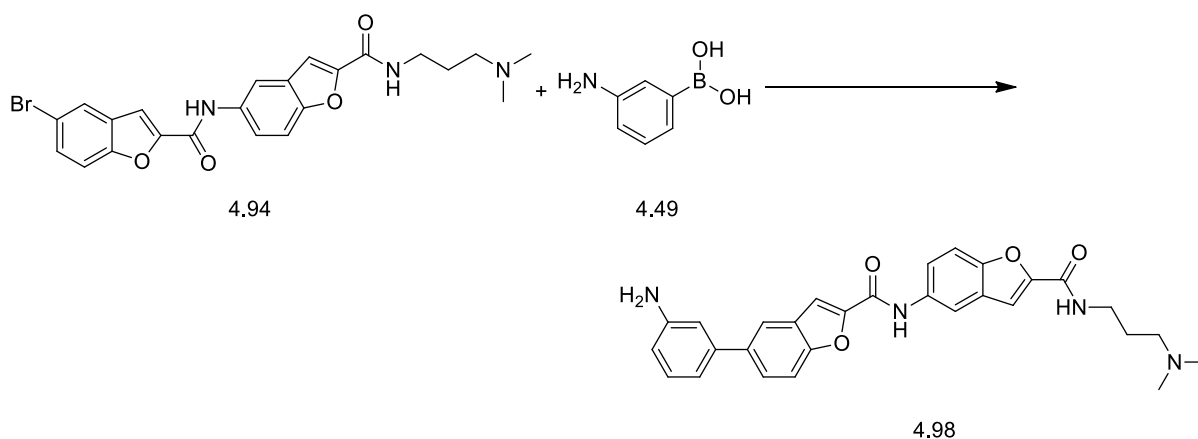


Light brown oil. IR (FTIR, $\nu_{\text{max}}/\text{cm}^{-1}$) 694.14, 723.10, 783.14, 1023.36, 1095.15, 1119.04, 1156.21, 1232.16, 1317.96, 1443.85, 1474.62, 1543.70, 1633.71, 1738.02, 2361.04, 2939.06, 3225.60, 3327.85; ¹H NMR (400 MHz, DMSO-*d*₆, TMS); δ 1.51 (t, *J*=6.82 Hz, 2H), 2.04 (s, 6H), 2.10 - 2.13 (m, 2H), 3.20 - 3.25 (m, 2H), 6.57 - 6.59 (m, 1H), 6.59 - 6.61 (m, 1H), 6.92 (d, *J*=3.54 Hz, 1H), 7.06 - 7.08 (m, 1H), 7.08 - 7.09 (m, 1H), 7.09 - 7.12 (m, 1H), 7.33 (d, *J*=3.54 Hz, 1H), 7.38 - 7.42 (m, 1H), 7.44 (d, *J*=9.09 Hz, 1H), 7.51 (s, 2H), 7.52 (s, 1H), 7.54 - 7.58 (m, 1H), 7.62 - 7.65 (m, 2H), 7.73 (s, 1H), 7.92 (d, *J*=1.52 Hz, 1H), 10.03 (s, 1H), 11.68 (s, 1H); ¹³C NMR (100 MHz, DMSO-*d*₆); δ 26.50, 37.44, 45.01, 48.55, 56.76, 106.83, 109.38, 112.01, 114.46, 115.68, 116.07, 118.74, 119.93, 126.66, 126.85, 127.70, 128.58, 128.77, 129.92, 131.39, 131.49, 131.56, 131.97, 132.34, 133.92, 146.54, 147.49, 148.99, 149.77, 155.97, 161.43; *m/z* (+EI) calc. For C₃₁H₃₁N₅O₃ (M⁺) 521.61, found 521.71 (M+H)⁺; Yield: 95%.

Procedure for the synthesis of 5-(3-aminophenyl)-N-(2-((3-(dimethylamino)propyl)carbamoyl)benzofuran-5-yl)benzofuran-2-carboxamide (4.98)

A catalytic amount of tetrakis(triphenylphosphine)palladium, Pd(PPh₃)₄ (0.1 eq.) was added to a solution of **4.94** (1.0 eq., 40 mg) and **4.49** (2 eq., 23 mg) in a 9:3:1 combination of EtOH, toluene and water in the presence of K₂CO₃ (3.0 eq., 99 mg) in a 10 ml microwave vial containing a magnetic stirrer. The reaction vessel was flushed with nitrogen during each addition. The reaction mixture was sealed in an inert nitrogen environment and heated with microwave radiation in an EMRYSTM Optimizer Microwave Station (Personal Chemistry) at 100 °C for 20 minutes. After LCMS analysis revealed complete reaction, the cooled reaction mixture was passed through an IsoluteTM SCX-2 cartridge (500 mg) and washed with DCM (3x), DMF (3x) twice and finally MeOH (2x). The product was released from the cartridge using 5.0 ml 2M NH₃ in MeOH and concentrated *in vacuo* to obtain a crude product. The product was further purified by flash chromatography using DCM/2M NH₃ in methanol/MeOH at a ratio 9:0.5:0.5 to obtain product **4.98** (39 mg).

5-(3-Aminophenyl)-N-(2-((3-(dimethylamino)propyl)carbamoyl)benzofuran-5-yl)benzofuran-2-carboxamide (4.98):



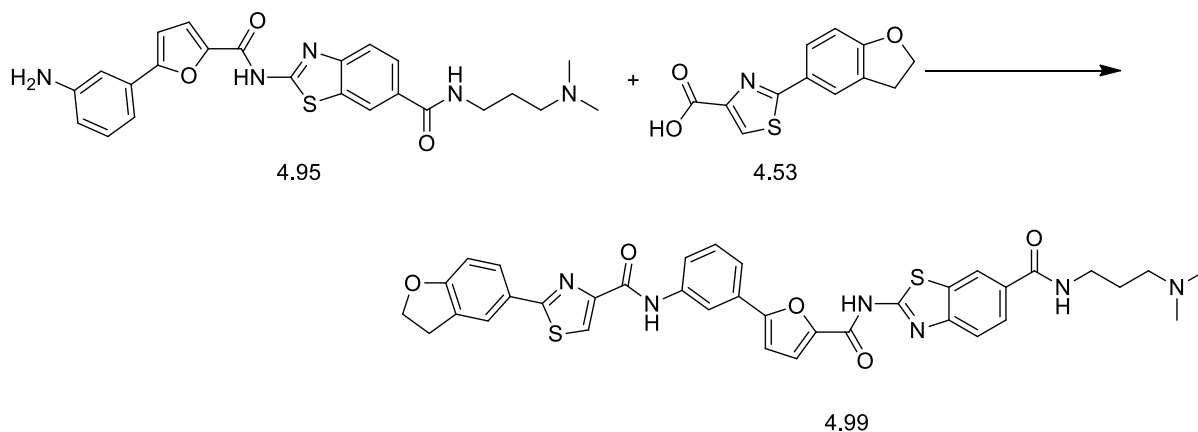
Brown oily mass. IR (FTIR, $\nu_{\text{max}}/\text{cm}^{-1}$) 612.14, 659.04, 697.55, 723.53, 869.62, 949.83, 993.81, 1093.22, 1153.36, 1259.61, 1301.05, 1384.90, 1436.08, 1469.27, 1580.46, 1656.83, 2358.18, 2927.52, 3342.83, 3439.02; ¹H NMR (400 MHz, DMSO-*d*₆, TMS); δ 1.68 (t, *J*=7.07 Hz, 2H), 2.14 - 2.17 (m, 6H), 2.25 - 2.30 (m, 2H), 2.89 (s, 2H), 6.57 - 6.61 (m, 1H), 6.94 - 6.97 (m, 1H), 6.97 - 7.00 (m, 1H), 7.10 - 7.16 (m, 1H), 7.54 - 7.56 (m, 1H), 7.65 (d, *J*=2.27 Hz, 1H), 7.66 - 7.69 (m, 1H), 7.70 (d, *J*=1.77 Hz, 1H), 7.79 (dd, *J*=1.89, 0.88 Hz, 1H), 7.82 - 7.84 (m, 1H), 7.96 (s, 1H), 7.97 (dd, *J*=1.89, 0.63 Hz, 1H), 8.27 - 8.30 (m, 1H), 8.78 (t,

$J=5.68$ Hz, 1H); ^{13}C NMR (100 MHz, $\text{DMSO}-d_6$); δ 26.75, 40.35, 45.15, 46.13, 57.83, 108.30, 109.58, 111.70, 112.0, 113.50, 114.06, 115.08, 116.03, 117.89, 119.62, 123.28, 128.26, 129.96, 130.67, 133.09, 136.75, 142.12, 148.93, 150.64, 151.21, 152.23, 156.40, 158.54, 163.92; m/z (+EI) calc. For $\text{C}_{29}\text{H}_{28}\text{N}_4\text{O}_4$ (M^+) 496.56, found 496.77 ($\text{M}+\text{H}$) $^+$; Yield: 98%.

Amide coupling was used for synthesizing compounds **4.99** to **4.104** to obtain the final molecules.

Procedure for the synthesis of 2-(5-(3-(2-(2,3-dihydrobenzofuran-5-yl)thiazole-4-carboxamido)phenyl)furan-2-carboxamido)-N-(3-(dimethylamino)propyl)benzo[d]thiazole-6-carboxamide (4.99) from **2-(5-(3-(dimethylamino)propyl)benzo[d]thiazole-6-carboxamide (4.95)** and **2-(2,3-dihydrobenzofuran-5-yl) thiazole-4-carboxylic acid (4.53)** 2.0 eq of HOBT and 1.75 eq. of DIC were added to a solution of **4.95** (1 eq., 40 mg) in DMF. After 30 minutes, 2.0 eq. (43 mg) of **4.53** was added and the reaction mixture was allowed to stand for 3 hours. After completion, the reaction mixture was passed through a SCX-2 cartridge (500 mg), which was washed with DCM (3x), DMF (3x) twice and finally MeOH (2x). The product **4.99** was released from the cartridge using 5.0 ml 2M NH_3 in MeOH. Further purification of the product was achieved using a silica column and DCM:MeOH:2M NH_3 as solvent system where the polarity of the system was changed from 18:1:1 to 17:2:1 gradually until the product was obtained in pure form. It was then concentrated *in vacuo* to obtain a light yellow oil (24 mg).

2-(5-(3-(2-(2,3-Dihydrobenzofuran-5-yl)thiazole-4-carboxamido)phenyl)furan-2-carboxamido)-N-(3-(dimethylamino)propyl)benzo[d]thiazole-6-carboxamide (4.99)

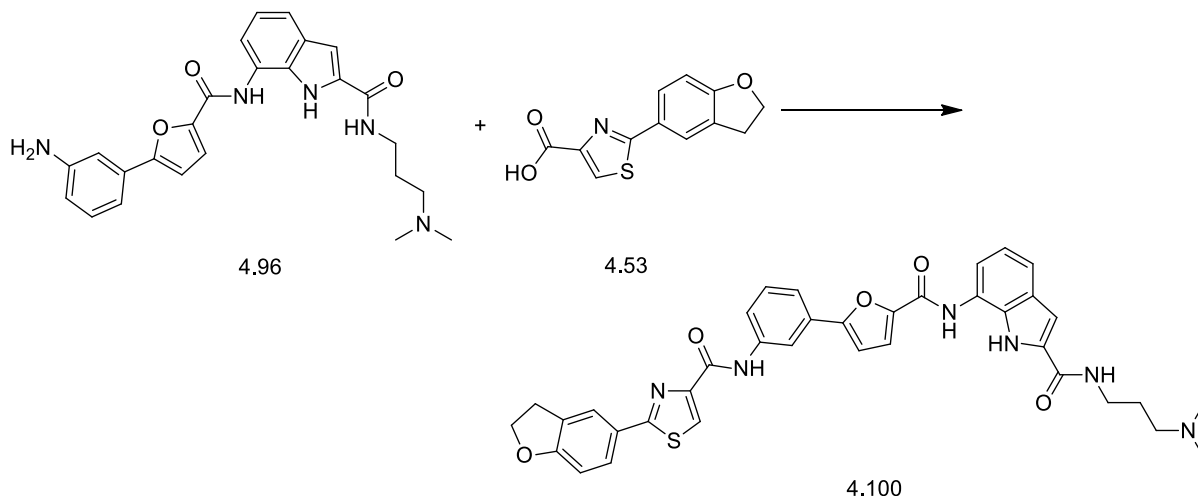


Light yellow oil. IR (FTIR, $\nu_{\text{max}}/\text{cm}^{-1}$) 616.50, 659.44, 694.73, 768.88, 941.23, 979.75, 1092.84, 1229.68, 1280.00, 1302.19, 1383.51, 1434.83, 1540.07, 1654.83, 1736.49, 2927.74, 3314.12, 3432.92; ^1H NMR (400 MHz, $\text{DMSO}-d_6$, TMS); δ 1.67 - 1.74 (m, 2H), 2.22 (s, 6H), 2.37 (t, $J=7.20$ Hz, 2H), 3.29 (d, $J=3.03$ Hz, 2H), 3.32 - 3.34 (m, 2H), 4.64 - 4.69 (m, 2H), 6.94 (d, $J=8.34$ Hz, 1H), 7.17 (d, $J=3.54$ Hz, 1H), 7.48 - 7.54 (m, 1H), 7.59 (d, $J=3.54$ Hz, 1H), 7.71 (d, $J=8.34$ Hz, 1H), 7.72 - 7.76 (m, 1H), 7.85 - 7.90 (m, 1H), 7.93 (d, $J=3.79$ Hz, 2H), 7.95 (s, 1H), 8.08 - 8.11 (m, 1H), 8.36 (t, $J=1.77$ Hz, 1H), 8.39 (s, 1H), 8.40 (d, $J=1.52$ Hz, 1H), 8.49 (t, $J=5.68$ Hz, 1H), 10.36 (s, 1H); ^{13}C NMR (100 MHz, $\text{DMSO}-d_6$); δ 26.85, 28.61, 38.88, 44.85, 44.92, 56.71, 71.75, 108.53, 109.45, 114.32, 119.64, 120.80, 121.0, 121.32, 121.50, 121.97, 123.45, 125.0, 127.3, 128.88, 129.49, 129.86, 130.51, 130.83, 131.43, 135.6, 149.89, 152.16, 156.18, 156.73, 159.21, 162.02, 167.73, 169.91, 174.03, 185.49; m/z (+EI) calc. For $\text{C}_{36}\text{H}_{32}\text{N}_6\text{O}_5\text{S}_2$ (M+) 692.81, found 692.56 (M+H) $^+$; Yield: 59%.

Procedure for the synthesis of 2-(2,3-dihydrobenzofuran-5-yl)-N-(3-(5-((3-(dimethylamino)propyl)carbamoyl)-1H-indol-7-yl)carbamoyl)furan-2-yl)phenylthiazole-4-carboxamide (4.100) from 7-(5-(3-aminophenyl)furan-2-carboxamido)-N-(3-(dimethylamino)propyl)-1H-indole-2-carboxamide (4.96) and 2-(2,3-dihydrobenzofuran-5-yl)thiazole-4-carboxylic acid (4.53)

2.0 eq of HOBT and 1.75 eq. of DIC were added to a solution of **4.96** (1 eq., 60 mg) in DMF. After 30 minutes, 2.0 eq. (128 mg) of **4.53** was added and the reaction mixture was allowed to stand for 3 hours. After completion, the reaction mixture was passed through a SCX-2 cartridge (2.0 gm), which was washed with DCM (3x), DMF (3x) twice and finally MeOH (2x). The product **4.100** was released from the cartridge using 5.0 ml 2M NH_3 in MeOH. Further purification of the product was achieved by passage through a silica column with DCM:MeOH:2M NH_3 as solvent system, where the polarity of the system was changed from 18:1:1 to 17:2:1, gradually, until the product was obtained in pure form. It was then concentrated *in vacuo* to obtain a brown oily mass (100 mg).

2-(2,3-Dihydrobenzofuran-5-yl)-N-(3-(5-((2-((3-(dimethylamino)propyl)carbamoyl)-1H-indol-7-yl)carbamoyl)furan-2-yl)phenyl)thiazole-4-carboxamide (4.100):

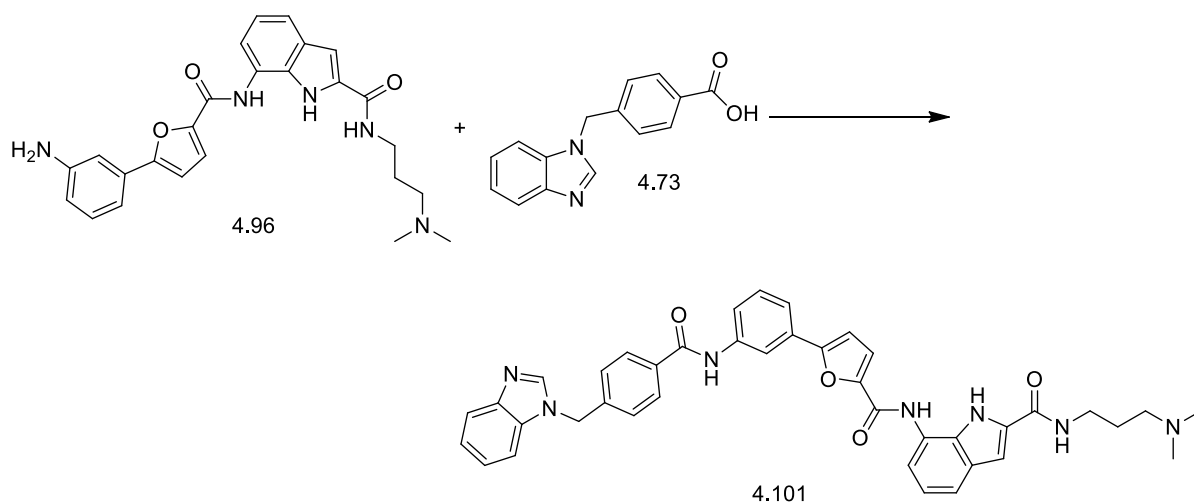


Brown oily mass. IR (FTIR, $\nu_{\text{max}}/\text{cm}^{-1}$) 638.74, 690.84, 734.16, 782.45, 821.24, 939.73, 1032.41, 1100.05, 1230.25, 1287.08, 1418.81, 1454.32, 1540.21, 1648.27, 1735.40, 2935.86, 3291.98; ^1H NMR (400 MHz, $\text{DMSO}-d_6$ TMS); δ 1.68 (t, $J=7.07$ Hz, 2H), 2.13 - 2.16 (m, 6H), 2.25 - 2.30 (m, 2H), 3.28 (br. s., 2H), 3.33 (br. s., 2H), 4.61 - 4.68 (m, 2H), 6.92 (d, $J=8.34$ Hz, 1H), 7.08 (t, $J=7.83$ Hz, 1H), 7.15 - 7.17 (m, 1H), 7.18 (d, $J=3.54$ Hz, 1H), 7.48 (d, $J=8.08$ Hz, 1H), 7.53 (d, $J=3.54$ Hz, 1H), 7.70 (d, $J=7.58$ Hz, 1H), 7.74 (d, $J=8.08$ Hz, 1H), 7.92 (dd, $J=8.34$, 2.02 Hz, 1H), 7.94 - 7.98 (m, 1H), 8.07 (s, 1H), 8.35 (t, $J=1.77$ Hz, 1H), 8.38 (s, 1H), 8.58 (t, $J=5.81$ Hz, 1H), 10.14 (s, 1H), 10.35 (s, 1H), 11.57 (s, 1H); ^{13}C NMR (100 MHz, $\text{DMSO}-d_6$); δ 27.36, 28.78, 37.47, 45.31, 45.31, 57.01, 82.78, 104.91, 109.56, 114.20, 114.96, 116.73, 120.04, 123.41, 123.91, 124.31, 125.39, 126.28, 127.59, 128.90, 129.01, 129.18, 130.01, 131.21, 133.76, 139.18, 145.76, 149.41, 150.43, 155.28, 156.66, 160.99, 162.01, 162.60, 167.92, 169.54, 186.31; m/z (+EI) calc. For $\text{C}_{37}\text{H}_{34}\text{N}_6\text{O}_5\text{S}$ (M^+) 674.77, found 675.30 ($\text{M}+\text{H}$) $^+$; Yield: 57%.

Procedure for the synthesis of 7-(5-(3-(4-((1*H*-benzo[d]imidazol-1-yl)methyl)benzamido)phenyl)furan-2-carboxamido)-*N*-(3-(dimethylamino)propyl)-1*H*-indole-2-carboxamide (4.101) from 7-(5-(3-aminophenyl)furan-2-carboxamido)-*N*-(3-(dimethylamino)propyl)-1*H*-indole-2-carboxamide (4.96) and 4-((1*H*-benzo[d]imidazol-1-yl)methyl)benzoic acid (4.73)

2.0 eq of HOBT and 1.75 eq. of DIC were added to a solution of **4.96** (1 eq., 115 mg) in DMF. After 30 minutes 2.0 eq. (131 mg) of **4.73** was added and the reaction mixture was allowed to stand for 3 hours. After completion, the reaction mixture was passed through a SCX-2 cartridge (2.0 gm), which was washed with DCM (3x), and DMF (3x) twice and finally MeOH (2x). The product **4.101** was released from the cartridge using 5.0 ml 2M NH₃ in MeOH. Further purification of the product was achieved by silica column chromatography using DCM:MeOH:2MNH₃ (18:1:1) as the solvent system until the product was obtained in pure form. It was then concentrated *in vacuo* to obtain yellow viscous material (150 mg).

7-(5-(3-(4-((1*H*-benzo[d]imidazol-1-yl)methyl)benzamido)phenyl)furan-2-carboxamido)-*N*-(3-(dimethylamino)propyl)-1*H*-indole-2-carboxamide (4.101):



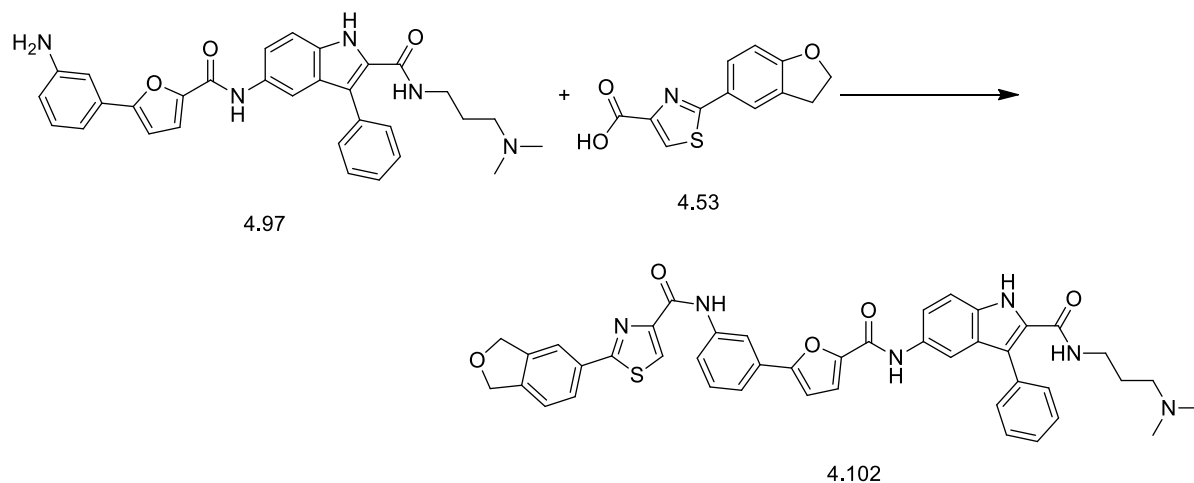
Yellow viscous material. IR (FTIR, $\nu_{\text{max}}/\text{cm}^{-1}$) 690.64, 734.31, 783.63, 963.41, 1020.59, 1088.21, 1145.61, 1176.84, 1258.75, 1287.39, 1415.61, 1496.78, 1549.21, 1633.90, 2941.34, 3279.15; ¹H NMR (400 MHz, DMSO-*d*₆, TMS); δ 1.71 (t, *J*=7.07 Hz, 2H), 2.23 (s, 6H), 2.40 (t, *J*=7.07 Hz, 2H), 3.40 (br. s., 2H), 5.61 (s, 2H), 7.07 (t, *J*=7.83 Hz, 1H), 7.13 (d, *J*=3.54 Hz, 1H), 7.16 (d, *J*=2.02 Hz, 1H), 7.19 - 7.22 (m, 2H), 7.44 (s, 1H), 7.46 (s, 2H), 7.48 (s, 1H),

7.49 - 7.50 (m, 1H), 7.53 (d, $J=3.54$ Hz, 1H), 7.65 - 7.68 (m, 1H), 7.69 (d, $J=2.53$ Hz, 1H), 7.71 (s, 1H), 7.81 (d, $J=8.08$ Hz, 1H), 7.95 (d, $J=8.34$ Hz, 2H), 8.25 (t, $J=1.77$ Hz, 1H), 8.45 (s, 1H), 8.60 (t, $J=5.56$ Hz, 1H), 10.11 (s, 1H), 10.38 (s, 1H), 11.57 (s, 1H); ^{13}C NMR (100 MHz, DMSO- d_6); δ 18.51, 44.72, 48.56, 55.99, 56.54, 62.77, 107.75, 110.64, 112.46, 116.15, 116.50, 116.88, 118.16, 119.51, 119.87, 120.04, 120.70, 121.62, 122.42, 123.24, 127.30, 128.10, 128.79, 128.92, 129.32, 129.67, 131.88, 133.58, 134.18, 139.70, 140.53, 143.58, 144.30, 146.82, 155.12, 156.48, 160.85, 163.08, 165.30, 171.20; m/z (+EI) calc. For $\text{C}_{40}\text{H}_{37}\text{N}_7\text{O}_4$ (M^+) 679.77, found 679.74 ($\text{M}+\text{H}$) $^+$; Yield: 89%.

Procedure for the synthesis of 2-(2,3-dihydrobenzofuran-5-yl)-*N*-(3-(5-((2-((3-(dimethylamino)propyl)carbamoyl)-3-phenyl-1*H*-indol-5-yl)carbamoyl)furan-2-yl)phenyl)thiazole-4-carboxamide (4.102) from 5-(5-(3-aminophenyl)furan-2-carboxamido)-*N*-(3-(dimethylamino)propyl)-3-phenyl-1*H*-indole-2-carboxamide (4.97) and 2-(2,3-dihydrobenzofuran-5-yl) thiazole-4-carboxylic acid (4.53)

2.0 eq of HOBt and 1.75 eq. of DIC were added to a solution of **4.97** (1 eq., 60 mg) in DMF. After 30 minutes, 2.0 eq. (57 mg) of **4.53** was added and the reaction mixture was allowed to stand for 3 hours. After completion, the reaction mixture was passed through a SCX-2 cartridge (2.0 gm), which was washed with DCM (3x), DMF (3x) twice and finally MeOH (2x). The product **4.102** was released from the cartridge using 5.0 ml 2M NH_3 in MeOH. Further purification of the product was made using a silica column and a DCM:MeOH:2M NH_3 solvent system where the polarity of the system was changed from 18:1:1 to 17:2:1, gradually, until the product was obtained in pure form. It was then concentrated *in vacuo* to obtain light brown oil (50 mg).

2-(2,3-Dihydrobenzofuran-5-yl)-N-(3-(5-((2-((3-(dimethylamino)propyl)carbamoyl)-3-phenyl-1*H*-indol-5-yl)carbamoyl)furan-2-yl)phenyl)thiazole-4-carboxamide (4.102):

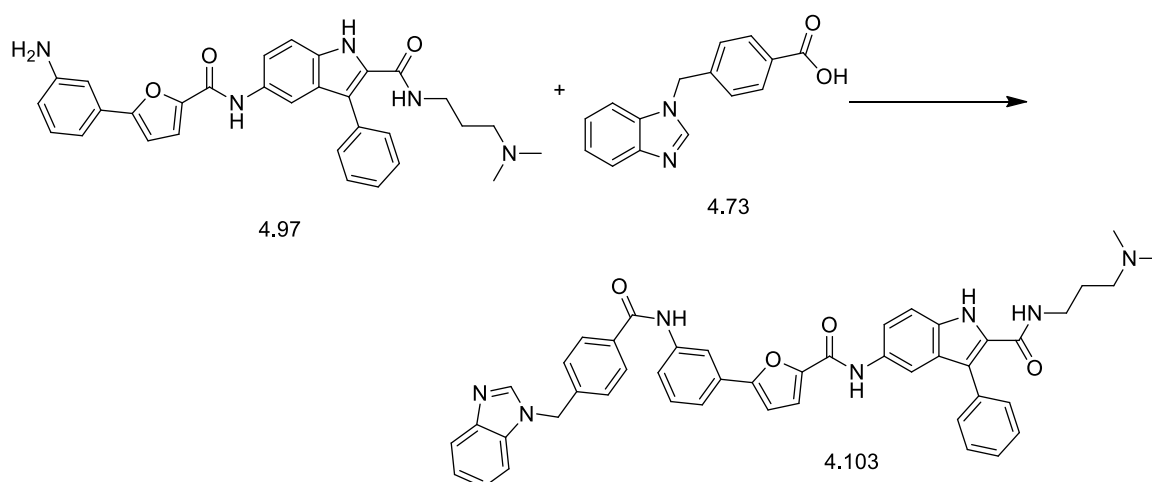


Light brown oil. IR (FTIR, $\nu_{\text{max}}/\text{cm}^{-1}$) 639.37, 659.92, 692.71, 786.69, 864.70, 939.80, 980.47, 1029.99, 1093.93, 1228.84, 1310.09, 1385.26, 1455.01, 1537.63, 1654.16, 2934.13, 3277.47; ^1H NMR (400 MHz, $\text{DMSO}-d_6$, TMS); δ 1.51 (quin, $J=6.88$ Hz, 2H), 2.04 (s, 6H), 2.10 - 2.12 (m, 2H), 2.13 - 2.17 (m, 2H), 3.19 - 3.25 (m, 2H), 4.65 (t, $J=8.84$ Hz, 2H), 6.93 (d, $J=8.34$ Hz, 1H), 7.11 (d, $J=3.54$ Hz, 1H), 7.31 (t, $J=5.56$ Hz, 1H), 7.37 - 7.41 (m, 2H), 7.46 (d, $J=8.59$ Hz, 1H), 7.50 - 7.51 (m, 2H), 7.52 (s, 2H), 7.63 (dd, $J=8.97, 1.89$ Hz, 1H), 7.72 - 7.76 (m, 1H), 7.92 (dd, $J=2.27, 1.26$ Hz, 1H), 7.93 - 7.94 (m, 1H), 7.95 (br. s., 1H), 8.08 (d, $J=1.52$ Hz, 1H), 8.29 (t, $J=1.77$ Hz, 1H), 8.38 (s, 1H), 10.11 (s, 1H), 10.31 (s, 1H), 11.70 (s, 1H); ^{13}C NMR (100 MHz, $\text{DMSO}-d_6$); δ 26.51, 30.73, 35.73, 45.02, 45.11, 56.78, 79.46, 180.34, 108.96, 109.39, 111.47, 112.07, 116.22, 116.61, 116.67, 118.85, 120.96, 123.74, 124.11, 125.22, 126.68, 126.86, 127.42, 128.60, 128.63, 128.75, 129.05, 129.29, 129.79, 129.93, 131.45, 132.42, 133.92, 138.87, 147.11, 149.87, 154.81, 155.89, 159.20, 161.44, 162.09, 162.28, 167.76; m/z (+EI) calc. For $\text{C}_{43}\text{H}_{38}\text{N}_6\text{O}_5\text{S}$ (M^+) 750.86, found 751.25 ($\text{M}+\text{H}^+$); Yield: 58%.

Procedure for the synthesis of 5-(5-(3-(4-((1*H*-benzo[*d*]imidazol-1-yl)methyl)benzamido)phenyl)furan-2-carboxamido)-*N*-(3-(dimethylamino)propyl)-3-phenyl-1*H*-indole-2-carboxamide (4.103) from 5-(5-(3-aminophenyl)furan-2-carboxamido)-*N*-(3-(dimethylamino)propyl)-3-phenyl-1*H*-indole-2-carboxamide (4.97) and 4-((1*H*-benzo[*d*]imidazol-1-yl)methyl)benzoic acid (4.73)

2.0 eq of HOBT and 1.75 eq. of DIC were added to a solution of **4.97** (1 eq., 75 mg) in DMF. After 30 minutes, 2.0 eq. (73 mg) of **4.73** was added and the reaction mixture was allowed to stand for 3 hours. After completion, the reaction mixture was passed through a SCX-2 cartridge (500 mg), which was washed with DCM (3x), DMF (3x) twice and finally MeOH (2x). The product **4.103** was released from the cartridge using 5.0 ml 2M NH₃ in MeOH. Further purification of the product was achieved using a silica column and DCM:MeOH:2MNH₃ as solvent system in which the polarity of the system was changed from 18:1:1 to 17:2:1, gradually, until the product was obtained in pure form. It was then concentrated *in vacuo* to obtain colourless, fluffy material (65 mg).

5-(5-(3-(4-((1*H*-benzo[*d*]imidazol-1-yl)methyl)benzamido)phenyl)furan-2-carboxamido)-*N*-(3-(dimethylamino)propyl)-3-phenyl-1*H*-indole-2-carboxamide (4.103):



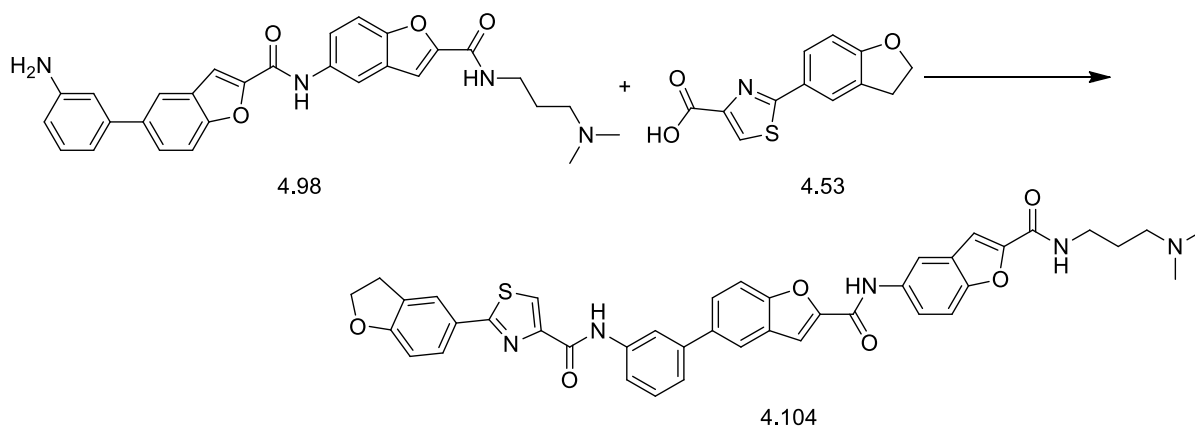
Colourless, fluffy material. IR (FTIR, $\nu_{\text{max}}/\text{cm}^{-1}$) 612.91, 692.98, 736.90, 788.56, 1018.45, 1214.76, 1256.08, 1306.23, 1372.32, 1426.56, 1472.01, 1538.07, 1643.54, 1744.28, 2956.07, 3250.64; ¹H NMR (400 MHz, DMSO-*d*₆, TMS); δ 1.50 (t, *J*=6.82 Hz, 2H), 2.03 (s, 6H), 2.11 (t, *J*=6.95 Hz, 2H), 3.20 - 3.26 (m, 2H), 5.62 (s, 2H), 7.05 (d, *J*=3.54 Hz, 1H), 7.19 - 7.23 (m, 2H), 7.31 (t, *J*=5.68 Hz, 1H), 7.37 - 7.39 (m, 1H), 7.39 - 7.40 (m, 1H), 7.43 - 7.46 (m, 2H), 7.46 - 7.48 (m, 2H), 7.50 (s, 2H), 7.51 - 7.52 (m, 2H), 7.53 (dd, *J*=2.78, 0.76 Hz, 1H), 7.63 (dd, *J*=8.84, 2.02 Hz, 1H), 7.66 - 7.71 (m, 2H), 7.75 - 7.78 (m, 1H), 7.92 (d, *J*=1.77 Hz, 1H),

7.93 - 7.96 (m, 2H), 8.20 (t, $J=1.77$ Hz, 1H), 8.46 (s, 1H), 10.08 (s, 1H), 10.34 (s, 1H); ^{13}C NMR (100 MHz, $\text{DMSO}-d_6$); δ 26.76, 37.67, 45.26, 47.50, 56.19, 57.01, 110.84, 111.56, 112.24, 116.27, 116.31, 116.49, 116.76, 118.94, 119.72, 120.23, 120.95, 121.82, 122.61, 126.85, 127.04, 127.49, 128.28, 128.77, 129.22, 129.43, 129.83, 129.89, 130.10, 131.67, 132.57, 133.78, 134.10, 134.31, 134.37, 137.73, 139.78, 140.74, 143.79, 144.35, 144.47, 147.24, 155.01, 156.06, 161.61, 165.44; m/z (+EI) calc. For $\text{C}_{46}\text{H}_{41}\text{N}_7\text{O}_4$ (M^+) 755.86, found 756.07 ($\text{M}+\text{H}$) $^+$; Yield: 60%.

Procedure for the synthesis of 2-(2,3-dihydrobenzofuran-5-yl)-N-(3-(2-((3-(dimethylamino)propyl)carbamoyl)benzofuran-5-yl)carbamoyl)benzofuran-5-yl)phenylthiazole-4-carboxamide (4.104) from 5-(3-aminophenyl)-N-(2-((3-(dimethylamino)propyl)carbamoyl)benzofuran-5-yl)benzofuran-2-carboxamide (4.98) and 2-(2,3-dihydrobenzofuran-5-yl) thiazole-4-carboxylic acid (4.53)

2.0 eq of HOBt and 1.75 eq. of DIC were added to a solution of **4.98** (1 eq., 38 mg) in DMF. After 30 minutes, 2.0 eq. (38 mg) of **4.53** was added and the reaction mixture was allowed to stand for 3 hours. After completion, the reaction mixture was passed through a SCX-2 cartridge (500 mg), which was washed with DCM (3x), DMF (3x) twice and finally MeOH (2x). The product **4.104** was released from the cartridge using 5.0 ml 2M NH_3 in MeOH. Further purification of the product was achieved using a silica column and DCM:MeOH:2M NH_3 (18:1:1) as solvent system to obtain the product in pure form. It was then concentrated *in vacuo* to obtain colourless oil (40 mg).

2-(2,3-Dihydrobenzofuran-5-yl)-N-(3-(2-((3-(dimethylamino)propyl)carbamoyl)benzofuran-5-yl)carbamoyl)benzofuran-5-yl)phenylthiazole-4-carboxamide (4.104):



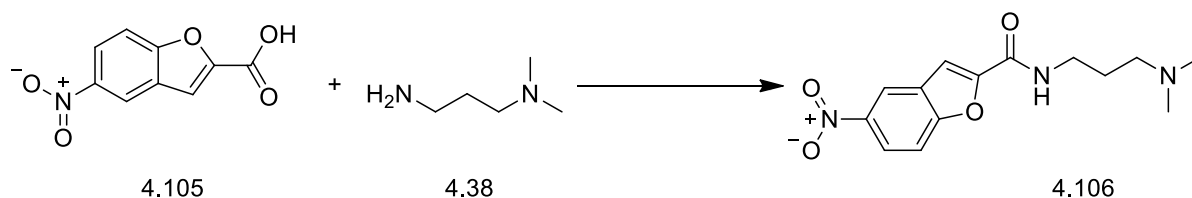
Colourless oil. IR (FTIR, $\nu_{\text{max}}/\text{cm}^{-1}$) 636.44, 691.10, 721.457, 785.24, 811.00, 870.28, 940.13, 1034.27, 1101.08, 1149.67, 1198.26, 1229.04, 1292.40, 1460.92, 1536.21, 1649.19, 2323.17, 2357.81, 2939.02, 3286.58; ^1H NMR (400 MHz, $\text{DMSO}-d_6$) δ 1.68 (t, $J=6.95$ Hz, 2H), 2.15 - 2.17 (m, 6H), 2.28 (t, $J=6.95$ Hz, 2H), 3.17 (s, 2H), 3.30 (br. s., 2H), 4.65 (t, $J=8.72$ Hz, 2H), 6.93 (d, $J=8.59$ Hz, 1H), 7.49 - 7.52 (m, 2H), 7.55 (d, $J=0.76$ Hz, 1H), 7.67 (d, $J=8.84$ Hz, 1H), 7.81 (d, $J=2.27$ Hz, 1H), 7.83 (d, $J=1.77$ Hz, 1H), 7.84 (s, 1H), 7.86 - 7.88 (m, 1H), 7.92 - 7.95 (m, 1H), 8.07 (d, $J=1.52$ Hz, 1H), 8.11 - 8.13 (m, 1H), 8.22 - 8.24 (m, 1H), 8.30 (d, $J=2.27$ Hz, 1H), 8.38 (s, 1H), 8.78 (t, $J=5.68$ Hz, 1H), 10.28 (s, 1H), 10.69 (s, 1H); ^{13}C NMR (100 MHz, $\text{DMSO}-d_6$) δ 26.91, 28.63, 37.36, 45.10, 45.10, 56.87, 71.76, 109.38, 110.85, 111.76, 112.32, 114.04, 119.16, 120.70, 120.81, 122.59, 123.73, 124.00, 125.22, 126.36, 127.28, 127.42, 127.85, 128.72, 128.84, 129.29, 131.49, 131.59, 134.24, 136.28, 138.97, 140.57, 149.51, 150.07, 151.03, 154.15, 156.60, 157.90, 159.17, 162.09, 167.78; m/z (+EI) calc. For $\text{C}_{41}\text{H}_{35}\text{N}_5\text{O}_6\text{S}$ (M^+) 725.81, found 726.98 ($\text{M}+\text{H}$) $^+$; Yield: 72%.

4.1.6.2 Sub type 3 Library synthesis

General procedure for the synthesis of *N*-(3-(dimethylamino)propyl)-5-nitrobenzofuran-2-carboxamide (4.106) from 5-nitrobenzofuran-2-carboxylic acid (4.105) and *N,N*-dimethylpropane-1,3-diamine (4.38) (Amide coupling)

2.0 eq of HOBT (522 mg) and 1.75 eq. of DIC (525 μl) were added to a solution of **4.105** (1 eq., 400 mg) in DMF. After 30 minutes, 1.0 eq. (242 μl) of **4.38** was added and the reaction mixture was allowed to stand for 3 hours. After completion, the reaction mixture was passed through a SCX-2 cartridge (5.0 gm), which was washed with DCM (3x), DMF (3x) twice and finally MeOH (2x). The product **4.106** was released from the cartridge using 5.0 ml 2M NH_3 in MeOH and concentrated *in vacuo* to obtain a bright yellow oil (336 mg).

***N*-(3-(dimethylamino)propyl)-5-nitrobenzofuran-2-carboxamide (4.106):**



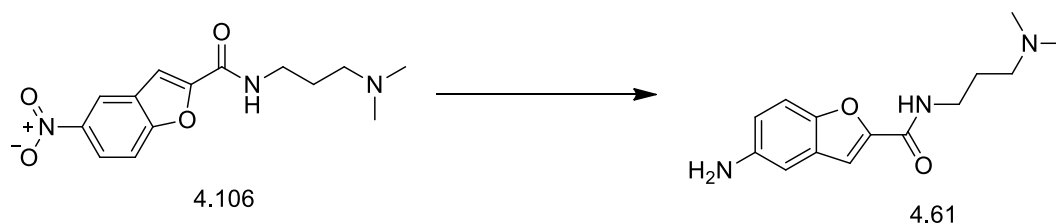
Bright yellow oil. IR (FTIR, $\nu_{\text{max}}/\text{cm}^{-1}$) 682.50, 737.70, 766.18, 827.94, 861.61, 889.94, 916.66, 939.92, 955.81, 990.36, 1038.20, 1060.33, 1097.24, 1132.03, 1162.55, 1247.81, 1270.14, 1301.05, 1338.74, 1453.72, 1521.19, 1600.55, 1660.00, 2360.22, 2779.28, 2819.37,

2856.77, 2952.05; ^1H NMR (400 MHz, CDCl_3 , TMS); δ 1.80 (quin, $J=6.13$ Hz, 2H), 2.34 (s, 6H), 2.49 - 2.55 (m, 2H), 3.61 (td, $J=6.06, 5.31$ Hz, 2H), 7.53 (d, $J=1.01$ Hz, 1H), 7.58 (d, $J=9.09$ Hz, 1H), 8.33 (dd, $J=9.09, 2.27$ Hz, 1H), 8.61 - 8.63 (m, 1H); ^{13}C NMR (100 MHz, CDCl_3); δ 25.11, 39.64, 44.50, 45.10, 58.62, 109.59, 111.83, 118.84, 121.73, 127.76, 144.37, 152.20, 156.91, 157.31; m/z (+EI) calc. For $\text{C}_{14}\text{H}_{17}\text{N}_3\text{O}_4$ (M^+) 291.30, found 292.29 ($\text{M}+\text{H}^+$); Yield: 84%.

General procedure for the synthesis of 5-amino-*N*-(3-(dimethylamino)propyl)benzofuran-2-carboxamide (4.61) from *N*-(3-(dimethylamino)propyl)-5-nitrobenzofuran-2-carboxamide (4.106) by hydrogenation.

N-(3-(Dimethylamino)propyl)-5-nitrobenzofuran-2-carboxamide (1.0 eq., 336 mg) (**4.106**) was dissolved in a minimum amount of ethanol (30 ml) and a catalytic amount of 10% Pd/C (34 mg) was added as a slurry, also in ethanol. The reaction mixture was shaken for 2 hours at 45 psi in a Parr hydrogenator. After completion of the reduction, the suspension was filtered through a layer of celite, with caution, using a Buchner flask and the filtrate was concentrated to obtain light yellow oil (**4.61**) (242 mg).

5-Amino-*N*-(3-(dimethylamino)propyl)benzofuran-2-carboxamide (4.61)



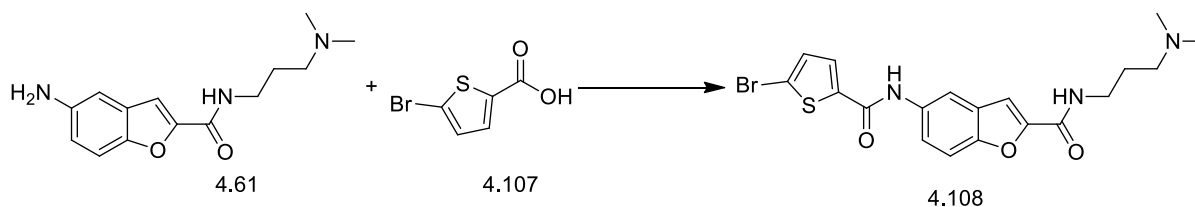
Light yellow oily mass. IR (FTIR, $\nu_{\text{max}}/\text{cm}^{-1}$) 630.65, 732.57, 809.43, 853.13, 1038.19, 1097.61, 1160.32, 1208.16, 1243.22, 1298.70, 1385.67, 1454.19, 1477.56, 1526.06, 1584.13, 1650.06, 2780.36, 2821.70, 2863.04, 2940.10, 3240.31, 3333.30; ^1H NMR (400 MHz, CDCl_3 , TMS); δ 1.73 - 1.81 (m, 2H), 2.29 (s, 6H), 2.46 (t, $J=6.44$ Hz, 2H), 3.50 - 3.53 (m, 2H), 6.76 (dd, $J=8.84, 2.53$ Hz, 1H), 6.87 (d, $J=2.27$ Hz, 1H), 7.21 - 7.25 (m, 2H), 8.11 (br. s., 1H); ^{13}C NMR (100 MHz, CDCl_3); δ 25.70, 38.51, 44.80, 44.83, 57.80, 106.06, 108.84, 111.46, 115.76, 128.08, 142.39, 148.87, 149.19, 158.63; m/z (+EI) calc. For $\text{C}_{14}\text{H}_{19}\text{N}_3\text{O}_2$ (M^+) 261.32, found 261.76 ($\text{M}+\text{H}^+$); Yield: 72%.

The following molecule was synthesized according to the general procedure of amide coupling.

Procedure for the synthesis of 5-(5-bromothiophene-2-carboxamido)-N-(3-(dimethylamino)propyl)benzofuran-2-carboxamide (4.108) from 5-amino-N-(3-(dimethylamino)propyl)benzofuran-2-carboxamide (4.61) and 5-bromothiophene-2-carboxylic acid (4.107)

2.0 eq of HOBT and 1.75 eq. of DIC were added to a solution of **4.61** (1eq., 23 mg) in DMF. After 30 minutes, 2.0 eq. (46 mg) of **4.107** was added and the reaction mixture was allowed to stand for 3 hours. After completion, the reaction mixture was passed through a SCX-2 cartridge (500 mg), which was washed with DCM (3x), DMF (3x) twice and finally MeOH (2x). The product **4.108** was released from the cartridge using 5.0 ml 2M NH₃ in MeOH and concentrated *in vacuo* to obtain colourless oil (32 mg).

5-(5-Bromothiophene-2-carboxamido)-N-(3-(dimethylamino)propyl)benzofuran-2-carboxamide (4.108):

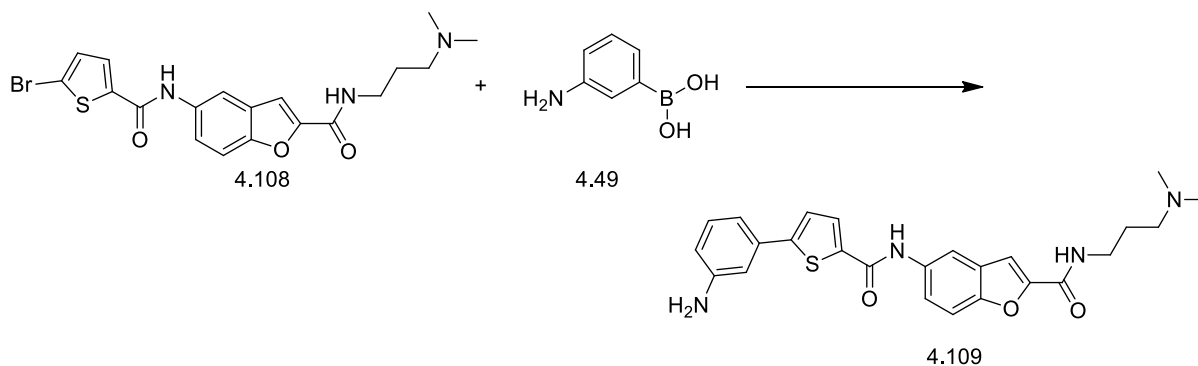


Colourless oil. IR (FTIR, $\nu_{\text{max}}/\text{cm}^{-1}$) 613.47, 626.39, 731.75, 765.13, 802.99, 815.89, 831.82, 850.11, 874.64, 947.04, 976.41, 1003.66, 1036.05, 1064.10, 1084.09, 1125.55, 1166.82, 1205.36, 1273.79, 1315.82, 1326.04, 1345.86, 1413.10, 1434.02, 1462.30, 1513.71, 1548.17, 1591.92, 1636.09, 2361.33, 2764.52, 2813.65, 2939.02, 2968.56, 3316.76, 3358.41; ¹H NMR (400 MHz, DMSO-*d*₆, TMS); 1.67 (t, *J*=6.95 Hz, 2H), 2.16 (s, 6H), 2.29 (t, *J*=6.95 Hz, 2H), 3.26 - 3.29 (m, 2H), 7.38 (d, *J*=4.04 Hz, 1H), 7.52 (s, 1H), 7.61 - 7.65 (m, 1H), 7.66 - 7.70 (m, 1H), 7.87 (d, *J*=4.04 Hz, 1H), 8.14 (d, *J*=2.02 Hz, 1H), 8.77 (t, *J*=5.81 Hz, 1H), 10.38 (s, 1H); ¹³C NMR (100 MHz, DMSO-*d*₆); δ 26.84, 37.29, 45.03, 45.06, 56.81, 109.32, 111.74, 113.91, 117.70, 120.52, 123.45, 127.29, 129.78, 131.68, 134.24, 150.92, 157.86, 158.74, 162.41; *m/z* (+EI) calc. For C₁₉H₂₀BrN₃O₃S (M⁺) 450.35, found 449.60 (M+H)⁺; Yield: 81%.

General procedure for Suzuki coupling for the synthesis of 5-(5-(3-aminophenyl)thiophene-2-carboxamido)-N-(3-(dimethylamino)propyl)benzofuran-2-carboxamide (4.109) from 5-(5-bromothiophene-2-carboxamido)-N-(3-(dimethylamino)propyl)benzofuran-2-carboxamide (4.108) and (3-aminophenyl)boronic acid (4.49)

A catalytic amount of tetrakis(triphenylphosphine)palladium, Pd(PPh₃)₄ (0.1 eq., 6 mg) was added to a solution of **4.108** (1.0 eq., 25 mg) and **4.49** (1.2 eq., 26 mg) in a 9:3:1 combination of EtOH, toluene and water in the presence of K₂CO₃ (3.0 eq., 23 mg) in a 10 ml microwave vial containing a magnetic stirrer. The reaction vessel was flushed with nitrogen during each addition. The reaction mixture was sealed in an inert nitrogen environment and heated with microwave radiation in an EMRYSTM Optimizer Microwave Station (Personal Chemistry) at 100 °C for 15 minutes. After LCMS analysis revealed complete reaction the cooled reaction mixture was passed through an IsoluteTM SCX-2 cartridge (500 mg) and washed with DCM (3x), DMF (3x) twice and finally MeOH (2x). The product was released from the cartridge using 5.0 ml 2M NH₃ in MeOH and concentrated in *vacuo* to obtain product **4.109** (22 mg).

5-(5-(3-aminophenyl)thiophene-2-carboxamido)-N-(3-(dimethylamino)propyl)benzofuran-2-carboxamide (4.109):



Dark brown, oily mass. IR (FTIR, $\nu_{\text{max}}/\text{cm}^{-1}$) 660.50, 709.32, 721.47, 779.45, 867.24, 993.11, 1094.01, 1159.72, 1239.43, 1298.48, 1343.95, 1385.70, 1440.55, 1548.38, 1598.54, 1653, 2341.46, 2363.08, 2859.75, 2932.92, 3342.51; ¹H NMR (400 MHz, DMSO-*d*₆, TMS); δ 1.68 (t, *J*=6.82 Hz, 2H), 2.18 (s, 6H), 2.31 (t, *J*=6.82 Hz, 2H), 2.89 (s, 2H), 6.57 - 6.59 (m, 1H), 6.95 - 6.96 (m, 1H), 7.10 (t, *J*=7.83 Hz, 1H), 7.45 (d, *J*=3.79 Hz, 1H), 7.52 - 7.54 (m, 1H), 7.64 (d, *J*=9.09 Hz, 1H), 7.70 (d, *J*=2.02 Hz, 1H), 7.73 (s, 1H), 7.95 (s, 1H), 8.00 (d, *J*=4.04 Hz, 1H), 8.19 (d, *J*=2.27 Hz, 1H), 8.78 (d, *J*=2.78 Hz, 1H), 10.32 (s, 1H); ¹³C NMR (100 MHz, DMSO-*d*₆); δ 26.60, 35.53, 44.78, 44.81, 56.57, 111.47, 113.54, 114.16, 115.47,

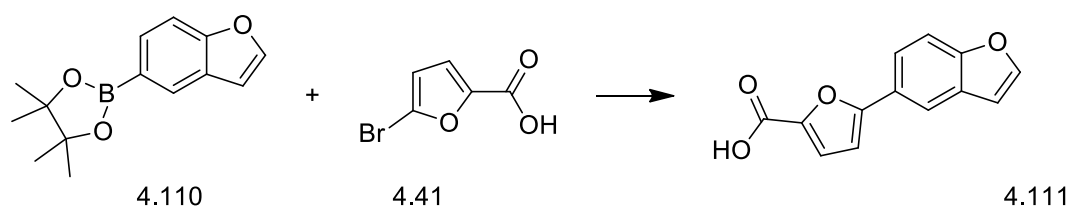
119.72, 121.63, 123.30, 127.06, 127.50, 129.49, 129.83, 133.22, 137.74, 147.29, 149.12, 149.35, 149.76, 157.70, 159.54, 162.05; m/z (+EI) calc. For $C_{25}H_{26}N_4O_3S$ (M^+) 462.56, found 462.81 ($M+H$)⁺; Yield: 86%.

A similar Suzuki coupling condition was followed for the following reaction.

Procedure for the synthesis of 5-(benzofuran-5-yl)furan-2-carboxylic acid (4.111) from 2-(benzofuran-5-yl)-4,4,5,5-tetramethyl-1,3,2-dioxaborolane (4.110) and 5-bromofuran-2-carboxylic acid (4.41)

A catalytic amount of tetrakis(triphenylphosphine)palladium, $Pd(PPh_3)_4$ (0.1 eq.) was added to a solution of **4.110** (1.0 eq., 100 mg) and **4.41** (1.5 eq., 117 mg) in a 9:3:1 combination of EtOH, toluene and water in the presence of K_2CO_3 (3.0 eq.) in a 10 ml microwave vial containing a magnetic stirrer. The reaction vessel was flushed with nitrogen during each addition. The reaction mixture was sealed in an inert nitrogen environment and heated with microwave radiation in an EMRYSTM Optimizer Microwave Station (Personal Chemistry) at 100 °C for 15 minutes. After LCMS analysis revealed complete reaction the cooled reaction mixture was dried over vacuum. A silica column was used to purify the product **4.111**. Initially the Palladium catalyst was trapped over a silica bed, which was washed with ethyl acetate to obtain the crude reaction mixture. This was then dried and purified using column chromatography, with ethyl acetate as the solvent system. Purification was very tricky, but a reasonable amount (89 mg) of pure product was obtained.

5-(Benzofuran-5-yl)furan-2-carboxylic acid (4.111):



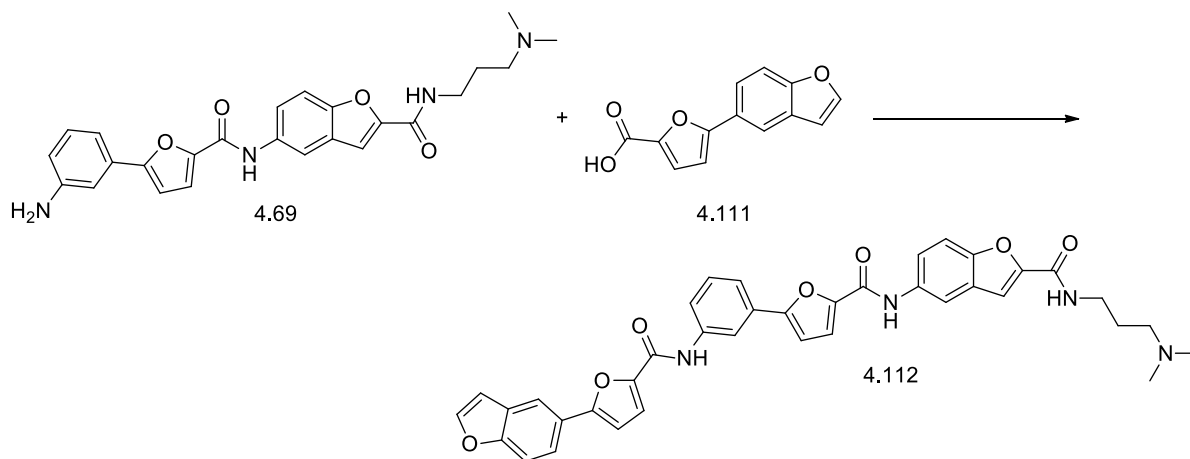
Colourless oily mass. IR (FTIR, ν_{max}/cm^{-1}) 690.47, 789.10, 881.54, 1021.07, 1204.42, 1263.83, 2361.94; 1H NMR (400 MHz, DMSO- d_6 , TMS); δ 7.05 (dd, $J=2.15, 0.88$ Hz, 1H), 7.12 (d, $J=3.54$ Hz, 1H), 7.32 (d, $J=3.54$ Hz, 1H), 7.70 (d, $J=8.84$ Hz, 1H), 7.78 (dd, $J=8.59, 1.77$ Hz, 1H) 8.06 (d, $J=2.27$ Hz, 1H), 8.11 (d, $J=1.52$ Hz, 1H); ^{13}C NMR (100 MHz, DMSO- d_6); δ 107.01, 107.08, 111.98, 117.40, 121.33, 127.51, 128.64, 128.76, 131.38, 131.48, 147.15, 156.68, 159.25; m/z (+EI) calc. For $C_{13}H_8O_4$ (M^+) 228.20, found 228.78 ($M+H$)⁺; Yield: 95%.

Amide coupling was used for synthesising compounds **4.112** to **4.117**.

Procedure for the synthesis of 5-(5-(3-(5-(benzofuran-5-yl)furan-2-carboxamido)phenyl)furan-2-carboxamido)-N-(3-(dimethylamino)propyl)benzofuran-2-carboxamide (4.112) from 5-(5-(3-aminophenyl)furan-2-carboxamido)-N-(3-(dimethylamino)propyl)benzofuran-2-carboxamide (4.69) and-(benzofuran-5-yl)furan-2-carboxylic acid (4.111)

2.0 eq of HOBT, 1.75 eq. of DIC, 2eq.of **4.69** (78 mg) and 1.0 eq. (20 mg) of **4.111** were added to DMF and the reaction mixture was allowed to stand for 3 hours. After completion, the reaction mixture was passed through a SCX-2 cartridge (500 mg), which was washed with DCM (3x), DMF (3x) twice and finally MeOH (2x). The product **4.112** was released from the cartridge using 5.0 ml 2M NH₃ in MeOH and concentrated *in vacuo* to obtain a crude product. The product was purified using a silica column and 18:1:1 DCM:MeOH:2M NH₃ as solvent system to obtain a colourless viscous material (40 mg).

5-(5-(3-(5-(Benzofuran-5-yl)furan-2-carboxamido)phenyl)furan-2-carboxamido)-N-(3-(dimethylamino)propyl)benzofuran-2-carboxamide (4.112):



Colourless, viscous material. IR (FTIR, $\nu_{\text{max}}/\text{cm}^{-1}$) 734.63, 864.86, 881.54, 956.09, 1021.07, 1111.18, 1129.52, 1168.32, 1204.42, 1233.90, 1263.83, 1297.11, 1343.91, 1434.31, 1467.89, 1546.23, 1584.18, 1648.75, 2361.94, 2780.36, 2816.53, 2857.88, 2932.13, 3121.44, 3278.35; ¹H NMR (400 MHz, Acetone-*d*₄, TMS); δ 1.78 (quin, *J*=6.63 Hz, 2H), 2.24 (d, *J*=1.01 Hz, 6H), 2.42 (td, *J*=6.51, 1.39 Hz, 2H), 3.46 - 3.50 (m, 2H), 6.98 (dd, *J*=2.02, 1.01 Hz, 1H), 7.04 (d, *J*=3.54 Hz, 1H), 7.06 (d, *J*=3.79 Hz, 1H), 7.35 (d, *J*=3.54 Hz, 1H), 7.39 (d, *J*=3.79 Hz, 1H), 7.42 - 7.43 (m, 1H), 7.47 (t, *J*=8.08 Hz, 1H), 7.53 (d, *J*=8.84 Hz, 1H), 7.64 (dt, *J*=8.59,

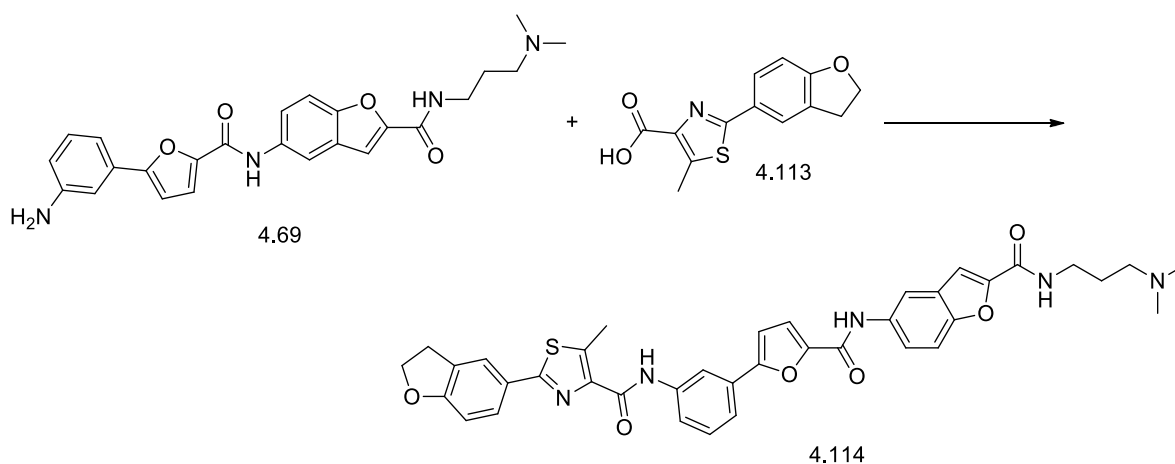
0.76 Hz, 1H), 7.67 - 7.70 (m, 1H), 7.82 - 7.86 (m, 1H), 7.90 (d, $J=2.02$ Hz, 1H), 7.91 (d, $J=2.27$ Hz, 1H), 7.92 (d, $J=1.77$ Hz, 1H), 8.24 (d, $J=1.52$ Hz, 1H), 8.28 - 8.30 (m, 1H), 8.33 (s, 1H), 9.76 (d, $J=11.37$ Hz, 1H); ^{13}C NMR (100 MHz, Acetone- d_4); δ 35.78, 48.88, 97.94, 97.98, 98.83, 100.19, 102.56, 102.81, 104.78, 104.89, 107.50, 107.60, 107.68, 108.26, 108.81, 111.20, 111.53, 111.71, 111.80, 112.70, 116.23, 118.98, 119.26, 120.42, 121.39, 125.85, 130.40, 137.83, 138.61, 142.56, 146.16, 146.67, 147.48, 196.11, 196.30, 196.32, 196.49, 196.70; m/z (+EI) calc. For $\text{C}_{38}\text{H}_{32}\text{N}_4\text{O}_7$ (M^+) 656.68, found 656.87 ($\text{M}+\text{H}$) $^+$; Yield: 51%.

Procedure for the synthesis of 2-(2,3-dihydrobenzofuran-5-yl)-*N*-(3-(5-((2-((3-(dimethylamino)propyl)

carbamoyl)benzofuran-5-yl)carbamoyl)furan-2-yl)phenyl)-5-methylthiazole-4-carboxamide (4.114) from 4.69 and 2-(2,3-dihydrobenzofuran-5-yl)-5-methylthiazole-4-carboxylic acid (4.113)

2.0 eq of HOBT and 1.75 eq. of DIC were added to a solution of **4.69** (1eq., 31 mg) in DMF. After 30 minutes, 2.0 eq. (36 mg) of **4.113** was added and the reaction mixture was allowed to stand for 3 hours. After completion, the reaction mixture was passed through a SCX-2 cartridge (500 mg), which was washed with DCM (3x), DMF (3x) twice and finally MeOH (2x). The product **4.114** was released from the cartridge using 5.0 ml 2M NH_3 in MeOH and concentrated *in vacuo* to obtain colourless oil (26 mg).

2-(2,3-Dihydrobenzofuran-5-yl)-*N*-(3-(5-((2-((3-(dimethylamino)propyl)
carbamoyl)benzofuran-5-yl)carbamoyl)furan-2-yl)phenyl)-5-methylthiazole-4-
carboxamide (4.114):

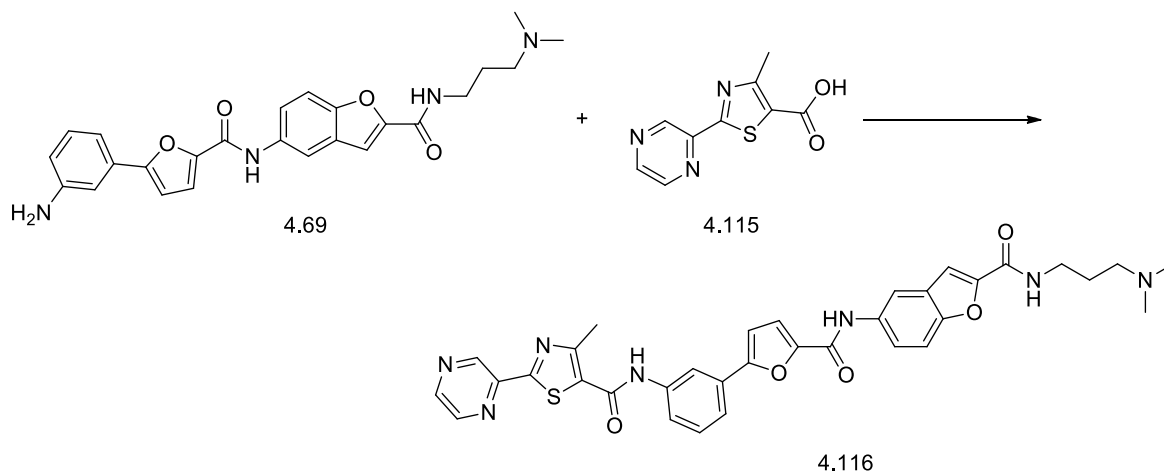


Colourless oil. IR (FTIR, $\nu_{\text{max}}/\text{cm}^{-1}$) 689.85, 736.01, 786.86, 861.17, 939.68, 1020.63, 1101.77, 1231.67, 1301.82, 1432.25, 1460.44, 1529.72, 1584.25, 1649.65, 2357.05, 2780.48, 2817.07, 2943.15, 3280.48; ^1H NMR (400 MHz, DMSO- d_6 , TMS); δ 1.67 (t, $J=7.07$ Hz, 2H), 2.15 (s, 6H), 2.28 (t, $J=6.95$ Hz, 2H), 2.66 (s, 3H), 3.25 - 3.29 (m, 2H), 3.33 (br. s., 2H), 4.63 (t, $J=8.84$ Hz, 2H), 6.90 (d, $J=8.34$ Hz, 1H), 7.13 (d, $J=3.54$ Hz, 1H), 7.47 (d, $J=3.54$ Hz, 1H), 7.50 (d, $J=8.08$ Hz, 1H), 7.53 (d, $J=0.76$ Hz, 1H), 7.65 (d, $J=9.09$ Hz, 1H), 7.69 - 7.70 (m, 1H), 7.71 - 7.73 (m, 1H), 7.75 (d, $J=2.02$ Hz, 1H), 7.76 - 7.78 (m, 1H), 7.88 (d, $J=1.52$ Hz, 1H), 8.18 (d, $J=2.02$ Hz, 2H), 8.77 (t, $J=5.68$ Hz, 1H), 10.30 (s, 1H), 10.31 (s, 1H); ^{13}C NMR (100 MHz, DMSO- d_6); δ 17.21, 26.90, 28.58, 37.34, 40.14, 45.10, 56.87, 71.81, 108.01, 109.29, 109.55, 111.67, 114.04, 116.86, 120.76, 121.09, 123.33, 124.45, 125.14, 127.07, 127.25, 128.96, 129.36, 129.69, 134.32, 139.21, 140.0, 146.76, 148.72, 150.01, 150.90, 155.01, 155.93, 156.13, 157.88, 160.16, 162.26, 166.85; m/z (+EI) calc. For $\text{C}_{38}\text{H}_{35}\text{N}_5\text{O}_6\text{S}$ (M^+) 689.78, found 690.93 ($\text{M}+\text{H}$) $^+$; Yield: 54%.

Procedure for the synthesis of *N*-(3-(5-((2-((3-(dimethylamino)propyl)carbamoyl)benzofuran-5-yl)carbamoyl)furan-2-yl)phenyl)-4-methyl-2-(pyrazin-2-yl)thiazole-5-carboxamide (4.116) from 4.69 and 4-methyl-2-(pyrazin-2-yl)thiazole-5-carboxylic acid (4.115)

2.0 eq of HOBT and 1.75 eq. of DIC were added to a solution of **4.69** (1eq., 35 mg) in DMF. After 30 minutes, 2.0 eq. (35 mg) of **4.115** was added and the reaction mixture was allowed to stand for 3 hours. After completion, the reaction mixture was passed through a SCX-2 cartridge (500 mg), which was washed with DCM (3x), DMF (3x) twice and finally MeOH (2x). The product **4.116** was released from the cartridge using 5.0 ml 2M NH_3 in MeOH and concentrated *in vacuo* to obtain colourless, viscous material (40 mg).

***N*-(3-(5-((2-((3-(Dimethylamino)propyl)carbamoyl)benzofuran-5-yl)carbamoyl)furan-2-yl)phenyl)-4-methyl-2-(pyrazin-2-yl)thiazole-5-carboxamide (4.116):**



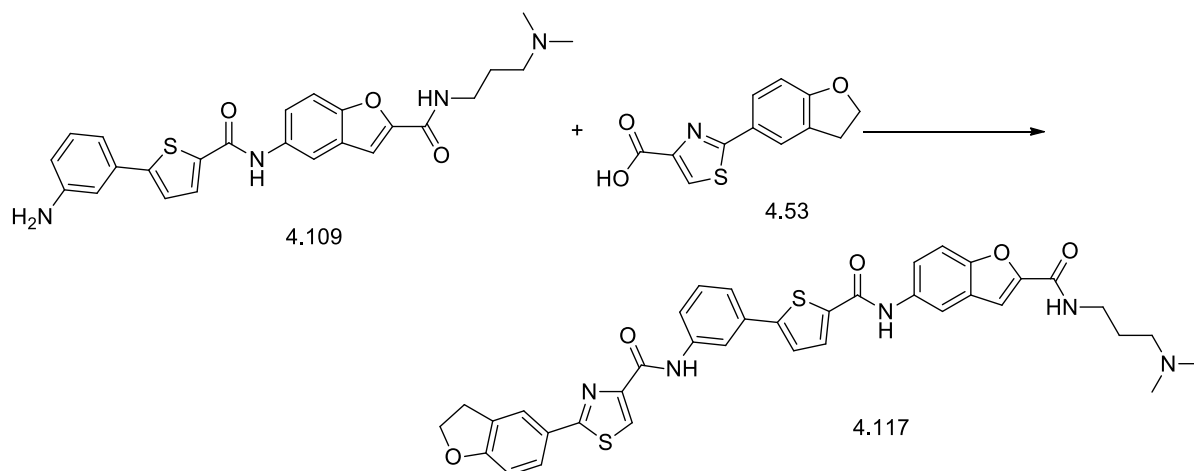
Colourless viscous mass. IR (FTIR, $\nu_{\text{max}}/\text{cm}^{-1}$) 685.21, 781.11, 880.83, 1013.16, 1104.28, 1166.05, 1203.46, 1234.17, 1300.57, 1348.24, 1434.26, 1469.72, 1513.77, 1557.36, 1584.31, 1644.68, 2356.80, 2936.00, 3266.89; ^1H NMR (400 MHz, $\text{DMSO}-d_6$, TMS); δ 1.70 (t, $J=6.95$ Hz, 2H), 2.22 (s, 6H), 2.37 (t, $J=7.07$ Hz, 2H), 2.73 (s, 3H), 3.30 (br. s., 2H), 7.14 (d, $J=3.54$ Hz, 1H), 7.48 (d, $J=3.54$ Hz, 1H), 7.51 (t, $J=7.96$ Hz, 1H), 7.54 (d, $J=0.76$ Hz, 1H), 7.65 (d, $J=9.09$ Hz, 1H), 7.72 (d, $J=2.02$ Hz, 1H), 7.74 - 7.76 (m, 1H), 7.77 (t, $J=1.64$ Hz, 1H), 8.19 (d, $J=2.02$ Hz, 1H), 8.21 (t, $J=1.77$ Hz, 1H), 8.76 - 8.80 (m, 2H), 8.82 (d, $J=2.53$ Hz, 1H), 9.36 (d, $J=1.52$ Hz, 1H), 10.30 (s, 1H), 10.52 (s, 1H); ^{13}C NMR (100 MHz, $\text{DMSO}-d_6$); δ 17.17, 26.60, 37.17, 40.14, 44.77, 56.60, 109.35, 111.67, 113.53, 114.03, 116.55, 116.72, 120.77, 127.25, 128.61, 129.73, 134.33, 136.43, 139.05, 140.65, 144.75, 145.28, 146.48, 146.78, 149.96, 150.90, 154.95, 156.13, 156.88, 157.92, 159.86, 161.32, 162.54, 164.90; m/z (+EI) calc. For $\text{C}_{34}\text{H}_{31}\text{N}_7\text{O}_5\text{S}$ (M^+) 649.72, found 649.61 ($\text{M}+\text{H}$) $^+$; Yield: 78%.

Procedure for the synthesis of 2-(2,3-dihydrobenzofuran-5-yl)-*N*-(3-(5-((2-((3-(dimethylamino)propyl)carbamoyl)benzofuran-5-yl)carbamoyl)thiophen-2-yl)phenyl)thiazole-4-carboxamide (4.117) from 5-(5-(3-aminophenyl)thiophene-2-carboxamido)-*N*-(3-(dimethylamino)propyl)benzofuran-2-carboxamide (4.109) and 2-(2,3-dihydrobenzofuran-5-yl)thiazole-4-carboxylic acid (4.53)

2.0 eq of HOBT and 1.75 eq. of DIC were added to a solution of **4.109** (1eq., 28 mg) in DMF. After 30 minutes, 2.0 eq. (30 mg) of **4.53** was added and the reaction mixture was allowed to stand for 3 hours. After completion, the reaction mixture was passed through a

SCX-2 cartridge (500 mg), which was washed with DCM (3x), DMF (3x) twice and finally MeOH (2x). The product **4.117** was released from the cartridge using 5.0 ml 2M NH₃ in MeOH and concentrated *in vacuo* to obtain a light green powder (30 mg).

2-(2,3-Dihydrobenzofuran-5-yl)-N-(3-(5-((2-((3-(dimethylamino)propyl)carbamoyl)benzofuran-5-yl)carbamoyl)thiophen-2-yl)phenyl)thiazole-4-carboxamide (4.117):



Light green powder. IR (FTIR, $\nu_{\text{max}}/\text{cm}^{-1}$) 622.10, 641.49, 677.69, 732.92, 747.39, 771.95, 804.76, 877.07, 941.35, 981.10, 103.92, 1112.12, 1163.00, 1194.23, 1237.39, 1255.95, 1276.28, 1299.08, 1347.58, 1415.86, 1434.30, 1454.00, 1550.54, 1590.48, 1638.51, 2361.62, 2768.29, 2815.15, 2941.68, 3318.34, 3353.65; ¹H NMR (400 MHz, DMSO-*d*₆, TMS); δ 1.68 (t, *J*=7.20 Hz, 2H), 2.16 (s, 6H), 2.29 (t, *J*=6.82 Hz, 2H), 3.28 (br. s., 4H), 4.65 (t, *J*=8.84 Hz, 2H), 6.94 (d, *J*=8.34 Hz, 1H), 7.45 - 7.51 (m, 1H), 7.53 - 7.55 (m, 1H), 7.63 - 7.65 (m, 1H), 7.66 (s, 1H), 7.71 - 7.75 (m, 1H), 7.92 - 7.93 (m, 1H), 7.93 - 7.97 (m, 2H), 8.06 - 8.09 (m, 2H), 8.21 (d, *J*=2.02 Hz, 1H), 8.29 (t, *J*=1.89 Hz, 1H), 8.39 (s, 1H), 8.78 (t, *J*=5.68 Hz, 1H), 10.32 (s, 1H), 10.39 (s, 1H); ¹³C NMR (100 MHz, DMSO-*d*₆); δ 26.88, 28.61, 37.33, 45.07, 45.10, 56.84, 71.76, 109.37, 111.71, 112.47, 113.80, 114.96, 116.29, 117.60, 120.50, 120.53, 122.75, 123.74, 124.21, 125.19, 126.28, 127.30, 127.44, 128.74, 130.18, 133.36, 137.25, 138.91, 139.23, 149.85, 150.00, 150.86, 157.91, 159.27, 162.09, 169.30, 187.84; *m/z* (+EI) calc. For C₃₇H₃₃N₅O₅S₂ (M⁺) 691.82, found 691.87 (M+H)⁺; Yield: 71%.

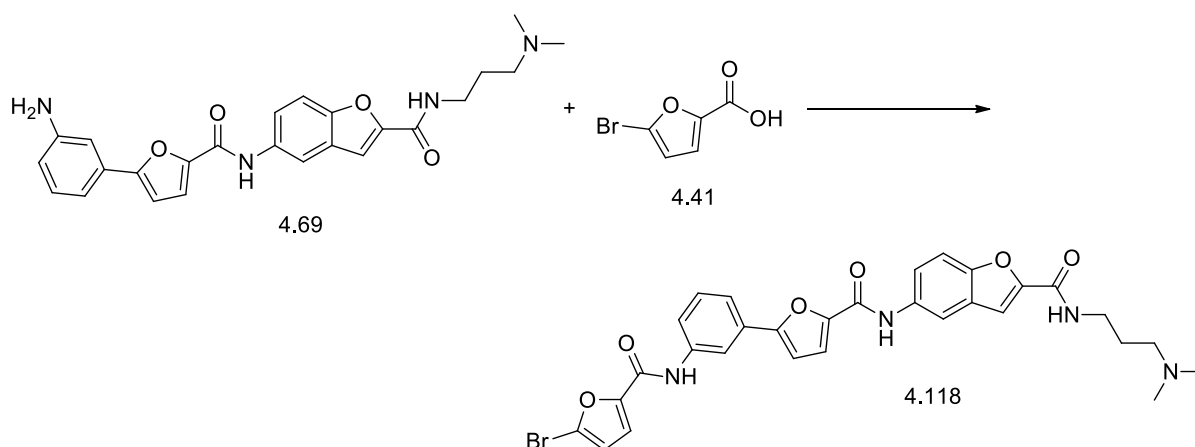
Again, intermediates **4.118** to **4.121** were synthesized by amide coupling reaction between 5-(5-(3-aminophenyl)furan-2-carboxamido)-*N*-(3-(dimethylamino)propyl)benzofuran-2-carboxamide (**4.69**) and 5-bromofuran-2-carboxylic acid (**4.41**), 5-bromothiophene-2-

carboxylic acid (**4.107**) and 2-bromo-4-methylthiazole-5-carboxylic acid (**4.120**), respectively.

Procedure for the synthesis of 5-(5-(3-(5-bromofuran-2-carboxamido)phenyl)furan-2-carboxamido)-N-(3-(dimethylamino)propyl)benzofuran-2-carboxamide (4.118**)**

2.0 eq of HOBT and 1.75 eq. of DIC were added to a solution of **4.69** (1eq., 196 mg) in DMF. After 30 minutes, 2.2 eq. (184 mg) of **4.41** was added and the reaction mixture was allowed to stand for 3 hours. After completion, the reaction mixture was passed through a SCX-2 cartridge (5 gm), which was washed with DCM (3x), DMF (3x) twice and finally MeOH (2x). The product **4.118** was released from the cartridge using 5.0 ml 2M NH₃ in MeOH and concentrated *in vacuo* to obtain 171 mg yellow oil.

5-(5-(3-(5-Bromofuran-2-carboxamido)phenyl)furan-2-carboxamido)-N-(3-(dimethylamino)propyl)benzofuran-2-carboxamide (4.118**):**



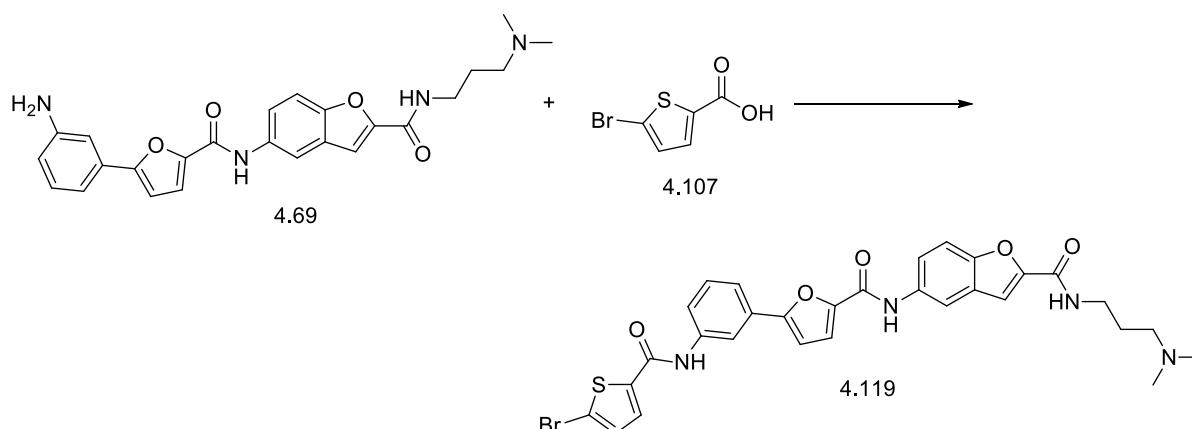
Yellow oil. IR (FTIR, $\nu_{\text{max}}/\text{cm}^{-1}$) 630.99, 682.65, 736.90, 863.46, 925.46, 959.04, 1108.85, 1168.26, 1204.42, 1295.06, 1431.73, 1462.73, 1514.39, 1585.91, 1644.03, 2356.58, 2940.56, 3278.85; ¹H NMR (400 MHz, DMSO-*d*₆, TMS); δ 1.67 (t, *J*=7.07 Hz, 2H), 2.15 (s, 6H), 2.28 (t, *J*=7.07 Hz, 2H), 3.27 - 3.31 (m, 2H), 6.86 (d, *J*=3.54 Hz, 1H), 7.12 (d, *J*=3.54 Hz, 1H), 7.42 (d, *J*=3.54 Hz, 1H), 7.46 - 7.48 (m, 1H), 7.48 - 7.51 (m, 1H), 7.54 (d, *J*=0.76 Hz, 1H), 7.66 (d, *J*=8.84 Hz, 1H), 7.73 (dt, *J*=8.02, 1.17 Hz, 1H), 7.74 - 7.78 (m, 1H), 7.80 (ddd, *J*=8.21, 2.02, 0.88 Hz, 1H), 8.17 - 8.19 (m, 2H), 8.77 (t, *J*=5.68 Hz, 1H), 10.29 (s, 1H), 10.38 (s, 1H); ¹³C NMR (100 MHz, DMSO-*d*₆); δ 26.68, 37.12, 39.62, 44.88, 56.65, 107.70, 109.08, 111.46, 113.83, 114.10, 116.28, 116.50, 117.08, 120.11, 120.55, 120.77, 125.25, 127.04, 129.14, 129.46, 134.11, 138.61, 146.55, 148.92, 149.80, 150.70, 154.79, 154.99,

155.91, 157.67; m/z (+EI) calc. For $C_{30}H_{27}BrN_4O_6$ (M^+) 619.46, found 618.35 ($M+H$)⁺; Yield: 63%.

Procedure for the synthesis of 5-(5-(3-(5-bromothiophene-2-carboxamido)phenyl)furan-2-carboxamido)-*N*-(3-(dimethylamino)propyl)benzofuran-2-carboxamide (4.119)

2.0 eq of HOBT and 1.75 eq. of DIC were added to a solution of **4.69** (1eq., 231 mg) in DMF. After 30 minutes, 2.0 eq. (214 mg) of **4.107** was added and the reaction mixture was allowed to stand for 3 hours. After completion, the reaction mixture was passed through a SCX-2 cartridge (500 mg), which was washed with DCM (3x), DMF (3x) twice and finally MeOH (2x). The product **4.119** was released from the cartridge using 5.0 ml 2M NH_3 in MeOH and concentrated *in vacuo* to obtain colourless oil (250 mg).

5-(5-(3-(5-Bromothiophene-2-carboxamido)phenyl)furan-2-carboxamido)-*N*-(3-(dimethylamino)propyl)benzofuran-2-carboxamide (4.119):



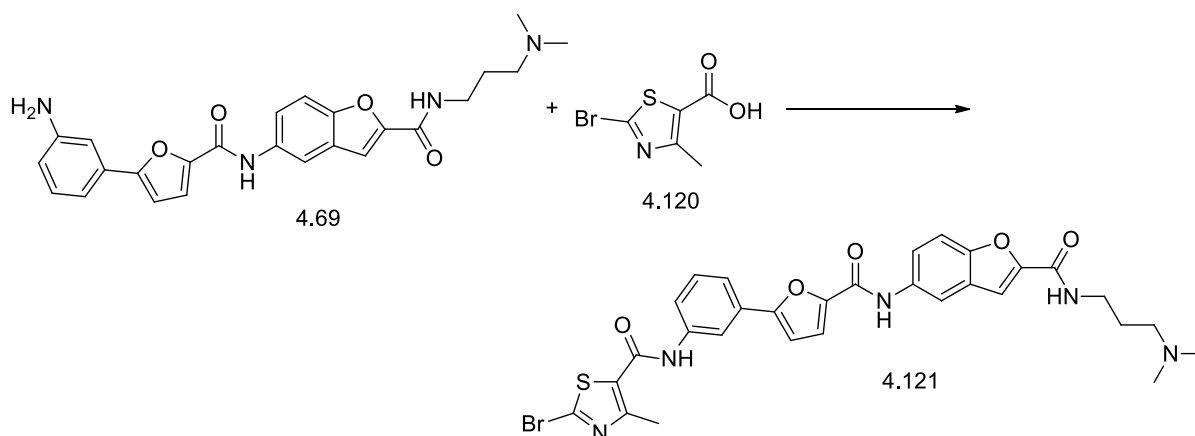
Colourless, oily mass. IR (FTIR, ν_{max}/cm^{-1}) 680.07, 734.02, 779.57, 801.47, 878.72, 976.56, 1027.73, 1099.49, 1170.07, 1201.84, 1234.21, 1262.43, 1293.07, 1352.23, 1425.53, 1469.49, 1513.61, 1555.87, 1585.63, 1638.76, 2346.25, 2775.19, 2816.53, 2857.88, 2934.17, 3279.67; 1H NMR (400 MHz, $DMSO-d_6$, TMS); δ 1.70 (t, $J=7.07$ Hz, 2H), 2.21 (s, 6H), 2.36 (t, $J=7.07$ Hz, 2H), 3.31 - 3.34 (m, 2H), 7.13 (d, $J=3.54$ Hz, 1H), 7.39 (d, $J=4.04$ Hz, 1H), 7.47 - 7.48 (m, 1H), 7.51 (d, $J=7.83$ Hz, 1H), 7.54 (d, $J=0.76$ Hz, 1H), 7.66 (d, $J=8.84$ Hz, 1H), 7.72 (d, $J=1.52$ Hz, 1H), 7.74 - 7.76 (m, 1H), 7.77 - 7.78 (m, 1H), 7.92 (d, $J=4.04$ Hz, 1H), 8.17 - 8.18 (m, 1H), 8.18 (d, $J=2.27$ Hz, 1H), 8.78 (t, $J=5.81$ Hz, 1H), 10.30 (s, 1H), 10.47 (s, 1H); ^{13}C NMR (100 MHz, $DMSO-d_6$); δ 26.66, 37.20, 41.12, 44.83, 56.66, 107.96, 109.34, 111.67, 114.03, 116.36, 116.69, 118.00, 119.45, 120.38, 120.77, 127.25, 129.73, 130.03,

131.75, 134.32, 138.94, 141.59, 145.27, 146.77, 149.97, 150.90, 154.97, 156.13, 157.91, 158.90; m/z (+EI) calc. For $C_{30}H_{27}BrN_4O_5S$ (M^+) 635.53, found 636.38 ($M+H$)⁺; Yield: 76%.

Procedure for the synthesis of 2-bromo-*N*-(3-(5-((2-((3-(dimethylamino)propyl)carbamoyl)benzofuran-5-yl)carbamoyl)furan-2-yl)phenyl)-4-methylthiazole-5-carboxamide (4.121)

2.0 eq of HOBT and 1.75 eq. of DIC were added to a solution of **4.69** (1eq., 100 mg) in DMF. After 30 minutes, 2.0 eq. (94 mg) of **4.120** was added and the reaction mixture was allowed to stand for 3 hours. After completion, the reaction mixture was passed through a SCX-2 cartridge (500 mg), which was washed with DCM (3x), DMF (3x) twice and finally MeOH (2x). The product **4.121** was released from the cartridge using 5.0 ml 2M NH_3 in MeOH and concentrated *in vacuo* to obtain colourless oil (63 mg).

2-Bromo-*N*-(3-(5-((2-((3-(dimethylamino)propyl)carbamoyl)benzofuran-5-yl)carbamoyl)furan-2-yl)phenyl)-4-methylthiazole-5-carboxamide (4.121):



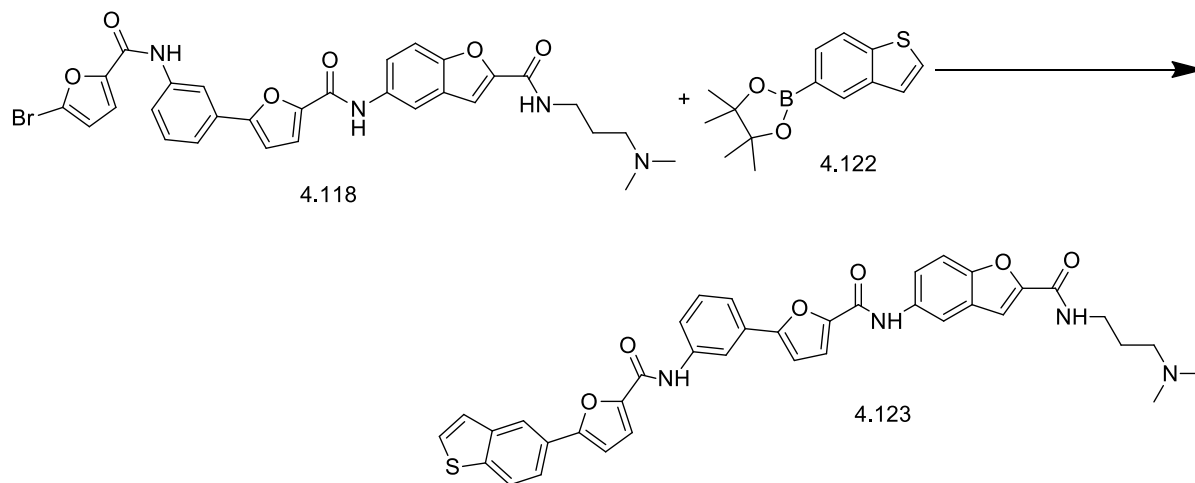
Colourless oil. IR (FTIR, ν_{max}/cm^{-1}) 630.65, 682.65, 785.93, 925.46, 1019.68, 1126.93, 1225.09, 1349.07, 1535.05, 1555.71, 1644.86, 1981.63, 2345.61, 2903.67, 3215.53; 1H NMR (400 MHz, $CDCl_3$, TMS); δ 1.70 - 1.73 (m, 2H), 2.28 (br. s., 6H), 2.40 - 2.46 (m, 2H), 2.50 (s, 3H), 3.50 - 3.52 (m, 2H), 7.13 - 7.15 (m, 1H), 7.35 (d, $J=3.03$ Hz, 1H), 7.53 (br. s., 1H), 7.57 - 7.59 (m, 1H), 7.60 - 7.65 (m, 1H), 7.70 - 7.73 (m, 1H), 7.83 - 7.93 (m, 1H), 8.23 - 8.36 (m, 2H), 8.44 (br. s., 1H); ^{13}C NMR (100 MHz, $CDCl_3$); δ 15.3, 26.54, 36.15, 43.02, 46.94, 56.80, 106.39, 109.45, 109.59, 113.24, 115.89, 118.09, 120.93, 121.55, 122.69, 126.67, 129.54, 131.12, 131.32, 138.12, 145.87, 150.32, 151.94, 156.38, 158.14, 159.33, 160.94, 161.57, 162.39, 168.49; m/z (+EI) calc. For $C_{30}H_{28}BrN_5O_5S$ (M^+) 650.54, found 651.59 ($M+H$)⁺; Yield: 63%.

From **4.118**, **4.119** and **4.121** intermediates final compounds **4.123** to **4.133** were synthesized by following the general conditions for the Suzuki coupling reaction.

Procedure for the synthesis of 5-(5-(3-(5-(benzo[*b*]thiophen-5-yl)furan-2-carboxamido)phenyl)furan-2-carboxamido)-*N*-(3-(dimethylamino)propyl)benzofuran-2-carboxamide (4.123**) from **4.118** and (2-(benzo[*b*]thiophen-5-yl)-4,5,5-trimethyl-1,3,2-dioxaborolan-4-yl)methylum (**4.122**)**

A catalytic amount of tetrakis(triphenylphosphine)palladium, Pd(PPh₃)₄ (0.1 eq.) was added to a solution of **4.118** (1.0 eq., 53 mg) and **4.122** (2.2 eq., 49 mg) in a 9:3:1 combination of EtOH, toluene and water in the presence of K₂CO₃ (3.0 eq.) in a 10 ml microwave vial containing a magnetic stirrer. The reaction vessel was flushed with nitrogen during each addition. The reaction mixture was sealed in an inert nitrogen environment and heated with microwave radiation in an EMRYS™ Optimizer Microwave Station (Personal Chemistry) at 100 °C for 15 minutes. After completion, the reaction mixture was passed through a SCX-2 cartridge (1 gm), which was washed with DCM (3x), DMF (3x) twice and finally MeOH (2x). The product **4.123** was released from the cartridge using 5.0 ml 2M NH₃ in MeOH and concentrated *in vacuo* to obtain a colourless, oily mass (56 mg).

5-(5-(3-(5-(Benzo[*b*]thiophen-5-yl)furan-2-carboxamido)phenyl)furan-2-carboxamido)-*N*-(3-(dimethylamino)propyl)benzofuran-2-carboxamide (4.123**):**



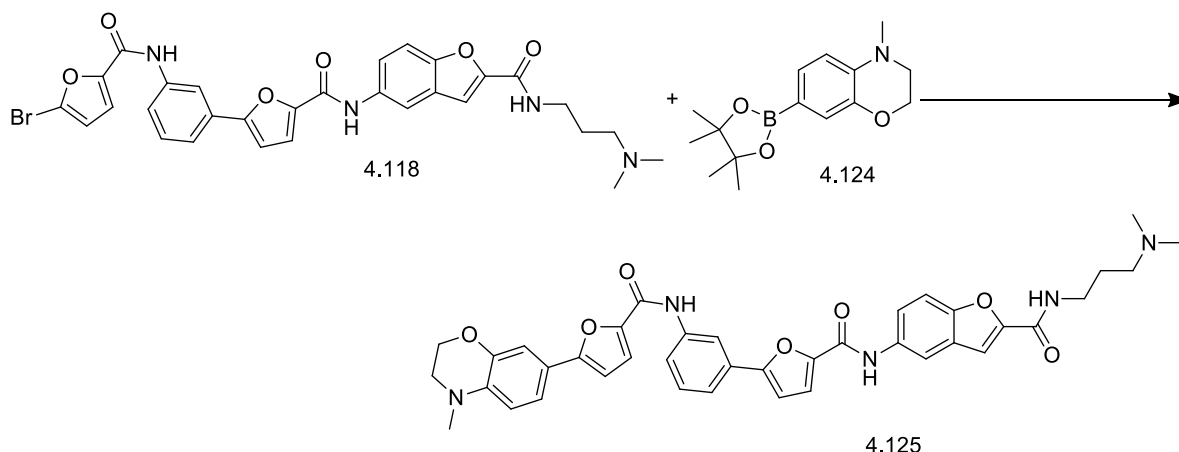
Colourless, oily mass. IR (FTIR, $\nu_{\text{max}}/\text{cm}^{-1}$) 694.15, 748.85, 794.36, 890.65, 954.96, 1020.00, 1120.48, 1203.74, 1265.07, 1297.37, 1348.72, 1434.80, 1469.53, 1523.97, 1586.29, 1643.98, 1738.82, 2360.24, 2768.29, 2938.91, 3279.54; ¹H NMR (400 MHz, DMSO-*d*₆, TMS); δ 1.68 (quin, *J*=7.07 Hz, 2H), 2.16 (s, 6H), 2.29 (t, *J*=7.07 Hz, 2H), 3.28 - 3.31 (m, 2H), 7.16 (d,

$J=3.54$ Hz, 1H), 7.25 (d, $J=3.54$ Hz, 1H), 7.48 (d, $J=2.27$ Hz, 1H), 7.49 (d, $J=2.27$ Hz, 1H), 7.50 - 7.53 (m, 1H), 7.54 (d, $J=1.01$ Hz, 1H), 7.55 - 7.57 (m, 1H), 7.59 - 7.63 (m, 1H), 7.66 (d, $J=9.09$ Hz, 1H), 7.76 (d, $J=2.02$ Hz, 1H), 7.86 (s, 1H), 7.87 - 7.88 (m, 1H), 7.99 (dd, $J=8.46$, 1.64 Hz, 1H), 8.15 (d, $J=8.59$ Hz, 1H), 8.20 (d, $J=2.02$ Hz, 1H), 8.25 (t, $J=1.77$ Hz, 1H), 8.52 (d, $J=1.52$ Hz, 1H), 8.78 (t, $J=5.81$ Hz, 1H), 10.31 (s, 1H), 10.39 (s, 1H); ^{13}C NMR (100 MHz, DMSO- d_6); δ 26.85, 37.31, 40.14, 45.04, 56.81, 107.74, 107.93, 109.31, 111.67, 114.07, 116.74, 116.78, 117.32, 119.20, 120.79, 121.31, 123.17, 125.76, 127.26, 128.64, 128.76, 129.33, 129.70, 131.48, 131.98, 132.20, 134.22, 138.99, 139.39, 146.37, 146.77, 150.01, 150.92, 155.08, 155.66, 156.15, 156.20, 157.90; m/z (+EI) calc. For $\text{C}_{38}\text{H}_{32}\text{N}_4\text{O}_6\text{S}$ (M^+) 672.75, found 672.61 ($\text{M}+\text{H}$) $^+$; Yield: 97%.

Procedure for the synthesis of *N*-(3-(dimethylamino)propyl)-5-(5-(3-(5-(4-methyl-3,4-dihydro-2*H*-benzo[*b*][1,4]oxazin-7-yl)furan-2-carboxamido)phenyl)furan-2-carboxamido)benzofuran-2-carboxamide (4.125) from 4.118 and 4-methyl-7-(4,4,5,5-tetramethyl-1,3,2-dioxaborolan-2-yl)-3,4-dihydro-2*H*-benzo[*b*][1,4]oxazine (4.124)

A catalytic amount of tetrakis(triphenylphosphine)palladium, $\text{Pd}(\text{PPh}_3)_4$ (0.1 eq.) was added to a solution of **4.118** (1.0 eq., 58 mg) and **4.124** (2.2 eq., 57 mg) in a 9:3:1 combination of EtOH, toluene and water in the presence of K_2CO_3 (3.0 eq.) in a 10 ml microwave vial containing a magnetic stirrer. The reaction vessel was flushed with nitrogen during each addition. The reaction mixture was sealed in an inert nitrogen environment and heated with microwave radiation in an EMRYSTM Optimizer Microwave Station (Personal Chemistry) at 100 °C for 15 minutes. After completion the reaction mixture was passed through a SCX-2 cartridge (1 gm), which was washed with DCM (3x), DMF (3x) twice and finally MeOH (2x). The product **4.125** was released from the cartridge using 5.0 ml 2M NH_3 in MeOH and concentrated *in vacuo* to obtain dark orange oil (59 mg).

***N*-(3-(Dimethylamino)propyl)-5-(5-(3-(5-(4-methyl-3,4-dihydro-2*H*-benzo[*b*][1,4]oxazin-7-yl)furan-2-carboxamido)phenyl)furan-2-carboxamido)benzofuran-2-carboxamide (4.125):**

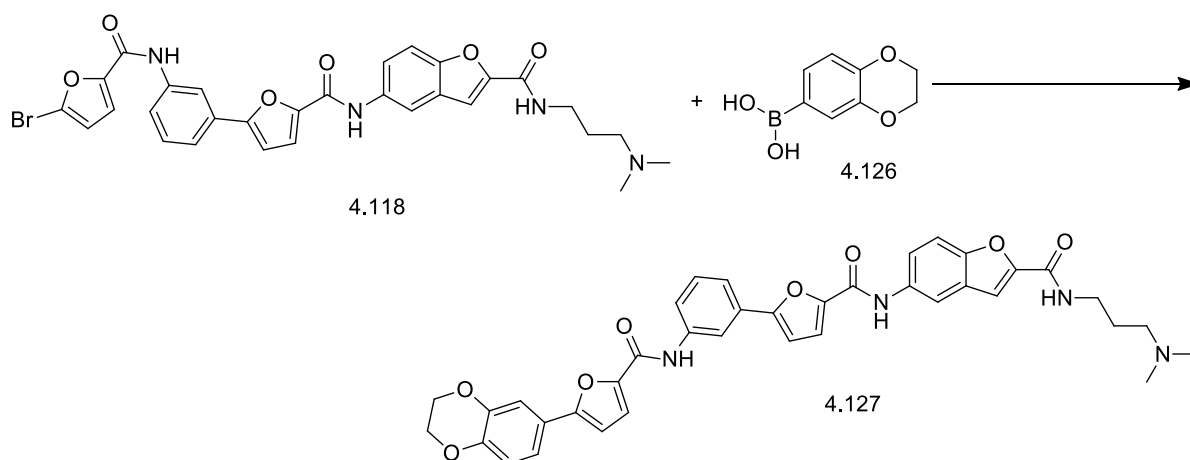


Dark orange oil. IR (FTIR, $\nu_{\text{max}}/\text{cm}^{-1}$) 631.52, 660.45, 693.76, 792.66, 865.52, 955.41, 1031.36, 1095.60, 1201.31, 1258.85, 1309.42, 13378.86, 1385.91, 1435.80, 1469.53, 1490.38, 1555.83, 1585.97, 1653.79, 2360.47, 2823.17, 2938.24, 3273.12; ^1H NMR (400 MHz, Acetone- d_4 , TMS); δ 1.77 (t, $J=6.69$ Hz, 2H), 2.22 (d, $J=0.76$ Hz, 6H), 2.39 (td, $J=6.44$, 1.26 Hz, 2H), 2.94 (s, 3H), 3.34 - 3.37 (m, 2H), 3.46 - 3.50 (m, 2H), 4.27 - 4.30 (m, 2H), 6.74 (d, $J=8.59$ Hz, 1H), 6.78 (d, $J=3.54$ Hz, 1H), 7.02 (d, $J=3.54$ Hz, 1H), 7.23 (d, $J=2.02$ Hz, 1H), 7.32 (d, $J=3.54$ Hz, 1H), 7.34 (t, $J=0.88$ Hz, 1H), 7.42 (s, 1H), 7.43 - 7.46 (m, 1H), 7.50 - 7.52 (m, 1H), 7.52 - 7.54 (m, 1H), 7.57 - 7.63 (m, 1H), 7.64 - 7.65 (m, 1H), 7.66 (d, $J=1.52$ Hz, 1H), 7.67 - 7.72 (m, 1H), 7.84 (d, $J=8.84$ Hz, 1H), 7.91 (d, $J=8.08$ Hz, 1H), 7.95 (s, 1H), 8.28 (t, $J=1.89$ Hz, 1H); ^{13}C NMR (100 MHz, Acetone- d_4); δ 26.68, 36.23, 40.06, 49.31, 49.34, 56.01, 96.37, 99.15, 102.91, 103.30, 103.51, 105.16, 105.26, 108.05, 108.83, 109.92, 110.70, 111.39, 111.92, 112.12, 119.33, 119.92, 120.04, 120.71, 121.65, 121.71, 123.19, 123.27, 129.08, 135.69, 137.36, 138.93, 142.24, 142.92, 147.09, 148.38, 149.38, 149.45, 153.31; m/z (+EI) calc. For $\text{C}_{39}\text{H}_{37}\text{N}_5\text{O}_7$ (M^+) 687.74, found 688.22 ($\text{M}+\text{H}$) $^+$; Yield: 92%.

Procedure for the synthesis of 5-(5-(3-(5-(2,3-dihydrobenzo[*b*][1,4]dioxin-6-yl)furan-2-carboxamido)phenyl)furan-2-carboxamido)-*N*-(3-(dimethylamino)propyl)benzofuran-2-carboxamide (4.127) from 4.118 and (2,3-dihydrobenzo[*b*][1,4]dioxin-6-yl)boronic acid (4.126)

A catalytic amount of tetrakis(triphenylphosphine)palladium, Pd(PPh₃)₄ (0.1 eq.) was added to a solution of **4.118** (1.0 eq., 50 mg) and **4.126** (2.2 eq., 30 mg) in a 9:3:1 combination of EtOH, toluene and water in the presence of K₂CO₃ (3.0 eq.) in a 10 ml microwave vial containing a magnetic stirrer. The reaction vessel was flushed with nitrogen during each addition. The reaction mixture was sealed in an inert nitrogen environment and heated with microwave radiation in an EMRYS™ Optimizer Microwave Station (Personal Chemistry) at 100 °C for 15 minutes. After completion, the reaction mixture was passed through a SCX-2 cartridge (1 gm), which was washed with DCM (3x), DMF (3x) twice and finally MeOH (2x). The product **4.127** was released from the cartridge using 5.0 ml 2M NH₃ in MeOH and concentrated *in vacuo* to obtain light green oil (43 mg).

5-(5-(3-(5-(2,3-Dihydrobenzo[*b*][1,4]dioxin-6-yl)furan-2-carboxamido)phenyl)furan-2-carboxamido)-*N*-(3-(dimethylamino)propyl)benzofuran-2-carboxamide (4.127):



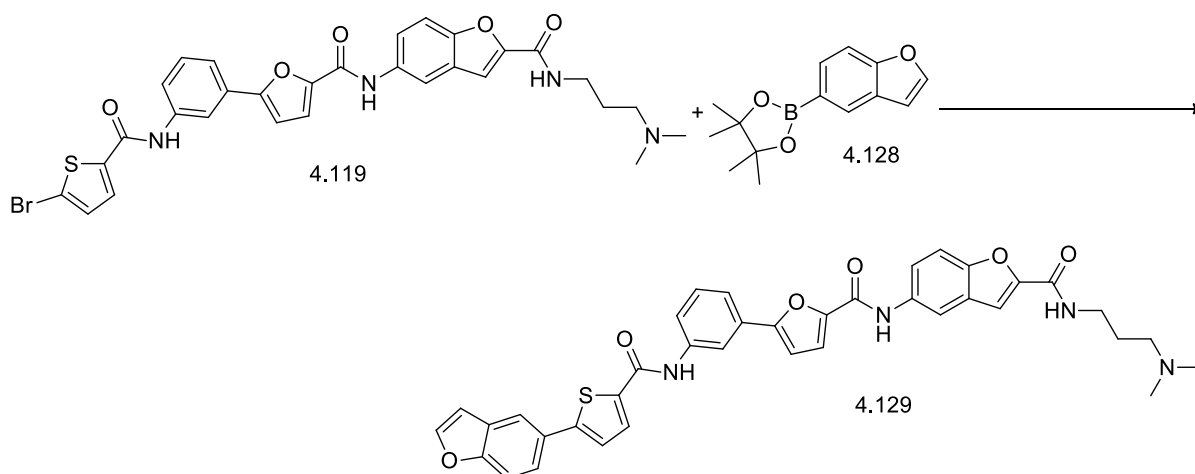
Light green oil. IR (FTIR, $\nu_{\text{max}}/\text{cm}^{-1}$) 689.88, 745.63, 789.78, 853.87, 890.10, 926.25, 954.27, 1020.45, 1067.83, 1126.25, 1226.86, 1243.88, 1280.53, 1308.81, 1352.43, 1435.54, 1468.54, 1547.72, 1582.32, 1650.68, 1705.46, 2357.65, 2938.77, 3293.76; ¹H NMR (400 MHz, Acetone-*d*₄, TMS); δ 1.75 - 1.82 (m, 2H), 2.24 (d, *J*=3.54 Hz, 6H), 2.39 - 2.43 (m, 2H), 3.47 - 3.51 (m, 2H), 4.32 (d, *J*=4.29 Hz, 4H), 6.92 (br. s., 1H), 7.03 (t, *J*=3.92 Hz, 1H), 7.31 - 7.35 (m, 2H), 7.37 - 7.39 (m, 1H), 7.41 - 7.43 (m, 2H), 7.52 - 7.55 (m, 2H), 7.68 (d, *J*=7.07 Hz, 2H), 7.79 - 7.85 (m, 1H), 7.88 (br. s., 1H), 7.95 (br. s., 1H), 8.25 - 8.29 (m, 2H), 8.43 (br. s.,

1H), 9.72 (br. s., 1H); ^{13}C NMR (100 MHz, Acetone- d_4); δ 29.38, 35.80, 48.88, 48.90, 55.61, 97.50, 98.83, 107.45, 107.66, 108.29, 108.71, 109.16, 111.38, 111.83, 114.33, 118.97, 119.53, 119.66, 120.39, 121.35, 122.80, 122.86, 125.72, 135.16, 135.68, 137.67, 138.55, 138.58, 142.54, 146.65, 146.91, 147.17, 147.23, 147.31, 153.74, 158.12, 160.14, 162.35; m/z (+EI) calc. For $\text{C}_{38}\text{H}_{34}\text{N}_4\text{O}_8$ (M+) 674.70, found 675.04 (M+H) $^+$; Yield: 84%.

Procedure for the synthesis of 5-(5-(3-(5-(benzofuran-5-yl)thiophene-2-carboxamido)phenyl)furan-2-carboxamido)-N-(3-(dimethylamino)propyl)benzofuran-2-carboxamide (4.129) from 4.119 and 2-(benzofuran-5-yl)-4,4,5,5-tetramethyl-1,3,2-dioxaborolane (4.128)

A catalytic amount of tetrakis(triphenylphosphine)palladium, $\text{Pd}(\text{PPh}_3)_4$ (0.1 eq.) was added to a solution of **4.119** (1.0 eq., 45 mg) and **4.128** (2.2 eq., 38 mg) in a 9:3:1 combination of EtOH, toluene and water in the presence of K_2CO_3 (3.0 eq.) in a 10 ml microwave vial containing a magnetic stirrer. The reaction vessel was flushed with nitrogen during each addition. The reaction mixture was sealed in an inert nitrogen environment and heated with microwave radiation in an EMRYSTM Optimizer Microwave Station (Personal Chemistry) at 100 °C for 15 minutes. After completion the reaction mixture was passed through a SCX-2 cartridge (1 gm), which was washed with DCM (3x), DMF (3x) twice and finally MeOH (2x). The product **4.129** was released from the cartridge using 5.0 ml 2M NH_3 in MeOH and concentrated *in vacuo* to obtain colourless oily mass (32 mg).

5-(5-(3-(5-(Benzofuran-5-yl)thiophene-2-carboxamido)phenyl)furan-2-carboxamido)-N-(3-(dimethylamino)propyl)benzofuran-2-carboxamide (4.129):



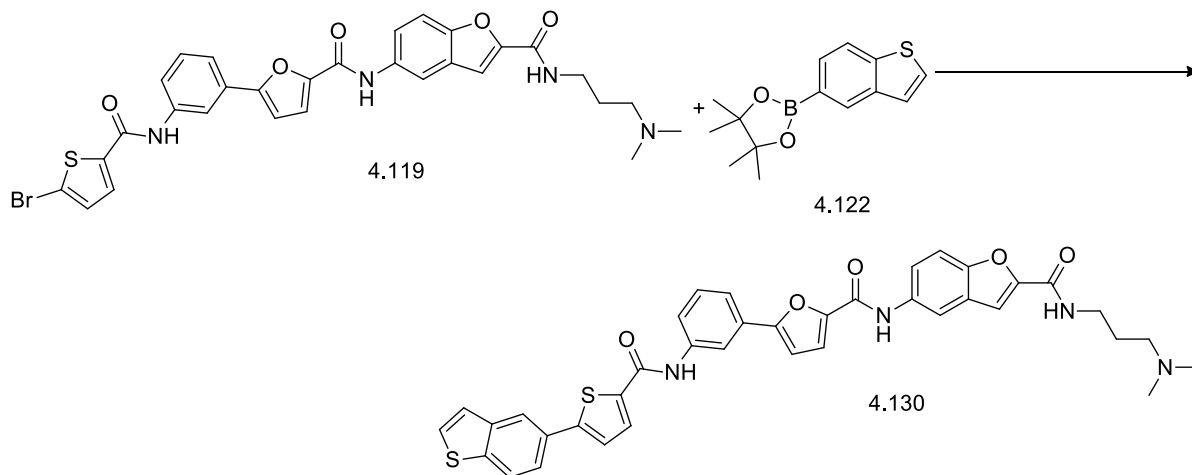
Colourless oil. IR (FTIR, $\nu_{\text{max}}/\text{cm}^{-1}$) 630.11, 681.17, 733.86, 777.78, 864.26, 955.93, 1027.61, 1109.57, 1129.86, 1170.41, 1234.15, 1259.95, 1294.38, 1350.84, 1438.17, 1469.68, 1513.19, 312

1539.15, 1585.07, 1640.35, 2361.40, 27774.39, 2817.07, 2853.65, 2931.22, 3286.35; ^1H NMR (400 MHz, DMSO- d_6 , TMS); δ 1.68 (t, $J=7.07$ Hz, 2H), 2.16 (s, 6H), 2.29 (t, $J=7.07$ Hz, 2H), 3.34 - 3.37 (m, 2H), 7.04 (dd, $J=2.02$, 0.76 Hz, 1H), 7.14 (d, $J=3.54$ Hz, 1H), 7.48 (d, $J=3.79$ Hz, 1H), 7.50 - 7.53 (m, 1H), 7.54 (d, $J=0.76$ Hz, 1H), 7.63 (d, $J=3.79$ Hz, 1H), 7.66 (d, $J=8.84$ Hz, 1H), 7.70 (s, 1H), 7.71 (d, $J=1.77$ Hz, 1H), 7.72 - 7.75 (m, 1H), 7.75 - 7.79 (m, 1H), 7.80 - 7.84 (m, 1H), 8.06 (dd, $J=1.64$, 0.88 Hz, 1H), 8.07 (d, $J=2.02$ Hz, 1H), 8.09 (d, $J=4.04$ Hz, 1H), 8.19 (d, $J=2.27$ Hz, 1H), 8.22 (t, $J=1.89$ Hz, 1H), 8.78 (t, $J=5.81$ Hz, 1H), 10.31 (s, 1H), 10.42 (s, 1H); ^{13}C NMR (100 MHz, DMSO- d_6); δ 26.86, 37.31, 45.05, 45.07, 56.83, 106.95, 109.29, 111.67, 112.03, 112.59, 116.29, 116.31, 116.70, 118.63, 120.76, 122.66, 124.09, 127.25, 127.89, 128.09, 128.24, 128.71, 129.37, 129.70, 130.42, 134.32, 138.11, 139.28, 146.75, 147.21, 150.00, 150.90, 154.38, 156.14, 157.88, 158.31, 159.86, 162.02; m/z (+EI) calc. For $\text{C}_{38}\text{H}_{32}\text{N}_4\text{O}_6\text{S}(\text{M}^+)$ 672.75, found 673.20 ($\text{M}+\text{H}$) $^+$; Yield: 67%.

Procedure for the synthesis of 5-(5-(3-(5-(benzo[*b*]thiophen-5-yl)thiophene-2-carboxamido)phenyl)furan-2-carboxamido)-*N*-(3-(dimethylamino)propyl)benzofuran-2-carboxamide (4.130) from 4.119 and 4.122

A catalytic amount of tetrakis(triphenylphosphine)palladium, $\text{Pd}(\text{PPh}_3)_4$ (0.1 eq.) was added to a solution of **4.119** (1.0 eq., 44 mg) and **4.122** (2.2 eq., 40 mg) in a 9:3:1 combination of EtOH, toluene and water in the presence of K_2CO_3 (3.0 eq.) in a 10 ml microwave vial containing a magnetic stirrer. The reaction vessel was flushed with nitrogen during each addition. The reaction mixture was sealed in an inert nitrogen environment and heated with microwave radiation in an EMRYSTM Optimizer Microwave Station (Personal Chemistry) at 100 °C for 20 minutes. After completion, the reaction mixture was passed through a SCX-2 cartridge (1 gm), which was washed with DCM (3x), DMF (3x) twice and finally MeOH (2x). The product **4.130** was released from the cartridge using 5.0 ml 2M NH_3 in MeOH and concentrated *in vacuo* to obtain a colourless oily mass (22 mg).

5-(5-(3-(5-(Benzo[*b*]thiophen-5-yl)thiophene-2-carboxamido)phenyl)furan-2-carboxamido)-*N*-(3-(dimethylamino)propyl)benzofuran-2-carboxamide (4.130):



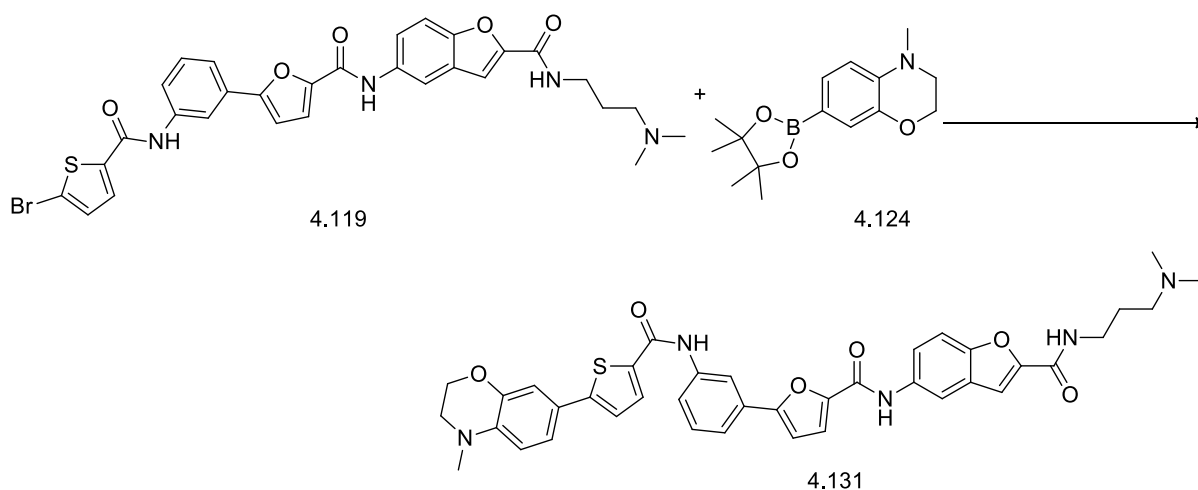
Colourless oily mass. IR (FTIR, $\nu_{\text{max}}/\text{cm}^{-1}$) 631.79, 680.33, 736.93, 774.51, 804/07, 854.27, 945.48, 1028.05, 1111.35, 1168.64, 1202.06, 1235.43, 1263.17, 1310.00, 1345.85, 1435.41, 1458.06, 1514.29, 1552.21, 1586.46, 1635.57, 2359.64, 2823.17, 2939.93, 3286.55; ^1H NMR (400 MHz, DMSO-*d*₆, TMS); δ 1.68 (t, $J=7.07$ Hz, 2H), 2.16 (s, 6H), 2.29 (t, $J=7.07$ Hz, 2H), 3.33 (br. s., 2H), 7.14 (d, $J=3.79$ Hz, 1H), 7.48 (d, $J=3.79$ Hz, 1H), 7.53 - 7.54 (m, 1H), 7.54 (d, $J=1.01$ Hz, 1H), 7.55 (s, 1H), 7.66 (d, $J=9.09$ Hz, 1H), 7.71 (d, $J=4.04$ Hz, 1H), 7.72 - 7.75 (m, 1H), 7.76 (d, $J=2.02$ Hz, 1H), 7.78 (d, $J=1.26$ Hz, 1H), 7.80 - 7.84 (m, 1H), 7.85 (d, $J=5.31$ Hz, 1H), 8.10 (d, $J=2.78$ Hz, 1H), 8.11 (d, $J=1.52$ Hz, 1H), 8.19 (d, $J=2.02$ Hz, 1H), 8.22 (t, $J=1.77$ Hz, 1H), 8.29 (d, $J=1.77$ Hz, 1H), 8.77 (t, $J=5.68$ Hz, 1H), 10.30 (s, 1H), 10.44 (s, 1H); ^{13}C NMR (100 MHz, DMSO-*d*₆); δ 26.87, 37.31, 45.06, 45.77, 56.84, 105.43, 107.57, 109.02, 109.30, 111.67, 114.03, 116.33, 116.71, 120.45, 122.12, 123.40, 124.16, 124.40, 127.26, 128.64, 128.76, 129.71, 130.45, 131.48, 134.33, 136.56, 138.32, 140.11, 142.84, 143.83, 146.76, 148.34, 150.01, 150.91, 155.08, 157.88, 166.59, 178.25; m/z (+EI) calc. For C₃₈H₃₂N₄O₅S (M+) 688.81, found 689.14 (M+H)⁺; Yield: 46%.

Procedure for the synthesis of *N*-(3-(dimethylamino)propyl)-5-(5-(3-(5-(4-methyl-3,4-dihydro-2*H*-benzo[*b*][1,4]oxazin-7-yl)thiophene-2-carboxamido)phenyl)furan-2-carboxamido)benzofuran-2-carboxamide (4.131) from 4.119 and 4.124

A catalytic amount of tetrakis(triphenylphosphine)palladium, Pd(PPh₃)₄ (0.1 eq.) was added to a solution of **4.119** (1.0 eq., 58 mg) and **4.124** (2.2 eq., 55 mg) in a 9:3:1 combination of

EtOH, toluene and water in the presence of K₂CO₃ (3.0 eq.) in a 10 ml microwave vial containing a magnetic stirrer. The reaction vessel was flushed with nitrogen during each addition. The reaction mixture was sealed in an inert nitrogen environment and heated with microwave radiation in an EMRYSTM Optimizer Microwave Station (Personal Chemistry) at 100 °C for 15 minutes. After completion the reaction mixture was passed through a SCX-2 cartridge (1 gm), which was washed with DCM (3x), DMF (3x) twice and finally MeOH (2x). The product **4.131** was released from the cartridge using 5.0 ml 2M NH₃ in MeOH and concentrated *in vacuo* to obtain a fluorescent yellow, oily mass (45 mg).

***N*-(3-(Dimethylamino)propyl)-5-(5-(3-(5-(4-methyl-3,4-dihydro-2*H*-benzo[*b*][1,4]oxazin-7-yl)thiophene-2-carboxamido)phenyl)furan-2-carboxamido)benzofuran-2-carboxamide (4.131):**



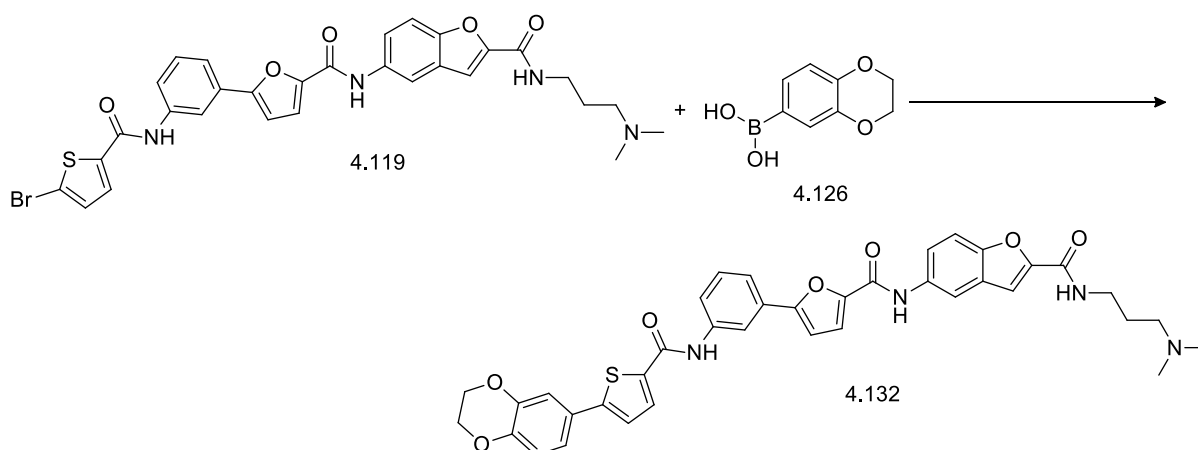
Fluorescent yellow oil. IR (FTIR, $\nu_{\text{max}}/\text{cm}^{-1}$) 692.14, 721.77, 791.11, 863.36, 959.84, 1028.48, 1119.25, 1161.63, 1224.86, 1253.39, 1301.41, 1444.25, 1510.52, 1539.91, 1584.90, 1651.50, 2341.46, 2358.62, 2817.07, 2871.95, 2941.73.3255.86; ¹H NMR (400 MHz, Acetone-*d*₆, TMS); δ 1.71 - 1.85 (m, 2H), 2.23 (d, *J*=4.55 Hz, 6H), 2.38 - 2.44 (m, 2H), 2.93 - 2.94 (m, 3H), 3.32 - 3.37 (m, 2H), 3.46 - 3.51 (m, 2H), 4.28 (d, *J*=4.29 Hz, 2H), 6.50 - 6.61 (m, 1H), 6.73 (dd, *J*=8.46, 4.93 Hz, 1H), 7.01 - 7.04 (m, 1H), 7.15 - 7.20 (m, 1H), 7.27 (t, *J*=4.04 Hz, 1H), 7.34 (t, *J*=4.29 Hz, 1H), 7.42 (d, *J*=4.80 Hz, 1H), 7.52 (br. s., 1H), 7.54 (br. s., 1H), 7.60 (d, *J*=6.06 Hz, 1H), 7.65 - 7.67 (m, 1H), 7.69 (d, *J*=4.80 Hz, 1H), 7.83 - 7.85 (m, 1H), 7.92 - 7.95 (m, 1H), 8.28 (br. s., 1H), 8.31 (br. s., 1H), 9.69 (br. s., 1H), 9.76 (br. s., 1H); ¹³C NMR (100 MHz, Acetone-*d*₆); δ 27.61, 38.63, 39.91, 45.70, 49.57, 58.76, 58.78, 65.63,

108.41, 108.70, 110.03, 110.14, 112.46, 113.31, 113.82, 114.70, 114.81, 114.94, 115.74, 117.23, 117.61, 120.31, 121.37, 121.48, 122.65, 123.98, 128.87, 129.48, 129.59, 130.28, 130.83, 132.73, 132.82, 145.39, 151.60, 152.47, 156.63, 159.02, 161.15; m/z (+EI) calc. For $C_{39}H_{37}N_5O_6S$ (M^+) 703.81, found 704.13 ($M+H$)⁺; Yield: 70%.

Procedure for the synthesis of 5-(5-(3-(5-(2,3-dihydrobenzo[*b*][1,4]dioxin-6-yl)thiophene-2-carboxamido)phenyl)furan-2-carboxamido)-*N*-(3-(dimethylamino)propyl)benzofuran-2-carboxamide (4.132) from 4.119 and 4.126

A catalytic amount of tetrakis(triphenylphosphine)palladium, $Pd(PPh_3)_4$ (0.1 eq.) was added to a solution of **4.119** (1.0 eq., 32 mg) and **4.126** (2.0 eq., 18 mg) in a 9:3:1 combination of EtOH, toluene and water in the presence of K_2CO_3 (3.0 eq.) in a 10 ml microwave vial containing a magnetic stirrer. The reaction vessel was flushed with nitrogen during each addition. The reaction mixture was sealed in an inert nitrogen environment and heated with microwave radiation in an EMRYS™ Optimizer Microwave Station (Personal Chemistry) at 100 °C for 15 minutes. After completion the reaction mixture was passed through a SCX-2 cartridge (1 gm), which was washed with DCM (3x), DMF (3x) twice and finally MeOH (2x). The product **4.132** was released from the cartridge using 5.0 ml 2M NH_3 in MeOH and concentrated *in vacuo* to obtain light brown mass (33 mg).

5-(5-(3-(5-(2,3-Dihydrobenzo[*b*][1,4]dioxin-6-yl)thiophene-2-carboxamido)phenyl)furan-2-carboxamido)-*N*-(3-(dimethylamino)propyl)benzofuran-2-carboxamide (4.132):



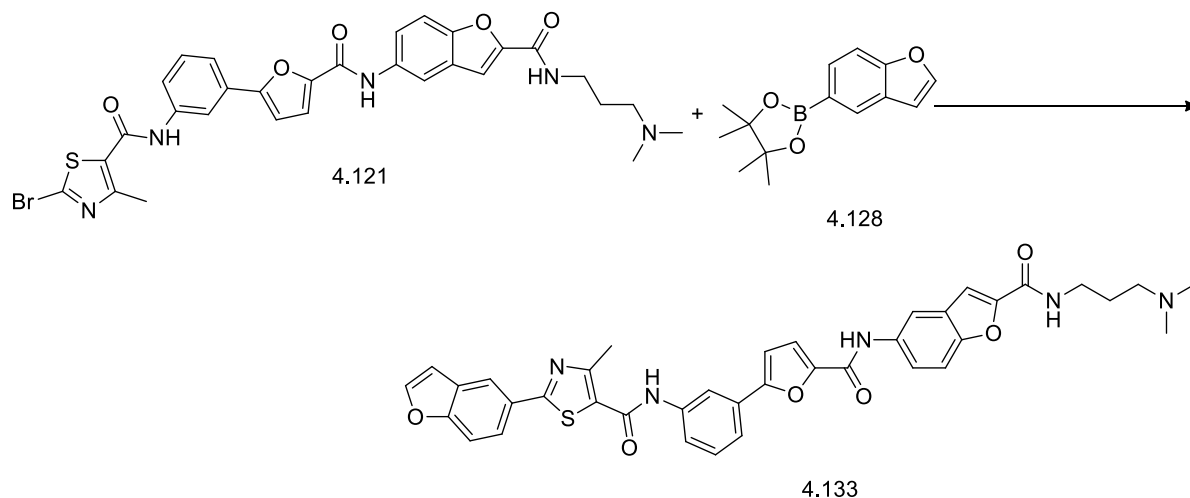
Light brown oil. IR (FTIR, ν_{max}/cm^{-1}) 663.77, 733.62, 793.48, 890.92, 1025.56, 1065.97, 1103.01, 1126.89, 1216.44, 1231.67, 1282.71, 1364.46, 1447.19, 1505.06, 1557.75, 1584.44,

1644.87, 1737.79, 2043.77, 2329.26, 2356.54, 2969.32, 3300.04, 3414.63; ^1H NMR (400 MHz, DMSO- d_6 , TMS); δ 1.67 (quin, $J=7.07$ Hz, 2H), 2.15 (s, 6H), 2.27 (t, $J=6.95$ Hz, 2H), 3.27 - 3.32 (m, 2H), 4.30 (s, 4H), 6.95 (d, $J=8.34$ Hz, 1H), 7.14 (d, $J=3.54$ Hz, 1H), 7.20 - 7.24 (m, 1H), 7.26 (d, $J=2.27$ Hz, 1H), 7.49 (d, $J=3.79$ Hz, 1H), 7.50 - 7.52 (m, 1H), 7.52 - 7.53 (m, 1H), 7.55 (d, $J=0.76$ Hz, 1H), 7.67 (d, $J=9.09$ Hz, 1H), 7.71 - 7.75 (m, 1H), 7.75 - 7.79 (m, 1H), 7.79 - 7.83 (m, 1H), 8.03 - 8.06 (m, 1H), 8.19 - 8.20 (m, 1H), 8.21 (d, $J=1.77$ Hz, 1H), 8.80 (t, $J=5.68$ Hz, 1H), 10.33 (s, 1H), 10.41 (s, 1H); ^{13}C NMR (100 MHz, DMSO- d_6); δ 26.96, 37.36, 45.16, 45.27, 56.90, 64.12, 64.24, 106.38, 109.34, 110.40, 111.71, 114.06, 114.26, 116.31, 116.76, 117.81, 119.04, 120.15, 120.39, 120.79, 123.64, 126.41, 127.28, 127.70, 130.42, 137.63, 143.76, 144.09, 146.76, 148.49, 150.02, 150.92, 155.09, 156.17, 157.90, 159.87, 161.49, 162.00; m/z (+EI) calc. For $\text{C}_{38}\text{H}_{34}\text{N}_4\text{O}_7\text{S}$ (M^+) 690.76, found 690.98 ($\text{M}+\text{H}$) $^+$; Yield: 94%.

Procedure for the synthesis of 2-(benzofuran-5-yl)-*N*-(3-(5-((2-((3-(dimethylamino)propyl)carbamoyl) benzofuran-5-yl)carbamoyl)furan-2-yl)phenyl)-4-methylthiazole-5-carboxamide (4.133) from 4.121 and 4.128

A catalytic amount of tetrakis(triphenylphosphine)palladium, $\text{Pd}(\text{PPh}_3)_4$ (0.1 eq.) was added to a solution of **4.121** (1.0 eq., 50 mg) and **4.128** (2.0 eq., 38 mg) in a 9:3:1 combination of EtOH, toluene and water in the presence of K_2CO_3 (3.0 eq.) in a 10 ml microwave vial containing a magnetic stirrer. The reaction vessel was flushed with nitrogen during each addition. The reaction mixture was sealed in an inert nitrogen environment and heated with microwave radiation in an EMRYSTM Optimizer Microwave Station (Personal Chemistry) at 100 °C for 20 minutes. After completion, the reaction mixture was passed through a SCX-2 cartridge (1 gm), which was washed with DCM (3x), DMF (3x) twice and finally MeOH (2x). The product **4.133** was released from the cartridge using 5.0 ml 2M NH_3 in MeOH and concentrated *in vacuo* to obtain the crude material. The crude was purified using a silica column and a DCM:MeOH:2M NH_3 (18:1:1) solvent system to obtain the pure product. The purification process was very difficult and only 8 mg was obtained as a pure, colourless, oily mass.

2-(Benzofuran-5-yl)-N-(3-(5-((2-((3-(dimethylamino)propyl)carbamoyl) benzofuran-5-yl)carbamoyl)furan-2-yl)phenyl)-4-methylthiazole-5-carboxamide (4.133):



Light yellow oil. IR (FTIR, $\nu_{\text{max}}/\text{cm}^{-1}$) 630.02, 691.10, 733.62, 784.05, 1028.19, 1107.94, 1207.37, 1237.47, 1305.91, 1435.14, 1465.50, 1540.09, 1585.10, 1651.37, 2329.26, 2358.05, 2774.39, 2823.17, 2859.75, 2945.12, 3276.00; ^1H NMR (400 MHz, Acetone- d_6 , TMS); δ 1.75 - 1.81 (m, 2H), 2.08 - 2.15 (m, 2H), 2.24 (br. s., 6H), 2.34 - 2.50 (m, 3H), 3.47 - 3.52 (m, 2H), 5.58 - 5.66 (m, 1H), 7.03 - 7.07 (m, 1H), 7.35 (d, $J=3.03$ Hz, 1H), 7.43 (br. s., 1H), 7.47 - 7.50 (m, 1H), 7.55 (d, $J=3.79$ Hz, 2H), 7.61 - 7.71 (m, 1H), 7.72 - 7.78 (m, 1H), 7.83 (br. s., 2H), 7.93 - 8.03 (m, 1H), 8.23 - 8.36 (m, 2H), 8.44 (br. s., 1H), 9.73 (d, $J=13.89$ Hz, 1H); ^{13}C NMR (100 MHz, Acetone- d_6); δ 16.32, 27.64, 37.51, 40.30, 45.73, 58.80, 106.63, 107.93, 108.44, 108.95, 110.98, 112.14, 112.97, 117.18, 117.90, 120.13, 120.98, 121.45, 121.99, 127.49, 129.22, 129.40, 130.23, 131.47, 136.72, 143.54, 146.94, 147.38, 150.78, 151.04, 156.10, 156.88, 158.94, 159.11, 161.04, 161.87, 162.31, 168.07; m/z (+EI) calc. For $\text{C}_{38}\text{H}_{33}\text{N}_5\text{O}_6\text{S}$ (M^+) 687.76, found 687.59 ($\text{M}+\text{H}$) $^+$; Yield: 16%.

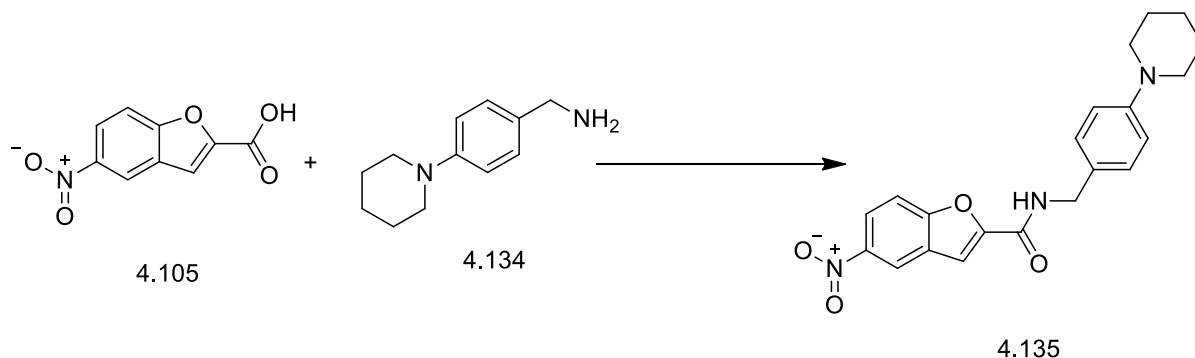
4.1.7 Type 3 Library synthesis

General procedure for the synthesis of 5-nitro-*N*-(4-(piperidin-1-yl)benzyl)benzofuran-2-carboxamide (4.135) from 5-nitrobenzofuran-2-carboxylic acid (4.105) and 4-(piperidin-1-yl)phenylmethanamine (4.134) (Amide coupling)

2.0 eq of HOBT (113 mg) and 1.75 eq. of DIC (114 μl) were added to a solution of **4.105** (1.2 eq., 104 mg) in DCM. After 30 minutes, 1.0 eq. (80.0 mg) of **4.134** was added and the reaction mixture was allowed to stand for 3 hours. After completion, the reaction mixture was

dried using a rotary evaporator to obtain the crude product. The product **4.135** was purified by flash chromatography using 100% DCM as mobile phase. The pure product was concentrated *in vacuo* to obtain a bright yellow powder (140 mg).

5-Nitro-*N*-(4-(piperidin-1-yl)benzyl)benzofuran-2-carboxamide (4.135):



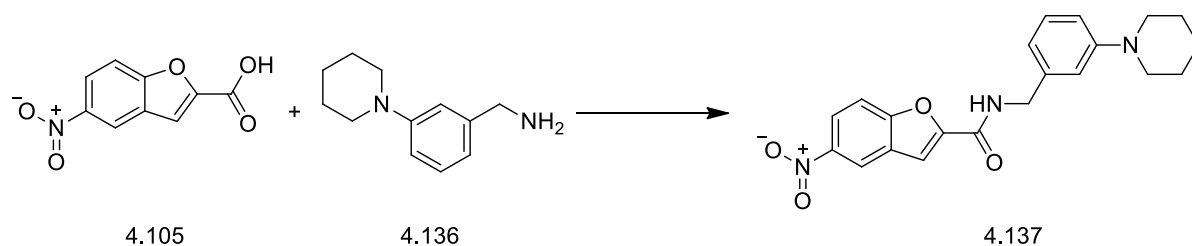
Bright yellow powder. IR (FTIR, $\nu_{\text{max}}/\text{cm}^{-1}$) 608.00, 674.43, 731.49, 749.75, 767.98, 821.84, 848.42, 900.34, 915.96, 986.39, 1040.69, 1067.76, 1125.60, 1173.83, 1227.49, 1275.81, 1303.14, 1339.96, 1385.92, 1442.03, 1516.97, 1598.47, 1647.69, 2361.37, 2857.53, 2941.60, 3096.52, 3316.04; ^1H NMR (400 MHz, CDCl_3 , TMS); δ 1.55 - 1.63 (m, 2H), 1.69 - 1.73 (m, 4H), 3.15 - 3.19 (m, 4H), 4.59 (d, $J=5.81$ Hz, 2H), 6.91 - 6.93 (m, 1H), 6.93 - 6.95 (m, 1H), 7.24 - 7.26 (m, 1H), 7.27 - 7.29 (m, 1H), 7.55 - 7.58 (m, 1H), 7.60 (d, $J=1.01$ Hz, 1H), 8.30 - 8.34 (m, 1H), 8.62 (dd, $J=2.27, 0.51$ Hz, 1H); ^{13}C NMR (100 MHz, CDCl_3); δ 24.24, 25.70, 25.70, 43.24, 50.36, 50.36, 110.24, 112.26, 116.43, 116.43, 119.23, 122.30, 127.16, 127.95, 129.13, 129.13, 144.75, 151.72, 151.91, 157.11, 157.40; m/z (+EI) calc. For $\text{C}_{21}\text{H}_{21}\text{N}_3\text{O}_4$ (M^+) 379.41, found 379.90 ($\text{M}+\text{H}$) $^+$; Yield: 88%.

A similar amide coupling reaction was used for synthesizing compounds **4.137** to **4.163**.

Procedure for the synthesis of 5-nitro-*N*-(3-(piperidin-1-yl)benzyl)benzofuran-2-carboxamide (4.137)

2.0 eq of HOBT and 1.75 eq. of DIC were added to a solution of **4.105** (1.2 eq., 196 mg) in DCM. After 30 minutes, 1.0 eq. (150 mg) of **4.136** was added and the reaction mixture was allowed to stand for 3 hours. After completion, the reaction mixture was dried using a rotary evaporator to obtain the crude product. The product **4.137** was purified by flash chromatography using 100% DCM as mobile phase. The pure product was concentrated *in vacuo* to obtain a light yellow powder (200 mg).

5-Nitro-*N*-(3-(piperidin-1-yl)benzyl)benzofuran-2-carboxamide (4.137):

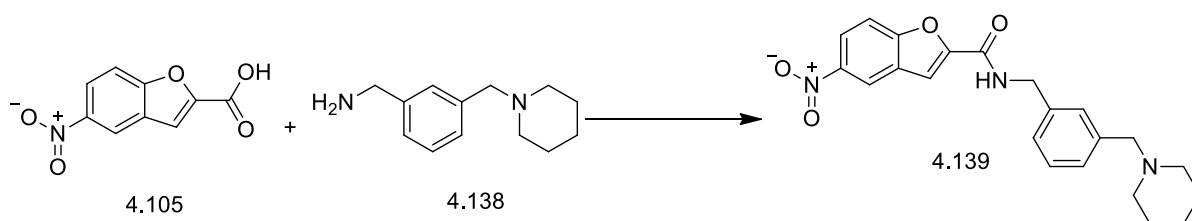


Light yellow powder. IR (FTIR, $\nu_{\text{max}}/\text{cm}^{-1}$) 681.96, 718.53, 749.00, 762.53, 819.63, 862.93, 906.60, 948.72, 992.73, 1004.41, 1027.84, 1070.65, 1118.06, 1192.30, 1244.35, 1279.61, 1323.54, 1343.91, 1421.23, 1442.23, 1492.39, 1525.67, 1571.32, 1596.17, 1621.56, 1736.85, 2335.91, 2359.63, 2801.03, 2857.88, 2932.70, 3095.60, 3268.47; ^1H NMR (400 MHz, CDCl_3 , TMS); δ 1.57 - 1.62 (m, 2H), 1.71 (dt, $J=11.18$, 5.65 Hz, 4H), 3.17 - 3.21 (m, 4H), 4.63 (d, $J=5.56$ Hz, 2H), 6.83 (d, $J=7.58$ Hz, 1H), 6.90 (dd, $J=8.34$, 2.53 Hz, 1H), 6.94 - 6.96 (m, 1H), 7.24 - 7.29 (m, 2H), 7.59 (d, $J=9.09$ Hz, 1H), 7.63 (d, $J=0.76$ Hz, 1H), 8.34 (dd, $J=9.09$, 2.53 Hz, 1H), 8.63 (d, $J=2.27$ Hz, 1H); ^{13}C NMR (100 MHz, CDCl_3); δ 24.24, 25.79, 25.79, 44.15, 50.42, 50.42, 110.89, 112.33, 115.75, 116.15, 118.64, 119.28, 123.37, 127.97, 129.63, 137.98, 144.80, 151.64, 152.71, 157.15, 157.48; m/z (+EI) calc. For $\text{C}_{21}\text{H}_{21}\text{N}_3\text{O}_4$ (M^+) 379.41, found 380.00 ($\text{M}+\text{H}^+$); Yield: 67%.

Procedure for the synthesis of 5-nitro-*N*-(3-(piperidin-1-ylmethyl)benzyl)benzofuran-2-carboxamide (4.139)

2.0 eq of HOBT and 1.75 eq. of DIC were added to a solution of **4.105** (1.2 eq., 195 mg) in DCM. After 30 minutes, 1.0 eq. (160 mg) of **4.138** was added and the reaction mixture was allowed to stand for 3 hours. After completion, the reaction mixture was dried using a rotary evaporator to obtain the crude product. The product **4.139** was purified by flash chromatography using 100% DCM as mobile phase. The pure product was concentrated *in vacuo* to obtain a light yellow oil (275 mg).

5-Nitro-*N*-(3-(piperidin-1-ylmethyl)benzyl)benzofuran-2-carboxamide (4.139):

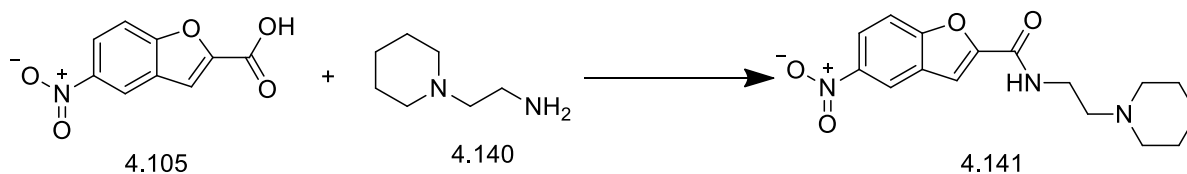


Light yellow oil. IR (FTIR, $\nu_{\text{max}}/\text{cm}^{-1}$) 631.71, 683.83, 705.86, 730.93, 750.39, 821.62, 898.70, 991.70, 1039.18, 1068.48, 1111.10, 1174.95, 1224.97, 1275.17, 1300.54, 1344.03, 1444.32, 1521.46, 1569.73, 1600.27, 1659.35, 1711.16, 2355.29, 2756.09, 2792.68, 2835.65, 2931.81, 3103.65, 3299.95; ^1H NMR (400 MHz, CDCl_3 , TMS); δ 1.40 - 1.46 (m, 2H), 1.57 (quin, $J=5.62$ Hz, 4H), 2.38 (br. s., 4H), 3.47 (s, 2H), 4.67 (d, $J=5.81$ Hz, 2H), 7.25 - 7.26 (m, 1H), 7.28 (d, $J=7.83$ Hz, 2H), 7.30 - 7.33 (m, 1H), 7.34 (s, 1H), 7.57 (dt, $J=9.09$, 0.76 Hz, 1H), 7.61 (d, $J=1.01$ Hz, 1H), 8.31 (dd, $J=9.09$, 2.27 Hz, 1H), 8.59 - 8.61 (m, 1H); ^{13}C NMR (100 MHz, CDCl_3); δ 24.20, 25.77, 30.82, 43.50, 54.47, 63.52, 110.84, 112.27, 119.20, 122.29, 126.53, 127.87, 128.60, 128.71, 128.75, 137.15, 139.27, 144.69, 151.53, 157.09, 157.55, 206.85; m/z (+EI) calc. For $\text{C}_{22}\text{H}_{23}\text{N}_3\text{O}_4$ (M^+) 393.44 found 393.33 ($\text{M}+\text{H}$) $^+$; Yield: 89%.

Procedure for the synthesis of 5-nitro-*N*-(2-(piperidin-1-yl)ethyl)benzofuran-2-carboxamide (4.141)

2.0 eq of HOBT and 1.75 eq. of DIC were added to a solution of **4.105** (1.0 eq., 100 mg) in DCM. After 30 minutes 1.0 eq. (62 mg) of **4.140** was added and the reaction mixture was allowed to stand for 3 hours. After completion, the reaction mixture was dried using a rotary evaporator to obtain the crude product. The product **4.141** was purified by flash chromatography using 100% DCM as mobile phase. The pure product was concentrated *in vacuo* to obtain a yellow, viscous oil (150 mg).

5-Nitro-*N*-(2-(piperidin-1-yl)ethyl)benzofuran-2-carboxamide (4.141):

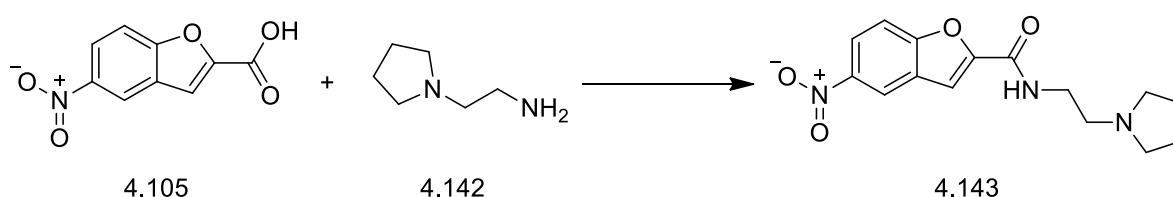


Yellow, viscous oil. IR (FTIR, $\nu_{\text{max}}/\text{cm}^{-1}$) 631.40, 683.60, 747.94, 822.76, 897.61, 940.13, 1069.98, 1096.85, 1127.98, 1176.98, 1275.81, 1342.86, 1445.64, 1523.21, 1599.61, 1651.54, 2329.26, 2359.18, 2935.23, 3241.62; ^1H NMR (500 MHz, CDCl_3 , TMS); δ 1.51 (br. s., 2H), 1.67 (quin, $J=5.60$ Hz, 4H), 2.60 (br. s., 4H), 2.69 - 2.76 (m, 2H), 3.66 (q, $J=5.36$ Hz, 2H), 7.25 - 7.27 (m, 1H), 7.55 (d, $J=0.95$ Hz, 1H), 8.28 (dd, $J=9.14$, 2.52 Hz, 1H), 8.58 (d, $J=2.21$ Hz, 1H); ^{13}C NMR (100 MHz, CDCl_3); δ 23.46, 23.89, 25.42, 35.66, 42.12, 54.22, 56.91, 110.42, 112.37, 112.38, 119.11, 122.11, 127.85, 151.82, 157.18, 157.85; m/z (+EI) calc. For $\text{C}_{16}\text{H}_{19}\text{N}_3\text{O}_4$ (M^+) 317.34, found 317.99 ($\text{M}+\text{H}$) $^+$; Yield: 98%.

Procedure for the synthesis of 5-nitro-*N*-(2-(pyrrolidin-1-yl)ethyl)benzofuran-2-carboxamide (4.143)

2.0 eq of HOBT and 1.75 eq. of DIC were added to a solution of **4.105** (1.0 eq., 60 mg) in DCM. After 30 minutes, 1.0 eq. (33 mg) of **4.142** was added and the reaction mixture was allowed to stand for 3 hours. After completion, the reaction mixture was dried using a rotary evaporator to obtain the crude product. The product **4.143** was purified by flash chromatography using 100% DCM as mobile phase. The pure product was concentrated *in vacuo* to obtain a yellow, viscous oil (85 mg).

5-Nitro-*N*-(2-(pyrrolidin-1-yl)ethyl)benzofuran-2-carboxamide (4.143):

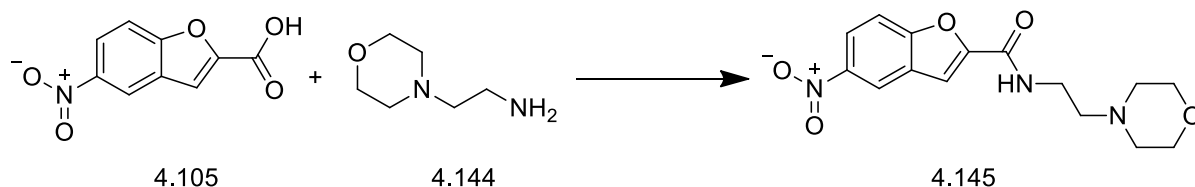


Yellow, viscous oil. IR (FTIR, $\nu_{\text{max}}/\text{cm}^{-1}$) 631.54, 683.84, 749.27, 822.30, 1034.27, 1069.66, 1095.59, 1170.90, 1275.71, 1342.93, 1445.92, 1523.21, 1573.61, 1599.68, 1614.31, 1653.96, 2804.87, 2965.94, 3097.56, 3337.71, 3647.90, 3734.74; ^1H NMR (500 MHz, CDCl_3 , TMS); δ 1.85 - 1.90 (m, 4H), 2.72 (br. s., 4H), 2.85 (t, $J=5.67$ Hz, 2H), 3.67 (q, $J=5.46$ Hz, 2H), 7.52 (d, $J=8.83$ Hz, 1H), 7.56 - 7.57 (m, 1H), 8.30 (dd, $J=9.14$, 2.52 Hz, 1H), 8.60 (d, $J=2.21$ Hz, 1H); ^{13}C NMR (100 MHz, CDCl_3); δ 23.47, 37.82, 42.18, 50.77, 53.98, 54.60, 110.51, 111.07, 112.42, 119.15, 122.17, 127.89, 151.78, 157.19, 157.93; m/z (+EI) calc. For $\text{C}_{15}\text{H}_{17}\text{N}_3\text{O}_4$ (M^+) 303.31, found 304.04 ($\text{M}+\text{H}$) $^+$; Yield: 97%.

Procedure for the synthesis of *N*-(2-morpholinoethyl)-5-nitrobenzofuran-2-carboxamide (4.145)

2.0 eq of HOBT and 1.75 eq. of DIC were added to a solution of **4.105** (1.0 eq., 60 mg) in DCM. After 30 minutes, 1.0 eq. (38 mg) of **4.144** was added and the reaction mixture was allowed to stand for 3 hours. After completion, the reaction mixture was dried using a rotary evaporator to obtain the crude product. The product **4.145** was purified by flash chromatography using 100% DCM as mobile phase. The pure product was concentrated *in vacuo* to obtain a light yellow oil (90 mg).

***N*-(2-morpholinoethyl)-5-nitrobenzofuran-2-carboxamide (4.145):**

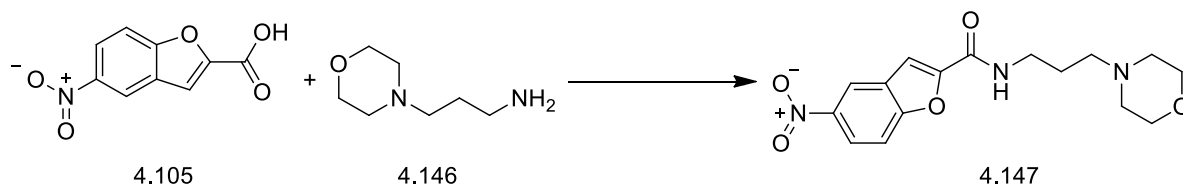


Light yellow oil. IR (FTIR, $\nu_{\text{max}}/\text{cm}^{-1}$) 637.26, 683.21, 748.84, 824.00, 860.39, 936.56, 1034.88, 1068.93, 1113.89, 1172.89, 1234.95, 1272.65, 1304.39, 1341.33, 1445.57, 1520.17, 1597.68, 1651.80, 2810.97, 2859.75, 2939.35, 3103.65, 3298.78, 3647.93, 3734.18; ^1H NMR (500 MHz, CDCl_3 , TMS); δ 2.56 (br. s., 4H), 2.66 (t, $J=5.99$ Hz, 2H), 3.62 (q, $J=5.88$ Hz, 2H), 3.76 - 3.80 (m, 4H), 7.23 (br. s., 1H), 7.58 - 7.61 (m, 1H), 7.64 (d, $J=9.14$ Hz, 1H), 8.35 (dd, $J=8.98, 2.36$ Hz, 1H), 8.63 (d, $J=2.21$ Hz, 1H); ^{13}C NMR (100 MHz, CDCl_3); δ 23.47, 35.59, 42.18, 53.32, 56.73, 66.91, 110.66, 112.39, 119.24, 122.28, 127.93, 144.69, 151.73, 157.18, 157.72; m/z (+EI) calc. For $\text{C}_{15}\text{H}_{17}\text{N}_3\text{O}_5$ (M^+) 319.31, found 319.93 ($\text{M}+\text{H}$) $^+$; Yield: 97%.

Procedure for the synthesis of *N*-(3-morpholinopropyl)-5-nitrobenzofuran-2-carboxamide (4.147)

2.0 eq of HOBT and 1.75 eq. of DIC were added to a solution of **4.105** (1.0 eq., 100 mg) in DCM. After 30 minutes, 1.0 eq. (70 mg) of **4.146** was added and the reaction mixture was allowed to stand for 3 hours. After completion, the reaction mixture was dried using a rotary evaporator to obtain the crude product. The product **4.147** was purified by flash chromatography using 100% DCM as mobile phase. The pure product was concentrated *in vacuo* to obtain a light green oil (160 mg).

***N*-(3-morpholinopropyl)-5-nitrobenzofuran-2-carboxamide (4.147):**



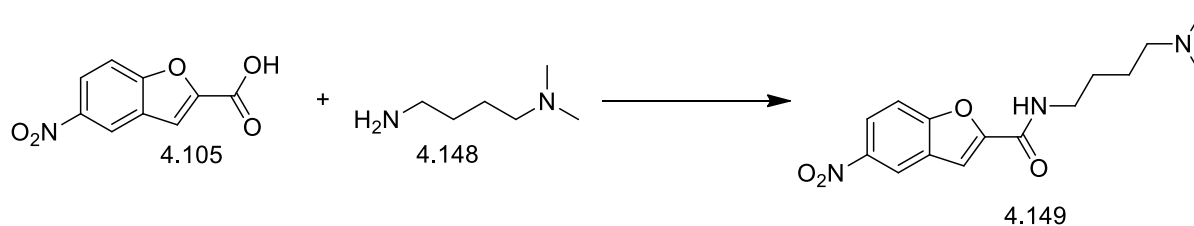
Light green oil. IR (FTIR, $\nu_{\text{max}}/\text{cm}^{-1}$) 608.40, 681.75, 731.38, 751.03, 767.71, 818.07, 829.06, 864.26, 887.58, 953.91, 988.10, 1029.56, 1061.79, 1089.81, 1170.75, 1223.50, 1274.25, 1302.82, 1338.89, 1359.75, 1439.24, 1455.69, 1516.01, 1601.22, 1659.76, 1980.26, 2354.22, 2821.99, 2856.04, 2946.05, 3201.74; ^1H NMR (400 MHz, CDCl_3 , TMS); δ 1.83 (dt, $J=11.77$,

5.82 Hz, 2H), 2.59 (br. s., 4H), 2.62 - 2.66 (m, 2H), 3.59 - 3.66 (m, 2H), 3.90 (t, $J=4.66$ Hz, 4H), 7.58 (d, $J=1.01$ Hz, 1H), 7.60 (d, $J=9.32$ Hz, 1H), 8.34 (dd, $J=9.06$, 2.52 Hz, 1H), 8.63 (d, $J=2.27$ Hz, 1H), 8.97 (br. s., 1H); ^{13}C NMR (100 MHz, CDCl_3); δ 23.47, 23.71, 35.10, 40.44, 53.78, 58.77, 66.84, 110.34, 111.96, 119.26, 122.26, 128.07, 144.71, 152.34, 157.09, 157.55; m/z (+EI) calc. For $\text{C}_{16}\text{H}_{19}\text{N}_3\text{O}_5$ (M^+) 333.34, found 334.18 ($\text{M}+\text{H}$) $^+$; Yield: 99%.

Procedure for the synthesis of *N*-(4-(dimethylamino)butyl)-5-nitrobenzofuran-2-carboxamide (4.149)

2.0 eq of HOBT and 1.75 eq. of DIC were added to a solution of **4.105** (1.0 eq., 100 mg) in DMF. After 30 minutes, 0.88 eq. (45 mg) of **4.148** was added and the reaction mixture was allowed to stand for 3 hours. After completion, the reaction mixture was purified using the ‘catch and release’ method over a SCX cartridge. The product **4.149** was released from the cartridge using 10 ml 2M NH_3 . The pure product was concentrated *in vacuo* to obtain a colourless oil (100 mg).

***N*-(4-(dimethylamino)butyl)-5-nitrobenzofuran-2-carboxamide (4.149):**



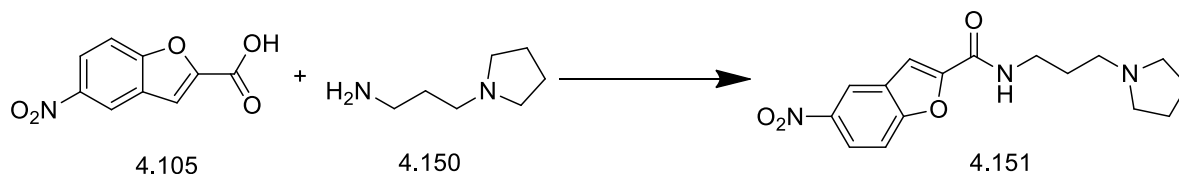
Colourless oil. IR (FTIR, $\nu_{\text{max}}/\text{cm}^{-1}$) 425.03, 681.97, 737.24, 771.79, 814.53, 853.40, 889.80, 956.24, 1023.76, 1065.00, 1155.70, 1170.81, 1231.20, 1264.50, 1338.62, 1441.72, 1461.00, 1519.75, 1651.97, 2778.8, 2821.20, 2857.40, 2924.00, 3108.30; ^1H NMR (400 MHz, CDCl_3) δ 1.69 (q, $J=6.13$ Hz, 2H), 1.72 - 1.79 (m, 2H), 2.35 (s, 6H), 2.42 (t, $J=6.42$ Hz, 2H), 3.50 (q, $J=5.79$ Hz, 2H), 7.56 - 7.57 (m, 1H), 7.59 (d, $J=9.06$ Hz, 1H), 8.33 (dd, $J=9.06$, 2.52 Hz, 1H), 8.55 (br. s., 1H), 8.62 (d, $J=2.27$ Hz, 1H); ^{13}C NMR (100 MHz, CDCl_3) δ 25.39, 287.40, 39.45, 45.18, 45.29, 59.06, 110.24, 112.11, 119.19, 122.08, 128.07, 144.64, 152.41, 157.18, 157.81; m/z (+EI) calc. For $\text{C}_{15}\text{H}_{19}\text{N}_3\text{O}_4$ (M^+) 305.33, found ($\text{M}+\text{H}$) $^+$ 306.1; Yield: 68%.

Procedure for the synthesis of 5-nitro-*N*-(3-(pyrrolidin-1-yl)propyl)benzofuran-2-carboxamide (4.151)

2.0 eq of HOBT and 1.75 eq. of DIC were added to a solution of **4.105** (1.0 eq., 100 mg) in DMF. After 30 minutes, 0.80 eq. (50 mg) of **4.150** was added and the reaction mixture was allowed to stand for 3 hours. After completion, the reaction mixture was purified using the ‘catch and release’ method over a SCX cartridge (1 gm). The product **4.151** was released

from the cartridge using 10 ml 2M NH₃. The pure product was concentrated *in vacuo* to obtain a light yellow powder (105 mg).

5-Nitro-*N*-(3-(pyrrolidin-1-yl)propyl)benzofuran-2-carboxamide (4.151):

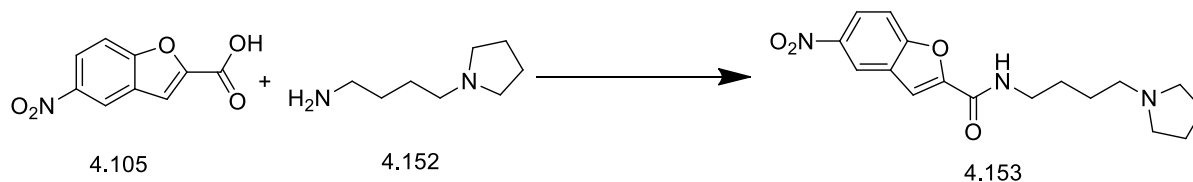


Light yellow powder. IR (FTIR, $\nu_{\text{max}}/\text{cm}^{-1}$) 423.90, 566.25, 682.16, 731.76, 818.48, 895.49, 913.85, 1004.50, 1064.83, 1143.60, 1170.77, 1261.08, 1272.24, 1292.89, 1338.73, 1439.80, 1521.94, 1594.00, 1665.27, 2788.00, 2812.00, 2872.50, 2945.00, 2966.20, 3111.30; ¹H NMR (400 MHz, CDCl₃) δ 1.84 (dt, $J=11.71$, 5.98 Hz, 2H), 1.94 (dt, $J=6.74$, 3.30 Hz, 4H), 2.66 (br. s., 4H), 2.74 - 2.81 (m, 2H), 3.60 - 3.67 (m, 2H), 7.52 (s, 1H), 7.54 (s, 1H), 8.32 (dd, $J=9.19$, 2.39 Hz, 1H), 8.62 (d, $J=2.27$ Hz, 1H), 9.35 (br. s., 1H); ¹³C NMR (100 MHz, CDCl₃) δ 23.48, 23.58, 25.98, 40.42, 54.02, 54.12, 55.71, 109.96, 111.95, 119.17, 122.06, 128.12, 144.60, 152.64, 157.20, 157.61; m/z (+EI) calc. For C₁₆H₁₉N₃O₄ (M⁺) 317.34, found (M+H)⁺ 318.10; Yield: 69%.

Procedure for the synthesis of 5-nitro-*N*-(4-(pyrrolidin-1-yl)butyl)benzofuran-2-carboxamide (4.153)

2.0 eq of HOBT and 1.75 eq. of DIC were added to a solution of **4.105** (1.0 eq., 100 mg) in DMF. After 30 minutes, 0.9 eq. (62 mg) of **4.152** was added and the reaction mixture was allowed to stand for 3 hours. After completion, the reaction mixture was purified using the ‘catch and release’ method over a SCX cartridge (1 gm). The product **4.153** was released from the cartridge using 10 ml 2M NH₃. The pure product was concentrated *in vacuo* to obtain colourless solid (110 mg).

5-Nitro-*N*-(4-(pyrrolidin-1-yl)butyl)benzofuran-2-carboxamide (4.153):



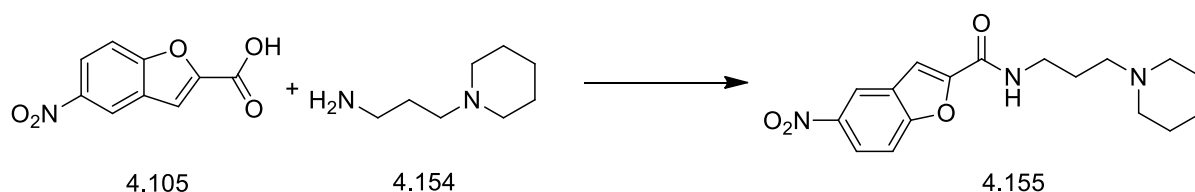
Colourless solid. IR (FTIR, $\nu_{\text{max}}/\text{cm}^{-1}$) 415.30, 487.31, 553.01, 587.97, 619.20, 687.12, 754.24, 806.37, 892.17, 1009.24, 1056.87, 1125.38, 1289.37, 1497.32, 1505.67, 1543.02, 1668.23, 2821.48, 2859.00, 3211.10, 3330.28; ¹H NMR (400 MHz, CDCl₃) δ 1.52 – 1.62 (m, 2H), 1.68 – 1.72 (m, 4H), 1.84 – 1.95 (m, 2H), 2.50 – 2.64 (m, 4H), 3.12 (br. s., 2H), 3.60 -

3.67 (m, 2H), 7.57 (s, 1H), 7.84 (d, $J=9.0$ Hz, 1H), 8.20 (d, $J=9.0$ Hz, 1H), 8.56 (s, 1H); ^{13}C NMR (100 MHz, CDCl_3) δ 23.00, 23.51, 24.98, 27.56, 40.10, 54.58, 55.12, 56.27, 108.47, 112.30, 116.04, 120.37, 130.56, 145.62, 150.14, 158.07, 163.30; m/z (+EI) calc. For $\text{C}_{17}\text{H}_{21}\text{N}_3\text{O}$ (M^+) 331.37, found ($\text{M}+\text{H}$) $^+$ 332.10; Yield: 69%.

Procedure for the synthesis of 5-nitro-*N*-(3-(piperidin-1-yl)propyl)benzofuran-2-carboxamide (4.155)

2.0 eq of HOBT and 1.75 eq. of DIC were added to a solution of **4.105** (1.0 eq., 100 mg) in DMF. After 30 minutes, 0.80 eq. (55 mg) of **4.154** was added and the reaction mixture was allowed to stand for 3 hours. After completion, the reaction mixture was purified using the ‘catch and release’ method over a SCX cartridge (1 gm). The product **4.155** was released from the cartridge using 10 ml 2M NH_3 . The pure product was concentrated *in vacuo* to obtain light yellow powder (136g).

5-Nitro-*N*-(3-(piperidin-1-yl)propyl)benzofuran-2-carboxamide (4.155):

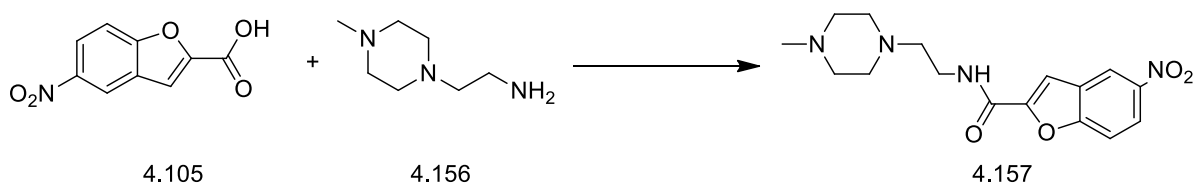


Light yellow powder. IR (FTIR, $\nu_{\text{max}}/\text{cm}^{-1}$) 422.91, 517.88, 681.44, 751.75, 819.17, 890.08, 1062.13, 1118.69, 1170.78, 1251.20, 1340.48, 1436.80, 1515.88, 1599.37, 1661.51, 2760.70, 2806.00, 2857.40, 2921.00, 3111.30; ^1H NMR (400 MHz, CDCl_3) δ 1.60 (br. s., 2H), 1.73 - 1.79 (m, 4H), 1.79 - 1.84 (m, 2H), 2.54 (br. s., 4H), 2.59 - 2.63 (m, 2H), 3.57 - 3.66 (m, 2H), 7.50 (d, $J=9.06$ Hz, 1H), 7.56 (d, $J=1.01$ Hz, 1H), 8.32 (dd, $J=9.06$, 2.52 Hz, 1H), 8.62 (d, $J=2.27$ Hz, 1H), 9.48 (br. s., 1H); ^{13}C NMR (100 MHz, CDCl_3) δ 22.89, 23.47, 23.71, 24.27, 25.71, 40.70, 42.13, 54.67, 110.00, 111.82, 119.19, 122.07, 128.13, 144.60, 152.63, 157.16, 157.63; m/z (+EI) calc. For $\text{C}_{17}\text{H}_{21}\text{N}_3\text{O}_4$ (M^+) 331.37, found ($\text{M}+\text{H}$) $^+$ 332.0; Yield: 85%.

Procedure for the synthesis of *N*-(2-(4-methylpiperazin-1-yl)ethyl)-5-nitrobenzofuran-2-carboxamide (4.157)

2.0 eq of HOBT and 1.75 eq. of DIC were added to a solution of **4.105** (1.0 eq., 100 mg) in DMF. After 30 minutes, 0.9 eq. (62 mg) of **4.156** was added and the reaction mixture was allowed to stand for 3 hours. After completion, the reaction mixture was purified using the ‘catch and release’ method over a SCX cartridge (1 gm). The product **4.157** was released from the cartridge using 10 ml 2M NH_3 . The pure product was concentrated *in vacuo* to obtain light yellow oil (141mg).

***N*-(2-(4-methylpiperazin-1-yl)ethyl)-5-nitrobenzofuran-2-carboxamide (4.157):**

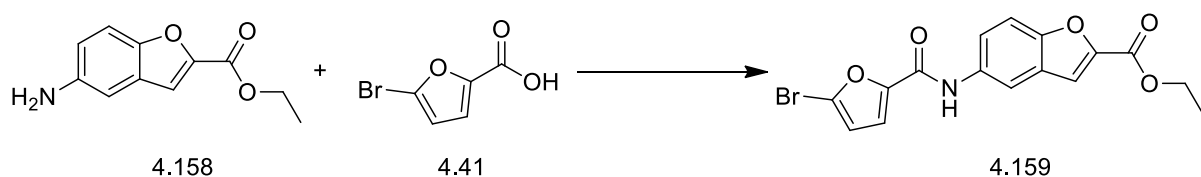


Light yellow oil. IR (FTIR, $\nu_{\text{max}}/\text{cm}^{-1}$) 424.01, 587.40, 681.92, 731.18, 751.55, 819.27, 890.27, 913.85, 953.15, 977.33, 1068.00, 1119.38, 1171.27, 1255.40, 1305.30, 1339.75, 1439.80, 1516.34, 1600.21, 1662.08, 2739.50, 2766.80, 2812.00, 2851.40, 2921.00, 3108.30, 3223.20, 3335.00; ^1H NMR (400 MHz, CDCl_3) δ 2.32 - 2.35 (m, 2H), 2.52 (br. s., 4H), 2.58 (br. s., 3H), 2.64 (br. s., 2H), 2.64 - 2.67 (m, 2H), 3.60 (q, $J=5.62$ Hz, 2H), 7.21 - 7.26 (m, 1H), 7.55 - 7.60 (m, 1H), 7.65 (d, $J=9.32$ Hz, 1H), 8.35 (dd, $J=9.06, 2.52$ Hz, 1H), 8.63 (d, $J=2.52$ Hz, 1H); ^{13}C NMR (100 MHz, CDCl_3) δ 23.47, 26.68, 35.95, 45.98, 52.78, 55.10, 56.14, 110.54, 112.39, 119.22, 122.23, 127.97, 144.70, 151.86, 157.20, 157.69; m/z (+EI) calc. For $\text{C}_{16}\text{H}_{20}\text{N}_4\text{O}_4$ (M^+) 332.35, found ($\text{M}+\text{H}$) $^+$ 333.1; Yield: 88%.

Procedure for the synthesis of ethyl 5-(5-bromofuran-2-carboxamido)benzofuran-2-carboxylate (4.159)

2.0 eq of HOBT and 1.75 eq. of DIC were added to a solution of **4.158** (1.0 eq., 200 mg) in DCM. After 30 minutes, 2.0 eq. (186 mg) of **4.41** was added and the reaction mixture was allowed to stand for 3 hours. After completion, the reaction mixture was dried using a rotary evaporator to obtain the crude product. The product **4.159** was purified by flash chromatography using 100% DCM as mobile phase. The pure product was concentrated *in vacuo* to obtain brown oil (267 mg).

Ethyl 5-(5-bromofuran-2-carboxamido)benzofuran-2-carboxylate (4.159):



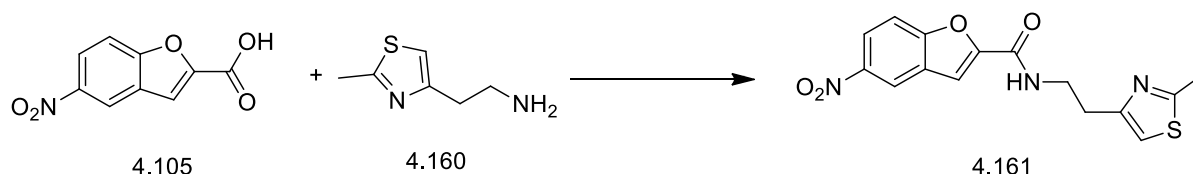
Brown oil. IR (FTIR, $\nu_{\text{max}}/\text{cm}^{-1}$) 439.30, 493.68, 545.09, 662.97, 736.31, 806.02, 816.02, 880.60, 919.90, 950.13, 1009.50, 1095.20, 1110.30, 1179.71, 1213.00, 1313.29, 1394.59, 1478.40, 1560.00, 1665.48, 1712.46, 2470.50, 2497.70, 2902.80, 2969.30, 2987.40, 3117.40, 3350.10; ^1H NMR (400 MHz, Methanol- d_4) δ 1.40 (t, $J=7.05$ Hz, 3H), 4.40 (q, $J=7.05$ Hz, 2H), 6.65 (d, $J=3.53$ Hz, 1H), 7.25 (d, $J=3.53$ Hz, 1H), 7.57 (s, 2H), 7.68 (dd, $J=8.94, 2.14$ Hz, 1H), 8.12 (d, $J=2.27$ Hz, 1H); ^{13}C NMR (100 MHz, Methanol- d_4) δ 14.92, 62.99, 113.42,

115.30, 115.84, 116.63, 118.88, 123.82, 127.36, 128.87, 135.57, 148.14, 151.05, 154.59, 158.09, 161.17; m/z (+EI) calc. For $C_{16}H_{12}BrNO_5$ (M^+) 378.12, found ($M+H$)⁺ 380.10; Yield: 72%.

Procedure for the synthesis of *N*-(2-(2-methylthiazol-4-yl)ethyl)-5-nitrobenzofuran-2-carboxamide (4.161)

2.0 eq of HOBT and 1.75 eq. of DIC were added to a solution of **4.105** (1.0 eq., 100 mg) in DCM. After 30 minutes, 0.9 eq. (62 mg) of **4.160** was added and the reaction mixture was allowed to stand for 3 hours. After completion, the reaction mixture was purified using the ‘catch and release’ method over a SCX cartridge (1 gm). The product **4.161** was released from the cartridge using 10 ml 2M NH_3 . The pure product was concentrated *in vacuo* to obtain light yellow powder (159 mg).

***N*-(2-(2-methylthiazol-4-yl)ethyl)-5-nitrobenzofuran-2-carboxamide (4.161):**

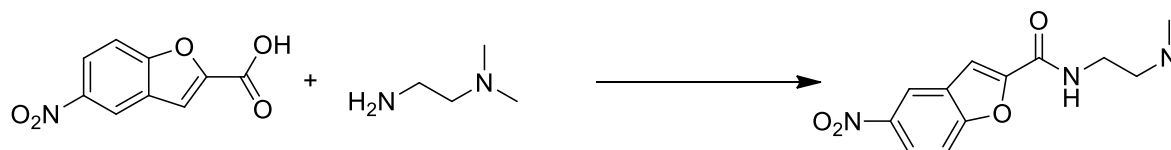


Light yellow powder. IR (FTIR, ν_{max}/cm^{-1}) 402.67, 428.73, 568.70, 683.67, 737.32, 767.53, 820.50, 891.05, 960.33, 1067.35, 1132.00, 1179.91, 1234.50, 1274.45, 1311.33, 1340.26, 1445.40, 1516.52, 1531.93, 1578.00, 1599.00, 1651.48, 1620.00, 1689.40, 3042.00, 3114.30, 3216.70, 3349.30; 1H NMR (400 MHz, $CDCl_3$) δ 2.76 (s, 3H), 3.05 (t, $J=6.42$ Hz, 2H), 3.81 - 3.86 (m, 2H), 6.88 (d, $J=0.76$ Hz, 1H), 7.58 (d, $J=0.76$ Hz, 1H), 7.59 - 7.63 (m, 1H), 8.31 - 8.35 (m, 1H), 8.61 - 8.62 (m, 1H); ^{13}C NMR (100 MHz, $CDCl_3$) δ 19.16, 23.40, 42.07, 110.42, 112.28, 114.16, 119.21, 122.21, 127.94, 151.90, 153.43, 157.17, 157.23, 157.72, 166.53; m/z (+EI) calc. For $C_{15}H_{13}N_3O_4S$ (M^+) 331.35, found ($M+H$)⁺ 331.90; Yield: 99%.

Procedure for the synthesis of *N*-(2-(dimethylamino)ethyl)-5-nitrobenzofuran-2-carboxamide (4.163)

2.0 eq of HOBT and 1.75 eq. of DIC were added to a solution of **4.105** (1.0 eq., 100 mg) in DCM. After 30 minutes, 0.9 eq. (38 mg) of **4.162** was added and the reaction mixture was allowed to stand for 3 hours. After completion, the reaction mixture was purified using the ‘catch and release’ method over a SCX cartridge (1 gm). The product **4.163** was released from the cartridge using 10 ml 2M NH_3 . The pure product was concentrated *in vacuo* to obtain light yellow powder (130 mg).

***N*-(2-(dimethylamino)ethyl)-5-nitrobenzofuran-2-carboxamide (4.163):**

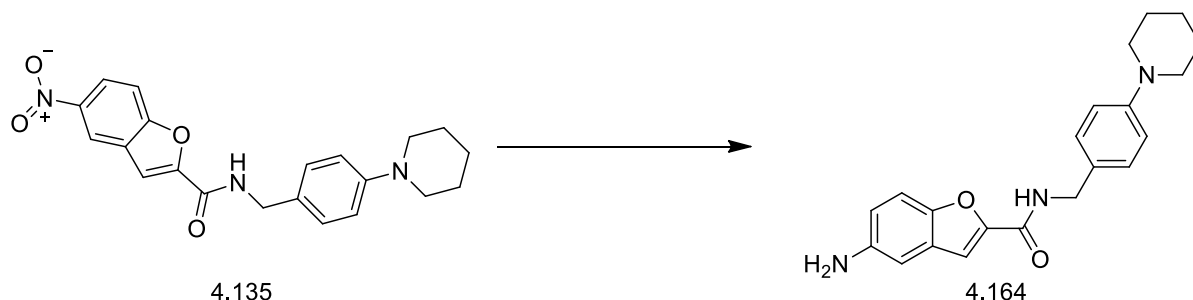


Light yellow powder. IR (FTIR, $\nu_{\text{max}}/\text{cm}^{-1}$) 423.63, 496.73, 551.13, 569.27, 611.59, 682.93, 726.45, 745.91, 825.92, 889.67, 944.08, 965.24, 1041.04, 1104.30, 1122.40, 1167.80, 1237.30, 1262.99, 1292.44, 1340.72, 1437.17, 1497.13, 1523.40, 1599.14, 1670.85, 2772.80, 2784.9, 2824.20, 2857.40, 2942.00, 2969.30, 3114.40, 3392.40; ^1H NMR (400 MHz, CDCl_3) δ 2.33 (s, 6H), 2.59 (t, $J=5.92$ Hz, 2H), 3.59 (q, $J=5.37$ Hz, 2H), 7.57 (d, $J=1.01$ Hz, 1H), 7.62 (d, $J=9.06$ Hz, 1H), 8.33 (dd, $J=9.19, 2.39$ Hz, 1H), 8.61 (d, $J=2.52$ Hz, 1H); ^{13}C NMR (100 MHz, CDCl_3) δ 36.70, 45.16, 45.16, 57.54, 110.49, 112.41, 119.17, 122.19, 127.94, 144.64, 151.84, 157.20, 157.78; m/z (+EI) calc. For $\text{C}_{13}\text{H}_{15}\text{N}_3\text{O}_4$ (M^+) 277.28, found ($\text{M}+\text{H}$) $^+$ 278.10; Yield: 97%.

General procedure for the synthesis of 5-amino-*N*-(4-(piperidin-1-yl)benzyl)benzofuran-2-carboxamide (4.164) from 5-nitro-*N*-(4-(piperidin-1-yl)benzyl)benzofuran-2-carboxamide (4.135) by hydrogenation.

5-Nitro-*N*-(4-(piperidin-1-yl)benzyl)benzofuran-2-carboxamide (1.0 eq., 113 mg) (**4.135**) was dissolved in a minimum amount of ethanol (25 ml) and a catalytic amount of 10% Pd/C (20 mg) was added as a slurry, also in ethanol. The reaction mixture was shaken for 1.5-2.5 hours at 45 psi in a Parr hydrogenator. After completion of the reduction, the suspension was filtered through a layer of celite, with caution, using a Buchner flask and the filtrate was concentrated to obtain a light brown viscous oil (**4.164**) (104 mg). Pd/C waste was discarded following the standard procedure of the university described earlier in the chapter.

5-Amino-*N*-(4-(piperidin-1-yl)benzyl)benzofuran-2-carboxamide (4.164):



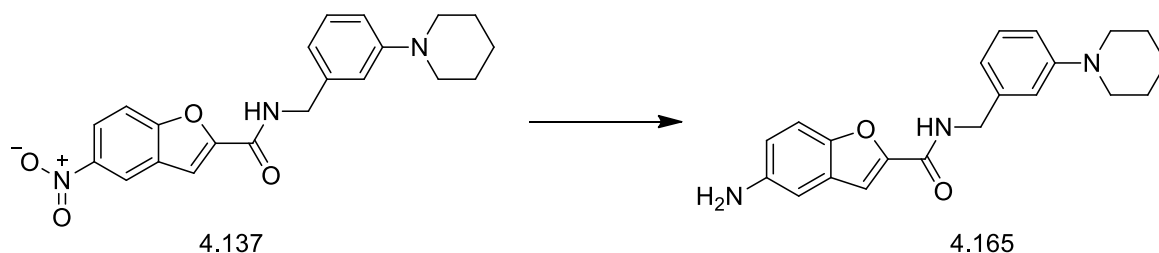
Light brown oil. IR (FTIR, $\nu_{\text{max}}/\text{cm}^{-1}$) 732.74, 804.97, 857.88, 919.38, 1026.00, 1044.26, 1128.77, 1158.02, 1231.67, 1298.26, 1327.23, 1383.60, 1452.22, 1474.74, 1512.93, 1583.30, 1646.33, 1731.49, 2359.93, 2804.87, 2847.56, 2930.66, 3336.41; ^1H NMR (400 MHz, CDCl_3 , TMS); δ 1.57 - 1.62 (m, 2H), 1.71 (quin, $J=5.62$ Hz, 4H), 3.14 - 3.19 (m, 4H), 4.56 (d, $J=5.56$ Hz, 2H), 6.78 (dd, $J=8.84$, 2.27 Hz, 2H), 6.88 - 6.91 (m, 1H), 6.93 (d, $J=8.59$ Hz, 2H), 7.21 - 7.24 (m, 1H), 7.26 (d, $J=7.07$ Hz, 2H), 7.33 (d, $J=1.01$ Hz, 1H); ^{13}C NMR (100 MHz, CDCl_3); δ 24.56, 26.03, 26.03, 39.58, 43.30, 50.89, 103.16, 106.88, 110.26, 112.29, 115.78, 116.69, 116.87, 128.83, 129.36, 143.07, 149.21, 149.48, 149.62, 152.04, 159.04; m/z (+EI) calc. For $\text{C}_{21}\text{H}_{23}\text{N}_3\text{O}_2$ (M^+) 349.43, found 349.23 ($\text{M}+\text{H}$) $^+$; Yield: 100%.

A similar hydrogenation process was followed for the synthesis of compounds **4.165** to **4.177** as mentioned below.

Procedure for the synthesis of 5-amino-*N*-(3-(piperidin-1-yl)benzyl)benzofuran-2-carboxamide (4.165)

5-Nitro-*N*-(4-(piperidin-1-yl)benzyl)benzofuran-2-carboxamide (1.0 eq., 170 mg) (**4.137**) was dissolved in a minimum amount of ethanol (35 ml) and a catalytic amount of 10% Pd/C (17 mg) was added as a slurry, also in ethanol. The reaction mixture was shaken for 1.5-2.5 hours at 45 psi in a Parr hydrogenator. After completion of the reduction, the suspension was filtered through a layer of celite, with caution, using a Buchner flask and the filtrate was concentrated to obtain a light brown, viscous oil (**4.165**) (120 mg). Pd/C waste was discarded following the standard procedure of the university described earlier in the chapter.

5-Amino-*N*-(3-(piperidin-1-yl)benzyl)benzofuran-2-carboxamide (4.165):



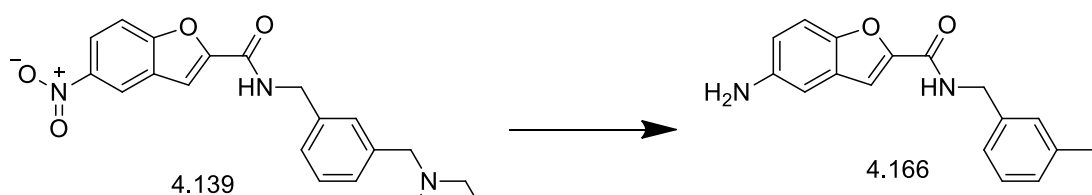
Light brown viscous mass. IR (FTIR, $\nu_{\text{max}}/\text{cm}^{-1}$) 630.11, 694.14, 733.75, 776.13, 855.09, 921.90, 952.27, 994.79, 1128.18, 1158.78, 1243.33, 1301.51, 1353.14, 1450.99, 1476.87, 1519.98, 1586.98, 1651.21, 2363.94, 2804.87, 2847.56, 2931.97, 3325.96; ^1H NMR (400 MHz, CDCl_3 , TMS); δ 1.56 - 1.62 (m, 2H), 1.71 (dt, $J=11.24$, 5.75 Hz, 4H), 3.15 - 3.21 (m, 4H), 4.60 (d, $J=5.81$ Hz, 2H), 6.79 (dd, $J=8.72$, 2.40 Hz, 1H), 6.83 (d, $J=7.33$ Hz, 1H), 6.87 -

6.90 (m, 1H), 6.91 (dd, $J=2.53, 0.51$ Hz, 1H), 6.95 (s, 1H), 7.22 - 7.24 (m, 1H), 7.24 - 7.27 (m, 1H), 7.34 (d, $J=0.76$ Hz, 1H); ^{13}C NMR (100 MHz, CDCl_3); δ 24.26, 25.80, 25.81, 43.87, 50.51, 50.52, 106.57, 110.03, 112.02, 115.83, 116.13, 116.42, 118.71, 128.51, 129.48, 138.52, 142.78, 145.39, 149.09, 149.33, 158.78; m/z (+EI) calc. For $\text{C}_{21}\text{H}_{23}\text{N}_3\text{O}_2$ (M^+) 349.43, found 349.01 ($\text{M}+\text{H}$) $^+$; Yield: 77%.

Procedure for the synthesis of 5-amino-*N*-(3-(piperidin-1-ylmethyl)benzyl)benzofuran-2-carboxamide (4.166)

5-Nitro-*N*-(4-(piperidin-1-yl)benzyl)benzofuran-2-carboxamide (1.0 eq., 100 mg) (**4.139**) was dissolved in a minimum amount of ethanol (25 ml) and a catalytic amount of 10% Pd/C (10 mg) was added as a slurry, also in ethanol. The reaction mixture was shaken for 1.5-2.5 hours at 45 psi in a Parr hydrogenator. After completion of the reduction, the suspension was filtered through a layer of celite, with caution, using a Buchner flask and the filtrate was concentrated to obtain a colourless, viscous mass (**4.166**) (63 mg). Pd/C waste was discarded following the standard procedure of the university described earlier in the chapter.

5-Amino-*N*-(3-(piperidin-1-ylmethyl)benzyl)benzofuran-2-carboxamide (4.166):

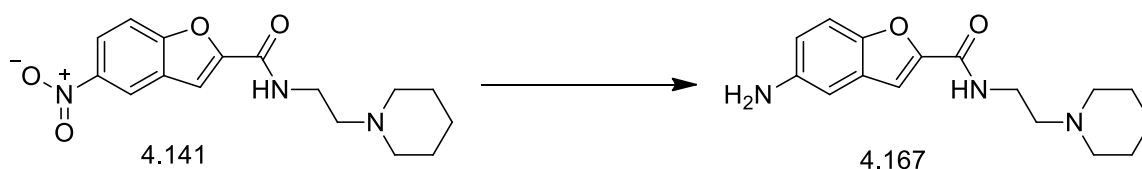


Colourless, viscous mass. IR (FTIR, $\nu_{\text{max}}/\text{cm}^{-1}$) 631.85, 702.51, 802.98, 858.45, 993.18, 1039.03, 1112.04, 1160.99, 1239.43, 1299.10, 1361.23, 1477.42, 1520.42, 1580.91, 1649.95, 1708.38, 2798.78, 2847.56, 2933.49, 3331.44; ^1H NMR (400 MHz, CDCl_3 , TMS); δ 1.41 - 1.48 (m, 2H), 1.60 (quin, $J=5.62$ Hz, 4H), 2.41 (br. s., 4H), 3.50 (s, 2H), 4.65 (d, $J=6.06$ Hz, 2H), 6.79 (dd, $J=8.84, 2.27$ Hz, 1H), 6.90 - 6.92 (m, 2H), 7.25 (d, $J=8.84$ Hz, 1H), 7.29 (d, $J=7.58$ Hz, 2H), 7.34 (br. s., 1H), 7.35 (d, $J=0.76$ Hz, 1H); ^{13}C NMR (100 MHz, CDCl_3); δ 24.21, 25.71, 30.88, 43.32, 54.47, 63.55, 77.20, 106.60, 110.17, 112.00, 116.50, 126.65, 128.49, 128.61, 128.72, 128.88, 137.73, 138.78, 142.78, 148.98, 149.35, 158.91; m/z (+EI) calc. For $\text{C}_{22}\text{H}_{25}\text{N}_3\text{O}_2$ (M^+) 363.45, found 364.12 ($\text{M}+\text{H}$) $^+$; Yield: 68%.

Procedure for the synthesis of 5-amino-*N*-(2-(piperidin-1-yl)ethyl)benzofuran-2-carboxamide (4.167)

5-Nitro-*N*-(4-(piperidin-1-yl)benzyl)benzofuran-2-carboxamide (1.0 eq., 150 mg) (**4.141**) was dissolved in a minimum amount of ethanol (25 ml) and a catalytic amount of 10% Pd/C (15 mg) was added as a slurry, also in ethanol. The reaction mixture was shaken for 1.5-2.5 hours at 45 psi in a Parr hydrogenator. After completion of the reduction, the suspension was filtered through a layer of celite, with caution, using a Buchner flask and the filtrate was concentrated to obtain a light brown oil (**4.167**) (134 mg). Pd/C waste was discarded following the standard procedure of the university described earlier in the chapter.

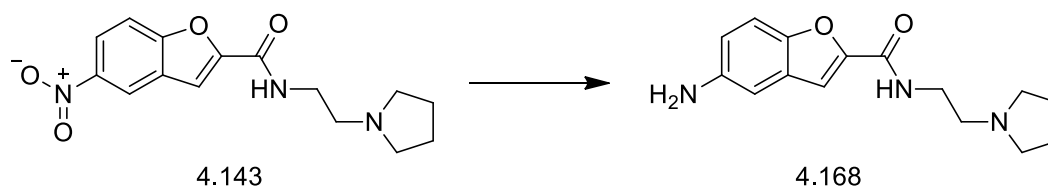
5-Amino-*N*-(2-(piperidin-1-yl)ethyl)benzofuran-2-carboxamide (4.167):



Light brown oil. IR (FTIR, $\nu_{\text{max}}/\text{cm}^{-1}$) 745.15, 809.54, 865.62, 957.87, 1043.72, 1090.91, 1129.07, 1165.74, 1242.60, 1303.60, 1325.43, 1360.35, 1383.35, 1456.02, 1577.87, 1615.12, 1647.72, 1709.67, 1732.75, 2358.94, 2931.49, 2966.59, 3336.21; ¹H NMR (500 MHz, CDCl₃, TMS); δ 1.50 (br. s., 2H), 1.67 (quin, $J=5.60$ Hz, 4H), 2.61 (br. s., 4H), 2.72 (t, $J=5.67$ Hz, 2H), 3.64 (q, $J=5.88$ Hz, 2H), 6.76 (dd, $J=8.83, 2.21$ Hz, 1H), 6.87 (d, $J=2.21$ Hz, 1H), 7.18 (d, $J=8.51$ Hz, 1H), 7.25 - 7.30 (m, 2H); ¹³C NMR (100 MHz, CDCl₃); δ 23.47, 23.85, 25.26, 35.56, 42.12, 54.23, 57.13, 106.45, 109.66, 112.10, 116.29, 128.38, 142.60, 149.16, 149.36, 159.18; m/z (+EI) calc. For C₁₆H₂₁N₃O₂ (M⁺) 287.36, found 287.87 (M+H)⁺; Yield: 99%.

Procedure for the synthesis of 5-amino-*N*-(2-(pyrrolidin-1-yl)ethyl)benzofuran-2-carboxamide (4.168)

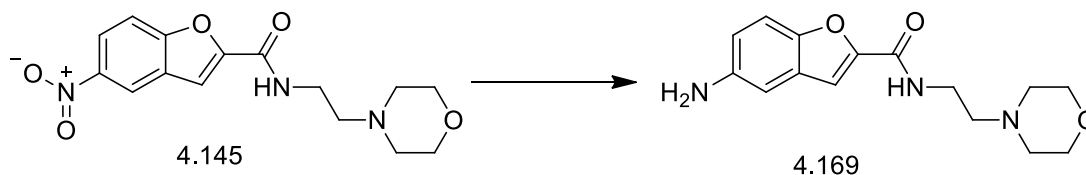
5-Nitro-*N*-(4-(piperidin-1-yl)benzyl)benzofuran-2-carboxamide (1.0 eq., 80 mg) (**4.143**) was dissolved in a minimum amount of ethanol (25 ml) and a catalytic amount of 10% Pd/C (10 mg) was added as a slurry, also in ethanol. The reaction mixture was shaken for 1.5-2.5 hours at 45 psi in a Parr hydrogenator. After completion of the reduction, the suspension was filtered through a layer of celite, with caution, using a Buchner flask and the filtrate was concentrated to obtain a light brown oil (**4.168**) (70 mg). Pd/C waste was discarded following the standard procedure of the university described earlier in the chapter.

5-Amino-*N*-(2-(pyrrolidin-1-yl)ethyl)benzofuran-2-carboxamide (4.168):

Light brown oil. IR (FTIR, $\nu_{\text{max}}/\text{cm}^{-1}$) 639.47, 745.76, 851.20, 936.02, 1045.22, 1093.04, 1164.42, 1208.19, 1242.12, 1301.53, 1382.70, 1453.88, 1475.18, 1522.15, 1583.94, 1617.35, 1646.12, 1733.50, 2329.26, 2360.62, 2798.78, 2871.95, 2932.92, 2966.50, 3337.73; ^1H NMR (500 MHz, CDCl_3 , TMS); δ 1.86 (dt, $J=6.46$, 3.39 Hz, 4H), 2.70 (br. s., 4H), 2.82 (t, $J=5.99$ Hz, 2H), 3.63 (q, $J=5.89$ Hz, 2H), 6.77 (dd, $J=8.67$, 2.36 Hz, 1H), 6.88 (d, $J=2.21$ Hz, 1H), 7.21 - 7.26 (m, 2H), 7.29 (d, $J=0.95$ Hz, 1H); ^{13}C NMR (100 MHz, CDCl_3); δ 23.71, 23.73, 37.96, 42.41, 54.26, 55.06, 106.74, 109.99, 112.36, 116.56, 128.67, 142.89, 149.43, 149.60, 159.45; m/z (+EI) calc. For $\text{C}_{15}\text{H}_{19}\text{N}_3\text{O}_2$ (M^+) 273.33, found 273.01 ($\text{M}+\text{H}$) $^+$; Yield: 97%.

Procedure for the synthesis of 5-amino-*N*-(2-morpholinoethyl)benzofuran-2-carboxamide (4.169)

5-Nitro-*N*-(4-(piperidin-1-yl)benzyl)benzofuran-2-carboxamide (1.0 eq., 85 mg) (**4.145**) was dissolved in a minimum amount of ethanol (25 ml) and a catalytic amount of 10% Pd/C (10 mg) was added as a slurry, also in ethanol. The reaction mixture was shaken for 1.5-2.5 hours at 45 psi in a Parr hydrogenator. After completion of the reduction, the suspension was filtered through a layer of celite, with caution, using a Buchner flask and the filtrate was concentrated to obtain a brown oil (**4.169**) (70 mg). Pd/C waste was discarded following the standard procedure of the university described earlier in the chapter.

5-Amino-*N*-(2-morpholinoethyl)benzofuran-2-carboxamide (4.169):

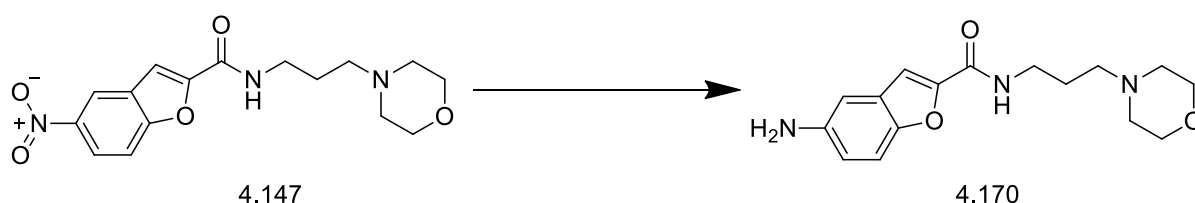
Brown oil. IR (FTIR, $\nu_{\text{max}}/\text{cm}^{-1}$) 632.69, 747.19, 807.52, 857.95, 935.17, 1045.39, 1114.07, 1146.63, 1163.00, 1208.45, 1301.96, 1361.11, 1454.23, 1476.05, 1522.16, 1583.94, 1645.97, 1732.90, 2335.36, 2810.97, 2859.75, 2967.14, 3334.37; ^1H NMR (500 MHz, CDCl_3 , TMS); δ 2.57 (br. s., 4H), 2.65 (t, $J=6.15$ Hz, 2H), 3.57 - 3.63 (m, 2H), 3.75 - 3.79 (m, 4H), 6.79 (dd,

$J=8.67$, 2.36 Hz, 1H), 6.89 (dd, $J=2.21$, 0.63 Hz, 1H), 7.26 - 7.28 (m, 2H), 7.29 (d, $J=0.95$ Hz, 1H); ^{13}C NMR (100 MHz, CDCl_3); δ 23.45, 35.39, 42.12, 53.29, 56.97, 66.76, 106.50, 109.82, 112.03, 116.36, 128.41, 142.72, 149.09, 149.30, 159.06; m/z (+EI) calc. For $\text{C}_{15}\text{H}_{19}\text{N}_3\text{O}_3$ (M^+) 289.33, found 289.02 ($\text{M}+\text{H}$) $^+$; Yield: 91%.

Procedure for the synthesis of 5-amino-*N*-(3-morpholinopropyl)benzofuran-2-carboxamide (4.170)

5-Nitro-*N*-(4-(piperidin-1-yl)benzyl)benzofuran-2-carboxamide (1.0 eq., 180 mg) (**4.147**) was dissolved in a minimum amount of ethanol (25 ml) and a catalytic amount of 10% Pd/C (20 mg) was added as a slurry, also in ethanol. The reaction mixture was shaken for 1.5-2.5 hours at 45 psi in a Parr hydrogenator. After completion of the reduction, the suspension was filtered through a layer of celite, with caution, using a Buchner flask and the filtrate was concentrated to obtain a light brown viscous oil (**4.170**) (160 mg). Pd/C waste was discarded following the standard procedure of the university described earlier in the chapter.

5-Amino-*N*-(3-morpholinopropyl)benzofuran-2-carboxamide (4.170):



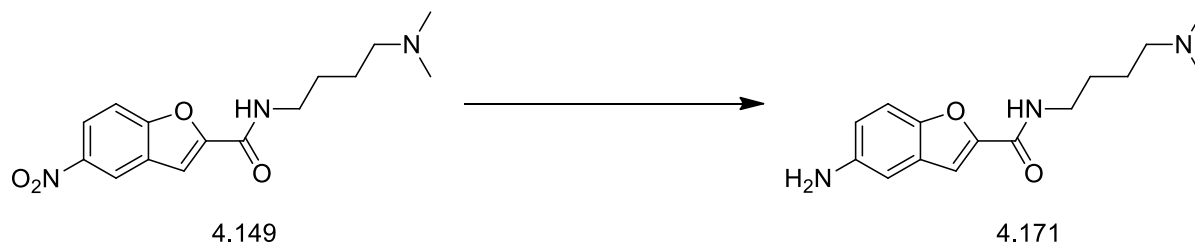
Light yellow oil. IR (FTIR, $\nu_{\text{max}}/\text{cm}^{-1}$) 690.95, 800.41, 832.64, 859.99, 896.24, 911.72, 919.67, 961.36, 983.85, 1029.91, 1072.11, 1129.99, 1153.90, 1208.56, 1242.79, 1266.55, 1292.30, 1360.10, 1342.03, 1455.24, 1474.70, 1522.95, 1582.71, 1618.43, 1654.22, 2013.55, 2357.79, 2818.34, 2951.52, 3340.12, 3434.10; ^1H NMR (400 MHz, CDCl_3 , TMS); δ 1.78 (dt, $J=11.90$, 6.01 Hz, 2H), 2.54 (br. s., 4H), 2.56 - 2.60 (m, 2H), 3.54 - 3.60 (m, 2H), 3.86 (t, $J=4.66$ Hz, 4H), 6.77 (dd, $J=8.69$, 2.39 Hz, 1H), 6.89 (d, $J=2.27$ Hz, 1H), 7.25 (d, $J=2.52$ Hz, 1H), 8.65 (br. s., 1H); ^{13}C NMR (100 MHz, CDCl_3); δ 23.45, 24.04, 39.97, 42.12, 53.76, 58.64, 66.75, 106.62, 109.49, 111.72, 116.22, 128.56, 142.74, 149.20, 149.66, 158.90; m/z (+EI) calc. For $\text{C}_{16}\text{H}_{21}\text{N}_3\text{O}_3$ (M^+) 303.36, found 303.45 ($\text{M}+\text{H}$) $^+$; Yield: 98%.

Procedure for the synthesis of 5-amino-*N*-(4-(dimethylamino)butyl)benzofuran-2-carboxamide (4.171)

5-Nitro-*N*-(4-(piperidin-1-yl)benzyl)benzofuran-2-carboxamide (1.0 eq., 100 mg) (**4.149**) was dissolved in a minimum amount of ethanol (25 ml) and a catalytic amount of 10% Pd/C (10 mg) was added as a slurry, also in ethanol. The reaction mixture was shaken for 1.5-2.5 hours

at 45 psi in a Parr hydrogenator. After completion of the reduction, the suspension was filtered through a layer of celite, with caution, using a Buchner flask and the filtrate was concentrated to obtain a light brown oil (**4.171**) (81 mg). Pd/C waste was discarded following the standard procedure of the university described earlier in the chapter.

5-Amino-*N*-(4-(dimethylamino)butyl)benzofuran-2-carboxamide (4.171**):**

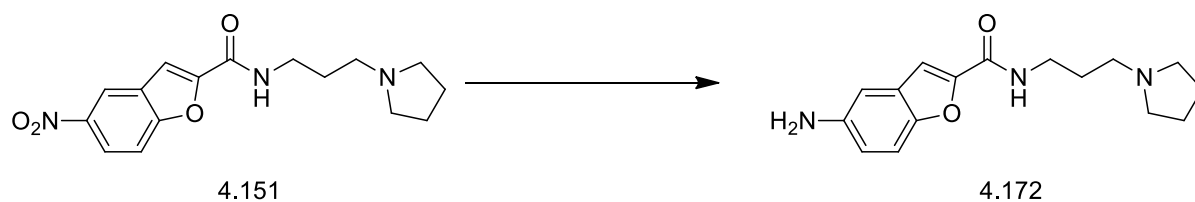


Light brown oil. IR (FTIR, $\nu_{\text{max}}/\text{cm}^{-1}$) 429.04, 518.60, 562.05, 615.46, 732.61, 807.58, 1019.6, 1164.70, 1206.97, 1241.29, 1306.80, 1454.78, 1478.58, 1531.65, 1584.87, 1639.00, 2778.8, 2824.2, 2863.50, 2939.00, 3332.00; ^1H NMR (400 MHz, CDCl_3) δ : 1.63 - 1.68 (m, 2H), 1.68 - 1.74 (m, 2H), 2.33 (s, 6H), 2.42 (t, $J=6.67$ Hz, 2H), 3.48 (q, $J=6.29$ Hz, 2H), 6.79 (dd, $J=8.69, 2.39$ Hz, 1H), 6.91 (d, $J=2.52$ Hz, 1H), 7.27 - 7.28 (m, 1H), 7.29 (d, $J=0.76$ Hz, 1H), 7.84 (br. s., 1H); ^{13}C NMR (100 MHz, CDCl_3) δ 20.83, 27.76, 39.47, 45.39, 45.41, 59.31, 106.92, 109.83, 112.21, 112.84, 116.47, 128.89, 142.99, 149.93, 159.06; m/z (+EI) calc. For $\text{C}_{15}\text{H}_{21}\text{N}_3\text{O}_2$ (M^+) 275.35, found ($\text{M}+\text{H}$) $^+$ 276.1; Yield: 90%.

Procedure for the synthesis of 5-amino-*N*-(3-(pyrrolidin-1-yl)propyl)benzofuran-2-carboxamide (4.172**)**

5-Nitro-*N*-(4-(piperidin-1-yl)benzyl)benzofuran-2-carboxamide (1.0 eq., 100 mg) (**4.151**) was dissolved in a minimum amount of ethanol (25 ml) and a catalytic amount of 10% Pd/C (10 mg) was added as a slurry, also in ethanol. The reaction mixture was shaken for 1.5-2.5 hours at 45 psi in a Parr hydrogenator. After completion of the reduction, the suspension was filtered through a layer of celite, with caution, using a Buchner flask and the filtrate was concentrated to obtain a colourless oil (**4.172**) (90 mg). Pd/C waste was discarded following the standard procedure of the university described earlier in the chapter.

5-Amino-*N*-(3-(pyrrolidin-1-yl)propyl)benzofuran-2-carboxamide (4.172**):**

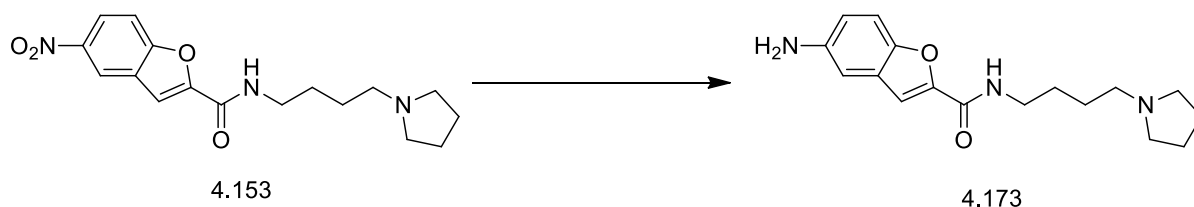


Colourless oil. IR (FTIR, $\nu_{\text{max}}/\text{cm}^{-1}$) 428.48, 519.74, 571.26, 614.54, 731.89, 749.11, 807.30, 859.45, 1161.70, 1210.00, 1242.62, 1300.80, 1454.31, 1475.64, 1524.20, 1583.61, 1638.63, 2803.00, 2878.60, 2930.00, 2957.20, 3232.20, 3335.00; ^1H NMR (400 MHz, CDCl_3) δ 1.85 (dt, $J=12.15$, 6.14 Hz, 2H), 1.89 - 1.98 (m, 4H), 2.69 (br. s., 4H), 2.77 (t, $J=6.17$ Hz, 2H), 3.56 - 3.63 (m, 2H), 6.78 (dd, $J=8.69$, 2.39 Hz, 1H), 6.90 (d, $J=2.52$ Hz, 1H), 7.24 (d, $J=8.81$ Hz, 1H), 8.71 (br. s., 1H); ^{13}C NMR (100 MHz, CDCl_3) δ 23.33, 23.48, 26.51, 50.91, 53.97, 54.31, 59.11, 104.25, 106.60, 109.24, 111.82, 116.10, 128.60, 142.61, 149.34, 154.99; m/z (+EI) calc. For $\text{C}_{16}\text{H}_{21}\text{N}_3\text{O}$ (M^+) 287.36, found ($\text{M}+\text{H}$) $^+$ 288.10; Yield: 99%.

Procedure for the synthesis of 5-amino-*N*-(4-(pyrrolidin-1-yl)butyl)benzofuran-2-carboxamide (4.173)

5-Nitro-*N*-(4-(piperidin-1-yl)benzyl)benzofuran-2-carboxamide (1.0 eq., 100 mg) (**4.153**) was dissolved in a minimum amount of ethanol (25 ml) and a catalytic amount of 10% Pd/C (10 mg) was added as a slurry, also in ethanol. The reaction mixture was shaken for 1.5-2.5 hours at 45 psi in a Parr hydrogenator. After completion of the reduction, the suspension was filtered through a layer of celite, with caution, using a Buchner flask and the filtrate was concentrated to obtain a light yellow powder (**4.173**) (85 mg). Pd/C waste was discarded following the standard procedure of the university described earlier in the chapter.

5-Amino-*N*-(4-(pyrrolidin-1-yl)butyl)benzofuran-2-carboxamide (4.173):

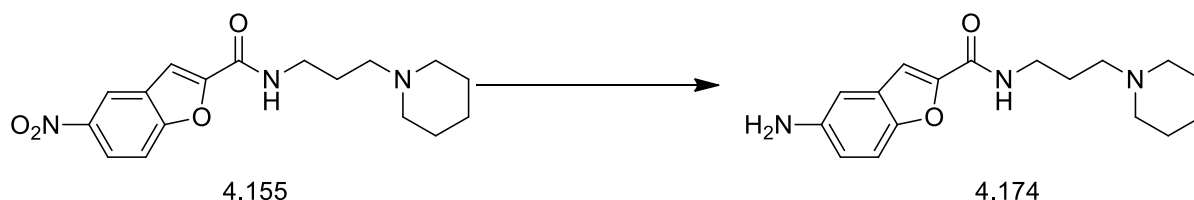


Light yellow powder. IR (FTIR, $\nu_{\text{max}}/\text{cm}^{-1}$) 416.34, 564.89, 678.00, 725.24, 809.64, 946.27, 1009.49, 1079.28, 1197.34, 1342.00, 1469.31, 1507.60, 1534.00, 1687.01, 1732.08, 2764.058, 2834.00, 2964.32; ^1H NMR (400 MHz, CDCl_3) δ 1.52 – 1.62 (m, 2H), 1.68 – 1.72 (m, 4H), 1.84 – 1.97 (m, 2H), 2.50 – 2.64 (m, 4H), 3.12 (br. s., 2H), 3.60 - 3.67 (m, 2H), 6.39 (d, $J=9.0$ Hz, 1H), 7.41 (d, $J=9.0$ Hz, 1H), 7.59 (s, 1H), 7.65 (s, 1H); ^{13}C NMR (100 MHz, CDCl_3) δ 23.00, 23.51, 24.98, 27.56, 40.10, 54.58, 55.12, 56.27, 108.47, 112.30, 116.04, 120.37, 130.56, 145.62, 150.14, 158.07, 163.30; m/z (+EI) calc. For $\text{C}_{17}\text{H}_{23}\text{N}_3\text{O}_2$ (M^+) 301.38, found ($\text{M}+\text{H}$) $^+$ 302.20; Yield: 93%.

Procedure for the synthesis of 5-amino-*N*-(3-(piperidin-1-yl)propyl)benzofuran-2-carboxamide (4.174)

5-Nitro-*N*-(4-(piperidin-1-yl)benzyl)benzofuran-2-carboxamide (1.0 eq., 130 mg) (**4.155**) was dissolved in a minimum amount of ethanol (25 ml) and a catalytic amount of 10% Pd/C (15 mg) was added as a slurry, also in ethanol. The reaction mixture was shaken for 1.5-2.5 hours at 45 psi in a Parr hydrogenator. After completion of the reduction, the suspension was filtered through a layer of celite, with caution, using a Buchner flask and the filtrate was concentrated to obtain a colourless oil (**4.174**) (45 mg). Pd/C waste was discarded following the standard procedure of the university described earlier in the chapter.

5-Amino-*N*-(3-(piperidin-1-yl)propyl)benzofuran-2-carboxamide (4.174):



Colourless oil. IR (FTIR, $\nu_{\text{max}}/\text{cm}^{-1}$) 429.22, 519.24, 614.89, 729.66, 805.38, 856.42, 913.85, 962.22, 1040.80, 1089.20, 1125.40, 1159.32, 1208.82, 1243.96, 1297.70, 1453.63, 1474.84, 1521.02, 1583.60, 1640.04, 2766.80, 2812.00, 2857.40, 2933.00, 3226.20, 3341.00; ^1H NMR (400 MHz, CDCl_3) δ ppm 1.23 - 1.29 (m, 2H), 1.55 (br. s., 2H), 1.72 - 1.77 (m, 4H), 1.78 - 1.83 (m, 2H), 2.52 (br. s., 2H), 2.56 - 2.60 (m, 2H), 3.53 - 3.59 (m, 2H), 6.75 - 6.79 (m, 1H), 6.90 (d, $J=2.27$ Hz, 1H), 7.18 - 7.22 (m, 1H), 7.28 (d, $J=0.76$ Hz, 1H), 8.98 (br. s., 1H); ^{13}C NMR (100 MHz, CDCl_3) δ 23.51, 24.21, 24.28, 25.47, 40.06, 42.11, 54.62, 58.66, 106.67, 109.31, 111.72, 116.14, 128.65, 142.66, 149.33, 149.89, 159.07; m/z (+EI) calc. For $\text{C}_{17}\text{H}_{23}\text{N}_3\text{O}_2$ (M^+) 301.38, found ($\text{M}+\text{H}$) $^+$ 302.20; Yield: 38%.

Procedure for the synthesis of 5-amino-*N*-(2-(4-methylpiperazin-1-yl)ethyl)benzofuran-2-carboxamide (4.175)

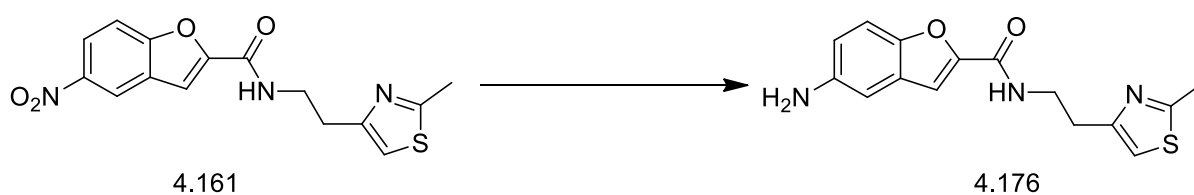
5-Nitro-*N*-(4-(piperidin-1-yl)benzyl)benzofuran-2-carboxamide (1.0 eq., 130 mg) (**4.157**) was dissolved in a minimum amount of ethanol (25 ml) and a catalytic amount of 10% Pd/C (13 mg) was added as a slurry, also in ethanol. The reaction mixture was shaken for 1.5-2.5 hours at 45 psi in a Parr hydrogenator. After completion of the reduction, the suspension was filtered through a layer of celite, with caution, using a Buchner flask and the filtrate was concentrated to obtain a light brown oil (**4.175**) (112 mg). Pd/C waste was discarded following the standard procedure of the university described earlier in the chapter.

5-Amino-N-(2-(4-methylpiperazin-1-yl)ethyl)benzofuran-2-carboxamide (4.175):

Light brown oil. IR (FTIR, $\nu_{\text{max}}/\text{cm}^{-1}$) 428.83, 519.83, 614.36, 729.61, 753.00, 805.33, 1038.70, 1089.90, 1123.00, 1159.20, 1208.58, 1243.81, 1300.80, 1453.79, 1474.69, 1521.54, 1583.66, 1639.52, 2810.00, 2852.20, 2936.60, 3231.80, 3346.30; ^1H NMR (400 MHz, CDCl_3) δ 2.31 (s, 3H), 2.37 - 2.59 (m, 8H), 2.59 - 2.62 (m, 2H), 3.54 (q, $J=5.96$ Hz, 2H), 6.77 (dd, $J=8.94, 2.39$ Hz, 1H), 6.88 (d, $J=2.27$ Hz, 1H), 7.08 (br. s., 1H), 7.28 - 7.30 (m, 1H); ^{13}C NMR (100 MHz, CDCl_3) δ 23.51, 26.78, 35.89, 45.88, 52.68, 55.00, 56.44, 106.59, 109.79, 112.08, 116.36, 128.52, 142.76, 149.27, 149.37, 159.07; m/z (+EI) calc. For $\text{C}_{16}\text{H}_{22}\text{N}_4\text{O}$ (M^+) 302.37, found ($\text{M}+\text{H}$) $^+$ 303.10; Yield: 95%.

Procedure for the synthesis of 5-amino-N-(2-(2-methylthiazol-4-yl)ethyl)benzofuran-2-carboxamide (4.176)

5-Nitro-N-(4-(piperidin-1-yl)benzyl)benzofuran-2-carboxamide (1.0 eq., 150 mg) (**4.161**) was dissolved in a minimum amount of ethanol (25 ml) and a catalytic amount of 10% Pd/C (15 mg) was added as a slurry, also in ethanol. The reaction mixture was shaken for 1.5-2.5 hours at 45 psi in a Parr hydrogenator. After completion of the reduction, the suspension was filtered through a layer of celite, with caution, using a Buchner flask and the filtrate was concentrated to obtain a colourless oil (**4.176**) (130 mg). Pd/C waste was discarded following the standard procedure of the university described earlier in the chapter.

5-Amino-N-(2-(2-methylthiazol-4-yl)ethyl)benzofuran-2-carboxamide (4.176):

Colourless oil. IR (FTIR, $\nu_{\text{max}}/\text{cm}^{-1}$) 432.79, 612.62, 631.97, 755.94, 792.94, 819.88, 865.29, 1059.70, 1129.49, 1158.79, 1235.998, 1303.80, 1321.80, 1385.10, 1453.09, 1522.15, 1561.45, 1617.00, 1637.45, 2918.50, 2966.70, 3334.20; ^1H NMR (400 MHz, CDCl_3) δ 2.74 (s, 3H), 3.04 (t, $J=6.55$ Hz, 2H), 3.79 - 3.82 (m, 2H), 6.79 (dd, $J=8.69, 2.39$ Hz, 1H), 6.86 (s, 1H), 6.89 - 6.90 (m, 1H), 7.28 (s, 1H), 7.29 (d, $J=1.01$ Hz, 1H); ^{13}C NMR (100 MHz, CDCl_3) δ 19.17, 23.47, 42.07, 106.54, 109.68, 111.98, 114.00, 116.32, 128.47, 142.70, 149.25,

153.60, 156.99, 159.03, 166.14; m/z (+EI) calc. For $C_{15}H_{15}N_3O_2S$ (M^+) 301.36, found ($M+H$)⁺ 302.00; Yield: 95%.

Procedure for the synthesis of 5-amino-*N*-(2-(dimethylamino)ethyl)benzofuran-2-carboxamide (4.177)

5-Nitro-*N*-(4-(piperidin-1-yl)benzyl)benzofuran-2-carboxamide (1.0 eq., 120 mg) (**4.163**) was dissolved in a minimum amount of ethanol (25 ml) and a catalytic amount of 10% Pd/C (12 mg) was added as a slurry, also in ethanol. The reaction mixture was shaken for 1.5-2.5 hours at 45 psi in a Parr hydrogenator. After completion of the reduction, the suspension was filtered through a layer of celite, with caution, using a Buchner flask and the filtrate was concentrated to obtain a light brown, viscous oil (**4.177**) (105 mg). Pd/C waste was discarded following the standard procedure of the university described earlier in the chapter.

5-Amino-*N*-(2-(dimethylamino)ethyl)benzofuran-2-carboxamide (4.177):



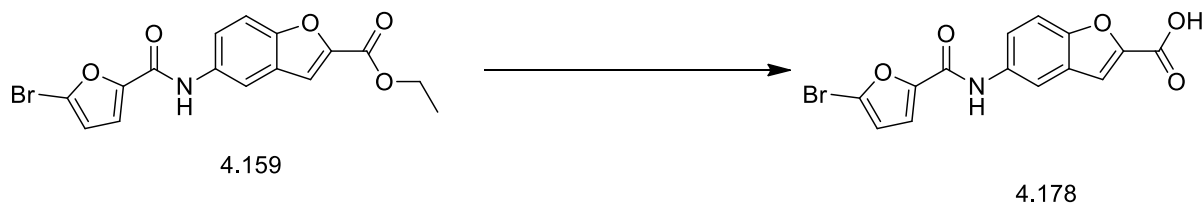
Colourless oil. IR (FTIR, $\nu_{\max}/\text{cm}^{-1}$) 432.79, 612.62, 631.97, 755.94, 792.94, 819.88, 865.29, 1059.70, 1129.49, 1158.79, 1235.998, 1303.80, 1321.80, 1385.10, 1453.09, 1522.15, 1561.45, 1617.00, 1637.45, 2918.50, 2966.70, 3334.20; ^1H NMR (400 MHz, CDCl_3) δ 3.04 (t, $J=6.55$ Hz, 2H), 3.79 - 3.82 (m, 2H), 6.79 (dd, $J=8.69, 2.39$ Hz, 1H), 6.86 (s, 1H), 6.89 - 6.90 (m, 1H), 7.28 (s, 1H), 7.29 (d, $J=1.01$ Hz, 1H); ^{13}C NMR (100 MHz, CDCl_3) δ 19.17, 23.47, 42.07, 106.54, 109.68, 111.98, 114.00, 116.32, 128.47, 142.70, 149.25, 153.60, 156.99, 159.03, 166.14; m/z (+EI) calc. For $C_{13}H_{17}N_3O_2$ (M^+) 247.29, found ($M+H$)⁺ 247.00; Yield: 98%.

General procedure for the synthesis of (5-bromofuran-2-carboxamido)benzofuran-2-carboxylic acid (4.178) from ethyl 5-(5-bromofuran-2-carboxamido)benzofuran-2-carboxylate (4.159) by hydrolysis

Ethyl 5-(5-bromofuran-2-carboxamido)benzofuran-2-carboxylate (267 mg, 1 eq.) (**4.159**) was dissolved in equal volumes of 1,4-dioxane and 0.5M NaOH (5 ml + 5 ml) in a round bottom flask. This reaction mixture was stirred for 3.0 hours at which point LCMS and TLC showed completion of the reaction. The reaction mixture was then diluted with 10.0 ml of distilled

water and 0.5M HCL acid solution was added drop by drop to reach a pH near 3.0. At this point, the product (**4.178**) precipitated and was collected by filtering on a sintered funnel. The pink powder was scraped from the funnel and dried overnight in a vacuum oven at 40 °C. The final weight of the dried product was 208 mg.

(5-Bromofuran-2-carboxamido)benzofuran-2-carboxylic acid (4.178):

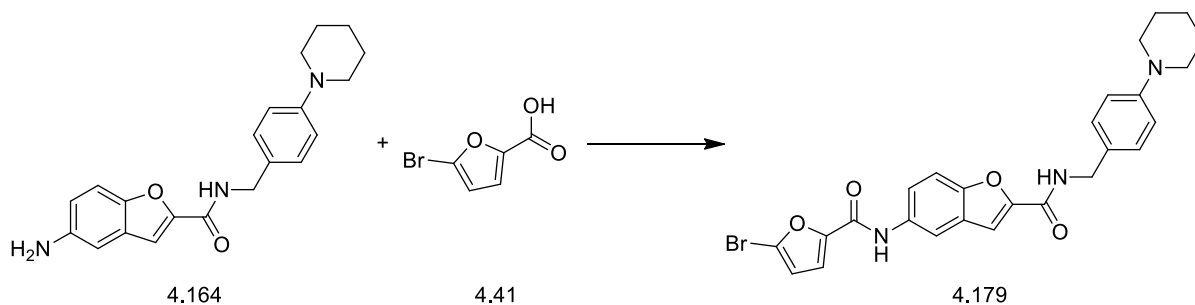


Light pink powder. IR (FTIR, $\nu_{\max}/\text{cm}^{-1}$) 420.58, 457.43, 543.29, 611.59, 740.94, 790.56, 876.66, 942.62, 1034.80, 1110.30, 1182.71, 1227.81, 1340.00, 1406.70, 1473.32, 1565.30, 1593.81, 1655.13, 2491.70, 2917.90, 3093, 3365.20; ^1H NMR (400 MHz, Methanol- d_4) δ 6.65 - 6.68 (m, 1H), 7.27 (d, $J=3.53$ Hz, 1H), 7.53 (s, 1H), 7.57 (d, $J=9.06$ Hz, 1H), 7.69 (dd, $J=8.94$, 2.14 Hz, 1H), 8.11 (d, $J=2.27$ Hz, 1H); ^{13}C NMR (100 MHz, Methanol- d_4) δ 113.15, 114.35, 115.62, 116.46, 118.64, 123.30, 135.14, 137.23, 146.06, 149.47, 154.36, 157.96, 161.67, 165.32; m/z (+EI) calc. For $\text{C}_{14}\text{H}_8\text{BrNO}_5$ (M^+) 350.12, found ($M+H$) $^+$ 351.90; Yield: 84%.

Amide coupling was used to obtain the following intermediates (**4.179** to **4.194**).

Procedure for the synthesis of 5-(5-bromofuran-2-carboxamido)-*N*-(4-(piperidin-1-yl)benzyl)benzofuran-2-carboxamide (4.179) from 5-amino-*N*-(4-(piperidin-1-yl)benzyl)benzofuran-2-carboxamide (4.164) and 5-bromofuran-2-carboxylic acid (4.41) 97 mg (1.0 eq.) **4.164**, 80 mg (1.50 eq.) **4.41**, 2.0 eq. HOBt and 1.75 eq. DIC were mixed in a round bottomed flask to which a minimum amount of DCM was added to make a clear solution. The reaction mixture was then stirred for 3 hours. In between, the progress of the reaction was checked using LCMS. When the reaction was completed after 3 hours the mixture was dried using a rotary evaporator and the product dried in a vacuum. The product **4.179** was then purified using a silica column with a DCM:ethylacetate solvent systems of different polarities. Finally, 130 mg product was obtained as bright yellow oil.

5-(5-Bromofuran-2-carboxamido)-N-(4-(piperidin-1-yl)benzyl)benzofuran-2-carboxamide (4.179)

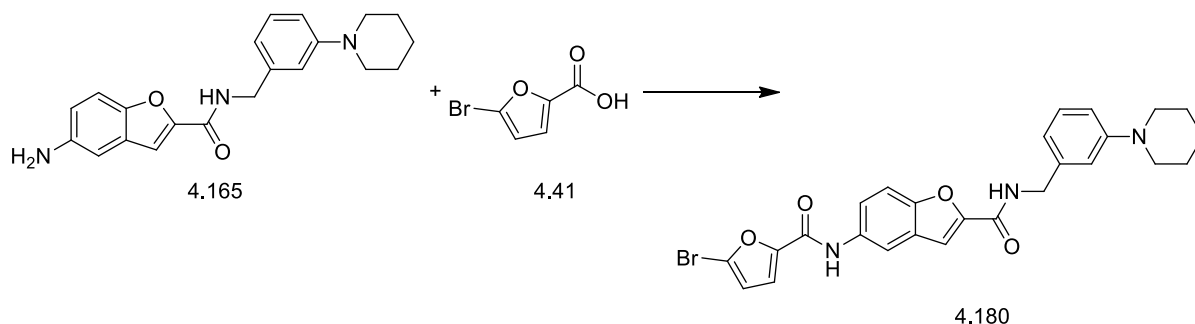


Bright yellow oil. IR (FTIR, $\nu_{\text{max}}/\text{cm}^{-1}$) 630.36, 700.21, 733.62, 781.24, 802.60, 865.75, 922.28, 946.81, 1010.97, 1100.52, 1125.37, 1167.24, 1201.39, 1234.31, 1359.23, 1466.33, 1514.09, 1567.77, 1614.10, 1657.00, 1710.07, 2329.26, 2359.13, 2935.98, 2963.41, 3339.21; ^1H NMR (400 MHz, CDCl_3 , TMS); δ 1.61 (q, $J=5.89$ Hz, 2H), 1.78 (dt, $J=11.37$, 5.68 Hz, 4H), 3.20 - 3.24 (m, 4H), 3.77 (dt, $J=13.01$, 6.38 Hz, 2H), 4.59 (d, $J=5.56$ Hz, 2H), 6.43 (d, $J=3.54$ Hz, 1H), 6.51 (d, $J=3.54$ Hz, 1H), 7.04 - 7.07 (m, 2H), 7.13 (d, $J=3.54$ Hz, 1H), 7.22 (d, $J=3.54$ Hz, 1H), 7.41 (d, $J=8.84$ Hz, 1H), 7.47 (d, $J=1.01$ Hz, 1H), 7.57 (dd, $J=8.97$, 2.15 Hz, 1H), 8.06 (d, $J=2.02$ Hz, 1H); ^{13}C NMR (100 MHz, CDCl_3); δ 23.23, 23.60, 25.09, 42.49, 42.97, 52.06, 110.69, 112.02, 113.80, 114.17, 114.61, 117.66, 117.82, 119.65, 120.47, 124.98, 126.29, 126.83, 128.01, 129.16, 149.18, 149.48, 151.87, 157.88, 158.63, 160.79; m/z (+EI) calc. For $\text{C}_{26}\text{H}_{24}\text{BrN}_3\text{O}_4$ (M^+) 522.39, found 523.87 ($\text{M}+\text{H}$) $^+$; Yield: 90%.

Procedure for the synthesis of 5-(5-bromofuran-2-carboxamido)-N-(3-(piperidin-1-yl)benzyl)benzofuran-2-carboxamide (3.180) from 5-amino-N-(3-(piperidin-1-yl)benzyl)benzofuran-2-carboxamide (3.165) and 5-bromofuran-2-carboxylic acid (3.41)

112 mg (1.0 eq.) **4.165**, 92 mg (1.50 eq.) **4.41**, 2.0 eq. HOBt and 1.75 eq. DIC were mixed in a round bottomed flask to which a minimum amount of DCM was added to make a clear solution. The reaction mixture was then stirred for 3 hours. In between, the progress of the reaction was checked using LCMS. When the reaction was completed after 3 hours the mixture was dried using a rotary evaporator and the product dried in a vacuum. The product **4.180** was then purified using a silica column and DCM:ethylacetate solvent systems of different polarities. Finally, 150 mg product was obtained as an orange, viscous mass.

5-(5-Bromofuran-2-carboxamido)-N-(3-(piperidin-1-yl)benzyl)benzofuran-2-carboxamide (3.180):

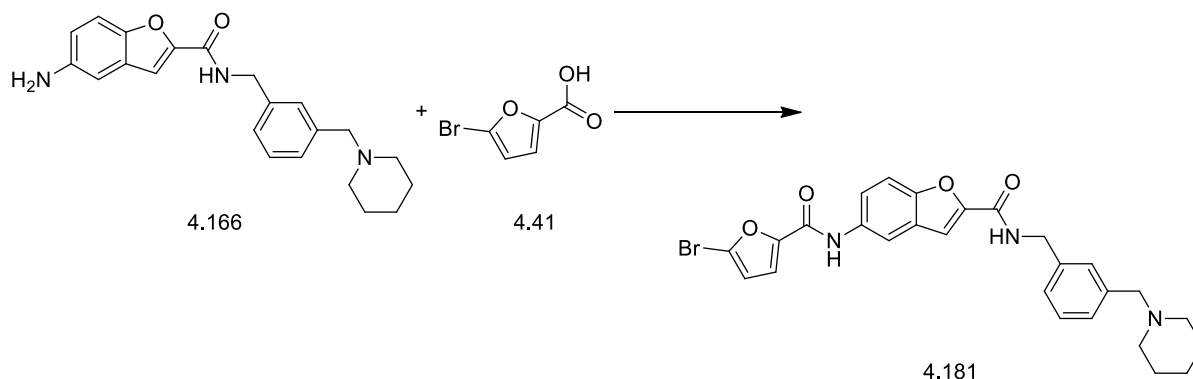


Orange, viscous mass. IR (FTIR, $\nu_{\text{max}}/\text{cm}^{-1}$) 630.60, 747.98, 865.74, 923.99, 1045.20, 1129.01, 1166.98, 1243.73, 1324.91, 1360.25, 1383.75, 1462.31, 1521.54, 1559.65, 1613.65, 2358.91, 2929.33, 2966.77, 3337.38; ^1H NMR (400 MHz, CDCl_3 , TMS); δ 1.56 - 1.62 (m, 2H), 1.71 (dt, $J=11.18$, 5.65 Hz, 4H), 3.15 - 3.21 (m, 4H), 4.62 (d, $J=5.56$ Hz, 2H), 6.53 (dd, $J=3.54$, 0.51 Hz, 1H), 6.84 (d, $J=7.83$ Hz, 1H), 6.88 - 6.92 (m, 1H), 6.95 (s, 1H), 7.22 (dd, $J=3.54$, 0.51 Hz, 1H), 7.44 - 7.47 (m, 1H), 7.49 (s, 1H), 7.57 (dd, $J=8.84$, 2.27 Hz, 1H), 7.69 (d, $J=8.84$ Hz, 1H), 7.91 (d, $J=8.59$ Hz, 1H), 8.09 (d, $J=2.27$ Hz, 1H), 8.11 (s, 1H); ^{13}C NMR (100 MHz, CDCl_3); δ 23.45, 24.24, 25.78, 42.23, 50.51, 50.54, 112.07, 114.08, 114.67, 117.65, 120.30, 124.47, 124.91, 129.54, 133.24, 135.47, 137.29, 137.62, 138.34, 139.83, 140.94, 147.50, 149.68, 155.00, 157.03, 158.44; m/z (+EI) calc. For $\text{C}_{26}\text{H}_{24}\text{BrN}_3\text{O}_4$ (M^+) 522.39, found 523.74 ($\text{M}+\text{H}$) $^+$; Yield: 89.58%.

Procedure for the synthesis of 5-(5-bromofuran-2-carboxamido)-N-(3-(piperidin-1-yl)methyl)benzyl)benzofuran-2-carboxamide (4.181) from 5-amino-N-(3-(piperidin-1-yl)methyl)benzyl)benzofuran-2-carboxamide (4.166) and 5-bromofuran-2-carboxylic acid (4.41)

59 mg (1.0 eq.) **4.166**, 46 mg (1.50 eq.) **4.41**, 2.0 eq. HOBt and 1.75 eq. DIC were mixed in a round bottomed flask to which a minimum amount of DCM was added to make a clear solution. The reaction mixture was then stirred for 3 hours. In between, the progress of the reaction was checked using LCMS. When the reaction was completed after 3 hours the mixture was dried using a rotary evaporator and the product dried in a vacuum. The product **4.181** was then purified using a silica column and DCM:ethylacetate solvent systems of different polarities. Finally, 55 mg product was obtained as a bright viscous mass.

5-(5-Bromofuran-2-carboxamido)-*N*-(3-(piperidin-1-ylmethyl)benzyl)benzofuran-2-carboxamide (4.181):

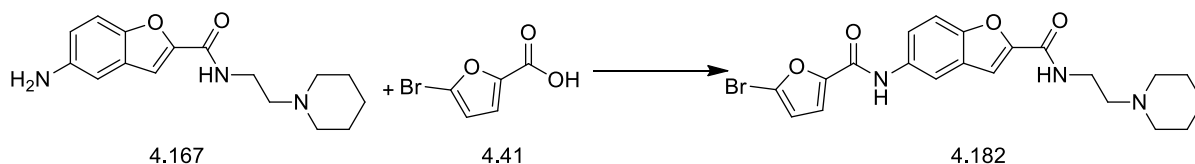


Brown, viscous mass. IR (FTIR, $\nu_{\text{max}}/\text{cm}^{-1}$) 632.88, 744.08, 806.50, 865.66, 923.54, 944.49, 1012.57, 1098.86, 1129.15, 1167.57, 1245.67, 1324.92, 1360.04, 1383.64, 1463.05, 1565.72, 1614.10, 1659.33, 2926.82, 2967.03, 3338.39; ^1H NMR (400 MHz, CDCl_3 , TMS); δ 2.89 (m, 2H), 2.96 (s, 2H), 3.49 (s, 4H), 3.80 (dt, $J=12.95$, 6.54 Hz, 4H), 4.55 (d, $J=6.06$ Hz, 1H), 6.46 - 6.52 (m, 1H), 7.17 - 7.19 (m, 1H), 7.29 - 7.31 (m, 1H), 7.32 - 7.33 (m, 1H), 7.35 (dd, $J=5.81$, 1.26 Hz, 1H), 7.37 - 7.40 (m, 1H), 7.45 (d, $J=0.76$ Hz, 1H), 7.49 (dd, $J=8.97$, 2.15 Hz, 1H), 7.64 - 7.68 (m, 2H), 7.80 - 7.84 (m, 2H), 8.01 - 8.04 (m, 1H); ^{13}C NMR (100 MHz, CDCl_3); δ 22.72, 23.36, 31.48, 36.51, 42.33, 50.78, 55.25, 110.60, 112.13, 113.67, 114.35, 118.21, 122.11, 126.24, 127.95, 128.21, 128.83, 129.18, 130.03, 133.01, 139.45, 142.27, 149.26, 151.93, 155.06, 157.32, 158.98; m/z (+EI) calc. For $\text{C}_{27}\text{H}_{26}\text{BrN}_3\text{O}_4$ (M^+) 536.42, found 537.58 ($\text{M}+\text{H}$) $^+$; Yield: 63%.

Procedure for the synthesis of 5-(5-bromofuran-2-carboxamido)-*N*-(2-(piperidin-1-yl)ethyl)benzofuran-2-carboxamide (4.182) from 5-amino-*N*-(2-(piperidin-1-yl)ethyl)benzofuran-2-carboxamide (4.167) and 5-bromofuran-2-carboxylic acid (4.41)

130 mg (1.0 eq.) **4.167**, 129 mg (1.50 eq.) **4.41**, 2.0 eq. HOBt and 1.75 eq. DIC were mixed in a round bottomed flask in which a minimum amount of DCM was added to make a clear solution. The reaction mixture was then stirred for 3 hours. In between, the progress of the reaction was checked using LCMS. When the reaction was completed after 3 hours it was dried using a rotary evaporator and the residue dried in a vacuum. The product **4.182** was then purified using a silica column and DCM:ethyl acetate as the solvent system of different polarities. Finally, 138 mg product was obtained as brown, viscous oil.

5-(5-Bromofuran-2-carboxamido)-N-(2-(piperidin-1-yl)ethyl)benzofuran-2-carboxamide (4.182):

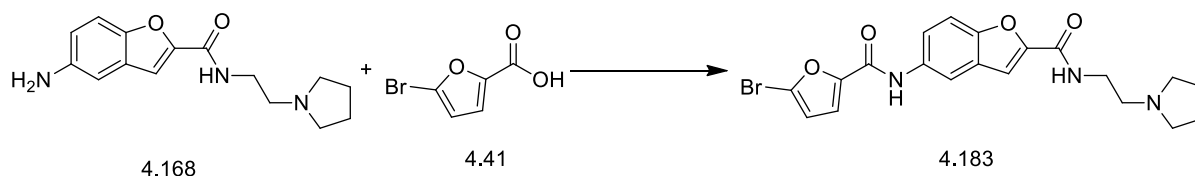


Brown, viscous oil. IR (FTIR, $\nu_{\text{max}}/\text{cm}^{-1}$) 631.14, 740.72, 807.85, 925.21, 1029.33, 1105.98, 1203.85, 1237.87, 1301.03, 1350.38, 1462.47, 1541.35, 1586.51, 1651.73, 2201.22, 2323.17, 2359.75, 2810.97, 2934.03, 3290.65; ^1H NMR (500 MHz, CDCl_3 , TMS); δ 1.47 - 1.52 (m, 2H), 1.64 (quin, $J=5.60$ Hz, 4H), 2.47 (br. s., 4H), 2.56 - 2.61 (m, 2H), 3.57 (q, $J=5.88$ Hz, 2H), 6.53 (d, $J=3.78$ Hz, 1H), 7.22 (d, $J=3.78$ Hz, 1H), 7.44 (d, $J=0.95$ Hz, 1H), 7.52 (d, $J=8.83$ Hz, 1H), 7.58 (dd, $J=8.83$, 2.21 Hz, 1H), 8.08 (d, $J=1.89$ Hz, 2H); ^{13}C NMR (100 MHz, CDCl_3); δ 23.46, 24.35, 26.00, 30.94, 35.99, 54.32, 56.97, 110.14, 112.14, 113.95, 114.68, 117.64, 120.03, 124.86, 128.16, 132.98, 149.21, 150.04, 151.89, 154.95, 158.63; m/z (+EI) calc. For $\text{C}_{21}\text{H}_{22}\text{BrN}_3\text{O}_4$ (M^+) 460.32, found 461.49 ($\text{M}+\text{H}$) $^+$; Yield: 66%.

Procedure for the synthesis of 5-(5-bromofuran-2-carboxamido)-N-(2-(pyrrolidin-1-yl)ethyl)benzofuran-2-carboxamide (4.183) from 5-amino-N-(2-(pyrrolidin-1-yl)ethyl)benzofuran-2-carboxamide (4.168) and 5-bromofuran-2-carboxylic acid (4.41)

70 mg (1.0 eq.) **4.168**, 73 mg (1.50 eq.) **4.41**, 2.0 eq. HOBt and 1.75 eq. DIC were mixed in a round bottomed flask in which a minimum amount of DCM was added to make a clear solution. The reaction mixture was then stirred for 3 hours. In between, the progress of the reaction was checked using LCMS. When the reaction was completed after 3 hours it was dried using a rotary evaporator and the residue dried in a vacuum. The product **4.183** was then purified using a silica column and DCM:ethylacetate solvent systems of different polarities. Finally, 112 mg product was obtained as light yellow, viscous oil.

5-(5-Bromofuran-2-carboxamido)-N-(2-(pyrrolidin-1-yl)ethyl)benzofuran-2-carboxamide (4.183):

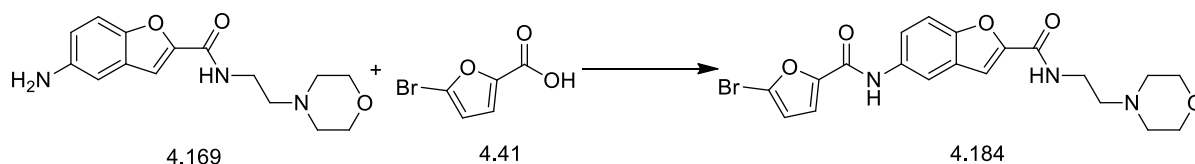


Light yellow viscous oil. IR (FTIR, $\nu_{\text{max}}/\text{cm}^{-1}$) 658.41, 739.93, 747.93, 757.97, 791.79, 810.73, 849.88, 864.54, 882.30, 925.33, 938.77, 960.55, 1031.30, 1105.85, 1135.00, 1169.21, 1205.89, 1223.16, 1240.07, 1279.43, 1308.79, 1337.97, 1354.97, 1436.07, 1460.66, 1569.95, 1593.26, 1638.43, 1650.22, 2335.36, 2357.05, 2803.26, 2871.95, 2939.62, 3311.23; ^1H NMR (500 MHz, CDCl_3 , TMS); δ 1.84 (dt, $J=7.01$, 3.27 Hz, 4H), 2.57 - 2.63 (m, 4H), 2.74 (t, $J=6.15$ Hz, 2H), 3.58 - 3.63 (m, 2H), 6.53 (d, $J=3.47$ Hz, 1H), 7.15 (t, $J=5.04$ Hz, 1H), 7.22 (d, $J=3.47$ Hz, 1H), 7.45 (d, $J=0.95$ Hz, 1H), 7.50 - 7.53 (m, 1H), 7.56 - 7.60 (m, 1H), 8.07 (br. s., 1H), 8.08 (d, $J=1.89$ Hz, 1H); ^{13}C NMR (100 MHz, CDCl_3); δ 23.80, 24.40, 38.33, 40.75, 54.23, 54.86, 110.48, 112.42, 114.22, 114.94, 117.91, 120.31, 125.12, 128.43, 133.24, 149.47, 150.24, 152.13, 155.20, 158.95; m/z (+EI) calc. For $\text{C}_{20}\text{H}_{20}\text{BrN}_3\text{O}_4$ (M^+) 446.29, found 445.98 ($\text{M}+\text{H}$) $^+$; Yield: 98%.

Procedure for the synthesis of 5-(5-bromofuran-2-carboxamido)-*N*-(2-morpholinoethyl)benzofuran-2-carboxamide (4.184) from 5-amino-*N*-(2-morpholinoethyl)benzofuran-2-carboxamide (4.169) and 5-bromofuran-2-carboxylic acid (4.41)

70 mg (1.0 eq.) **4.169**, 69 mg (1.50 eq.) **4.41**, 2.0 eq. HOBt and 1.75 eq. DIC were mixed in a round bottomed flask in which a minimum amount of DCM was added to make a clear solution. The reaction mixture was then stirred for 3 hours. In between, the progress of the reaction was checked using LCMS. When the reaction was completed after 3 hours it was dried using a rotary evaporator and dried in a vacuum. The product **4.184** was then purified using a silica column and DCM:ethylacetate solvent systems of different polarities. Finally, 105 mg product was obtained as light yellow oil.

5-(5-Bromofuran-2-carboxamido)-*N*-(2-morpholinoethyl)benzofuran-2-carboxamide (4.184):



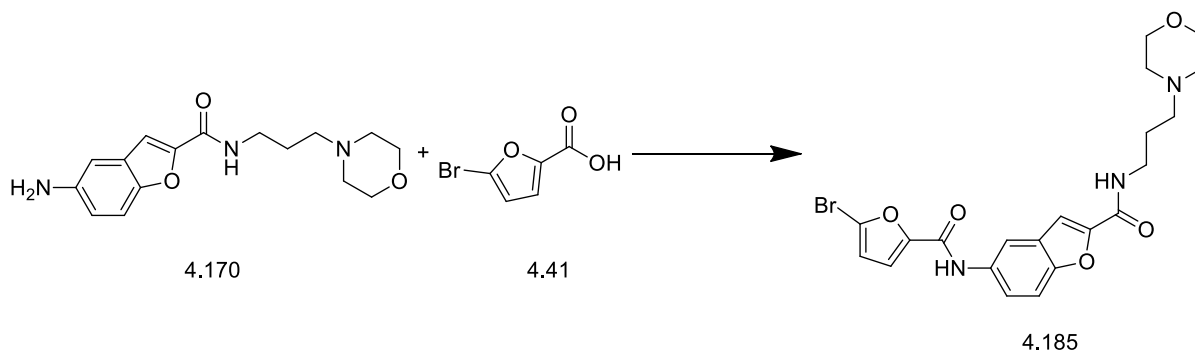
Light yellow oil. IR (FTIR, $\nu_{\text{max}}/\text{cm}^{-1}$) 615.82, 657.68, 750.47, 792.38, 807.91, 866.04, 912.80, 965.19, 1006.70, 1067.97, 1112.31, 1172.63, 1217.73, 1287.83, 1311.12, 1342.18, 1459.43, 1519.63, 1537.85, 1592.94, 149.90, 2335.36, 2356.42, 2810.97, 2859.75, 2947.35, 3316.47; ^1H NMR (500 MHz, CDCl_3 , TMS); δ 2.54 (br. s., 4H), 2.63 (t, $J=6.15$ Hz, 2H), 3.57 - 3.63 (m, 2H), 3.78 (t, $J=4.57$ Hz, 4H), 6.53 (d, $J=3.78$ Hz, 1H), 7.23 (d, $J=3.47$ Hz, 1H),

7.46 (d, $J=0.95$ Hz, 1H), 7.52 (d, $J=8.83$ Hz, 1H), 7.59 (dd, $J=8.83$, 2.21 Hz, 1H), 8.10 (d, $J=2.21$ Hz, 1H); ^{13}C NMR (100 MHz, CDCl_3); δ 35.56, 35.60, 53.36, 56.89, 66.99, 67.01, 110.37, 112.12, 114.00, 114.69, 117.68, 120.15, 124.89, 128.14, 133.06, 149.18, 149.84, 151.86, 154.96, 158.63; m/z (+EI) calc. For $\text{C}_{20}\text{H}_{20}\text{BrN}_3\text{O}_5$ (M^+) 462.29, found 461.96 ($\text{M}+\text{H}^+$); Yield: 94%.

Procedure for the synthesis of 5-(5-bromofuran-2-carboxamido)-*N*-(3-morpholinopropyl)benzofuran-2-carboxamide (4.185) from 5-amino-*N*-(3-morpholinopropyl)benzofuran-2-carboxamide (4.170) 5-bromofuran-2-carboxylic acid (4.41)

160 mg (1.0 eq.) **4.170**, 201 mg (2.0 eq.) **4.41**, 2.0 eq. HOBt and 1.75 eq. DIC were mixed in a round bottomed flask in which a minimum amount of DCM was added to make a clear solution. The reaction mixture was then stirred for 3 hours. In between, the progress of the reaction was checked using LCMS. When the reaction was completed after 3 hours it was dried using a rotary evaporator and the residue dried in a vacuum. The product **4.185** was then purified using a silica column and DCM:MeOH solvent systems of different polarities. Finally, 250 mg product was obtained as light brown oil.

5-(5-Bromofuran-2-carboxamido)-*N*-(3-morpholinopropyl)benzofuran-2-carboxamide (4.185):



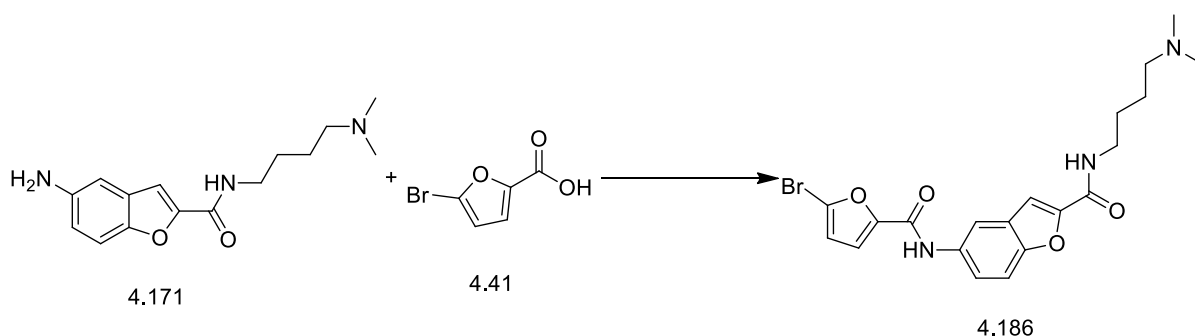
Light brown oil. IR (FTIR, $\nu_{\text{max}}/\text{cm}^{-1}$) 627.74, 711.22, 746.50, 761.76, 791.89, 806.52, 861.61, 913.75, 927.07, 956.92, 987.27, 1028.60, 1067.84, 1104.38, 1132.80, 1171.94, 1204.03, 1223.18, 1276.02, 1301.46, 1359.58, 1465.78, 1551.11, 1572.36, 1587.57, 1667.37, 1755.58, 2361.59, 2809.69, 2875.54, 2923.38, 3316.40, 3537.21; ^1H NMR (400 MHz, CDCl_3 , TMS); δ 1.82 (dt, $J=11.83$, 5.92 Hz, 2H), 2.58 (br. s., 4H), 2.60 - 2.64 (m, 2H), 3.57 - 3.65 (m, 2H), 3.90 (t, $J=4.53$ Hz, 4H), 6.52 (d, $J=3.53$ Hz, 1H), 7.22 (d, $J=3.53$ Hz, 1H), 7.44 (d, $J=1.01$ Hz, 1H), 7.47 (d, $J=9.06$ Hz, 1H), 7.56 (dd, $J=8.94$, 2.14 Hz, 1H), 8.11 (d, $J=2.01$ Hz, 1H), 8.14 (s, 1H), 8.78 (t, $J=4.28$ Hz, 1H); ^{13}C NMR (100 MHz, CDCl_3); δ 23.47, 23.96,

40.16, 53.80, 58.73, 66.82, 74.41, 110.08, 111.14, 114.17, 114.66, 117.65, 120.14, 124.87, 128.24, 133.06, 150.35, 151.35, 151.77, 155.00, 158.52; m/z (+EI) calc. For $C_{21}H_{22}BrN_3O_5$ (M+) 476.32, found 475.77 (M+H)⁺; Yield: 48%.

Procedure for the synthesis of 5-(5-bromofuran-2-carboxamido)-N-(4-(dimethylamino)butyl)benzofuran-2-carboxamide (4.186) from 5-amino-N-(4-(dimethylamino)butyl)benzofuran-2-carboxamide (4.171) and 5-bromofuran-2-carboxylic acid (4.41)

71 mg (1.0 eq.) **4.171**, 123 mg (2.50 eq.) **4.41**, 2.0 eq. HOBt and 1.75 eq. DIC were mixed in a round bottomed flask in which a minimum amount of DMF was added to make a clear solution. The reaction mixture was then stirred for 3 hours. In between, the progress of the reaction was checked using LCMS. When the reaction was completed after 3 hours it was poured over an Isolute SCX (2 gm) cartridge for purification. The product **4.186** was then purified using the 'catch and release' method and the product was released from the cartridge using 2M NH_3 in MeOH (10 ml). Finally, 76.0 mg product was obtained as light brown oil.

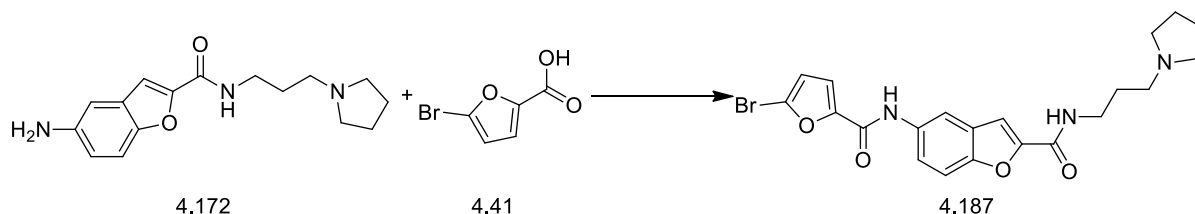
5-(5-Bromofuran-2-carboxamido)-N-(4-(dimethylamino)butyl)benzofuran-2-carboxamide (4.186):



Light brown oil. IR (FTIR, ν_{max}/cm^{-1}) 428.84, 569.57, 735.64, 803.56, 924.18, 957.32, 1014.6, 1102.0, 1235.18, 1298.54, 1436.96, 1462.23, 1536.26, 1569.04, 1586.57, 1645.55, 2780.0, 2825.1, 2855.2, 2924.5, 3265.0; 1H NMR (400 MHz, $CDCl_3$) δ 1.66 (q, $J=6.55$ Hz, 2H), 1.69 - 1.76 (m, 2H), 2.29 - 2.32 (m, 6H), 2.37 (t, $J=6.55$ Hz, 2H), 3.49 (q, $J=6.04$ Hz, 2H), 6.53 (dd, $J=3.53$, 0.50 Hz, 1H), 7.22 (dd, $J=3.53$, 0.50 Hz, 1H), 7.43 (d, $J=1.01$ Hz, 1H), 7.44 - 7.48 (m, 1H), 7.58 (dd, $J=8.94$, 2.14 Hz, 1H), 8.07 (d, $J=2.27$ Hz, 1H), 8.11 (s, 1H), 8.18 (br. s., 1H); ^{13}C NMR (100 MHz, $CDCl_3$) δ 25.51, 27.51, 39.39, 45.31, 45.32, 59.19, 109.98, 111.88, 114.03, 114.66, 117.63, 119.98, 124.86, 129.37, 132.24, 132.98, 149.23, 150.36, 151.84, 158.71; m/z (+EI) calc. For $C_{20}H_{22}BrN_3O_4$ (M+) 448.31, found (M+H)⁺ 449.8; Yield: 66%.

Procedure for the synthesis of 5-(5-bromofuran-2-carboxamido)-*N*-(3-(pyrrolidin-1-yl)propyl)benzofuran-2-carboxamide (4.187) from 5-amino-*N*-(3-(pyrrolidin-1-yl)propyl)benzofuran-2-carboxamide (4.172) and 5-bromofuran-2-carboxylic acid (4.41) 85 mg (1.0 eq.) **4.172**, 141 mg (2.50 eq.) **4.41**, 2.0 eq. HOBt and 1.75 eq. DIC were mixed in a round bottomed flask in which a minimum amount of DMF was added to make a clear solution. The reaction mixture was then stirred for 3 hours. In between, the progress of the reaction was checked using LCMS. When the reaction was completed after 3 hours it was poured over an Isolute SCX (2 gm) cartridge for purification. The product **4.187** was then purified using the 'catch and release' method and the product was released from the cartridge using 2M NH₃ in MeOH (10 ml). Finally, 90.0 mg product was obtained as light brown oil.

5-(5-Bromofuran-2-carboxamido)-*N*-(3-(pyrrolidin-1-yl)propyl)benzofuran-2-carboxamide (4.187):

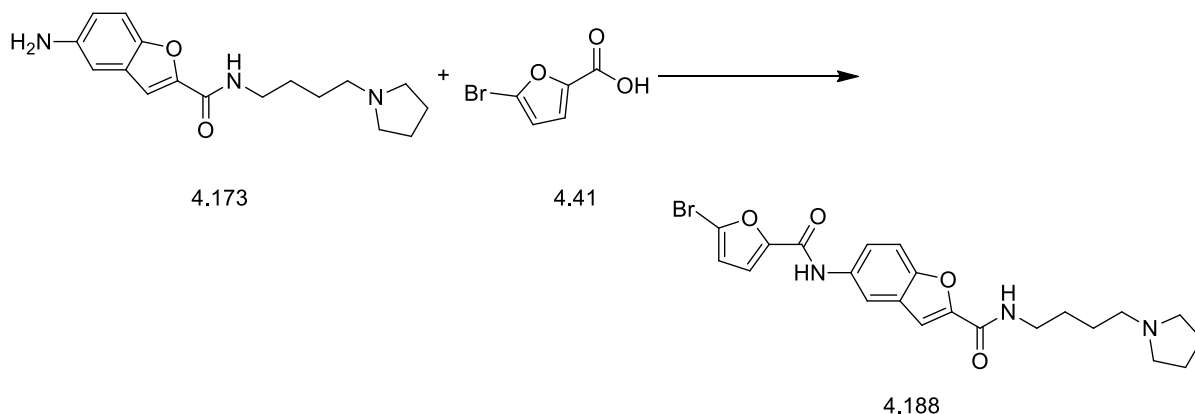


Light brown oil. IR (FTIR, $\nu_{\text{max}}/\text{cm}^{-1}$) 431.07, 431.07, 569.50, 729.72, 801.71, 865.50, 925.94, 1010.60, 1101.30, 1167.81, 1202.57, 1237.55, 1296.87, 1346.00, 1460.34, 1528.14, 1568.46, 1645.86, 1742.00, 2851.40, 2918.83, 3271.50; ¹H NMR (400 MHz, CDCl₃) δ 1.82 (dt, $J=11.71, 5.98$ Hz, 2H), 1.89 - 1.96 (m, 4H), 2.63 (br. s., 4H), 2.71 - 2.77 (m, 2H), 3.58 - 3.64 (m, 2H), 6.52 (d, $J=3.53$ Hz, 1H), 7.22 (d, $J=3.53$ Hz, 1H), 7.40 (d, $J=1.01$ Hz, 1H), 7.41 - 7.44 (m, 1H), 7.57 (dd, $J=8.94, 2.14$ Hz, 1H), 8.06 (d, $J=2.27$ Hz, 1H), 8.12 (s, 1H) 9.04 (br. s., 1H); ¹³C NMR (100 MHz, CDCl₃) δ 23.56, 23.59, 26.39, 40.19, 54.07, 54.09, 55.71, 109.71, 111.79, 114.07, 114.68, 117.64, 119.98, 124.88, 128.30, 132.96, 150.67, 151.91, 153.82, 155.03, 158.58; m/z (+EI) calc. For C₂₁H₂₂BrN₃O₄ (M⁺) 460.32, found (M+H)⁺ 460.10; Yield: 66%.

Procedure for the synthesis of 5-(5-bromofuran-2-carboxamido)-*N*-(4-(pyrrolidin-1-yl)butyl)benzofuran-2-carboxamide (4.188) from 5-amino-*N*-(4-(pyrrolidin-1-yl)butyl)benzofuran-2-carboxamide (4.173) and 5-bromofuran-2-carboxylic acid (4.41) 112 mg (1.0 eq.) **4.173**, 177 mg (2.50 eq.) **4.41**, 2.0 eq. HOBt and 1.75 eq. DIC were mixed in a round bottomed flask in which a minimum amount of DMF was added to make a clear solution. The reaction mixture was then stirred for 3 hours. In between, the progress of the reaction was checked using LCMS. When the reaction was completed after 3 hours it was

poured over an Isolute SCX (2 gm) cartridge for purification. The product **4.188** was then purified using the 'catch and release' method and the product was released from the cartridge using 2M NH₃ in MeOH (10 ml). Finally, 134.0 mg product was obtained as dark brown oil.

5-(5-Bromofuran-2-carboxamido)-N-(4-(pyrrolidin-1-yl)butyl)benzofuran-2-carboxamide (4.188):

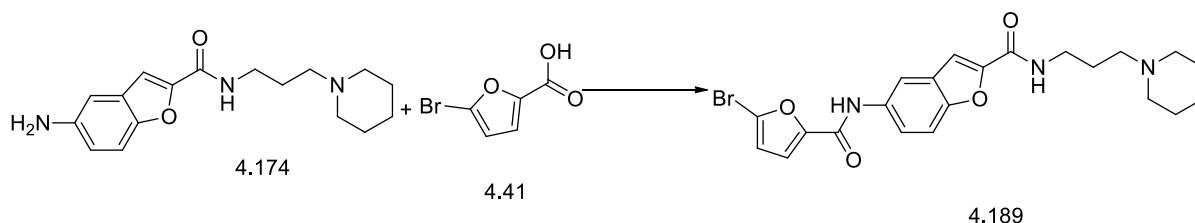


Dark brown oil. IR (FTIR, $\nu_{\text{max}}/\text{cm}^{-1}$) 429.14, 629.22, 728.10, 798.84, 909.12, 921.17, 1011.50, 1102.00, 1123.00, 1168.20, 1202.05, 1240.14, 1295.68, 1349.00, 1435.83, 1460.78, 1525.87, 1569.04, 1585.54, 16454.16, 1737.60, 2855.20, 2924.50, 3274.00; ¹H NMR (400 MHz, CDCl₃) δ 1.60 – 1.69 (m, 2H), 1.75 – 1.85 (m, 4H), 1.90 – 2.10 (m, 2H), 2.30 – 2.44 (m, 4H), 3.12 – 3.25 (m, 2H), 3.60 - 3.67 (br. s., 2H), 6.74 (d, $J=3.9$ Hz, 1H), 7.29 (d, $J=3.9$ Hz, 1H), 7.59 (s, 1H), 7.57 (d, $J=9.0$ Hz, 1H), 7.65 (d, $J=9.0$ Hz, 1H), 8.03 (s, 1H), 8.83 (s, 1H), 9.03 (s, 1H); ¹³C NMR (100 MHz, CDCl₃) δ 23.0, 23.08, 25.27, 27.34, 40.12, 54.36, 56.07, 57.34, 107.89, 111.23, 112.56, 113.37, 117.54, 118.01, 122.45, 130.0, 132.28, 149.67, 150.27, 152.64, 158.37, 162.45; m/z (+EI) calc. For C₂₂H₂₄BrN₃O₄ (M⁺) 474.35, found (M+H)⁺ 474.00; Yield: 76%.

Procedure for the synthesis of 5-(5-bromofuran-2-carboxamido)-N-(3-(piperidin-1-yl)propyl)benzofuran-2-carboxamide (4.189) from 5-amino-N-(3-(piperidin-1-yl)propyl)benzofuran-2-carboxamide (4.174) and 5-bromofuran-2-carboxylic acid (4.41)
39 mg (1.0 eq.) **4.174**, 62 mg (2.50 eq.) **4.41**, 2.0 eq. HOBt and 1.75 eq. DIC were mixed in a round bottomed flask in which a minimum amount of DMF was added to make a clear solution. The reaction mixture was then stirred for 3 hours. In between, the progress of the reaction was checked using LCMS. When the reaction was completed after 3 hours it was poured over an Isolute SCX (2 gm) cartridge for purification. The product **4.189** was then

purified using the 'catch and release' method and the product was released from the cartridge using 2M NH₃ in MeOH (10 ml). Finally, 50.0 mg product was obtained as brown oil.

5-(5-Bromofuran-2-carboxamido)-N-(3-(piperidin-1-yl)propyl)benzofuran-2-carboxamide (4.189):

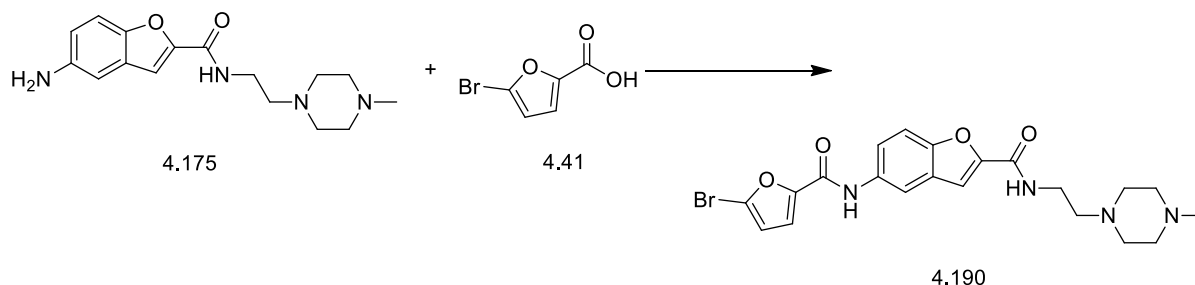


Brown oil. IR (FTIR, $\nu_{\text{max}}/\text{cm}^{-1}$) 429.52, 692.22, 795.86, 862.67, 963.35, 1011.50, 1039.92, 1099.00, 1165.20, 1201.67, 1237.50, 1296.17, 1346.00, 1462.51, 1531.25, 1585.34, 1645.39, 2770.9, 2810.00, 2855.20, 2933.05, 3274.00; ¹H NMR (400 MHz, Methanol-d₄) δ 1.50 (br. s., 2H), 1.65 (quin, $J=5.67$ Hz, 4H), 1.84 (quin, $J=7.05$ Hz, 2H), 2.12 - 2.14 (m, 2H), 2.45 - 2.50 (m, 4H), 3.45 (t, $J=6.67$ Hz, 2H), 6.66 (d, $J=3.53$ Hz, 1H), 7.26 (d, $J=3.53$ Hz, 1H), 7.44 (d, $J=0.76$ Hz, 1H), 7.53 (d, $J=8.81$ Hz, 1H), 7.69 (dd, $J=8.94, 2.14$ Hz, 1H), 8.08 (d, $J=2.01$ Hz, 1H); ¹³C NMR (100 MHz, Methanol-d₄) δ 25.54, 26.88, 27.18, 31.04, 39.80, 40.83, 55.89, 58.67, 111.60, 113.09, 115.84, 116.54, 118.87, 123.16, 124.67, 129.38, 134.57, 135.48, 151.35, 153.87, 158.13, 161.28; m/z (+EI) calc. For C₂₂H₂₄BrN₃O₄ (M⁺) 474.35, found (M+H)⁺ 475.70; Yield: 81%.

Procedure for the synthesis of 5-(5-bromofuran-2-carboxamido)-N-(2-(4-methylpiperazin-1-yl)ethyl)benzofuran-2-carboxamide (4.190) from 5-amino-N-(2-(4-methylpiperazin-1-yl)ethyl)benzofuran-2-carboxamide (4.175) and 5-bromofuran-2-carboxylic acid (4.41)

102 mg (1.0 eq.) **4.175**, 161 mg (2.50 eq.) **4.41**, 2.0 eq. HOBt and 1.75 eq. DIC were mixed in a round bottomed flask in which a minimum amount of DMF was added to make a clear solution. The reaction mixture was then stirred for 3 hours. In between, the progress of the reaction was checked using LCMS. When the reaction was completed after 3 hours it was poured over an Isolute SCX (2 gm) cartridge for purification. The product **4.190** was then purified using the 'catch and release' method and the product was released from the cartridge using 2M NH₃ in MeOH (10 ml). Finally, 130.0 mg product was obtained as light brown oil.

5-(5-Bromofuran-2-carboxamido)-N-(2-(4-methylpiperazin-1-yl)ethyl)benzofuran-2-carboxamide (4.190):

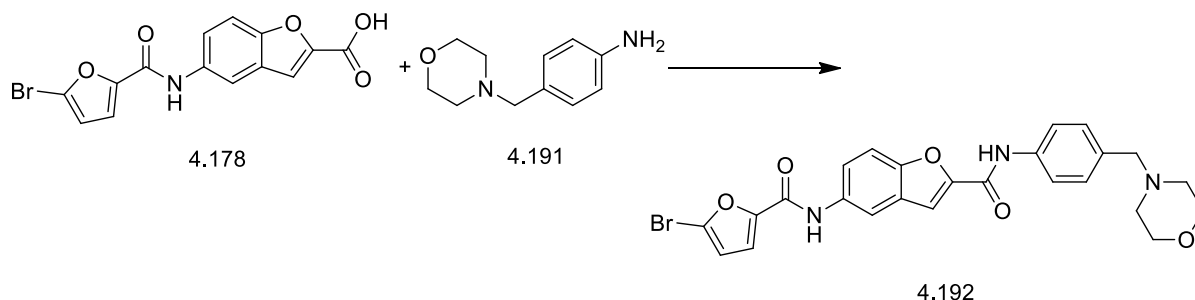


Light brown oil. IR (FTIR, $\nu_{\text{max}}/\text{cm}^{-1}$) 418.60, 427.81, 569.76, 594.81, 609.96, 628.54, 738.59, 801.50, 919.90, 1007.60, 1104.30, 1149.60, 1167.80, 1204.00, 1237.30, 1283.72, 1349.10, 1460.03, 1536.50, 1569.16, 1586.01, 1644.98, 2809.00, 2945.00, 3283.60; ^1H NMR (400 MHz, Methanol- d_4) δ 2.12 - 2.19 (m, 4H), 2.32 (s, 3H), 2.54 (m, 4H), 2.64 (t, $J=6.67$ Hz, 2H), 3.54 - 3.59 (m, 2H), 6.67 (d, $J=3.53$ Hz, 1H), 7.27 (d, $J=3.53$ Hz, 1H), 7.46 (d, $J=1.01$ Hz, 1H), 7.55 - 7.60 (m, 1H), 7.68 - 7.73 (m, 1H), 8.08 (d, $J=2.01$ Hz, 1H); ^{13}C NMR (100 MHz, Methanol- d_4) δ 31.05, 34.01, 37.72, 46.32, 54.01, 56.00, 58.39, 111.68, 113.20, 115.84, 116.55, 118.31, 118.88, 120.07, 123.21, 127.37, 129.35, 137.88, 151.10, 151.27, 153.92; m/z (+EI) calc. For $\text{C}_{21}\text{H}_{23}\text{BrN}_4\text{O}_4$ (M^+) 475.34, found ($\text{M}+\text{H}$) $^+$ 475.00; Yield: 81%.

Procedure for the synthesis of 5-(5-bromofuran-2-carboxamido)-N-(4-(morpholinomethyl)phenyl)benzofuran-2-carboxamide (4.192) from 5-(5-bromofuran-2-carboxamido)benzofuran-2-carboxylic acid (4.178) and 4-(morpholinomethyl)aniline (4.191)

70 mg (1.0 eq.) **4.178**, 35 mg (0.90 eq.) **4.191**, 2.0 eq. HOBt and 1.75 eq. DIC were mixed in a round bottomed flask in which a minimum amount of DMF was added to make a clear solution. The reaction mixture was then stirred for 3 hours. In between, the progress of the reaction was checked using LCMS. When the reaction was completed after 3 hours it was poured over an Isolute SCX (2 gm) cartridge for purification. The product **4.192** was then purified using the 'catch and release' method and the product was released from the cartridge using 2M NH_3 in MeOH (10 ml). Finally, 36.0 mg product was obtained as light yellow oil.

5-(5-Bromofuran-2-carboxamido)-N-(4-(morpholinomethyl)phenyl)benzofuran-2-carboxamide (4.192):

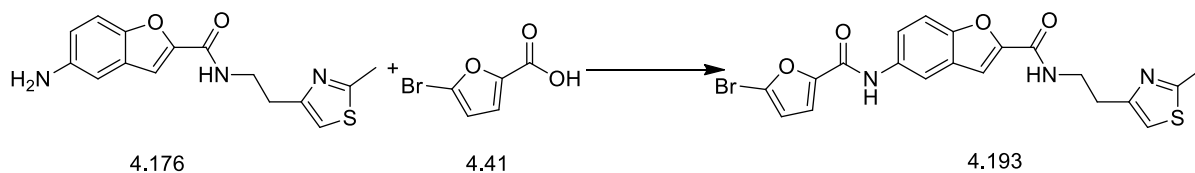


Light yellow oil. IR (FTIR, $\nu_{\text{max}}/\text{cm}^{-1}$) 443.01, 463.23, 496.31, 561.57, 580.52, 598.99, 614.15, 737.42, 746.84, 793.63, 805.50, 827.54, 913.85, 953.15, 998.49, 1034.80, 1104.30, 1240.30, 1325.00, 1400.50, 1436.80, 1470.00, 1515.40, 1584.90, 1606.00, 1651.40, 2464.50, 2803.00, 2917.90, 2957.20, 3335.00; ^1H NMR (400 MHz, METHANOL- d_4) δ 2.47 (br. s., 4H), 3.51 - 3.56 (m, 2H), 3.67 - 3.70 (m, 4H), 6.69 (d, $J=8.06$ Hz, 1H), 7.07 (d, $J=8.56$ Hz, 1H), 7.20 (m, $J=8.56$ Hz, 2H), 7.24 - 7.28 (m, 2H), 7.43 (m, $J=8.56$ Hz, 2H) 8.83 (s, 1H); ^{13}C NMR (100 MHz, METHANOL- d_4) δ 54.52, 55.71, 64.50, 67.21, 67.34, 108.54, 110.27, 112.38, 113.25, 115.97, 117.64, 120.31, 121.13, 122.65, 129.67, 129.84, 130.04, 132.58, 134.09, 136.27, 149.08, 150.70, 152.38, 160.38, 162.13; m/z (+EI) calc. For $\text{C}_{25}\text{H}_{22}\text{BrN}_3\text{O}_5$ (M^+) 524.36, found ($M+H$) $^+$ 525.80; Yield: 34%.

Procedure for the synthesis of 5-(5-bromofuran-2-carboxamido)-N-(2-(2-methylthiazol-4-yl)ethyl)benzofuran-2-carboxamide (4.193) from 5-amino-N-(2-(2-methylthiazol-4-yl)ethyl)benzofuran-2-carboxamide (4.176) and 5-bromofuran-2-carboxylic acid (4.41)

125 mg (1.0 eq.) **4.176**, 198 mg (2.5 eq.) **4.41**, 2.0 eq. HOBt and 1.75 eq. DIC were mixed in a round bottomed flask in which a minimum amount of DMF was added to make a clear solution. The reaction mixture was then stirred for 3 hours. In between, the progress of the reaction was checked using LCMS. When the reaction was completed after 3 hours it was poured over an Isolute SCX (2 gm) cartridge for purification. The product **4.193** was then purified using the 'catch and release' method and the product was released from the cartridge using 2M NH_3 in MeOH (10 ml). Finally, 163.0 mg product was obtained as colourless powder.

5-(5-Bromofuran-2-carboxamido)-N-(2-(2-methylthiazol-4-yl)ethyl)benzofuran-2-carboxamide (4.193):

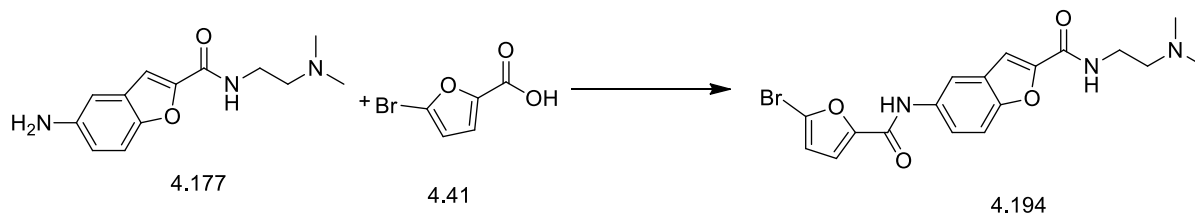


Colourless powder. IR (FTIR, $\nu_{\text{max}}/\text{cm}^{-1}$) 423.83, 479.58, 625.01, 741.08, 820.62, 854.90, 872.97, 927.20, 951.30, 1041.70, 1108.00, 1132.00, 1177.20, 1240.50, 1343.00, 1402.82, 1426.56, 1448.26, 1466.36, 1551.25, 1567.82, 1590.64, 1638.27, 2460.60, 2502.80, 2927.50, 2966.70, 3340.30; ^1H NMR (400 MHz, CDCl_3) δ 2.74 (s, 3H), 3.05 (t, $J=6.55$ Hz, 2H), 3.78 - 3.82 (m, 2H), 6.52 (d, $J=3.53$ Hz, 1H), 6.89 (s, 1H), 7.22 (d, $J=3.78$ Hz, 1H), 7.42 - 7.44 (m, 1H), 7.47 (s, 1H), 7.58 (dd, $J=8.81, 2.27$ Hz, 1H), 7.72 (d, $J=8.56$ Hz, 1H), 8.07 (d, $J=2.01$ Hz, 1H), 8.18 (s, 1H); ^{13}C NMR (100 MHz, CDCl_3) δ 19.05, 23.36, 42.42, 110.32, 112.09, 114.11, 114.28, 114.69, 117.69, 120.28, 124.97, 126.78, 133.08, 149.22, 149.81, 151.92, 153.31, 155.08, 158.81, 166.70; m/z (+EI) calc. For $\text{C}_{20}\text{H}_{16}\text{BrN}_3\text{O}_4\text{S}$ (M^+) 474.33, found ($\text{M}+\text{H}$) $^+$ 476.10; Yield: 83%.

Procedure for the synthesis of 5-(5-bromofuran-2-carboxamido)-N-(2-(dimethylamino)ethyl)benzofuran-2-carboxamide (4.194) from 5-amino-N-(2-(dimethylamino)ethyl)benzofuran-2-carboxamide (4.177) and 5-bromofuran-2-carboxylic acid (4.41)

101 mg (1.0 eq.) **4.177**, 195 mg (2.5 eq.) **4.41**, 2.0 eq. HOBt and 1.75 eq. DIC were mixed in a round bottomed flask in which a minimum amount of DMF was added to make a clear solution. The reaction mixture was then stirred for 3 hours. In between, the progress of the reaction was checked using LCMS. When the reaction was completed after 3 hours it was poured over an Isolute SCX (2 gm) cartridge for purification. The product **4.195** was then purified using the 'catch and release' method and the product was released from the cartridge using 2M NH_3 in MeOH (10 ml). Finally, 150.0 mg product was obtained as light brown oil.

5-(5-Bromofuran-2-carboxamido)-N-(2-(dimethylamino)ethyl)benzofuran-2-carboxamide (4.194):

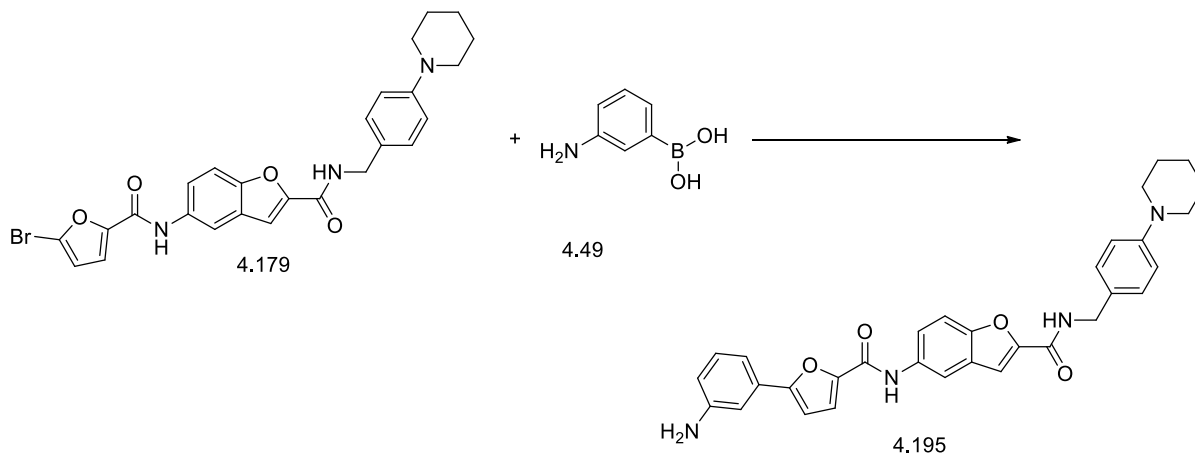


Light brown oil. IR (FTIR, $\nu_{\text{max}}/\text{cm}^{-1}$) 426.88, 571.60, 727.61, 798.98, 863.93, 924.18, 1011.50, 1105.00, 1202.13, 1236.56, 1298.04, 1349.00, 1436.39, 1459.49, 1531.12, 1569.01, 1585.74, 1647.01, 2777.00, 2825.10, 2861.30, 2936.60, 3274.00; ^1H NMR (400 MHz, CDCl_3) δ 2.31 (s, 6H), 2.54 (t, $J=5.92$ Hz, 2H), 3.56 (q, $J=5.54$ Hz, 2H), 6.52 (d, $J=3.53$ Hz, 1H), 7.16 (t, $J=4.28$ Hz, 1H), 7.21 (d, $J=3.53$ Hz, 1H), 7.42 - 7.44 (m, 1H), 7.51 (s, 1H), 7.55 - 7.60 (m, 1H), 8.07 (d, $J=2.01$ Hz, 1H), 8.16 (s, 1H); ^{13}C NMR (100 MHz, CDCl_3) δ 36.72, 45.25, 45.28, 57.74, 110.22, 112.13, 114.00, 114.63, 117.60, 120.14, 124.85, 128.11, 133.01, 149.23, 149.89, 151.87, 154.99, 158.70; m/z (+EI) calc. For $\text{C}_{18}\text{H}_{18}\text{BrN}_3\text{O}_4$ (M^+) 420.26, found ($\text{M}+\text{H}$) $^+$ 421.80; Yield: 87%.

General procedure for Suzuki coupling for the synthesis of 5-(5-(3-aminophenyl)furan-2-carboxamido)-N-(4-(piperidin-1-yl)benzyl)benzofuran-2-carboxamide (4.195) from 5-(5-bromofuran-2-carboxamido)-N-(4-(piperidin-1-yl)benzyl)benzofuran-2-carboxamide (4.179) and (3-aminophenyl)boronic acid (4.49)

A catalytic amount of tetrakis(triphenylphosphine)palladium, $\text{Pd}(\text{PPh}_3)_4$ (0.1 eq., 31 mg) was added to a solution of **4.179** (1.0 eq., 140 mg) and **4.49** (1.5 eq., 75 mg) in a 9:3:1 combination of EtOH, toluene and water in the presence of K_2CO_3 (3.0 eq., 111 mg) in a 10 ml microwave vial containing a magnetic stirrer. The reaction vessel was flushed with nitrogen during each addition. The reaction mixture was sealed in an inert nitrogen environment and heated with microwave radiation in an EMRYSTM Optimizer Microwave Station (Personal Chemistry) at 100 °C for 13 minutes. LCMS analysis revealed completion of reaction and the cooled reaction mixture was passed through a layer of celite and dried to obtain the crude product. This was then purified by flash chromatography using a DCM and ethyl acetate solvent mixture (100% DCM, then 10% ethyl acetate in DCM and 20% ethyl acetate in DCM) to obtain the pure product **4.195** (130 mg).

5-(5-(3-Aminophenyl)furan-2-carboxamido)-N-(4-(piperidin-1-yl)benzyl)benzofuran-2-carboxamide (4.195):



Light green, viscous material. IR (FTIR, $\nu_{\text{max}}/\text{cm}^{-1}$) 609.11, 668.16, 746.24, 781.38, 807.01, 863.29, 919.84, 1037.30, 1116.70, 1205.66, 1237.73, 1286.79, 1338.77, 1461.79, 1517.13, 1590.08, 1645.15, 1732.38, 2335.36, 2359.55, 2930.11, 3341.16; ^1H NMR (400 MHz, CDCl_3 , TMS); δ 1.57 - 1.63 (m, 2H), 1.72 (dt, $J=11.18$, 5.65 Hz, 4H), 3.15 - 3.20 (m, 4H), 4.58 (d, $J=5.81$ Hz, 2H), 6.68 - 6.73 (m, 1H), 6.74 (d, $J=3.54$ Hz, 1H), 6.81 (t, $J=5.68$ Hz, 1H), 6.91 - 6.96 (m, 2H), 7.08 (s, 1H), 7.13 - 7.18 (m, 1H), 7.23 (d, $J=7.83$ Hz, 1H), 7.26 (s, 1H), 7.27 - 7.29 (m, 1H), 7.32 (d, $J=3.54$ Hz, 1H), 7.44 (d, $J=8.84$ Hz, 1H), 7.47 (d, $J=0.76$ Hz, 1H), 7.63 (dd, $J=8.97$, 2.15 Hz, 1H), 8.08 (d, $J=2.02$ Hz, 1H), 8.18 (s, 1H); ^{13}C NMR (100 MHz, CDCl_3); δ 24.27, 25.73, 25.74, 43.08, 50.48, 50.54, 107.73, 110.50, 110.79, 111.95, 114.00, 115.09, 115.74, 116.50, 116.76, 117.49, 120.36, 127.69, 128.12, 129.07, 129.09, 129.90, 130.41, 133.42, 146.47, 146.89, 149.71, 151.76, 151.84, 156.14, 156.26, 158.40; m/z (+EI) calc. For $\text{C}_{32}\text{H}_{30}\text{N}_4\text{O}_4$ (M^+) 534.61, found 534.94 ($\text{M}+\text{H}$) $^+$; Yield: 70%.

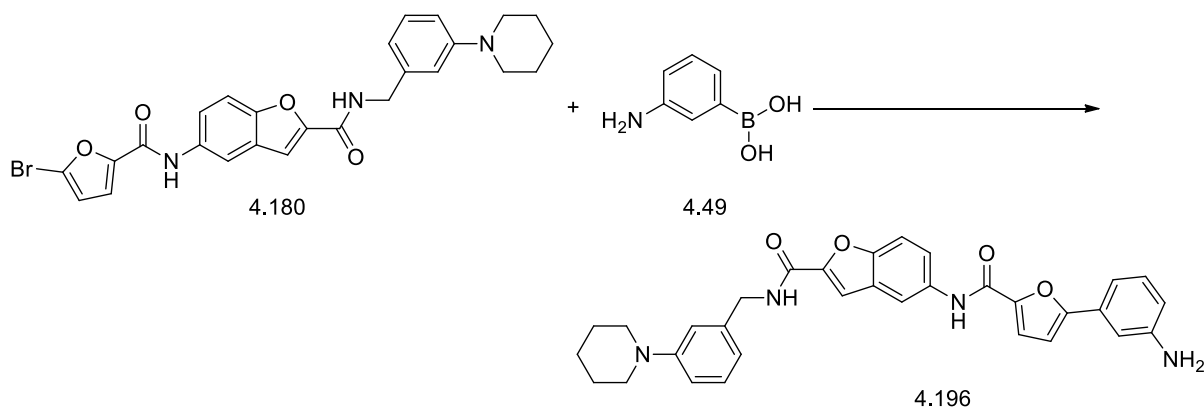
Similar Suzuki coupling reaction conditions were applied for compounds **4.196** to **4.209** using (3-aminophenyl)boronic acid (**4.49**) as the boronic acid.

Procedure for the synthesis of 5-(5-(3-aminophenyl)furan-2-carboxamido)-N-(3-(piperidin-1-yl)benzyl)benzofuran-2-carboxamide (4.196)

A catalytic amount of tetrakis(triphenylphosphine)palladium, $\text{Pd}(\text{PPh}_3)_4$ (0.1 eq.) was added to a solution of **4.180** (1.0 eq., 146 mg) and **4.49** (1.5 eq., 57 mg) in a 9:3:1 combination of EtOH, toluene and water in the presence of K_2CO_3 (3.0 eq.) in a 10 ml microwave vial containing a magnetic stirrer. The reaction vessel was flushed with nitrogen during each

addition. The reaction mixture was sealed in an inert nitrogen environment and heated with microwave radiation in an EMRYS™ Optimizer Microwave Station (Personal Chemistry) at 100 °C for 20 minutes. LCMS analysis revealed completion of reaction and the cooled reaction mixture was passed through a layer of celite and dried to obtain the crude product. This was then purified by flash chromatography using DCM and ethyl acetate solvent mixtures (100% DCM, then 10% ethyl acetate in DCM and 20% ethyl acetate in DCM) to obtain the pure product **4.196** (140 mg).

5-(5-(3-Aminophenyl)furan-2-carboxamido)-N-(3-(piperidin-1-yl)benzyl)benzofuran-2-carboxamide (4.196):



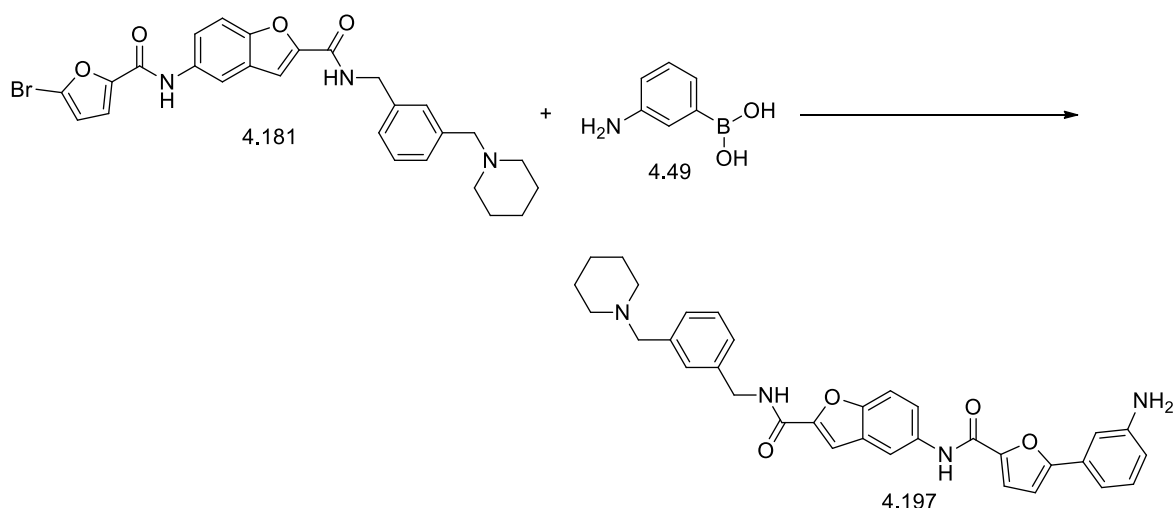
Light yellow powder. IR (FTIR, $\nu_{\text{max}}/\text{cm}^{-1}$) 632.54, 749.14, 897.79, 934.00, 1050.21, 1135.10, 1163.68, 1223.63, 1326.41, 1363.35, 1385.62, 1476.14, 1525.64, 1560.61, 1615.655, 2359.00, 2930.31.2968.97, 3339.58; ^1H NMR (400 MHz, CDCl_3 , TMS); δ 1.59 - 1.63 (m, 2H), 1.80 (dt, $J=11.18$, 5.65 Hz, 4H), 3.45 - 3.48 (m, 4H), 4.13 (s, 2H), 6.59 (dd, $J=3.54$, 0.51 Hz, 1H), 6.89 (d, $J=7.83$ Hz, 1H), 6.90 - 6.92 (m, 1H), 7.05 (s, 1H), 7.34 (dd, $J=3.54$, 0.51 Hz, 1H), 7.44 (m, 1H), 7.46 (m, 1H), 7.55 - 7.57 (m, 1H), 7.60 (s, 1H), 7.63 (dd, $J=8.84$, 2.27 Hz, 1H), 7.80 (d, $J=8.84$ Hz, 1H), 7.93 (d, $J=8.59$ Hz, 1H), 8.00 (d, $J=2.27$ Hz, 1H), 8.09 (s, 1H); ^{13}C NMR (100 MHz, CDCl_3) δ : 24.0, 25.35, 25.5, 43.12, 53.12, 55.03, 106.32, 108.9, 109.67, 110.25, 111.27, 112.54, 119.32, 119.54, 120.48, 121.00, 123.14, 126.57, 126.58, 128.64, 129.08, 135.27, 136.58, 140.59, 141.87, 145.69, 148.69, 150.46, 156.37, 159.02, 162.87, 170.39; m/z (+EI) calc. For $\text{C}_{32}\text{H}_{30}\text{N}_4\text{O}_4$ (M^+) 534.61, found 534.98 ($\text{M}+\text{H}^+$); Yield: 94%.

Procedure for the synthesis of 5-(5-(3-aminophenyl)furan-2-carboxamido)-N-(3-(piperidin-1-ylmethyl)benzyl)benzofuran-2-carboxamide (4.197)

A catalytic amount of tetrakis(triphenylphosphine)palladium, $\text{Pd}(\text{PPh}_3)_4$ (0.1 eq.) was added to a solution of **4.181** (1.0 eq., 49 mg) and **4.49** (1.5 eq., 19 mg) in a 9:3:1 combination of

EtOH, toluene and water in the presence of K_2CO_3 (3.0 eq.) in a 10 ml microwave vial containing a magnetic stirrer. The reaction vessel was flushed with nitrogen during each addition. The reaction mixture was sealed in an inert nitrogen environment and heated with microwave radiation in an EMRYSTM Optimizer Microwave Station (Personal Chemistry) at 100 °C for 10 minutes. LCMS analysis revealed completion of reaction and the cooled reaction mixture was passed through a layer of celite and dried to obtain the crude product. This was then purified by flash chromatography using DCM and ethyl acetate solvent mixtures (100% DCM, then 10% ethyl acetate in DCM and 20% ethyl acetate in DCM) to obtain the pure product **4.197** (35 mg).

5-(5-(3-Aminophenyl)furan-2-carboxamido)-N-(3-(piperidin-1-ylmethyl)benzyl)benzofuran-2-carboxamide (4.197):



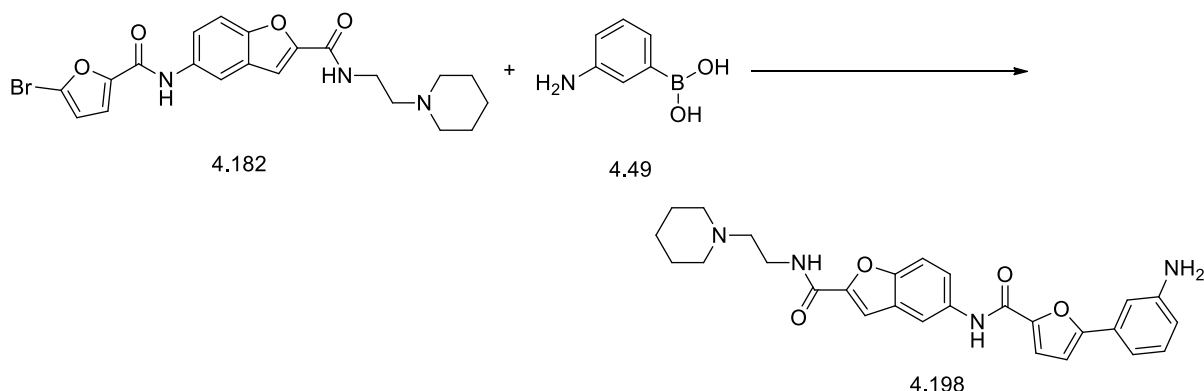
Light green, viscous material. IR (FTIR, $\nu_{\max}/\text{cm}^{-1}$) 692.51, 740.17, 779.93, 800.43, 861.72, 992.65, 1019.19, 1110.60, 1168.93, 1204.33, 1228.81, 1297.69, 1344.01, 1438.17, 1465.50, 1540.23, 1581.99, 1651.88, 1711.12, 1738.82, 2358.09, 2853.65, 2922.60, 3317.71; ^1H NMR (400 MHz, CDCl_3 , TMS); δ 1.43 - 1.49 (m, 2H), 1.59 (dt, $J=10.80$, 5.59 Hz, 4H), 2.40 (br. s., 4H), 3.50 (s, 2H), 4.68 (d, $J=5.81$ Hz, 2H), 6.72 (ddd, $J=7.83$, 2.27, 1.01 Hz, 1H), 6.76 (d, $J=3.79$ Hz, 1H), 7.08 (t, $J=1.89$ Hz, 1H), 7.16 (dt, $J=8.02$, 1.17 Hz, 1H), 7.24 (d, $J=7.83$ Hz, 1H), 7.31 (d, $J=7.33$ Hz, 2H), 7.33 (d, $J=3.54$ Hz, 1H), 7.35 (s, 1H), 7.47 (d, $J=9.09$ Hz, 1H), 7.51 (d, $J=1.01$ Hz, 1H), 7.64 (dd, $J=9.09$, 2.27 Hz, 1H), 8.11 (d, $J=2.02$ Hz, 1H), 8.15 (s, 1H); ^{13}C NMR (100 MHz, CDCl_3) δ 24.75, 25.87, 30.91, 43.43, 54.54, 68.74, 73.48, 105.86, 107.78, 110.79, 112.02, 114.02, 115.12, 117.51, 119.60, 120.41, 124.58, 125.08, 126.90, 128.16, 128.64, 128.80, 129.94, 130.43, 133.47, 136.07, 139.58, 146.89, 149.61, 151.82,

156.16, 156.24, 162.49; m/z (+EI) calc. For $C_{33}H_{32}N_4O_4$ (M^+) 548.63, found 548.79 ($M+H$)⁺; Yield: 70%.

Procedure for the synthesis of 5-(5-(3-aminophenyl)furan-2-carboxamido)-*N*-(2-(piperidin-1-yl)ethyl)benzofuran-2-carboxamide (4.198)

A catalytic amount of tetrakis(triphenylphosphine)palladium, $Pd(PPh_3)_4$ (0.1 eq.) was added to a solution of **4.182** (1.0 eq., 138 mg) and **4.49** (1.5 eq., 62 mg) in a 9:3:1 combination of EtOH, toluene and water in the presence of K_2CO_3 (3.0 eq.) in a 10 ml microwave vial containing a magnetic stirrer. The reaction vessel was flushed with nitrogen during each addition. The reaction mixture was sealed in an inert nitrogen environment and heated with microwave radiation in an EMRYSTM Optimizer Microwave Station (Personal Chemistry) at 100 °C for 15 minutes. LCMS analysis revealed completion of reaction and the cooled reaction mixture was passed through a layer of celite and dried to obtain the crude product. This was then purified by flash chromatography using DCM and ethyl acetate solvent mixtures (100% DCM, then 10% ethyl acetate in DCM and 20% ethyl acetate in DCM) to obtain the pure product **4.198** (100 mg).

5-(5-(3-Aminophenyl)furan-2-carboxamido)-*N*-(2-(piperidin-1-yl)ethyl)benzofuran-2-carboxamide (4.198):



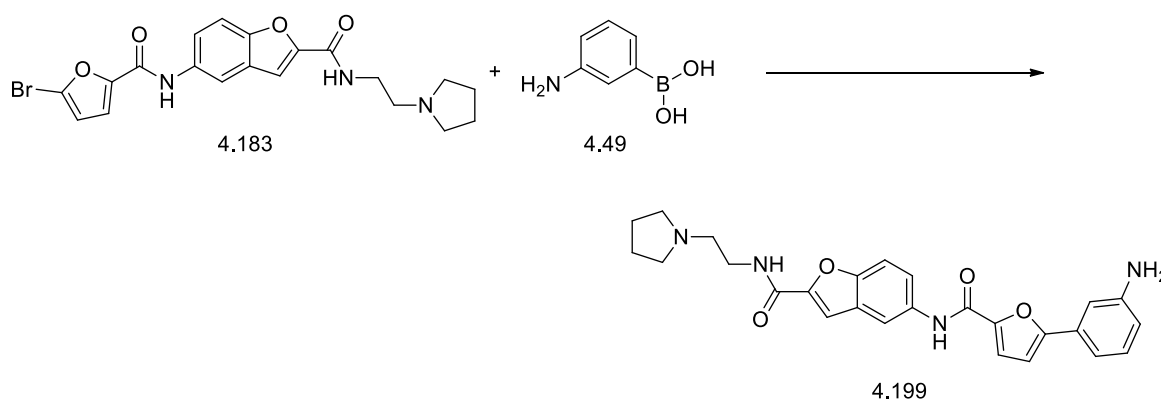
Brown, viscous oil. IR (FTIR, ν_{max}/cm^{-1}) 688.06, 724.54, 781.76, 855.14, 925.50, 993.93, 1026.73, 1117.67, 1168.35, 1232.38, 1302.65, 1435.04, 1467.91, 1540.30, 1582.46, 1651.53, 2335.36, 2362.03, 2931.98, 3327.86; 1H NMR (500 MHz, $CDCl_3$, TMS); δ 1.50 (br. s., 2H), 1.66 (dt, $J=11.19$, 5.44 Hz, 4H), 2.36 (s, 2H), 2.50 (br. s., 2H), 2.59 - 2.64 (m, 2H), 3.56 - 3.63 (m, 2H), 6.71 (ddd, $J=7.88$, 2.52, 0.95 Hz, 1H), 6.76 (d, $J=3.47$ Hz, 1H), 7.09 (t, $J=1.89$ Hz, 1H), 7.17 (ddt, $J=2.36$, 1.50, 0.75, 0.75 Hz, 1H), 7.19 (s, 1H), 7.25 - 7.27 (m, 1H), 7.33 - 7.34 (m, 1H), 7.45 - 7.47 (m, 1H), 7.47 - 7.48 (m, 1H), 7.53 - 7.55 (m, 1H), 7.55 - 7.58 (m,

1H), 7.66 (d, $J=1.26$ Hz, 1H) 7.67 - 7.69 (m, 1H), 8.09 (d, $J=2.21$ Hz, 1H); ^{13}C NMR (100 MHz, CDCl_3); δ 21.70, 24.51, 26.12, 36.18, 51.12, 54.60, 57.31, 108.02, 110.46, 111.01, 112.38, 115.33, 115.99, 117.79, 120.47, 125.53, 128.46, 128.70, 128.80, 129.27, 132.29, 132.37, 147.13, 152.10, 156.35, 156.51, 159.00; m/z (+EI) calc. For $\text{C}_{27}\text{H}_{29}\text{N}_4\text{O}_4$ (M^+) 472.54, found 472.78 ($\text{M}+\text{H}$) $^+$; Yield: 71%.

Procedure for the synthesis of 5-(5-(3-aminophenyl)furan-2-carboxamido)-N-(2-(pyrrolidin-1-yl)ethyl)benzofuran-2-carboxamide (4.199)

A catalytic amount of tetrakis(triphenylphosphine)palladium, $\text{Pd}(\text{PPh}_3)_4$ (0.1 eq.) was added to a solution of **4.183** (1.0 eq., 100 mg) and **4.49** (1.5 eq., 46 mg) in a 9:3:1 combination of EtOH, toluene and water in the presence of K_2CO_3 (3.0 eq.) in a 10 ml microwave vial containing a magnetic stirrer. The reaction vessel was flushed with nitrogen during each addition. The reaction mixture was sealed in an inert nitrogen environment and heated with microwave radiation in an EMRYSTM Optimizer Microwave Station (Personal Chemistry) at 100 °C for 10 minutes. LCMS analysis revealed completion of reaction and the cooled reaction mixture was passed through a SCX (2 gm) cartridge for purification and 2M NH_3 in MeOH was used to release the pure product **4.199** (100 mg) from the cartridge.

5-(5-(3-Aminophenyl)furan-2-carboxamido)-N-(2-(pyrrolidin-1-yl)ethyl)benzofuran-2-carboxamide (4.199):



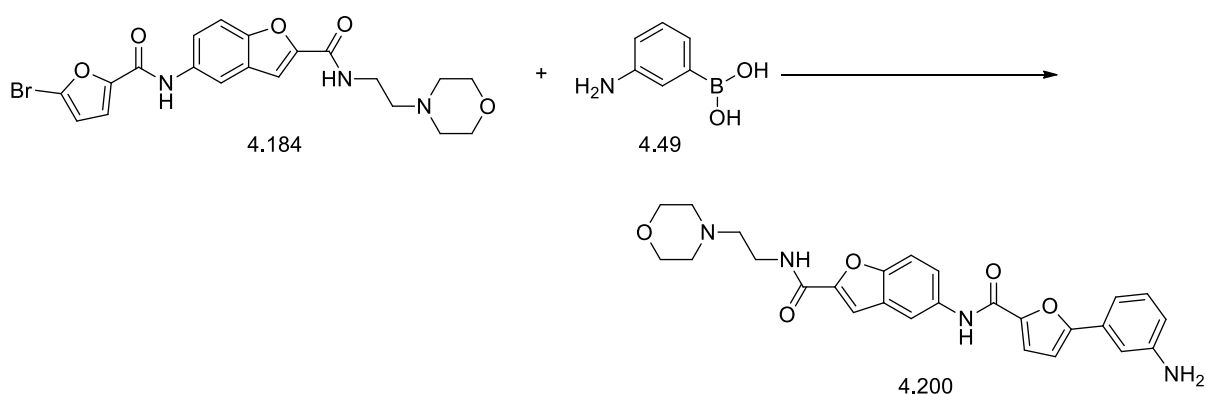
Dark brown oil. IR (FTIR, $\nu_{\text{max}}/\text{cm}^{-1}$) 688.09, 722.28, 782.02, 863.39, 952.05, 1021.96, 1113.01, 1153.97, 1204.33, 1296.88, 1344.03, 1441.21, 1467.52, 1488.16, 1540.88, 1578.94, 1648.13, 2335.36, 2357.07, 2817.07, 2932.59, 3042.68, 3225.60, 3345.79; ^1H NMR (500 MHz, CDCl_3 , TMS); δ 1.84 (dt, $J=6.62, 3.31$ Hz, 4H), 2.62 (br. s., 4H), 2.76 (t, $J=5.99$ Hz, 2H), 3.59 - 3.64 (m, 2H), 6.72 (ddd, $J=7.88, 2.21, 0.95$ Hz, 1H), 6.76 (d, $J=3.78$ Hz, 1H), 7.00 (t, $J=7.88$ Hz, 1H), 7.08 - 7.09 (m, 1H), 7.15 - 7.18 (m, 1H), 7.24 (d, $J=7.88$ Hz, 1H),

7.33 (d, $J=3.47$ Hz, 1H), 7.46 (d, $J=0.95$ Hz, 1H), 7.47 - 7.50 (m, 1H), 7.52 (d, $J=9.14$ Hz, 1H), 7.62 - 7.66 (m, 1H), 7.67 - 7.70 (m, 1H), 8.09 (d, $J=2.21$ Hz, 1H), 8.17 (s, 1H); ^{13}C NMR (100 MHz, CDCl_3); δ 21.84, 23.53, 38.02, 48.13, 53.99, 54.67, 107.79, 110.28, 110.75, 112.13, 113.95, 115.09, 115.75, 117.55, 120.21, 128.15, 128.46, 128.55, 129.94, 130.39, 132.12, 133.29, 146.45, 146.86, 149.87, 156.10; m/z (+EI) calc. For $\text{C}_{26}\text{H}_{26}\text{N}_4\text{O}_4$ (M^+) 458.51, found 459.21 ($\text{M}+\text{H}$) $^+$; Yield: 97%.

Procedure for the synthesis of 5-(5-(3-aminophenyl)furan-2-carboxamido)-*N*-(2-morpholinoethyl)benzofuran-2-carboxamide (4.200)

A catalytic amount of tetrakis(triphenylphosphine)palladium, $\text{Pd}(\text{PPh}_3)_4$ (0.1 eq.) was added to a solution of **4.184** (1.0 eq., 100 mg) and **4.49** (1.5 eq., 44 mg) in a 9:3:1 combination of EtOH, toluene and water in the presence of K_2CO_3 (3.0 eq.) in a 10 ml microwave vial containing a magnetic stirrer. The reaction vessel was flushed with nitrogen during each addition. The reaction mixture was sealed in an inert nitrogen environment and heated with microwave radiation in an EMRYSTM Optimizer Microwave Station (Personal Chemistry) at 100 °C for 13 minutes. LCMS analysis revealed completion of reaction and the cooled reaction mixture was passed through a SCX (2 gm) cartridge for purification and 2M NH_3 in MeOH was used to release the pure product **4.200** (100 mg) from the cartridge.

5-(5-(3-Aminophenyl)furan-2-carboxamido)-*N*-(2-morpholinoethyl)benzofuran-2-carboxamide (4.200):



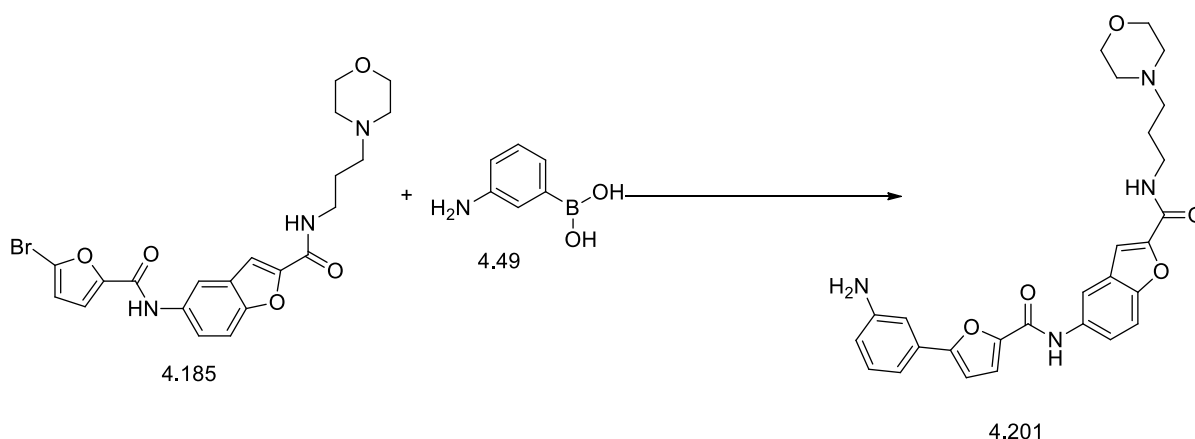
Dark brown oil. IR (FTIR, $\nu_{\text{max}}/\text{cm}^{-1}$) 630.36, 784.23, 863.10, 961.38, 1024.14, 1113.62, 1167.89, 1204.99, 1234.37, 1309.71, 1441.21, 1540.36, 1582.62, 1651.32, 2335.36, 2356.50, 2817.07, 2938.98, 3347.83; ^1H NMR (500 MHz, CDCl_3) δ 2.55 (br. s., 4H), 2.64 (t, $J=5.99$ Hz, 2H), 3.58 - 3.63 (m, 2H), 3.76 - 3.80 (m, 4H), 6.71 (ddd, $J=7.88, 2.52, 0.95$ Hz, 1H), 6.76

(d, $J=3.47$ Hz, 1H), 7.08 (t, $J=1.89$ Hz, 1H), 7.14 - 7.18 (m, 2H), 7.23 - 7.27 (m, 1H), 7.33 (d, $J=3.47$ Hz, 1H), 7.46 (d, $J=0.95$ Hz, 1H), 7.47 - 7.50 (m, 1H), 7.51 - 7.54 (m, 1H), 7.64 - 7.70 (m, 2H), 8.10 (d, $J=1.89$ Hz, 1H), 8.21 (s, 1H); ^{13}C NMR (100 MHz, CDCl_3) δ 35.31, 35.36, 53.11, 56.65, 66.70, 66.73, 107.52, 110.16, 110.49, 111.81, 114.82, 115.49, 117.32, 120.07, 127.86, 128.31, 129.67, 130.12, 131.77, 133.13, 146.15, 146.62, 149.49, 151.55, 155.88, 158.46; m/z (+EI) calc. For $\text{C}_{26}\text{H}_{26}\text{N}_4\text{O}_5$ (M^+) 474.51, found 475.10 ($\text{M}+\text{H}$) $^+$; Yield: 97%.

Procedure for the synthesis of 5-(5-(3-aminophenyl)furan-2-carboxamido)-*N*-(3-morpholinopropyl)benzofuran-2-carboxamide (4.201)

A catalytic amount of tetrakis(triphenylphosphine)palladium, $\text{Pd}(\text{PPh}_3)_4$ (0.1 eq.) was added to a solution of **4.185** (1.0 eq., 250 mg) and **4.49** (1.5 eq., 108 mg) in a 9:3:1 combination of EtOH, toluene and water in the presence of K_2CO_3 (3.0 eq.) in a 10 ml microwave vial containing a magnetic stirrer. The reaction vessel was flushed with nitrogen during each addition. The reaction mixture was sealed in an inert nitrogen environment and heated with microwave radiation in an EMRYSTM Optimizer Microwave Station (Personal Chemistry) at 100 °C for 20 minutes. LCMS analysis revealed completion of reaction and the cooled reaction mixture was passed through a SCX (2 gm) cartridge for purification and 2M NH_3 in MeOH was used to release the pure product **4.201** (181 mg) from the cartridge.

5-(5-(3-Aminophenyl)furan-2-carboxamido)-*N*-(3-morpholinopropyl)benzofuran-2-carboxamide (4.201):



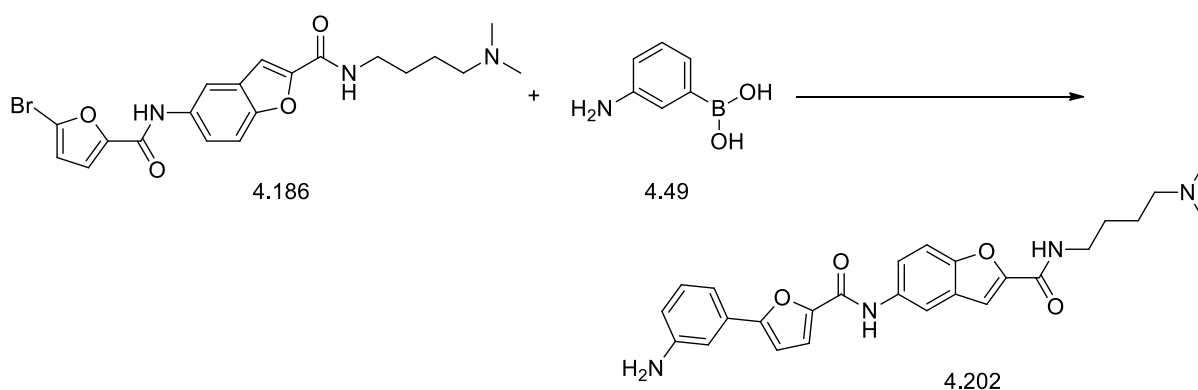
Light brown oil. IR (FTIR, $\nu_{\text{max}}/\text{cm}^{-1}$) 636.84, 689.46, 782.66, 862.50, 986.84, 1028.57, 1112.71, 1171.05, 1201.75, 1231.34, 1300.00, 1343.49, 1465.78, 1538.49, 1584.76, 1643.85, 2011.96, 2359.98, 3329.63; ^1H NMR (400 MHz, CDCl_3 , TMS); δ 1.81 (quin, $J=5.79$ Hz, 2H), 2.57 (br. s., 4H), 2.59 - 2.64 (m, 2H), 3.58 - 3.65 (m, 2H), 3.91 (t, $J=4.66$ Hz, 4H), 6.71

(ddd, $J=7.93, 2.39, 1.01$ Hz, 1H), 6.75 (d, $J=3.78$ Hz, 1H), 7.08 - 7.10 (m, 1H), 7.15 - 7.18 (m, 1H), 7.22 - 7.27 (m, 1H), 7.33 (d, $J=3.53$ Hz, 1H), 7.45 - 7.46 (m, 1H), 7.46 - 7.51 (m, 2H), 7.61 - 7.65 (m, 1H), 7.66 - 7.71 (m, 1H), 8.11 (d, $J=2.01$ Hz, 1H), 8.22 (s, 1H), 8.81 (t, $J=4.41$ Hz, 1H); ^{13}C NMR (100 MHz, CDCl_3); δ 23.97, 29.69, 40.23, 50.69, 53.84, 58.79, 66.87, 107.76, 110.12, 110.46, 110.77, 111.70, 114.16, 115.09, 115.74, 117.56, 120.28, 128.24, 128.45, 130.39, 131.99, 132.11, 133.37, 146.43, 146.87, 150.28, 156.29; m/z (+EI) calc. For $\text{C}_{27}\text{H}_{28}\text{N}_4\text{O}_5$ (M^+) 488.54, found 489.06 ($\text{M}+\text{H}^+$); Yield: 71%.

Procedure for the synthesis of 5-(5-(3-aminophenyl)furan-2-carboxamido)-*N*-(4-(dimethylamino)butyl)benzofuran-2-carboxamide (4.202)

A catalytic amount of tetrakis(triphenylphosphine)palladium, $\text{Pd}(\text{PPh}_3)_4$ (0.1 eq.) was added to a solution of **4.186** (1.0 eq., 76 mg) and **4.49** (2.5 eq., 58 mg) in a 9:3:1 combination of EtOH, toluene and water in the presence of K_2CO_3 (3.0 eq.) in a 10 ml microwave vial containing a magnetic stirrer. The reaction vessel was flushed with nitrogen during each addition. The reaction mixture was sealed in an inert nitrogen environment and heated with microwave radiation in an EMRYSTM Optimizer Microwave Station (Personal Chemistry) at 100 °C for 20 minutes. LCMS analysis revealed completion of reaction and the cooled reaction mixture was passed through a SCX (2 gm) cartridge for purification and 2M NH_3 in MeOH was used to release the pure product **4.202** (76 mg) from the cartridge.

5-(5-(3-Aminophenyl)furan-2-carboxamido)-*N*-(4-(dimethylamino)butyl)benzofuran-2-carboxamide (4.202):



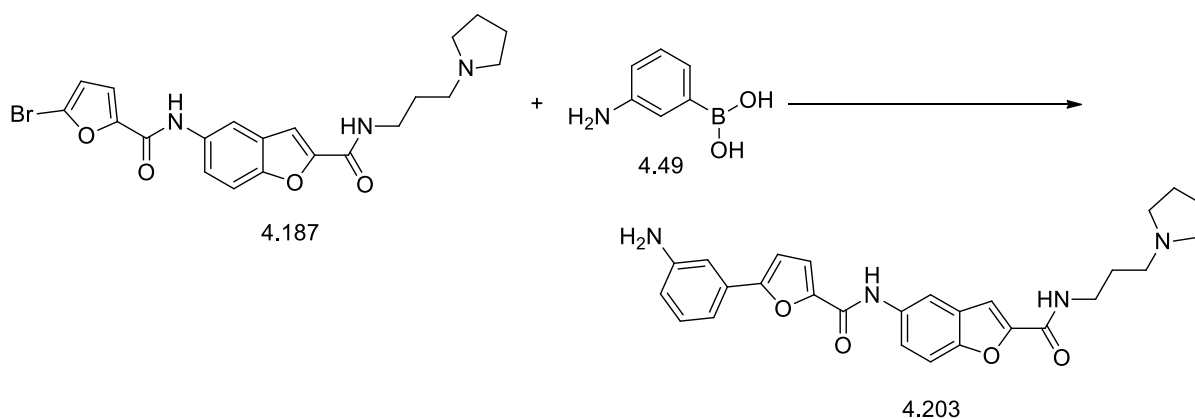
Light brown oil. IR (FTIR, $\nu_{\text{max}}/\text{cm}^{-1}$) 406.01, 416.24, 427.69, 524.08, 535.29, 600.15, 611.67, 688.72, 777.83, 847.36, 959.20, 1019.60, 1107.30, 1152.60, 1231.20, 1300.80, 1442.80, 1468.62, 1536.50, 1581.90, 2851.40, 2921.00, 3214.10, 3347.10; ^1H NMR (400 MHz, CDCl_3) δ 1.66 - 1.67 (m, 2H), 1.69 - 1.76 (m, 2H), 2.29 (s, 6H), 2.56 (t, $J=6.55$ Hz, 2H), 3.09 (m, 2H), 6.53 (dd, $J=3.53, 0.50$ Hz, 1H), 6.89 (dd, $J=0.50, 1.50$ Hz, 1H), 7.22 (dd,

$J=3.53$, 0.50 Hz, 1H), 7.43 (d, $J=1.01$ Hz, 1H), 7.44 - 7.48 (m, 1H), 7.50 (m, 1H), 7.58 (dd, $J=8.94$, 2.14 Hz, 1H), 7.64 (m, 1H), 7.57 (m, 1H), 8.07 (d, $J=2.27$ Hz, 1H), 8.11 (s, 1H), 8.18 (br. s., 1H); ^{13}C NMR (100 MHz, CDCl_3) δ 24.1, 27.5, 42.3, 47.6, 47.8, 57.6, 106.8, 108.2, 108.9, 110.12, 113.0, 114.5, 116.8, 118.4, 118.9, 130.4, 130.8, 131.0, 132.3, 133.0, 145.8, 148.2, 150.0, 156.3, 158.2, 160.9; m/z (+EI) calc. For $\text{C}_{26}\text{H}_{28}\text{N}_4\text{O}_4$ (M^+) 460.52, found ($\text{M}+\text{H}$) $^+$ 461.20; Yield: 98%.

Procedure for the synthesis of 5-(5-(3-aminophenyl)furan-2-carboxamido)-*N*-(3-(pyrrolidin-1-yl)propyl)benzofuran-2-carboxamide (4.203)

A catalytic amount of tetrakis(triphenylphosphine)palladium, $\text{Pd}(\text{PPh}_3)_4$ (0.1 eq.) was added to a solution of **4.187** (1.0 eq., 36 mg) and **4.49** (2.5 eq., 27 mg) in a 9:3:1 combination of EtOH, toluene and water in the presence of K_2CO_3 (3.0 eq.) in a 10 ml microwave vial containing a magnetic stirrer. The reaction vessel was flushed with nitrogen during each addition. The reaction mixture was sealed in an inert nitrogen environment and heated with microwave radiation in an EMRYSTM Optimizer Microwave Station (Personal Chemistry) at 100 °C for 15 minutes. LCMS analysis revealed completion of reaction and the cooled reaction mixture was passed through a SCX (1 gm) cartridge for purification and 2M NH_3 in MeOH was used to release the pure product **4.203** (30 mg) from the cartridge.

5-(5-(3-Aminophenyl)furan-2-carboxamido)-*N*-(3-(pyrrolidin-1-yl)propyl)benzofuran-2-carboxamide (4.203):



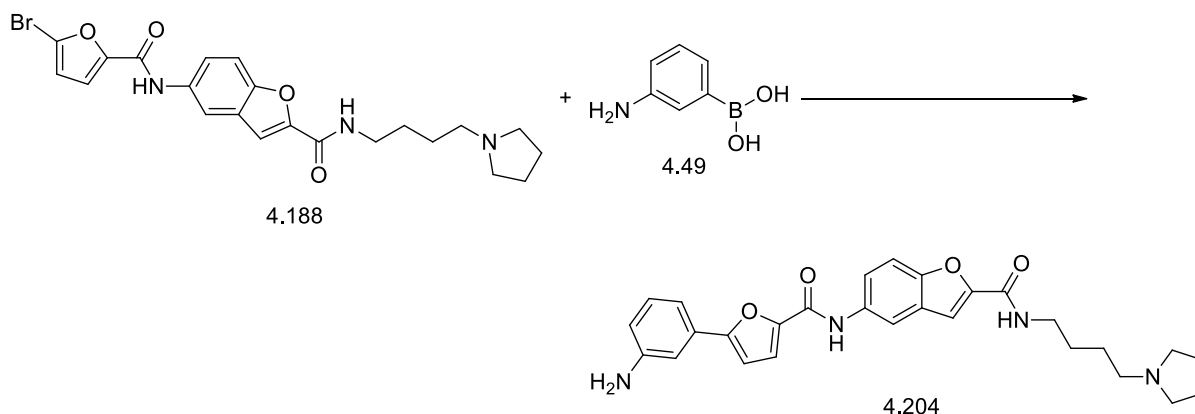
Brown oil. IR (FTIR, $\nu_{\text{max}}/\text{cm}^{-1}$) 427.50, 568.59, 691.98, 738.15, 779.05, 863.60, 953.15, 1022.70, 1107.30, 1170.80, 1203.76, 1233.02, 1296.69, 1469.51, 1538.84, 1581.52, 1645.17, 2809.00, 2936.00, 2963.20, 3220.20, 3347.10; ^1H NMR (400 MHz, CDCl_3) δ 1.74 – 1.78 (m, 2H), 1.80 - 1.93 (m, 4H), 2.63 – 2.75 (m, 4H), 2.81 - 2.87 (m, 2H), 3.64 - 3.84 (m, 2H), 6.52 (dd, $J=8.5$, 2.1 Hz, 1H), 6.80 (d, $J=2.1$ Hz, 1H), 7.13 (d, $J=3.53$ Hz, 1H), 7.38 (d, $J=3.53$ Hz,

1H), 7.40 (d, $J=1.01$ Hz, 1H), 7.41 - 7.44 (m, 1H), 7.50 (dd, $J=7.8$, 8.5 Hz, 1H), 7.57 (dd, $J=8.94$, 2.14 Hz, 1H), 7.68 (dd, $J=7.8$, 8.5 Hz, 1H), 8.06 (d, $J=2.27$ Hz, 1H), 8.12 (s, 1H) 9.04 (br. s., 1H); ^{13}C NMR (100 MHz, CDCl_3) δ 23.50, 23.60, 26.90, 40.10, 40.29, 56.61, 56.68, 106.31, 108.52, 108.64, 110.92, 111.13, 113.82, 114.67, 118.54, 118.90, 130.52, 131.12, 132.00, 132.12, 145.91, 148.23, 150.00, 152.36, 156.28, 158.37, 162.12; m/z (+EI) calc. For $\text{C}_{27}\text{H}_{28}\text{N}_4\text{O}_4$ (M^+) 472.54, found ($\text{M}+\text{H}$) $^+$ 473.20; Yield: 81%.

Procedure for the synthesis of 5-(5-(3-aminophenyl)furan-2-carboxamido)-*N*-(4-(pyrrolidin-1-yl)butyl)benzofuran-2-carboxamide (4.204)

A catalytic amount of tetrakis(triphenylphosphine)palladium, $\text{Pd}(\text{PPh}_3)_4$ (0.1 eq.) was added to a solution of **4.188** (1.0 eq., 124 mg) and **4.49** (2.5 eq., 90 mg) in a 9:3:1 combination of EtOH, toluene and water in the presence of K_2CO_3 (3.0 eq.) in a 10 ml microwave vial containing a magnetic stirrer. The reaction vessel was flushed with nitrogen during each addition. The reaction mixture was sealed in an inert nitrogen environment and heated with microwave radiation in an EMRYSTM Optimizer Microwave Station (Personal Chemistry) at 100 °C for 15 minutes. LCMS analysis revealed completion of reaction and the cooled reaction mixture was passed through a SCX (2 gm) cartridge for purification and 2M NH_3 in MeOH was used to release the pure product **4.204** (120 mg) from the cartridge.

5-(5-(3-Aminophenyl)furan-2-carboxamido)-*N*-(4-(pyrrolidin-1-yl)butyl)benzofuran-2-carboxamide (4.204):



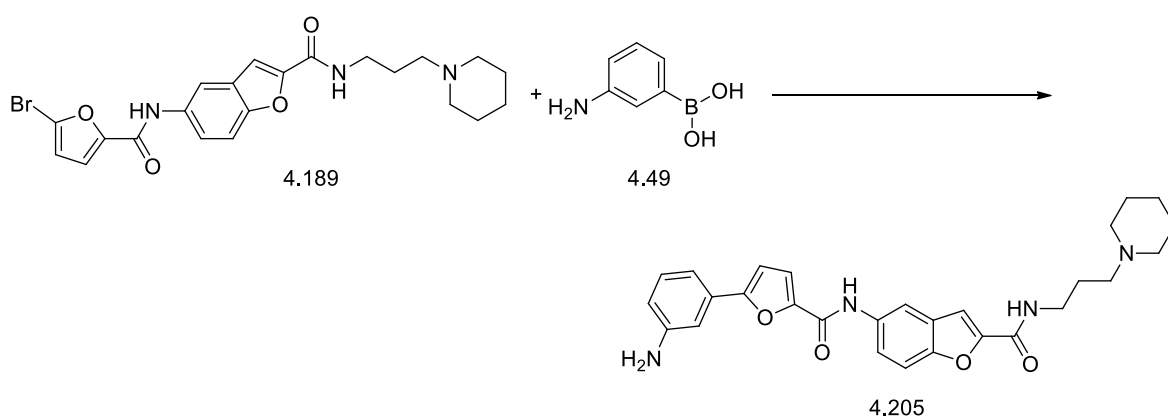
Orange oil. IR (FTIR, $\nu_{\text{max}}/\text{cm}^{-1}$) 425.46, 524.20, 568.14, 616.52, 690.36, 729.91, 778.48, 856.42, 956.17, 1022.70, 1113.40, 1204.00, 1234.30, 1296.59, 1346.00, 1436.15, 1468.45, 1519.98, 1542.95, 1580.42, 2812.00, 2851.40, 2936.00, 3223.20, 3350.10; ^1H NMR (400 MHz, CDCl_3) δ 1.59 (br. s., 2H), 1.78 (dt, $J=11.20$, 5.48 Hz, 6H), 2.50 (br. s., 2H), 2.54 - 2.59 (m, 2H), 3.57 - 3.63 (m, 2H), 3.83 (br. s., 2H), 6.26 (dd, $J=8.06$, 2.27 Hz, 1H), 6.67

(ddd, $J=7.99, 2.33, 1.01$ Hz, 1H), 6.71 (ddd, $J=7.93, 2.39, 1.01$ Hz, 1H), 6.95 - 6.99 (m, 1H), 7.09 (t, $J=1.89$ Hz, 1H), 7.15 - 7.18 (m, 1H), 7.24 (d, $J=8.06$ Hz, 1H), 7.33 (d, $J=3.53$ Hz, 1H), 7.41 (d, $J=8.81$ Hz, 1H), 7.44 (d, $J=0.76$ Hz, 1H), 7.66 (dd, $J=8.81, 2.27$ Hz, 1H), 8.04 (d, $J=2.01$ Hz, 1H), 8.20 (s, 1H), 9.28 (br. s., 1H); ^{13}C NMR (100 MHz, CDCl_3) δ 23.96, 24.04, 25.79, 27.57, 38.56, 54.80, 55.41, 56.61, 105.69, 107.59, 107.76, 109.75, 110.77, 111.60, 113.89, 114.05, 115.08, 117.52, 117.64, 120.15, 129.52, 130.26, 130.40, 133.22, 146.46, 150.58, 156.11, 158.63; m/z (+EI) calc. For $\text{C}_{28}\text{H}_{30}\text{N}_4\text{O}_4$ (M^+) 486.56, found ($\text{M}+\text{H}$) $^+$ 487.20; Yield: 94%.

Procedure for the synthesis of 5-(5-(3-aminophenyl)furan-2-carboxamido)-*N*-(3-(piperidin-1-yl)propyl)benzofuran-2-carboxamide (4.205)

A catalytic amount of tetrakis(triphenylphosphine)palladium, $\text{Pd}(\text{PPh}_3)_4$ (0.1 eq.) was added to a solution of **4.1889** (1.0 eq., 41 mg) and **4.49** (2.5 eq., 30 mg) in a 9:3:1 combination of EtOH, toluene and water in the presence of K_2CO_3 (3.0 eq.) in a 10 ml microwave vial containing a magnetic stirrer. The reaction vessel was flushed with nitrogen during each addition. The reaction mixture was sealed in an inert nitrogen environment and heated with microwave radiation in an EMRYSTM Optimizer Microwave Station (Personal Chemistry) at 100 °C for 15 minutes. LCMS analysis revealed completion of reaction and the cooled reaction mixture was passed through a SCX (1 gm) cartridge for purification and 2M NH_3 in MeOH was used to release the pure product **4.205** (41 mg) from the cartridge.

5-(5-(3-aminophenyl)furan-2-carboxamido)-*N*-(3-(piperidin-1-yl)propyl)benzofuran-2-carboxamide (4.205):



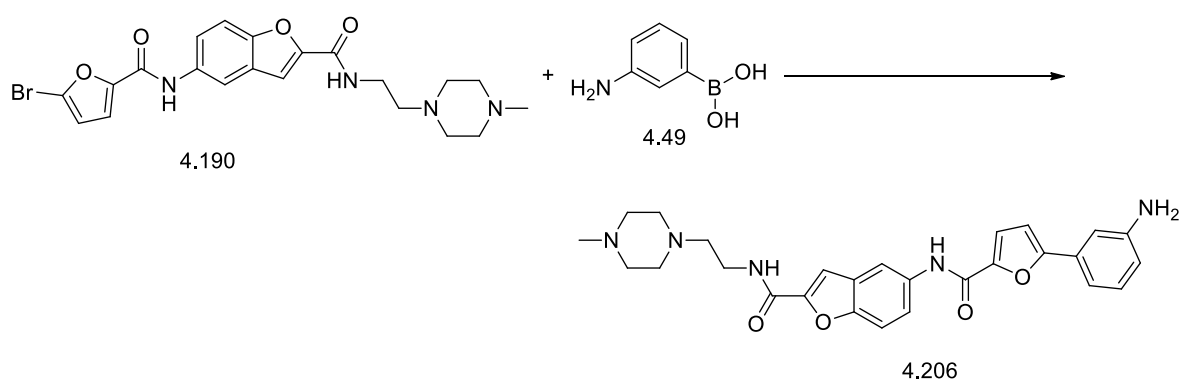
Dark brown oil. IR (FTIR, $\nu_{\text{max}}/\text{cm}^{-1}$) 408.82, 422.32, 533.24, 690.93, 780.86, 1022.70, 1116.40, 1024.45, 1230.97, 1303.09, 1343.00, 1469.65, 1543.54, 1582.47, 1639.41, 2497.70, 2936.00, 3349.01; ^1H NMR (400 MHz, Methanol- d_4) δ 1.52 (br. s., 2H), 1.63 - 1.70 (m, 4H),

1.82 - 1.90 (m, 2H), 2.13 - 2.15 (m, 2H), 2.47 - 2.51 (m, 4H), 3.43 - 3.50 (m, 2H), 6.72 - 6.76 (m, 1H), 6.89 (d, $J=3.53$ Hz, 1H), 7.16 - 7.21 (m, 1H), 7.23 - 7.26 (m, 1H), 7.27 (d, $J=1.76$ Hz, 1H), 7.35 (d, $J=3.78$ Hz, 1H), 7.47 (d, $J=0.50$ Hz, 1H), 7.57 (d, $J=9.06$ Hz, 1H), 7.75 (dd, $J=8.94$, 2.14 Hz, 1H), 8.13 (d, $J=2.01$ Hz, 1H); ^{13}C NMR (100 MHz, Methanol- d_4) δ 26.69, 26.99, 28.06, 30.82, 35.21, 40.60, 55.70, 56.69, 104.44, 108.18, 111.42, 112.88, 113.75, 116.70, 118.49, 120.09, 123.11, 127.11, 129.22, 131.77, 138.92, 142.23, 145.37, 147.63, 150.48, 153.67, 158.90, 162.33; m/z (+EI) calc. For $\text{C}_{28}\text{H}_{30}\text{N}_4\text{O}_4$ (M^+) 486.56, found ($M+H$) $^+$ 487.20; Yield: 97%.

Procedure for the synthesis of 5-(5-(3-aminophenyl)furan-2-carboxamido)-*N*-(2-(4-methylpiperazin-1-yl)ethyl)benzofuran-2-carboxamide (4.206)

A catalytic amount of tetrakis(triphenylphosphine)palladium, $\text{Pd}(\text{PPh}_3)_4$ (0.1 eq.) was added to a solution of **4.190** (1.0 eq., 120 mg) and **4.49** (2.5 eq., 86 mg) in a 9:3:1 combination of EtOH, toluene and water in the presence of K_2CO_3 (3.0 eq.) in a 10 ml microwave vial containing a magnetic stirrer. The reaction vessel was flushed with nitrogen during each addition. The reaction mixture was sealed in an inert nitrogen environment and heated with microwave radiation in an EMRYSTM Optimizer Microwave Station (Personal Chemistry) at 100 °C for 15 minutes. LCMS analysis revealed completion of reaction and the cooled reaction mixture was passed through a SCX (2 gm) cartridge for purification and 2M NH_3 in MeOH was used to release the pure product **4.206** (120 mg) from the cartridge.

5-(5-(3-aminophenyl)furan-2-carboxamido)-*N*-(2-(4-methylpiperazin-1-yl)ethyl)benzofuran-2-carboxamide (4.206):



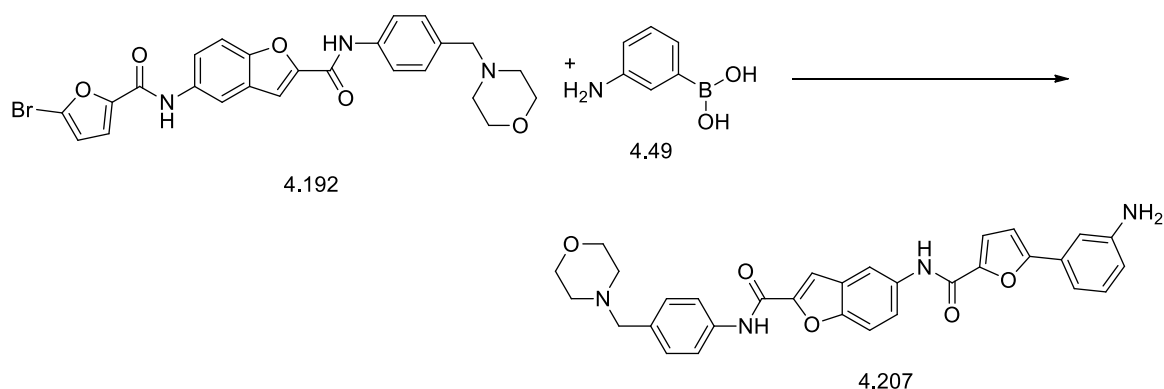
Yellow oil. IR (FTIR, $\nu_{\text{max}}/\text{cm}^{-1}$) 419.02, 447.53, 523.28, 572.34, 690.98, 719.37, 781.06, 863.93, 954.30, 1008.50, 1023.60, 1108.00, 1153.10, 1204.40, 1235.08, 1285.37, 1343.00, 1443.95, 1463.29, 1538.70, 1582.12, 1641.20, 1740.60, 2849.20, 2917.47, 3219.70, 3337.20; ^1H NMR (400 MHz, CDCl_3) δ 2.31 - 2.35 (s, 3H), 2.53 (m, 8H), 2.64 (t, $J=6.04$ Hz, 2H), 3.55

- 3.63 (m, 2H), 6.75 (d, $J=3.78$ Hz, 1H), 7.08 (t, $J=2.01$ Hz, 1H), 7.16 - 7.21 (m, 2H), 7.22 - 7.27 (m, 1H), 7.33 (d, $J=3.52$ Hz, 1H), 7.45 (d, $J=0.76$ Hz, 1H), 7.52 (d, $J=8.81$ Hz, 1H), 7.66 (dd, $J=8.81, 2.27$ Hz, 1H), 8.08 (d, $J=2.01$ Hz, 1H), 8.22 (s, 1H); ^{13}C NMR (100 MHz, CDCl_3) δ 29.99, 31.87, 36.22, 40.54, 53.08, 55.37, 56.66, 108.08, 110.63, 111.09, 112.31, 114.32, 114.37, 115.39, 116.07, 117.88, 117.96, 120.62, 128.43, 129.83, 130.23, 133.67, 136.34, 147.19, 150.12, 152.14, 159.04; m/z (+EI) calc. For $\text{C}_{27}\text{H}_{29}\text{N}_5\text{O}_4$ (M^+) 487.55, found ($\text{M}+\text{H}$) $^+$ 488.20; Yield: 97%.

Procedure for the synthesis of 5-(5-(3-aminophenyl)furan-2-carboxamido)-N-(4-(morpholinomethyl)phenyl)benzofuran-2-carboxamide (4.207)

A catalytic amount of tetrakis(triphenylphosphine)palladium, $\text{Pd}(\text{PPh}_3)_4$ (0.1 eq.) was added to a solution of **4.192** (1.0 eq., 28 mg) and **4.49** (2.5 eq., 18 mg) in a 9:3:1 combination of EtOH, toluene and water in the presence of K_2CO_3 (3.0 eq.) in a 10 ml microwave vial containing a magnetic stirrer. The reaction vessel was flushed with nitrogen during each addition. The reaction mixture was sealed in an inert nitrogen environment and heated with microwave radiation in an EMRYSTM Optimizer Microwave Station (Personal Chemistry) at 100 °C for 15 minutes. LCMS analysis revealed completion of reaction and the cooled reaction mixture was passed through a SCX (1 gm) cartridge for purification and 2M NH_3 in MeOH was used to release the pure product **4.207** (25 mg) from the cartridge.

5-(5-(3-Aminophenyl)furan-2-carboxamido)-N-(4-(morpholinomethyl)phenyl)benzofuran-2-carboxamide (4.207):



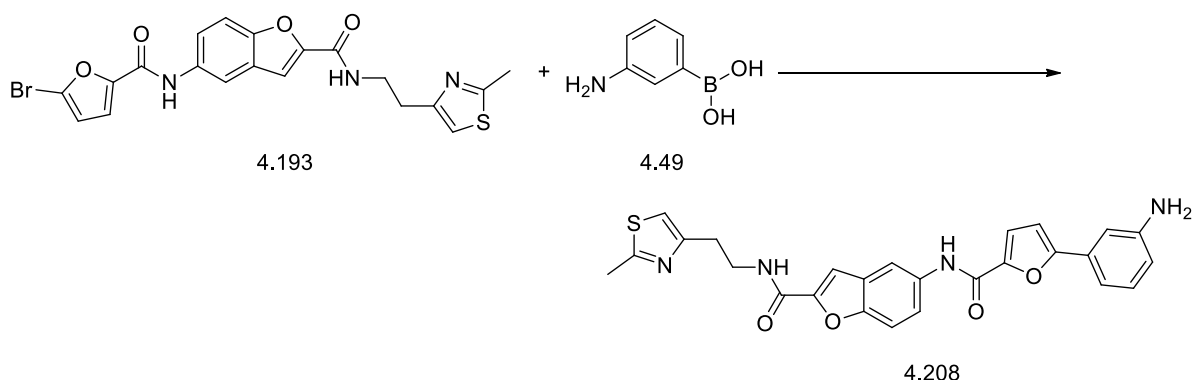
Dark brown oil. IR (FTIR, $\nu_{\text{max}}/\text{cm}^{-1}$) 418.52, 462.16, 507.35, 538.60, 623.09, 695.62, 775.43, 862.43, 1002.08, 1071.00, 1071.00, 1111.14, 1170.80, 1261.50, 1288.70, 1328.00, 1433.80, 1451.90, 1482.10, 1517.27, 1579.09, 1598.39, 2815.10, 2863.50, 2924.00, 2932.20, 3032.70, 3217.10, 3344.00; ^1H NMR (400 MHz, $\text{METHANOL}-d_4$) δ 2.45 (d, $J=16.37$ Hz, 4H), 3.51 (s, 2H), 3.65 - 3.72 (m, 4H), 6.67 - 6.71 (m, 2H), 6.88 - 6.92 (m, 2H), 6.94 (t, $J=1.89$ Hz,

2H), 7.06 (d, $J=8.31$ Hz, 2H), 7.13 (t, $J=7.81$ Hz, 2H), 7.33 - 7.40 (m, 2H), 7.64 - 7.69 (m, 1H), 7.74 (d, $J=8.56$ Hz, 1H); ^{13}C NMR (100 MHz, METHANOL- d_4) δ 5.01, 55.64, 64.58, 66.34, 66.89, 108.02, 108.23, 108.65, 111.08, 113.84, 114.28, 115.39, 117.13, 118.91, 121.51, 121.67, 129.35, 129.82, 130.25, 130.56, 131.25, 132.84, 134.29, 136.19, 146.35, 148.09, 150.00, 152.23, 156.38, 160.02, 162.34; m/z (+EI) calc. For $\text{C}_{31}\text{H}_{28}\text{N}_4\text{O}_5$ (M^+) 536.58, found ($\text{M}+\text{H}$) $^+$ 537.30; Yield: 87%.

Procedure for the synthesis of 5-(5-(3-aminophenyl)furan-2-carboxamido)-*N*-(2-(2-methylthiazol-4-yl)ethyl)benzofuran-2-carboxamide (4.208)

A catalytic amount of tetrakis(triphenylphosphine)palladium, $\text{Pd}(\text{PPh}_3)_4$ (0.1 eq.) was added to a solution of **4.193** (1.0 eq., 120 mg) and **4.49** (2.5 eq., 86 mg) in a 9:3:1 combination of EtOH, toluene and water in the presence of K_2CO_3 (3.0 eq.) in a 10 ml microwave vial containing a magnetic stirrer. The reaction vessel was flushed with nitrogen during each addition. The reaction mixture was sealed in an inert nitrogen environment and heated with microwave radiation in an EMRYSTM Optimizer Microwave Station (Personal Chemistry) at 100 °C for 15 minutes. LCMS analysis revealed completion of reaction and the cooled reaction mixture was passed through a SCX (2 gm) cartridge for purification and 2M NH_3 in MeOH was used to release the pure product **4.208** (120 mg) from the cartridge.

5-(5-(3-Aminophenyl)furan-2-carboxamido)-*N*-(2-(2-methylthiazol-4-yl)ethyl)benzofuran-2-carboxamide (4.208):



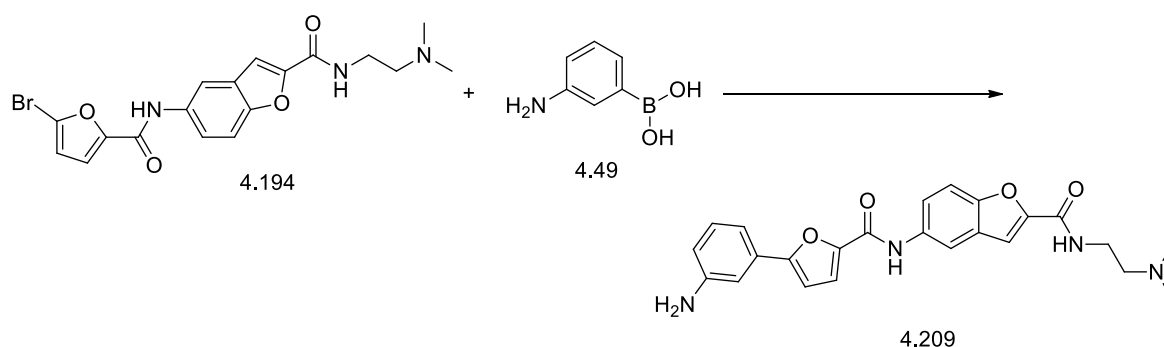
Colourless oil. IR (FTIR, $\nu_{\text{max}}/\text{cm}^{-1}$) 430.17, 567.72, 691.73, 784.31, 863.97, 939.25, 1041.70, 1110.35, 1235.58, 1297.75, 1343.75, 1459.57, 1542.11, 1584.32, 1647.94, 2852.20, 2921.50, 3319.20; ^1H NMR (400 MHz, CDCl_3) δ 2.77 (s, 3H), 3.06 (t, $J=6.29$ Hz, 2H), 3.80 - 3.86 (m,

2H), 6.72 (ddd, $J=7.99, 2.33, 1.01$ Hz, 1H), 6.76 (d, $J=3.53$ Hz, 1H), 6.88 (s, 1H), 7.08 (t, $J=1.89$ Hz, 1H), 7.15 - 7.18 (m, 1H), 7.24 (d, $J=7.81$ Hz, 1H), 7.33 (d, $J=3.78$ Hz, 1H), 7.46 (d, $J=1.01$ Hz, 1H), 7.49 (d, $J=9.06$ Hz, 1H), 7.53 (t, $J=5.54$ Hz, 1H), 7.65 (dd, $J=8.94, 2.14$ Hz, 1H), 8.09 (d, $J=2.01$ Hz, 1H), 8.17 (s, 1H); ^{13}C NMR (100 MHz, CDCl_3) δ 19.54, 25.86, 41.44, 107.04, 110.54, 111.09, 112.33, 114.38, 115.43, 117.88, 118.71, 120.57, 124.94, 129.53, 130.26, 132.94, 136.05, 144.96, 146.76, 147.19, 151.26, 153.96, 155.89, 159.01, 163.10, 163.96; m/z (+EI) calc. For $\text{C}_{26}\text{H}_{22}\text{N}_4\text{O}_4\text{S}$ (M^+) 486.54, found ($\text{M}+\text{H}$) $^+$ 487.20; Yield: 97%.

Procedure for the synthesis of 5-(5-(3-aminophenyl)furan-2-carboxamido)-*N*-(2-(dimethylamino)ethyl)benzofuran-2-carboxamide (4.209)

A catalytic amount of tetrakis(triphenylphosphine)palladium, $\text{Pd}(\text{PPh}_3)_4$ (0.1 eq.) was added to a solution of **4.194** (1.0 eq., 58 mg) and **4.49** (2.5 eq., 47 mg) in a 9:3:1 combination of EtOH, toluene and water in the presence of K_2CO_3 (3.0 eq.) in a 10 ml microwave vial containing a magnetic stirrer. The reaction vessel was flushed with nitrogen during each addition. The reaction mixture was sealed in an inert nitrogen environment and heated with microwave radiation in an EMRYSTM Optimizer Microwave Station (Personal Chemistry) at 100 °C for 15 minutes. LCMS analysis revealed completion of reaction and the cooled reaction mixture was passed through a SCX (1 gm) cartridge for purification and 2M NH_3 in MeOH was used to release the pure product **4.209** (59 mg) from the cartridge.

5-(5-(3-Aminophenyl)furan-2-carboxamido)-*N*-(2-(dimethylamino)ethyl)benzofuran-2-carboxamide (4.209):



Dark brown oil. IR (FTIR, $\nu_{\text{max}}/\text{cm}^{-1}$) 403.30, 417.76, 566.25, 691.90, 725.72, 780.99, 862.93, 1020.95, 1107.30, 1203.56, 1231.81, 1298.49, 1343.00, 1468.45, 1539.09, 1581.34, 1644.83, 2784.90, 2827.2, 2942.00, 3223.20, 3338.00; ^1H NMR (400 MHz, CDCl_3) δ 2.32 (s, 6H), 2.55 (t, $J=5.92$ Hz, 2H), 3.57 (q, $J=5.62$ Hz, 2H), 6.71 (dd, $J=7.81, 1.26$ Hz, 1H), 6.75 (d,

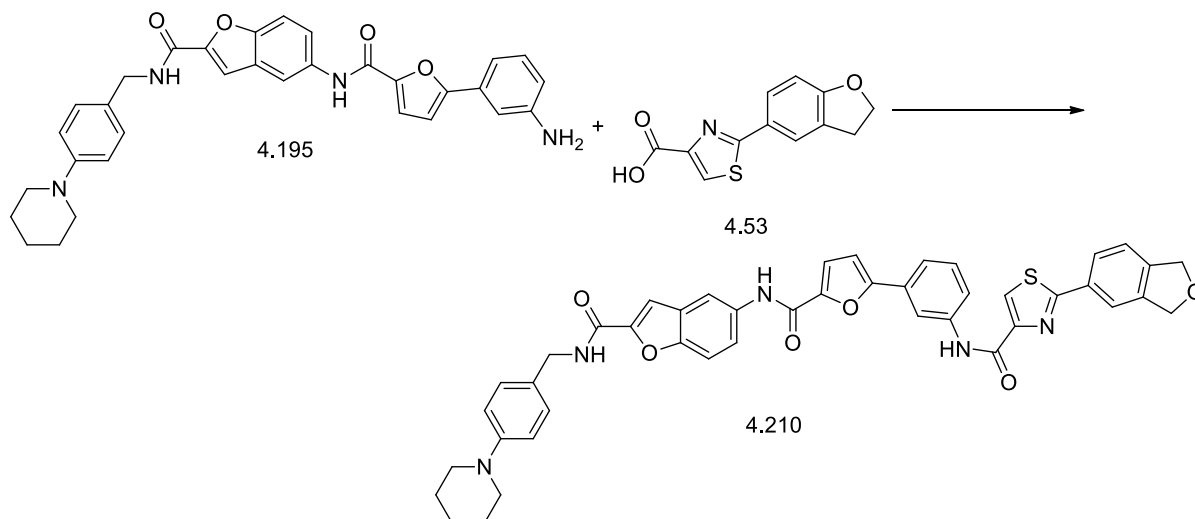
$J=3.52$ Hz, 1H), 7.08 (s, 1H), 7.16 (d, $J=7.55$ Hz, 2H), 7.24 (t, $J=7.81$ Hz, 1H), 7.33 (d, $J=3.78$ Hz, 1H), 7.45 (s, 1H), 7.52 (d, $J=9.06$ Hz, 1H), 7.64 (dd, $J=8.81, 2.01$ Hz, 1H) 8.09 (d, $J=2.01$ Hz, 1H), 8.21 (s, 1H); ^{13}C NMR (100 MHz, CDCl_3) δ 22.18, 34.99, 45.27, 57.77, 107.75, 110.25, 112.11, 113.95, 114.65, 115.72, 117.52, 120.25, 128.13, 129.91, 133.32, 136.06, 141.20, 146.88, 151.83, 152.84, 156.11, 158.76, 161.37, 173.26; m/z (+EI) calc. For $\text{C}_{24}\text{H}_{24}\text{N}_4\text{O}_4$ (M^+) 432.47, found ($\text{M}+\text{H}$) $^+$ 433.10; Yield: 99%.

The general procedure for the amide coupling reaction was followed for the synthesis of the following final compounds (**4.210** to **4.224**) from reactions between several heterocyclic amines and 2-(2,3-dihydrobenzofuran-5-yl)thiazole-4-carboxylic acid (**4.53**).

General procedure for the synthesis of 2-(2,3-dihydrobenzofuran-5-yl)-*N*-(3-(5-((2-((4-(piperidin-1-yl)benzyl)carbamoyl)benzofuran-5-yl)carbamoyl)furan-2-yl)phenyl)thiazole-4-carboxamide (4.210**) from **4.195** and **4.53****

81 mg (1.0 eq.) of **4.195** and 75 mg (2.0 eq.) of **4.53** were added to a reaction vessel. Along with these, 2.0 eq. of HOBt and 1.75 eq. of DIC were added and a clear solution was made by dissolving these reactants in a minimum amount of DMF. The reaction mixture was stirred for 3 hours with occasional monitoring of the progress of the reaction by LCMS. After completion of the reaction, it was dried using a vacuum. The crude product was purified by silica column chromatography using DCM and ethyl acetate solvent mixtures (100% DCM, then 10% ethyl acetate in DCM and 20% ethyl acetate in DCM) to obtain the pure product **4.210** (50 mg).

2-(2,3-Dihydrobenzofuran-5-yl)-N-(3-(5-((2-((4-(piperidin-1-yl)benzyl)carbamoyl)benzofuran-5-yl)carbamoyl)furan-2-yl)phenyl)thiazole-4-carboxamide (4.210):

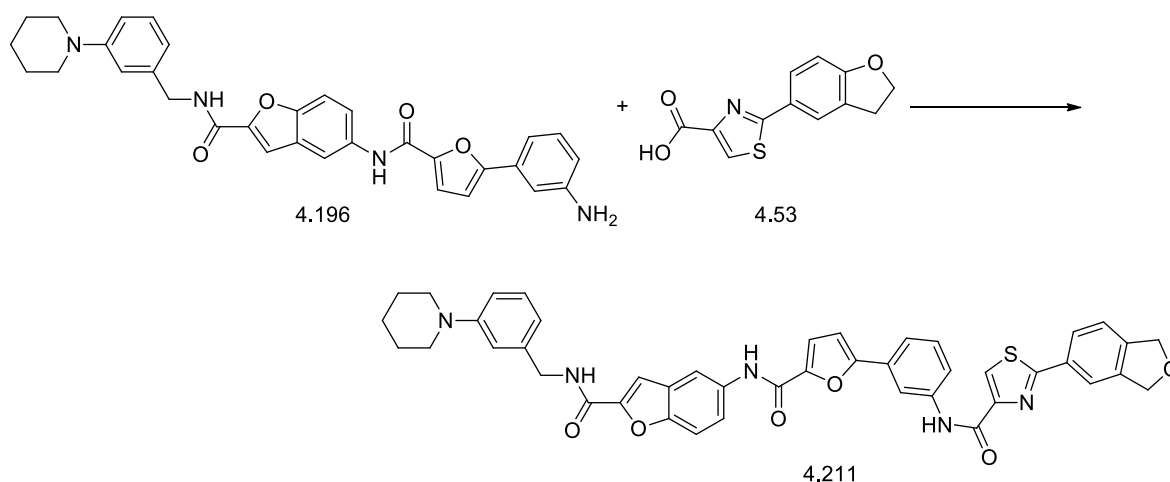


Colourless, viscous oil. IR (FTIR, $\nu_{\text{max}}/\text{cm}^{-1}$) 643.91, 669.74, 692.45, 742.38, 798.55, 832.96, 873.86, 921.32, 975.95, 1024.45, 1106.40, 1128.04, 1172.39, 1198.74, 1233.28, 1299.98, 1345.64, 1473.61, 1550.55, 1591.58, 1645.62, 1679.74, 2361.31, 2790.69, 2852.71, 2932.16, 3111.11, 3317.64; ^1H NMR (400 MHz, CDCl_3 , TMS); δ 1.60 (q, $J=5.89$ Hz, 2H), 1.75 (dt, $J=11.24, 5.75$ Hz, 4H), 3.18 - 3.23 (m, 4H), 3.31 (t, $J=8.84$ Hz, 2H), 4.59 (d, $J=5.81$ Hz, 2H), 4.69 (t, $J=8.84$ Hz, 2H), 6.86 - 6.88 (m, 1H), 6.99 - 7.02 (m, 2H), 7.26 - 7.27 (m, 1H), 7.27 - 7.28 (m, 1H), 7.35 - 7.37 (m, 1H), 7.38 (d, $J=1.77$ Hz, 1H), 7.39 (s, 1H), 7.40 (d, $J=1.77$ Hz, 1H), 7.41 - 7.44 (m, 2H), 7.48 (d, $J=0.76$ Hz, 1H), 7.52 - 7.56 (m, 1H), 7.74 - 7.76 (m, 2H), 7.87 (d, $J=1.52$ Hz, 1H), 8.09 (d, $J=2.27$ Hz, 1H), 8.15 (s, 1H), 8.28 (t, $J=1.77$ Hz, 1H), 8.33 (s, 1H); ^{13}C NMR (100 MHz, CDCl_3); δ 23.81, 25.31, 25.34, 29.31, 43.02, 44.25, 51.63, 71.95, 108.38, 109.86, 111.42, 111.57, 111.95, 114.37, 115.97, 115.99, 116.75, 117.39, 117.65, 120.31, 122.47, 123.01, 123.56, 123.57, 126.35, 126.48, 127.65, 128.03, 128.35, 128.45, 129.16, 129.65, 133.36, 138.37, 141.70, 149.08, 149.47, 150.09, 151.88, 155.59, 155.64, 158.64, 159.32, 160.31; m/z (+EI) calc. For $\text{C}_{44}\text{H}_{37}\text{N}_5\text{O}_6\text{S}$ (M^+) 763.86, found 764.15 ($\text{M}+\text{H}$) $^+$; Yield: 43%.

Procedure for the synthesis of 2-(2,3-dihydrobenzofuran-5-yl)-N-(3-(5-((2-((3-(piperidin-1-yl)benzyl)carbamoyl)benzofuran-5-yl)carbamoyl)furan-2-yl)phenyl)thiazole-4-carboxamide (4.211) from 4.196 and 4.53

55 mg (1.0 eq.) of **4.196** and 51 mg (2.0 eq.) of **4.53** were added to a reaction vessel. Along with these, 2.0 eq. of HOBt and 1.75 eq. of DIC were added and a clear solution was made by dissolving these reactants in a minimum amount of DMF. The reaction mixture was stirred for 3 hours with occasional monitoring of the progress of the reaction by LCMS. After completion of the reaction it was dried using vacuum. The crude product was purified by silica column chromatography using DCM and ethyl acetate solvent mixtures (100% DCM, then 10% ethyl acetate in DCM and 20% ethyl acetate in DCM) to obtain pure product **4.211** (50 mg).

2-(2,3-Dihydrobenzofuran-5-yl)-N-(3-(5-((2-((3-(piperidin-1-yl)benzyl)carbamoyl)benzofuran-5-yl)carbamoyl)furan-2-yl)phenyl)thiazole-4-carboxamide (4.211):



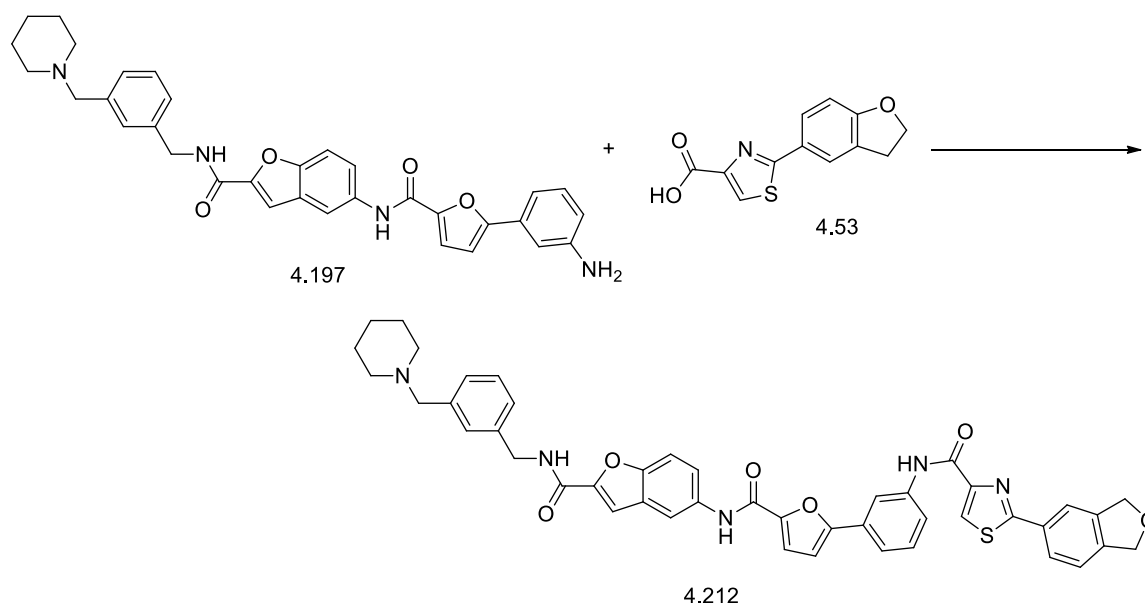
Colourless mass. IR (FTIR, $\nu_{\text{max}}/\text{cm}^{-1}$) 636.44, 691.10, 727.54, 785.24, 864.20, 941.37, 979.60, 1000.86, 1016.05, 1111.68, 1167.89, 1233.44, 1295.44, 1350.10, 1468.86, 1537.87, 1586.98, 1650.13, 1665.94, 2335.36, 2363.10, 2930.65, 3329.26; ^1H NMR (400 MHz, CDCl_3 , TMS); δ 1.56 - 1.62 (m, 2H), 1.69 - 1.73 (m, 4H), 3.14 - 3.22 (m, 4H), 3.31 (t, $J=8.59$ Hz, 2H), 4.62 (d, $J=5.56$ Hz, 2H), 4.66 - 4.70 (m, 2H), 6.84 - 6.87 (m, 2H), 6.87 - 6.89 (m, 2H), 6.95 - 6.96 (m, 1H), 7.23 - 7.26 (m, 1H), 7.34 (d, $J=3.79$ Hz, 1H), 7.42 - 7.43 (m, 1H), 7.45 (d, $J=2.02$ Hz, 1H), 7.48 (d, $J=0.76$ Hz, 1H), 7.53 (dt, $J=7.83$, 1.39 Hz, 1H), 7.65 - 7.66 (m, 1H), 7.66 - 7.68 (m, 1H), 7.68 (d, $J=2.02$ Hz, 1H), 7.78 (dd, $J=8.34$, 2.02 Hz, 1H), 7.86 (d, $J=1.52$ Hz, 1H), 8.11 (d, $J=2.02$ Hz, 1H), 8.13 (s, 1H), 8.27 (t, $J=1.77$ Hz, 1H), 8.37 (s,

1H), 9.38 (s, 1H); ^{13}C NMR (100 MHz, CDCl_3); δ 23.47, 24.25, 25.79, 29.29, 42.18, 43.94, 50.45, 71.94, 108.31, 109.83, 110.61, 111.91, 114.23, 115.64, 115.88, 116.10, 117.52, 118.66, 120.22, 120.65, 122.91, 123.54, 125.52, 127.63, 128.05, 128.33, 128.42, 128.54, 129.50, 129.61, 130.39, 132.03, 132.13, 133.46, 138.38, 146.91, 149.56, 150.14, 151.80, 152.65, 156.27, 158.48, 159.22, 162.66; m/z (+EI) calc. For $\text{C}_{44}\text{H}_{37}\text{N}_5\text{O}_6\text{S}$ (M^+) 763.86, found 763.79 ($\text{M}+\text{H}$) $^+$; Yield: 64%.

Procedure for the synthesis of 2-(2,3-dihydrobenzofuran-5-yl)-N-(3-(5-((2-((3-(piperidin-1-ylmethyl)benzyl)carbamoyl)benzofuran-5-yl)carbamoyl)furan-2-yl)phenyl)thiazole-4-carboxamide (4.212) from 4.197 and 4.53

27 mg (1.0 eq.) of **4.197** and 18 mg (1.5 eq.) of **4.53** were added to a reaction vessel. Along with these, 2.0 eq. of HOBT and 1.75 eq. of DIC were added and a clear solution was made by dissolving these reactants in a minimum amount of DMF. The reaction mixture was stirred for 3 hours with occasional monitoring of the progress of the reaction by LCMS. After completion of the reaction it was dried using vacuum. The crude product was purified by silica column chromatography using DCM and ethyl acetate solvent mixtures (100% DCM, then 10% ethyl acetate in DCM and 20% ethyl acetate in DCM) to obtain the pure product **4.212** (26 mg).

2-(2,3-Dihydrobenzofuran-5-yl)-N-(3-(5-((2-((3-(piperidin-1-ylmethyl)benzyl)carbamoyl)benzofuran-5-yl)carbamoyl)furan-2-yl)phenyl)thiazole-4-carboxamide (4.212):

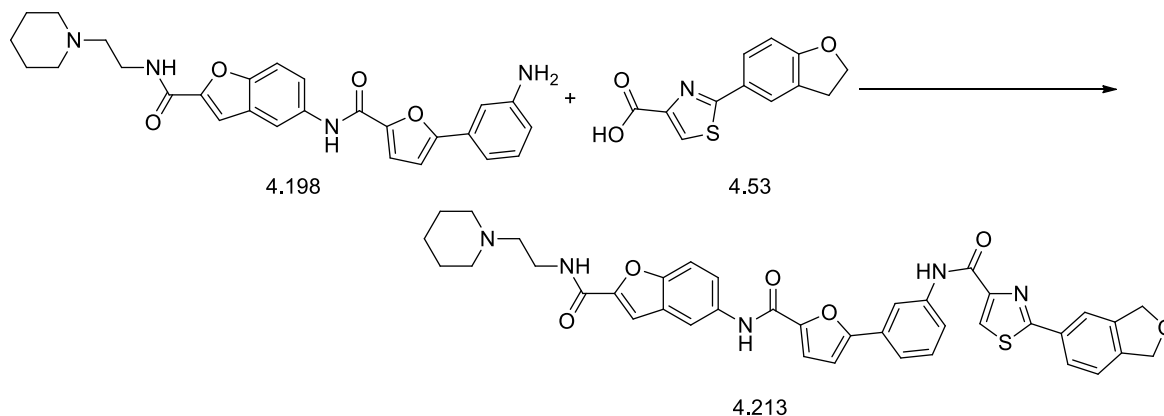


Colourless oil. IR (FTIR, $\nu_{\text{max}}/\text{cm}^{-1}$) 639.47, 744.49, 865.93, 958.54, 1037.66, 1097.90, 1129.57, 1167.45, 1243.19, 1325.31, 1360.51, 1383.56, 1462.80, 1559.65, 1612.68, 2335.36, 2357.70, 2932.92, 2966.89, 3336.27; ^1H NMR (500 MHz, DMSO- d_6 , TMS); δ 1.12 - 1.20 (m, 4H), 1.45 - 1.48 (m, 2H), 3.28 - 3.31 (m, 2H), 3.63 (dq, $J=7.68$, 6.59, 6.59, 6.59, 6.59 Hz, 4H), 4.36 (s, 2H), 4.64 (t, $J=8.83$ Hz, 2H), 6.93 (d, $J=8.20$ Hz, 1H), 7.16 (d, $J=3.47$ Hz, 1H), 7.19 - 7.23 (m, 1H), 7.25 - 7.28 (m, 1H), 7.46 - 7.47 (m, 1H), 7.47 - 7.50 (m, 2H), 7.52 (t, $J=7.88$ Hz, 1H), 7.61 - 7.63 (m, 1H), 7.63 - 7.66 (m, 1H), 7.66 - 7.69 (m, 1H), 7.75 - 7.77 (m, 1H), 7.85 - 7.87 (m, 1H), 7.91 - 7.93 (m, 1H), 7.94 (d, $J=1.89$ Hz, 1H), 8.06 - 8.09 (m, 2H), 8.21 (d, $J=2.21$ Hz, 1H), 8.31 - 8.32 (m, 1H), 8.39 (s, 1H), 9.30 (t, $J=6.15$ Hz, 1H), 10.33 (s, 1H), 10.35 (s, 1H); ^{13}C NMR (100 MHz, DMSO- d_6); δ 21.18, 23.51, 28.82, 29.48, 36.35, 45.02, 51.14, 52.60, 68.40, 107.46, 107.96, 109.18, 109.44, 109.61, 109.99, 110.45, 111.97, 113.52, 114.80, 119.12, 119.29, 119.91, 120.55, 121.11, 121.30, 121.93, 122.33, 122.48, 123.24, 124.30, 125.23, 126.41, 128.60, 129.90, 131.80, 134.25, 138.11, 144.43, 148.36, 151.20, 154.34, 156.98, 160.69, 162.29, 188.33; m/z (+EI) calc. For $\text{C}_{45}\text{H}_{39}\text{N}_5\text{O}_5\text{S}$ (M^+) 777.89, found 778.21 ($M+H$) $^+$; Yield: 69%.

Procedure for the synthesis of 2-(2,3-dihydrobenzofuran-5-yl)-N-(3-(5-((2-((2-(piperidin-1-yl)ethyl)carbamoyl)benzofuran-5-yl)carbamoyl)furan-2-yl)phenyl)thiazole-4-carboxamide (4.213) from 4.198 and 4.53

82 mg (1.0 eq.) of **4.198** and 85 mg (2.0 eq.) of **4.53** were added to a reaction vessel. Along with this, 2.0 eq. of HOBt and 1.75 eq. of DIC were added and a clear solution was made by dissolving these reactants in a minimum amount of DMF. The reaction mixture was stirred for 3 hours with occasional monitoring of the progress of the reaction by LCMS. After completion of the reaction it was dried using vacuum. The crude product was purified by using a SCX cartridge (2 gm) by the catch and release method, as described earlier in the chapter. Ten ml 2M NH_3 was used to release the product from the cartridge. Purification of the product **4.213** (40 mg) was finally made using flash chromatography with DCM:MeOH:2M NH_3 (18:1:1) as the solvent system.

2-(2,3-Dihydrobenzofuran-5-yl)-N-(3-(5-((2-((2-(piperidin-1-yl)ethyl)carbamoyl)benzofuran-5-yl)carbamoyl)furan-2-yl)phenyl)thiazole-4-carboxamide (4.213):



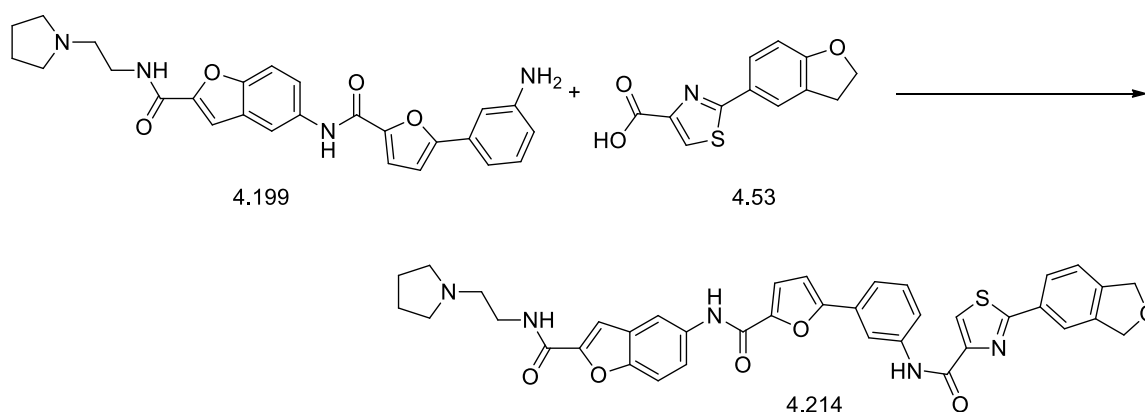
Colourless oil. IR (FTIR, $\nu_{\text{max}}/\text{cm}^{-1}$) 691.66, 735.84, 785.97, 863.06, 939.92, 1015.54, 1110.70, 1231.48, 1537.77, 1584.59, 1650.61, 2175.94, 2929.57, 3300.69; ^1H NMR (500 MHz, DMSO- d_6 , TMS); δ 1.38 (d, $J=3.47$ Hz, 2H), 1.49 (quin, $J=5.52$ Hz, 4H), 2.38 (br. s., 2H), 2.44 (t, $J=6.94$ Hz, 2H), 3.30 (t, $J=8.20$ Hz, 2H), 3.36 - 3.42 (m, 4H), 4.65 (t, $J=8.67$ Hz, 2H), 6.93 (d, $J=8.51$ Hz, 1H), 7.16 (d, $J=3.47$ Hz, 1H), 7.47 (d, $J=3.78$ Hz, 1H), 7.52 (t, $J=8.04$ Hz, 1H), 7.55 (d, $J=0.95$ Hz, 1H), 7.67 (d, $J=9.14$ Hz, 1H), 7.75 - 7.78 (m, 2H), 7.92 - 7.96 (m, 2H), 8.09 (d, $J=1.58$ Hz, 1H), 8.20 (d, $J=2.21$ Hz, 1H), 8.32 (t, $J=1.89$ Hz, 1H), 8.39 (s, 1H), 8.59 (t, $J=5.83$ Hz, 1H), 10.32 (s, 1H), 10.35 (s, 1H); ^{13}C NMR (100 MHz, DMSO- d_6); δ 21.15, 25.75, 28.81, 30.89, 54.22, 55.11, 57.42, 57.71, 60.64, 109.72, 111.95, 114.34, 115.82, 117.14, 119.81, 119.95, 121.08, 123.94, 125.40, 125.81, 125.96, 126.79, 127.47, 127.63, 128.63, 128.97, 129.57, 129.91, 138.06, 139.12, 141.33, 141.61, 146.94, 150.03, 150.10, 151.12, 152.06, 152.78, 162.29; m/z (+EI) calc. For $\text{C}_{39}\text{H}_{35}\text{N}_5\text{O}_6\text{S}$ (M^+) 701.79, found 702.18 ($\text{M}+\text{H}$) $^+$; Yield: 41%.

Procedure for the synthesis of 2-(2,3-dihydrobenzofuran-5-yl)-N-(3-(5-((2-((2-(pyrrolidin-1-yl)ethyl)carbamoyl)benzofuran-5-yl)carbamoyl)furan-2-yl)phenyl)thiazole-4-carboxamide (4.214) from 4.199 and 4.53

60 mg (1.0 eq.) of **4.199** and 65 mg (2.0 eq.) of **4.53** were added to a reaction vessel. Along with these, 2.0 eq. of HOBt and 1.75 eq. of DIC were added and a clear solution was made by dissolving these reactants in a minimum amount of DMF. The reaction mixture was stirred for 3 hours with occasional monitoring of the progress of the reaction by LCMS. The crude product was purified by using a SCX cartridge (2 gm) by the catch and release method, as

described earlier in the chapter. Ten ml 2M NH₃ was used to release the product from the cartridge. Purification of product **4.214** (50 mg) was finally made using flash chromatography with DCM:MeOH:2M NH₃ (18:1:1) as the solvent system.

2-(2,3-Dihydrobenzofuran-5-yl)-N-(3-(5-((2-((2-(pyrrolidin-1-yl)ethyl)carbamoyl)benzofuran-5-yl)carbamoyl)furan-2-yl)phenyl)thiazole-4-carboxamide (4.214):

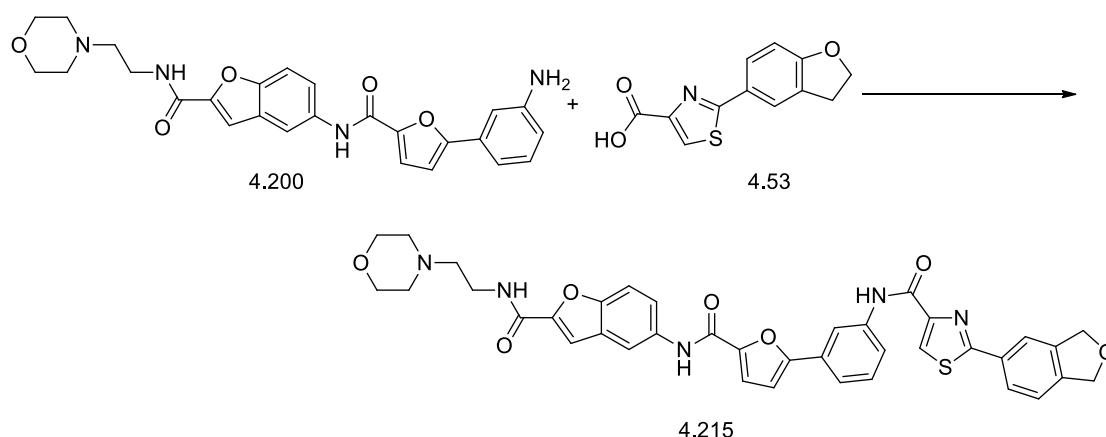


Light yellow oil. IR (FTIR, $\nu_{\text{max}}/\text{cm}^{-1}$) 634.44, 660.73, 691.69, 740.32, 785.58, 864.16, 939.32, 979.60, 1022.12, 1095.97, 1167.89, 1204.33, 1232.84, 1299.84, 1347.07, 1383.51, 1463.93, 1539.90, 1585.93, 1650.75, 2335.36, 2358.58, 2804.87, 2859.75, 2922.10, 2957.31, 3115.85, 3286.58; ¹H NMR (500 MHz, CDCl₃, TMS); δ 1.88 (br. s., 4H), 2.75 (br. s., 2H), 2.96 (s, 4H), 3.29 - 3.35 (m, 2H), 3.67 (d, $J=5.36$ Hz, 2H), 4.69 (t, $J=8.83$ Hz, 2H), 6.87 (d, $J=3.78$ Hz, 1H), 6.89 (d, $J=8.20$ Hz, 1H), 7.36 (d, $J=3.78$ Hz, 1H), 7.43 - 7.46 (m, 1H), 7.48 (d, $J=7.88$ Hz, 1H), 7.54 - 7.56 (m, 1H), 7.63 (dd, $J=8.67$, 2.05 Hz, 1H), 7.67 - 7.70 (m, 1H), 7.79 (dd, $J=8.20$, 1.89 Hz, 1H), 7.87 - 7.88 (m, 1H), 8.03 (s, 1H), 8.10 (d, $J=2.21$ Hz, 1H), 8.15 (s, 1H), 8.28 (t, $J=1.73$ Hz, 1H), 8.32 (s, 1H), 9.40 (s, 1H); ¹³C NMR (100 MHz, CDCl₃); δ 23.74, 29.54, 31.67, 36.73, 51.12, 54.29, 55.04, 72.21, 108.62, 110.10, 110.59, 112.32, 114.38, 116.09, 117.80, 118.35, 120.47, 120.71, 120.88, 123.20, 123.79, 125.75, 1227.88, 128.28, 128.59, 129.91, 130.64, 133.49, 138.65, 147.14, 150.36, 152.11, 155.74, 156.47, 159.47, 162.74, 162.90, 169.10; m/z (+EI) calc. For C₃₈H₃₃N₅O₆S (M⁺) 687.76, found 687.99 (M+H)⁺; Yield: 56%.

Procedure for the synthesis of 2-(2,3-dihydrobenzofuran-5-yl)-N-(3-(5-((2-((2-morpholinoethyl)carbamoyl)benzofuran-5-yl)carbamoyl)furan-2-yl)phenyl)thiazole-4-carboxamide (4.215) from 4.200 and 4.53

77 mg (1.0 eq.) of **4.200** and 60 mg (1.5 eq.) of **4.53** were added to a reaction vessel. Along with these, 2.0 eq. of HOBt and 1.75 eq. of DIC were added and a clear solution was made by dissolving these reactants in a minimum amount of DMF. The reaction mixture was stirred for 3 hours with occasional monitoring of the progress of the reaction by LCMS. The crude product was purified by using a SCX cartridge (2 gm) by the catch and release method, as described earlier in the chapter. Ten ml 2M NH₃ was used to release the product from the cartridge. Purification of the product **4.215** (37 mg) was finally achieved using flash chromatography with DCM:MeOH:2M NH₃ (18:1:1) as solvent system.

2-(2,3-Dihydrobenzofuran-5-yl)-N-(3-(5-((2-((2-morpholinoethyl)carbamoyl)benzofuran-5-yl)carbamoyl)furan-2-yl)phenyl)thiazole-4-carboxamide (4.215):



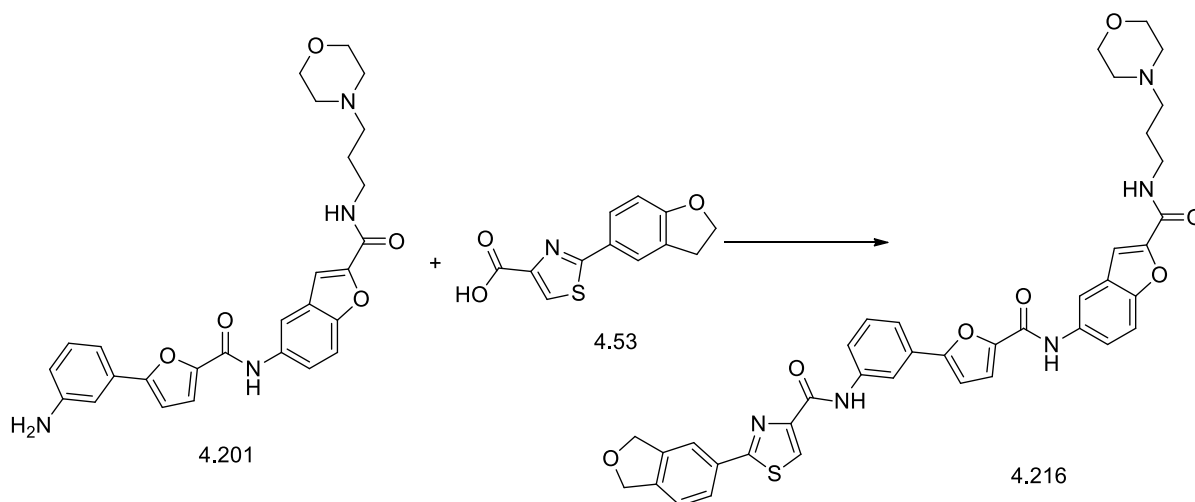
Light yellow oil. IR (FTIR, $\nu_{\text{max}}/\text{cm}^{-1}$) 660.03, 691.98, 740.58, 788.04, 862.95, 939.05, 979.60, 1027.26, 1111.93, 1170.96, 1300.58, 1344.03, 1384.84, 1465.10, 1539.46, 1585.38, 1653.79, 2335.36, 2359.56, 2817.07, 2853.65, 2929.41, 3282.17; ¹H NMR (500 MHz, CDCl₃, TMS); δ 2.55 (br. s., 4H), 2.64 (t, $J=5.99$ Hz, 2H), 3.33 (t, $J=8.67$ Hz, 2H), 3.58 - 3.63 (m, 2H), 3.75 - 3.80 (m, 4H), 4.70 (t, $J=8.67$ Hz, 2H), 6.87 - 6.89 (m, 1H), 7.14 (t, $J=5.20$ Hz, 1H), 7.37 (d, $J=3.78$ Hz, 1H), 7.47 (d, $J=0.95$ Hz, 1H), 7.47 - 7.49 (m, 1H), 7.52 - 7.57 (m, 2H), 7.66 - 7.71 (m, 2H), 7.80 (dd, $J=8.51, 1.89$ Hz, 1H), 7.88 (d, $J=1.26$ Hz, 1H), 8.03 (s, 1H), 8.13 (d, $J=2.21$ Hz, 1H), 8.15 (s, 1H), 8.30 (t, $J=1.73$ Hz, 1H), 8.31 (s, 1H), 9.41 (s, 1H); ¹³C NMR (100 MHz, CDCl₃); δ 29.29, 31.42, 35.56, 36.47, 53.37, 56.91, 67.01, 71.96, 107.59, 109.85, 110.41, 112.03, 114.22, 115.83, 117.62, 120.55, 122.96, 123.55,

125.49, 127.63, 128.09, 128.34, 129.66, 130.38, 133.34, 137.39, 146.85, 149.74, 150.10, 151.85, 153.56, 155.10, 155.52, 156.24, 158.69, 159.22, 162.65, 168.86; m/z (+EI) calc. For $C_{38}H_{33}N_5O_7S$ (M^+) 703.76, found 703.97 ($M+H$)⁺; Yield: 48%.

Procedure for the synthesis of 2-(2,3-dihydrobenzofuran-5-yl)-N-(3-(5-((2-((3-morpholinopropyl)carbamoyl)benzofuran-5-yl)carbamoyl)furan-2-yl)phenyl)thiazole-4-carboxamide (4.216) from 4.201 and 4.53

181 mg (1.0 eq.) of **4.201** and 183 mg (2.0 eq.) of **4.53** were added to a reaction vessel. Along with these, 2.0 eq. of HOBT and 1.75 eq. of DIC were added and a clear solution was made by dissolving these reactants in a minimum amount of DMF. The reaction mixture was stirred for 3 hours with occasional monitoring of the progress of the reaction by LCMS. The crude product was purified by using a SCX cartridge (2 gm) by the catch and release method, as described earlier in the chapter. Ten ml 2M NH_3 was used to release the product from the cartridge. Purification of the product **4.216** (200 mg) was finally achieved using flash chromatography with DCM:MeOH:2M NH_3 (18:1:1) as solvent system.

2-(2,3-Dihydrobenzofuran-5-yl)-N-(3-(5-((2-((3-morpholinopropyl)carbamoyl)benzofuran-5-yl)carbamoyl)furan-2-yl)phenyl)thiazole-4-carboxamide (4.216):



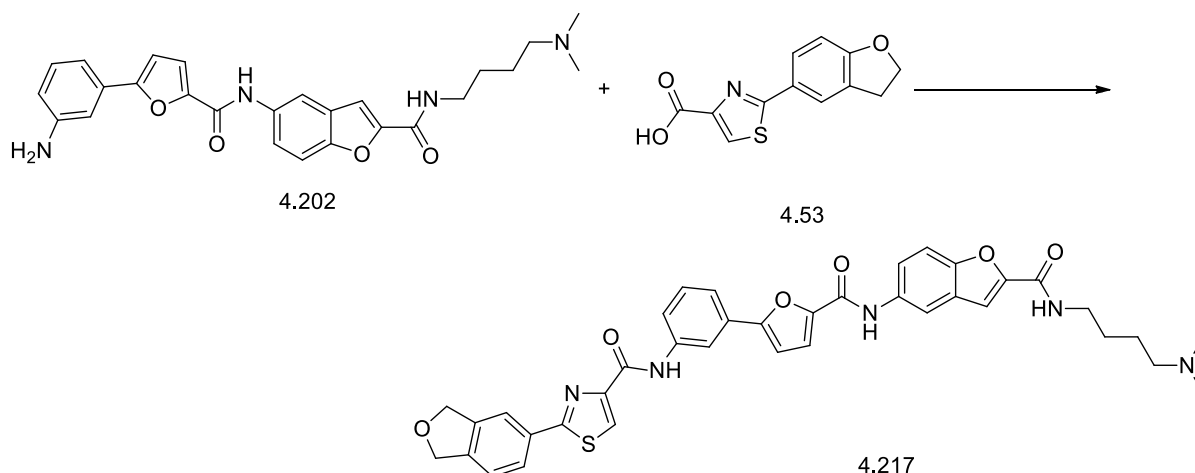
Light brown oil. IR (FTIR, ν_{max}/cm^{-1}) 630.70, 777.26, 862.45, 930.18, 985.92, 1029.19, 1109.90, 1173.90, 1230.17, 1299.11, 1343.38, 1435.03, 1469.44, 1503.94, 1519.59, 1557.48, 1585.11, 1634.61, 2006.35, 2331.65, 2823.88, 3329.29; 1H NMR (400 MHz, $CDCl_3$, TMS); δ 1.78 - 1.84 (m, 2H), 2.57 (br. s., 4H), 2.59 - 2.63 (m, 2H), 3.31 (t, $J=8.69$ Hz, 2H), 3.58 - 3.65 (m, 2H), 3.91 (t, $J=4.66$ Hz, 4H), 4.69 (t, $J=8.69$ Hz, 2H), 6.86 (d, $J=3.53$ Hz, 1H), 6.88 (d, $J=8.31$ Hz, 1H), 7.35 (d, $J=3.78$ Hz, 1H), 7.43 - 7.45 (m, 1H), 7.46 (d, $J=4.53$ Hz, 1H), 7.48

(d, $J=5.29$ Hz, 1H), 7.52 - 7.56 (m, 1H), 7.62 - 7.66 (m, 1H), 7.68 (dd, $J=8.81$, 2.27 Hz, 1H), 7.78 (dd, $J=8.31$, 2.01 Hz, 1H), 7.85 - 7.87 (m, 1H), 8.13 (d, $J=2.01$ Hz, 1H), 8.14 (s, 1H), 8.31 (t, $J=1.76$ Hz, 1H), 8.43 (s, 1H), 8.78 (t, $J=5.04$ Hz, 1H), 9.39 (s, 1H); ^{13}C NMR (100 MHz, CDCl_3); δ 14.32, 24.31, 29.61, 54.16, 59.09, 66.06, 67.20, 72.27, 73.94, 110.15, 111.94, 114.70, 116.17, 117.87, 120.86, 123.29, 123.57, 123.85, 125.82, 127.93, 128.49, 128.65, 129.93, 130.71, 133.72, 135.05, 139.97, 142.53, 147.21, 150.40, 150.56, 155.80, 156.42, 156.62, 158.90, 159.54, 163.84, 169.15, 185.36; m/z (+EI) calc. For $\text{C}_{39}\text{H}_{35}\text{N}_5\text{O}_7\text{S}$ (M^+) 717.79, found 718.25 ($\text{M}+\text{H}$) $^+$; Yield: 75%.

Procedure for the synthesis of 2-(2,3-dihydrobenzofuran-5-yl)-*N*-(3-(5-((2-((4-(dimethylamino)butyl)carbamoyl)benzofuran-5-yl)carbamoyl)furan-2-yl)phenyl)thiazole-4-carboxamide (4.217) from 4.202 and 4.53

73 mg (1.0 eq.) of **4.202** and 96 mg (2.5 eq.) of **4.53** were added to a reaction vessel. Along with these, 2.0 eq. of HOBt and 1.75 eq. of DIC were added and a clear solution was made by dissolving these reactants in a minimum amount of DMF. The reaction mixture was stirred for 3 hours with occasional monitoring of the progress of the reaction by LCMS. The crude product was purified by using a SCX cartridge (2 gm) by the catch and release method, as described earlier in the chapter. Ten ml 2M NH_3 was used to release the product from the cartridge. Purification of the product **4.217** (82 mg) was finally achieved using flash chromatography with DCM:MeOH:2M NH_3 (18:1:1) as solvent system.

2-(2,3-Dihydrobenzofuran-5-yl)-*N*-(3-(5-((2-((4-(dimethylamino)butyl)carbamoyl)benzofuran-5-yl)carbamoyl)furan-2-yl)phenyl)thiazole-4-carboxamide (4.217):

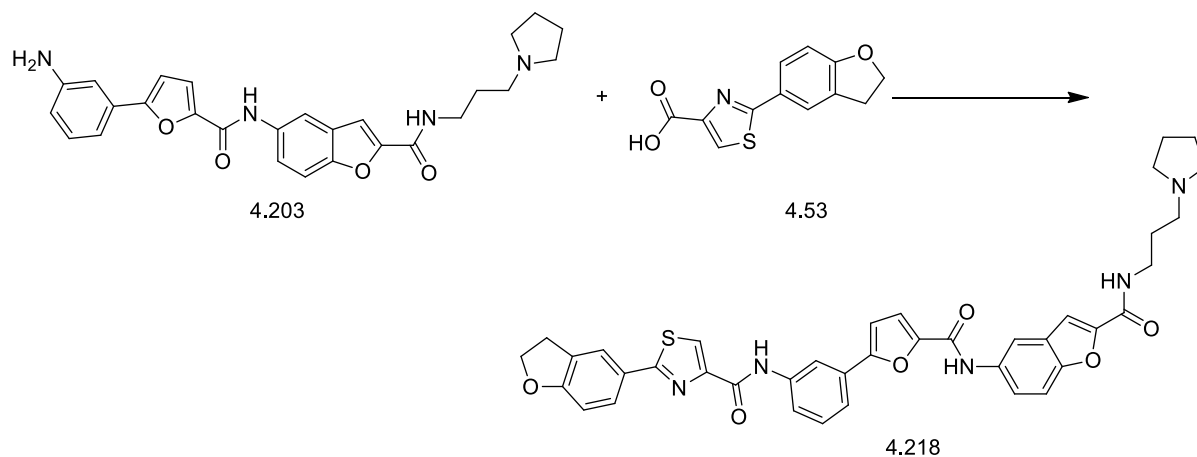


Brown oil. IR (FTIR, $\nu_{\text{max}}/\text{cm}^{-1}$) 420.75, 562.35, 593.45, 635.77, 690.07, 736.98, 786.44, 863.70, 938.04, 1016.60, 1109.32, 1201.00, 1231.27, 1297.86, 1466.34, 1534.91, 1584.89, 1654.59, 2781.90, 2821.20, 2857.4, 2930.00, 3120.40, 3286.60; ^1H NMR (400 MHz, CDCl_3) δ 1.62 - 1.68 (m, 2H), 1.69 - 1.76 (m, 2H), 2.20 - 2.22 (m, 2H), 2.28 - 2.32 (m, 6H), 2.37 (t, $J=6.55$ Hz, 2H), 3.31 (t, $J=8.69$ Hz, 2H), 3.46 - 3.52 (m, 2H), 4.65 - 4.71 (m, 2H), 6.86 (d, $J=3.53$ Hz, 1H), 6.88 (d, $J=8.31$ Hz, 1H), 7.34 (d, $J=3.78$ Hz, 1H), 7.42 (d, $J=1.01$ Hz, 1H), 7.44 - 7.45 (m, 1H), 7.46 - 7.47 (m, 1H), 7.52 - 7.55 (m, 1H), 7.65 (ddd, $J=7.99, 2.08, 1.01$ Hz, 1H), 7.69 (dd, $J=9.06, 2.27$ Hz, 1H), 7.78 (dd, $J=8.31, 1.76$ Hz, 1H), 7.85 - 7.87 (m, 1H), 8.08 (d, $J=2.27$ Hz, 1H), 8.12 - 8.13 (m, 1H), 8.28 (t, $J=1.76$ Hz, 1H), 9.39 (s, 1H); ^{13}C NMR (100 MHz, CDCl_3) δ 23.56, 26.41, 40.17, 47.13, 54.07, 55.69, 60.82, 65.98, 103.11, 105.77, 107.75, 109.70, 110.77, 111.71, 112.33, 113.87, 114.05, 114.58, 115.08, 115.72, 117.51, 117.63, 120.11, 127.45, 128.25, 129.51, 129.91, 133.24, 137.75, 142.59, 146.46, 146.57, 148.65, 150.55, 151.81, 152.52, 155.97, 156.11; m/z (+EI) calc. For $\text{C}_{38}\text{H}_{35}\text{N}_5\text{O}_6\text{S}$ (M^+) 689.78, found ($\text{M}+\text{H}$) $^+$ 690.30; Yield: 77%.

Procedure for the synthesis of 2-(2,3-dihydrobenzofuran-5-yl)-N-(3-(5-(((3-(pyrrolidin-1-yl)propyl)carbamoyl)benzofuran-5-yl)carbamoyl)furan-2-yl)phenyl)thiazole-4-carboxamide (4.218) from 4.203 and 4.53

60 mg (1.0 eq.) of **4.203** and 78 mg (2.5 eq.) of **4.53** were added to a reaction vessel. Along with these, 2.0 eq. of HOBt and 1.75 eq. of DIC were added and a clear solution was made by dissolving these reactants in a minimum amount of DMF. The reaction mixture was stirred for 3 hours with occasional monitoring of the progress of the reaction by LCMS. The crude product was purified by using a SCX cartridge (2 gm) by the catch and release method, as described earlier in the chapter. Ten ml 2M NH_3 was used to release the product from the cartridge. Purification of the product **4.218** (71 mg) was finally made using flash chromatography with DCM:MeOH:2M NH_3 (18:1:1) as the solvent system.

2-(2,3-Dihydrobenzofuran-5-yl)-N-(3-(5-((2-((3-(pyrrolidin-1-yl)propyl)carbamoyl)benzofuran-5-yl)carbamoyl)furan-2-yl)phenyl)thiazole-4-carboxamide (4.218):



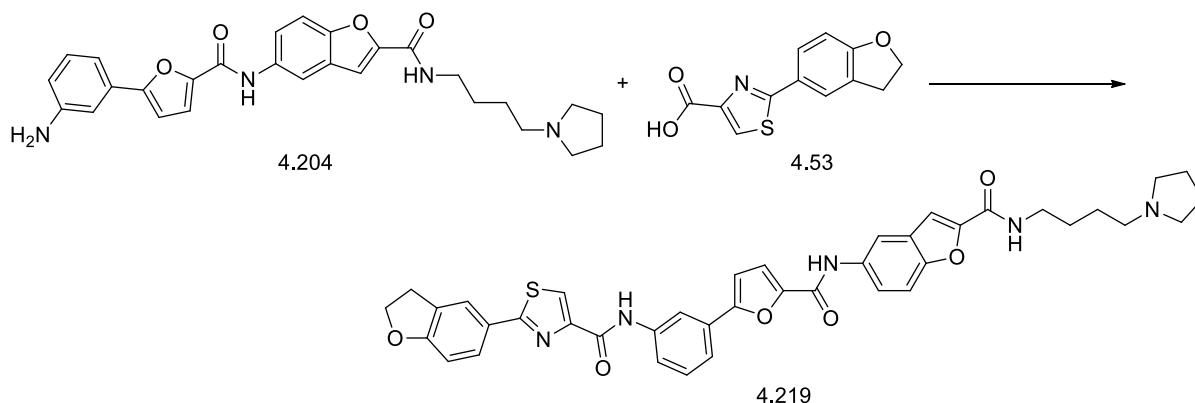
Light yellow oil. IR (FTIR, $\nu_{\text{max}}/\text{cm}^{-1}$) 417.98, 427.08, 563.79, 562.30, 642.39, 691.16, 725.18, 786.88, 865.50, 907.80, 983.38, 1016.60, 1107.30, 1140.60, 1204.00, 1231.64, 1291.70, 1465.31, 1538.74, 1584.76, 1648.80, 2800.00, 2927.00, 2963.20, 3277.60; ^1H NMR (400 MHz, CDCl_3) δ 1.78 - 1.84 (m, 2H), 1.88 - 1.96 (m, 4H), 2.62 (br. s., 4H), 2.73 (t, $J=5.92$ Hz, 2H), 3.21 - 3.37 (m, 2H), 3.57 - 3.64 (m, 2H), 4.60 - 4.76 (m, 2H), 6.84 - 6.87 (m, 1H), 7.34 (d, $J=3.53$ Hz, 1H), 7.40 (s, 1H), 7.41 (d, $J=8.31$ Hz, 1H), 7.45 (d, $J=8.06$ Hz, 1H), 7.51 - 7.54 (m, 1H), 7.64 (ddd, $J=7.93, 2.14, 1.01$ Hz, 1H), 7.69 (dd, $J=8.81, 2.01$ Hz, 1H), 7.78 (dd, $J=8.31, 1.76$ Hz, 1H), 7.86 (d, $J=1.51$ Hz, 1H), 8.07 (d, $J=2.01$ Hz, 1H), 8.13 (s, 1H), 8.29 (t, $J=1.89$ Hz, 1H), 8.45 (s, 1H), 9.02 (t, $J=4.66$ Hz, 1H), 9.39 (s, 1H); ^{13}C NMR (100 MHz, CDCl_3) δ 23.48, 23.56, 40.17, 54.07, 55.54, 55.69, 60.82, 103.11, 105.77, 106.78, 107.75, 109.55, 109.70, 110.77, 111.71, 112.33, 113.87, 114.06, 114.58, 115.08, 115.72, 117.51, 117.63, 118.53, 120.11, 127.45, 128.07, 128.25, 129.51, 129.91, 133.24, 137.75, 142.59, 146.46, 146.57, 150.55, 155.97, 156.11, 160.42; m/z (+EI) calc. For $\text{C}_{39}\text{H}_{35}\text{N}_5\text{O}_6\text{S}$ (M^+) 701.79, found ($\text{M}+\text{H}$) $^+$ 702.40; Yield: 80%.

Procedure for the synthesis of 2-(2,3-dihydrobenzofuran-5-yl)-N-(3-(5-((2-((4-(pyrrolidin-1-yl)butyl)carbamoyl)benzofuran-5-yl)carbamoyl)furan-2-yl)phenyl)thiazole-4-carboxamide (4.219) from 4.204 and 4.53

79 mg (1.0 eq.) of **4.204** and 100 mg (2.5 eq.) of **4.53** were added to a reaction vessel. Along with these, 2.0 eq. of HOBt and 1.75 eq. of DIC were added and a clear solution was made by dissolving these reactants in a minimum amount of DMF. The reaction mixture was stirred

for 3 hours with occasional monitoring of the progress of the reaction by LCMS. The crude product was purified by using a SCX cartridge (2 gm) by the catch and release method, as described earlier in the chapter. Ten ml 2M NH₃ was used to release the product from the cartridge. Purification of the product **4.219** (105 mg) was finally achieved using flash chromatography with DCM:MeOH:2MNH₃ (18:1:1) as the solvent system.

2-(2,3-Dihydrobenzofuran-5-yl)-N-(3-(5-((2-((4-(pyrrolidin-1-yl)butyl)carbamoyl)benzofuran-5-yl)carbamoyl)furan-2-yl)phenyl)thiazole-4-carboxamide (4.219):

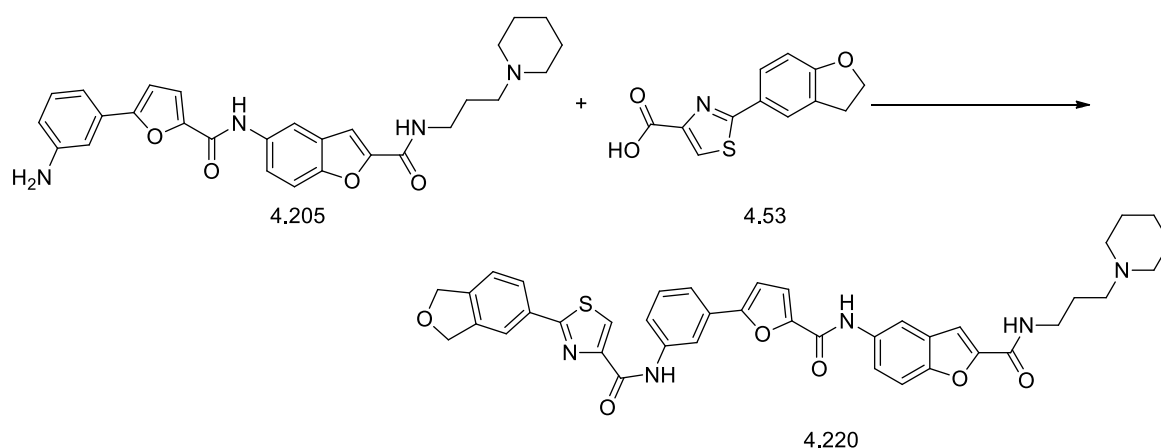


Light yellow oil. IR (FTIR, $\nu_{\text{max}}/\text{cm}^{-1}$) 430.10, 563.16, 631.16, 690.60, 737.16, 786.28, 863.93, 981.42, 1110.54, 1231.51, 1295.24, 1465.97, 1541.08, 1584.71, 1648.11, 2924.5; ¹H NMR (400 MHz, CDCl₃) δ 1.58 (br. s., 2H), 1.74 - 1.80 (m, 6H), 2.48 (br. s., 2H), 2.53 - 2.57 (m, 2H), 3.30 (t, $J=8.81$ Hz, 2 H), 3.55 - 3.62 (m, 2H), 4.65 - 4.71 (m, 2H), 6.84 - 6.87 (m, 1H), 6.88 (s, 1H), 7.34 (d, $J=3.53$ Hz, 1H), 7.39 (d, $J=9.06$ Hz, 1H), 7.41 - 7.43 (m, 1H), 7.44 - 7.47 (m, 1H), 7.51 - 7.55 (m, 1H), 7.66 (d, $J=7.81$ Hz, 1H), 7.70 (dd, $J=8.94$, 2.14 Hz, 1H), 7.77 (dd, $J=8.31$, 1.76 Hz, 1H), 7.84 - 7.86 (m, 1H), 8.06 (d, $J=2.01$ Hz, 1H), 8.12 (s, 1H), 8.27 (s, 1H), 8.41 (s, 1H), 9.28 (br. s., 1H), 9.38 (s, 1H); ¹³C NMR (100 MHz, CDCl₃) δ 22.21, 24.04, 24.47, 25.84, 29.27, 54.81, 55.40, 59.30, 68.83, 71.93, 109.69, 109.80, 111.50, 114.27, 115.83, 117.47, 119.33, 120.18, 120.37, 120.60, 122.91, 123.51, 125.47, 127.59, 128.21, 128.32, 129.60, 130.37, 133.24, 138.36, 146.91, 150.09, 150.56, 151.79, 155.45, 156.28, 158.58, 159.20, 162.63, 168.80; m/z (+EI) calc. For C₄₀H₃₇N₅O₆S (M⁺) 715.82, found (M+H)⁺ 716.40; Yield: 91%.

Procedure for the synthesis of 2-(2,3-dihydrobenzofuran-5-yl)-N-(3-(5-((2-((3-(piperidin-1-yl)propyl)carbamoyl)benzofuran-5-yl)carbamoyl)furan-2-yl)phenyl)thiazole-4-carboxamide (4.220) from 4.205 and 4.53

36 mg (1.0 eq.) of **4.205** and 46 mg (2.5 eq.) of **4.53** were added to a reaction vessel. Along with these, 2.0 eq. of HOBT and 1.75 eq. of DIC were added and a clear solution was made by dissolving these reactants in a minimum amount of DMF. The reaction mixture was stirred for 3 hours with occasional monitoring of the progress of the reaction by LCMS. The crude product was purified by using a SCX cartridge (2 gm) by the catch and release method, as described earlier in the chapter. Ten ml 2M NH₃ was used to release the product from the cartridge. Purification of the product **4.220** (50 mg) was finally achieved using flash chromatography with DCM:MeOH:2MNH₃ (18:1:1) as the solvent system.

2-(2,3-Dihydrobenzofuran-5-yl)-N-(3-(5-((2-((3-(piperidin-1-yl)propyl)carbamoyl)benzofuran-5-yl)carbamoyl)furan-2-yl)phenyl)thiazole-4-carboxamide (4.220);



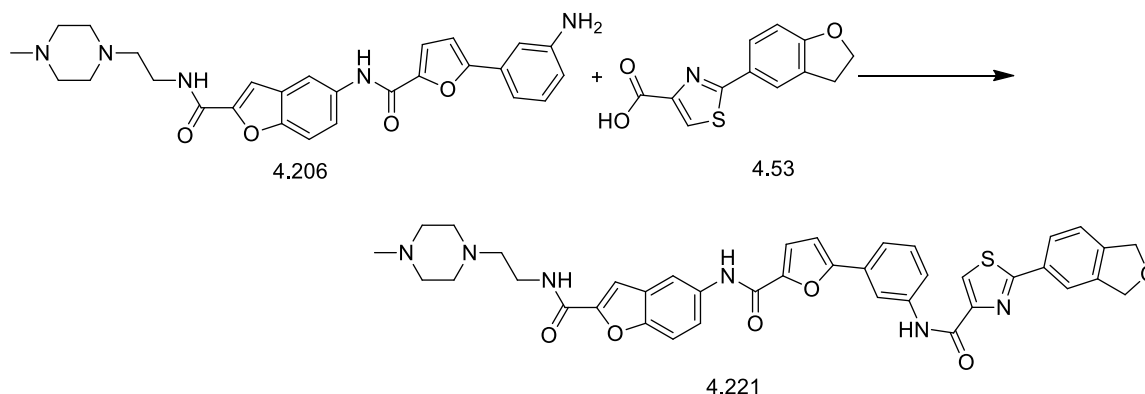
Light yellow oil. IR (FTIR, $\nu_{\text{max}}/\text{cm}^{-1}$) 414.05, 430.07, 593.93, 641.84, 690.99, 725.88, 788.11, 859.45, 907.80, 1016.60, 1110.68, 1198.00, 1237.58, 1297.70, 1343.00, 1466.02, 1535.68, 1584.66, 1653.61, 2854.40, 2927.00, 3295.7; ¹H NMR (400 MHz, CDCl₃) δ 1.60 (br. s., 2H), 1.75 - 1.83 (m, 6H), 2.54 (br. s., 2H), 2.57 - 2.61 (m, 2H), 3.32 (t, $J=8.69$ Hz, 2H), 3.57 - 3.63 (m, 2H), 3.72 (s, 2H), 4.69 (t, $J=8.81$ Hz, 2H), 6.86 - 6.90 (m, 2H), 7.35 (d, $J=3.53$ Hz, 1H), 7.41 (d, $J=9.06$ Hz, 1H), 7.43 (s, 1H), 7.47 (d, $J=7.81$ Hz, 1H), 7.53 - 7.57 (m, 1H), 7.65 (dd, $J=2.01, 1.01$ Hz, 1H), 7.67 - 7.70 (m, 1H), 7.79 (dd, $J=8.31, 2.01$ Hz, 1H), 7.86 - 7.88 (m, 1H), 8.06 - 8.09 (m, 1H), 8.14 (s, 1H), 8.29 - 8.31 (m, 1H), 8.35 (s, 1H), 9.40 (s, 1H); ¹³C NMR (100 MHz, CDCl₃) δ 22.83, 24.12, 24.85, 27.22, 34.49, 50.49, 53.03, 55.99, 60.59, 64.87, 102.22, 104.51, 106.75, 108.00, 108.12, 109.82, 110.07, 110.41, 114.28,

115.69, 119.45, 120.62, 121.72, 122.93, 124.77, 125.31, 126.50, 131.43, 132.24, 135.26, 143.26, 143.93, 146.89, 147.71, 150.14, 150.93, 151.19, 152.84, 154.97, 161.00; m/z (+EI) calc. For $C_{40}H_{37}N_5O_6S$ (M^+) 715.82, found $(M+H)^+$ 716.40; Yield: 94%.

Procedure for the synthesis of 2-(2,3-dihydrobenzofuran-5-yl)-N-(3-(5-((2-(4-methylpiperazin-1-yl)ethyl)carbamoyl)benzofuran-5-yl)carbamoyl)furan-2-yl)phenyl)thiazole-4-carboxamide (4.221) from 4.206 and 4.53

151 mg (1.0 eq.) of **4.206** and 192 mg (2.5 eq.) of **4.53** were added to a reaction vessel. Along with these, 2.0 eq. of HOBt and 1.75 eq. of DIC were added and a clear solution was made by dissolving these reactants in a minimum amount of DMF. The reaction mixture was stirred for 3 hours with occasional monitoring of the progress of the reaction by LCMS. The crude product was purified by using a SCX cartridge (2 gm) by the catch and release method, as described earlier in the chapter. Ten ml 2M NH_3 was used to release the product from the cartridge. Purification of the product **4.221** (120 mg) was finally achieved using flash chromatography with DCM:MeOH:2M NH_3 (18:1:1) as the solvent system.

2-(2,3-Dihydrobenzofuran-5-yl)-N-(3-(5-((2-(4-methylpiperazin-1-yl)ethyl)carbamoyl)benzofuran-5-yl)carbamoyl)furan-2-yl)phenyl)thiazole-4-carboxamide (4.221):



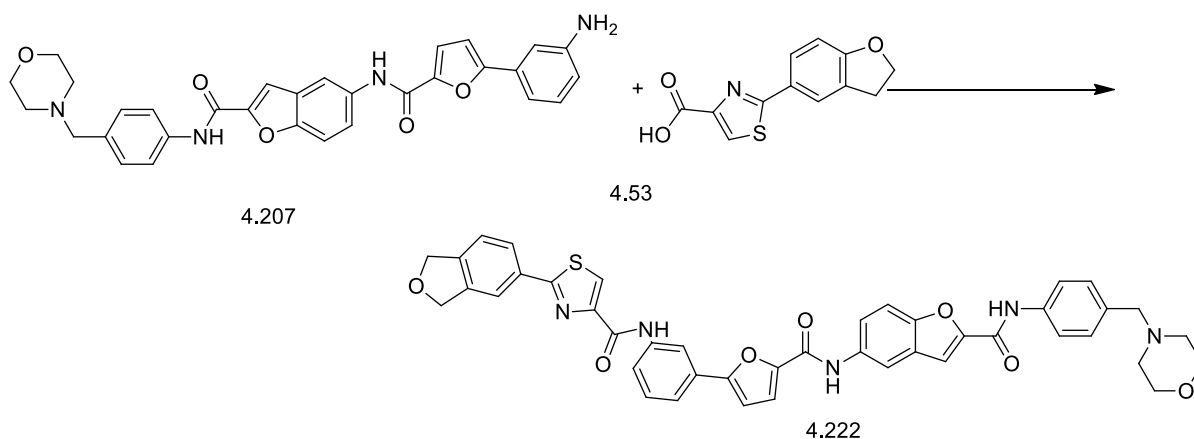
Light yellow oil. IR (FTIR, ν_{max}/cm^{-1}) 418.35, 563.04, 593.92, 630.45, 691.07, 738.46, 786.93, 862.47, 941.06, 980.35, 1010.60, 1107.30, 1146.60, 1164.70, 1207.00, 1234.17, 1283.68, 1346.00, 1462.59, 1538.96, 1584.71, 1648.96, 2806.00, 2851.40, 2924.00, 3120.40, 3283.60; 1H NMR (400 MHz, $CDCl_3$) δ 2.26 - 2.30 (m, 2H), 2.31 (s, 3H), 2.47 - 2.53 (m, 2H), 2.53 - 2.63 (m, 6H), 3.28 (t, $J=8.81$ Hz, 2H), 3.56 (q, $J=5.79$ Hz, 2H), 4.65 (t, $J=8.81$ Hz, 2H), 6.80 (d, $J=3.53$ Hz, 1H), 6.85 (d, $J=8.31$ Hz, 1H), 7.21 (t, $J=4.78$ Hz, 1H), 7.30 (d, $J=3.78$ Hz, 1H), 7.37 - 7.42 (m, 2H), 7.44 - 7.50 (m, 2H), 7.55 (dt, $J=8.31, 1.38$ Hz, 1H), 7.74

(dd, $J=8.31$, 2.01 Hz, 1H), 7.71 (dd, $J=8.94$, 2.14 Hz, 1H), 7.81 (s, 1H), 8.00 (s, 1H), 8.09 (s, 1H), 8.31 (t, $J=1.76$ Hz, 1H), 8.74 (s, 1H), 9.38 (s, 1H); ^{13}C NMR (100 MHz, CDCl_3) δ 29.0, 46.57, 53.00, 55.61, 56.40, 56.47, 56.87, 56.91, 78.13, 106.32, 108.11, 108.61, 110.94, 113.27, 114.02, 117.35, 118.94, 119.37, 120.31, 121.13, 125.01, 127.09, 127.42, 128.37, 129.58, 130.10, 130.25, 130.50, 132.47, 135.29, 146.08, 150.07, 150.36, 152.37, 155.94, 162.07, 162.64, 169.87, 183.91; m/z (+EI) calc. For $\text{C}_{39}\text{H}_{36}\text{N}_6\text{O}_6\text{S}$ (M^+) 716.80, found ($\text{M}+\text{H}$) $^+$ 717.30; Yield: 54%.

Procedure for the synthesis of 2-(2,3-dihydrobenzofuran-5-yl)-*N*-(3-(5-((2-((4-(morpholinomethyl)phenyl)carbamoyl)benzofuran-5-yl)carbamoyl)furan-2-yl)phenyl)thiazole-4-carboxamide (4.222) from 4.207 and 4.53

32 mg (1.0 eq.) of **4.207** and 38 mg (2.5 eq.) of **4.53** were added to a reaction vessel. Along with these, 2.0 eq. of HOBt and 1.75 eq. of DIC were added and a clear solution was made by dissolving these reactants in a minimum amount of DMF. The reaction mixture was stirred for 3 hours with occasional monitoring of the progress of the reaction by LCMS. The crude product was purified by using a SCX cartridge (2 gm) by the catch and release method, as described earlier in the chapter. Ten ml 2M NH_3 was used to release the product from the cartridge. Purification of the product **4.222** (36 mg) was finally achieved using flash chromatography with DCM:MeOH:2M NH_3 (18:1:1) as the solvent system.

2-(2,3-Dihydrobenzofuran-5-yl)-*N*-(3-(5-((2-((4-(morpholinomethyl)phenyl)carbamoyl)benzofuran-5-yl)carbamoyl)furan-2-yl)phenyl)thiazole-4-carboxamide (4.222):



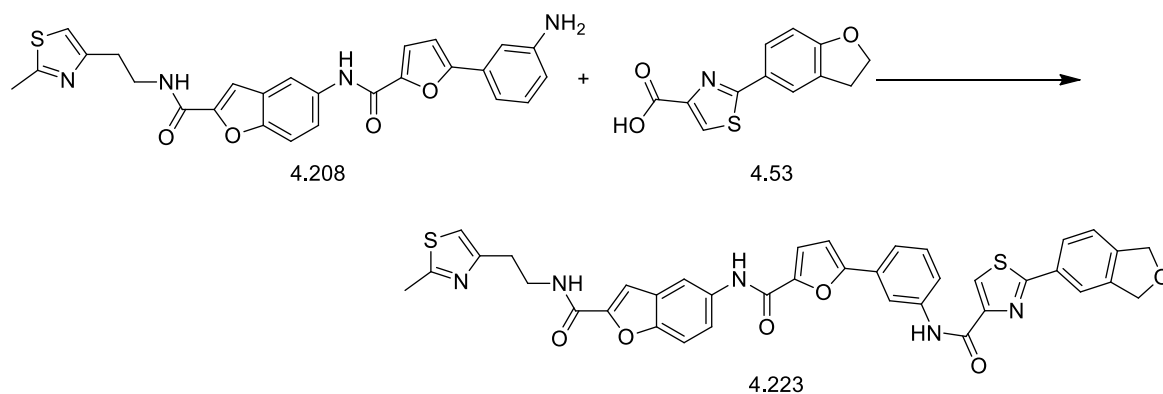
Colourless oil. IR (FTIR, $\nu_{\text{max}}/\text{cm}^{-1}$) 420.21, 456.34, 658.24, 697.01, 824.12, 976.24, 1112.65, 1112.87, 113.01, 1343.00, 1458.17, 1492.08, 1550.21, 1567.37, 1634.13, 27.14, 2824.38,

2954.37, 3335.25; ^1H NMR (400 MHz, $\text{DMSO}-d_6$) δ 2.30 - 2.39 (m, 4H), 3.44 (s, 2H), 3.52 - 3.64 (m, 4H), 4.65 (t, $J=8.69$ Hz, 2H), 6.94 (d, $J=8.56$ Hz, 1H), 7.17 (d, $J=3.53$ Hz, 1H), 7.30 (d, $J=8.56$ Hz, 2H), 7.49 (d, $J=3.78$ Hz, 1H), 7.53 (t, $J=8.06$ Hz, 1H), 7.59 (s, 1H), 7.73 - 7.76 (m, 1H), 7.77 (d, $J=8.56$ Hz, 2H), 7.79 (s, 1H), 7.80 - 7.81 (m, 1H), 7.92 - 7.97 (m, 2H), 8.08 - 8.10 (m, 1H), 8.25 (d, $J=2.01$ Hz, 1H), 8.33 (t, $J=1.76$ Hz, 1H), 8.40 (s, 1H), 10.36 (s, 1H), 10.53 (s, 1H); ^{13}C NMR (100 MHz, $\text{DMSO}-d_6$) δ 29.01, 56.50, 57.02, 64.00, 65.23, 66.19, 80.10, 108.20, 108.64, 109.11, 111.84, 113.14, 114.50, 119.14, 119.26, 120.08, 121.03, 121.34, 121.56, 121.98, 124.90, 127.54, 128.34, 129.26, 129.65, 129.81, 129.97, 130.03, 130.13, 132.32, 134.19, 136.35, 136.52, 146.25, 150.12, 150.32, 152.69, 156.37, 160.25, 162.23, 162.38, 168.91, 184.00; m/z (+EI) calc. For $\text{C}_{43}\text{H}_{35}\text{N}_5\text{O}_7\text{S}$ (M^+) 765.83, found ($\text{M}+\text{H}$) $^+$ 766.40; Yield: 76%.

Procedure for the synthesis of 2-(2,3-dihydrobenzofuran-5-yl)-N-(3-(5-((2-((2-(2-methylthiazol-4-yl)ethyl)carbamoyl)benzofuran-5-yl)carbamoyl)furan-2-yl)phenyl)thiazole-4-carboxamide (4.223) from 4.208 and 4.53

256 mg (1.0 eq.) of **4.208** and 326 mg (2.5 eq.) of **4.53** were added to a reaction vessel. Along with these, 2.0 eq. of HOBt and 1.75 eq. of DIC were added and a clear solution was made by dissolving these reactants in a minimum amount of DMF. The reaction mixture was stirred for 3 hours with occasional monitoring of the progress of the reaction by LCMS. The crude product was purified by using a SCX cartridge (5 gm) by the catch and release method, as described earlier in the chapter. Ten ml 2M NH_3 was used to release the product from the cartridge. Purification of the product **4.223** (300 mg) was finally achieved using flash chromatography with $\text{DCM}:\text{MeOH}:\text{2MNH}_3$ (18:1:1) as the solvent system.

2-(2,3-Dihydrobenzofuran-5-yl)-N-(3-(5-((2-((2-(2-methylthiazol-4-yl)ethyl)carbamoyl)benzofuran-5-yl)carbamoyl)furan-2-yl)phenyl)thiazole-4-carboxamide (4.223):



Colourless oil. IR (FTIR, $\nu_{\text{max}}/\text{cm}^{-1}$) 428.54, 473.28, 498.28, 561.90, 629.13, 684.51, 743.99, 780.18, 935.01, 980.35, 1013.60, 1104.30, 1185.90, 1239.05, 1300.80, 1393.90, 1427.26, 1471.73, 1524.40, 1584.90, 1641.70, 1666.50, 2851.4, 2924.00, 2957.2, 3120.40, 3323.00; ^1H NMR (400 MHz, CDCl_3) δ 2.70 (s, 3H), 3.05 (t, $J=7.18$ Hz, 2H), 3.73 (t, $J=7.05$ Hz, 2H), 4.10 (q, $J=7.05$ Hz, 2H), 4.64 (t, $J=8.69$ Hz, 2H), 6.84 (d, $J=8.31$ Hz, 1H), 7.03 (d, $J=3.53$ Hz, 1H), 7.10 (s, 1H), 7.37 (d, $J=3.53$ Hz, 1H), 7.45 (d, $J=1.01$ Hz, 1H), 7.46 (d, $J=1.01$ Hz, 1H), 7.48 - 7.49 (m, 1H), 7.52 (dd, $J=8.81, 1.51$ Hz, 1H), 7.58 (d, $J=9.06$ Hz, 1H), 7.72 (dt, $J=2.01, 1.26$ Hz, 1H), 7.74 (d, $J=2.27$ Hz, 1H), 7.75 - 7.78 (m, 1H), 7.80 (dd, $J=8.06, 1.26$ Hz, 1H), 7.86 (d, $J=8.31$ Hz, 1H), 8.00 (d, $J=1.51$ Hz, 1H), 8.13 (d, $J=2.01$ Hz, 1H), 8.24 (s, 1H), 8.34 (t, $J=1.76$ Hz, 1H); ^{13}C NMR (100 MHz, CDCl_3) δ 19.43, 28.80, 29.24, 40.19, 79.25, 106.35, 108.24, 108.54, 110.58, 113.24, 114.78, 115.27, 117.45, 119.63, 120.08, 121.31, 121.84, 125.40, 127.36, 127.60, 129.03, 129.50, 130.21, 130.32, 132.01, 136.38, 146.28, 150.07, 150.30, 152.34, 152.36, 156.28, 158.54, 162.03, 162.35, 163.28, 169.84, 184.50; m/z (+EI) calc. For $\text{C}_{38}\text{H}_{29}\text{N}_5\text{O}_6\text{S}_2$ (M^+) 715.80, found ($\text{M}+\text{H}$) $^+$ 716.20; Yield: 79%.

Procedure for the synthesis of 2-(2,3-dihydrobenzofuran-5-yl)-N-(3-(5-((2-(dimethylamino)ethyl)carbamoyl)benzofuran-5-yl)carbamoyl)furan-2-yl)phenyl)thiazole-4-carboxamide (4.224) from 4.209 and 4.53

59 mg (1.0 eq.) of **4.209** and 84 mg (2.5 eq.) of **4.53** were added to a reaction vessel. Along with these, 2.0 eq. of HOBt and 1.75 eq. of DIC were added and a clear solution was made by dissolving these reactants in a minimum amount of DMF. The reaction mixture was stirred for 3 hours with occasional monitoring of the progress of the reaction by LCMS. The crude product was purified by using a SCX cartridge (2 gm) by the catch and release method, as described earlier in the chapter. Ten ml 2M NH_3 was used to release the product from the cartridge. Purification of the product **4.224** (60 mg) was finally achieved using flash chromatography with DCM:MeOH:2M NH_3 (18:1:1) as the solvent system.

The reaction scheme shows the synthesis of compound 4.224. On the left, compound 4.209 (N-(4-((4-aminophenyl)furan-2-yl)methyl)furan-2-carbonyl)-2-methylpropan-1-amine) reacts with compound 4.53 (4-(4-((4-((4-aminophenyl)furan-2-yl)methyl)furan-2-carbonyl)amino)phenyl)-2-methylpropan-1-amine). The reaction arrow points to the right, leading to the product 4.224, which is a dimeric structure where two units of the 4.209 moiety are linked via an amide bond at the 4-position of the central phenyl ring.

4.2 Experimental-Biophysical

Although a large number of techniques are used for the biophysical evaluation of the G-quadruplex ligands, this thesis focuses on high-throughput fluorescence-resonance-energy-transfer (FRET) melting experiments and a biophysical modified telomere-repeat-

amplification-protocol (TRAP) (discussed in chapter 2). Additionally, ultraviolet (UV), melting and circular dichroism (CD) experiments are discussed, as they remain the most experimentally feasible and informative techniques amongst isothermal/viscosimetry titration calorimetry, voltametric, DNA footprinting and surface plasmon resonance (SPR) techniques.

4.2.1.1 Fluorescence resonance energy transfer (FRET) assay

The principles and application of the FRET melting assay have been described previously in chapter 2.

4.2.1.1.1 Choice of FRET sequences

The aryl-polyamide series was screened by FRET against several oligonucleotides, as follows:

i) F21T; telomeric DNA – For quadruplex ligands to function as telomerase-inhibitors they must show significant quadruplex-stabilizing ability. This sequence is indicative of telomeric-DNA. Good-quadruplex ligands show greater than $\sim \Delta T_m 25^\circ \text{C}$ [$c=1 \mu\text{M}$].

ii) Hairpin duplex DNA – G-quadruplex ligands must demonstrate selectivity towards quadruplex DNA from duplex DNA. Favourable G-quadruplex ligands will, therefore, not bind duplex DNA and demonstrate high $\Delta T_{m[\text{Quadruplex}]}: \Delta T_{m[\text{Duplex}]}$ ratios.

iii) TERRA HTelo – When these non-coding telomeric repeat-containing RNA (TERRA) sequences are transcribed, they can regulate telomere maintenance, binding TRF1 and TRF2 and interfere with telomere elongation.

iv) cKit1 and cKit2 – PQS have been identified within the promoter region of the c-kit oncogene. cKit is a dominant oncogene in gastrointestinal-stromal (GIST) tumours and melanomas promoting cell survival, proliferation and differentiation.

v) Heat shock protein 90 (HSP90a) - PQS have been identified within the promoter region of HSP90. HSP90 is a molecular chaperone involved in the folding of proteins. Cancer-causing oncoproteins require HSP90 as a result of destabilizing mutant genetic aberrations. Tumour cells are, therefore, dependent on HSP90. 17AAG is a HSP90 inhibitor in the clinic highlighting proof-of-principle for HSP90 inhibition.

vi) **k-Ras (KR32)** - PQS have been identified within the promoter region of the c-kit oncogene. k-Ras is a dominant oncogene in pancreatic tumours, promoting cell growth.

4.2.1.1.2 Materials and methods

4.2.1.1.2.1 Compound preparation and long-term storage

All compounds were dissolved in 10 mM stock solutions in 100% dimethyl sulfoxide (DMSO) and stored at -20 °C. Compounds were then diluted in 1 mM dH₂O (10% DMSO) prior to use.

4.2.1.1.2.2 Oligonucleotide sequences used for the FRET assay

The following oligonucleotide sequences were purchased from Eurogentec, Southampton, UK.

i) **F21T (Human telomeric sequence):** 5'-FAM-GGG TTA GGG TTA GGG TTA GGG-TAMRA-3'

ii) **T-Loop (Duplex DNA):** 5'-FAM-TAT AGC TATA TTT TTT TATA GCT ATA-TAMRA-3'

iii) **k-Ras F32RT (KR32):** 5'-FAM- AGG GCG GTG TGG GAA GAG GGA AGA GGG GGA GG-TAMRA

iv) **k-Ras F33RT (KR33):** 5'-FAM-AGG GCG GTG TGG GAA GAG GGA AGA GGG GGA GGC-TAMRA

v) **HSP90a:** 5'-FAM- GGG CCA AAG GGA AGG GGT GGG-TAMRA

vi) **HSP90b:** 5'-FAM- GGG CGG GCC AAA GGG AAG GGG-TAMRA

vii) **HSP90c:** 5'-FAM-AGG GCG GGC CAA AGG GAA GGG GTG GGC-TAMRA

viii) **cKit-1:** 5'-FAM-AGA GGG AGG GCG CTG GGA GGA GGG GCT-TAMRA

ix) cKit-2: 5'-FAM-CCC GGG CGG GCG CGA GGG AGG GGA GG-TAMRA

x) DRH: TTA-GGG-TTAGGG-TTT-TTT-CCC-UAA-CCC-UAA

xi) CDRH: TTA-GGG-TTAGGG-TTT-TTT-CCC-TAA-CCC-TAA

xii) Cmyc: TGG-GGA-GGG-TGG-GGAGGG-TGG-GGA-AGG

x) RNA hTelo (TERRA): 5'-FAM-d(GGG[UUAGGG]3)-TAMRA

4.2.1.1.2.3 Preparation of FRET-buffer

TAMRA (6-carboxytetramethylrhodamine) is an acceptor fluorophore, whereas FAM (6-carboxyfluorescein) is a donor fluorophore. From 20 μM stock solutions, 400 nM solutions in FRET buffer (optimised as 50 mM potassium, 50 mM cacodylate, pH 7.4) were prepared prior to use. The buffer was stored in the freezer at -20 °C.

4.2.1.1.2.4 Annealing of DNA

The fluorescence tagged sequences were diluted in two steps with sterile water (DNA Grade, Fisher Scientific) to obtain first 100 μM , then 20 μM solutions. These solutions were then further diluted to 400 nM using FRET-buffer. The sequences were annealed by heating at 85 °C for 5 minutes, followed by cooling to room temperature over two hours (Grant Bio PCH-2 Dry Block Heating/Cooling System).

4.2.1.1.2.5 Preparation of ligand solutions

For all the synthesized biaryl polyamides, ligand stock solutions of 20 mM were made with dimethyl sulfoxide ($\geq 99.9\%$, A.C.S. spectrophotometric grade, Sigma-Aldrich). From these stock solutions, the following dilutions were prepared using FRET buffer: 100 μM , 50 μM , 25 μM , 15 μM , 10 μM , 5 μM and 2 μM , for some compounds, and also 1 μM . These concentrations represent double the concentration needed for the final assay.

4.2.1.1.2.6 Fluorescent Resonance Energy Transfer (FRET)-Based DNA Melting Assay

For the FRET-based DNA melting assay, 50 μ l of annealed DNA was placed in each well of a 96-well plate (Bio-Rad Laboratories), and then 50 μ l of ligand solution was added to each well. Different concentrations of each compound were tested, each concentration being tested in triplicate. Pure FRET buffer instead of ligand solution was added to all wells of the first line (A) of the plate to serve as blank. After 15 minutes of incubation at room-temperature, the well plate was processed in the DNA Engine Opticon (Continuous Fluorescence Detector, MJ Research) and fluorescence measurements were taken over a temperature range from 30 °C to 100 °C at intervals of 0.5 °C. Prior to each measurement, the temperature was kept constant for 30 seconds. The incident radiation was emitted at 450-495 nm and detection measured at 515-545 nm.

4.2.1.1.2.7 Data processing

The data were analysed using the program Origin – Scientific Graphing and Analysis Software (Version 7.0, OriginLab Corp.). The increases in the melting temperatures (ΔT_m) were obtained by subtracting the value of the blank from the measured values of each sample. For each concentration of every compound the average of ΔT_m was calculated from the three corresponding values.

4.2.1.2 F21T Competition assay with calf thymus-DNA

For compound KN-88 an additional competition assay was performed with F21T and duplex DNA of calf thymus. The aim of this experiment was to clarify whether the affinity between the ligand KN-88 and the DNA sequence F21T is affected by the simultaneous presence of duplex DNA.

A 800 nM solution of F21T in FRET-buffer was annealed and a ligand solution of 2 μ M from KN-88 was made. A solution of calf thymus-DNA (CT-DNA) was prepared by dissolving a small amount with unknown mass of calf thymus-DNA sodium salt (Type I, Highly Polymerized, fibrous preparation) in 20 ml FRET-buffer. On the following day, the solution was filtered (0.45 μ m). To determine its purity and concentration, UV measurements at wavelengths of 260 nm and 280 nm were taken from 1:100 and 1:10 dilutions (Biochrom Libra S22 UV/Vis Spectrophotometer). Considering the determined concentration, the calf

thymus-DNA solution was then further diluted with FRET-buffer to obtain solutions of the following concentrations: 800 μM (corresponds to a concentration ratio F21T: CT-DNA = 1:1000), 80 μM (1:100), 8 μM (1:10) and 800 nM (1:1).

A well-plate was filled as depicted in Table 4.1. Thereby, the calf thymus-DNA-solutions were added 2 minutes after all other components. The well plate was processed in the DNA Engine Opticon and the data analysed as described above.

Table 4.1: F21T competition assay with calf thymus-DNA: Filling of the well-plate.

	1	2	3
A - blank	25 μl F21T 800 nM + 75 μl FRET-buffer		
B - 1:0	25 μl F21T 800 nM + 50 μl KN-88 2 μM + 25 μl FRET-buffer		
C - 1:1	25 μl F21T 800 nM + 50 μl KN-88 2 μM + 25 μl CT-DNA 800 nM		
D - 1:10	25 μl F21T 800 nM + 50 μl KN-88 2 μM + 25 μl CT-DNA 8 μM		
E - 1:100	25 μl F21T 800 nM + 50 μl KN-88 2 μM + 25 μl CT-DNA 80 μM		
F - 1:1000	25 μl F21T 800 nM + 50 μl KN-88 2 μM + 25 μl CT-DNA 800 μM		

4.2.1.3 Telomere repeat amplification protocol (trap) assay

Since it was established that quadruplex-ligands contaminate the second-stage of the traditional TRAP assay, a modified three-stage assay coined TRAP–LIG was proposed [240]. The first-stage involved TS primer elongation by telomerase in the presence of the ligand. The second and novel-introduction was the subsequent removal of the ligand. Finally, the elongated artifacts were amplified via polymerase-chain-reaction (PCR).

4.2.1.4 Materials and Methods

Telomerase-dependent elongation was carried out by preparing a master mix containing 0.1 μg TS forward primer (5'-AAT CCG TCG AGC AGA GTT-3'), TRAP buffer (20 mM Tris–HCl [pH 8.3], 68 mM KCl, 1.5 mM MgCl_2 , 1 mM EGTA, and 0.05% [v/v] Tween 20), 0.05 μg bovine serum albumin (BSA), dNTPs (125 μM), and protein extract (500 ng/ μl) diluted in lysis buffer (10 mM Tris–HCl [pH 7.5], 1 mM MgCl_2 , 1 mM EGTA, 0.5% Chaps, 10% glycerol, 5 mM β -mercaptoethanol, and 0.1 mM 4-(2-aminoethyl)-benzenesulfonyl fluoride [AEBSF]). The elongation master mix was added to freshly prepared ligands at various

concentrations diluted in dH₂O, a negative control (no telomerase) and a positive control (no ligand). Elongation occurred for 30 mins at 30 °C, followed by 94 °C for 5 mins and the final mixture was maintained at 20 °C.

The elongated TRAP products were purified to remove ligands in the QIA quick nucleotide purification kit (Qiagen) in accordance with the manufacturer's instructions. The QIA quick kit is designed for the purification of oligonucleotides more than 17 bases in length. An initial high-salt buffer binds the negatively charged oligonucleotides to the positively charged spin tube membrane. Further centrifugation ensures all other components, including positively charged and neutral ligand molecules are eluted. Then, an ethanol-based buffer is washed through the spin-tube to wash any impurities away before the DNA is eluted using a low-salt concentration solution. Since the TRAP assay is sensitive to trace amounts of ethanol, the purified samples were dissolved in DEPC H₂O and precipitated in a centrifuged vacuum at 30 °C and then re-dissolved in 40 µL PCR-grade water at room temperature prior to the amplification step.

The purified extended artifacts were then amplified *via* PCR. The amplification master-mix was comprised of 1 µM ACX reverse primer (5'-GCG CGG [CTTACC]3 CTA ACC-3'), 0.1 µg TS forward primer (5'-AAT CCG TCG AGC AGA GTT-3'), TRAP buffer, 5 µg BSA, 0.5 mM dNTPs, and 2 units of *Taq* polymerase (RedHot, ABgene, UK). A 10 µl aliquot of the 5X master mix was added to the 40 µL purified telomerase extended samples and amplified for 35 cycles of 94 °C for 30 s, of 61 °C for 1 min, and of 72 °C for 1 min.

TRAP products were separated by a 10% w/w PAGE and visualized with 1xSYBR Green I nucleic acid gel stain (Sigma-Aldrich, S9430). Gels were quantified using a gel scanner and Gene Tool software (Syngene, UK). Densitometry analysis was obtained by integrating the total intensity of each PCR product ladder in the denaturing gels. Drug samples were normalized against positive control (no ligand). Lanes were background-corrected through subtracting the integrated total intensity of the negative control (no telomerase). The biophysical TRAP-LIG data for the aryl polyamide series of ligands were collected at a range of concentrations to obtain dose-response curves from which EC₅₀ values (the concentrations required for 50% enzyme inhibition, corresponding to a 50% decrease in total integrated ladder intensity); 25 µM was the highest concentration chosen.

4.3 Experimental-Biological

4.3.1 Assays for the biological evaluation of G-quadruplex ligands

Although biophysical assays (discussed in earlier section) provide relatively fast, ‘proof-of-principle’ information in assessing G-quadruplex stabilization and acute telomerase inhibition, the next level of evaluation is the introduction of G-quadruplex ligands into cells. Initially, biophysical assays were used to screen large libraries of small molecules and identify potentially active small-molecules. Subsequently, this focused range of small molecules was examined in cell-culture studies.

Prior to clinical evaluation, lead-molecules must be identified by pre-clinical studies. The purpose is to emphasize and consolidate the biophysical proof-of-principle studies. In anti-cancer drug discovery, the initial paradigm of any new class of agents is to demonstrate significant ($<1 \mu\text{M}$) toxicity in a range of tumour cell lines while having little adverse effects/toxicity in a healthy fibroblast cell line. Further, we must identify and validate the molecular target and mechanism of action of the compound for pre-clinical investigations. Toxicity screens can offer preliminary insight into the mechanism of action of ligands through observing selectivity/potency in a range of cell lines.

The principles of the biological assays used to assess the activity of the G-quadruplex binding ligands have been described in Chapter 2.

4.3.2 Materials and methods

4.3.2.1 Cell Culture

The aryl polyamide series was evaluated against a varied panel of cell lines: MCF7 (human breast adenocarcinoma), A549 (human lung adenocarcinoma), and MIA-Pa-Ca-2 (human pancreatic) were obtained from the European Collection of Cell Cultures, and WI38 (healthy fibroblast), RCC4 (human renal) and HPAC (human pancreatic) cell lines were obtained from the American Type Culture Collection. All adherent cell-lines were maintained in monolayer culture in 75 cm² flasks (TPP, Switzerland) under a humidified 5% CO₂ atmosphere at 37°C. Unless otherwise specified, all incubations were made under these conditions. For MCF7 and

A549, Dulbecco's MEM medium (GIBCO 21969, Invitrogen, UK) was used, supplemented with L-glutamine (2 mM, GIBCO 25030, Invitrogen, UK), essential amino acids (1%, GIBCO 11140, Invitrogen, UK), foetal calf serum (10%, S1810, Biosera, UK) and hydrocortisone (0.5 µg/mL, Acros Organics, UK). For MIA-Pa-Ca-2, Dulbecco's MEM, supplemented with L-glutamine (2mM) and foetal calf serum (10%) was used. For WI38 the medium MEM (M2279, Sigma, UK) with added L-glutamine (2mM), essential amino acids (1%) and foetal calf serum (10%) was used. For HPAC the medium D-MEM/F12 (1:1) (21331, Invitrogen, UK) supplemented with L-glutamine (2mM), insulin (0.002 mg/ml, GIBCO 12585-014, Invitrogen, UK), transferrin (0.005 mg/ml, 11108-016, Invitrogen, UK), hydrocortisone (40 ng/ml), epidermal growth factor (10 ng/ml, 53003-018, Invitrogen, UK) and foetal calf serum (10%) was used. For RCC4 the medium employed was RPMI 1640 (GIBCO 31870, Invitrogen, UK), supplemented with L-glutamine (2 mM), foetal calf serum (10%) and cultured in G418 (0.5 mg/ml) (10131-027, Invitrogen, UK). For passaging, cells were washed with PBS (GIBCO 14040, Invitrogen, UK), incubated with trypsin (GIBCO 25300, Invitrogen, UK), and re-seeded into fresh medium. For seeding, cells were counted using a Neubauer haemocytometer (Assistant, Germany) by microscopy on a non-adherent suspension of cells that was washed in PBS, trypsinised, centrifuged at 8 °C at 8000 rpm for 3 mins and re-suspended in fresh medium.

4.3.2.2 Sulphorhodamine B assay (SRB)

MCF7, A549, MIA-Pa-Ca-2, WI38, RCC4 and HPAC were counted and diluted to the required concentration in 20 mL medium, as 160 µL medium (containing a pre-determined number of cells) was seeded into each well of a 96 well plate (Nunc, Denmark). After 24 h incubation, the polyamide series was subjected to a series of dilutions as 40 µL of medium containing variant drug concentrations was added and the cells incubated for 96 h. The medium was then removed and the cells fixed by incubation with TCA (10%, Sigma-Aldrich, UK) in water for 30 mins at 4 °C. After the TCA was removed, cells were washed 5 times with deionised water and dried at 60 °C for 1 h. Sulphorhodamine B (80 µL, 0.4% in 1% acetic acid, Acros Organics, UK) was then added to the cells for 15 mins at RT. The SRB was then removed as the wells were washed with 1% acetic acid (200 µL), and dried at 60°C for 1 h. Tris-base (100 µL, 10 mM, Acros Organics, UK) solution was then added, and the plates shaken for 5 mins. The absorbance at 540 nm was then measured with a plate reader

(Spectrostar Omega, BMG Labtech, Germany). All data were normalized to the value of 100 for the control experiment (untreated cells), and the IC₅₀ values were obtained as the concentration leading to an absorbance intensity of 50%. Individual data sets were averaged in quadruplicate with the assay performed on three independent occasions.

4.3.2.3 Long-term treatment profiles and population doublings studies

In initial experiments, varying numbers of cells were seeded in T25 and T75 flasks to predetermine the optimum number of cells required for the following experiments. Long-term cell studies occurred using the MIA-PaCa 2 cell line. Several treatment profiles were utilized; (*re-treatment involved discarding the medium, washing the cells with PBS and applying the drug in fresh medium).

- i) 0.6 x IC₅₀ for a total of 7 days. Cells were re-treated* with the drug on day 3 and day 5.
- ii) 1 x IC₅₀ for 1, 3 and 5 days. The 5-day study was re-treated* on day 3.
- iii) Varying concentrations of drug for 4-days with re-treatment on day 2; the 4-day treatment cycle was repeated to observe the long-term effect on cell population.

Treatment profile **iii)** was utilized in a long-term pd study. Cells were counted on day 4, as described, and re-seeded (1 x 10⁴ cells in T25 flasks and 1x10⁵ cells in T75 flasks to ensure ~80% confluency after 4-days) in their respective treatment profiles for the duration of the experiment. Two-seeding densities were used, and each condition repeated in triplicate and averaged. Pd was then calculated using the formula:

$$N_f = N_0 2^{pd}; \quad pd = \log (N_f/N_0) / \log 2$$

N₀ is 1x10⁵; N_f is the number of cells at time of counting; pd is number of population doubling

4.3.2.4 Modified telomere repeat amplification protocol (TRAP)

The materials and methods performed were as previously described in **4.2.1.4**. Protein extracts were a result of treatment profiles **i)** and **ii)** outlined in **4.3.2.3**.

4.3.2.5 β -Galactosidase senescence studies

Senescence was detected and quantified using a commercially available kit (β -galactosidase senescence staining kit, Cell Signalling Technology, MA, USA) in accordance with the manufacturers' instructions. Following appropriate treatment of the cells, 1×10^5 cells were seeded in a 35 mm well within 6-well plates in 2 ml of medium and incubated for 24 h. Afterwards, the medium was removed and the cells washed with 2 ml of PBS, and then treated with 1 ml of fixative solution (2% formaldehyde and 2% glutaraldehyde in PBS) for 15 mins at room temperature. The fixative was then removed and the cells washed with PBS. Afterwards, freshly prepared staining solution (930 μ L of 500 mM potassium ferrocyanide, 10 μ L 500 mM potassium ferricyanide and 50 μ L of 20 mg/ml 5-bromo-4-chloro-3-indolyl- β -D-galactopyranoside in DMF, final volume of 1 ml) was added to the cells and incubated overnight. The number of senescent cells, as indicated by blue pigmentation, was quantified by microscopy.

4.3.2.6 Western blots; protein expression studies

Western blots were conducted to investigate the relative expression of telomerase (hTERT) and k-Ras. Whole cell nuclear extracts were extracted using the RIPA lysis buffer system (sc-24948, Santa-Cruz Biotechnology, USA) and quantified using the BCA protein assay (23225, Pierce, Thermo Scientific, USA). Prior to gel-loading, ~ 150 μ g of protein sample was vortexed in a 1:1 mixture with 2 x Laemmli samples buffer and heated to 90 °C for 5 mins. Samples were run on Mini-Protean TGX Any kD Precast Gels (456-9033, BioRad, USA) at 200v for 40 mins, and subsequently transferred onto nitrocellulose membranes at 40 mV for 120 mins at room-temperature. The nitrocellulose membrane was then blocked with 3% (w/v) non-fat dried milk in Tris buffered saline (TBS) buffer (50 mM tris, pH 7.2, 150 mM NaCl). Incubation with primary antibody, 1/200 anti-k-Ras (F234; sc-30, Santa-Cruz Biotechnology, USA; Mouse), 1/200 anti-hTERT (600401252, Rockland Immunochemicals, USA; Rabbit) and 1/100 anti-actin (AC-15, ab6276, Abcam, USA; mouse) was conducted overnight at 4 °C. After incubation with the primary antibody, the membrane was washed twice for 5 mins with TBS, and treated with secondary antibody for 2 h. Proteins were detected using Super-Signal West Pico Chemiluminescent (ECL) substrate (34080, Pierce, Thermo Scientific, USA).

5.0 Conclusion and Future Work

After careful modification of the first generation biaryl polyamides, a total of 66 molecules containing novel benzofused biaryl moiety were synthesized using a solution phase combinatorial approach. Most molecules were obtained in good yield and purity utilizing established synthetic procedures. The structures of these compounds were unambiguously confirmed using a range of spectroscopic techniques. Initial assessment of the G-quadruplex binding ligands was carried out using a FRET melting assay. KN-242, which is a hybrid benzofused compound containing biaryl building blocks, provided significant G-quadruplex stabilization of human telomeric G-quadruplex by 34.43 °C at 1 μ M concentration, while showing no binding affinity towards duplex DNA. Analysis of the molecules with other oligonucleotide sequences such as ckit-1, ckit-2, cmc, DRH and CDRH by FRET melting further confirmed their ability to selectively stabilize telomeric quadruplexes. Biophysical studies of some of the molecules by TRAP and modified-TRAP assays showed some degree of telomerase inhibition, while short term growth inhibitory assays against six different cancer cell lines (MiaPaCa2, A549, MCF7, HeLa, U87MG and A431) provided low micromolar IC₅₀ values, and between 5-8 fold selectivity for cancer cell lines compared to the non-tumor cell line. Molecules such as these, with good G-quadruplex stabilizing potential, binding selectivity, cytotoxicity and drug like properties have potential as therapeutic agents in the oncology area.

As these initial results have demonstrated significant activity against a panel of pancreatic tumour cell lines, future biological investigations will be undertaken against the promoter kRAS G-quadruplex sequences. Biological evaluation of some of the ligands is presently underway at the University of Mississippi (USA) in which they are being studied in a kras model. Although a limited SAR has already been established based on available data, a complete SAR has yet to be established by compiling all the biological results. Future work will also focus on establishing the precise mechanism of action of these ligands at the cellular level.

References

1. Kinzler, K.W. and Bert, V., The genetic basis of human cancer, 2002 (2sw): p. 5. McGraw-Hill Medical.
2. Croce, C.M, Molecular origins of cancer: Oncogenes and cancer. New England Journal of Medicine, 2008. 358 (5): p. 502-511.
3. Hanahan, D. and R.A. Weinberg, The hallmarks of cancer. Cell, 2000. 100 (1): p. 57-70.
4. Hanahan, D. and R.A. Weinberg, Hallmarks of Cancer: The Next Generation. Cell, 2011. 144 (5): p. 646-674.
5. Takimoto C, Calvo E (2008) Principles of Oncologic Pharmacotherapy. Ch 3 Appendix 3, in Pazdur R, Wagman LD, Camphausen KA, Hoskins WJ (Eds) Cancer Management: A Multidisciplinary Approach, 11th edition. Available: <http://www.cancernetwork.com/cancermanagement-11/>.
6. Rich, A., *DNA comes in many forms*. Gene, 1993. **135** (1-2): p. 99-109.
7. Mills, M., et al., *Unusual DNA conformations: implications for telomeres*. Current Medicinal Chemistry. Anti-Cancer Agents, 2002. **2** (5): p. 627-644.
8. Patel, D.J., A.T. Phan, and V. Kuryavyi, *Human telomere, oncogenic promoter and 5'-UTR G-quadruplexes: Diverse higher order DNA and RNA targets for cancer therapeutics*. Nucleic Acids Research, 2007. **35** (22): p. 7429-7455.
9. Frank-Kamenetskii, M.D., *DNA Structure: Sequence Effects*. In: eLS. John Wiley & Sons Ltd, Chichester, <http://www.els.net> [doi: 10.1038/npg.els.0002976], 2005.
10. Watson, J.D. and F.H.C. Crick, *Molecular structure of nucleic acids - a structure for deoxyribose nucleic acid*. Nature, 1953. **171** (4356): p. 737-738.
11. Mandelkern, M., et al., *The dimensions of DNA in solution*. Journal of Molecular Biology, 1981. **152** (1): p. 153-161.
12. Ghosh, A. and M. Bansal, *A glossary of DNA structures from A to Z*. Acta Crystallographica Section D-Biological Crystallography, 2003. **59**: p. 620-626.
13. Yakovchuk, P., E. Protozanova, and M.D. Frank-Kamenetskii, *Base-stacking and base-pairing contributions into thermal stability of the DNA double helix*. Nucleic Acids Research, 2006. **34** (2): p. 564-574.
14. Alberts B., Johnson A., Lewis J., Raff, M., Roberts, K. and Walter, P., *The Structure and Function of DNA*. Molecular Biology of the Cell. 4th edition. New York: Garland Science, 2002.

15. Arnott, S. and E. Selsing, *Structures for polynucleotide complexes poly(dA).poly(dT) and poly(dT).poly(dA).poly(dT)*. Journal of Molecular Biology, 1974. **88** (2): p. 509-&.
16. Morgan, A.R. and R.D. Wells, *Specificity of 3-stranded complex formation between double stranded DNA and single stranded RNA containing repeating nucleotide sequences*. Journal of Molecular Biology, 1968. **37** (1): p. 63-80.
17. Chamberlin, Mj. and Patterson, Dl. *Physical and chemical characterization of ordered complexes formed between polyinosinic acid and polycytidylic acid and their deoxyribo-analogues*. Journal of Molecular Biology, 1965. **12** (2): p. 410-428.
18. Felsenfeld, G., D.R. Davies, and A. Rich, *Formation of a 3-stranded polynucleotide molecule*. Journal of the American Chemical Society, 1957. **79** (8): p. 2023-2024.
19. Vazquez, K.M. and J.H. Wilson, *Triplex-directed modification of genes and gene activity*. Trends in Biochemical Sciences, 1998. **23** (1): p. 4-9.
20. Raghavan, S.C., et al., *Evidence for a triplex DNA conformation at the bcl-2 major breakpoint region of the t(14;18) translocation*. Journal of Biological Chemistry, 2005. **280** (24): p. 22749-22760.
21. Faucon, B., J.L. Mergny, and C. Helene, *Effect of third strand composition on triple helix formation: Purine versus pyrimidine oligodeoxynucleotides*. Nucleic Acids Research, 1996. **24** (16): p. 3181-3188.
22. Dayn, A., G.M. Samadashwily, and S.M. Mirkin, *Intramolecular DNA triplexes-unusual sequence requirements and influence of DNA polymerization*. Proceedings of the National Academy of Sciences of the United States of America, 1992. **89**(23): p. 11406-11410.
23. Asensio, J.L., et al., *The contribution of cytosine protonation to the stability of parallel DNA triple helices*. Journal of Molecular Biology, 1998. **275**(5): p. 811-822.
24. Taylor, R., *DNA triplexes in chemistry biology and medicine*, in Chemistry 2011, University of Southampton. p. 323.
25. Rich, A., *The molecular structure of polyinosinic acid*. Biochimica et Biophysica Acta, 1958. **29** (3): p. 502-509.
26. Zimmerman, S.B., G.H. Cohen, and D.R. Davies, *X-ray fibre diffraction and model-building study of polyguanilic acid and polyinosinic acid*. Journal of Molecular Biology, 1975. **92** (2): p. 181-192.

27. Tera, M., et al., *Synthesis of a potent G-quadruplex-binding macrocyclic heptaotazole*. ChemBioChem, 2009. **10** (3): p. 431-435.
28. Murat, P., Y. Singh, and E. Defrancq, *Methods for investigating G-quadruplex DNA/ligand interactions*. Chemical Society Reviews, 2011. **40** (11): p. 5293-5307.
29. Balasubramanian, S., L.H. Hurley, and S. Neidle, *Targeting G-quadruplexes in gene promoters: a novel anticancer strategy?* Nature Reviews Drug Discovery, 2011. **10** (4): p. 261-275.
30. Huppert, J.L., *Four-stranded nucleic acids: structure, function and targeting of G-quadruplexes*. Chemical Society Reviews, 2008. **37** (7): p. 1375-1384.
31. Burge, S., et al., *Quadruplex DNA: sequence, topology and structure*. Nucleic Acids Research, 2006. **34** (19): p. 5402-5415.
32. Haider, S., G.N. Parkinson, and S. Neidle, *Crystal structure of the potassium form of an Oxytricha nova G-quadruplex*. Journal of Molecular Biology, 2002. **320** (2): p. 189-200.
33. *Fundamentals of Quadruplex Structures*, in *Quadruplex Nucleic Acids*, S. Neidle and S. Balasubramanian, Editors. 2006, The Royal Society of Chemistry. p. 1-30.
34. Parkinson, G.N., M.P.H. Lee, and S. Neidle, *Crystal structure of parallel quadruplexes from human telomeric DNA*. Nature, 2002. **417** (6891): p. 876-880.
35. Phan, A.T. and D.J. Patel, *Two-repeat human telomeric d(TAGGGTTAGGGT) sequence forms interconverting parallel and antiparallel G-quadruplexes in solution: Distinct topologies, thermodynamic properties, and folding/unfolding kinetics*. Journal of the American Chemical Society, 2003. **125** (49): p. 15021-15027.
36. Phan, A.T., Y.S. Modi, and D.J. Patel, *Two-repeat Tetrahymena telomeric d(TGGGGTTGGGGT) sequence interconverts between asymmetric dimeric G-quadruplexes in solution*. Journal of Molecular Biology, 2004. **338** (1): p. 93-102.
37. Adrian, M., B. Heddi, and A.T. Phan, *NMR spectroscopy of G-quadruplexes*. Methods, 2012. **57** (1): p. 11-24.
38. Rawal, P., et al., *Genome-wide prediction of G4 DNA as regulatory motifs: Role in Escherichia coli global regulation*. Genome Research, 2006. **16** (5): p. 644-655.
39. Todd, A.K., M. Johnston, and S. Neidle, *Highly prevalent putative quadruplex sequence motifs in human DNA*. Nucleic Acids Research, 2005. **33** (9): p. 2901-2907.
40. Fry, M., *Tetraplex DNA and its interacting proteins*. Frontiers in Bioscience-Landmark, 2007. **12**: p. 4336-4351.

41. Henderson, E., et al., *Telomeric DNA oligonucleotides form novel intramolecular structures containing guanine base-pairs*. Cell, 1987. **51** (6): p. 899-908.
42. Sundquist, W.I. and A. Klug, *Telomeric DNA dimerizes by formation of guanine tetrads between hairpin loops*. Nature, 1989. **342** (6251): p. 825-829.
43. Williamson, J.R., M.K. Raghuraman, and T.R. Cech, *Mono-valent cation induced structure of telomeric DNA- the G-quartet model*. Cell, 1989. **59** (5): p. 871-880.
44. Schaffitzel, C., et al., *In vitro generated antibodies specific for telomeric guanine-quadruplex DNA react with Stylonychia lemnae macronuclei*. Proceedings of the National Academy of Sciences of the United States of America, 2001. **98** (15): p. 8572-8577.
45. Yang, D.Z. and K. Okamoto, *Structural insights into G-quadruplexes: towards new anticancer drugs*. Future Medicinal Chemistry, 2010. **2** (4): p. 619-646.
46. Maizels, N., *Dynamic roles for G4 DNA in the biology of eukaryotic cells*. Nature Structural & Molecular Biology, 2006. **13** (12): p. 1055-1059.
47. Lipps, H.J. and D. Rhodes, *G-quadruplex structures: in vivo evidence and function*. Trends in Cell Biology, 2009. **19** (8): p. 414-422.
48. Eddy, J. and N. Maizels, *Gene function correlates with potential for G4 DNA formation in the human genome*. Nucleic Acids Research, 2006. **34** (14): p. 3887-3896.
49. Simonsson, T., P. Pecinka, and M. Kubista, *DNA tetraplex formation in the control region of c-myc*. Nucleic Acids Research, 1998. **26** (5): p. 1167-1172.
50. Siddiqui-Jain, A., et al., *Direct evidence for a G-quadruplex in a promoter region and its targeting with a small molecule to repress c-MYC transcription*. Proceedings of the National Academy of Sciences of the United States of America, 2002. **99** (18): p. 11593-11598.
51. Phan, A.T., Y.S. Modi, and D.J. Patel, *Propeller-type parallel-stranded g-quadruplexes in the human c-myc promoter*. Journal of the American Chemical Society, 2004. **126** (28): p. 8710-8716.
52. Lemarteleur, T., et al., *Stabilization of the c-myc gene promoter quadruplex by specific ligands' inhibitors of telomerase*. Biochemical and Biophysical Research Communications, 2004. **323** (3): p. 802-808.
53. Zahler, A.M., et al., *Inhibition of telomerase by G-quartet DNA structures*. Nature, 1991. **350** (6320): p. 718-720.

54. Phatak, P. and A.M. Burger, *Telomerase and its potential for therapeutic intervention*. British Journal of Pharmacology, 2007. **152**: p. 1003-1011.
55. Oganessian, L. and T.M. Bryan, *Physiological relevance of telomeric G-quadruplex formation: a potential drug target*. Bioessays, 2007. **29** (2): p. 155-165.
56. Moon, I.K. and M.B. Jarstfer, *The human telomere and its relationship to human disease, therapy, and tissue engineering*. Frontiers in Bioscience, 2007. **12**: p. 4595-4620.
57. Julie E. Reed, S.N. Ramon Vilar, *Stabilisation of human telomeric quadruplex DNA and inhibition of telomerase by a platinum–phenanthroline complex*. Chemical Communications, 2007: p. 4366-4368.
58. Yanez, G.H., et al., *DNA structure-dependent recruitment of telomeric proteins to single-stranded/double-stranded DNA junctions*. Biochemical and Biophysical Research Communications, 2005. **328** (1): p. 49-56.
59. Neidle, S. and G. Parkinson, *Telomere maintenance as a target for anticancer drug discovery*. Nature reviews. Drug discovery, 2002. **1**(5): p. 383-393.
60. Gehring, K., J.-L. Leroy, and M. Gueron, *A tetrameric DNA structure with protonated cytosine-cytosine base pairs*. Nature, 1993. **363** (6429): p. 561-565.
61. Guéron, M. and J.-L. Leroy, *The i-motif in nucleic acids*. Current Opinion in Structural Biology, 2000. **10** (3): p. 326-331.
62. Brooks, T.A. and L.H. Hurley, *The role of supercoiling in transcriptional control of MYC and its importance in molecular therapeutics*. Nature reviews. Cancer, 2009. **9** (12): p. 849-861.
63. Choi, J., et al., *pH-Induced intramolecular folding dynamics of i-motif DNA*. Journal of the American Chemical Society, 2011. **133** (40): p. 16146-16153.
64. Phan, A.T. and J.L. Mergny, *Human telomeric DNA: G-quadruplex, i-motif and Watson–Crick double helix*. Nucleic Acids Research, 2002. **30** (21): p. 4618-4625.
65. Huppert, J.L. and S. Balasubramanian, *G-quadruplexes in promoters throughout the human genome*. Nucleic Acids Research, 2007. **35** (2): p. 406-413.
66. Wang, A.H.J., et al., *Molecular-structure of a left handed double helical DNA fragment at atomic resolution*. Nature, 1979. **282** (5740): p. 680-686.
67. Hascheme, Ae and A. Rich, *Nucleoside confirmations-an analysis of steric barriers to rotation about glycosidic bond*. Journal of Molecular Biology, 1967. **27** (2): p. 369-384.

68. Rahmouni, A.R. and R.D. Wells, *Stabilization of Z DNA in vivo by localized supercoiling*. Science, 1989. **246** (4928): p. 358-363.
69. Ho, P.S., et al., *A computer aided thermodynamic approach for predicting the formation of Z-DNA in naturally occurring sequences*. Embo Journal, 1986. **5** (10): p. 2737-2744.
70. Herbert, A.G., et al., *Z-DNA binding-protein from chicken blood nuclei*. Proceedings of the National Academy of Sciences of the United States of America, 1993. **90** (8): p. 3339-3342.
71. Watson, J.D. and F.H.C. Crick, *Genetical implications of the structure of deoxyribonucleic acid*. Nature, 1953. **171** (4361): p. 964-967.
72. Watson, J.D., *Origin of concatemeric T7 DNA*. Nature-New Biology, 1972. **239** (94): p. 197-201.
73. Olovniko, Am, *Theory of marginotomy - Incomplete copying of template margin in enzymic-synthesis of polynucleotides and biological significance of phenomenon*. Journal of Theoretical Biology, 1973. **41** (1): p. 181-190.
74. Makarov, V.L., Y. Hirose, and J.P. Langmore, *Long G tails at both ends of human chromosomes suggest a C strand degradation mechanism for telomere shortening*. Cell, 1997. **88** (5): p. 657-666.
75. Sfeir, A.J., et al., *Telomere-end processing: The terminal nucleotides of human chromosomes*. Molecular Cell, 2005. **18** (1): p. 131-138.
76. Harley, C.B., A.B. Futcher, and C.W. Greider, *Telomeres shorten during aging of human fibroblasts*. Nature, 1990. **345** (6274): p. 458-460.
77. Hayflick, L. and P.S. Moorhead, *Serial cultivation of human diploid cell strains*. Experimental Cell Research, 1961. **25** (3): p. 585-621.
78. Naasani, I., *Telomerase inhibitors: Forcing the end to put an end*. Drug News & Perspectives, 2000. **13** (7): p. 389-394.
79. Blackburn, E.H. and J.G. Gall, *Tandemly repeated sequence at termini of extrachromosomal ribosomal-Rna genes in Tetrahymena*. Journal of Molecular Biology, 1978. **120** (1): p. 33-53.
80. Moyzis, R.K., et al., *A highly conserved repetitive DNA-sequence, (Ttaggg)_N, present at the telomeres of human-chromosomes*. Proceedings of the National Academy of Sciences of the United States of America, 1988. **85** (18): p. 6622-6626.

81. Griffith, J.D., et al., *Mammalian telomeres end in a large duplex loop*. Cell, 1999. **97** (4): p. 503-514.
82. de Lange, T., *Shelterin: the protein complex that shapes and safeguards human telomeres*. Genes & Development, 2005. **19** (18): p. 2100-2110.
83. Blasco, M.A., *Mammalian telomeres and telomerase: why they matter for cancer and aging*. European Journal of Cell Biology, 2003. **82** (9): p. 441-446.
84. Choi, K.H., et al., *Characterization of the DNA binding specificity of Shelterin complexes*. Nucleic Acids Research, 2011. **39**(21):9206-9023.
85. Cesare, A.J. and R.R. Reddel, *Alternative lengthening of telomeres: models, mechanisms and implications*. Nature reviews. Genetics, 2010. **11** (5): p. 319-330.
86. Collins, K., *The biogenesis and regulation of telomerase holoenzymes*. Nature Reviews Molecular Cell Biology, 2006. **7** (7): p. 484-494.
87. Shay, J.W., et al., *Telomerase and cancer*. Human Molecular Genetics, 2001. **10** (7): p. 677-685.
88. Wai, L.K., *Telomeres, telomerase, and tumorigenesis -- A review*. MedGenMed., 2004. **6**(3): p. 19.
89. Dahse, R., W. Fiedler, and G. Ernst, *Telomeres and telomerase: biological and clinical importance*. Clinical Chemistry, 1997. **43** (5): p. 708-714.
90. Hahn, W.C., *Role of telomeres and telomerase in the pathogenesis of human cancer*. Journal of Clinical Oncology, 2003. **21** (10): p. 2034-2043.
91. Zvereva, M.I., D.M. Shcherbakova, and O.A. Dontsova, *Telomerase: Structure, functions, and activity regulation*. Biochemistry-Moscow, 2010. **75** (13): p. 1563-1583.
92. Cong, Y.S., W.E. Wright, and J.W. Shay, *Human telomerase and its regulation*. Microbiology and Molecular Biology Reviews, 2002. **66** (3): p. 407-425.
93. Feng, J.L., et al., *The Rna component of human telomerase*. Science, 1995. **269** (5228): p. 1236-1241.
94. Ueda, C.T. and R.W. Roberts, *Analysis of a long-range interaction between conserved domains of human telomerase RNA*. Rna-a Publication of the Rna Society, 2004. **10** (1): p. 139-147.
95. Antal, M., et al., *Analysis of the structure of human telomerase RNA in vivo*. Nucleic Acids Research, 2002. **30** (4): p. 912-920.

96. Tesmer, V.M., et al., *Two inactive fragments of the integral RNA cooperate to assemble active telomerase with the human protein catalytic subunit (hTERT) in vitro*. Molecular and Cellular Biology, 1999. **19** (9): p. 6207-6216.
97. Bachand, F. and C. Autexier, *Functional regions of human telomerase reverse transcriptase and human telomerase RNA required for telomerase activity and RNA-protein interactions*. Molecular and Cellular Biology, 2001. **21** (5): p. 1888-1897.
98. Chen, J.-L. and C.W. Greider, *An emerging consensus for telomerase RNA structure*. Proceedings of the National Academy of Sciences of the United States of America, 2004. **101** (41): p. 14683-14684.
99. Blackburn, E.H., *Switching and signaling at the telomere*. Cell, 2001. **106** (6): p. 661-673.
100. McEachern, M.J. and E.H. Blackburn, *Runaway telomere elongation caused by telomerase Rna gene-mutations*. Nature, 1995. **376** (6539): p. 403-409.
101. Evans, S.K. and V. Lundblad, *Positive and negative regulation of telomerase access to the telomere*. Journal of Cell Science, 2000. **113** (19): p. 3357-3364.
102. Smogorzewska, A., et al., *Control of human telomere length by TRF1 and TRF2*. Molecular and Cellular Biology, 2000. **20** (5): p. 1659-1668.
103. Zhou, X.Z. and K.P. Lu, *The Pin2/TRF1-interacting: Protein PinX1 is a potent telomerase inhibitor*. Cell, 2001. **107** (3): p. 347-359.
104. Henson, J.D., et al., *Alternative lengthening of telomeres in mammalian cells*. Oncogene, 2002. **21** (4): p. 598-610.
105. Bryan, T.M., et al., *Evidence for an alternative mechanism for maintaining telomere length in human tumors and tumor-derived cell lines*. Nature Medicine, 1997. **3** (11): p. 1271-1274.
106. Dunham, M.A., et al., *Telomere maintenance by recombination in human cells*. Nature Genetics, 2000. **26** (4): p. 447-450.
107. Tarsounas, M., et al., *Telomere maintenance requires the RAD51D recombination/repair protein*. Cell, 2004. **117** (3): p. 337-347.
108. Wang, Y. and D.J. Patel, *Solution structure of the human telomeric repeat D[Ag(3)(T(2)Ag(3))3] G-tetraplex structure*, 1993. **1** (4): p. 263-282.
109. Phan, A.T. and D.J. Patel, *Two-repeat human telomeric d(TAGGGTTAGGGT) sequence forms interconverting parallel and antiparallel G-quadruplexes in solution:*

- Distinct topologies, thermodynamic properties, and folding/unfolding kinetics.* Journal of the American Chemical Society, 2003. **125** (49): p. 15021-15027.
110. Xu, Y. and M. Komiyama, *Structure, function and targeting of human telomere RNA.* Methods, 2012. **57** (1): p. 100-105.
 111. Ambrus, A., et al., *Human telomeric sequence forms a hybrid-type intramolecular G-quadruplex structure with mixed parallel/antiparallel strands in potassium solution.* Nucleic Acids Research, 2006. **34** (9): p. 2723-2735.
 112. Neidle, S., *The structures of quadruplex nucleic acids and their drug complexes.* Current Opinion in Structural Biology, 2009. **19** (3): p. 239-250.
 113. Luu, K.N., et al., *Structure of the human telomere in K⁺ solution: An intramolecular (3 + 1) G-quadruplex scaffold.* Journal of the American Chemical Society, 2006. **128** (30): p. 9963-9970.
 114. Huppert, J.L. and S. Balasubramanian, *Prevalence of quadruplexes in the human genome.* Nucleic Acids Research, 2005. **33** (9): p. 2908-2916.
 115. McLuckie, K.I.E., et al., *G-Quadruplex-binding benzo[a]phenoxazines down-regulate c-KIT expression in human gastric carcinoma cells.* Journal of the American Chemical Society, 2011. **133** (8): p. 2658-2663.
 116. Rankin, S., et al., *Putative DNA quadruplex formation within the human c-kit oncogene.* Journal of the American Chemical Society, 2005. **127** (30): p. 10584-10589.
 117. Fernando, H., et al., *A conserved quadruplex motif located in a transcription activation site of the human c-kit oncogene.* Biochemistry, 2006. **45** (25): p. 7854-7860.
 118. Todd, A.K., et al., *Sequence occurrence and structural uniqueness of a G-quadruplex in the human c-kit promoter.* Nucleic Acids Research, 2007. **35**: p. 5799-5808.
 119. Phan, A.T., et al., *Structure of an unprecedented G-quadruplex scaffold in the human c-kit promoter.* Journal of the American Chemical Society, 2007. **129** (14): p. 4386-4392.
 120. Hsu, S.-T.D., et al., *A G-rich sequence within the c-kit oncogene promoter forms a parallel G-quadruplex having asymmetric G-tetrad dynamics.* Journal of the American Chemical Society, 2009. **131** (37): p. 13399-13409.

121. Tuveson, D.A., et al., *STI571 inactivation of the gastrointestinal stromal tumor c-KIT oncoprotein: biological and clinical implications*. *Oncogene*, 2001. **20** (36): p. 5054-5058.
122. Bejugam, M., et al., *Trisubstituted isoalloxazines as a new class of G-quadruplex binding ligands: Small molecule regulation of c-kit oncogene expression*. *Journal of the American Chemical Society*, 2007. **129**: p. 12926-12927.
123. Mallesham Bejugam, M.G., et al., *Targeting the c-kit promoter G-quadruplexes with 6-substituted indenoisoquinolines*. *ACS Medicinal Chemistry Letters*, 2010. **1**(7):306-310.
124. Gonzalez, V. and L.H. Hurley, *The c-MYC NHE III1: Function and regulation*. *Annual Review of Pharmacology and Toxicology*, 2010. **50**: p. 111-129.
125. Michelotti, G.A., et al., *Multiple single-stranded cis elements are associated with activated chromatin of the human c-myc gene in vivo*. *Molecular and Cellular Biology*, 1996. **16** (6): p. 2656-2669.
126. Chen, W.-J., et al., *Disubstituted 1,8-dipyrazolcarbazole derivatives as a new type of c-myc G-quadruplex binding ligands*. *Bioorganic & Medicinal Chemistry*, 2012. **20** (9): p. 2829-2836.
127. Seto, M., et al., *Alternative promoters and exons, somatic mutation and deregulation of the BCL-2-IG fusion gene in lymphoma*. *Embo Journal*, 1988. **7** (1): p. 123-131.
128. Jing, N., Zhu, Q., Yuan, P., Y. Li, L. Mao, and D. J. Tweardy, *Targeting signal transducer and activator of transcription 3 with G-tetrad oligonucleotides: a potential novel therapy for head and neck cancer*. *Molecular Cancer Therapy*, 2006. **5**: p. 279–286.
129. Kim, J., C. Cheong, and P.B. Moore, *Tetramerization of an RNA oligonucleotide containing a GGGG sequencebbvvvvvnbvf*. *Nature*, 1991. **351** (6324): p. 331-332.
130. Bugaut, A. and S. Balasubramanian, *5'-UTR RNA G-quadruplexes: translation regulation and targeting*. *Nucleic Acids Research*, 2012. **40**(11):4727-4741.
131. Gros, J., et al., *G-quadruplex formation interferes with P1 helix formation in the RNA component of telomerase hTERC*. *Chembiochem*, 2008. **9** (13): p. 2075-2079.
132. Zhang, A.Y.Q., A. Bugaut, and S. Balasubramanian, *A sequence-independent analysis of the loop length dependence of intramolecular RNA G-quadruplex stability and topology*. *Biochemistry*, 2011. **50** (33): p. 7251-7258.

133. Zhang, D.H. and G.Y. Zhi, *Structure monomorphism of RNA G-quadruplex that is independent of surrounding condition*. Journal of Biotechnology, 2010. **150** (1): p. 6-10.
134. Zhang, D.H., et al., *Monomorphic RNA G-quadruplex and polymorphic DNA G-quadruplex structures responding to cellular environmental factors*. Biochemistry, 2010. **49** (21): p. 4554-4563.
135. Joachimi, A., A. Benz, and J.S. Hartig, *A comparison of DNA and RNA quadruplex structures and stabilities*. Bioorganic & Medicinal Chemistry, 2009. **17** (19): p. 6811-6815.
136. Arora, A. and S. Maiti, *Differential biophysical behavior of human telomeric RNA and DNA quadruplex*. Journal of Physical Chemistry B, 2009. **113** (30): p. 10515-10520.
137. Armitage, B.A., *The rule of four*. Nature Chemical Biology, 2007. **3** (4): p. 203-204.
138. Kumari, S., et al., *An RNA G-quadruplex in the 5[prime] UTR of the NRAS proto-oncogene modulates translation*. Nature Chemical Biology, 2007. **3** (4): p. 218-221.
139. Duchler, M., *G-quadruplexes: targets and tools in anticancer drug design*. Journal of Drug Targeting, 2012. **20** (5): p. 389-400.
140. Sun, D.Y., et al., *Inhibition of human telomerase by a G-quadruplex-interactive compound*. Journal of Medicinal Chemistry, 1997. **40** (14): p. 2113-2116.
141. Han, H., A. Rangan, and L.H. Hurley, *Selective interaction of cationic porphyrins with different types of G-quadruplex structures*. Clinical Cancer Research, 1999. **5**: p. 3852S-3852S.
142. Han, H.Y., R.J. Bennett, and L.H. Hurley, *Inhibition of unwinding of G-quadruplex structures by Sgs1 helicase in the presence of N,N '-bis 2-(1-piperidino)ethyl - 3,4,9,10-perylenetetracarboxylic diimide, a G-quadruplex-interactive ligand*. Biochemistry, 2000. **39** (31): p. 9311-9316.
143. Shin-ya, K., et al., *Telomestatin, a novel telomerase inhibitor from Streptomyces anulatus*. Journal of the American Chemical Society, 2001. **123** (6): p. 1262-1263.
144. Kim, M.Y., et al., *Telomestatin, a potent telomerase inhibitor that interacts quite specifically with the human telomeric intramolecular G-quadruplex*. Journal of the American Chemical Society, 2002. **124** (10): p. 2098-2099.
145. Han, H.Y. and L.H. Hurley, *G-quadruplex DNA: a potential target for anti-cancer drug design*. Trends in Pharmacological Sciences, 2000. **21** (4): p. 136-142.

146. Ou, T.-m., et al., *G-quadruplexes: Targets in anticancer drug design*. ChemMedChem, 2008. **3** (5): p. 690-713.
147. Gavathiotis, E., et al., *Drug recognition and stabilisation of the parallel-stranded DNA quadruplex d(TTAGGGT)(4) containing the human telomeric repeat*. Journal of Molecular Biology, 2003. **334** (1): p. 25-36.
148. Haider, S.M., G.N. Parkinson, and S. Neidle, *Structure of a G-quadruplex-ligand complex*. Journal of Molecular Biology, 2003. **326** (1): p. 117-125.
149. Schouten, J.A., et al., *G-quadruplex-specific peptide-hemicyanine ligands by partial combinatorial selection*. Journal of the American Chemical Society, 2003. **125** (19): p. 5594-5595.
150. Perry, P.J., et al., *2,7-Disubstituted amidofluorenone derivatives as inhibitors of human telomerase*. Journal of Medicinal Chemistry, 1999. **42** (14): p. 2679-2684.
151. Harrison, R.J., et al., *Human telomerase inhibition by substituted acridine derivatives*. Bioorganic & Medicinal Chemistry Letters, 1999. **9** (17): p. 2463-2468.
152. Harrison, R.J., et al., *Trisubstituted acridine derivatives as potent and selective telomerase inhibitors*. Journal of Medicinal Chemistry, 2003. **46** (21): p. 4463-4476.
153. Perry, P.J., et al., *Design, synthesis and evaluation of human telomerase inhibitors based upon a tetracyclic structural motif*. Anti-Cancer Drug Design, 1999. **14** (4): p. 373-382.
154. Caprio, V., et al., *A novel inhibitor of human telomerase derived from 10H-indolo 3,2-b quinoline*. Bioorganic & Medicinal Chemistry Letters, 2000. **10** (18): p. 2063-2066.
155. Guyen, B., et al., *Synthesis and evaluation of analogues of 10H-indolo[3,2-b]-quinoline as G-quadruplex stabilising ligands and potential inhibitors of the enzyme telomerase*. Organic & Biomolecular Chemistry, 2004. **2** (7): p. 981-988.
156. Zhou, J.M., et al., *Senescence and telomere shortening induced by novel potent G-quadruplex interactive agents, quindoline derivatives, in human cancer cell lines*. Oncogene, 2006. **25** (4): p. 503-511.
157. Zhou, J.L., et al., *Synthesis and evaluation of quindoline derivatives as G-quadruplex inducing and stabilizing ligands and potential inhibitors of telomerase*. Journal of Medicinal Chemistry, 2005. **48** (23): p. 7315-7321.
158. Dixon, I.M., et al., *A G-quadruplex ligand with 10000-fold selectivity over duplex DNA*. Journal of the American Chemical Society, 2007. **129** (6): p. 1502-1503.

159. Seenisamy, J., et al., *Design and synthesis of an expanded porphyrin that has selectivity for the c-MYC G-quadruplex structure*. Journal of the American Chemical Society, 2005. **127** (9): p. 2944-2959.
160. Goncalves, D.P.N., et al., *Tetramethylpyridiniumporphyrazines - a new class of G-quadruplex inducing and stabilising ligands*. Chemical Communications, 2006 (45): p. 4685-4687.
161. Ren, L.G., et al., *Quaternary ammonium zinc phthalocyanine: Inhibiting telomerase by stabilizing G quadruplexes and inducing G-quadruplex structure transition and formation*. Chembiochem, 2007. **8** (7): p. 775-780.
162. Cocco, M.J., et al., *Specific interactions of distamycin with G-quadruplex DNA*. Nucleic Acids Research, 2003. **31**(11): p. 2944-2951.
163. Ma, Y., et al., *9-N-Substituted berberine derivatives: Stabilization of G-quadruplex DNA and down-regulation of oncogene c-myc*. Bioorganic & Medicinal Chemistry, 2008. **16** (16): p. 7582-7591.
164. Franceschin, M., et al., *Natural and synthetic G-quadruplex interactive berberine derivatives*. Bioorganic & Medicinal Chemistry Letters, 2006. **16** (6): p. 1707-1711.
165. Naasani, I., et al., *FJ5002: A potent telomerase inhibitor identified by exploiting the disease-oriented screening program with COMPARE analysis*. Cancer Research, 1999. **59** (16): p. 4004-4011.
166. Barbieri, C.M., et al., *Defining the mode, energetics and specificity with which a macrocyclic hexaoxazole binds to human telomeric G-quadruplex DNA*. Nucleic Acids Research, 2007. **35** (10): p. 3272-3286.
167. Tera, M., et al., *Design and synthesis of telomestatin derivatives and their inhibitory activity of telomerase*. Heterocycles, 2006. **69** (1): p. 505-514.
168. Zhang, W.J., et al., *9-substituted berberine derivatives as G-quadruplex stabilizing ligands in telomeric DNA*. Bioorganic & Medicinal Chemistry, 2007. **15** (16): p. 5493-5501.
169. Riou, J.F., et al., *Cell senescence and telomere shortening induced by a new series of specific G-quadruplex DNA ligands*. Proceedings of the National Academy of Sciences of the United States of America, 2002. **99** (5): p. 2672-2677.
170. De Cian, A., et al., *Highly efficient G-quadruplex recognition by bisquinolinium compounds*. Journal of the American Chemical Society, 2007. **129** (7): p. 1856-1857.

171. Rahman, K.M., et al., *Biaryl polyamides as a new class of DNA quadruplex-binding ligands*, Chemical Communications, 2009. p. 4097-4099.
172. Moore, M.J.B., et al., *Synthesis of distamycin A polyamides targeting G-quadruplex DNA*. Organic & Biomolecular Chemistry, 2006. **4**: p. 3479-3488.
173. Luedtke, N.W., *Targeting G-quadruplex DNA with small molecules*. Chimia, 2009. **63** (3): p. 134-139.
174. Guo, Q., et al., *Interaction of the dye ethidium-bromide with DNA containing guanine repeats*. Biochemistry, 1992. **31** (9): p. 2451-2455.
175. Ren, J.S. and J.B. Chaires, *Sequence and structural selectivity of nucleic acid binding ligands*. Biochemistry, 1999. **38** (49): p. 16067-16075.
176. Franceschin, M., *G-Quadruplex DNA structures and organic chemistry: More than one connection*. European Journal of Organic Chemistry, 2009 (14): p. 2225-2238.
177. Gowan, S.M., et al., *A G-quadruplex-interactive potent small-molecule inhibitor of telomerase exhibiting in vitro and in vivo antitumor activity*. Molecular Pharmacology, 2002. **61** (5): p. 1154-1162.
178. Burger, A.M., et al., *The G-quadruplex-interactive molecule BRACO-19 inhibits tumor growth, consistent with telomere targeting and interference with telomerase function*. Cancer Research, 2005. **65** (4): p. 1489-1496.
179. S. Neidle, Read, M.A., *G-Quadruplexes as therapeutic targets*. . Biopolymers (Nucleic Acid Sciences), 2001. **56**: p. 195–208.
180. Reed, J.E., S. Neidle, and R. Vilar, *Stabilisation of human telomeric quadruplex DNA and inhibition of telomerase by a platinum-phenanthroline complex*. Chemical Communications, 2007 (42): p. 4366-4368.
181. Wu, H.L., et al., *Berberine-induced apoptosis of human leukemia HL-60 cells is associated with down-regulation of nucleophosmin/B23 and telomerase activity*. International Journal of Cancer, 1999. **81** (6): p. 923-929.
182. Han, H.Y., C.L. Cliff, and L.H. Hurley, *Accelerated assembly of G-quadruplex structures by a small molecule*. Biochemistry, 1999. **38** (22): p. 6981-6986.
183. Tera, M., et al., *Macrocyclic hexaoxazoles as sequence- and mode-selective G-quadruplex binders*. Angewandte Chemie-International Edition, 2008. **47** (30): p. 5557-5560.

184. Kieltyka, R., et al., *A platinum supramolecular square as an effective G-quadruplex binder and telomerase inhibitor*. Journal of the American Chemical Society, 2008. **130** (31): p. 10040-10041.
185. Yu, H.J., et al., *Chiral metallo-supramolecular complexes selectively recognize human telomeric G-quadruplex DNA*. Nucleic Acids Research, 2008. **36** (17): p. 5695-5703.
186. Drewe, W.C., et al., *Rational design of substituted diarylureas: A scaffold for binding to G-quadruplex motifs*. Journal of Medicinal Chemistry, 2008. **51** (24): p. 7751-7767.
187. Laronze-Cochard, M., et al., *Synthesis and biological evaluation of novel 4,5-bis(dialkylaminoalkyl)-substituted acridines as potent telomeric G-quadruplex ligands*. European Journal of Medicinal Chemistry, 2009. **44** (10): p. 3880-3888.
188. Gunaratnam, M., et al., *Targeting human gastrointestinal stromal tumor cells with a quadruplex-binding small molecule*. Journal of Medicinal Chemistry, 2009. **52** (12): p. 3774-3783.
189. Rahman, K.M., et al., *Biaryl polyamides as a new class of DNA quadruplex-binding ligands*. Chemical Communications, 2009 (27): p. 4097-4099.
190. Bhattacharya, S., et al., *Symmetrical bisbenzimidazoles with benzenediyl spacer: The role of the shape of the ligand on the stabilization and structural alterations in telomeric G-quadruplex DNA and telomerase inhibition*. Bioconjugate Chemistry, 2009. **21**(7): p. 1148-1159.
191. Bianco, S., et al., *Bis-phenanthroline derivatives as suitable scaffolds for effective G-quadruplex recognition*. Dalton Transactions, 2010. **39** (25): p. 5833-5841.
192. Yaku, H., et al., *Anionic phthalocyanines targeting G-quadruplexes and inhibiting telomerase activity in the presence of excessive DNA duplexes*. Chemical Communications, 2010. **46** (31): p. 5740-5742.
193. Agarwal, T., et al., *Selective targeting of G-quadruplex using furan-based cyclic homooligopeptides: Effect on c-MYC expression*. Biochemistry, 2010. **49** (38): p. 8388-8397.
194. Chen, S.-B., et al., *Pharmacophore-based discovery of triaryl-substituted imidazole as new telomeric G-quadruplex ligand*. Bioorganic & Medicinal Chemistry Letters, 2011. **21** (3): p. 1004-1009.

195. Wu, W.-B., et al., *Disubstituted 2-phenyl-benzopyranopyrimidine derivatives as a new type of highly selective ligands for telomeric G-quadruplex DNA*. Organic & Biomolecular Chemistry, 2011. **9** (8): p. 2975-2986.
196. Dash, J., et al., *Synthesis and binding studies of novel diethynyl-pyridine amides with genomic promoter DNA G-quadruplexes*. Chemistry – A European Journal, 2011. **17** (16): p. 4571-4581.
197. Keith I. E., et al., *G-Quadruplex-binding benzo[a]phenoxazines down-regulated c-KIT expression in human gastric carcinoma cells*. Journal of the American Chemical Society 2011. **133** (8): p. 2658-2663.
198. Ma, Y., et al., *Quinolino-benzo-[5, 6]-dihydroisoquinolium compounds derived from berberine: A new class of highly selective ligands for G-quadruplex DNA in c-myc oncogene*. European Journal of Medicinal Chemistry, 2011. **46** (5): p. 1906-1913.
199. Czerwinska, I., S. Sato, and S. Takenaka, *Improving the affinity of naphthalene diimide ligand to telomeric DNA by incorporating Zn²⁺ ions into its dipicolylamine groups*. Bioorganic & Medicinal Chemistry, 2012. **20** (21): p. 6416-6422.
200. Ma, D.-L., et al., *Discovery of a natural product-like c-myc G-quadruplex DNA groove-binder by molecular docking*. PLoS ONE, 2012. **7** (8): p. e43278.
201. Yuan, F., et al., *Synthesis of a ruthenium(II) polypyridine complex with 1,10-phenanthroline-selenazole as ligand and investigation of its G-quadruplex DNA-binding properties*. Journal of Coordination Chemistry, 2012. **65** (7): p. 1246-1257.
202. Rahman, K.M., et al., *The prenylated dioxopiperazine alkaloid Cristatin A has selective telomeric DNA G-quadruplex stabilising properties*. Chemical Communications, 2012. **48** (70): p. 8760-8762.
203. Jantos, K., et al., *Oxazole-based peptide macrocycles: A new class of G-quadruplex binding ligands*. Journal of the American Chemical Society, 2006. **128** (42): p. 13662-13663.
204. Kim, M.Y., et al., *Design, synthesis, and biological evaluation of a series of fluoroquinoanthroxazines with contrasting dual mechanisms of action against topoisomerase II and G-quadruplexes*. Journal of Medicinal Chemistry, 2003. **46** (4): p. 571-583.
205. Drygin, D., et al., *Anticancer activity of CX-3543: A direct inhibitor of rRNA biogenesis*. Cancer Research, 2009. **69** (19): p. 7653-7661.

206. Jaumot, J. and R. Gargallo, *Experimental methods for studying the interactions between G-quadruplex structures and ligands*. Current Pharmaceutical Design, 2012. **18** (14): p. 1900-1916.
207. Paramasivan, S., I. Rujan, and P.H. Bolton, *Circular dichroism of quadruplex DNAs: Applications to structure, cation effects and ligand binding*. Methods, 2007. **43** (4): p. 324-331.
208. White, E.W., et al., *Structure-specific recognition of quadruplex DNA by organic cations: Influence of shape, substituents and charge*. Biophysical Chemistry, 2007. **126** (1-3): p. 140-153.
209. Rachwal, P.A. and K.R. Fox, *Quadruplex melting*. Methods, 2007. **43** (4): p. 291-301.
210. Förster, T., *Zwischenmolekulare Energiewanderung und Fluoreszenz (Intermolecular Energy Migration and Fluorescence)*. Annalen der Physik, 1948. **437** (1-2): p. 55-75.
211. Mergny, J.-L. and J.-C. Maurizot, *Fluorescence resonance energy transfer as a probe for G-quartet formation by a telomeric repeat*. Chembiochem, 2001. **2** (2): p. 124-132.
212. Mergny, J.L., et al., *Telomerase inhibitors based on quadruplex ligands selected by a fluorescence assay*. Proceedings of the National Academy of Sciences of the United States of America, 2001. **98** (6): p. 3062-3067.
213. De Cian, A., et al., *Fluorescence-based melting assays for studying quadruplex ligands*. Methods, 2007. **42** (2): p. 183-195.
214. Monchaud, D., C. Allain, and M.-P. Teulade-Fichou, *Development of a fluorescent intercalator displacement assay (G4-FID) for establishing quadruplex-DNA affinity and selectivity of putative ligands*. Bioorganic & Medicinal Chemistry Letters, 2006. **16** (18): p. 4842-4845.
215. Tse, W.C. and D.L. Boger, *A fluorescent intercalator displacement assay for establishing DNA binding selectivity and affinity*. Accounts of Chemical Research, 2004. **37** (1): p. 61-69.
216. Tran, P.L.T., et al., *Fluorescence intercalator displacement assay for screening G4 ligands towards a variety of G-quadruplex structures*. Biochimie, 2011. **93** (8): p. 1288-1296.

217. Muller, W. and D.M. Crothers, *Interactions of the heterochromatic-compounds with nucleic acids. 1. Influence of heteroatoms and polarizability on base specificity of interacting ligands*. European Journal of Biochemistry, 1975. **54** (1): p. 267-277.
218. Ragazzon, P.A., N.C. Garbett, and J.B. Chaires, *Competition dialysis: A method for the study of structural selective nucleic acid binding*. Methods, 2007. **42** (2): p. 173-182.
219. Rosu, F., E. De Pauw, and V. Gabelica, *Electrospray mass spectrometry to study drug-nucleic acids interactions*. Biochimie, 2008. **90** (7): p. 1074-1087.
220. Salim, N.N. and A.L. Feig, *Isothermal titration calorimetry of RNA*. Methods, 2009. **47** (3): p. 198-205.
221. Buurma, N.J. and I. Haq, *Advances in the analysis of isothermal titration calorimetry data for ligand-DNA interactions*. Methods, 2007. **42** (2): p. 162-172.
222. Pagano, B., et al., *Targeting DNA quadruplexes with distamycin A and its derivatives: An ITC and NMR study*. Biochimie, 2008. **90** (8): p. 1224-1232.
223. Karlsson, R., *SPR for molecular interaction analysis: a review of emerging application areas*. Journal of Molecular Recognition, 2004. **17** (3): p. 151-161.
224. Homola, J., S.S. Yee, and G. Gauglitz, *Surface plasmon resonance sensors: review*. Sensors and Actuators B-Chemical, 1999. **54** (1-2): p. 3-15.
225. Redman, J.E., *Surface plasmon resonance for probing quadruplex folding and interactions with proteins and small molecules*. Methods, 2007. **43** (4): p. 302-312.
226. Campbell, N.H., et al., *Structural basis of DNA quadruplex recognition by an acridine drug*. Journal of the American Chemical Society, 2008. **130** (21): p. 6722-6724.
227. Collie, G., et al., *Selectivity in small molecule binding to human telomeric RNA and DNA quadruplexes*. Chemical Communications, 2009 (48): p. 7482-7484.
228. da Silva, M.W., *NMR methods for studying quadruplex nucleic acids*. Methods, 2007. **43** (4): p. 264-277.
229. Hounsou, C., et al., *G-quadruplex recognition by quinacridines: a SAR, NMR, and biological study*. ChemMedChem, 2007. **2** (5): p. 655-666.
230. Trotta, R., et al., *A more detailed picture of the interactions between virtual screening-derived hits and the DNA G-quadruplex: NMR, molecular modelling and ITC studies*. Biochimie, 2011. **93** (8): p. 1280-1287.

231. Carrasco, B. and J.G. de la Torre, *Hydrodynamic properties of rigid particles: Comparison of different modeling and computational procedures*. Biophysical Journal, 1999. **76** (6): p. 3044-3057.
232. Redon, S., et al., *Platination of the (T(2)G(4))(4) telomeric sequence: A structural and cross-linking study*. Biochemistry, 2001. **40** (29): p. 8463-8470.
233. Jennerwein, M.M. and A. Eastman, *A polymerase chain reaction based method to detect cisplatin adducts in specific genes*. Nucleic Acids Research, 1991. **19** (22): p. 6209-6214.
234. Gomez, D., et al., *Telomerase downregulation induced by the G-quadruplex ligand 12459 in A549 cells is mediated by hTERT RNA alternative splicing*. Nucleic Acids Research, 2004. **32** (1): p. 371-379.
235. Gomez, D., J.-L. Mergny, and J.-F. Riou, *Detection of telomerase inhibitors based on G-quadruplex ligands by a modified telomeric repeat amplification protocol assay*. Cancer Research, 2002. **62** (12): p. 3365-3368.
236. Kim, N., et al., *Specific association of human telomerase activity with immortal cells and cancer*. Science, 1994. **266** (5193): p. 2011-2015.
237. Burger, A.M., *Standard TRAP assay*. T telomeres and Telomerase, 2002. p. 109-124.
238. De Cian, A., et al., *Targeting telomeres and telomerase*. Biochimie, 2008. **90** (1): p. 131-155.
239. De Cian, A., et al., *Reevaluation of telomerase inhibition by quadruplex ligands and their mechanisms of action*. Proceedings of the National Academy of Sciences of the United States of America, 2007. **104** (44): p. 17347-17352.
240. Reed, J., et al., *TRAP-LIG, a modified telomere repeat amplification protocol assay to quantitate telomerase inhibition by small molecules*. Analytical Biochemistry, 2008. **380** (1): p. 99-105.
241. Cheng, M.K., et al., *Antitumor polycyclic acridines. 20. Search for DNA quadruplex binding selectivity in a series of 8,13-dimethylquino 4,3,2-kl acridinium salts: Telomere-targeted agents*. Journal of Medicinal Chemistry, 2008. **51** (4): p. 963-975.
242. Skehan, P., et al., *New colorimetric cytotoxicity assay for anticancer-drug screening*. Journal of the National Cancer Institute, 1990. **82** (13): p. 1107-1112.
243. Vichai, V. and K. Kirtikara, *Sulforhodamine B colorimetric assay for cytotoxicity screening*. Nature Protocols, 2006. **1** (3): p. 1112-1116.

244. Cookson, J.C., et al., *Pharmacodynamics of the G-quadruplex-stabilizing telomerase inhibitor 3,11-difluoro-6,8,13-trimethyl-8H-quino 4,3,2-kl acridinium methosulfate (RHPS4) in vitro: Activity in human tumor cells correlates with telomere length and can be enhanced, or antagonized, with cytotoxic agents.* Molecular Pharmacology, 2005. **68** (6): p. 1551-1558.
245. Gottesfeld, J.M., et al., *Regulation of gene expression by small molecules.* Nature, 1997. **387**(6629): p. 202-205
246. Dervan, P.B. and B.S. Edelson, *Recognition of the DNA minor groove by pyrrole-imidazole polyamides.* Current Opinion in Structural Biology, 2003. **13**(3): p. 284-299.
247. Cocco, M.J., et al., *Specific interactions of distamycin with G-quadruplex DNA.* Nucleic Acids Research, 2003. **31**(11): p. 2944-2951.
248. Reed, J.E., et al., *Stabilization of G-Quadruplex DNA and Inhibition of Telomerase Activity by Square-Planar Nickel(II) Complexes.* Journal of the American Chemical Society, 2006. **128**(18): p. 5992-5993.
249. Pagano, B. and C. Giancola, *Energetics of quadruplex-drug recognition in anticancer therapy.* Current cancer drug targets, 2007. **7**(6): p. 520-540.
250. Francisco, C., CRUK Biomolecular Structure Group, School of Pharmacy, University of London, 2008.
251. Hampel, S., CRUK Biomolecular Structure Group, School of Pharmacy, University of London, 2011.
252. Gunaratnam, M., et al., *Mechanism of acridine-based telomerase inhibition and telomere shortening.* Biochemical Pharmacology, 2007. **74**(5): p. 679-689.
253. Incles, C.M., et al., *A G-quadruplex telomere targeting agent produces p16-associated senescence and chromosomal fusions in human prostate cancer cells.* Molecular Cancer Therapeutics, 2004. **3**(10): p. 1201-1206.
254. Lim, K.W., et al., *Coexistence of Two Distinct G-Quadruplex Conformations in the hTERT Promoter.* Journal of the American Chemical Society, 2010. **132**(35): p. 12331-12342.

Appendix

Table AP1: ΔT_m values for Duplex at 5 μm , 2 μm , and 1 μm concentration with standard deviations

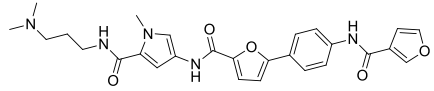
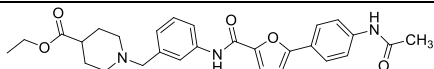
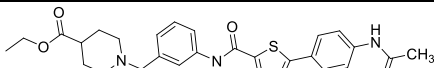
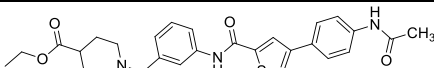
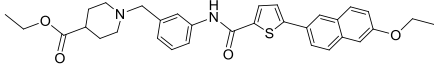
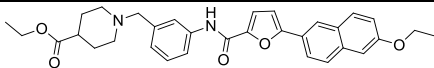
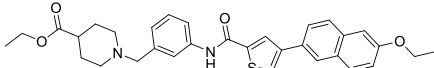
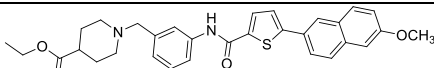
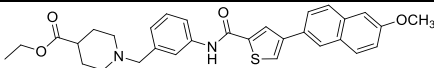
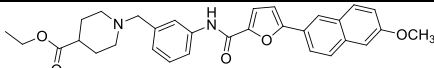
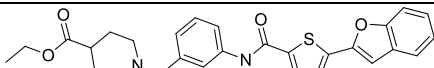
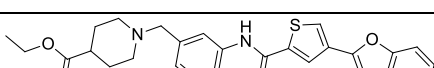
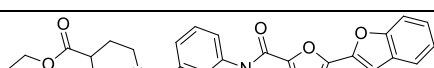
ΔT_m values for Control Duplex DNA sequence					
Code	Structure	MW	5 μm	2 μm	1 μm
KN-24		504.02	0.07 ± 0.20	0.00 ± 0.00	0.20 ± 0.00
KN-39		491.11	0.00 ± 0.00	0.13 ± 0.15	0.37 ± 0.58
KN-40		507.38	0.20 ± 0.10	0.07 ± 0.08	0.17 ± 0.13
KN-41		507.15	0.40 ± 0.00	0.30 ± 0.00	0.23 ± 0.05
KN-45		543.00	0.23 ± 0.11	0.47 ± 0.08	-1.53 ± 0.05
KN-46		527.10	0.23 ± 0.08	0.33 ± 0.15	0.533 ± 0.08
KN-47		543.05	-1.53 ± 0.58	-1.533 ± 0.15	-1.50 ± 0.10
KN-48		529.96	-1.33 ± 0.08	0.33 ± 0.05	0.13 ± 0.05
KN-49		528.94	-0.43 ± 0.92	-1.40 ± 0.00	0.27 ± 0.05
KN-50		512.99	0.17 ± 0.05	0.23 ± 0.08	0.43 ± 0.58
KN-51		489.17	0.00 ± 0.20	0.30 ± 0.08	0.17 ± 0.0
KN-52		490.14	0.00 ± 0.58	0.13 ± 0.13	0.37 ± 0.00
KN-53		473.13	-1.33 ± 0.13	-1.63 ± 0.00	-1.33 ± 0.10

Table AP1: ΔT_m values for Duplex at 5 μm , 2 μm , and 1 μm concentration with standard deviations (continued)

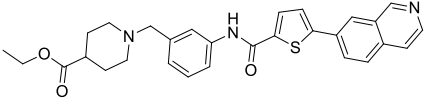
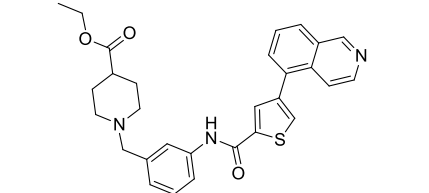
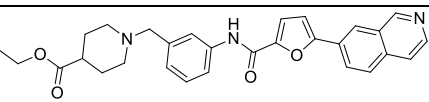
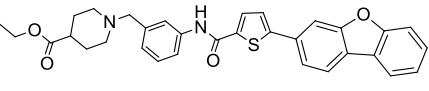
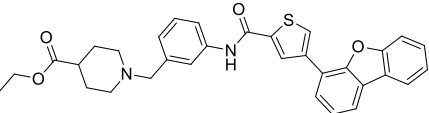
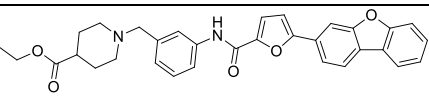
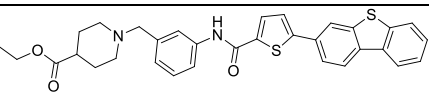
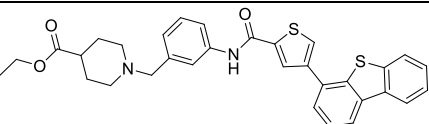
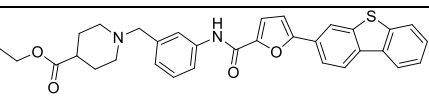
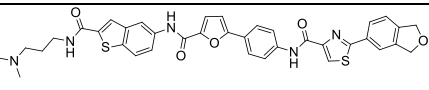
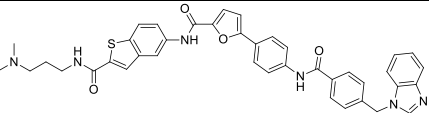
ΔT_m values for Control Duplex DNA sequence					
Code	Structure	MW	5μm	2 μm	1 μm
KN-54		499.85	-1.37 ± 0.08	-1.50 ± 0.05	-1.50 ± 0.40
KN-55		499.92	-1.53 ± 0.20	-1.30 ± 0.11	-1.27 ± 0.29
KN-56		483.88	-1.60 ± 0.05	-1.33 ± 0.10	-1.33 ± 0.00
KN-57		539.09	-1.50 ± 0.05	-1.70 ± 0.20	-1.53 ± 0.10
KN-58		539.09	-1.33 ± 0.17	-1.53 ± 0.00	-1.60 ± 0.08
KN-59		523.12	-1.53 ± 0.10	-1.33 ± 0.00	-1.40 ± 0.21
KN-60		554.99	-1.67 ± 0.58	-1.57 ± 0.08	-1.26 ± 0.13
KN-61		554.99	-1.67 ± 0.10	-1.67 ± 0.10	-1.50 ± 0.05
KN-62		539.05	-1.63 ± 0.13	-1.57 ± 0.10	-1.33 ± 0.08
KN-78		692.55	-1.20 ± 0.15	-1.07 ± 0.00	-1.26 ± 0.00
KN-79		697.81	-1.40 ± 0.58	-1.37 ± 0.10	-1.13 ± 0.08

Table AP1: ΔT_m values for Duplex at 5 μm , 2 μm , and 1 μm concentration with standard deviations (continued)

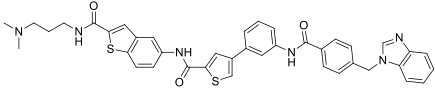
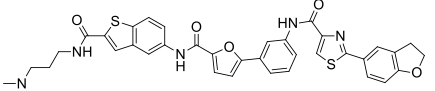
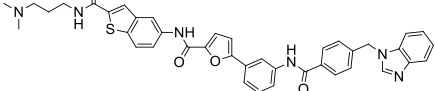
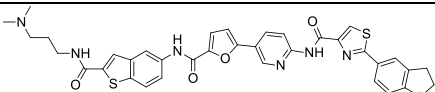
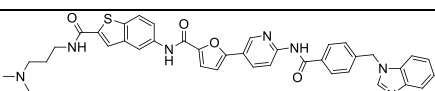
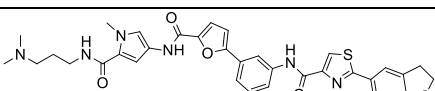
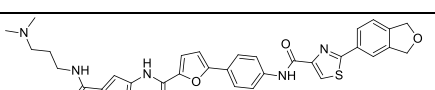
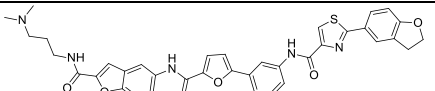
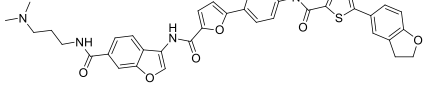
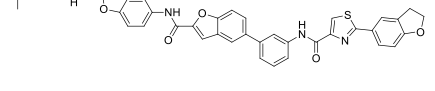
ΔT_m values for Control Duplex DNA sequence					
Code	Structure	MW	5 μm	2 μm	1 μm
KN-83		713.39	-1.37 ± 0.00	-1.40 ± 0.58	-1.56 ± 0.26
KN-88		692.72	0.71 ± 0.08	0.40 ± 0.08	0.40 ± 0.05
KN-89		697.57	0.40 ± 0.08	-0.80 ± 0.97	-1.17 ± 0.00
KN-90		693.30	0.12 ± 0.11	0.08 ± 0.12	0.06 ± 0.13
KN-91		698.53	0.07 ± 0.15	0.26 ± 0.05	0.30 ± 0.11
KN-110		639.33	0.10 ± 0.00	0.09 ± 0.00	0.03 ± 0.00
KN-112		639.32	0.43 ± 0.05	0.34 ± 0.00	0.15 ± 0.10
KN-119		676.13	-0.33 ± 0.08	0.20 ± 0.15	0.33 ± 0.00
KN-120		676.21	0.33 ± 0.00	0.67 ± 0.08	0.17 ± 0.05
KN-136		725.81	0.24 ± 0.00	0.19 ± 0.08	0.02 ± 0.00

Table AP1: ΔT_m values for Duplex at 5 μm , 2 μm , and 1 μm concentration with standard deviations (continued)

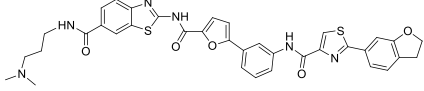
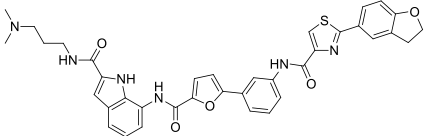
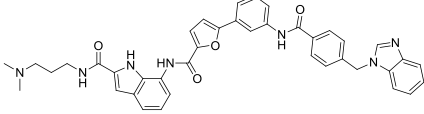
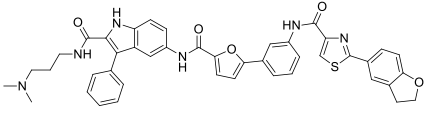
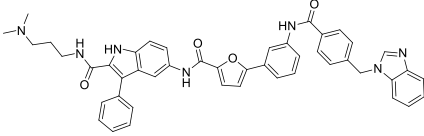
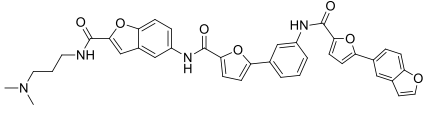
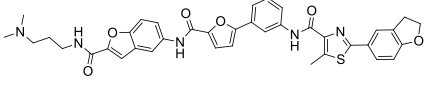
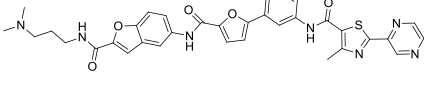
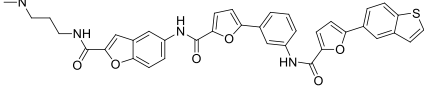
ΔT_m values for Control Duplex DNA sequence					
Code	Structure	MW	5μm	2 μm	1 μm
KN-130		692.81	0.33 ± 0.00	0.36 ± 0.05	0.267 ± 0.05
KN-143		674.77	0.33 ± 0.10	0.67 ± 0.58	0.37 ± 0.08
KN-144		679.77	0.83 ± 0.10	0.37 ± 0.08	0.47 ± 0.15
KN-145		750.86	0.53 ± 0.00	0.43 ± 0.00	0.433 ± 0.10
KN-146		755.86	0.67 ± 0.15	0.40 ± 0.58	0.30 ± 0.58
KN-148		656.68	1.47 ± 0.05	1.83 ± 0.00	0.40 ± 0.58
KN-149		689.78	0.33 ± 0.10	0.53 ± 0.00	0.33 ± 0.10
KN-150		649.72	0.50 ± 0.08	0.33 ± 0.10	0.53 ± 0.00
KN-154		672.75	0.48 ± 0.05	0.23 ± 0.00	0.10 ± 0.10

Table AP1: ΔT_m values for Duplex at 5 μm , 2 μm , and 1 μm concentration with standard deviations (continued)

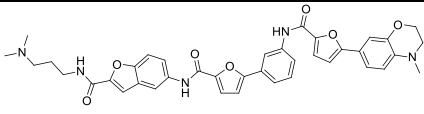
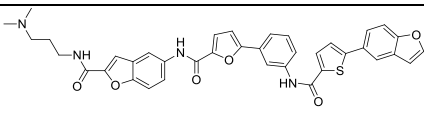
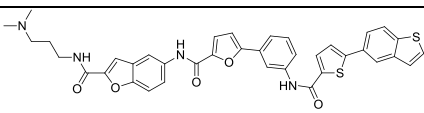
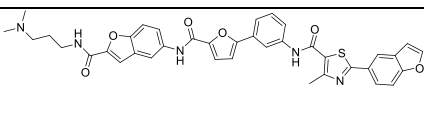
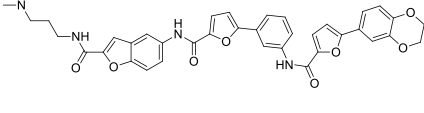
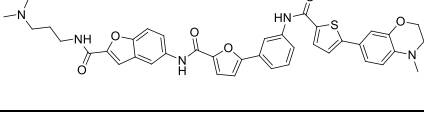
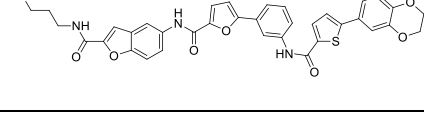
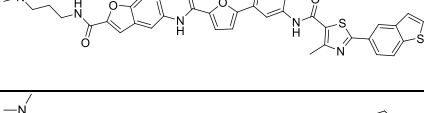
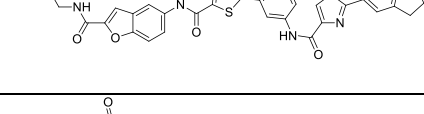
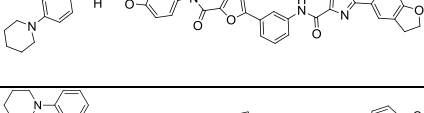
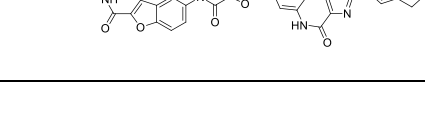
ΔT_m values for Control Duplex DNA sequence					
Code	Structure	MW	5μm	2 μm	1 μm
KN-155		687.74	0.23 ± 0.00	0.19 ± 0.00	0.02 ± 0.08
KN-156		672.75	0.27 ± 0.53	0.33 ± 0.00	0.21 ± 0.08
KN-157		688.81	0.52 ± 0.15	0.32 ± 0.10	0.13 ± 0.08
KN-158		687.76	0.93 ± 0.00	0.01 ± 0.05	0.09 ± 0.12
KN-159		674.70	0.52 ± 0.00	0.41 ± 0.10	0.24 ± 0.00
KN-160		703.81	0.27 ± 0.08	0.27 ± 0.58	0.33 ± 0.00
KN-161		690.76	0.38 ± 0.00	-0.67 ± 0.10	0.17 ± 0.15
KN-164		703.19	0.00 ± 0.08	0.03 ± 0.00	0.06 ± 0.10
KN-176		691.82	0.57 ± 0.58	-0.47 ± 0.00	0.27 ± 0.08
KN-200		763.86	0.00 ± 0.13	0.23 ± 0.00	0.23 ± 0.00
KN-202		763.86	0.03 ± 0.10	0.17 ± 0.53	0.43 ± 0.00

Table AP1: ΔT_m values for Duplex at 5 μm , 2 μm , and 1 μm concentration with standard deviations (continued)

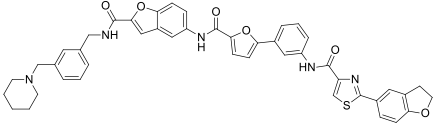
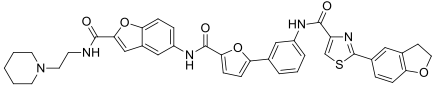
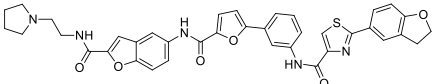
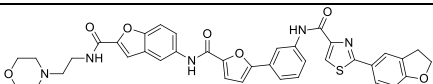
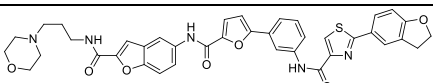
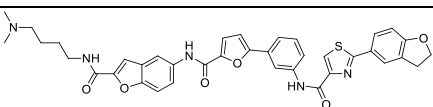
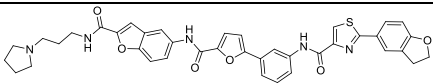
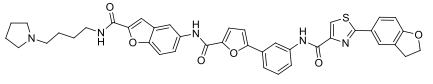
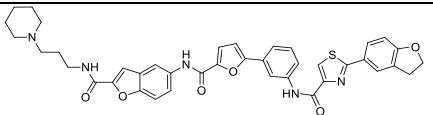
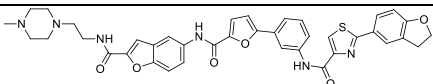
ΔT_m values for Control Duplex DNA sequence					
Code	Structure	MW	5μm	2 μm	1 μm
KN-207		777.89	0.23 ± 0.00	0.10 ± 0.08	0.31 ± 0.08
KN-212		701.79	0.50 ± 0.08	0.30 ± 0.58	0.37 ± 0.58
KN-217		687.76	0.43 ± 0.10	0.67 ± 0.05	0.41 ± 0.15
KN-222		703.76	0.31 ± 0.08	0.45 ± 0.15	0.60 ± 0.08
KN-227		717.79	0.35 ± 0.05	0.45 ± 0.05	0.48 ± 0.10
KN-232		689.78	0.350 ± 0.265	0.883 ± 0.603	0.217 ± 0.702
KN-237		701.79	0.98 ± 0.41	0.33 ± 0.61	0.58 ± 0.76
KN-242		715.82	1.57 ± 1.20	0.50 ± 0.64	0.20 ± 0.63
KN-247		715.25	0.60 ± 1.48	0.03 ± 1.26	-0.07 ± 0.51
KN-252		716.80	1.30 ± 0.48	0.13 ± 0.05	-0.17 ± 0.47

Table AP1: ΔT_m values for Duplex at 5 μm , 2 μm , and 1 μm concentration with standard deviations (continued)

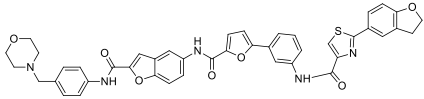
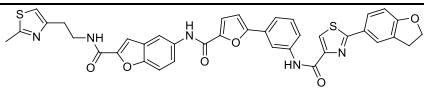
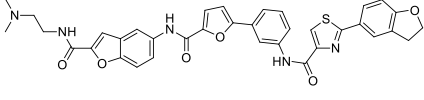
ΔT_m values for Control Duplex DNA sequence					
Code	Structure	MW	5 μm	2 μm	1 μm
KN-257		765.83	0.10 ± 0.46	-0.17 ± 0.66	-0.05 ± 0.61
KN-267		715.80	-0.37 ± 0.53	-0.83 ± 1.26	0.27 ± 0.51
KN-272		661.73	-0.17 ± 1.09	0.13 ± 0.75	0.83 ± 0.28

Table AP2: ΔT_m values for C-Kit1 at 5 μm , 2 μm , and 1 μm concentration with standard deviations

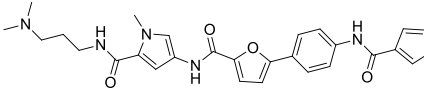
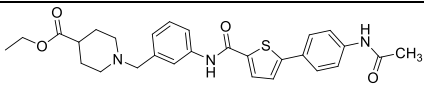
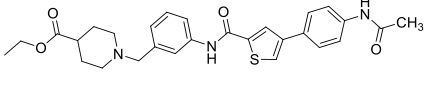
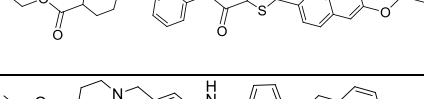
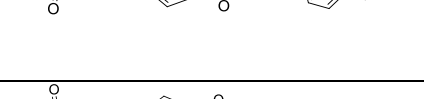
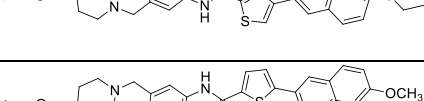
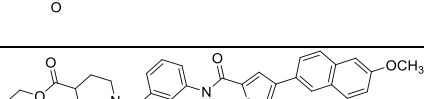

ΔT_m values for C-kit1					
Code	Structure	MW	5 μm	2 μm	1 μm
KN-24		504.02	0.48 ± 0.00	0.00 ± 0.10	0.14 ± 0.05
KN-40		507.38	0.00 ± 0.05	0.00 ± 0.11	0.00 ± 0.22
KN-41		507.15	0.00 ± 0.17	0.00 ± 0.00	0.00 ± 0.26
KN-45		543.00	0.00 ± 0.12	0.00 ± 0.52	0.00 ± 0.100
KN-46		527.10	0.00 ± 0.05	0.00 ± 0.10	0.00 ± 0.36
KN-47		543.05	0.00 ± 0.20	0.00 ± 0.00	0.00 ± 0.59
KN-48		529.96	0.00 ± 0.05	0.00 ± 0.17	0.00 ± 0.12
KN-49		528.94	0.00 ± 0.10	0.00 ± 0.16	0.00 ± 0.36

Table AP2: ΔT_m values for C-Kit1 at 5 μm , 2 μm , and 1 μm concentration with standard deviations (continued)

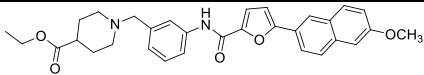
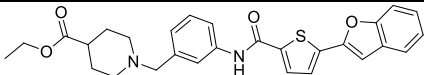
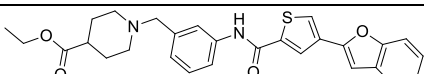
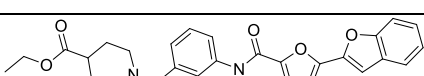
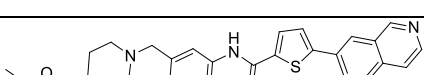
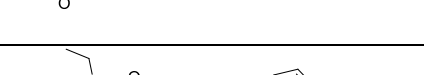
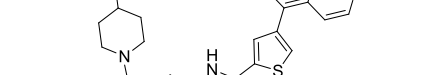
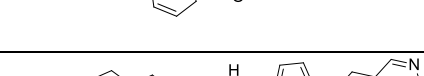
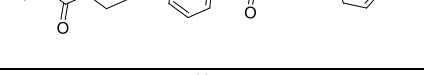
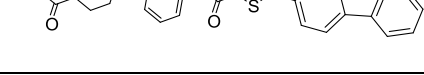
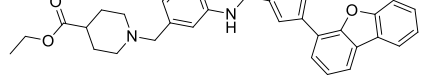
ΔT_m values for C-kit1					
Code	Structure	MW	5 μm	2 μm	1 μm
KN-50		512.99	0.01 ± 0.00	0.00 ± 0.05	0.00 ± 0.52
KN-51		489.17	0.00 ± 0.25	0.00 ± 0.15	0.00 ± 0.30
KN-52		490.14	0.00 ± 0.25	0.00 ± 0.20	0.00 ± 0.00
KN-53		473.13	0.00 ± 0.10	0.00 ± 0.36	0.00 ± 0.01
KN-54		499.85	0.00 ± 0.00	0.00 ± 0.17	0.00 ± 0.12
KN-55		499.92	0.00 ± 0.11	0.00 ± 0.05	0.00 ± 0.10
KN-56		483.88	0.06 ± 0.10	0.20 ± 0.20	0.00 ± 0.22
KN-57		539.09	0.00 ± 0.12	0.00 ± 0.00	0.00 ± 0.26
KN-58		539.09	0.00 ± 0.08	0.00 ± 0.35	0.00 ± 0.19
KN-59		523.12	0.00 ± 0.20	0.00 ± 0.11	0.00 ± 0.10
KN-60		554.99	0.00 ± 0.10	0.00 ± 0.17	0.00 ± 0.25

Table AP2: ΔT_m values for C-Kit1 at 5 μm , 2 μm , and 1 μm concentration with standard deviations (continued)

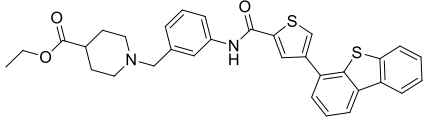
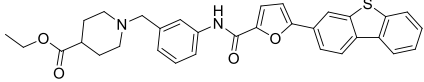
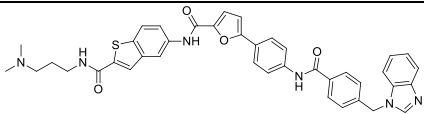
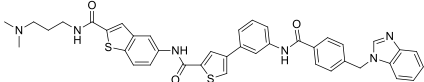
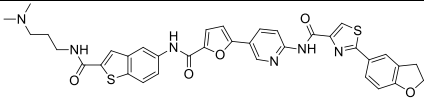
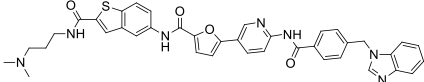
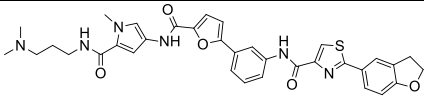
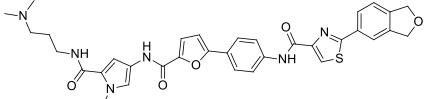
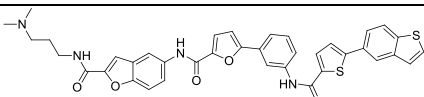
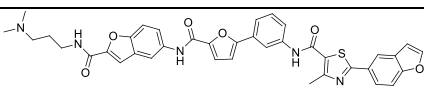
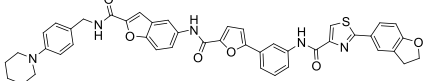
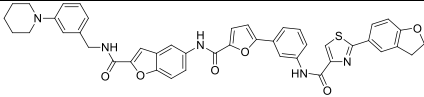
ΔT_m values for C-kit1					
Code	Structure	MW	5μm	2 μm	1 μm
KN-61		554.99	0.00 ± 0.26	0.00 ± 0.15	0.00 ± 0.23
KN-62		539.05	0.05 ± 0.52	0.00 ± 0.00	0.00 ± 0.36
KN-79		697.81	1.27 ± 0.20	0.90 ± 0.22	0.52 ± 0.51
KN-83		713.39	2.54 ± 0.52	0.00 ± 0.10	0.00 ± 0.08
KN-90		693.30	0.21 ± 0.08	0.00 ± 0.25	0.00 ± 0.65
KN-91		698.53	0.34 ± 0.17	0.00 ± 0.22	0.00 ± 0.00
KN-110		639.33	0.00 ± 0.10	0.22 ± 0.11	0.00 ± 0.05
KN-112		639.32	2.43 ± 0.00	1.133 ± 0.08	0.92 ± 0.10
KN-157		688.81	4.03 ± 0.71	1.41 ± 0.11	0.68 ± 0.36
KN-158		687.76	1.17 ± 0.52	1.33 ± 1.02	0.83 ± 0.36
KN-200		763.86	1.93 ± 0.25	0.92 ± 0.73	0.43 ± 0.15
KN-202		763.86	2.22 ± 0.08	1.06 ± 0.26	0.54 ± 0.61

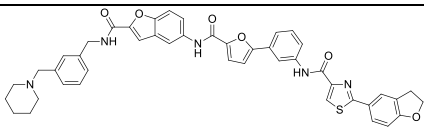
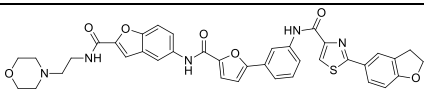
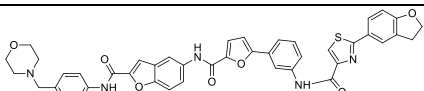
Table AP2: ΔT_m values for C-Kit1 at 5 μm, 2 μm, and 1 μm concentration with standard deviations (continued)					
T_m values for C-kit1					
Code	Structure	MW	5μm	2 μm	1 μm
KN-207		777.89	1.51 ± 0.00	1.22 ± 0.15	0.59 ± 0.10
KN-222		703.76	1.62 ± 0.56	1.06 ± 0.29	0.61 ± 0.63
KN-257		765.83	2.37 ± 0.71	0.17 ± 0.20	-0.10 ± 0.15

Table AP3: ΔT_m values for C-Kit2 at 5 μm , 2 μm , and 1 μm concentration with standard deviations

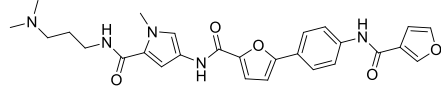
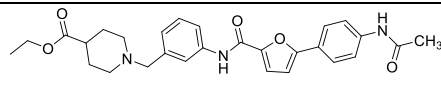
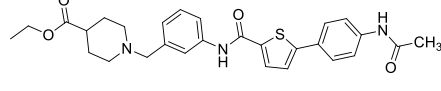
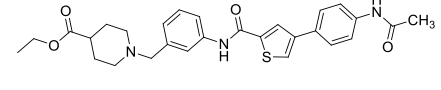
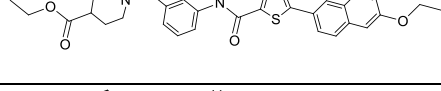
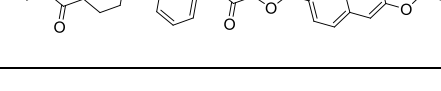
ΔT_m values for C-kit2					
Code	Structure	MW	5μm	2 μm	1 μm
KN-24		504.02	0.00 ± 0.05	0.00 ± 0.00	0.00 ± 0.27
KN-39		491.11	0.00 ± 0.65	0.00 ± 0.15	0.00 ± 0.50
KN-40		507.38	0.42 ± 0.15	0.35 ± 0.71	0.40 ± 0.63
KN-41		507.15	0.00 ± 0.16	0.00 ± 0.93	0.00 ± 0.13
KN-45		543.00	0.46 ± 0.30	0.30 ± 0.00	0.10 ± 0.12
KN-46		527.10	0.00 ± 0.02	0.00 ± 0.12	0.00 ± 0.10

Table AP3: ΔT_m values for C-Kit2 at 5 μm , 2 μm , and 1 μm concentration with standard deviations (continued)

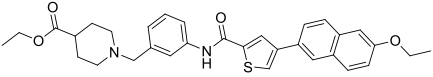
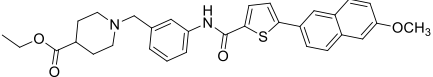
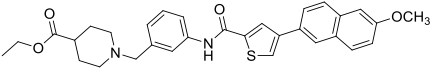
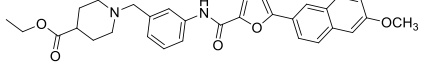
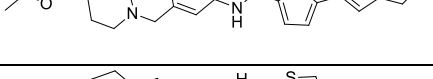
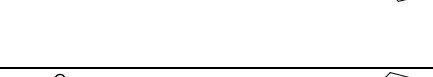
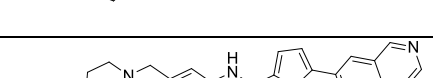
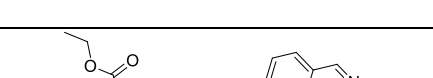
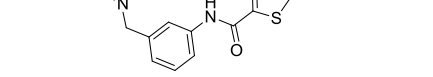
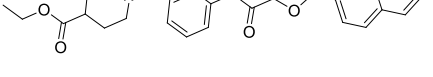
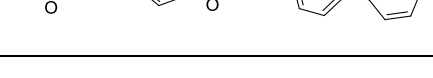
ΔT_m values for C-kit2					
Code	Structure	MW	5 μm	2 μm	1 μm
KN-47		543.05	0.00 ± 0.92	0.00 ± 0.08	0.00 ± 0.15
KN-48		529.96	0.00 ± 0.08	0.00 ± 0.15	0.00 ± 0.16
KN-49		528.94	0.00 ± 0.65	0.00 ± 0.62	0.00 ± 0.51
KN-50		512.99	0.00 ± 0.10	0.00 ± 0.00	0.00 ± 0.08
KN-51		489.17	0.00 ± 0.52	0.00 ± 0.32	0.00 ± 0.33
KN-52		490.14	0.00 ± 0.15	0.00 ± 0.40	0.00 ± 0.08
KN-53		473.13	0.00 ± 0.15	0.00 ± 0.10	0.00 ± 0.58
KN-54		499.85	0.30 ± 0.38	0.00 ± 0.16	0.00 ± 0.32
KN-55		499.92	0.00 ± 0.05	0.00 ± 0.22	0.00 ± 0.39
KN-56		483.88	0.00 ± 0.21	0.00 ± 0.15	0.00 ± 0.06
KN-57		539.09	0.43 ± 0.92	0.42 ± 0.10	0.14 ± 0.13

Table AP3: ΔT_m values for C-Kit2 at 5 μm , 2 μm , and 1 μm concentration with standard deviations (continued)

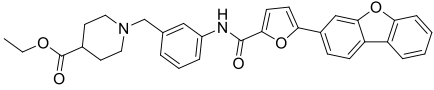
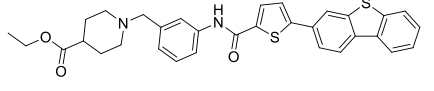
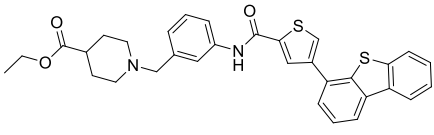
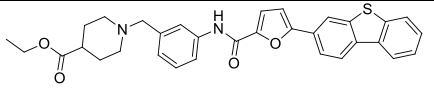
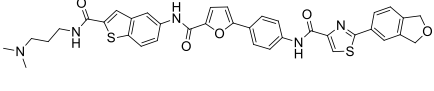
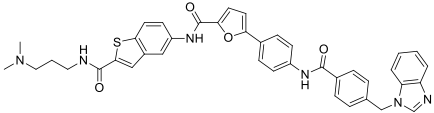
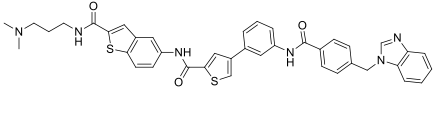
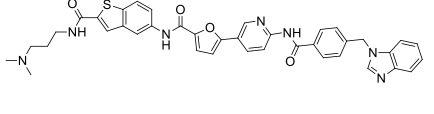
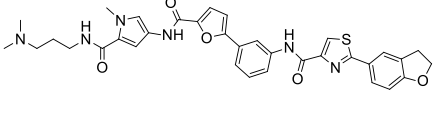
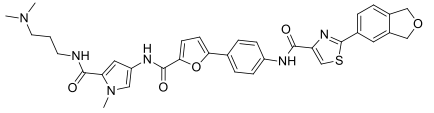
ΔT_m values for C-kit2					
Code	Structure	MW	5 μm	2 μm	1 μm
KN-59		523.12	0.12 ± 0.13	0.00 ± 0.15	0.00 ± 0.90
KN-60		554.99	0.03 ± 0.11	0.00 ± 0.34	0.00 ± 0.00
KN-61		554.99	0.02 ± 0.13	0.00 ± 0.08	0.00 ± 0.23
KN-62		539.05	0.00 ± 0.10	0.00 ± 0.90	0.00 ± 0.05
KN-78		692.55	0.52 ± 0.00	2.72 ± 0.15	0.40 ± 0.15
KN-79		697.81	0.46 ± 0.80	0.00 ± 0.03	0.00 ± 0.06
KN-83		713.39	2.98 ± 0.05	2.01 ± 0.15	0.91 ± 0.25
KN-91		698.53	1.34 ± 0.15	0.18 ± 0.17	0.44 ± 0.12
KN-110		639.33	2.27 ± 0.00	0.44 ± 0.25	0.16 ± 0.13
KN-112		639.32	3.026 ± 0.10	2.340 ± 0.08	0.911 ± 0.25

Table AP3: ΔT_m values for C-Kit2 at 5 μm , 2 μm , and 1 μm concentration with standard deviations (continued)

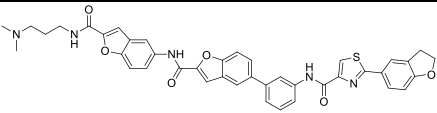
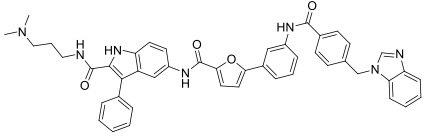
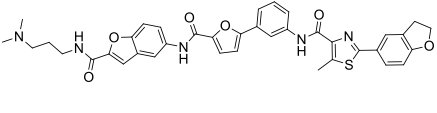
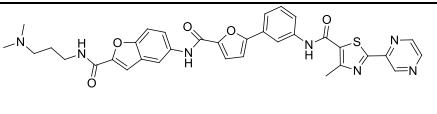
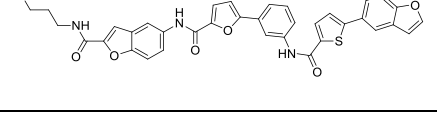
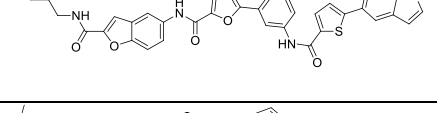
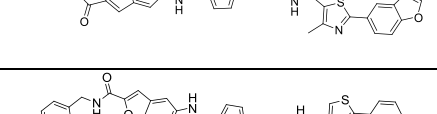
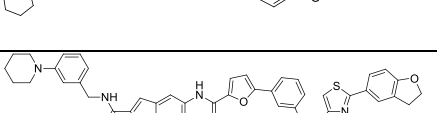
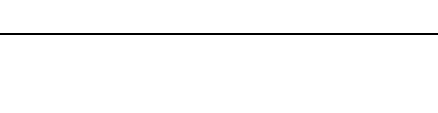
ΔT_m values for C-kit2					
Code	Structure	MW	5 μm	2 μm	1 μm
KN-136		725.81	4.01 ± 0.00	1.42 ± 0.06	0.36 ± 0.13
KN-146		755.86	5.83 ± 0.01	1.39 ± 0.11	0.31 ± 0.12
KN-149		689.78	2.30 ± 0.28	1.92 ± 0.00	0.41 ± 0.10
KN-150		649.72	3.13 ± 0.71	1.10 ± 0.10	1.34 ± 0.13
KN-156		672.75	2.83 ± 0.20	1.02 ± 0.19	0.62 ± 0.39
KN-157		688.81	2.43 ± 0.65	0.86 ± 0.04	0.35 ± 0.15
KN-158		687.76	2.58 ± 0.70	0.98 ± 0.15	0.53 ± 0.00
KN-200		763.86	0.60 ± 0.20	-0.10 ± 0.20	0.50 ± 0.26
KN-202		763.86	1.43 ± 0.31	0.70 ± 0.0	0.60 ± 0.26

Table AP4: ΔT_m values for DRH at 5 μm , 2 μm , and 1 μm concentration with standard deviations

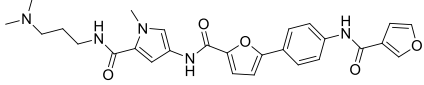
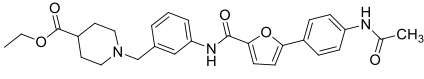
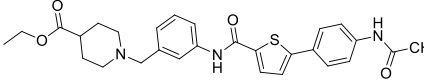
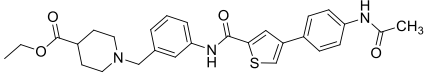
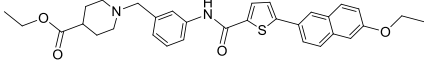
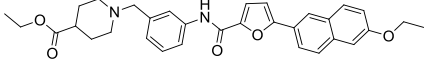
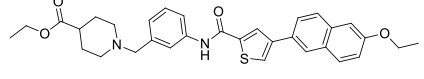
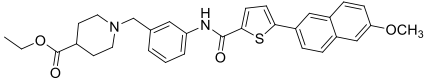
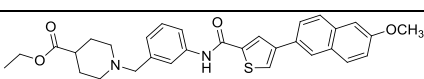
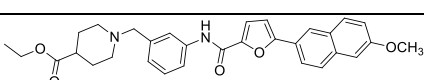
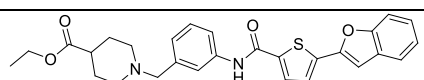
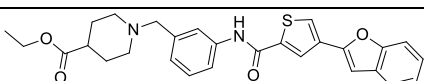
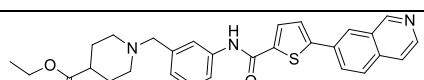
ΔT_m values for DRH					
Code	Structure	MW	5 μm	2 μm	1 μm
KN-24		504.02	0.07 ± 0.15	0.25 ± 0.00	0.05 ± 0.73
KN-39		491.11	-0.03 ± 0.15	0.03 ± 0.08	0.37 ± 0.08
KN-40		507.38	0.21 ± 0.08	0.03 ± 0.08	0.11 ± 0.08
KN-41		507.15	0.30 ± 0.00	0.27 ± 0.58	0.03 ± 0.08
KN-45		543.00	0.08 ± 0.28	0.35 ± 0.00	0.25 ± 0.00
KN-46		527.10	0.25 ± 0.00	0.23 ± 0.05	0.28 ± 0.05
KN-47		543.05	0.23 ± 0.08	0.17 ± 0.08	0.10 ± 0.00
KN-48		529.96	0.17 ± 0.21	0.27 ± 0.08	0.20 ± 0.00
KN-49		528.94	0.13 ± 0.15	0.83 ± 0.58	0.20 ± 0.00
KN-50		512.99	0.27 ± 0.08	0.11 ± 0.13	-0.10 ± 0.25
KN-51		489.17	-0.37 ± 0.00	-0.17 ± 0.00	-0.13 ± 0.05
KN-52		490.14	-0.07 ± 0.20	-0.23 ± 0.11	-0.13 ± 0.05
KN-54		499.85	-0.10 ± 0.08	-0.03 ± 0.08	0.10 ± 0.13

Table AP4: ΔT_m values for DRH at 5 μm , 2 μm , and 1 μm concentration with standard deviations (continued)

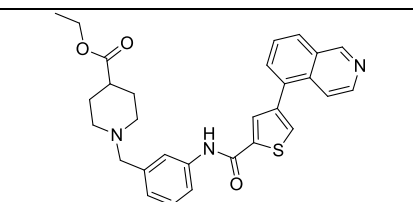
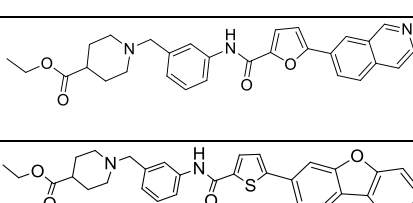
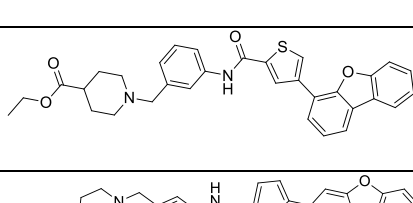
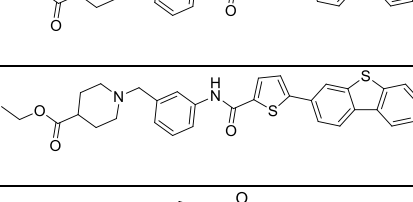
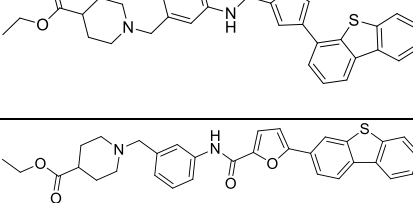
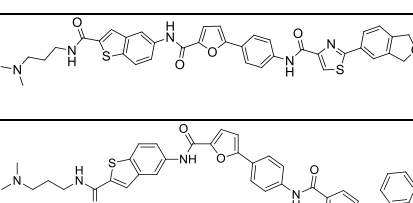
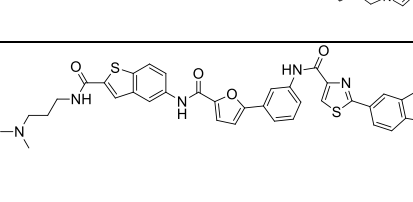

ΔT_m values for DRH					
Code	Structure	MW	5 μm	2 μm	1 μm
KN-55		499.92	-0.07 ± 0.00	-0.03 ± 0.08	0.10 ± 0.08
KN-56		483.88	0.10 ± 0.13	-0.67 ± 0.00	0.03 ± 0.100
KN-57		539.09	0.23 ± 0.00	0.20 ± 0.15	0.00 ± 0.05
KN-58		539.09	0.33 ± 0.00	0.17 ± 0.53	0.20 ± 0.15
KN-59		523.12	-0.03 ± 0.08	0.17 ± 0.13	0.07 ± 0.13
KN-60		554.99	0.07 ± 0.15	0.00 ± 0.15	0.10 ± 0.15
KN-61		554.99	0.20 ± 0.20	-0.03 ± 0.00	0.26 ± 0.00
KN-62		539.05	-0.07 ± 0.25	-0.20 ± 0.58	0.30 ± 0.05
KN-78		692.55	0.67 ± 0.13	0.47 ± 0.10	0.43 ± 0.08
KN-79		697.81	0.37 ± 0.00	0.67 ± 0.10	0.47 ± 0.10
KN-88		692.72	0.57 ± 0.08	0.37 ± 0.13	0.31 ± 0.58

Table AP4: ΔT_m values for DRH at 5 μm , 2 μm , and 1 μm concentration with standard deviations (continued)

ΔT_m values for DRH					
Code	Structure	MW	5 μm	2 μm	1 μm
KN-89		697.57	0.33 ± 0.53	0.33 ± 0.15	0.50 ± 0.08
KN-90		693.30	0.23 ± 0.15	0.18 ± 0.08	0.14 ± 0.15
KN-91		698.53	0.33 ± 0.15	0.37 ± 0.05	0.00 ± 0.00
KN-110		639.33	0.33 ± 0.08	0.90 ± 0.00	0.16 ± 0.13
KN-112		639.32	0.43 ± 0.15	0.93 ± 0.58	0.06 ± 0.00
KN-119		676.13	-0.67 ± 0.58	0.03 ± 0.13	0.67 ± 0.08
KN-120		676.21	0.30 ± 0.00	0.00 ± 0.00	0.00 ± 0.10
KN-130		692.81	0.30 ± 0.00	0.20 ± 0.00	0.33 ± 0.58
KN-136		725.81	0.43 ± 0.58	0.36 ± 0.15	0.10 ± 0.00
KN-143		674.77	0.37 ± 0.53	0.33 ± 0.08	0.23 ± 0.08
KN-144		679.77	0.87 ± 0.08	0.67 ± 0.08	0.23 ± 0.58

Table AP4: ΔT_m values for DRH at 5 μm , 2 μm , and 1 μm concentration with standard deviations (continued)

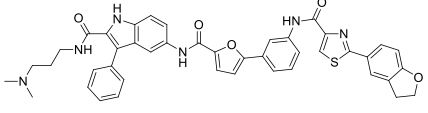
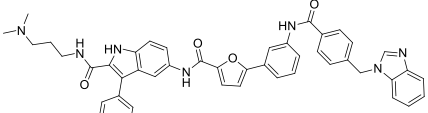
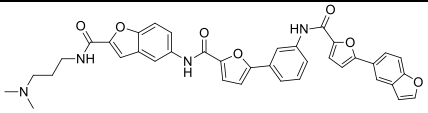
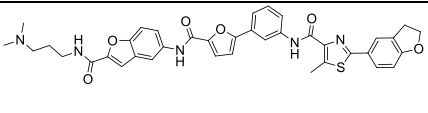
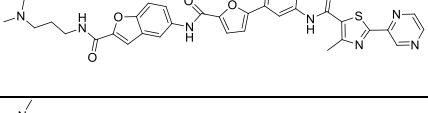
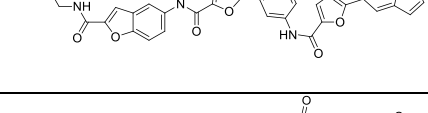
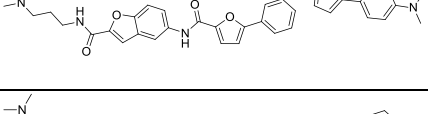
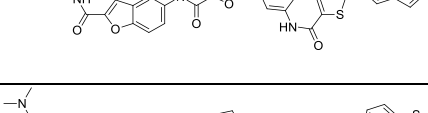
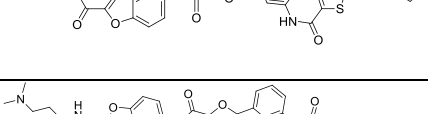
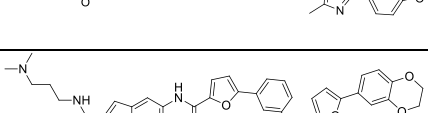
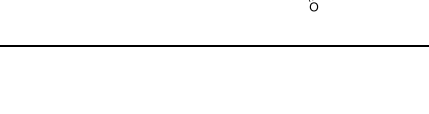
ΔT_m values for DRH					
Code	Structure	MW	5 μm	2 μm	1 μm
KN-145		750.86	0.63 ± 0.08	0.30 ± 0.08	0.30 ± 0.00
KN-146		755.86	0.60 ± 0.10	0.33 ± 0.08	0.17 ± 0.08
KN-148		656.68	2.93 ± 0.00	1.50 ± 0.51	0.17 ± 0.13
KN-149		689.78	0.47 ± 0.08	0.23 ± 0.08	0.1 ± 0.05
KN-150		649.72	0.57 ± 0.58	0.33 ± 0.08	0.27 ± 0.15
KN-154		672.75	0.30 ± 0.08	0.20 ± 0.58	0.10 ± 0.08
KN-155		687.74	0.67 ± 0.00	0.17 ± 0.00	0.17 ± 0.13
KN-156		672.75	0.33 ± 0.15	0.37 ± 0.00	0.26 ± 0.10
KN-157		688.81	0.43 ± 0.05	0.40 ± 0.08	0.23 ± 0.08
KN-158		687.76	0.40 ± 0.08	0.67 ± 0.10	0.33 ± 0.11
KN-159		674.70	0.67 ± 0.25	0.57 ± 0.00	0.43 ± 0.13

Table AP4: ΔT_m values for DRH at 5 μm , 2 μm , and 1 μm concentration with standard deviations (continued)

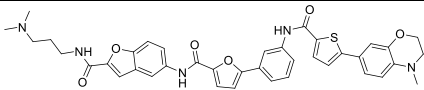
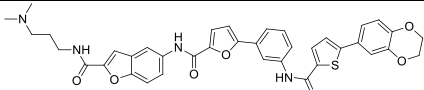
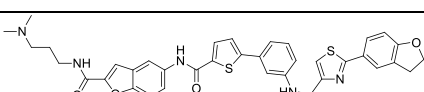
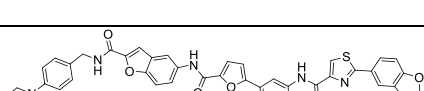
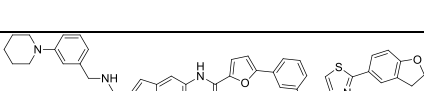
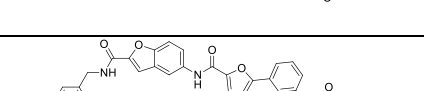

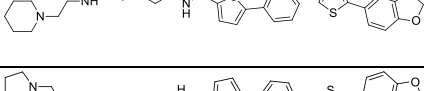
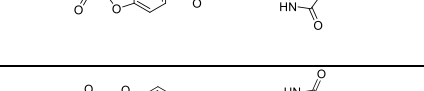
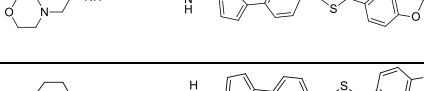
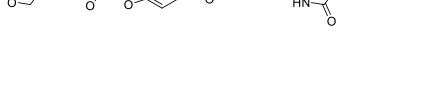
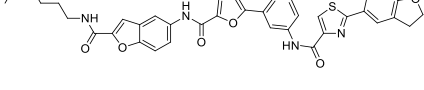
ΔT_m values for DRH					
Code	Structure	MW	5 μm	2 μm	1 μm
KN-160		703.81	0.66 ± 0.10	0.60 ± 0.08	0.40 ± 0.05
KN-161		690.76	0.73 ± 0.28	0.50 ± 0.05	0.37 ± 0.00
KN-176		691.82	1.20 ± 0.11	0.76 ± 0.00	0.27 ± 0.00
KN-200		763.86	0.25 ± 0.11	0.18 ± 0.00	-0.17 ± 0.20
KN-202		763.86	0.01 ± 0.05	-0.05 ± 0.31	0.30 ± 0.11
KN-207		777.89	0.38 ± 0.10	-0.01 ± 0.26	0.13 ± 0.10
KN-212		701.79	0.23 ± 0.00	0.27 ± 0.58	0.10 ± 0.05
KN-217		687.76	0.31 ± 0.08	0.28 ± 0.10	0.28 ± 0.00
KN-222		703.76	0.33 ± 0.10	0.20 ± 0.15	0.20 ± 0.05
KN-227		717.79	0.31 ± 0.08	0.23 ± 0.00	0.250 ± 0.08
KN-232		689.78	0.78 ± 0.40	-0.17 ± 0.00	-0.37 ± 0.14
KN-237		701.79	0.08 ± 0.28	-0.61 ± 0.00	-1.07 ± 0.35

Table AP4: ΔT_m values for DRH at 5 μm , 2 μm , and 1 μm concentration with standard deviations (continued)

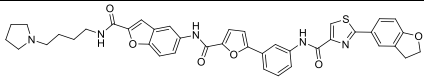
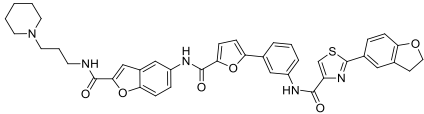
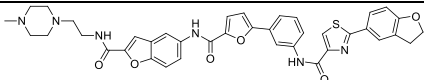
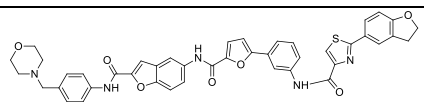
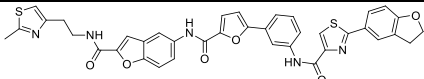
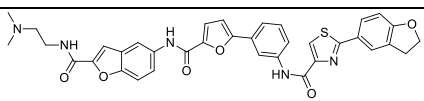
ΔT_m values for DRH					
Code	Structure	MW	5 μm	2 μm	1 μm
KN-242		715.82	16.43 ± 1.14	-0.96 ± 0.34	-0.67 ± 0.14
KN-247		715.25	-3.31 ± 1.41	-0.16 ± 0.35	-1.21 ± 0.42
KN-252		716.80	11.98 ± 2.54	-0.36 ± 0.35	-0.67 ± 0.00
KN-257		765.83	-1.07 ± 0.14	-0.47 ± 0.00	-0.71 ± 0.00
KN-267		715.80	-0.36 ± 0.07	-0.67 ± 0.23	0.13 ± 0.35
KN-272		661.73	-0.96 ± 0.62	-0.41 ± 0.14	-0.91 ± 0.14

Table AP5: ΔT_m values for CDRH at 5 μm , 2 μm , and 1 μm concentration with standard deviations

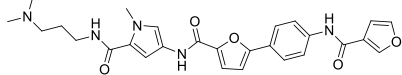
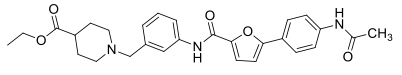
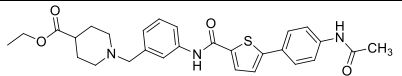
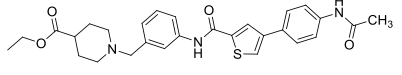
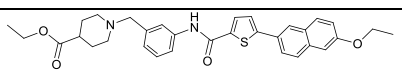
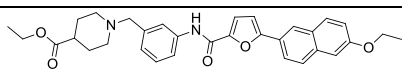
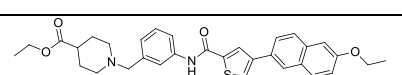
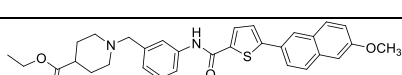
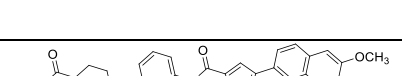
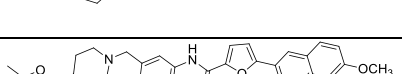
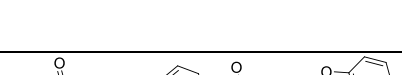
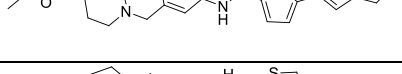
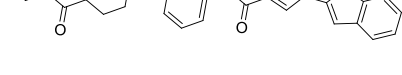
ΔT_m values for CDRH					
Code	Structure	MW	5 μm	2 μm	1 μm
KN-24		504.02	0.71 ± 0.08	0.83 ± 0.58	0.60 ± 0.10
KN-39		491.11	0.83 ± 0.08	0.17 ± 0.13	1.11 ± 0.05
KN-40		507.38	1.00 ± 0.10	0.73 ± 0.08	0.90 ± 0.00
KN-41		507.15	1.07 ± 0.05	1.28 ± 0.13	0.70 ± 0.10
KN-45		543.00	0.87 ± 0.58	0.50 ± 0.10	0.83 ± 0.08
KN-46		527.10	0.88 ± 0.05	0.90 ± 0.10	1.18 ± 0.05
KN-47		543.05	1.11 ± 0.05	1.01 ± 0.08	1.50 ± 0.10
KN-48		529.96	1.10 ± 0.10	0.91 ± 0.08	0.83 ± 0.05
KN-49		528.94	0.30 ± 0.94	0.90 ± 0.00	0.83 ± 0.08
KN-50		512.99	1.05 ± 0.36	1.51 ± 0.11	1.63 ± 0.05
KN-51		489.17	-0.23 ± 0.10	0.15 ± 0.08	0.17 ± 0.00
KN-52		490.14	-0.00 ± 0.08	-0.07 ± 0.13	0.50 ± 0.05
KN-53		473.13	-0.10 ± 0.15	0.07 ± 0.00	0.01 ± 0.10

Table AP5: ΔT_m values for CDRH at 5 μm , 2 μm , and 1 μm concentration with standard deviations (continued)

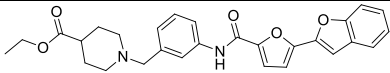
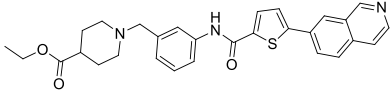
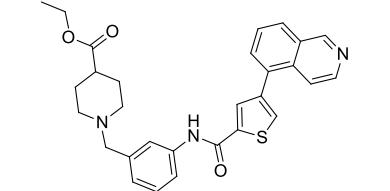
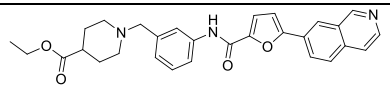
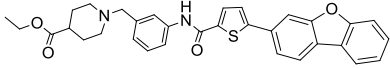
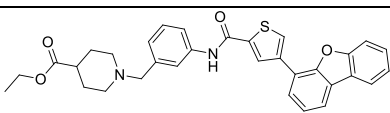
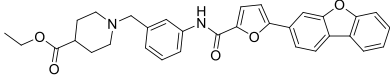
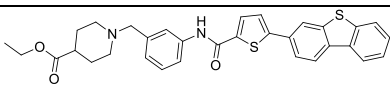
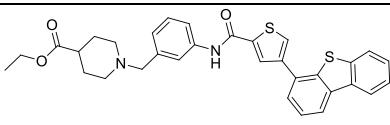
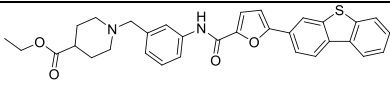
ΔT_m values for CDRH					
Code	Structure	MW	5 μm	2 μm	1 μm
KN-53		473.13	-0.15 ± 0.15	0.07 ± 0.00	0.07 ± 0.10
KN-54		499.85	0.15 ± 0.08	0.27 ± 0.48	-0.21 ± 0.08
KN-55		499.92	-0.20 ± 0.08	-0.05 ± 0.08	-0.05 ± 0.05
KN-56		483.88	-0.15 ± 0.05	-0.15 ± 0.05	-0.01 ± 0.05
KN-57		539.09	-0.03 ± 0.00	-0.03 ± 0.00	-0.03 ± 0.10
KN-58		539.09	-0.01 ± 0.05	-0.11 ± 0.08	-0.17 ± 0.05
KN-59		523.12	-0.20 ± 0.05	-0.00 ± 0.08	-0.17 ± 0.11
KN-60		554.99	-0.21 ± 0.05	-0.15 ± 0.05	-0.01 ± 0.15
KN-61		554.99	-1.15 ± 0.10	0.15 ± 0.00	-0.07 ± 0.08
KN-62		539.05	-0.18 ± 0.11	-0.05 ± 0.10	0.15 ± 0.10

Table AP5: ΔT_m values for CDRH at 5 μm , 2 μm , and 1 μm concentration with standard deviations (continued)

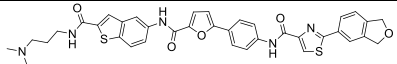
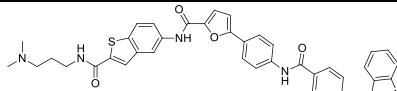
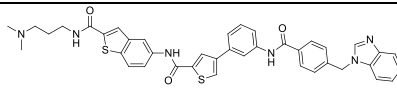
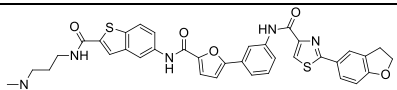
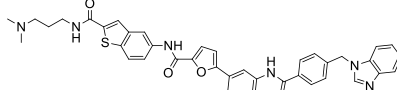
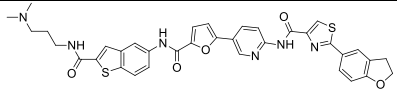
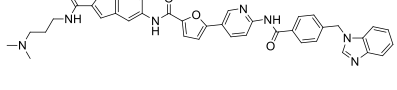
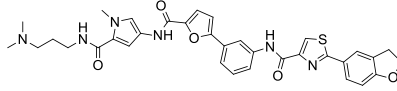
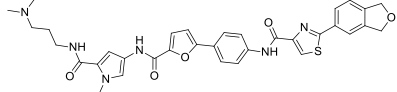
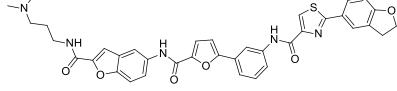
ΔT_m values for CDRH					
Code	Structure	MW	5 μm	2 μm	1 μm
KN-78		692.55	0.20 ± 0.20	0.23 ± 0.08	0.08 ± 0.05
KN-79		697.81	-0.28 ± 0.2	0.01 ± 0.05	0.15 ± 0.10
KN-83		713.39	0.11 ± 0.05	0.07 ± 0.05	0.08 ± 0.05
KN-88		692.72	3.50 ± 0.05	1.96 ± 0.05	3.16 ± 0.05
KN-89		697.57	0.11 ± 0.08	0.28 ± 0.28	0.48 ± 0.05
KN-90		693.30	0.35 ± 0.05	0.13 ± 0.23	0.10 ± 0.00
KN-91		698.53	0.24 ± 0.05	0.13 ± 0.10	0.02 ± 0.05
KN-110		639.33	0.27 ± 0.05	0.83 ± 0.23	0.80 ± 0.00
KN-112		639.32	0.16 ± 0.05	0.03 ± 0.03	0.00 ± 0.00
KN-119		676.13	3.55 ± 0.05	2.47 ± 0.23	1.11 ± 0.11

Table AP5: ΔT_m values for CDRH at 5 μm , 2 μm , and 1 μm concentration with standard deviations (continued)

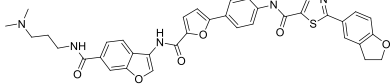
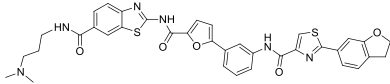
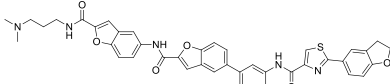

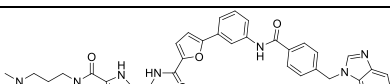
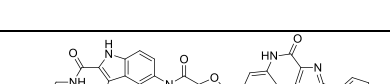
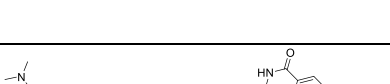


ΔT_m values for CDRH					
Code	Structure	MW	5 μm	2 μm	1 μm
KN-120		676.21	1.21 ± 0.10	0.92 ± 0.05	0.46 ± 0.23
KN-130		692.81	0.25 ± 0.10	0.31 ± 0.05	0.14 ± 0.10
KN-136		725.81	0.27 ± 0.05	0.13 ± 0.231	0.08 ± 0.00
KN-143		674.77	0.21 ± 0.45	0.18 ± 0.08	0.20 ± 0.11
KN-144		679.77	0.11 ± 0.05	0.10 ± 0.10	0.11 ± 0.05
KN-145		750.86	0.56 ± 0.23	0.23 ± 0.15	0.13 ± 0.00
KN-146		755.86	0.47 ± 0.11	0.36 ± 0.10	0.13 ± 0.05
KN-148		656.68	1.30 ± 0.05	2.93 ± 0.26	3.30 ± 0.32
KN-149		689.78	-0.05 ± 0.05	-0.15 ± 0.15	0.08 ± 0.15

Table AP5: ΔT_m values for CDRH at 5 μm , 2 μm , and 1 μm concentration with standard deviations (continued)

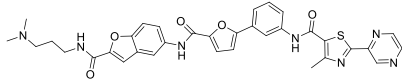
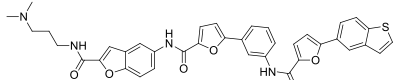
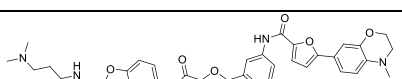
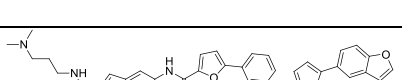
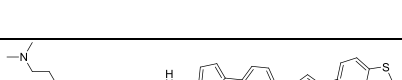
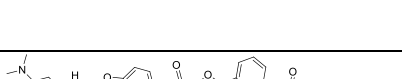
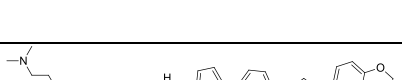
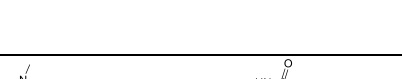

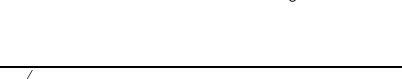
ΔT_m values for CDRH					
Code	Structure	MW	5 μm	2 μm	1 μm
KN-150		649.72	0.28 ± 0.23	0.11 ± 0.05	0.19 ± 0.08
KN-154		672.75	-0.03 ± 0.15	-0.03 ± 0.05	-0.20 ± 0.10
KN-155		687.74	0.03 ± 0.11	-0.33 ± 0.05	-0.10 ± 0.10
KN-156		672.75	-0.23 ± 0.37	-0.30 ± 0.26	-0.50 ± 0.10
KN-157		688.81	-0.20 ± 0.10	-0.36 ± 0.05	-0.33 ± 0.05
KN-158		687.76	-0.13 ± 0.25	-0.53 ± 0.25	-0.70 ± 0.26
KN-159		674.70	0.20 ± 0.00	0.00 ± 0.28	0.20 ± 0.00
KN-160		703.81	0.30 ± 0.11	0.30 ± 0.00	0.66 ± 0.23
KN-161		690.76	0.26 ± 0.05	0.83 ± 0.23	0.80 ± 0.00
KN-176		691.82	0.00 ± 0.10	0.00 ± 0.00	-0.17 ± 0.08

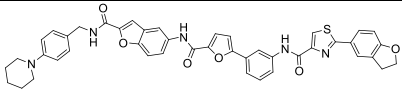
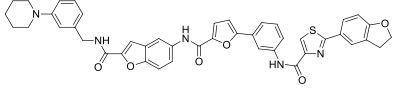
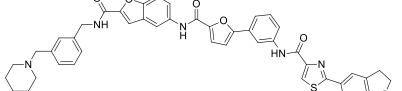
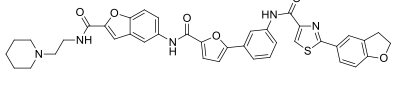
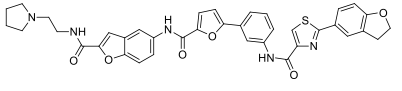
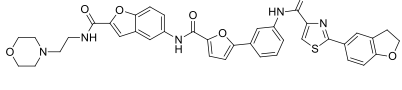
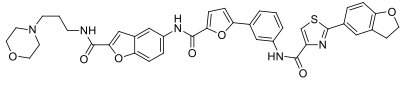
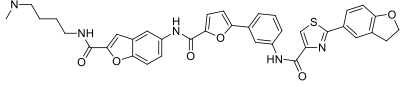
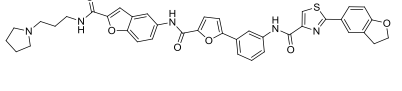
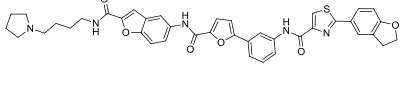
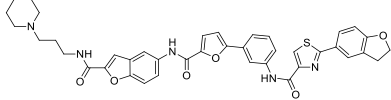
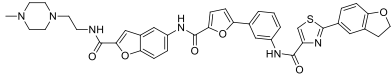
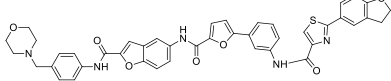
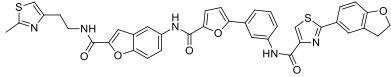
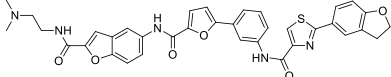
Table AP5: ΔT_m values for CDRH at 5 μm, 2 μm, and 1 μm concentration with standard deviations (continued)					
ΔT_m values for CDRH					
Code	Structure	MW	5μm	2 μm	1 μm
KN-200		763.86	2.53 ± 0.10	1.30 ± 0.05	3.03 ± 0.08
KN-202		763.86	2.90 ± 0.05	1.60 ± 0.15	3.17 ± 0.05
KN-207		777.89	3.33 ± 0.00	1.77 ± 0.08	2.97 ± 0.08
KN-212		701.79	4.33 ± 0.25	2.53 ± 0.10	3.30 ± 0.11
KN-217		687.76	3.40 ± 0.08	2.07 ± 0.05	3.20 ± 0.08
KN-222		703.76	3.00 ± 0.08	1.80 ± 0.58	3.23 ± 0.00
KN-227		717.79	3.10 ± 0.05	1.76 ± 0.05	3.13 ± 0.10
KN-232		689.78	0.83 ± 0.20	0.35 ± 0.63	0.17 ± 0.11
KN-237		701.79	0.89 ± 0.10	0.53 ± 0.00	0.33 ± 0.15
KN-242		715.82	0.51 ± 0.21	0.25 ± 0.10	0.15 ± 0.03

Table AP5: ΔT_m values for CDRH at 5 μm, 2 μm, and 1 μm concentration with standard deviations (continued)					
ΔT_m values for CDRH					
Code	Structure	MW	5 μm	2 μm	1 μm
KN-247		715.25	0.68 ± 0.45	0.43 ± 0.26	0.317 ± 0.11
KN-252		716.80	0.35 ± 0.05	0.18 ± 0.58	0.07 ± 0.13
KN-257		765.83	0.10 ± 0.43	-0.01 ± 0.66	-0.05 ± 0.36
KN-267		715.80	0.33 ± 0.11	0.21 ± 0.20	0.11 ± 0.05
KN-272		661.73	0.11 ± 0.05	0.10 ± 0.00	0.08 ± 0.00